PHOTOSYNTHESIS IN A CHANGING GLOBAL CLIMATE: A MATTER OF SCALE

EDITED BY: Iker Aranjuelo, Marouane Baslam and Alvaro Sanz-Saez

PUBLISHED IN: Frontiers in Plant Science

frontiers Research Topics

frontiers

ISSN 1664-8714
ISBN 978-2-88966-513-6
DOI 10.3389/978-2-88966-513-6

About Frontiers

Frontiers is more than just an open-access publisher of scholarly articles: it is a pioneering approach to the world of academia, radically improving the way scholarly research is managed. The grand vision of Frontiers is a world where all people have an equal opportunity to seek, share and generate knowledge. Frontiers provides immediate and permanent online open access to all its publications, but this alone is not enough to realize our grand goals.

Frontiers Journal Series

The Frontiers Journal Series is a multi-tier and interdisciplinary set of open-access, online journals, promising a paradigm shift from the current review, selection and dissemination processes in academic publishing. All Frontiers journals are driven by researchers for researchers; therefore, they constitute a service to the scholarly community. At the same time, the Frontiers Journal Series operates on a revolutionary invention, the tiered publishing system, initially addressing specific communities of scholars, and gradually climbing up to broader public understanding, thus serving the interests of the lay society, too.

Dedication to Quality

Each Frontiers article is a landmark of the highest quality, thanks to genuinely collaborative interactions between authors and review editors, who include some of the world's best academicians. Research must be certified by peers before entering a stream of knowledge that may eventually reach the public - and shape society; therefore, Frontiers only applies the most rigorous and unbiased reviews.
Frontiers revolutionizes research publishing by freely delivering the most outstanding research, evaluated with no bias from both the academic and social point of view. By applying the most advanced information technologies, Frontiers is catapulting scholarly publishing into a new generation.

What are Frontiers Research Topics?

Frontiers Research Topics are very popular trademarks of the Frontiers Journals Series: they are collections of at least ten articles, all centered on a particular subject. With their unique mix of varied contributions from Original Research to Review Articles, Frontiers Research Topics unify the most influential researchers, the latest key findings and historical advances in a hot research area! Find out more on how to host your own Frontiers Research Topic or contribute to one as an author by contacting the Frontiers Editorial Office: frontiersin.org/about/contact

PHOTOSYNTHESIS IN A CHANGING GLOBAL CLIMATE: A MATTER OF SCALE

Topic Editors:
Iker Aranjuelo, Superior Council of Scientific Investigations, Spain
Marouane Baslam, Niigata University, Japan
Alvaro Sanz-Saez, Auburn University, United States

Citation: Aranjuelo, I., Baslam, M., Sanz-Saez, A., eds. (2021). Photosynthesis in a Changing Global Climate: a Matter of Scale. Lausanne: Frontiers Media SA.
doi: 10.3389/978-2-88966-513-6

Table of Contents

frontiers in Plant Science

ORIGINAL RESEARCH
published: 06 August 2019
doi: 10.3389/fpls.2019.01012

Performance Index and PSII Connectivity Under Drought and Contrasting Light Regimes in the CAM Orchid *Phalaenopsis*

*Nathalie Ceusters[1], Roland Valcke[2], Mario Frans[1], Johan E. Claes[3], Wim Van den Ende[4] and Johan Ceusters[1,5]**

[1] Department of Biosystems, Division of Crop Biotechnics, Research Group for Sustainable Crop Production & Protection, KU Leuven, Geel, Belgium, [2] Molecular and Physical Plant Physiology, UHasselt, Diepenbeek, Belgium, [3] Department of Microbial and Molecular Systems, Bioengineering Technology TC, KU Leuven, Geel, Belgium, [4] Laboratory of Molecular Plant Biology, Department of Biology, KU Leuven, Leuven, Belgium, [5] Centre for Environmental Sciences, Environmental Biology, UHasselt, Diepenbeek, Belgium

OPEN ACCESS

Edited by:
Marouane Baslam,
Niigata University, Japan

Reviewed by:
Jim Leebens-Mack,
University of Georgia, United States
Jie He,
Nanyang Technological University, Singapore

***Correspondence:**
Johan Ceusters
johan.ceusters@kuleuven.be

Specialty section:
This article was submitted to Plant Abiotic Stress, a section of the journal Frontiers in Plant Science

Received: 20 March 2019
Accepted: 18 July 2019
Published: 06 August 2019

Citation:
Ceusters N, Valcke R, Frans M, Claes JE, Van den Ende W and Ceusters J (2019) Performance Index and PSII Connectivity Under Drought and Contrasting Light Regimes in the CAM Orchid Phalaenopsis. Front. Plant Sci. 10:1012. doi: 10.3389/fpls.2019.01012

Crassulacean acid metabolism (CAM) is a specialized mode of photosynthesis characterized by improved water use efficiency mediated by major nocturnal CO_2 fixation. Due to its inherent metabolic plasticity CAM represents a successful physiological strategy for plant adaptation to abiotic stress. The present study reports on the impact of drought stress and different light intensities (PPFD 50 and 200 μmol m^{-2} s^{-1}) on the photosynthetic performance of the obligate CAM orchid *Phalaenopsis* "Edessa" by integrating diel gas exchange patterns with assessments of the light reactions by analyzing fast chlorophyll *a* fluorescence induction. Parameters such as PI_{abs} (performance index), different energy fluxes per active reaction centre (RC) reflecting the electron flow from photosystem II to photosystem I and the energetic communication between PSII complexes defined as connectivity were considered for the first time in a CAM plant. A higher PS II connectivity for plants grown under low light ($p \sim 0.51$) compared to plants grown under high light ($p \sim 0.31$) brought about similar specific energy fluxes of light absorbance, dissipation and processing through the electron transport chain, irrespective of the light treatment. With a 25% higher maximum quantum yield and comparable biomass formation, low light grown plants indeed proved to process light energy more efficiently compared to high light grown plants. The performance index was identified as a very reliable and sensitive parameter to indicate the onset and progress of drought stress. Under restricted CO_2 availability (due to closed stomata) leaves showed higher energy dissipation and partial inactivation of PSII reaction centres to reduce the energy input to the electron transport chain and as such aid in avoiding overexcitation and photodamage. Especially during CAM idling there is a discrepancy between continuous input of light energy but severely reduced

availability of both water and CO_2, which represents the ultimate electron acceptor. Taken together, our results show a unique flexibility of CAM plants to optimize the light reactions under different environmental conditions in a dual way by either attenuating or increasing energy flux.

Keywords: chlorophyll fluorescence, crassulacean acid metabolism, *Phalaenopsis*, performance index, PSII connectivity, specific energy fluxes

INTRODUCTION

Plants thrive in a variety of environments, each associated with certain characteristics and limitations (e.g., rainforest, desert, and arctic conditions). Due to their sessile nature they need to be extremely adaptable to their continuously changing environment. Crassulacean acid metabolism (CAM), which is characterized by an optimized water use efficiency by taking up CO_2 predominantly at night is an important physiological strategy for plant adaptation (Cushman and Borland, 2002; Borland et al., 2011; Ceusters et al., 2017). Traditionally, diel CAM has been defined within a four-phase framework to describe the photosynthetic performance (Osmond, 1978): (i) phase I – open stomata in the dark and external CO_2 fixation via phospho*enol*pyruvate carboxylase (PEPC) into C_4 acids (mostly malic acid); (ii) phase 2 – open stomata at the start of the light period and external CO_2 fixation by combination of PEPC and ribulose-1,5-bisphosphate carboxylase-oxygenase (RubisCO); (iii) phase 3 – closed stomata in the middle of the day whilst malic acid is decarboxylated [catalyzed by NAD(P)-malic enzyme (ME) or phospho*enol*pyruvate carboxykinase] and refixation of CO_2 by RubisCO; and (iv) phase 4 – stomata open toward the end of the day and external CO_2 is fixed via RubisCO and/or PEPC. An ubiquitous feature of CAM is the integration of circadian and metabolite control over nocturnal C_4 and daytime C_3 carboxylation processes, hereby providing plasticity for optimizing carbon gain and water use by extending or curtailing the period of net CO_2 uptake over any 24-h period (Borland et al., 1999; Ceusters et al., 2009a, 2010; Haydon et al., 2011; Ceusters et al., 2014; Yang et al., 2015). When experiencing severe drought stress CAM plants enter the stage of CAM-idling, showing no net CO_2 uptake and recycling respiratory CO_2 behind closed stomates during the complete diel cycle to minimize any further water loss (Ting, 1985; Ceusters et al., 2009a,b).

Plant photosynthesis is generally characterized by two linked key processes, i.e., (1) light energy capture and use in the electron transport chains to provide energy and reducing power and (2) CO_2 sequestration into triose phosphates (**Figure 1**). Non-destructive methods like chlorophyll fluorescence and leaf gas exchange analyses can easily be applied to investigate photosynthetic performance. Chlorophyll fluorescence analyses allow to obtain detailed information about the primary light mediated reactions of photosynthesis. Basically, light energy absorbed by the sun can be dissipated by either photochemical (i.e., photosynthesis) or non-photochemical processes (i.e., heat or fluorescence) (Maxwell and Johnson, 2000). As these processes occur in close competition, abiotic stress factors such as deviations of the optimal temperature, light and water availability can easily cause imbalances between the absorption of light energy by chlorophyll and the subsequent use of energy in CO_2 fixation (**Figure 1**; Cornic and Massacci, 1996; Falk et al., 1996). Evaluation of the response of the photosynthetic apparatus to different conditions has generally been performed by analyzing parameters describing the maximum quantum efficiency of photosystem II (PSII) photochemistry (F_v/F_m), the effective quantum yield of PSII photochemistry (Φ_{PSII}), electron transport rate (ETR), photochemical quenching (qP) and non-photochemical quenching (qN). In addition different authors suggested that (1) the performance index (PI_{abs}) parameter, which quantifies the overall functionality of the electron flow through PSII, might be a sensitive parameter of plant homeostasis; and (2) that it is also interesting to evaluate specific energy fluxes per reaction centre (RC) i.e., absorption (ABS/RC), trapping (Tr_0/RC), electron transport (Et_0/RC), reduction of end electron acceptors (Re_0/RC) and dissipation (Di_0/RC) to obtain information about the response of the photosynthetic apparatus under different environmental conditions (Krüger et al., 1997; Rapacz, 2007; Zivcak et al., 2008, 2014a,b; Campos et al., 2014; Chondrogiannis and Grammatikopoulos, 2016). The specific energy fluxes measured per active PSII reaction centre are all interconnected and can be considered as expressing the behavior of the PSII system when all RCs are open (i.e., at the onset of excitation). In healthy plants (**Figure 1A**), part of the flux of absorbed photons (ABS) will be channeled as trapping flux to the RC (TR) and another part of this excitation energy is dissipated, mainly as heat (DI). An electron transport will be created within the RCs (ET) and further to PSI (RE), ultimately leading to CO_2 fixation (Strasser et al., 2000). Another intriguingly topic is the possibility of energetic communication (also known as "grouping" or "connectivity" and "overall grouping probability") between different PSII complexes (Stirbet, 2013), allowing the transfer of excitation energy from a closed PSII RC to an open (active) PSII RC (**Figures 1B,C**). Zivcak et al. (2014a) demonstrated that the omission of connectivity can lead to misinterpretation of the JIP-test results in mature barley plants. The JIP test, which stands for the major inflection points in the fluorescence induction curve, is based on the theory of energy fluxes in the photosynthetic apparatus (Strasser et al., 2000; Stirbet and Govindjee, 2011). The concept of PSII connectivity is still under discussion in scientific literature and has not yet been taken into account in studies with CAM plants which are exceptionally well adapted to environmental stresses.

In CAM ecophysiology, chlorophyll fluorescence has already been explored to some extent regarding adaptation and survival strategy in response to variations in the natural

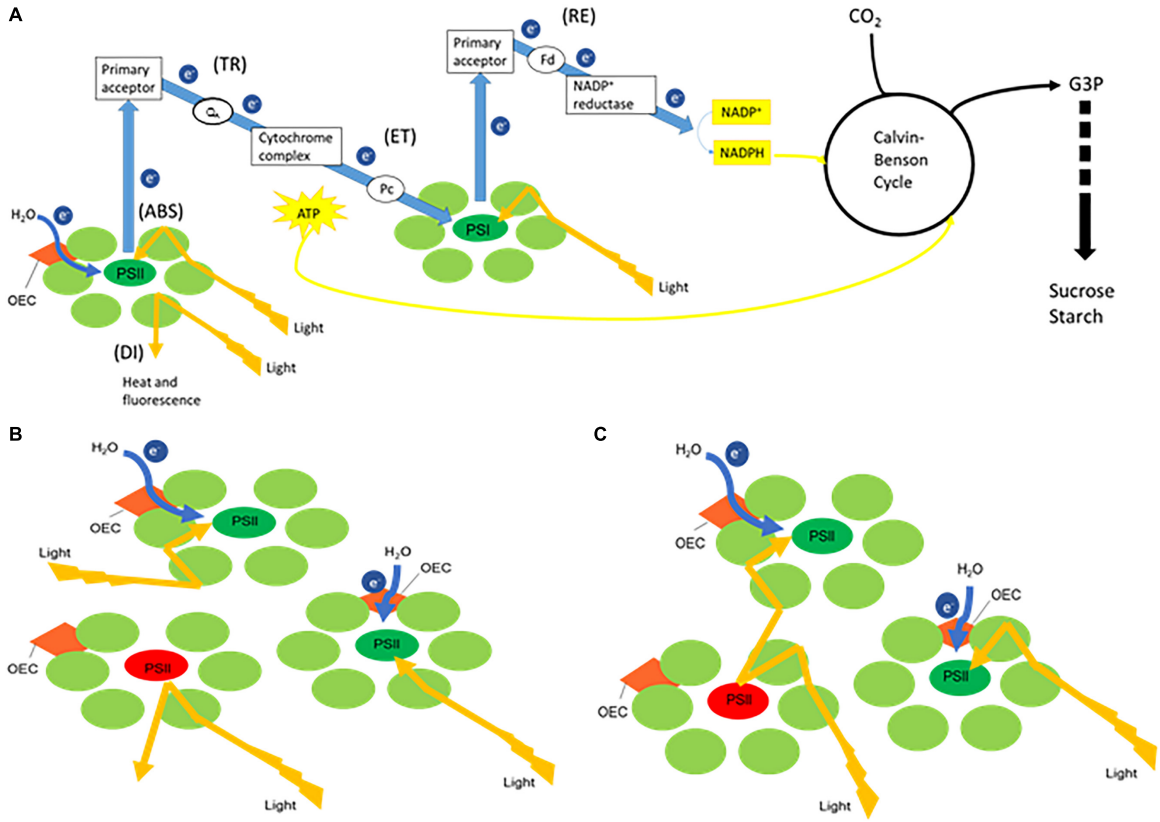

FIGURE 1 | Simplified schemes representing **(A)** the electron transport chain creating ATP and NADH, linked with carbon fixation where the measured energy fluxes are indicated between brackets. When receiving light, part of the flux of photons absorbed by photosystem II (PSII) (ABS) will be utilized to drive the electron transport chain. Trapping flux (TR) indicates the initial electron flow where plastoquinone A (Q_A) will be reduced. The electrons will further proceed to cytochrome complex followed by further transport mediated by plastocyanin (Pc) to photosystem I (PSI) (ET). Part of the original excitation energy is not utilized in the photochemical reactions and is dissipated, mainly as heat (DI). The splitting of water by the oxygen-evolving complex (OEC) releases electrons (e^-) to feed the electron transport chain. Finally in PSI the reduction of the end electron acceptors (RE) via ferredoxin (Fd) mediates the production of NADPH by $NADP^+$ reductase activity. ATP (created by ATP synthase fueled by a proton gradient resulting from the electron transport chain) and NADPH will provide energy and reducing power for the synthesis of glyceraldehyde 3-phosphate (G3P) during the Calvin-Benson cycle, which will lead to the synthesis of sucrose and starch. Panels **(B,C)** both represent a few PSII units with one closed reaction centre (red) and two open reaction centres (green). **(B)** Without connectivity between the three PSII units, excitation energy that encounters a closed reaction centre will be dissipated. **(C)** Taking connectivity into account, excitation energy from a closed RC will be transferred to an open (active) PSII RC.

environment. Measurements of chlorophyll fluorescence quenching confirmed the existence of diverse photoprotective mechanisms in CAM involving non-radiative excess energy dissipation and xanthophyll cycling (Winter et al., 1990; Adams and Demmig-Adams, 1996; Barker and Adams, 1997; Masrahi et al., 2015). Changes in the electron transport rates in CAM, related to CO_2 reduction rates in chloroplasts, were shown to result primarily in alterations in the rates of non-radiative energy dissipation so that consequently the reduction state of the primary electron acceptor of PSII was maintained at relatively low and constant levels (Winter and Demmig, 1987). The extra requirements of ATP for CAM plants are reflected by high values of total qN, which can be twice as much as compared to C3 (Keiller et al., 1994; Heber et al., 1996; Skillman and Winter, 1997). Chlorophyll fluorescence measurements also revealed the negative impact of abiotic stress, related to water and light availability, on the photosynthetic capacity of different CAM plants by significantly reducing photosynthetic electron transport rate and the overall effective quantum yield of PSII photochemistry, despite an increased capacity in dissipating excess energy (Osmond, 1982; de Mattos et al., 1999; Pollet et al., 2009; Arias-Moreno et al., 2017; Zheng et al., 2019).

The purpose of the present work was to gain more insight in the functioning of the photosynthetic apparatus in the CAM orchid *Phalaenopsis* "Edessa" under different light conditions and under drought stress, by evaluating performance indices (PI_{abs}) and specific energy fluxes as described above. Therefore a detailed study was performed integrating diel gas exchange patterns with analyses of fast chlorophyll *a* fluorescence induction. Under both environmental conditions, specific fluxes were calculated without and with connectivity to investigate the importance of energetic communication between PSII complexes in the CAM orchid *Phalaenopsis* "Edessa."

MATERIALS AND METHODS

Plant Material and Experimental Setup

Phalaenopsis "Edessa" is an obligate CAM plant and belongs to the family of the Orchidaceae. Vegetative plants of 16 weeks old were cultivated in a growth room with a day/night temperature of 28°C, a relative humidity of 75% and a 12-h photoperiod with photosynthetic photon flux density (PPFD) of 100 μmol m^{-2} s^{-1} at leaf level. Watering was performed twice a week; one time with a nutrient solution Peters 20N-8.7P-16.6K of 1 mS cm^{-1} and once with water. Following a 2 months acclimation to these conditions, plants were divided into two groups to investigate the possible effect of light intensity on the photosynthetic performance: (1) PPFD of 50 μmol m^{-2} s^{-1} (low light: LL) and (2) PPFD of 200 μmol m^{-2} s^{-1} (high light: HL). As total diel CO_2 uptake for *Phalaenopsis* has earlier been noticed to saturate around 200 μmol m^{-2} s^{-1}, this light intensity is further considered as high light treatment for *Phalaenopsis* "Edessa" (Guo et al., 2012). To determine chlorophyll content and titratable acidity samples were taken from the upper one-third of young fully expanded leaves (n = 5 plants) at week 0, 4, 6, and 10. In addition a drought experiment was performed with other plants kept at 100 μmol m^{-2} s^{-1}, which had also been divided into two groups: (1) control group which continued to receive watering twice a week and (2) a treatment group which was attributed to drought stress by withholding water. Samples were taken from the upper one-third of young fully expanded leaves (n = 5 plants) to determine chlorophyll content and titratable acidity at week 0, 4, and 6. Leaf discs (n = 5 plants) were punched out just beneath the sample position to determine relative water content (RWC). At week six, the oldest and most wilted leaves of the treatment group were also included to analyze chlorophyll *a* fluorescence.

Gas Exchange Measurements and Titratable Acidity

For both light and drought experiments, gas exchange was measured on the youngest fully expanded leaves after 10 and 6 weeks, respectively, using a LCi Portable Photosynthesis System (ADC BioScientific Ltd., United Kingdom). The top part of the leaf was enclosed in a broad leaf chamber (6.25 cm^2) and the incoming air was passed through a 20-l bottle to buffer short-term fluctuations in the CO_2 concentration. Gas exchange data were collected over a 24-h period with measurements obtained at 15-min intervals (n = 3 plants). By integrating specific areas under the CO_2 exchange curves, net gas exchange was calculated per phase as well as total net gas exchange during the 24-h time course. Nocturnal CO_2 uptake was also assessed by analyzing the nocturnal increase in titratable acidity (ΔH^+) by titration of methanol extracts against 0.005 M NaOH with phenolphthalein as indicator.

Relative Water Content Determination

Relative water content was determined by sampling the youngest fully expanded leaves (n = 5 plants) and calculated with the formula: (fresh mass – dry mass)/(turgid mass – dry mass) according to Ceusters et al. (2008). Leaf parts (95 mm^2) were floated in plastic tubes filled with demineralized water for 6 h in darkness at 4°C to determine turgid mass.

Determination of Chlorophyll Content and Plant Growth

For the calculation of leaf chlorophyll contents, plant pigments were extracted by immersing leaf material in N,N-dimethylformamide (DMFA) at room temperature for 72 h in darkness (n = 5 plants). The supernatant was used to determine absorbance at 647 nm (A_{647}) and 664 nm (A_{664}) (Genesys 10S UV-VIS, Thermo Fisher Scientific, United States). These data were used to calculate the content of chlorophyll *a*, chlorophyll *b* and total chlorophyll by means of the empirical formulas: C_a = 11.65 A_{664} – 2.69 A_{647}; C_b = 20.81 A_{647} – 4.53 A_{664}; $C = C_a + C_b$ (Moran and Porath, 1980; Porra et al., 1989; Wellburn, 1994).

Differences in plant growth, after growing for 10 weeks under different light conditions, were evaluated on basis of differences in above ground fresh and dry mass (g). Above ground plant material was separated from the roots, weighed and dried at 70°C to a constant mass after 8 days (n = 5 plants).

Chlorophyll *a* Fluorescence

Chlorophyll *a* fluorescence measurements were carried out by means of a Handy PEA fluorometer (Plant Efficiency Analyser, *Hansatech*, King's Lynn, United Kingdom) and were taken on the adaxial side, always on the left side of the main vein, of young fully developed leaves (n = 15 plants). Measurements were performed using a saturating pulse of 3 000 μmol m^{-2} s^{-1}, pulse duration of 1 s, and fixed gain (1.2×). Induction curve analysis (Handy PEA software V1.10) allowed to evaluate the effectiveness of fluorescence saturation during measurements. Before carrying out measurements, leaves were always allowed to dark adapt for 20 min using light-withholding clips (*Hansatech*). The light level of the saturating pulse and the minimal dark period had experimentally been determined for *Phalaenopsis* "Edessa" beforehand in order to obtain true values for the chlorophyll *a* fluorescence parameters. During the light experiment chlorophyll measurements were taken at 08.00 h (Phase II) on week 0, week 4, week 6, and week 10. All chlorophyll fluorescence data was assembled at 08.00 h because additional measurements at 12.00 h (Phase III) revealed no significant differences for these parameters in the different CAM phases (**Supplementary Table 1**). To study the progression of drought stress, chlorophyll fluorescence measurements were also taken at 08.00 h on week 0, week 4, and week 6.

The measured fast chlorophyll fluorescence induction curves (F_0 to F_m) were analyzed by the JIP test, which is based on the theory of energy fluxes in the photosynthetic apparatus (Strasser et al., 2000; Stirbet and Govindjee, 2011). When receiving light, part of the flux of photons absorbed by PSII antenna pigments (ABS) is dissipated (DI), mainly as heat, and another part is converted to redox energy by reducing the electron acceptor Q_A (TR). This electron acceptor is then reoxidized creating an electron transport (ET) until the reduction of the end electron acceptors at the PSI electron

acceptor side (RE) (**Figure 1A**). This stepwise flow of energy through PSII can also be expressed per RC, defined as following specific energy fluxes: ABS/RC, Tr_0/RC, Di_0/RC, Et_0/RC, and Re_0/RC. All these specific fluxes refer to time zero, i.e., the onset of fluorescence induction. In a logarithmic time scale, fast chlorophyll fluorescence induction curves have a typical shape which shows the steps O, J, I, P (Strasser and Strasser, 1995; Srivastava et al., 1999; Strasser et al., 2000, 2004, 2010), making it possible to collect following cardinal points: maximal fluorescence intensity (F_m, when all RCs are closed), minimum fluorescence intensity (F_0, when all RCs are open), fluorescence intensity at 2 and 30 ms (F_J and F_I, respectively) and at 50 and 300 μs ($F_{50\ \mu s}$ and $F_{300\ \mu s}$). These primary data were used to calculate chlorophyll fluorescence parameters describing maximum quantum efficiency of PSII (F_v/F_m), performance index (PI_{abs}) and the afore mentioned specific energy fluxes (Chondrogiannis and Grammatikopoulos, 2016). Definitions and equations of the measured and calculated JIP parameters are described in **Table 1**.

Since fluorescence induction data may be affected by the existence of PSII excitonic connectivity (**Figures 1B,C**), i.e., transfer of excitation energy from a closed PSII RC to an open (active) PSII RC (Stirbet, 2013), it was interesting to take this process into account. Connectivity parameters were calculated to allow comparison between results without and with taking connectivity into account (**Table 1**). Based on Zivcak et al. (2014a) the curvature constant (C) of the initial phase of the O-J curve (from 0.05 to 2 ms) was used to correct the values of the specific fluxes for connectivity, i.e., multiplying the specific flux values by 1 + C (**Table 1**).

Statistical Analyses

Where appropriate, data were analyzed using the statistical software package IBM SPSS Statistics V23. Before carrying out statistical tests, normality of the data was checked by means of the Kolmogorov-Smirnoff statistic ($p > 0.01$). Since our goal was to interpret the chlorophyll fluorescence data in function of the specific treatments (control/drought and different light intensities) and exclude non-treatment effects (plant age, time effects, ...), results were always compared between treatments from the same age by independent sample *t*-test or Tukey's Studentized range test, both at the 1% probability level. All replicates considered in our study were independent biological replicates originating from different plants.

RESULTS

Light

Gas Exchange Measurements and Titratable Acidity

For both investigated PPFD conditions (i.e., LL: 50 μmol m^{-2} s^{-1} and HL: 200 μmol m^{-2} s^{-1}) a traditional diel CAM pattern was observed (**Figure 2**). A complete 24 h CAM cycle occurred with nocturnal CO_2 fixation (Phase I) and net CO_2 loss during the day (Phase III), accompanied by two intermediate phases (Phases II and IV). During Phase I, extending from 20.00 h

TABLE 1 | Definitions and equations of measured and calculated parameters derived from fast fluorescence kinetics.

Parameter	Name and basic physiological interpretation
Basic JIP-test parameters	
$V_t = (F_t - F_{50\ \mu s})/(F_m - F_{50\ \mu s})$	Relative variable fluorescence at time t (V_J, V_I at 2, 30 ms)
$M_0 = dV/dt_0$	Approximate value of the initial slope of relative variable fluorescence curve Vt (for $F_0 = F_{50\ \mu s}$)
Specific energy fluxes (per active PSII reaction centre)	
$ABS/RC = (M_0/V_J) \times (1/\varphi P0)$	Absorbed photon flux per RC
$Tr_0/RC = M_0/V_J$	Trapped excitation flux (leading to Q_A reduction) of absorbed photons per RC
$Et_0/RC = (M_0/V_J) \times (1 - V_J)$	Electron transport flux (from reduced Q_A to Q_B) per RC
$Re_0/RC = (M_0/V_J) \times (1 - V_I)$	Electron flux reducing end electron acceptors at the PSI acceptor side, per RC
$Di_0/RC = (ABS/RC - Tr_0/RC)$	Dissipated energy flux per RC
Performance index	
$PI_{ABS} = RC/ABS \times [\varphi P_0/(1 - \varphi P_0)] \times [\Psi E_0/(1 - \Psi E_0)]$	Performance index for energy conservation from photons absorbed by PSII antenna, to the reduction of Q_B
Quantum yields and probabilities	
$\varphi P_0 = F_V/Fm$	Maximum quantum efficiency of primary PSII photochemistry; maximum efficiency at which light absorbed by PSII is used for reduction of Q_A
$\Psi E_0 = 1 - V_J$	Probability with which a PSII trapped electron is transferred from reduced Q_A to Q_B
Connectivity among PSII units	
$W_E = 1 - [(F_J - F_{300\ \mu s})/(F_J - F_{50\ \mu s})]^{1/5}$	Model-derived value of relative variable fluorescence at 100 μs calculated for unconnected PSII units
$W = (F_{100\ \mu s} - F_{50\ \mu s})/(F_J - F_{50\ \mu s})$	Relative variable fluorescence at 100 μs
$C = (W_E - W)/[V_J \times W \times (1 - W_E)]$	Curvature constant of intial phase of the O-J curve
$p_{2G} = C \times [F_{50\ \mu s}/(F_J - F_{50\ \mu s})]$	Overall grouping probability between PSII units when they are all open
$p = [p_{2G} \times (F_m/F_{50\ \mu s} - 1)]/[1 + p_{2G} \times (F_m/F_{50\ \mu s} - 1)]$	Connectivity parameter
$\omega = p \times [(F_m - F_{50\ \mu s})/F_m]$	Probability of the connectivity among PSII units when they are all closed

Based on information presented by Strasser et al.(1995, 2000, 2004, 2010), Strasser and Stirbet (2001), Stirbet and Govindjee (2011), Stirbet (2013).

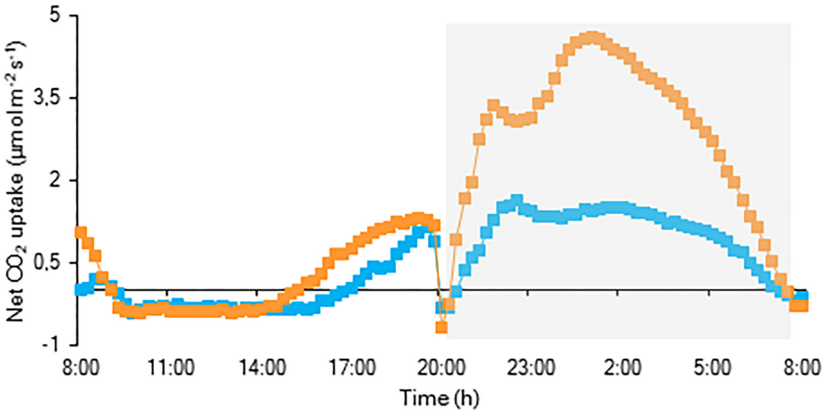

FIGURE 2 | Net 24 h CO_2 uptake (µmol m^{-2} s^{-1}) for young fully expanded leaves of *Phalaenopsis* "Edessa" 10 weeks after growing under different light conditions i.e., PPFD of 50 µmol m^{-2} s^{-1} (blue) and PPFD of 200 µmol m^{-2} s^{-1} (orange). The dark period is indicated in gray. Gas exchange curves are representative of three replicate runs with SE < 15%.

to 8.00 h, nocturnal CO_2 uptake of LL grown plants was only approximately one third that of plants grown under HL. This difference was also reflected in the nocturnal increase of titratable acidity which was already significantly higher for HL plants after 4 weeks (**Figure 3**). In addition, during Phase II, CO_2 uptake was lowered by 80% when grown under LL after 10 weeks. Phase IV was also delayed with 2 h under LL, resulting in only 44% CO_2 uptake in comparison to plants grown under HL. As a consequence, total daily CO_2 gain of HL plants was three times higher compared to LL plants (129 ± 20 mmol m^{-2} and 41 ± 19 mmol m^{-2} respectively; **Figure 2**).

Chlorophyll *a* Fluorescence Parameters

Comparing the two light conditions, no significant differences were observed for the maximum quantum efficiency of PSII photochemistry (F_v/F_m) and for the performance index for absorption (PI_{abs}) (**Figure 4** and **Table 1**). However, regarding the specific energy fluxes (per active RC) (**Figure 1A** and **Table 1**), significantly higher values were obtained for plants grown under HL (**Figure 4A**). After 6 weeks, a significant increase was noticed for photon absorption (ABS/RC) for plants grown under HL, concomitantly with a slight increase in the activity of energy dissipation (Di_0/RC). A significant rise was also calculated for the electron trapping efficiency (Tr_0/RC) after 10 weeks grown under HL. For the activity of electron transport within the reaction centre (Et_0/RC) and the flow of electrons further than PSII (Re_0/RC) significant differences were observed from week 4. Also for these parameters, the highest values were calculated for plants grown under HL.

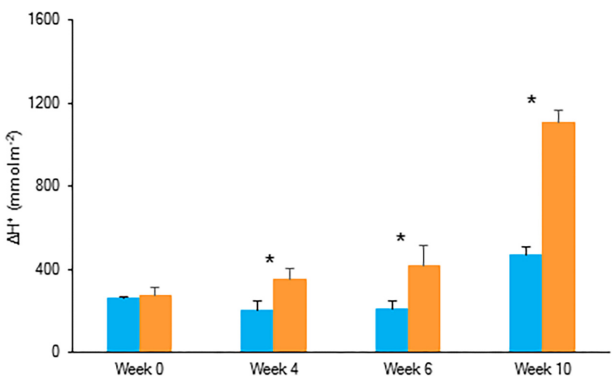

FIGURE 3 | Nocturnal increase (between 20.00 h and 08.00 h) in titratable acidity (mmol H$^+$ m^{-2}) in young fully expanded leaves of *Phalaenopsis* "Edessa" at 0, 4, 6, and 10 weeks after growing under different light conditions, i.e., PPFD of 50 µmol m^{-2} s^{-1} (blue) and PPFD of 200 µmol m^{-2} s^{-1} (orange). Data are means ± SD (n = 5 plants). Asteriks indicate significant differences per week between different light conditions at $P < 0.01$ according to the independent sample t-test.

To estimate the connectivity among PSII units, the first part of fast chlorophyll fluorescence induction curve was used (from 0.05 to 2 ms) as described above (Strasser and Stirbet, 2001; Joliot and Joliot, 2003; Stirbet, 2013). From week 6, calculated values of parameters associated with connectivity (**Table 1**), i.e., overall grouping probability of PSII units – p_{2G}, connectivity parameter – p, probability of connectivity among PSII units – ω (as defined by Strasser and Stirbet, 2001), were ∼1.5 times higher in plants grown under LL compared to those grown under HL (**Figure 5**). After correction for connectivity, i.e., multiplying the specific flux values by 1 + C (Zivcak et al., 2014a), all values obtained under LL became higher (**Figure 4B**) and eliminated the significant differences in the activity of energy dissipation (Di_0/RC) and electron transport (Et0/RC) originating from not considering connectivity. At week 6 photon absorption (ABS/RC) was equally for both light conditions and trapping efficiency was significantly increased in LL plants when taking connectivity into account.

Chlorophyll Content and Plant Growth

After 10 weeks of growing under different light conditions, significantly lower values in content of chlorophyll *a*, chlorophyll *b* and total chlorophyll were observed for plants grown under the highest light condition (**Figure 6**). The Chl *a*/*b* ratio remained

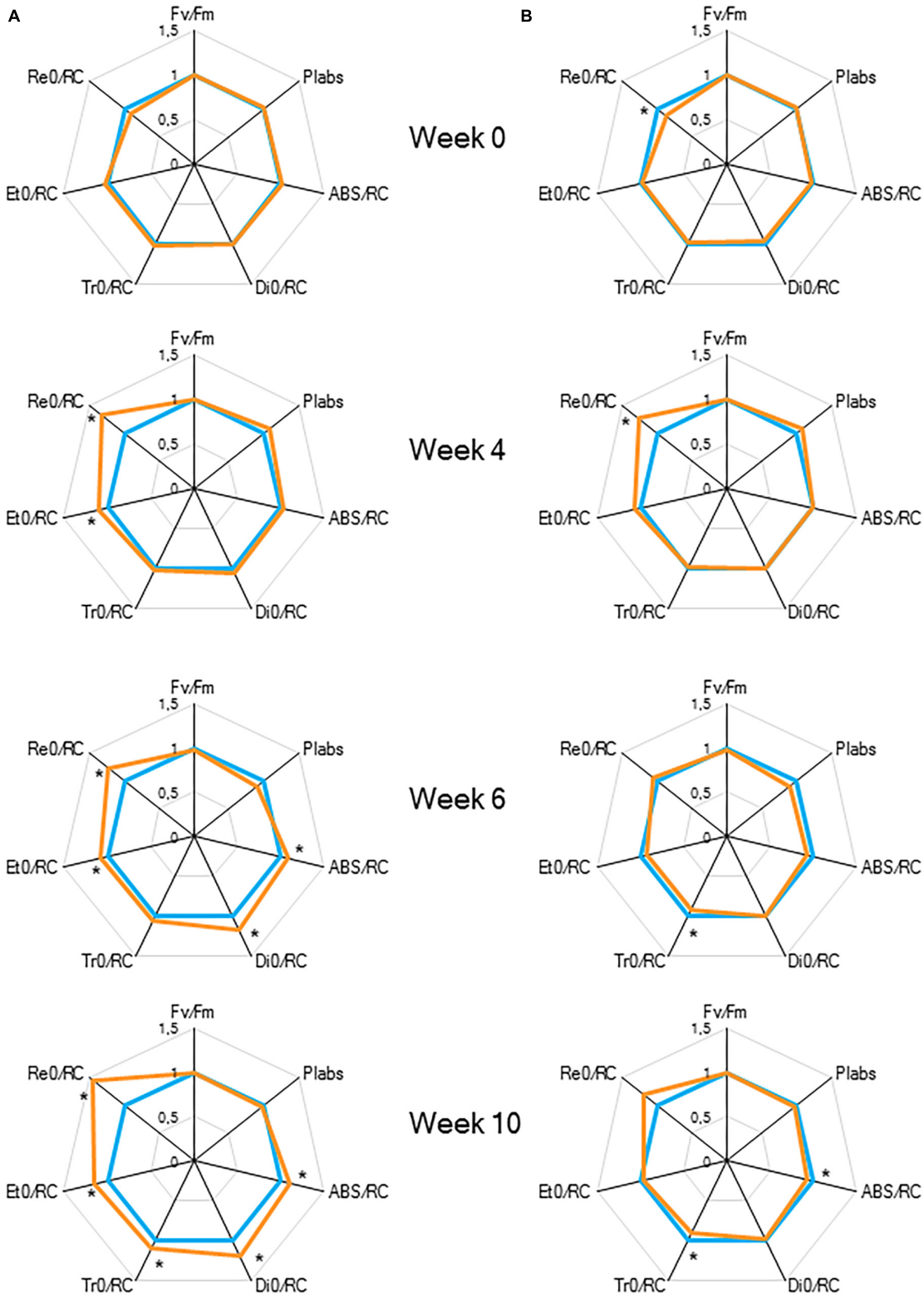

FIGURE 4 | "Spider plots" of selected chlorophyll *a* fluorescence transients parameters measured at 08.00 h in young fully expanded leaves of *Phalaenopsis* "Edessa" at 0, 4, 6, and 10 weeks after growing under different light conditions, i.e., PPFD of 50 μmol m^{-2} s^{-1} (blue) and PPFD of 200 μmol m^{-2} s^{-1} (orange). Parameters are calculated without connectivity **(A)** and corrected for connectivity between PSII units **(B)**. All values are shown as percent of PPFD of 50 μmol m^{-2} s^{-1} (n = 15 plants). Asteriks indicate significant differences between different light conditions at $P < 0.01$ according to the independent sample t-test.

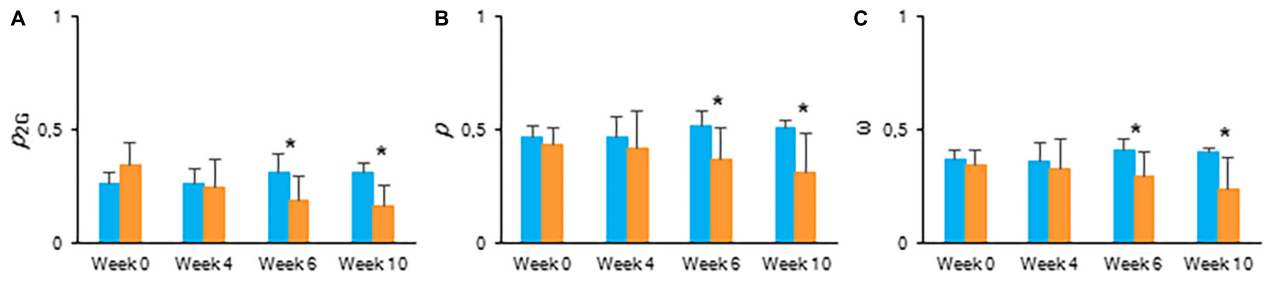

FIGURE 5 | Calculated connectivity parameters derived from fast fluorescence kinetics measured at 08.00 h in young fully expanded leaves of *Phalaenopsis* "Edessa" at 0, 4, 6, and 10 weeks after growing under different light conditions, i.e., PPFD of 50 μmol m^{-2} s^{-1} (blue) and PPFD of 200 μmol m^{-2} s^{-1} (orange). **(A)** Overall grouping probability of PSII units when they are all open. **(B)** Connectivity parameter. **(C)** Probability of connectivity among PSII units when they are all closed (Strasser and Stirbet, 2001; Stirbet and Govindjee, 2011; Stirbet, 2013). Data are means ± SD (n = 15 plants). Asteriks indicate significant differences between different light conditions at $P < 0.01$ according to the independent sample t-test.

unaffected by light condition. Both fresh and dry mass of the shoots showed an overall similar plant growth for plants grown under LL and HL after 10 weeks (**Table 2**).

Drought

Gas Exchange Measurements and Titratable Acidity

The CO_2 uptake pattern of *Phalaenopsis* "Edessa" grown under standard conditions (PPFD 100 μmol m^{-2} s^{-1}; 12-h photoperiod), watered twice a week, fitted the four-phase CAM framework as earlier described (**Figure 7**). After 6 weeks of withholding water no net CO_2 uptake occurred, indicating that the plants were in the CAM-idling mode with closed stomata during the complete diel cycle. In accordance with the gas exchange data, the nocturnal increase in titratable acidity was reduced by >80% when grown under drought stress (**Figure 8A**).

Chlorophyll *a* Fluorescence Parameters and Relative Water Content

To indicate the onset of water stress, RWC was measured and showed a significant decrease from 4 weeks of withholding water supply (**Figure 8B**). During progression of drought the

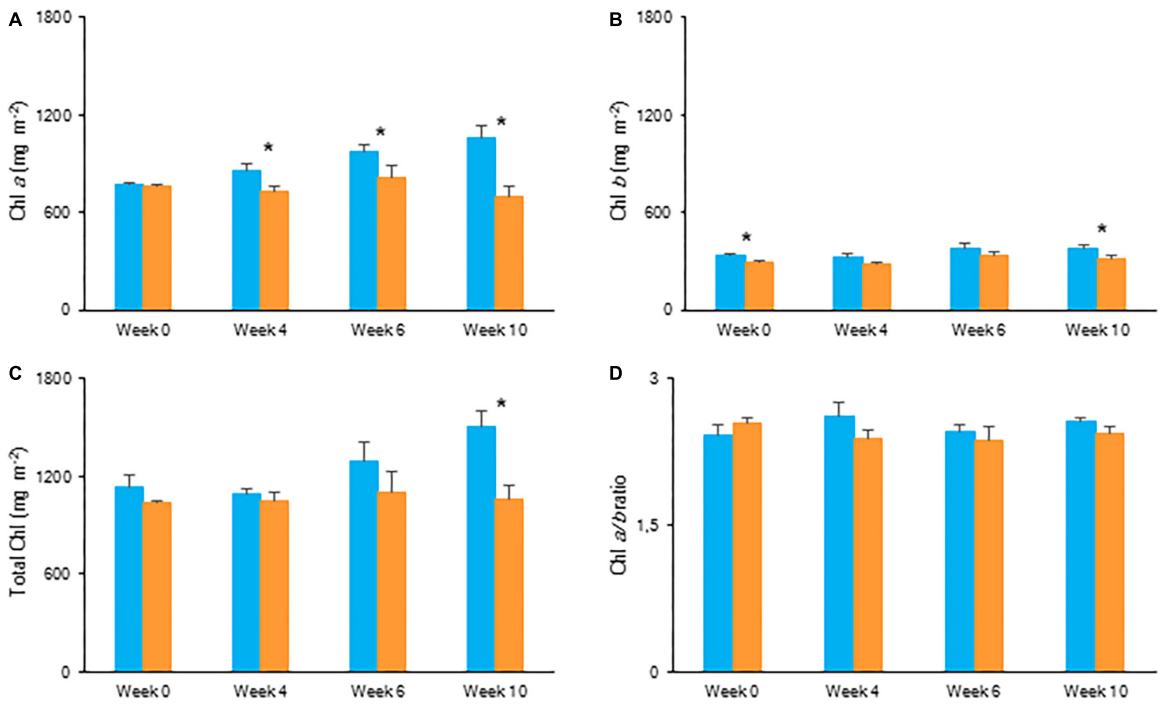

FIGURE 6 | Content (mg m^{-2}) of chlorophyll *a* **(A)**, chlorophyll *b* **(B)**, total chlorophyll **(C),** and chlorophyll *a*/*b* ratio **(D)** measured in young fully expanded leaves of *Phalaenopsis* "Edessa" at 0, 4, 6, and 10 weeks after growing under different light conditions, i.e., PPFD of 50 μmol m^{-2} s^{-1} (blue) and PPFD of 200 μmol m^{-2} s^{-1} (orange). Data are means ± SD (n = 5 plants). Asteriks indicate significant differences between different light conditions at $P < 0.01$ according to the independent sample t-test.

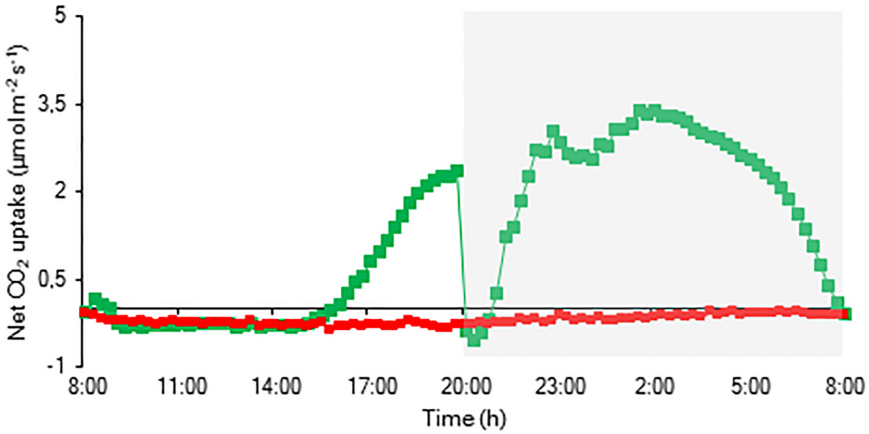

FIGURE 7 | Net 24 h CO_2 uptake (µmol m^{-2} s^{-1}) for young fully expanded leaves of *Phalaenopsis* "Edessa" 6 weeks after drought stress (red) compared with the controls (green). The dark period is indicated in gray. Gas exchange curves are representative of three replicate runs with *SE* < 15%.

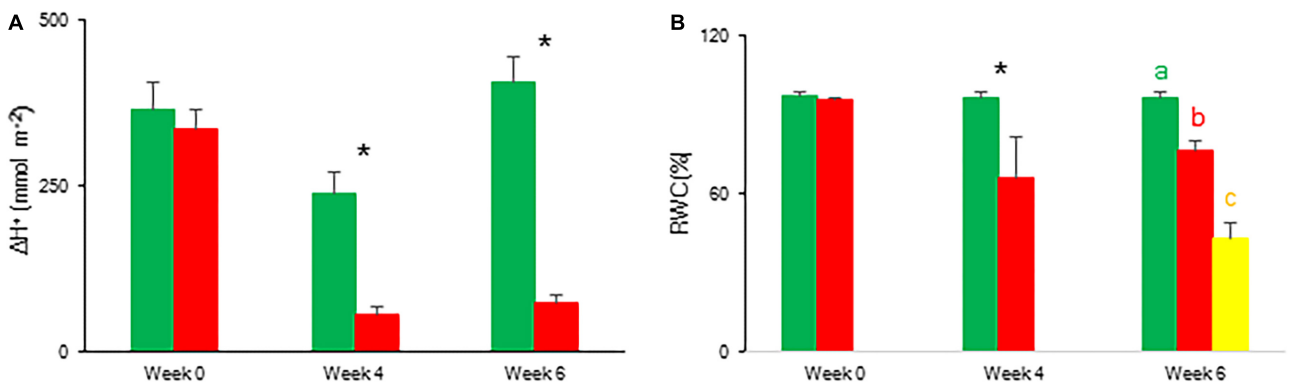

FIGURE 8 | Nocturnal increase (between 20.00 h and 08.00 h) in titratable acidity (mmol H^+ m^{-2}) **(A)** and relative water content (%) **(B)** measured at 08.00 h in young fully expanded leaves of *Phalaenopsis* "Edessa" after 0, 4, and 6 weeks for controls (green) or drought stressed plants (red). At week 6 additional measurements were also made for the oldest, most wilted leaves (yellow) for relative water content. Data are means ± SD (n = 5 plants). Asteriks indicate significant differences between control and drought at $P < 0.01$ according to the independent sample t-test. At week 6 values were compared between control, drought and wilted according to Tukey's Studentized range test at $P < 0.01$ marked by different letters.

TABLE 2 | Biomass on fresh and dry mass (g) basis for above ground material of *Phalaenopsis* "Edessa" grown for 10 weeks under different light conditions, i.e., PPFD 50 µmol m^{-2} s^{-1} or 200 µmol m^{-2} s^{-1}.

	PPFD (µmol m^{-2} s^{-1})	
	50	**200**
Fresh	94 ± 13	74 ± 5
Dry	4.4 ± 0.6	4.0 ± 0.4

Data are means ± SD (n = 5 plants) and no significant differences between the different light conditions were detected at P < 0.01 according to the independent sample t-test.

maximal quantum efficiency of PSII photochemistry (F_v/F_m) remained unaffected (**Figure 9** and **Table 1**). In contrast, the PI_{abs} parameter was already significantly lower after 4 weeks of drought stress in comparison to control plants (**Figure 9**). Drought stress also affected the specific energy fluxes within and related to PSII (**Figure 1A** and **Table 1**). After 4 weeks of drought stress, a significant increase was observed for photon absorption (ABS/RC) compared to control plants (**Figure 9A**). Also for the trapping efficiency (Tr_0/RC) and the flow of electrons further than PSII (Re_0/RC), significantly higher values were obtained at week 4 in the leaves of plants exposed to drought stress (**Figure 9A**). At week ten Tr_0/RC was significantly higher in the most wilted leaves whilst Re_0/RC and Et_0/RC remained unaffected. Activity of energy dissipation (Di_0/RC) showed a significant increase in the most wilted leaves compared to the measurements in plants grown under control conditions.

The calculated connectivity parameters (**Table 1**) of measurements performed at week 6 in leaves of control plants were ∼1.3 times higher compared to measurements performed on the youngest fully expanded leaves of plants exposed to drought stress, and ∼7.6 times higher compared to measurements on the most wilted leaves of plants exposed to

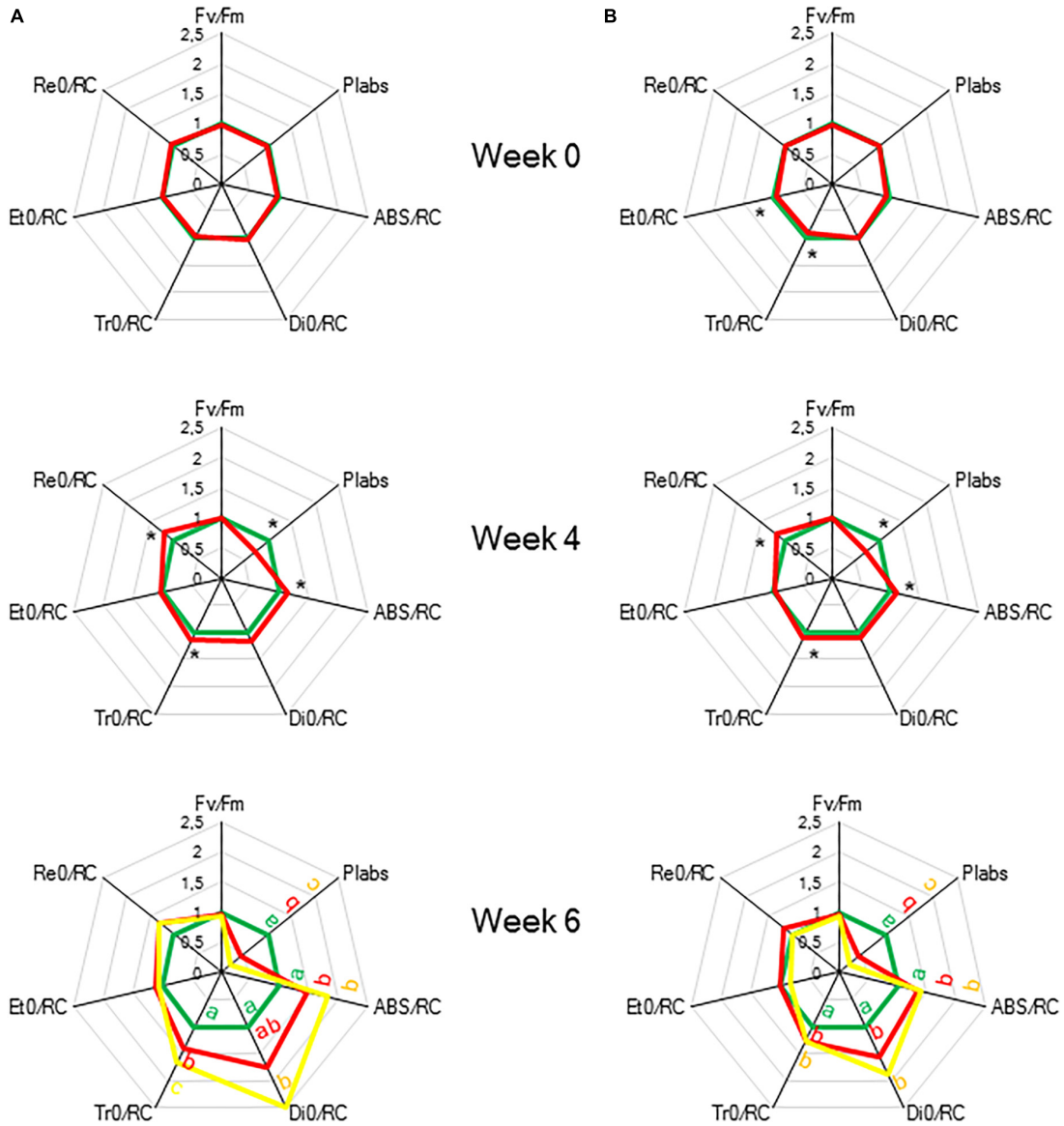

FIGURE 9 | "Spider plots" of selected chlorophyll *a* fluorescence transients parameters measured at 08.00 h in young fully expanded leaves of *Phalaenopsis* "Edessa" after 0, 4, and 6 weeks for controls (green) or drought stressed plants (red). At week 6 additional measurements were also made for the oldest, most wilted leaves (yellow). Parameters are calculated without connectivity **(A)** and corrected for connectivity between PSII units **(B)**. All values are shown as percent of control. Asteriks indicate significant differences between control and drought at $P < 0.01$ according to the independent sample *t*-test. At week 6 values were compared between control, drought and wilted according to Tukey's Studentized range test at $P < 0.01$ marked by different letters.

drought stress (**Figure 10**). As a consequence, the increase of the calculated fluxes after correction for connectivity, was the highest in the control leaves and the lowest in the most wilted leaves (**Figure 9B**).Taking connectivity into account showed an increased energy dissipation (Di_0/RC) for drought stressed plants and indicated an equal trapping efficiency (Tr_0/RC) for drought and wilted leaves at week six (**Figure 9B**).

Chlorophyll Content

Overall, the content of photosynthetic pigments remained unaffected during the 6 weeks of drought stress. No significant differences were observed for Chl *a*, Chl *b*, and total Chl between control and drought stressed plants (**Figure 11**).

DISCUSSION

Chlorophyll fluorescence measurements in CAM plants mainly report photochemical and non-photochemical quenching (qP and qN), the maximum quantum efficiency (F_v/F_m) and the effective quantum yield (Φ_{PSII}) of PSII photochemistry (**Table 1**; Winter and Demmig, 1987; Winter et al., 1990; Keiller et al., 1994;

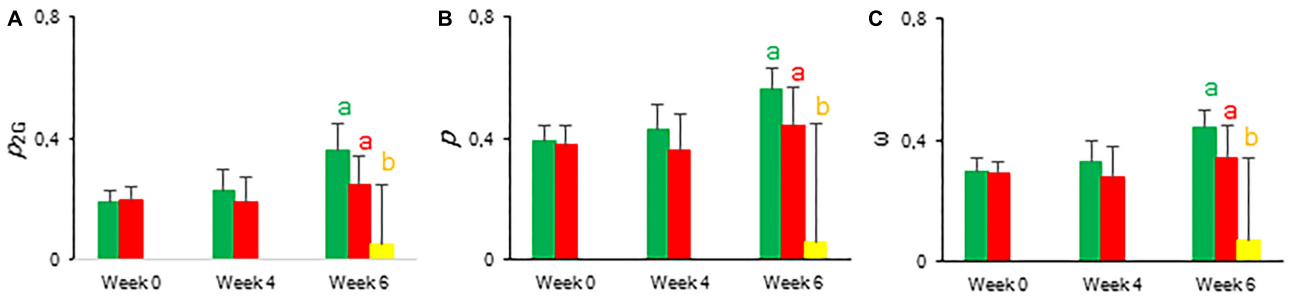

FIGURE 10 | Calculated connectivity parameters derived from fast fluorescence kinetics measured at 08.00 h in young fully expanded leaves of *Phalaenopsis* "Edessa" after 0, 4, and 6 weeks for controls (green) or drought stressed plants (red). At week 6 additional measurements were also made for the oldest, most wilted leaves (yellow). **(A)** Overall grouping probability of PSII units when they are all open. **(B)** Connectivity parameter. **(C)** Probability of connectivity among PSII units when they are all closed (Strasser and Stirbet, 2001; Stirbet and Govindjee, 2011; Stirbet, 2013). Data are means ± SD (n = 15 plants). No significant differences were detected between control and drought at $P < 0.01$ according to the independent sample t-test. At week 6 values were compared between control, drought and wilted according to Tukey's Studentized range test at $P < 0.01$ marked by different letters.

Adams and Demmig-Adams, 1996; Heber et al., 1996; Barker and Adams, 1997; Skillman and Winter, 1997; de Mattos et al., 1999; Lin and Hsu, 2004; Masrahi et al., 2015; Liu et al., 2016; Arias-Moreno et al., 2017). A detailed investigation of the performance index, specific energy fluxes related to PSII processing and the concept of connectivity between PSII units (**Figure 1** and **Table 1**) revealed important PSII related adaptations concerning the initial light reactions in CAM plants under different environmental conditions.

Increased PSII Connectivity Under Light Limitation

Chlorophyll fluorescence measurements were performed to investigate the effects of low light (LL: PPFD 50 μmol m^{-2} s^{-1}) and high light (HL: PPFD 200 μmol m^{-2} s^{-1}) on the photosynthetic performance of the CAM plant *Phalaenopsis* "Edessa." Our detailed energy flux analyses focused on the efficiency of energy capture and the electron transport in PSII system when all RCs are open (i.e., at the onset of excitation). Comparing these parameters between LL and HL (**Figure 4**), stresses the importance of the energetic communication between PSII complexes defined as connectivity when evaluating specific energy fluxes in CAM plants (**Figure 1**). Without taking connectivity into account (**Figure 4A**), all values of specific energy fluxes were significantly lower after 10 weeks of growing under LL compared to the HL treatment, indicating an affected energy processing through PSII upon light limitation. However, taking into account higher connectivity of LL grown plants (**Figure 5**), higher values were recorded for all energy fluxes (**Figure 4B**) and as such these plants seemed to process light energy more efficiently compared to plants grown under the high light conditions. This was also reflected in a 25% higher maximum quantum yield for plants under LL as indicated by relating the daily CO_2 gain of a leaf to the amount of photons absorbed per day (Skillman, 2008). Plants grown under LL realized an overall similar biomass on both fresh and dry mass basis (**Table 2**) despite a triple decrease in CO_2 fixation in the measured source leaves for plants under LL (**Figure 2**). However, HL grown plants were typically characterized by several layers of leaf pairs largely shading each other whilst LL grown plants showed an improved architecture with less underlying sink leaves and larger source leaves. Under LL, total chlorophyll content in source leaves after 10 weeks was also 140% in comparison to contents of plants grown under HL (**Figure 6C**), which was also reflected by the higher photon absorption flux (ABS/RC) for plants grown under LL (**Figure 4B**). The increase in total chlorophyll content was mainly due to a significant increase in Chl *a* (**Figure 6A**), which can reflect an increase in active RC's. As a consequence, the higher connectivity in plants grown under LL is consistent with the absence of a difference in the performance index PI_{abs} (**Figure 4** and **Table 1**), due to their more efficient energy processing. Without considering connectivity an increase in PI_{abs} would be expected for HL, since both trapping efficiency and electron transport increased significantly by HL and only the parameter RC/ABS decreased. Taking connectivity into account changed the concentration of reaction centres per chlorophyll (RC/ABS) and trapping efficiency (Tr_0/RC) in the opposite direction, whilst the other parameters remained unaffected and no difference was observed for PI_{abs}. As such, the question can be raised whether a higher connectivity for plants grown under low light conditions might underpin the adaptive radiation of CAM plants from full sun to deep shade conditions. Several species from the Bromeliaceae are excellent examples of CAM representatives thriving in light limited environments such as wet cloud forests and shaded understoreys of tropical rainforests (Pierce et al., 2002; Ceusters et al., 2011).

Increased Energy Dissipation and Partial Inactivation of PSII Reaction Centres to Reconcile Energy and Carbon Requirements During Drought Stress

To evaluate the effects of drought stress on the photosynthetic performance in the CAM plant *Phalaenopsis* "Edessa," chlorophyll fluorescence parameters (**Table 1**) were compared between control plants (watered twice a week) and drought stressed plants. In contrast to the maximum quantum efficiency

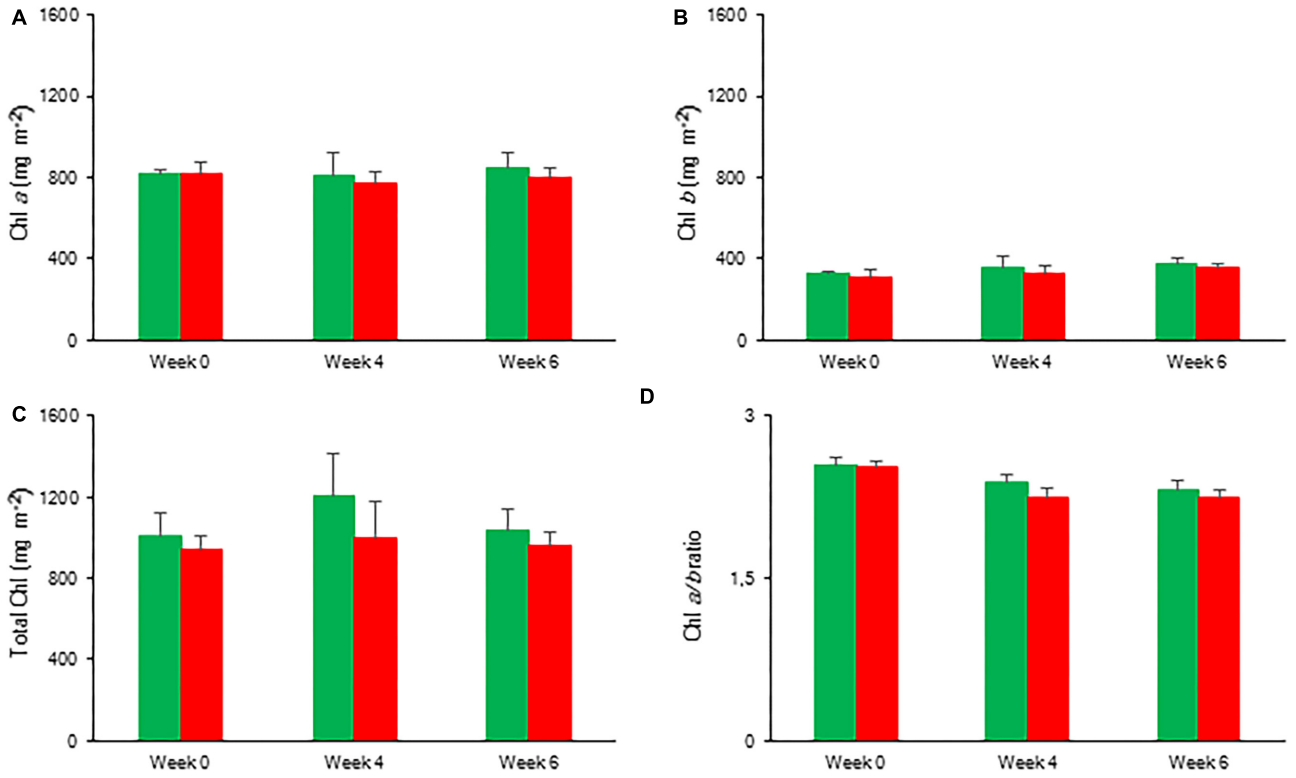

FIGURE 11 | Content (mg m^{-2}) of chlorophyll *a* **(A)**, chlorophyll *b* **(B)**, total chlorophyll **(C)**, and chlorophyll *a*/*b* ratio **(D)** measured in young fully expanded leaves of *Phalaenopsis* "Edessa" after 0, 4, and 6 weeks for controls (green) or drought stressed plants (red). Data are means ± SD (n = 5 plants). No significant differences were detected between control and drought at $P < 0.01$ according to the independent sample t-test.

of PSII (F_v/F_m) which remained unaffected, the performance index PI_{abs} reflected the reduction of RWC for drought stressed plants (**Figure 9**). These results corroborate investigations in C3 plants where the performance index PI_{abs} has already been proposed a reliable and sensitive parameter to evaluate plant homeostasis with regard to moderate abiotic stress (Zivcak et al., 2008; Campos et al., 2014; Jedmowski et al., 2015). As indicated in **Table 1**, the performance index takes into account three dependent characteristics: the concentration of reaction centres per chlorophyll (RC/ABS), a parameter related to primary photochemistry (φP_0) and a parameter related to electron transport (ψE_0) (Strasser et al., 2004). As a consequence, changes in environmental conditions which influence either antenna properties (ABS/RC), trapping efficiency (Tr_0/RC) or electron transport beyond Q_A in PSII (Et_0/RC and Re_0/RC) (**Figure 1**) will have an impact on the current state of plant performance and PI_{abs} will decrease under stress. Mathematically, the observed decrease in performance index could not be explained by merely looking at the three separate parameters on which PI_{abs} is based (**Table 1**). Only the trapping efficiency (Tr_0/RC) significantly increased under drought whilst RC/ABS was only significantly different between control and drought, and the parameter Et_0/RC remained unaffected (**Figure 9A**). Taking connectivity into account eliminated the observed significant difference for Tr_0/RC between drought and wilted but could not fully explain the observed significant decrease in PI_{abs} (**Figure 9B**). From these data it can be concluded that other components or processes, such as oxygen-evolving complex (OEC); transition from active to non-Q_A-reducing centres; carotenoids and PSI may also influence the performance index (**Figure 1**). Different studies revealed that drought can indeed result in damage to the OEC and block further electron transport. This phenomenon is mostly characterized by an increase in the specific fluxes for trapping, absorption and dissipation (Guissé et al., 1995; Wang et al., 2012; Guha et al., 2013).

Our data also demonstrate that enhanced protection of photochemistry in the CAM plant *Phalaenopsis* "Edessa" is also achieved by adjusting the energy distribution between photosystems. Two possible explanations can be presented for the observed increase in ABS/RC under drought stress (**Figure 9B**): (1) inactivation of some PSII RC's, considering that the ABS/RC ratio is calculated as the total number of photons absorbed by Chl molecules in all RC's divided by total number of active RC's, or (2) an increase in antenna size (van Heerden et al., 2007; Gomes et al., 2012). The latter seems to be less plausible since no significant differences were obtained in the content of photosynthetic pigments between the two treatments (**Figure 11**). The inactivation of some PSII RC's, becoming non-Q_A-reducing centres, can explain the observed increase in Tr_0/RC under drought. Down-regulation of photochemical

activity together with a significant increase in thermal dissipation may play a critical role in protecting plants exposed to drought stress from over-excitation and photodamage (van Heerden et al., 2007; Zivcak et al., 2014b; Wang et al., 2017; Kalaji et al., 2018). As such, the performance index depicts a downregulation of PSII related energy fluxes as a physiological response to drought stress. Especially for CAM plants during CAM idling the Calvin-Benson cycle, for which the end products of the electron transport chain (ATP and NADH) are indispensable (**Figure 1A**), is seriously compromised by carbon and water limitation (**Figure 7**). In this physiological mode of survival, inactivation of several PSII RC's adds in overcoming severe drought periods by attenuating energy fluxes in consistence with the very low CO_2 availability, due to stomatal closure during day and night, in the leaf mesophyll cells.

CONCLUSION

The results presented in this paper suggest a clear physiological role for PSII connectivity (energetic communication between PSII complexes) in the CAM plant *Phalaenopsis* "Edessa." A higher connectivity for plants grown under low light ($p \sim 0.51$) compared to plants grown under high light ($p \sim 0.31$) resulted in similar specific energy fluxes irrespective of the light treatment. With a 25% higher maximum quantum yield and comparable biomass formation, low light grown plants proved to process light energy more efficiently compared to high light grown plants. As such, taking into account PSII connectivity might help to better understand the adaptation of CAM plants to changing environmental conditions. The obtained results also indicate that PI_{abs} is a sensitive parameter to detect drought stress in the CAM plant *Phalaenopsis* "Edessa." Besides an enhanced thermal dissipation drought stressed plants also seemed to attenuate the electron flow from PSII toward PSI by partial inactivation of PSII reaction centres. This strategy might help to reconcile the light reactions and the carbon fixation reactions which are seriously compromised by carbon and water limitation during CAM-idling and as such minimize chances of photodamage to occur. Further research into the specific energy fluxes and the connectivity between different PSII units in CAM plants under combinations of abiotic stress factors is highly encouraged. This will enable to expand our physiological knowledge about the interplay of the light and carbon fixation reactions in CAM plants under changing environmental conditions.

DATA AVAILABILITY

The raw data supporting the conclusions of this manuscript will be made available by the authors, without undue reservation, to any qualified researcher.

AUTHOR CONTRIBUTIONS

NC, RV, and JC proposed the conceptual framework for the study and performed the data collection and analysis. NC and MF performed the experimental analyses. NC, RV, JEC, WVdE, and JC interpreted the data and wrote the manuscript.

FUNDING

This research was supported by the Research Fund KU Leuven.

ACKNOWLEDGMENTS

Microflor NV is acknowledged for supplying the plant materials.

SUPPLEMENTARY MATERIAL

The Supplementary Material for this article can be found online at: https://www.frontiersin.org/articles/10.3389/fpls.2019.01012/full#supplementary-material

REFERENCES

Adams, W. W., and Demmig-Adams, B. (1996). "Energy dissipation and the xanthophyll cycle in CAM plants," in *Crassulacean acid Metabolism. Ecological studies (Analysis and Synthesis)*, Vol. 114, eds K. Winter, and J. A. C. Smith, (Berlin: Springer).

Arias-Moreno, D. M., Jiménez-Bremont, J. F., Maruri-López, I., and Delgado-Sánchez, P. (2017). Effects of catalase on chloroplast arrangement in *Opuntia streptacantha* chlorenchyma cells under salt stress. *Sci. Rep.* 7:8656. doi: 10.1038/s41598-017-08744-x

Barker, D. H., and Adams, W. W. (1997). The xanthophyll cycle and energy dissipation in differently oriented faces of the cactus *Opuntia macrorhiza*. *Oecologia* 109, 353–361. doi: 10.1007/s004420050093

Borland, A. M., Hartwell, J., Jenkins, G. I., Wilkins, M. B., and Nimmo, H. G. (1999). Metabolite control overrides circadian regulation of phosphoenolpyruvate carboxylase kinase and CO2 fixation in crassulacean acid metabolism. *Plant Physiol.* 121, 889–896. doi: 10.1104/pp.121.3.889

Borland, A. M., Zambrano, V. A. B., Ceusters, J., and Shorrock, K. (2011). The photosynthetic plasticity of crassulacean acid metabolism: an evolutionary innovation for sustainable productivity in a changing world. *New Phytol.* 191, 619–633. doi: 10.1111/j.1469-8137.2011.03781.x

Campos, H., Trejo, C., Peña-Valdivia, C. B., García-Nava, R., Conde-Martínez, F. V., and Cruz-Ortega, M. D. R. (2014). Photosynthetic acclimation to drought stress in *Agave salmiana* otto ex Salm-Dyck seedlings is largely dependent on thermal dissipation and enhanced electron flux to photosystem I. *Photosynth. Res.* 122, 23–39. doi: 10.1007/s11120-014-0008-6

Ceusters, J., Borland, A. M., Ceusters, N., Verdoodt, V., Godts, C., and De Proft, M. P. (2010). Seasonal influences on carbohydrate metabolism in the CAM bromeliad *Aechmea* 'Maya': consequences for carbohydrate partitioning and growth. *Ann. Bot.* 105, 301–309. doi: 10.1093/aob/mcp275

Ceusters, J., Borland, A. M., and De Proft, M. P. (2009a). Drought adaptation in plants with crassulacean acid metabolism involved the flexible use of different storage carbohydrate pools. *Plant Signal. Behav.* 4, 212–214. doi: 10.4161/psb.4.3.7813

Ceusters, J., Borland, A. M., Londers, E., Verdoodt, V., Godts, C., and De Proft, M. P. (2009b). Differential usage of storage carbohydrates in the CAM bromeliad *Aechmea* 'Maya' during acclimation to drought and recovery from dehydration. *Physiol. Plant.* 135, 174–184. doi: 10.1111/j.1399-3054.2008.01186.x

Ceusters, J., Borland, A. M., Godts, C., Londers, E., Croonenborghs, S., Van Goethem, D., et al. (2011). Crassulacean acid metabolism under severe light

limitation: a matter of plasticity in the shadows? *J. Exp. Bot.* 62, 283–291. doi: 10.1093/jxb/erq264

Ceusters, J., Borland, A. M., Taybi, T., Frans, M., Godts, C., and De Proft, M. P. (2014). Light quality modulates metabolic synchronization over the diel phases of crassulacean acid metabolism. *J. Exp. Bot.* 65, 3705–3714. doi: 10.1093/jxb/eru185

Ceusters, J., Londers, E., Verdoodt, V., Ceusters, N., and De Proft, M. P. (2008). Seasonal impact on physiological leaf damage risk of *Aechmea* hybrid under greenhouse conditions. *Sci. Hortic.* 118, 242–245. doi: 10.1016/j.scienta.2008.06.006

Ceusters, N., Van den Ende, W., and Ceusters, J. (2017). "Exploration of sweet immunity to enhance abiotic stress tolerance in plants: lessons from CAM," in *Progress in Botany*. eds M. C. Francisco, U. Lüttge, and R. Matyssek, (Berlin: Springer), 78.

Chondrogiannis, C., and Grammatikopoulos, G. (2016). Photosynthesis in developing leaf of juveniles and adults of three Mediterranean species with different growth forms. *Photosynth. Res.* 130, 427–444. doi: 10.1007/s11120-016-0276-4

Cornic, G., and Massacci, A. (1996). "Leaf photosynthesis under drought stress," in *Photosynthesis and the Environment,* Edn 1, ed. N. R. Baker, (Netherlands: Springer).

Cushman, J. C., and Borland, A. M. (2002). Induction of crassulacean acid metabolism by water limitation. *Plant Cell Environ.* 25, 295–310. doi: 10.1046/j.0016-8025.2001.00760.x

de Mattos, E. A., Herzog, B., and Lüttge, U. (1999). Chlorophyll fluorescence during CAM –phases in *Clusia minor* L. *under drought stress. J. Exp. Bot.* 50, 253–261. doi: 10.1093/jexbot/50.331.253

Falk, S., Maxwell, D. P., Laudenbach, D. E., and Huner, N. P. A. (1996). "Photosynthetic adjustment to temperature," in *Photosynthesis and the Environment,* Edn 1, ed. N. R. Baker, (Netherlands: Springer).

Gomes, M. T. G., da Luz, A. C., dos Santos, M. R., Batitucci, M. D. C. P., Silva, D. M., and Falqueto, A. R. (2012). Drought tolerance of passion fruit plants assessed by the OJIP chlorophyll a transient. *Sci. Hortic.* 142, 49–56. doi: 10.1016/j.scienta.2012.04.026

Guha, A., Sengupta, D., and Reddy, A. R. (2013). Polyphasic chlorophyll a fluorescence kinetics and leaf protein analyses to track dynamics of photosynthetic performance in mulberry during progressive drought. *J. Photochem. Photobiol. B Biol.* 119, 71–83. doi: 10.1016/j.jphotobiol.2012.12.006

Guissé, B., Srivastava, A., and Strasser, R. J. (1995). "Effects of high temperature and water stress on the polyphasic chlorophyll a fluorescence transient of potato leaves," in *Photosynthesis: from light to biosphere*, ed. P. Mathis, (Dordrecht: Kluwer Academic Publishers), 913–916.

Guo, W. J., Lin, Y. Z., and Lee, N. (2012). Photosynthetic light requirements and effects of low irradiance and daylength on *Phalaenopsis amabilis*. *J. Am. Soc. Horticu. Sci.* 137, 465–472. doi: 10.21273/jashs.137.6.465

Haydon, M. J., Bell, L. J., and Webb, A. A. R. (2011). Interactions between plant circadian clocks and solute transport. *J. Exp. Bot.* 62, 2333–2348. doi: 10.1093/jxb/err040

Heber, U., Kaiser, W. M., and Neimanis, S. (1996). "Regulation of crassulacean acid metabolism in *Kalanchoë pinnata* as studied by gas exchange and measurements of chlorophyll fluorescence," in *Crassulacean acid metabolism. Ecological studies (Analysis and Synthesis)*, Vol. 114, eds K. Winter, and J. A. C. Smith, (Berlin: Springer).

Jedmowski, C., Ashoub, A., Momtaz, O., and Brüggemann, W. (2015). Impact of drought, heat and their combination on chlorophyll fluorescence and yield of wild barley (*Hordeum spontaneum*). *J. Bot.* 2015, 120868. doi: 10.1155/2015/120868

Joliot, P., and Joliot, A. (2003). Excitation transfer between photosynthetic units: the 1964 experiment. *Photosynth. Res.* 76, 241–245.

Kalaji, H. M., Rackova, L., Paganova, V., Swoczyna, T., Rusinowski, S., and Sitko, K. (2018). Can chlorophyll-a fluorescence parameters be used as bio-indicators to distinguish between drought and salinity stress in *Tillia cordata* Mill? *Environ. Exp. Bot.* 152, 149–157. doi: 10.1016/j.envexpbot.2017.11.001

Keiller, D. R., Slocombe, S. P., and Cockburn, W. (1994). Analysis of chlorophyll a fluorescence in C3 and CAM forms of *Mesembryanthemum crystallinum*. *J. Exp. Bot.* 45, 325–334. doi: 10.1093/jxb/45.3.325

Krüger, G. H. J., Tsimilli-Michael, M., and Strasser, R. J. (1997). Light stress provokes plastic and elastic modifications in structure and function of photosystem II in camellia leaves. *Physiol. Plant.* 101, 265–277. doi: 10.1034/j.1399-3054.1997.1010203.x

Lin, M. J., and Hsu, B. D. (2004). Photosynthetic plasticity of *Phalaenopsis* in response to different light environments. *J. Plant Physiol.* 161, 1259–1268. doi: 10.1016/j.jplph.2004.05.009

Liu, Y. C., Liu, C. H., Lin, Y. C., Lu, C. H., Chen, W. H., and Wang, H. L. (2016). Effect of low irradiance on the photosynthetic performance and spiking of *Phalaenopsis*. *Photosynthetica* 54, 259–266. doi: 10.1007/s11099-016-0079-z

Masrahi, Y. S., Al-Turki, T. A., and Sayed, O. H. (2015). Photosynthetic adaptation and survival strategy of *Duvalia velutina* in an extremely arid environment. *Photosynthetica* 53, 555–561. doi: 10.1007/s11099-015-0143-0

Maxwell, K., and Johnson, G. N. (2000). Chlorophyll fluorescence – a practical guide. *J. Exp. Bot.* 51, 659–668. doi: 10.1093/jexbot/51.345.659

Moran, R., and Porath, D. (1980). Chlorophyll determination in intact tissues extracted with N,N-dimethylformamide. *Plant Physiol.* 65, 478–479. doi: 10.1104/pp.65.3.478

Osmond, C. B. (1978). Crassulacean acid metabolism. a curiosity in context. *Annu. Rev. Plant Physiol. Plant Mol. Biol.* 29, 379–414. doi: 10.1093/jxb/ern052

Osmond, C. B. (1982). "Carbon cycling and stability of the photosynthetic apparatus in CAM," in *Crassulacean acid metabolism*, eds I. P. Ting, and M. Gibbs, (Rockville: American Society of Plant Physiologists), 112–127.

Pierce, S., Winter, K., and Griffiths, H. (2002). The role of CAM in high rainfall cloud forests: an in situ comparison of photosynthetic pathways in Bromeliaceae. *New Phytol.* 25, 1181–1189. doi: 10.1046/j.1365-3040.2002.00900.x

Pollet, B., Steppe, K., Van Labeke, M. C., and Lemeur, R. (2009). Diurnal cycle of chlorophyll fluorescence in *Phalaenopsis*. *Photosynthetica* 47, 309–312. doi: 10.1007/s11099-009-0048-x

Porra, R. J., Thompson, W. A., and Kriedemann, P. E. (1989). Determination of accurate extinction coefficients and simultaneous equation for assaying chlorophylls a and b extracted with four different solvents: Verification of the concentration of chlorophyll standards by atomic absorption spectroscopy. *Biochim. Biophys. Acta* 975, 384–394. doi: 10.1016/s0005-2728(89)80347-0

Rapacz, M. (2007). Chlorophyll a fluorescence transient during freezing and recovery in winter wheat. *Photosynthetica* 45, 409–418. doi: 10.1007/s11099-007-0069-2

Skillman, J. B. (2008). Quantum yield variation across the three pathways of photosynthesis: not yet out of the dark. *J. Exp. Bot.* 59, 1647–1661. doi: 10.1093/jxb/ern029

Skillman, J. B., and Winter, K. (1997). High photosynthetic capacity in a shade-tolerant crassulacean acid metabolism plant. *Plant Physiol.* 113, 441–450. doi: 10.1104/pp.113.2.441

Srivastava, A., Strasser, R. J., and Govindjee. (1999). Greening of peas: parallel measurements of 77K emission spectra, OJIP chlorophyll a fluorescence transient, period four oscillation of the initial fluorescence level, delayed light emission, and P700. *Photosynthetica* 37, 365–392.

Stirbet, A. (2013). Excitonic connectivity between photosystem II units: what is it, and how to measure it? *Photosynth. Res.* 116, 189–214. doi: 10.1007/s11120-013-9863-9

Stirbet, A., and Govindjee. (2011). On the relation between the Kautsky effect (chlorophyll a fluorescence induction) and Photosystem II: Basics and applications of the OJIP fluorescence transient. *J. Photochem. Photobiol. B Biol.* 104, 236–257. doi: 10.1016/j.jphotobiol.2010.12.010

Strasser, B. J., and Strasser, R. J. (1995). "Measuring fast fluorescence transients to address environmental questions: The JIP-test," in *Photosynthesis: From Light to Biosphere*, ed. P. Mathis, (Dordrecht: . Kluwer Academic Publishers), 977–980.

Strasser, R. J., Srivastava, A., and Govindjee, G. (1995). Polyphasic chlorophyll α fluorescence transients in plants and cyanobacteria. *Photochem. Photobiol.* 61, 32–42. doi: 10.1111/j.1751-1097.1995.tb09240.x

Strasser, R. J., Srivastava, A., and Tsimilli-Michael, M. (2000). "The fluorescence transient as a tool to characterize and screen photosynthetic samples," in *Probing photosynthesis: Mechanisms Regulation and Adaptation*, eds M. Yunus, U. Pathre, and P. Mohanty, (London: Taylor and Francis), 445–483.

Strasser, R. J., and Stirbet, A. D. (2001). Estimation of the energetic connectivity of PSII centres in plants using the fluorescence rise O-J-I-P. Fitting of experimental data to three different PSII models. *Math. Comput. Simulation* 56, 451–461.

Strasser, R. J., Tsimilli-Michael, M., Qiang, S., and Goltsev, V. (2010). Simultaneous in vivo recording of prompt and delayed fluorescence and 820 nm reflection changes during drying and after rehydration of the resurrection plant *Haberlea rhodopensis*. *Biochim. Biophys. Acta Bioenerg.* 1797, 1313–1326. doi: 10.1016/j.bbabio.2010.03.008

Strasser, R. J., Tsimilli-Michael, M., and Srivastava, A. (2004). "Analysis of the chlorophyll fluorescence transient," in *Chlorophyll a* fluorescence: a signature of photosynthesis, eds G. C. Papageorgiou, and Govindjee, (Netherlands: Springer Press), 321–362. doi: 10.1007/978-1-4020-3218-9_12

Ting, I. P. (1985). Crassulacean acid metabolism. *Annu. Rev. Plant Physiol.* 36, 595–622.

van Heerden, P. D. R., Swanepoel, J. W., and Krüger, G. H. J. (2007). Modulation of photosynthesis by drought in two desert scrub species exhibiting C3-mode CO2 assimilation. *Environ. Exp. Bot.* 61, 124–136. doi: 10.1016/j.envexpbot.2007.05.005

Wang, Y., Xu, C., Wu, M., and Chen, G. (2017). Characterization of photosynthetic performance during reproductive stage in high-yield hybrid rice LYJP exposed to drought stress probed by chlorophyll a fluorescence transient. *Plant Growth Regul.* 81, 489–499. doi: 10.1007/s10725-016-0226-3

Wang, Z. X., Chen, L., Ai, J., Qin, H. Y., Liu, Y. X., Xu, P. L., et al. (2012). Photosynthesis and activity of photosystem II in response to drought stress in Amur Grape (*Vitis amurensis* Rupr.). *Photosynthetica* 50, 189–196. doi: 10.1007/s11099-012-0023-9

Wellburn, A. R. (1994). The spectral determination of chlorophylls a and b, as well as total carotenoids, using various solvents with spectrophotometers of different resolution. *J. Plant Physiol.* 144, 307–313. doi: 10.1016/s0176-1617(11)81192-2

Winter, K., and Demmig, B. (1987). Reduction state of Q and nonradiative energy dissipation during photosynthesis in leaves of a crassulacean acid metabolism plant, kalanchoë daigremontiana hamet et perr. *Plant Physiol.* 85, 1000–1007. doi: 10.1104/pp.85.4.1000

Winter, K., Lesch, M., and Diaz, M. (1990). Changes in xanthophyll-cycle components and in fluorescence yield in leaves of a crassulacean-acid-metabolism plant, clusia rosea Jacq., throughout a 12-hour photoperiod of constant irradiance. *Planta* 182, 181–185. doi: 10.1007/BF00197108

Yang, X., Cushman, J. C., Borland, A. M., Edwards, E. J., Wullschleger, S. D., Tuskan, G. A., et al. (2015). A roadmap for research on crassulacean acid metabolism (CAM) to enhance sustainable food and bioenergy production in a hotter, drier world. *New Phytologist.* 207, 491–504. doi: 10.1111/nph.13393

Zheng, L., Ceusters, J., and Van Labeke, M. C. (2019). Light quality affects light harvesting and carbon sequestration during the diel cycle of crassulacean acid metabolism in *Phalaenopsis*. *Photosynth. Res.* doi: 10.1007/s11120-019-00620-1 [Epub ahead of print].

Zivcak, M., Brestic, M., Kalaji, H. M., and Govindjee. (2014a). Photosynthetic responses of sun- and shade-grown barley leaves to high light: is the lower PSII connectivity in shade leaves associated with protection against excess of light? *Photosynth. Res.* 119, 339–354. doi: 10.1007/s11120-014-9969-8

Zivcak, M., Kalaji, H. M., Shao, H. B., Olsovska, K., and Brestic, M. (2014b). Photosynthetic proton and electron transport in wheat leaves under prolonged moderate drought stress. *J. Photochem. Photobiol. B Biol.* 137, 107–115. doi: 10.1016/j.jphotobiol.2014.01.007

Zivcak, M., Brestic, M., Olsovska, K., and Slamka, P. (2008). Performance index as a sensitive indicator of water stress in *Triticum aestivum* L. *Plant Soil Environ.* 54, 133–139. doi: 10.17221/392-pse

Conflict of Interest Statement: The authors declare that the research was conducted in the absence of any commercial or financial relationships that could be construed as a potential conflict of interest.

frontiers in Plant Science

SYSTEMATIC REVIEW
published: 06 September 2019
doi: 10.3389/fpls.2019.00957

Warming Treatment Methodology Affected the Response of Plant Ecophysiological Traits to Temperature Increases: A Quantitive Meta-Analysis

*Dan Wang[1], Hao Wang[1], Pengpeng Wang[2], Tianqi Ling[1], Wenhui Tao[1] and Zaiqiang Yang[1]**

[1] *Jiangsu Key Laboratory of Agricultural Meteorology, International Center for Ecology, Meteorology and Environment, Institute of Ecology, Nanjing University of Information Science and Technology, Nanjing, China,* [2] *Meteorological Bureau of Chengde City, Chengde, China*

OPEN ACCESS

Edited by:
Iker Aranjuelo, Institute of Agrobiotechnology, Superior Council of Scientific Investigations, Spain

Reviewed by:
Lina Fusaro, Sapienza University of Rome, Italy
Elisa Pellegrini, University of Pisa, Italy

***Correspondence:**
Zaiqiang Yang
yzq@nuist.edu.cn

Specialty section:
This article was submitted to Plant Abiotic Stress, a section of the journal Frontiers in Plant Science

Received: *18 February 2019*
Accepted: *09 July 2019*
Published: *06 September 2019*

Citation:
Wang D, Wang H, Wang P, Ling T, Tao W and Yang Z (2019) Warming Treatment Methodology Affected the Response of Plant Ecophysiological Traits to Temperature Increases: A Quantitive Meta-Analysis. Front. Plant Sci. 10:957. doi: 10.3389/fpls.2019.00957

Global mean temperature is expected to significantly increase by the end of the twenty-first century and could have dramatic impacts on a plant's growth, physiology, and ecosystem processes. Temperature manipulative experiments have been conducted to understand the responsive pattern of plant ecophysiology to climate warming. However, it remains unknown how different methodology used in these experiments will affect plants ecophysiological responses to warming. We conducted a comprehensive meta-analysis of the warming manipulative studies to synthesize the ecophysiological traits responses to warming treatment of different intensities, durations, and conducted for different species and under different experimental settings. The results indicated that warming enhanced leaf dark respiration (R_d) and specific leaf area (SLA) but decreased net photosynthetic rate (A_{net}) and leaf nitrogen content (LN). The positive and negative effects of warming on R_d and A_{net} were greater for C_4 species than C_3 species, respectively. The negative effect of warming treatment on A_{net} and LN and the positive effect on R_d were more evident under >1 year warming treatment. Negative effects of warming were more evident for plants grown at <10 L pots when experiment duration was longer than 1 year. The magnitude of warming treatment had a significant impact on most of the parameters that were investigated in the study. Overall, the results showed that warming effects on plant ecophysiological traits varied among different response variables and PFTs and affected by the magnitude of temperature change and experimental methodology. The results highlight the need for cautiously selecting the values of plant ecophysiological parameters in forecasting ecosystem function changes in future climate regimes and designing controlled experiments to realistically reflecting ecosystems responses to future global warming.

Keywords: photosynthesis, respiration, controlled experiment, climate warming, meta-analysis

INTRODUCTION

Based on the current trends in fossil energy production and use, deforestation, and population growth, it is expected that the increase of global mean surface temperatures for 2081–2100 relative to 1986–2005 is projected to be in the ranges of 0.3 to 1.7°C (RCP2.6), 1.1 to 2.6°C (RCP4.5), 1.4 to 3.1°C (RCP6.0), and 2.6 to 4.8°C (RCP8.5), which will have dramatic effects on economics, agriculture, and environment (AR5, IPCC, 2013). Plant traits are sensitive to climate warming and ecologists use plant trait-climate relationships to simulate plant physiology and growth in current and future climate situations (Farquhar and Sharkey, 1982; Wang et al., 2012; Jing et al., 2016). Therefore, understanding the patterns of plant physiological and morphological responses to global warming is of great importance in simulating and predicting the impact of global change on natural systems and agriculture.

Predictions of response to global warming may be derived from experimental and observational studies (Tilman, 1989; Wang et al., 2008, 2018; Knapp et al., 2012). While both types of study are common, relatively few authors have investigated whether they produce similar predictions or reflect reality (Dunne et al., 2004; Knapp et al., 2018). Experimental global change studies are typically limited in scope both spatially and temporally (Rustad et al., 2001). Observational studies often have broader spatial and temporal scales but suffer from a lack of control over covariates in biophysical and biochemical parameters of weather and soil. To minimize the weaknesses of each approach, it has been suggested that more research should explicitly unite observational and experimental work, perhaps by nesting experiments at multiple sites within a larger observational context or through summarized meta-analysis (Dunne et al., 2004; Jing et al., 2016).

Many manipulative experiments controlling physical and environmental factors have been conducted around the world to investigate the potential effects of global change on plants and terrestrial ecosystems (Sage and Kubien, 2007; Rustad, 2008; Wang et al., 2018). However, the methodology used in these experiments was different in their research settings, treatment intensities and durations and targeted species. The impact of short-term vs. long-term warming on plants traits would probably be different due to plants' acclimation capacity in photosynthesis, respiration and other physiological processes and these impacts would vary among different plant functional types (PFTs) under natural or controlled settings (Smith and Dukes, 2017). Plants' physiological and morphological responses to short-term warming treatment, however, are often used to parameterize the sub-models of photosynthesis, stomatal conductance, and respiration in plant growth and terrestrial ecosystem models, which would likely unrealistically simulate plant energy, carbon, and water fluxes in the long term. Indoor or outdoor settings and pot sizes could also affect the magnitude of ecophysiologial responses to temperature increase by implicating root growth and plant above-ground and below-ground tissue interactions (Arp, 1991). To accurately predict the impacts of climatic change and develop proper adaptive agricultural management practices, it is imperative to understand how temperature changes of different intensities and duration and changes manipulated under different experimental settings affect photosynthetic carbon gain, loss and allocation through a comprehensive analysis of relevant studies.

Previous research and meta-analyses have indicated that global warming will promote plant photosynthesis, dark respiration, leaf nitrogen content, specific leaf area, and other metabolisms (Poorter et al., 2012). It has been reported that the modulation of leaf traits and trait relationships by site climatic properties was modest (Wright et al., 2005). However, the modulation of leaf traits by warming treatment of different intensities and duration has not been extensively analyzed. Understanding how these processes vary among different species and plant functional types is a major goal for plant ecology and crucial for modeling how nutrient fluxes and vegetation boundaries will shift under global warming. The effect of the intensities and the treatment duration of global warming manipulative experiments on the plant physiology and growth among different plant functional groups, however, remain unclear. Therefore, the main objective of this study was to investigate the effects of global warming treatment with different magnitudes and durations on plant response in ecophysiological traits. Specifically, we aim to: (1) assess the impact of global warming of different magnitudes and durations on plant ecophysiological traits at leaf level; (2) detect the variations of ecophysiological traits response of different plant functional types to warming treatment of different durations; (3) explore the effect of different experimental settings on the response of a plant's traits to global warming. Accordingly, we propose: (1) due to plant acclimation capacity, short-term vs. long-term warming has different impacts on plant traits, with short-term warming having a more stimulating effect on the physiological functions of plants; (2) different experimental facilities may change the response of plants traits to warming treatment. To test these hypotheses, we conducted a comprehensive meta-analysis of the warming manipulating studies published from 1980 to 2018.

MATERIALS AND METHODS

Data Collection

Journal articles were searched on the Web of Science database with the keyword "leaf traits & warming," "leaf traits & temperature increase" and etc. The articles were later cross-checked with review articles and book chapters. The articles were imported into EndNote software and formed a database. All articles about warming effects on leaf traits were screened to ensure that all the articles available were included for the analysis. The articles published from 1980 to 2018 and meeting the following two conditions were included in the analysis: (1) the control group in the experiment was treated at ambient temperature situation; (2) physiological and morphological measurements were performed on both ambient and manipulated groups. Articles were rejected if: (1) plant physiological changes under warming treatments led to death of or severe damage to the plant; (2) there were other stressing factors impacting the warming treatments. Finally, 80 papers meeting the requirements were included in

the database (**Supplementary Material S1**). Data was obtained directly from the table or was extracted using the GetData Graph Digitizer software from the selected articles. In these studies, the magnitude of warming treatment ranged between 0.3 and 25°C, with only two studies showing a warming treatment above 20°C above AT (**Supplementary Material S1**). Response variables collected from these articles included net photosynthetic rate (A_{net}), stomatal conductance (G_s), leaf nitrogen (LN), dark respiration (R_d), and specific leaf area (SLA). When A_{net}, R_d, and G_s of one species with the same unit were all provided in the study (including measurements conducted on the same leaves/individuals and those across individuals), the R_d/A_{net}, and A_{net}/G_s in the control and warming treatments were calculated. In addition to the above responsive variables under different treatments, plant species, sample size, growth facilities, and duration of warming treatment were also collected. To ensure the independent nature of the data, we excluded duplicate results collected from the same studies. However, our analyses were not completely independent because individual study often provided data with more than one treatment (e.g., different warming treatment intensities) and/or different response variables. To examine the influence of non-independence of data, we first averaged those data from the same published study by PFTs so that only one comparison was used from a published study for each PFT. Nonetheless, we found that most of the response patterns were unchanged; therefore, all data were used in our study.

Categorization of the Studies

Temperature treatment was divided into two categories: AT (ambient temperature) and ET (elevated temperature). Plant species were classified into different photosynthetic pathways (C_3, C_4, or CAM), growth forms (herb or wood) and economic values (crop or non-crop). Experimental facilities were categorized into indoor (growth chambers or greenhouses) and outdoor (open top chambers or fully-open) settings and <10 L and >10 L growing pots. In our dataset, exposure time (i.e., how long plants were exposed to warming) ranged from <10 days to >10 years. To analyze the possible different responses under various warming durations, we banded the temperature treatment into two categories: short-term (<1 year) and long-term (>1 year). Warming treatments that were applied through air warming were included in the analyses. We listed the species, PFTs information and relevant experimental methodology used in this study (**Supplementary Material S1**).

Meta-Analysis Methods

To avoid the adverse effects of different units, we used the response ratio $r = X_t/X_c$ to estimate the magnitude of the effect of warming treatment, where X_t is the treatment mean and X_c is the control mean. For ease of comparison, we calculated the natural logarithm of the response ratio (lnr). The standard deviation (SD) and the sample size (n) for each observation were collected to calculate the variance of the effect size.

The lnr was calculated without and with being standardized by warming magnitude (Equations 1, 2).

$$\log_e r = \log_e\left(\frac{X_t}{X_c}\right) = \log_e(X_t) - \log_e(X_c) \quad (1)$$

$$\log_e r = \frac{\log_e\left(\frac{X_t}{X_c}\right)}{T_t - T_c} = \frac{\log_e(X_t)}{T_t - T_c} - \frac{\log_e(X_c)}{T_t - T_c} \quad (2)$$

where T_t and T_c are the temperature in the warming and control treatments, respectively.

Using METAWIN software 2.1 (Sinauer Associates, Inc. Sunderland, MA, USA), we calculated the effect size of the target variables and used a weighted fixed-effect model to assess the effect of plant functional types, experimental settings, and treatment duration. If the 95% confidence interval (CI) of the effect size produced by the fixed-effect model overlaps with 0, no significant effect was detected on the response variables. If the upper limit of 95% CI is less than 0, the effect is considered significantly negative. In contrast, if the lower limit of 95% CI is greater than 0, the effect is considered significantly positive. If the 95% CI of the effect size among different species, pot size, and treatment duration does not overlap, their response is considered significantly different. Unless otherwise indicated, significance level was set at $p < 0.05$. The publication bias for effect size (lnr) in this meta-analysis was also calculated. We calculated Spearman's rank order correlation (rs) which indicates the relationship between the effect size (lnr) and the sample size (Begg and Mazumdar, 1994), and Rosenthal's fail-safe number which represents the number of additional studies with a mean effect size of zero needed to eliminate the significance of a significant effect (Rosenthal, 1979). Publication bias was significant if p-value of rs was smaller than 0.05. However, the publication bias may be safely ignored if the fail-safe number is larger than a critical value of 5n+10 where n is the number of studies (Rosenberg, 2005).

Statistical Analysis

Original data collected from these studies were arranged into a database in which the value of response variables was lnr. The effect of warming duration on lnr was considered significant if the 95% confidence interval (CI) of lnr does not overlap with 0. And when the 95% confidence intervals (CI) of lnr of different PFTs, facilities or pot size did not overlap with each other, the response was considered significantly different among different categories, the means of the ratio of the R_d/A_{net} and A_{net}/G_s in the control and warming treatments were compared using paired t-test. The relationship between lnr of all the variables and the magnitude of warming treatments were evaluated by a second-degree polynomial or linear regression analysis with the R statistical programming language (R 3.2.2 for Windows GUI front-end).

RESULTS

Effects of the Duration of Warming Treatment on Plant Ecophysiological Traits Across Plant Functional Types (PFTs) and Growth Forms

Warming treatment increased dark respiration (R_d) and specific leaf area (SLA) and decreased net photosynthetic rate (A_{net}) and leaf N concentration (LN) across all the experiments (**Figure 1**). The response of standardized (triangle symbols) or unstandardized (circle symbols) rate of A_{net}, G_s, R_d, LN, and SLA to warming treatment differed with different warming durations (**Figure 2**). Long-term warming treatment (>1 year) had a greater positive effect on R_d than short-term (<1 year), regardless of whether the effect was standardized or unstandardized. LN was decreased by long-term warming but was increased or not changed by short-term warming treatment for unstandardized and standardized effect, respectively. Long-term warming treatment increased SLA, while short-term treatment had no effect on SLA. For standardized response of SLA, there was no difference between long and short-term treatments. For G_s, long term treatment had a positive but short-term treatment had a negative effect on the standardized effect size. However, for the unstandardized effect size, short-term treatment did not have a significant but long-term had a negative effect on G_s. Short-term had a positive and long-term treatment a negative effect on A_{net} for the unstandardized form of the effect. And for standardized effect of A_{net}, long-term treatment had a more negative effect than short-term treatment (**Figure 2**).

The response of A_{net}, G_s, R_d, LN, and SLA to warming treatment differed among PFTs with different photosynthetic pathways (**Figure 3**). Warming had a more positive effect on R_d for C_4 species than for C_3 species, regardless of whether the effect size was standardized. Warming had a negative effect for C_3 but a positive effect for C_4 species on LN, SLA, and G_s. In contrast, warming had a negative effect for C_4 but near-zero effect for C_3 species on A_{net} (**Figure 3**).

Warming duration had a significant effect on the response of A_{net}, G_s, R_d, LN, and SLA for PFTs with different photosynthetic pathways (**Figure 4**). Long term warming treatment had a more positive effect than short-term on R_d for both C_3 and C_4 species, regardless of whether the effect was standardized. For LN, long term treatment had a negative effect but short-term treatment had a positive effect for C_3 and C_4 species. For C_3 species, short term warming treatment had a positive and long-term had a negative effect on A_{net}; for C_4 species, long term warming treatment had a positive but short term a negative effect on A_{net}. Similar trend was found for standardized A_{net}, even though the magnitude of the effect differed.

Effects of Warming Duration on Plant Traits Across Different Experimental Settings

The responses of A_{net}, G_s, R_d, LN, and SLA to warming treatment differed among in-door and outdoor experimental settings (**Figure 5**). Warming had a more positive impact on R_d in the in-door than the out-door settings for unstandardized effect size. Warming had a positive effect on LN for in-door, but a negative effect for outdoor settings. Being standardized with temperature treatment, warming had no impact on LN for the in-door but negative impact on outdoor experimental settings. Warming had a positive effect on SLA for in-door settings but tended to have a negative effect for outdoor settings. G_s responded positively to warming under in-door but negatively under outdoor settings. Warming treatment had a positive effect on unstandardized A_{net} under in-door settings but a negative effect under outdoor settings. For standardized A_{net}, warming had a negative effect for both in-door and outdoor settings (**Figure 5**).

The response of A_{net}, G_s, R_d, LN, and SLA to warming treatment under indoor and outdoor experiment settings also differed with different treatment durations (**Figure 6**). Short-term warming had a positive effect but long-term had a negative effect on R_d for indoor experimental settings. Long-term warming had a more positive impact on R_d than short-term for outdoor experimental settings for both standardized and unstandardized effect size. Short-term warming treatment had a more positive impact than long-term treatment on A_{net} for unstandardized effect size but had no difference on standardized effect size. Short-term had a positive impact on A_{net} for outdoor settings, but long-term treatment had a negative impact on A_{net} for unstandardized effect. Long-term warming treatment had a more negative effect on standardized A_{net} than short term for outdoor settings (**Figure 6**).

Pot size had a significant impact on the responses of A_{net}, G_s, R_d, and LN to warming treatment (**Figure 7**). Warming had a positive impact on R_d for plants grown in pots larger than 10 L, while a negative effect for plants grown in pots smaller than 10 L. G_s responded positively to warming when grown at <10 L plots but negatively at >10 L plots. A_{net} of plants grown at >10 L pots responded negatively to warming. Warming had no impacts on unstandardized A_{net} but a negative effect on standardized A_{net} of plants grown at <10 L pots.

The response of A_{net}, G_s, LN, and SLA to warming treatment differed among different treatment durations when plants were grown in pots of different volumes (**Figure 8**). Short-term warming had a positive effect but long-term, a positive effect on LN for plants grown at both <10 L and >10 L pots. Short-term warming had a negative effect on SLA, but long-term a positive effect for both <10 L and >10 L pots. G_s responded positively with both short and long-term warming treatments at <10 L pots but negatively at >10 L pots. A_{net} responded positively to long-term warming treatment at <10 L pots but negatively at >10 L pots (**Figure 8**).

Effects of Warming Magnitude on Plant Traits Across Different Experimental Settings

A_{net}, R_d, LN, and SLA formed a quadratic relationship to warming treatment (**Figure 9**). The effect size of A_{net}, R_d, LN, and SLA to warming was highest or lowest when temperature change was 6.6, 2.5, 6.6, and 5.2°C above ambient temperature, respectively (**Figure 9**).

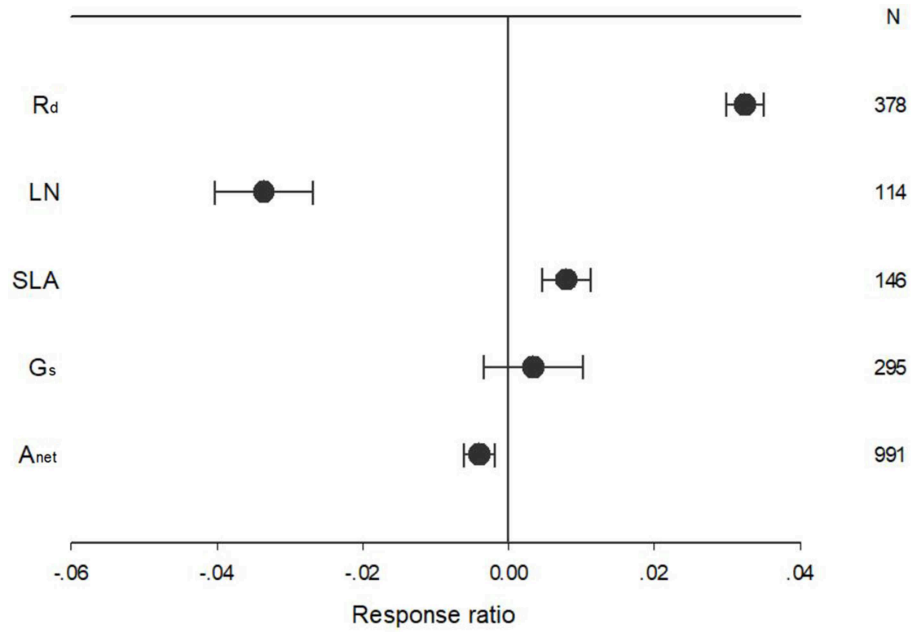

FIGURE 1 | Ecophysiological responses of net photosynthetic rate (A_{net}), stomatal conductance (G_S), leaf nitrogen content (LN), specific leaf area (SLA), and leaf dark respiration rate (R_d) to increased temperature. Each data point represents the mean ± 95% CI. The number of observations for each variable is given on the right of the graph.

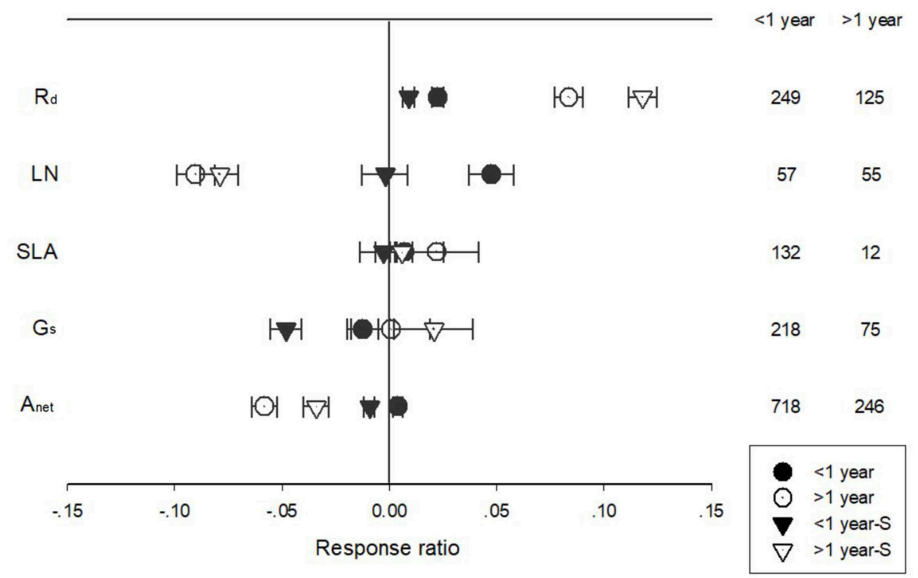

FIGURE 2 | Standardized (triangle symbols) and unstandardized (circle symbols) responses of net photosynthetic rate (A_{net}), stomatal conductance (G_S), leaf nitrogen content (LN), specific leaf area (SLA), and leaf dark respiration rate (R_d) to <1 year (closed symbols) and >1 year (open symbols) temperature treatment durations. Each data point represents the mean±95% CI. The number of observations for each variable is given on the right of the graph.

DISCUSSION

Several meta-analyses have investigated the general tendency of warming impacts on plant physiology and production (Rustad et al., 2001; Jing et al., 2016). However, it remains unclear how the experimental methodology of warming treatment affects the responses of plant ecophysiological traits to warming at leaf level. In this study, we collected data from warming manipulative studies and analyzed changes in the ecophysiological responses in the leaf traits. Overall, we found that (1) the direction and degree of the effect of warming treatment of different durations and settings on plant ecophysiological traits varied

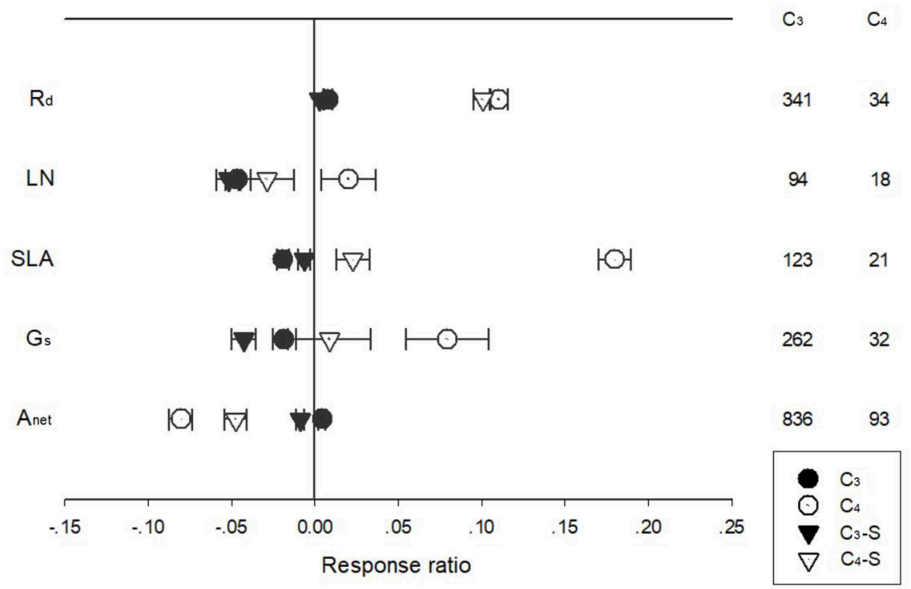

FIGURE 3 | Standardized (triangle symbols) and unstandardized (circle symbols) of net photosynthetic rate (A_{net}), stomatal conductance (G_s), leaf nitrogen content (LN), specific leaf area (SLA), and leaf dark respiration rate (R_d) of C_3 (closed symbols) and C_4 (open symbols) species to increased temperatures. Each data point represents the mean±95% CI. The number of observations for each variable is given on the right of the graph.

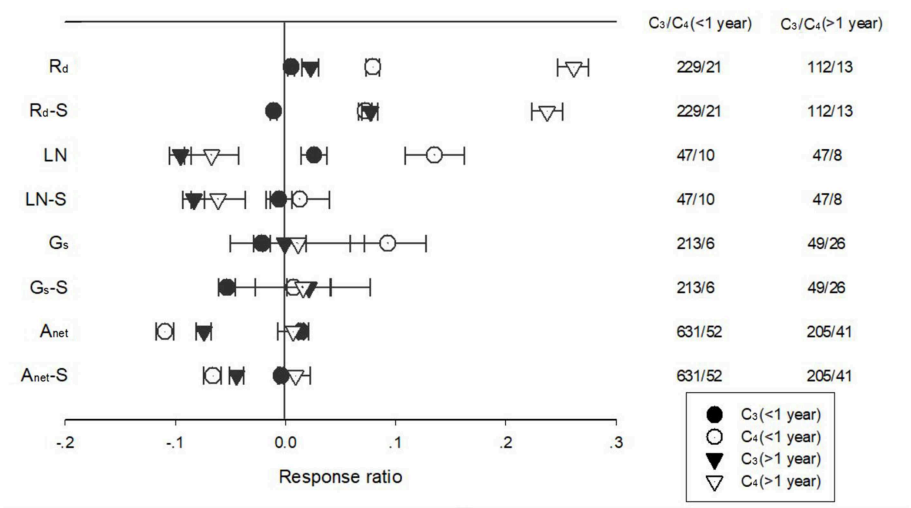

FIGURE 4 | Responses of net photosynthetic rate (A_{net}), stomatal conductance (G_s), leaf nitrogen content (LN), specific leaf area (SLA) and leaf dark respiration rate (R_d) of C_3 (closed symbols) and C_4 (open symbols) species to <1 year (circle symbols) and >1 year (triangle symbols) temperature treatment. Each data point represents the mean±95% CI. The number of observations for each variable is given on the right of the graph.

significantly; (2) there were significant variations among plant functional types in response to warming treatment of different methodology.

Consistent with previous findings from other studies, this meta-analysis confirmed that R_d and SLA were stimulated by warming treatment (Rustad et al., 2001; Jing et al., 2016). Increasing, decreasing or neutral impacts of experimental warming have been observed for net photosynthetic rates (Bruhn et al., 2007; Bronson and Gower, 2010; Li et al., 2013). The net photosynthetic rate in this analysis was significantly decreased by warming treatment. The decrease in plant photosynthetic capacity may be attributed to the decreased LN under warmed conditions. Many studies showed that plant photosynthetic capacity was positively related to leaf N concentrations (Kattge et al., 2009; Reich et al., 2009). Compared with the negative effect of warming for non-legumes, there was

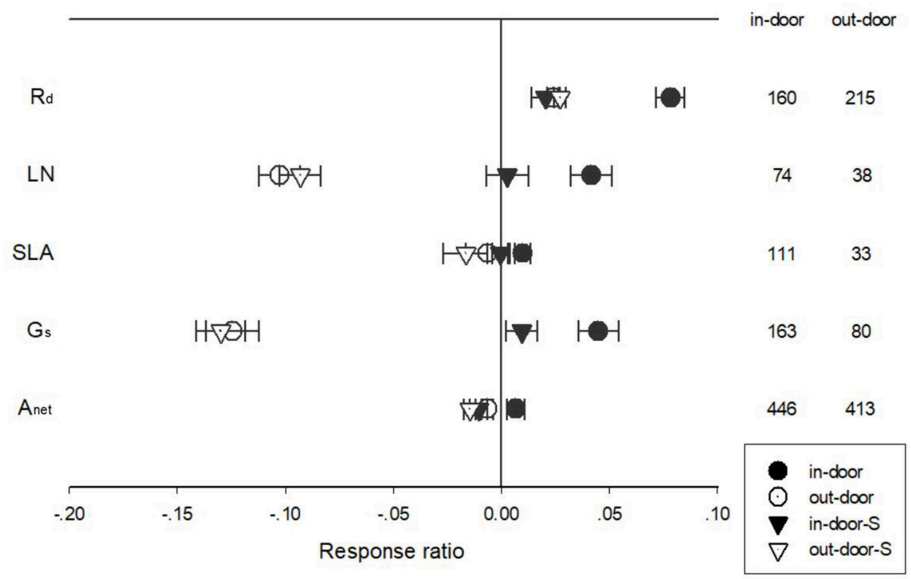

FIGURE 5 | Standardized (triangle symbols) and unstandardized (circle symbols) responses of net photosynthetic rate (A_{net}), stomatal conductance (G_s), leaf nitrogen content (LN), specific leaf area (SLA), and leaf dark respiration rate (R_d) to increased temperatures at in-door (closed symbols) and out-door (open symbols) experimental settings. Each data point represents the mean±95% CI. The number of observations for each variable is given on the right of the graph.

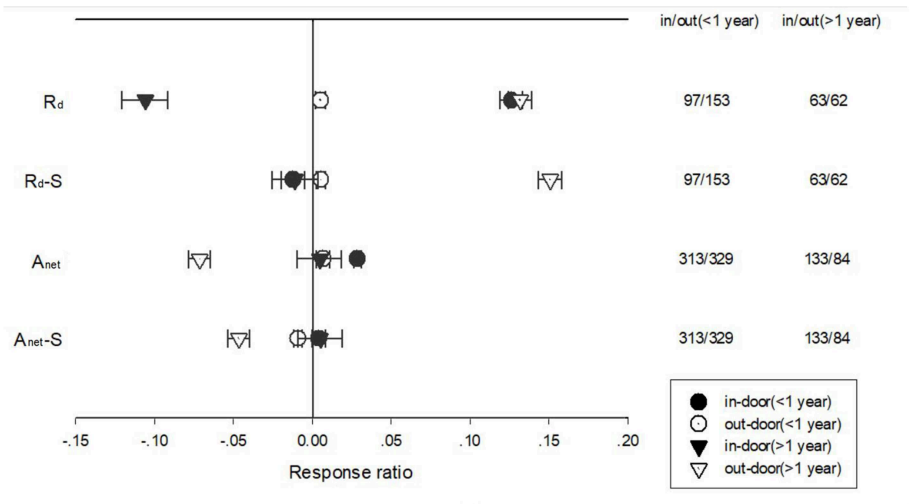

FIGURE 6 | Responses of net photosynthetic rate (A_{net}) and leaf dark respiration rate (R_d) to <1 year (circle symbols) and >1 year (triangle symbols) temperature treatment at in-door (closed symbols) and out-door (open symbols) experimental settings. Each data point represents the mean±95% CI. The number of observations for each variable is given on the right of the graph.

a positive or neutral effect on LN and A_{net} for legume species (**Supplementary Material S3**). Contrary to the expectations, stomatal conductance remained unchanged under warming, thus highlighting the key roles of biochemical and nutritional limitations on the negative responses of net photosynthesis to warming treatment. The response of G_s to global warming is critical for modeling ecosystem and landscape-scale water fluxes and CO_2 exchange. The ratio of respiration to photosynthesis (*R/P*) has been used to express the proportion of consumed to fixed C of plants (Atkin et al., 2007; Campbell et al., 2007) and shown to be enhanced (Danby and Hik, 2007; Wan et al., 2009), suppressed (Jochum et al., 2007), or maintained (He et al., 2005) by experimental warming. The ratio of R_d/A_{net} was increased at warming conditions (effect size is 0.3623, $n = 275$) in this study, suggesting that the respiration was more affected and a greater proportion of fixed C was consumed, implying a decline of the net amount of C fixed by leaves by warming, at least in the controlled experiments.

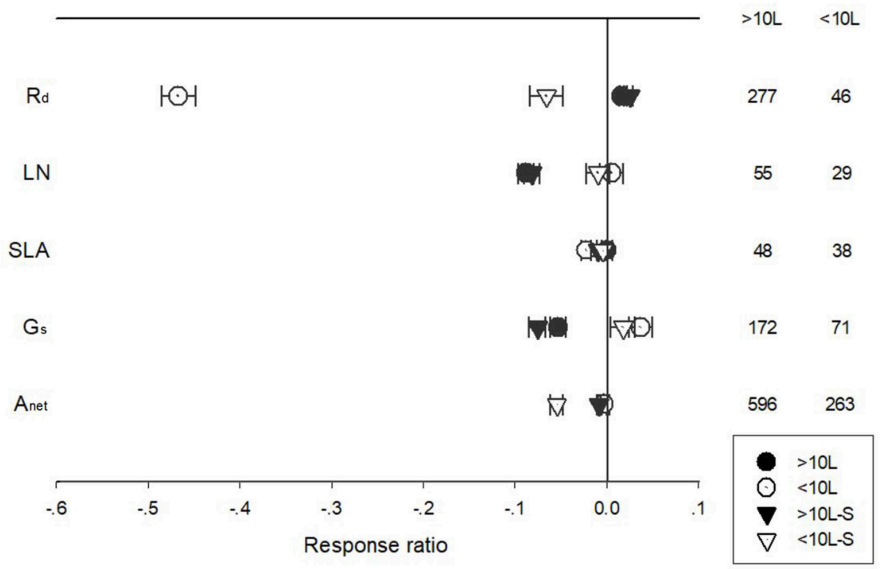

FIGURE 7 | Standardized (triangle symbols) and unstandardized (circle symbols) responses of net photosynthetic rate (A_{net}), stomatal conductance (G_S), leaf nitrogen content (LN), specific leaf area (SLA), and leaf dark respiration rate (R_d) to increased temperatures for plants grown at <10 L (closed symbols) and >10 L pots (open symbols). Each data point represents the mean±95% CI. The number of observations for each variable is given on the right of the graph.

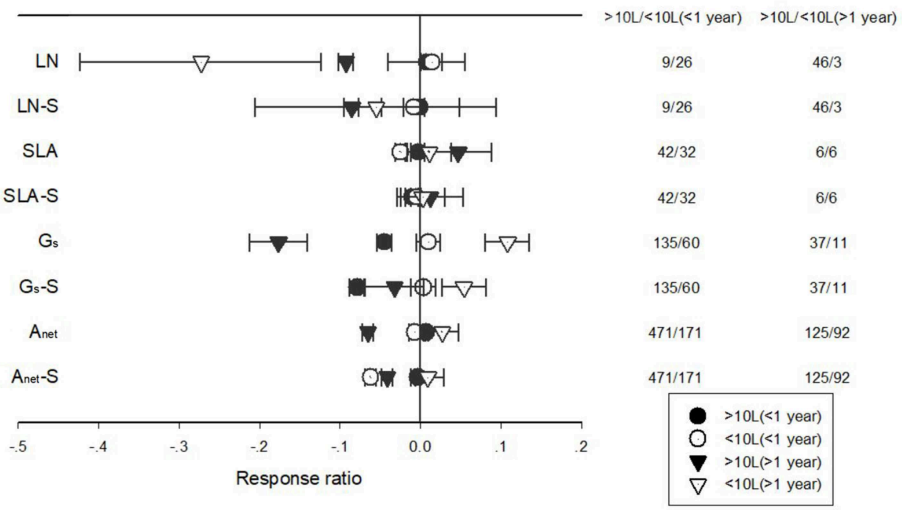

FIGURE 8 | Responses of net photosynthetic rate (A_{net}), stomatal conductance (G_S), leaf nitrogen content (LN), specific leaf area (SLA), and leaf dark respiration rate (R_d) to <1 year (circle symbols) and >1 year (triangle symbols) temperature treatment at in-door (closed symbols) and out-door (open symbols) experimental settings. Each data point represents the mean±95% CI. The number of observations for each variable is given on the right of the graph.

Ecophysiological traits responses of terrestrial plants to increased temperature varied among plant functional types with different photosynthetic pathways (PFTs; Wang et al., 2012; Jing et al., 2016). Previous studies indicated that global warming had stronger effects on A_{net} of C_3 species than C_4 species (Wahid et al., 2007). In this study, the positive and negative effects of warming on R_d and A_{net} were greater for C_4 species than C_3 species, in spite of positive or neutral effects of warming on LN, SLA, and G_S for C_4 and C_3 species, respectively. The contradictory findings posed great challenges for projecting the responses and feedbacks of terrestrial ecosystems to global warming. The more disadvantaged situation for C_4 species under warming might be associated with higher growth and treatment temperature applied in the experiment (**Supplementary Material S1**). The metabolic balance of the photosynthetic and respiratory processes under climate warming plays a critical role in regulating ecosystem carbon storage and cycling (Schimel, 1995; King et al., 2006).

Warming stimulated A_{net} in woody but suppressed it in herbaceous plants (**Supplementary Material S4**). The positive

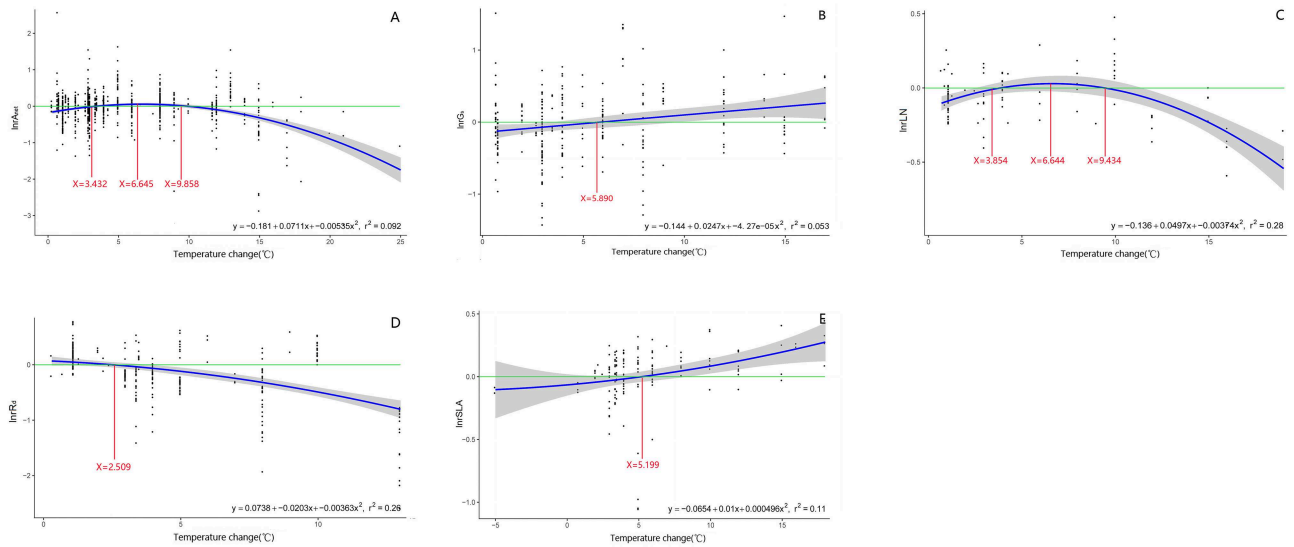

FIGURE 9 | Regression relationship between the magnitude of warming treatment and the effect size of net photosynthetic rate (**A:** A_{net}), stomatal conductance (**B:** G_s), leaf nitrogen content (**C:** LN), specific leaf area (**D:** SLA), and leaf dark respiration rate (**E:** R_d). Regression equation and variation coefficient are presented in the lower right corner of each graph. Different lines indicate x-value when y is the maximum (red line), crossing points of y = 0 (green line) and regression relationships (blue line).

effect of warming on A_{net} for woody species was unrelated to either G_s or LN, as G_s and LN both were decreased under warming treatments (**Supplementary Material S4**). The results from this study were similar to the trend reported for trees showing a lower percentage decrease in G_s compared to herbaceous species (Wang et al., 2012). Warming had a positive effect on G_s and LN for crops, while a negative effect for non-crops (**Supplementary Material S5**). The changes in G_s at warming treatment may alter leaf temperature and result in a change in latent heat loss through evaporation, which may further affect net carbon balance (Warren et al., 2011). Warming could influence vegetation dynamics and ecosystem structure through shifting competitive interactions among different functional groups in natural or agricultural systems. Therefore, knowledge of photosynthetic and stomatal responses to increased temperature of different PFTs instead of species will facilitate the prediction of terrestrial C- and water-cycle feedback to climate warming.

Ecophysiological trait responses of terrestrial plants to increased temperature varied among warming treatments of differing durations. The physiological acclimation can lead to smaller enhancements of plant photosynthesis and respiration under long term warmer conditions than predicted with photosynthesis/respiration-temperature relationships (Medlyn et al., 2002; Dwyer et al., 2007; Tjoelker and Zhou, 2007; Gunderson et al., 2010). The thermal acclimation of R_d could minimize the effects of climate warming on C loss via plant respiration (Gifford, 1995; Ziska and Bunce, 1998; Loveys et al., 2002) and mitigate the positive feedback between climate change and atmospheric CO_2 (King et al., 2006; Atkin et al., 2008).The findings in this meta-analysis indicated that the negative effect of warming treatment on A_{net} and LN and the positive effect on R_d were more evident under >1 year warming treatment and the trend was confirmed for both C_3 and C_4 species (**Figure 4**), which contrasted to other studies showing significant declines in the photosynthetic and/or respiratory response with increasing exposure time, a thermal acclimation to warming (Hikosaka et al., 2006; Gunderson et al., 2010).

Potential confounding factors must be accounted in the meta-analysis because many studies were conducted under variable conditions and targeted on different species. In this analysis, studies in which plants were grown under other environmental stresses such as drought, low nutrients, light deficiency or elevated ozone were excluded. In addition to the variation caused by plant functional types and treatment duration, different experimental facilities could be responsible for the responses of different PFTs (Cheesman and Klaus, 2013; Rehmani et al., 2014). This study mainly focused on the effects of pot size (<10 L vs. >10 L) and experimental settings (in-door vs. out-door) on plant ecophysiological responses. Warming had a negative and positive effect on LN and G_s when plants were grown at outdoor and in-door settings, respectively. Pot size significantly altered the responses of R_d, LN and SLA to warming treatments. Warming had a negative effect on R_d for plants grown at <10 L pots, while a positive effect at >10 L pot. For both LN and G_s, warming had a negative effect for plants grown at >10 L pots, while a neutral effect at <10 L pot. We were expecting that warming would have a more negative effect on LN and G_s in smaller pots or in-door settings considering that below-ground growth would be more constrained and thus limited the nutrients and water supply to the aboveground growth (Walters and Reich, 1989; Climent et al., 2011), the analysis indicated that this was true only when

experiment duration was longer than 1 year when negative effects of warming was more evident for plants grown at <10 L pots.

Warming treatment duration had a significant interactive effect with experimental settings (in-door vs. outdoor) on R_d and A_{net}. Long-term warming had a negative effect on R_d for in-door and on A_{net} for outdoor experimental settings. The findings in this meta-analysis indicated that the negative effect of warming treatment on A_{net} and LN and the positive effect on R_d were more evident under >1 year warming treatment and the trend was confirmed for both C_3 and C_4 species (**Figure 4**). The negative effect of warming on R_d could be related to the higher treatment temperature applied at the in-door settings (**Supplementary Material S2**). Temperature conditions in which plants live may be another possible reason for the contradictory findings (Rustad et al., 2001). The discrepancy of the response of A_{net} and R_d to warming treatment under different experimental settings provided difficulty in parameterizing ecosystem models and raised concerns in proper experimental designs when dealing with climate change questions.

The intensities of temperature treatment also had a significant impact on most of the parameters that were investigated in the study. The effect size of A_{net}, R_d, LN, and SLA responded to temperature increase in a quadratic relationship. Consistent with the results discussed before, the peak value of the ecophysiological traits of A_{net}, R_d, and LN occurred at temperatures higher than the ambient. Plant physiological responses to warming may also depend on the temperature regime they are grown at. Studies often report a positive response to warming in Rubisco carboxylation, photosynthesis, and growth in cool-climate species but reduced growth and carbon gain in species that exist in warm low-latitude climates (Way and Oren, 2010; Crous et al., 2018).

CONCLUSION

Overall, we found that warming treatment of different durations and settings had different impacts on plant ecophysiological traits and the responses varied significantly among different plant functional types. Warming stimulated R_d and SLA but suppressed A_{net} and LN and the effect varied among different PFTs and experimental designs. The positive and negative effects of warming on R_d and A_{net}, were greater for C_4 than C_3 species, in spite of the positive or neutral effects of warming on LN, SLA, and G_S for C_4 and C_3 species, respectively. The findings in this meta-analysis also indicated that the negative effect of warming treatment on A_{net} and LN and the positive effect on R_d were more evident under >1 year warming treatment and the trend was confirmed for both C_3 and C_4 species. Negative effect of warming was more evident for plants grown at <10 L pots only when experiment duration was longer than 1 year. The magnitude of temperature treatment did have an impact on most of the parameters that were investigated in the study. The functional type specific response patterns of plant traits to warming are critical for obtaining credible predictions of the changes in food production, carbon sequestration and climate regulation. This result also highlights the need for cautiously selecting parameter values in forecasting ecosystem function changes in future climate regimes, evaluating much more broadly what can and cannot be learned from experimental studies and designing controlled experiments to realistically reflecting ecosystems responses to future global warming.

DATA AVAILABILITY

All datasets for this study are included in the manuscript and the **Supplementary Files**.

AUTHOR CONTRIBUTIONS

DW and ZY conceived and wrote the paper. The rest of the authors helped collection data and ran data analysis.

ACKNOWLEDGMENTS

Funding for this research was provided by The National Natural Science Foundation of China (31500503 & 31770485), Nanjing University of Information Science and Technology (2013r115), Jiangsu Distinguished Professor Scholarship, Jiangsu six talent peaks (R2016L15), Jiangsu Natural Science Foundation (BK20150894), and the Jiangsu Overseas Research & Training Program for University Prominent Young & Middle-aged Teachers and Presidents through DW.

SUPPLEMENTARY MATERIAL

The Supplementary Material for this article can be found online at: https://www.frontiersin.org/articles/10.3389/fpls.2019.00957/full#supplementary-material

REFERENCES

An, Y. A., Wan, S. Q., Zhou, X. H., Subedar, A. A., Wallace, L. L., and Luo, Y. (2005). Plant nitrogen concentration, use efficiency, and contents in a tallgrass prairie ecosystem under experimental warming. *Glob. Chang. Biol.* 11, 1733–1744. doi: 10.1111/j.1365-2486.2005.01030.x

Anderson, L., and Cipollini, J. (2013). Gas exchange, growth, and defense responses of invasive Alliaria Petiolata (Brassicaceae) and native Geum Vernum (Rosaceae) to elevated atmospheric CO_2 and warm spring temperatures. *Am. J. Bot.* 100, 1544–1554. doi: 10.3732/ajb.1300014

Arp, W. J. (1991). Effects of source-sink relations on photosynthetic acclimation to elevated CO_2. *Plant Cell Environ.* 14, 869–875. doi: 10.1111/j.1365-3040.1991.tb01450.x

Atkin, O. K., Atkinson, L. J., Fisher, R. A., Campbell, C. D., Zaragoza-Castells, J., Pitchford, J. W., et al. (2008). Using temperaturedependent changes in leaf scaling relationships to quantitatively account for thermal acclimation of respiration in a coupled global climate-vegetation model. *Glob. Chang. Biol.* 14, 2709–2726. doi: 10.1111/j.1365-2486.2008.01664.x

Atkin, O. K., Scheurwater, I., and Pons, T. L. (2007). Respiration as a percentage of daily photosynthesis in whole plants is homeostatic at

moderate, but not high, growth temperatures. *New Phytol.* 174, 367–380. doi: 10.1111/j.1469-8137.2007.02011.x

Begg, C. B., and Mazumdar, M. (1994). Operating characteristic of a rand correlation test for publication bias. *Biometrics* 50, 1088–1101. doi: 10.2307/2533446

Bronson, D. R., and Gower, S. T. (2010). Ecosystem warming does not affect photosynthesis or aboveground autotrophic respiration for boreal black spruce. *Tree Physiol.* 30, 441–449. doi: 10.1093/treephys/tpq001

Bruhn, D., Egerton, J. J. G., Loveys, B. R., and Ball, M. C. (2007). Evergreen leaf respiration acclimates to long-term nocturnal warming under field conditions. *Glob. Chang. Biol.* 13, 1216–1223. doi: 10.1111/j.1365-2486.2007.01351.x

Campbell, C., Atkinson, L., Zaragoza-Castells, J., Lundmark, M., Atkin, O., and Hurry, V. (2007). Acclimation of photosynthesis and respiration is asynchronous in response to changes in temperature regardless of plant functional group. *New Phytol.* 176, 375–389. doi: 10.1111/j.1469-8137.2007.02183.x

Cheesman, A. W., and Klaus, W. (2013). Elevated night-time temperatures increase growth in seedlings of two tropical pioneer tree species. *New Phytol.* 197, 1185–1192. doi: 10.1111/nph.12098

Climent, J., Chambel, M. R., Pardos, M., Lario, F., and Villar-Salvador, P. (2011). Biomass allocation and foliage heteroblasty in hard pine species respond differentially to reduction in rooting volume. *Eur. J. For. Res.* 130, 841–850. doi: 10.1007/s10342-010-0476-y

Crous, K. Y., Drake, J. E., Aspinwall, M. J., Sharwood, R. E., Tjoelker, M. G., and Ghannoum, O. (2018). Photosynthetic capacity and leaf nitrogen decline along a controlled climate gradient in provenances of two widely distributed *Eucalyptus* species. *Glob. Change Biol.*24, 4626–4644. doi: 10.1111/gcb.14330

Danby, R. K., and Hik, D. S. (2007). Responses of white spruce (*Picea glauca*) to experimental warming at a subarctic alpine treeline. *Glob. Chang. Biol.* 13, 437–451. doi: 10.1111/j.1365-2486.2006.01302.x

Drake, J. E., Aspinwall, M. J., Pfautsch, S., Rymer, P. D., Reich, P. B., Smith, R. A., et al. (2015). The capacity to cope with climate warming declines from temperate to tropical latitudes in two widely distributed Eucalyptus species. *Glob. Chang. Biol.* 21, 459–472. doi: 10.1111/gcb.12729

Duan, B. L., Zhang, X. L., Li, Y. P., Li, L., Korpelainen, H., and Li, C. (2013). Plastic responses of *Populus yunnanensis* and *Abies faxoniana* to elevated atmospheric CO_2 and warming. *For. Ecol. Manage.* 296, 33–40. doi: 10.1016/j.foreco.2013.01.032

Dunne, J. A., Saleska, S. R., Fischer, M. L., and Harte, J. (2004). Integrating experimental and gradient methods in ecological climate change research. *Ecology* 85, 904–916. doi: 10.1890/03-8003

Dwyer, S. A., Ghannoum, O., Nicotra, A., and von Caemmerer, S. (2007). High temperature acclimation of C_4 photosynthesis is linked to changes in photosynthetic biochemistry. *Plant Cell Environ.* 30, 53–66. doi: 10.1111/j.1365-3040.2006.01605.x

Farquhar, G. D., and Sharkey, T. D. (1982). Stomatal conductance and photosynthesis. *Annu. Rev. Plant Physiol.* 33, 317–345. doi: 10.1146/annurev.pp.33.060182.001533

Flury, S., and Gessner, M. O. (2014). Effects of experimental warming and nitrogen enrichment on leaf and litter chemistry of a wetland grass, *Phragmites australis*. *Basic Appl. Ecol.* 15, 219–228. doi: 10.1016/j.baae.2014.04.002

Gifford, R. M. (1995). Whole plant respiration and photosynthesis of wheat under increased CO_2 concentration and temperature: longterm vs short-term distinctions for modelling. *Glob. Chang. Biol.* 1, 385–396. doi: 10.1111/j.1365-2486.1995.tb00037.x

Gunderson, C. A., O'Hara, K. H., Campion, C. M., Walker, A. V., and Edwards, N. T. (2010). Thermal plasticity of photosynthesis: the role of acclimation in forest responses to a warming climate. *Glob. Chang. Biol.* 16, 2272–2286. doi: 10.1111/j.1365-2486.2009.02090.x

Gunderson, C. A., Norby, R. J., and Wullschleger, S. D. (2000). Acclimation of photosynthesis and respiration to simulated climatic warming in northern and southern populations of *Acer saccharum*: laboratory and field evidence. *Tree Physiol.* 20, 87–96. doi: 10.1093/treephys/20.2.87

Han, S., Sun, J., Kyung, T., Han, S. H., Lee, J., Kim, S., et al. (2015). Species-specific growth and photosynthetic responses of first-year seedlings of four coniferous species to open-field experimental warming. *Turk. J. Agric. For.* 39, 342–349. doi: 10.3906/tar-1408-117

He, J. S., Wolfe-Bellin, K. S., and Bazzaz, F. A. (2005). Leaf-level physiology, biomass, and reproduction of *Phytolacca americana* under conditions of elevated CO_2 and altered temperature regimes. *Int. J. Plant Sci.* 166, 615–622. doi: 10.1086/430196

Hikosaka, K., Ishikawa, K., Borjigidai, A., Muller, O., and Onoda, Y. (2006). Temperature acclimation of photosynthesis: mechanisms involved in the changes in temperature dependence of photosynthetic rate. *J. Exp. Bot.* 57, 291–302. doi: 10.1093/jxb/erj049

IPCC (2013). *Climate Change 2013 AR5: The Physical Science Basis*. Intergovernmental Panel on Climate Change. Cambridge: Cambridge University Press, 548.

Jacques, M., Lapointe, L., Rice, K., and Montgomery, R. A., Stefanski, A., and Reich, P. B. (2015). Responses of two understory herbs, *Maianthemum canadense* and *Eurybia macrophylla*, to experimental forest warming: early emergence is the key to enhanced reproductive output. *Am. J. Bot.* 102, 1610–1624. doi: 10.3732/ajb.1500046

Jing, P., Wang, D., Zhu, C., and Chen, J. (2016). Plant physiological, morphological and yield-related responses to night temperature changes across different species and plant functional types. *Front. Plant Sci.* 7:1774. doi: 10.3389/fpls.2016.01774

Jochum, G. M., Mudge, K. W., and Thomas, R. B. (2007). Elevated temperatures increase leaf senescence and root secondary metabolite concentrations in the understory herb *Panax quinquefolius* (Araliaceae). *Am. J. Bot.* 94:819–826. doi: 10.3732/ajb.94.5.819

Kattge, J., Knorr, W., Raddatz, T., and Wirth, C. (2009). Quantifying photosynthetic capacity and its relationship to leaf nitrogen content for global-scale terrestrial biosphere models. *Glob. Chang. Biol.* 15, 976–991. doi: 10.1111/j.1365-2486.2008.01744.x

King, A. W., Gunderson, C. A., Post, W. M., Weston, D. J., and Wullschleger, S. D. (2006). Atmosphere: plant respiration in a warmer world. *Science* 312, 536–537. doi: 10.1126/science.1114166

Knapp, A. K., Carroll, C. J. W., Griffin-Nolan, R. J., Slette, I. J., Chaves, F. A., Baur, L. E., et al. (2018). A reality check for climate change experiments: do they reflect the real world? *Ecology* 99, 2145–2151. doi: 10.1002/ecy.2474

Knapp, A. K., Smith, M. D., Hobbie, S. E., Collins, S. L., Fahey, T. J., Hansen, G. J. A., et al. (2012). Past, present, and future roles of long-term experiments in the LTER network. *Bioscience* 62, 377–389. doi: 10.1525/bio.2012.62.4.9

Kroner, Y., and Way, D. A. (2016). Carbon fluxes acclimate more strongly to elevated growth temperatures than to elevated CO_2 concentrations in a northern conifer. *Glob. Chang. Biol.* 22, 2913–2928. doi: 10.1111/gcb.13215

Leon-Sanchez, L., Nicolas, E., Nortes, P. A., Maestre, F. T., and Querejeta, J. I., et al. (2016). Photosynthesis and growth reduction with warming are driven by nonstomatal limitations in a Mediterranean semi-arid shrub. *Ecol. Evol.* 6, 2725–2738. doi: 10.1002/ece3.2074

Li, Y., Zhang, Y., Zhang, X., Korpelainen, H., Berninger, F., and Li, C. (2013). Effects of elevated CO_2 and temperature on photosynthesis and leaf traits of an understory dwarf bamboo in subalpine forest zone, China. *Physiol. Plant.* 148, 261–272. doi: 10.1111/j.1399-3054.2012.01705.x

Loveys, B. R., Scheurwater, I., Pons, T. L., Fitter, A. H., and Atkin, O. K. (2002). Growth temperature influences the underlying components of relative growth rate: an investigation using inherently fast- and slow-growing plant species. *Plant Cell Environ.* 25, 975–987. doi: 10.1046/j.1365-3040.2002.00879.x

Maenpaa, M., Riikonen, J., Kontunen-Soppela, S., Rousi, M., and Oksanen, E. (2011). Vertical profiles reveal impact of ozone and temperature on carbon assimilation of *Betula pendula* and *Populus tremula*. *Tree Physiol.* 31, 808–818. doi: 10.1093/treephys/tpr075

Medlyn, B. E., Dreyer, E., Ellsworth, D., Forstreuter, M., Harley, P. C., Kirschbaum, M. U. F. et al. (2002). Temperature response of parameters of a biochemically based model of photosynthesis. II. A review of experimental data. *Plant Cell Environ.* 25, 1167–1179. doi: 10.1046/j.1365-3040.2002.00891.x

Niu, S., Li, Z., Xia, J., Han, Y., Wu, M., and Wan, S. (2008). Climatic warming changes plant photosynthesis and its temperature dependence in a temperate steppe of northern China. *Environ. Exp. Bot.* 63, 91–101. doi: 10.1016/j.envexpbot.2007.10.016

Poorter, H., Niklas, K. J., Reich, P. B., Oleksyn, J., Poot, P., and Mommer, L. (2012). Biomass allocation to leaves, stems and roots: meta-analyses of interspecific variation and environmental control. *New Phytol.* 193, 30–50. doi: 10.1111/j.1469-8137.2011.03952.x

Quentin, A. G., Crous, K. Y., Barton, C. V. M., and Ellsworth, D. S. (2015). Photosynthetic enhancement by elevated CO2 depends on seasonal temperatures for warmed and non-warmed *Eucalyptus globulus* trees. *Tree Physiol.* 35, 1249–1263. doi: 10.1093/treephys/tpv110

Rehmani, M. I. A., Wei, G., Hussain, N., Ding, C., Li, G., Liu, Z., et al. (2014). Yield and quality responses of two indica rice hybrids to post-anthesis asymmetric day and night open-field warming in lower reaches of Yangtze River delta. *Field Crops Res.* 156, 231–241. doi: 10.1016/j.fcr.2013.09.019

Reich, P. B., Oleksyn, J., and Wright, I. J. (2009). Leaf phosphorus influences the photosynthesis-nitrogen relation: a cross-biome analysis of 314 species. *Oecologia* 160, 207–212. doi: 10.1007/s00442-009-1291-3

Rodrigues, W. P., Martins, M. Q., and Fortunato, A. S. (2016). Long-term elevated air CO_2 strengthens photosynthetic functioning and mitigates the impact of supra-optimal temperatures in tropical Coffea arabica and *C. canephora* species. *Global Change Biol.* 22, 415–431. doi: 10.1111/gcb.13088

Rosenberg, M. S. (2005). The file-drawer problem revisited: a general weighted method for calculating fail-safe numbers in meta-analysis. *Evolution* 59, 464–486. doi: 10.1111/j.0014-3820.2005.tb01004.x

Rosenthal, R. (1979). The "file drawer problem" and tolerance for null results. *Psychol. Bull.* 86, 638–641. doi: 10.1037/0033-2909.86.3.638

Ruiz-Vera, U., Siebers, M., Matthew, H., and Drag, D. W. (2015). Canopy warming caused photosynthetic acclimation and reduced seed yield in maize grown at ambient and elevated CO_2. *Glob. Chang. Biol.* 21, 4237–4249. doi: 10.1111/gcb.13013

Rustad, L., Campbell, J., Marion, G., Norby, R., Mitchell, M., Hartley, A., et al. (2001). A meta-analysis of the response of soil respiration, net nitrogen mineralization, and aboveground plant growth to experimental ecosystem warming. *Oecologia* 126, 543–562. doi: 10.1007/s004420000544

Rustad, L. E. (2008). The response of terrestrial ecosystems to global climate change: towards an integrated approach. *Sci. Total Environ.* 404, 222–235. doi: 10.1016/j.scitotenv.2008.04.050

Sage, R. F., and Kubien, D. S. (2007). The temperature response of C_3 and C_4 photosynthesis. *Plant Cell Environ.* 30, 1086–1106. doi: 10.1111/j.1365-3040.2007.01682.x

Schimel, D. S. (1995). Terrestrial ecosystems and the carbon-cycle. *Glob. Chang. Biol.* 1, 77–91. doi: 10.1111/j.1365-2486.1995.tb00008.x

Shen, H., Klein, J. A., Zhao, X., and Tang, Y. (2009). Leaf photosynthesis and simulated carbon budget of Gentiana straminea from a decade-long warming experiment. *J. Plant Ecol.* 2, 207–216. doi: 10.1093/jpe/rtp025

Smith, N. G., and Dukes, J. S. (2017). Short-term acclimation to warmer temperatures accelerates leaf carbon exchange processes across plant types. *Glob. Chang. Biol.* 23, 4840–4853. doi: 10.1111/gcb.13735

Song, B., Niu, S., and Wan, S. (2016). Precipitation regulates plant gas exchange and its long-term response to climate change in a temperate grassland. *J. Plant Ecol.* 9, 531–541. doi: 10.1093/jpe/rtw010

Song, X., Wang, Y., and Lv, X. (2016). Responses of plant biomass, photosynthesis and lipid peroxidation to warming and precipitation change in two dominant species (*Stipa grandis* and *Leymus chinensis*) from North China Grasslands. *Ecol. Evol.* 6, 1871–1882. doi: 10.1002/ece3.1982

Tian, Y., Chen, J., Chen, C., Deng, A., Song, Z., Zheng, C., et al. (2012). Warming impacts on winter wheat phenophase and grain yield under field conditions in Yangtze Delta Plain, China. *Field Crops Res.* 134, 193–199. doi: 10.1016/j.fcr.2012.05.013

Tilman, D. (1989). "Ecological experimentation: strengths and conceptual problems," in *Long-Term Studies in Ecology,* ed G. E. Likens (New York, NY: Springer), 136–157. doi: 10.1007/978-1-4615-7358-6_6

Tjoelker, M. G., and Zhou, X. (2007). The many faces of climate warming. *New Phytol.* 176, 739–742. doi: 10.1111/j.1469-8137.2007.02279.x

Tjoelker, M. G., Oleksyn, J., Lorenc-Plucinska, G., and Reich, P. B. (2009). Acclimation of respiratory temperature responses in northern and southern populations of *Pinus banksiana*. *New Phytol.* 181, 218–229. doi: 10.1111/j.1469-8137.2008.02624.x

Valencia, E., Quero, J. L., and Maestre, F. T. (2016). Functional leaf and size traits determine the photosynthetic response of 10 dryland species to warming. *J. Plant Ecol.* 9, 773–783. doi: 10.1093/jpe/rtv081

Wahid, A., Gelani, S., Ashraf, M., and Foolad, M. R. (2007). Heat tolerance in plants: an overview. *Environ. Exp. Bot.* 61, 199–223. doi: 10.1016/j.envexpbot.2007.05.011

Walters, M. B., and Reich, P. B. (1989). Response of Ulmus americana seedlings to varying nitrogen and water status. 1 Photosynthesis and growth. *Tree Physiol.* 5, 159–172. doi: 10.1093/treephys/5.2.159

Wan, S., Xia, J., Liu, W., and Niu, S. (2009). Photosynthetic overcompensation under nocturnal warming enhances grassland carbon sequestration. *Ecology* 90, 2700–2710. doi: 10.1890/08-2026.1

Wang, D., Barua, D., Joshi, P., LaCroix, J., Hamilton, E. W., and Heckathorn, S. A. (2008). Effects of elevated CO_2 on the tolerance of photosynthesis to acute heat stress in 11 (C3, C4, and CAM) species. *Am. J. Bot.* 95, 1–13. doi: 10.3732/ajb.95.2.165

Wang, D., Heckathorn, S. A., Wang, X., and Philpott, S. M. (2012). A meta-analysis of plant physiological and growth responses to temperature and elevated CO_2. *Oecologia* 169, 1–13. doi: 10.1007/s00442-011-2172-0

Wang, D., Ling, T., Wang, P., Jing, P., Fan, J., Wang, H., et al. (2018). Effects of 8-year nitrogen and phosphorus treatments on the ecophysiological traits of two key species on Tibetan Plateau. *Front. Plant Sci.* 9:1290. doi: 10.3389/fpls.2018.01290

Warren, J. M., Norby, R. J., and Wullschleger, S. D. (2011). Elevated CO_2 enhances leaf senescence during extreme drought in a temperate forest. *Tree Physiol.* 31, 117–130. doi: 10.1093/treephys/tpr002

Way, D. A., and Oren, R. (2010). Differential responses to changes in growth temperature between trees from different functional groups and biomes: a review and synthesis of data. *Tree Physiol.* 30, 669–688. doi: 10.1093/treephys/tpq015

Wright, I. J., Reich, P. B., Cornelissen, J. H. C., Falster, D. S., Groom, P. K., Hikosaka, K., et al. (2005). Modulation of leaf economic traits and trait relationships by climate. *Glob. Ecol. Biogeogr.* 14, 411–421. doi: 10.1111/j.1466-822x.2005.00172.x

Xiong, F. S., Mueller, E. C., and Day, T. A. (2000). Photosynthetic and respiratory acclimation and growth response of Antarctic vascular plants to contrasting temperature regimes. *Am. J. Bot.* 87, 700–710. doi: 10.2307/2656856

Xu, X., Peng, G., Wu, C., and Han, Q. (2010). Global warming induces female cuttings of *Populus cathayana* to allocate more biomass, C and N to aboveground organs than do male cuttings. *Aust. J. Bot.* 58, 519–526. doi: 10.1071/BT10108

Xu, X., Yang, F., Xiao, X. W., Zhang, S., Korpelainen, H., and Li, C. (2008). Sex-specific responses of *Populus cathayana* to drought and elevated temperatures. *Plant Cell Environ.* 31, 850–860. doi: 10.1111/j.1365-3040.2008.01799.x

Zhou, X., Liu, X., Wallace, L. L., and Luo, Y. (2007). Photosynthetic and respiratory acclimation to experimental warming for four species in a tallgrass prairie ecosystem. *J. Integr. Plant Biol.* 49, 270–281. doi: 10.1111/j.1744-7909.2007.00374.x

Ziska, L. H., and Bunce, J. A. (1998). The influence of increasing growth temperature and CO_2 concentration on the ratio of respiration to photosynthesis in soybean seedlings. *Glob. Chang. Biol.* 4, 637–643. doi: 10.1046/j.1365-2486.1998.00179.x

Conflict of Interest Statement: The authors declare that the research was conducted in the absence of any commercial or financial relationships that could be construed as a potential conflict of interest.

frontiers in Plant Science

METHODS
published: 25 October 2019
doi: 10.3389/fpls.2019.01276

Measuring Rapid *A–Ci* Curves in Boreal Conifers: Black Spruce and Balsam Fir

Carole Coursolle[1], Guillaume Otis Prud'homme[1,2], Manuel Lamothe[1] and Nathalie Isabel[1]*

[1] Laurentian Forestry Centre, Canadian Forest Service, Natural Resources Canada, Québec City, QC, Canada, [2] Ministère des Forêts, de la Faune et des Parcs, Direction de la recherche forestière, Québec, QC, Canada

Climate change is steering tree breeding programs towards the development of families and genotypes that will be adapted and more resilient to changing environments. Making genotype–phenotype–environment connections is central to these predictions and it requires the evaluation of functional traits such as photosynthetic rates that can be linked to environmental variables. However, the ability to rapidly measure photosynthetic parameters has always been limiting. The estimation of $V_{c,max}$ and J_{max} using CO_2 response curves has traditionally been time consuming, taking anywhere from 30 min to more than an hour, thereby drastically limiting the number of trees that can be assessed per day. Technological advancements have led to the development of a new generation of portable photosynthesis measurement systems offering greater chamber environmental control and automated sampling and, as a result, the proposal of a new, faster, method (RACiR) for measuring $V_{c,max}$ and J_{max}. This method was developed using poplar trees and involves measuring photosynthetic responses to CO_2 over a range of CO_2 concentrations changing at a constant rate. The goal of the present study was to adapt the RACiR method for use on conifers whose measurement usually requires much larger leaf chambers. We demonstrate that the RACiR method can be used to estimate $V_{c,max}$ and J_{max} in conifers and provide recommendations to enhance the method. The use our method in conifers will substantially reduce measurement time, thus greatly improving genotype evaluation and selection capabilities based on photosynthetic traits. This study led to the developpement of an R package (RapidACi, https://github.com/ManuelLamothe/RapidACi) that facilitates the correction of multiple RACiR files and the post-measurement correction of leaf areas.

Keywords: rapid *A–C*$_i$ curves, boreal conifers, LI-6800, phenotyping, photosynthesis, V_{cmax}, J_{max}, phenomics

OPEN ACCESS

Edited by:
Alvaro Sanz-Saez, Auburn University, United States

Reviewed by:
Joseph Ronald Stinziano, University of New Mexico, United States
Amanda Cavanagh, University of Illinois at Urbana-Champaign, United States

****Correspondence:***
Carole Coursolle
Carole.Coursolle@Canada.ca

Specialty section:
This article was submitted to Plant Abiotic Stress, a section of the journal Frontiers in Plant Science

Received: *18 April 2019*
Accepted: *12 September 2019*
Published: *25 October 2019*

Citation:
Coursolle C, Otis Prud'homme G, Lamothe M and Isabel N (2019) Measuring Rapid A–Ci Curves in Boreal Conifers: Black Spruce and Balsam Fir. Front. Plant Sci. 10:1276. doi: 10.3389/fpls.2019.01276

INTRODUCTION

Climate change is steering tree breeding programs towards the development of families and genotypes that will be adapted and more resilient to the warming climate and thereby ensure the health and productivity of forests (Aitken and Bemmels, 2015). Despite the advances in genomics, the prediction of tree responses to future climate remains challenging because of the difficulty in measuring phenotypes related to adaptation. Making genotype–phenotype–environment connections is central to these predictions but the list of traits reflecting tree adaptation to environment that could be efficiently assessed is limited. Indeed, measuring ecophysiological traits can be laborious and time consuming, thus limiting the ability to establish relationships between

genotypes and plant response to environmental conditions. Rapid, large-scale screening, or plant phenomics (Furbank and Tester, 2011; Stinziano et al., 2017), are required to overcome these constraints.

Developing indicators for photosynthetic performance are of particular interest when trying to select genotypes that will be adapted to future climates. $V_{c,max}$, the maximum rate of ribulose-1,5-bisphosphate carboxylation (Rubisco) and J_{max}, the maximum rate of electron transport, are two such parameters (Long and Bernacchi, 2003). These two parameters are also incorporated into Earth System Models (Rogers, 2014) and can be used as "ground truthing" parameters for the development of phenotyping and forest health monitoring platforms using unmanned aerial vehicles (UAVs) and other types of mobile systems in combination with spectral measurements (Dash et al., 2017, Thompson et al., 2018), which is another incentive for the development of a method to obtain reliable estimates rapidly. Estimates of $V_{c,max}$ and J_{max} are obtained through the measurement and modelling of photosynthetic response to CO_2 concentration (A–C_i curves), which until recently could take anywhere from 30 min to more than 60 min per curve (depending on the number of CO_2 concentrations measured and the system used), thereby greatly limiting the number of measurements that can be made daily.

Recent technological advances have resulted in the development of a new generation of portable photosynthesis measurement systems. With better chamber environmental controls, automation, logging capabilities and computing power, they now permit much greater sampling densities as well as the possibility of accelerating measurement times. Stinziano et al. (2017) have proposed a new method (RACiR) for measuring A–C_i curves. By continuously increasing or decreasing the chamber CO_2 concentration (ramping), they were able to take less than 5 min for each curve. However, this method was developed using poplar leaves (*Populus deltoids* Barr.) and a small chamber (6 cm^2 leaf aperture), which is not really suitable for measuring most conifers where a much larger chamber (36 cm^2 leaf aperture in our case) is usually used. The larger leaf chamber volume causes larger differences in response times between the reference and sample chambers due to greater dilution. This, combined with their unique leaf physiology and geometry, requires that the RACiR method be tested on conifers. The objective of the present study was to develop and test the RACiR method on two boreal conifers, balsam fir (*Abies balsamea* (L.) Mill.) and black spruce (*Picea mariana* (Mill.) Britton), growing in a common garden experiment set up to test the effects of heating the seedling growth environment, using a larger chamber.

MATERIALS AND METHODS

Plant Material and Growth Conditions

The study was conducted using 5-year-old black spruce and balsam fir trees planted in a common garden experiment at the Valcartier experimental station in St-Gabriel-de-Valcartier, Québec (N 46°56′59.93″/W 71°29′53.88″). Bare-root seedlings were planted in triangular plots in May and June 2015. Starting in 2016, half the plots were heated from May to October of each year using 1000 W infrared lamps between May and October to produce a growing temperature 2 °C above ambient temperatures. A branch with at least 3 years of growth (2018, 2017, 2016) was sampled from seven different black spruce (BS) and seven different balsam fir (BF) trees, four growing in heated plots and three growing in unheated control plots. Branches were cut, placed in water, recut and inserted into floral water tubes while still underwater to avoid cavitation. Water levels in the floral tubes were monitored throughout the measuring period and the water was topped up as required using a syringe. All measurements were made on site under normal field conditions.

Gas Exchange Measurements

An LI-6800 portable photosynthesis system (LI-COR Inc., Lincoln, NE, USA) equipped with the Large Leaf and Needle Chamber (36 cm^2) and the large light source was used for all measurements. The dark respiration (Rd) and CO_2 response of photosynthesis (A–C_i) of 1-year-old needles were measured on site on July 16, 18 and 19, 2018. Two different methods were used to measure A–C_i: (1) The traditional method (A–C_i-TRAD), involving net assimilation (A_n) measurements at a predetermined set of CO_2 concentrations (ex. Long and Bernacchi, 2003) and (2) The rapid method (RACiR), involving continuous measurements over a programmed ramp of changing CO_2 concentrations (ex. Stinziano et al., 2017). Both a traditional and a RACiR curve were measured on the same set of needles from each shoot. The RACiR curve was measured first followed by the traditional curve. The same environmental conditions were used for both curve types: 1) 22 mmol mol^{-1} of H_2O in the reference cell producing between ~63% and 79% relative humidity (RH) in the leaf chamber, depending on the quantity of leaf surface area in the chamber, and producing a variation of ~2% to 3% in RH over the course of measurements for each shoot; 2) 1200 µmol m^{-2} s^{-1} of light, based on Benomar et al. (2017) and Sendall et al., 2015); 3) chamber air temperature of 25 °C; 4) flow rate of 600 µmol s^{-1}; and 5) fan speed of 13,000 rpm.

Rapid A–C_i Response Curves

The method used for the RACiR curves was adapted from the one developed by Stinziano et al. (2017) for *P. deltoides* Barr. leaves using the LI-6800 Portable Photosynthesis System and the Multiflash Fluorometer and Chamber (LI-COR Inc., Lincoln, NE, USA). Shoots were placed in the Large Leaf and Needle Chamber at 420 ppm CO_2 concentration ($[CO_2]$) and allowed to acclimate for ~5 min. The LI-6800's Autocontrol function was used to program a "down" ramp from 420 to 20 ppm at a rate of 200 ppm min^{-1} CO_2 and was immediately followed, approx. 10 to 15 s later, by an "up" ramp from 20 to 1,520 ppm at a rate of 100 ppm min^{-1}. The LI6800's Autolog feature was used to record measurements every 2 s. The reference and sample infrared gas analyzers (IRGAs) were matched before the start of each curve. Only the portion of

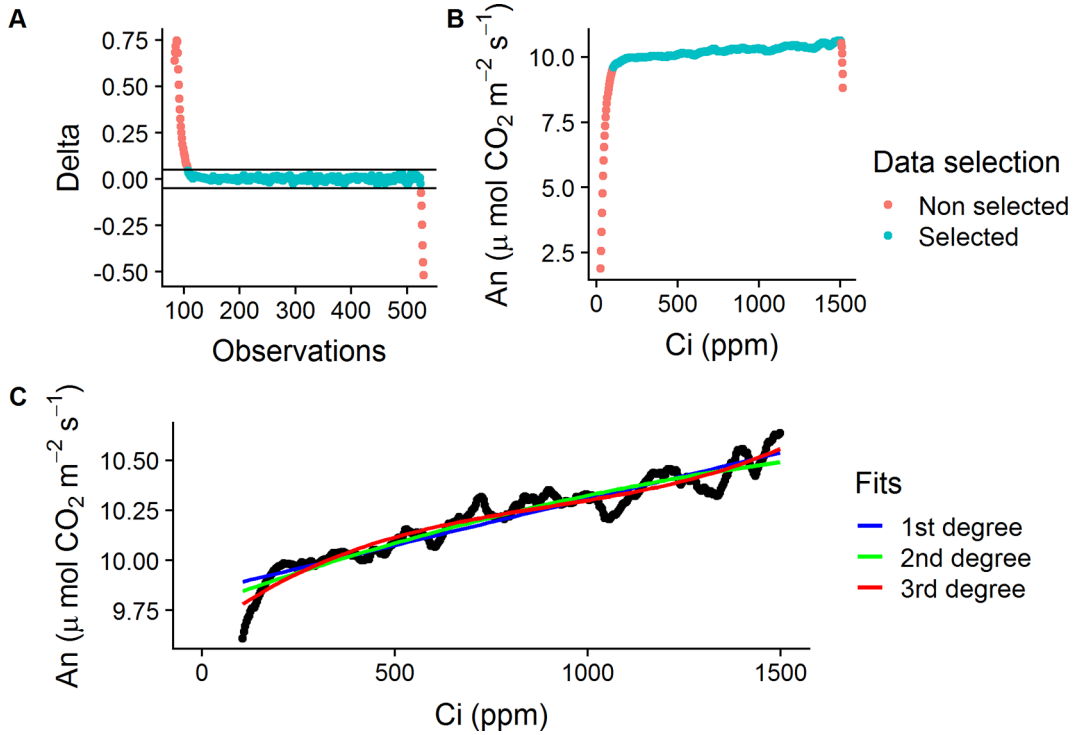

FIGURE 1 | Data selection process for the empty chamber (ECRC) and RACiR response curves. **(A)** Calculated delta values (± 0.05, An_i _ An_{i-1}) for a selected ECRC, red symbols indicate outliers, blue symbols indicate selected points. **(B)** A_n vs C_i for a selected ECRC curve, red symbols indicate non-steady state observations, blue symbols indicate selected points. **(C)** First, second and third degree polynomials fitted to a selected ECRC for correction of raw RACiR data.

data collected from the "up" ramps (20 to 1,520 ppm) were used to establish the CO_2 response curves. The raw data from these "up ramps" was filtered automatically using a delta threshold value (± 0.05, An_i _ An_{i-1}) to keep only the quasi-linear portion of the data, where the chamber mixing is at steady-state, and to also remove outliers (ex: **Figures 1A**, **B**).

The raw data obtained from the RACiR curve measurements must be corrected to account for measurement lags between the reference and sample [CO_2] (**Supplementary Figure 1**) caused by the mixing volume of the chamber, match offsets and system residual time delays (Stinziano et al., 2017). Data collected from the quasi-linear portion of a RACiR curve measured with the chamber empty (ECRC) was used for this correction. Following Stinziano et al. (2017) and Stinziano et al. (2018), we fitted 1st, 2nd and 3rd degree polynomials (**Figure 1C**) to this data and the best fitting model according to the Bayesian information criterion (BIC) was used to correct the quasi-linear portion of the RACiR curve measurements. The script used to make the corrections is available on Github (https://github.com/ManuelLamothe/RapidACi) it can be used to automatically correct multiple files at a time and to carry out post-measurement corrections to leaf area, which are required when measuring non-flat leaves. An example of the analysis can be found in the **Supplementary Material (Supplementary Data Sheet 1)**. ECRCs were carried out at the beginning, middle and end of each day using the same environmental conditions as for the actual measurements. Three sets of corrected response curve data, one for each empty chamber, were generated for each measured shoot. Each set of response curve data was corrected using empty chamber data obtained the same day.

Traditional A–C_i Response Curves

The LI-6800 CO_2 response program was used for the *A*–C_i–TRAD curves and the reference CO_2 concentrations were set to 420, 40, 20, 40, 60, 80, 100, 150, 200, 300, 420, 500, 700, 900, 1,100, 1,300, and 1,500 ppm. Minimum and maximum wait times were set at 60 to 120 s based on the stability of the CO_2 net assimilation rate and the difference between sample and reference CO_2 concentrations. The reference and sample infrared gas analyzers (IRGAs) were matched before the measurement at each concentration. The measured shoot was allowed to acclimate at 420 ppm for ~5 min. The *A*–C_i–TRAD curve was measured on the same needles immediately following the end of the RACiR curve.

Dark Respiration (R_{d_Meas}) Measurements

Shoots were removed from the chamber immediately following the *A*–C_i–TRAD measurement and dark adapted for at least 30 min by covering the measured shoot with aluminum foil. Shoots were then placed in the darkened LI6800 chamber and allowed to acclimate at 420 ppm [CO_2], 25 °C and 22 mmol mol^{-1} of H_2O in the reference before recording R_{d_meas}.

Parameter Estimation and Statistical Analysis

Timing of Empty Chamber Response Curve (ECRC)

Corrected CO_2 response curve data were fitted with the FvCB model using the fitaci function from the Plantecophys R Package (Duursma, 2015) with the default settings and R_{d_meas} as an input. $V_{c,max}$, J_{max}, and root mean square error (RMSE) were obtained for the three corrected curves (one for each ECRC) from each measured shoot. An analysis of variance on the effect of the timing of the empty chamber measurement series used to correct the RACiR curves was conducted using the nlme R Package (Pinheiro et al., 2018) for mixed models. The analysis was carried out on daily means of $V_{c,max}$, J_{max}, and RMSE, measurement day was considered a random effect and empty chamber timing (morning, mid-day and afternoon) was considered a fixed effect.

Comparison of Traditional and Rapid CO_2 Response Curve Parameters

$V_{c,max}$ and J_{max} were generated for the A–C_i–TRAD and RACiR curves by fitting the FvCB model using the Plantecophys R package (Duursma, 2015) with the default settings of the fitaci function and R_{d_meas} as an input. A third set of parameters was generated using the portion of the measured RACiR curve between 200 and 800 ppm of intercellular CO_2 concentration (C_i) (RACiR–Partial). An analysis of variance for repeated measures on the effect of the curve type was conducted using the nlme R Package (Pinheiro et al., 2018). Curve type was the repeated factor, tree was considered as a random effect and species, curve type and their interaction were considered fixed effects. The heating effect (main and interactions with curve type) was included as a fixed effect in the original ANOVA model but found to be non-significant ($V_{c,max}$: F = 0.6604, p = 0.4334 for the main effect and F = 2.4311, p = 0.1135 for the interaction; J_{max}: F = 1.2578, p = 0.2883 for the main effect and F = 1.7539, p = .1987 for the interaction) so it was removed from the final model.

Dark respiration estimates were also obtained using the Plantecophys R package (Duursma, 2015), with its default settings for each curve type, so as to provide additional information on the performance of the three curve fitting methods. An analysis of variance on the effect of the method used to estimate dark respiration, measured (R_{d_meas}) or estimated using A–C_i–TRAD (R_{d_aci}), RACiR (R_{d_racir}) and RACiR–Partial (R_{d_part}), was conducted using the same parameters as for $V_{c,max}$ and J_{max}. Again, the heating effect (main and interactions with measurement type) was included as a fixed effect in the original ANOVA model but found to be non-significant (F = 1.1313, p = 0.3125 for the main effect and F = 0.0782, p = 0.9713 for the interaction) so it was removed from the final model.

RESULTS

Timing of Empty Chamber Response Curve Measurements (ECRC)

Three ECRCs were generated per day in an attempt to determine how often an empty chamber response curve needed to be generated to correct the raw RACiR curve measurements. The analyses of variance indicated that the timing of the generation of the ECRC had no significant effect on $V_{c,max}$ (F = 0.7588, p = 0.5256) generated using the F_vCB model. However, ECRC timing had a significant effect on J_{max} (F = 7.8493, p = 0.0412), values generated using the morning ECRC being significantly higher ($p < 0.05$) than those generated using the mid-day ECRC (**Table 1**). Finally, RMSE of the fitted F_vCB models were not significantly affected by the timing of the ECRC (F = 1.25961, p = 0.3765, **Table 1**). **Figure 2** illustrates the correction effect on the net assimilation rates for a selected balsam fir and black spruce tree. The differences appear to be minimal. The mid-day empty chamber response curve was chosen to correct the RACiR curves for the comparison

TABLE 1 | LSmeans of $V_{c,max}$, J_{max} and RMSE generated using morning, mid-day and late afternoon empty chamber corrections are shown.

ECRC	$V_{c,max}$ (μmol m^{-2} s^{-1})		J_{max} (μmol m^{-2} s^{-1})		RMSE	
	Mean	SE	Mean	SE	Mean	SE
Morning	71.1841^{a}	4.5118	127.2851^{a}	5.9813	10.4003^{a}	1.4394
Mid-day	64.1333^{a}	4.5118	119.8836^{b}	5.9813	9.8551^{a}	1.4394
Late Afternoon	70.6677^{a}	4.5118	121.2287^{a,b}	5.9813	10.7410^{a}	1.4394

Means followed by the same letter are not significantly different ($p < 0.05$) for the variable in question.

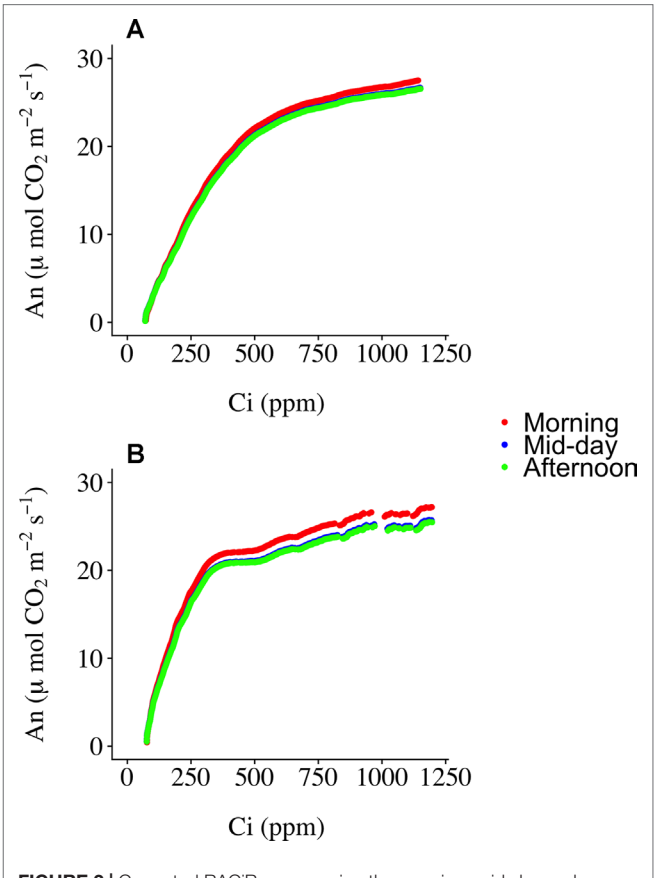

FIGURE 2 | Corrected RACiR curves using the morning, mid-day and afternoon empty chamber response curves (ECRC) for a selected balsam fir **(A)** and black spruce **(B)** shoot.

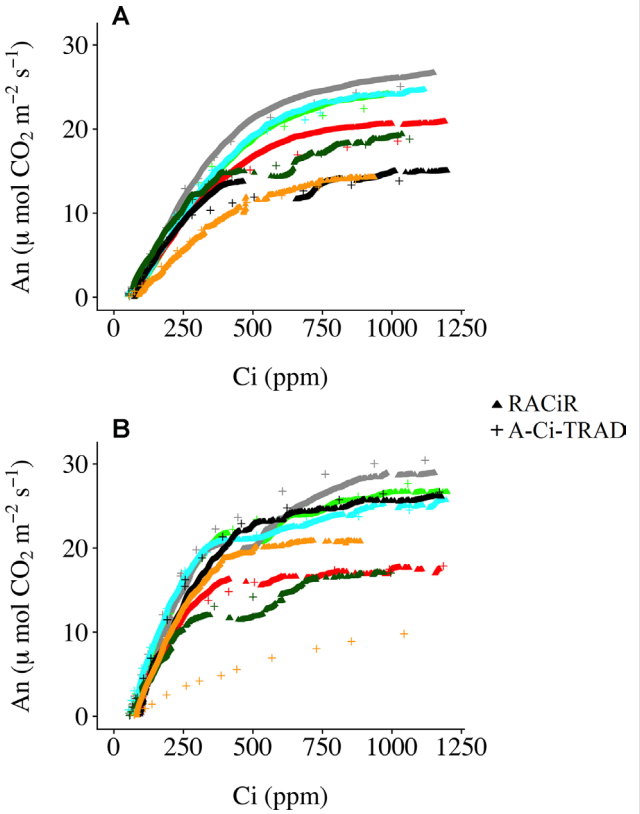

FIGURE 3 | Traditional (*A–C*$_i$–TRAD) and rapid (RACiR) CO_2 response curves for the seven balsam fir **(A)** and seven black spruce **(B)** shoots measured.

between traditional and rapid response curves since it was the measurement that was the closest in timing to the largest number of RACiR curves. Furthermore, the J_{max} generated by the morning empty chamber was the only parameter that was significantly different from the mid-day and afternoon empty chamber curves.

Comparison of Traditional and Rapid CO_2 Response Curves and Parameters

Figure 3 presents *A–C*$_i$–TRAD and corrected RACiR curves for the balsam fir (a) and black spruce (b) shoots measured. Generally, there is good agreement between the two types of curve when C_i is below 500 ppm and where $d\text{An}/dC_i$ is high. However, there is greater variability and deviation between the two types of curves at higher C_i concentrations. Also, small drops in net assimilation within the approximate range of 450–600 ppm C_i can be seen for the RACiR curves of some trees. These data points were considered erroneous and removed before fitting the FvCB model. **Figure 4** presents the fitted FvCB model using *A–C*$_i$–TRAD (a, d), RACiR (b, e) and RACiR–Partial (c, f) data for a selected balsam fir (a, b, c) and black spruce (d, e, f) shoot. RMSEs of the fitted FvCB models ranged from 2.224 to 13.746 for the *A–C*$_i$–TRAD curves, from 3.834 to 21.787 for the RACiR curves and from 3.243 to 15.065 for the RACiR–Partial curves.

An ANOVA conducted for the response curve parameters ($V_{c,max}$, J_{max}) and RMSE of the fitted models indicated that the response curve type did not significantly affect either $V_{c,max}$ or J_{max}, but the RMSE of the models were significantly different (**Tables 2**, **3**). The RMSEs of the fitted RACiR and RACiR–Partial curves were significantly but only slightly to moderately higher than the RMSE of the fitted *A–C*$_i$–TRAD curve.

The statistical analyses indicate that dark respiration was significantly affected (F = 5.4684, p = 0.0033) by the estimation method used. The *A–C*$_i$–TRAD curve yielded the lowest dark respiration (R_{d_aci}) value while R_{d_meas} was the highest. R_{d_aci} was the only dark respiration measurement that was significantly different from R_{d_meas} (**Table 4**). R_{d_part} was quite similar to R_{d_aci} while R_{d_racir} was closer to R_{d_meas}.

DISCUSSION

LI-6800 Configuration Considerations for Conifer Needle Measurements

Compared to previously published studies describing the RACiR method applied to flat leaves (Stinziano et al., 2017; Pilon et al., 2018), the needle-leaf geometry of conifer species requires a different instrument configuration for photosynthesis measurements. A much larger leaf chamber (193.7 cm^3, large needle and leaf chamber, vs 87.3 cm^3 for the fluorometer chamber, in our case) is generally used, thereby leading to a greater "lag time" required for the differences between the sample and reference [CO_2] to stabilize compared to the smaller chambers. We noted "lag times" of between 48 and 92 s. (Mean = 63.4, SE = 4.0) compared to the 20–30 s reported by Stinziano et al., 2017 for poplar leaves. The larger lag times caused by the larger cuvette mean that a greater number of potential data points at the start of the ramp (low *Ci* concentrations in our case) are lost, so preliminary tests should always be carried out to adequately identify the starting CO_2 concentration for the ramp. The same should apply for the identification of the ramp end point.

Preliminary tests using a controlled target leaf VPD revealed the existence of periodic noise in the empty chamber measurements caused by adjustments in the H_2O control loop and the large chamber volume (Pers. Comm: D. Lynch, LI-COR Inc., Lincoln, NE, USA). This led at times to unrealistic, negative C_i values and was remedied by controlling the H_2O content of the air in the reference cell instead. Preliminary tests allowed us to choose a target concentration (22 mmol mol^{-1}) which produced RHs between ~63 and 79% in the leaf chamber, thereby assuring that shoot samples were not stressed. This also produced stomatal conductances that were high enough to minimize noise in the H_2O analyzer, which minimized noise in the calculated C_i values (Pers. Comm: D. Lynch, LI-COR Inc., Lincoln, NE, USA).

Timing of Empty Chamber Response Curve Measurements (ECRC)

Determining the best moment to conduct the ECRC so as to keep the number of required ECRCs to a minimum is an important factor given that one of the main reasons for using the RACiR method is reducing the overall measurement time

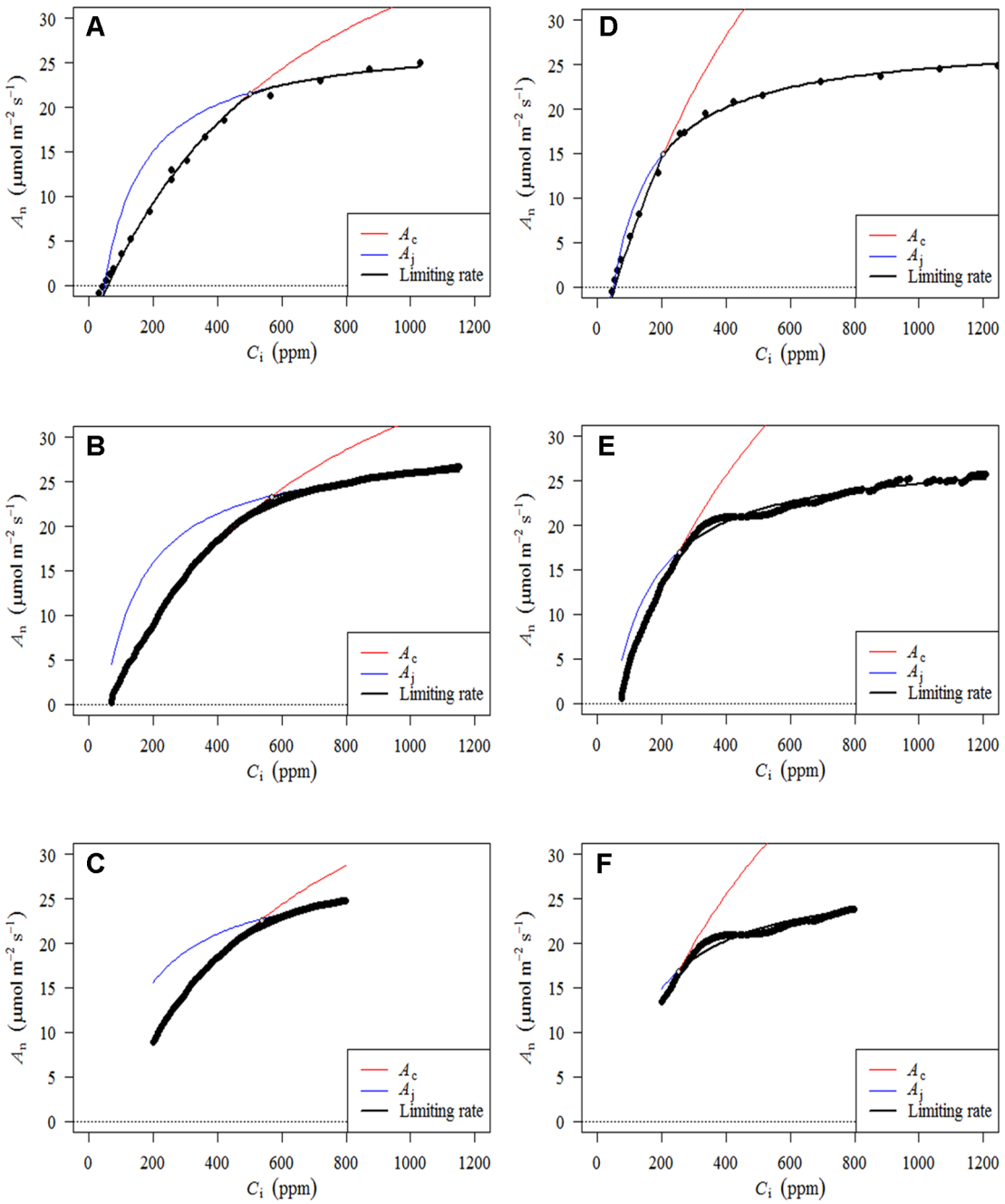

FIGURE 4 | Fitted FvCB models using *A–Ci*–TRAD **(A**, **D)**, RACiR **(B**, **E)** and RACiR–Partial **(C**, **F)** data for a selected Balsam fir **(A**, **B**, **C)** and black spruce **(D**, **E**, **F)** shoot. The graphs were generated by the fitaci function of the Plantecophys R package (Duursma, 2015) using the default settings and R_{d_meas} as an input.

TABLE 2 | Results of the ANOVA for the comparison of $V_{c,max}$, J_{max} and RMSE generated by the FvCB model using the three different response curve methods.

Fixed Effect	Num. DF	Den. DF	$V_{c,max}$		J_{max}		RMSE	
			F	p	F	p	F	p
Species	1	23	6.640	0.0242	1.763	0.2090	4.162	0.0640
Curve Type (CT)	2	23	0.006	0.9940	1.604	0.2220	28.084	<0.0001
Species*CT	2	23	0.051	0.9501	0.004	0.9961	0.081	0.9227

Num. DF, numerator degrees of freedom; Den. DF, denominator degrees of freedom.

TABLE 3 | LSmeans for $V_{c,max}$, J_{max} and RMSE generated by the 3 different types of curves.

Curve type	$V_{c,max}$ (μmol m^{-2} s^{-1})		J_{max} (μmol m^{-2} s^{-1})		RMSE	
	Mean	SE	Mean	SE	Mean	SE
A–Ci–TRAD	62.09[a]	1.09	112.60[a]	8.34	3.73[a]	1.14
RACiR	62.02[a]	1.09	119.59[a]	8.34	8.59[b]	1.14
RACiR–Partial	61.59[a]	1.09	118.42[a]	8.34	6.10[c]	1.14

Means followed by the same letter are not significantly different ($p < 0.05$) for the variable in question.

TABLE 4 | LSmeans for measured dark respiration (R_{d_meas}) and dark respiration estimated from the *A–Ci*–TRAD (R_{d_aci}), RACiR (R_{d_racir}) and RACiR–Partial (R_{d_part}) response curves.

	Dark Respiration	
Measurement Type	Mean (μmol m^{-2} s^{-1})	SE
Measured	2.19[a]	0.40
A–Ci–TRAD	0.52[b]	0.40
RACiR	1.85[a,b]	0.40
RACiR–Partial	0.78[a,b]	0.40

Means followed by the same letter are not significantly different ($p < 0.05$).

for producing photosynthetic parameters that can be used for phenotyping and health/stress monitoring. Three ECRCs were measured daily, one in the morning before the first shoot measurement, one around mid-day and one in the late afternoon after the last shoot measurement of the day. The J_{max} generated by the morning ECRC was the only parameter that was significantly different among the ECRCs (**Table 1**) and the A_n vs C_i relationships obtained from the three different corrected RACiR curves were quite similar (**Figure 2**). The significantly higher J_{max} generated by the morning ECRC may have resulted from the fact that we matched the reference and sample IRGAs before measuring each RACiR curve. In a letter published after the conclusion of our study, Stinziano et al., 2018 recommend using the same match for the ECRC and RACiR curves. In fact, we noticed that the largest match adjustments tended to occur towards the beginning of the day and would stabilize thereafter, which most likely explains the lack of significant differences between the RACiR parameters calculated using the mid-day and late afternoon ECRCs. Given our results, we feel that it is most likely feasible to conduct only one ECRC per measurement run per day as long as matches are checked regularly, remain constant and chamber settings do not change. It would also probably be best to run the LI-6800 at the desired chamber settings for several minutes and conduct more than one match before starting a measurement run.

RACiR Vs Traditional CO_2 Response Curves

Figure 3 presents the corrected "raw" response curve data generated by the RACiR and *A–Ci*–TRAD methods for the seven balsam fir a) and seven black spruce b) shoots. With the exception of one black spruce shoot, there is generally good agreement when dA_n/dC_i is high (at C_i values below ~500 ppm), the area related to Rubisco activity ($V_{c,max}$), but there is more variability at higher C_i values related to RuBP regeneration (J_{max}; Long and Bernacchi, 2003). These results are generally similar to those reported by Stinziano et al. (2017) and Taylor and Long (2018), using an LI-6800, and to Bunce, 2018, using a CIRAS-3. We believe that the divergence between the two response curve types for one of the black spruce shoots may be linked to a problem with the *A–Ci*–TRAD measurement and not the RACiR method, given the unusual form of the *A–Ci*–TRAD curve compared to the others. Contrary to Taylor and Long (2018), we did not observe significant offsets for CO_2 compensation points. CO_2 compensation points calculated using RACiR data were generally higher (62.5 without R_{d_meas} and 70.6 using $R_{d\_meas)}$ compared to *A–Ci*–TRAD (51.1 without R_{d_meas} and 68.1 using R_{d_meas}) data but not significantly different ($p = 0.06$ without R_{d_meas} and 0.39 using R_{d_meas}). This would seem to confirm the assertion by Stinziano et al. (2018) that ramp rates above 100 ppm min^{-1} can be problematic. Using measured values for dark respiration seems to reduce offsets.

Our results (**Table 4**) indicate that the dark respiration (R_d) estimated by the FvCB model using the RACiR method (1.85 μmol m^{-2} s^{-1}) was the closest estimate to, and not significantly different from, R_{d_meas} (2.19 μmol m^{-2} s^{-1}). Furthermore, although considerably lower, R_d estimated using the RACiR–Partial method (0.78 μmol m^{-2} s^{-1}) was not significantly different from R_{d_meas}. The R_d estimated using the *A–Ci*–TRAD method (0.52 μmol m^{-2} s^{-1}) was considerably lower and significantly different from R_{d_meas}. These results indicate that the RACiR method performs very well when used to estimate dark respiration and this better performance may be linked to the much larger number of data points available for the estimate compared to *A–Ci*–TRAD data.

We found that there were no significant differences among the $V_{c,max}$ and J_{max} values generated by the traditional or either of the two rapid response curve methods (**Tables 2** and **3**) when R_{d_meas} was used as an input to the FvCB model. $V_{c,max}$ values ranged from 61.59 to 62.02 μmol m^{-2} s^{-1} (SE = 1.09) and J_{max} values ranged between 112.6 and 119.59 μmol m^{-2} s^{-1} (SE = 8.34). However, a separate ANOVA looking at $V_{c,max}$ and J_{max} generated without using R_{d_meas} as an input revealed that the curve fitting method had a significant effect on the J_{max} generated ($F = 5.3946$, $p = 0.0116$), the RACiR method (Mean = 117.63, SE = 8.7215) producing a significantly greater J_{max} compared to the *A–Ci*–TRAD method (Mean = 103.02, SE = 8.72). This result is not surprising given that the *A–Ci*–TRAD method generated dark respiration estimates that were significantly lower than the measured values. Furthermore, an ANOVA conducted to analyze the effect of using R_{d_meas} vs estimated R_d on the generation of $V_{c,max}$ and J_{max} values by the *A–Ci*–TRAD method revealed that using R_{d_meas} had a significant ($V_{c,max}$: $F = 11.1819$, $p = 0.0074$; J_{max}: $F = 54.7402$, $p < 0.0001$) effect.

These results clearly show that the RACiR method can be used for a larger chamber size required by conifers and that measuring dark respiration so as to provide the most accurate input to the FvCB model improves the estimated J_{max}. Also, we believe that using the RACiR method when R_{d_meas} is not available would produce the best estimates of $V_{c,max}$ and J_{max} given that this method provides an estimate of dark respiration that is much closer to, and not significantly different from, the measured dark respiration when compared to the A–C_i–TRAD method.

Results concerning statistical comparisons involving the values generated by the RACiR–Partial method should be interpreted with caution. We did not generate a complete independent set of CO_2 response curves for this method but, instead, used a subset of the data that were generated by the RACiR curves. This may have led to some autocorrelation among the data, but we believe that the potential of using smaller [CO_2] ranges for CO_2 response curves of conifers should be further investigated, the smaller the required range, the faster the measurement.

CONCLUSIONS AND RECOMMENDATIONS

1) The RACiR method can be used for measuring conifers using large needle and leaf chambers, 193.7 cm^3 in our case. The exact length of the ramp as well as the appropriate chamber environmental conditions need to be identified during pre-tests and may vary depending on the species and size of chamber used.
2) Typically, a traditional A–C_i takes between 30 and 60 min, approx. 30 to 36 min (excluding acclimation time) in our case, depending on the number of points and wait times at each CO_2 concentration. A total maximum time of approximately 22 min was required to measure a full RACiR curve using the method we have developed. However, as shown by our analysis of the partial RACiR curves (between 200 and 800 ppm internal CO_2 concentration), we believe that total measurement time could be reduced by at least 50% by reducing the ramp range. This method could be used to obtain "ground truthed" photosynthetic capacity estimates to validate air-borne spectral measurements and thereby accelerate and facilitate the development of plant stress and phenotyping platforms.
3) As suggested by Stinziano et al. (2018), we believe that carrying out an empty chamber response curve measurement (ECRC) to correct the RACiR measurements should be carried out for each RACiR measurement series, i.e. at least once a day, and not necessarily after each RACiR measurement, and when environmental conditions in the chamber change. Our findings indicate that the timing is less important as long as the match adjustment remains constant for all of the measured curves in the series.
4) Whenever possible, we recommend measuring dark respiration independently so as to produce the best possible estimates of $V_{c,max}$ and J_{max}. This could be achieved by using a second photosynthesis measuring system so as to decrease measurement time.

DATA AVAILABILITY STATEMENT

The datasets generated for this study are available on request to the corresponding author. Also, data from one uncorrected RACiR curve and its corresponding ECRC and ACi-TRAD are provided at https://github.com/GuillaumeOtisPrudhomme/TestFiles for use with the example analyses in Data Sheet 1.

AUTHOR CONTRIBUTIONS

CC, with input from GP, contrived the study and wrote the manuscript. GP produced the figures. GP and CC collected and analyzed the data. ML provided input to the statistical analysis. ML and GP developed the scripts used to correct the RACiR curves with input from CC. GP and NI read and commented on the manuscript.

FUNDING

Funding was provided to NI by the Genomics Research and Development Initiative (GRDI) of the government of Canada.

ACKNOWLEDGMENTS

The authors would like to thank Doug Lynch (LI-COR Inc., Lincoln, NE, USA) for his suggestions concerning RACiR measurement methods and Gilbert Éthier (Faculté des sciences de l'agriculture et de l'alimentation, Université Laval, Québec, QC, Canada) for his suggestions concerning FvCB model fitting.

SUPPLEMENTARY MATERIAL

The Supplementary Material for this article can be found online at: https://www.frontiersin.org/articles/10.3389/fpls.2019.01276/full#supplementary-material

REFERENCES

Aitken, S. N., and Bemmels, J. B. (2015). Time to get moving: assisted gene flow of forest trees. *Evol. Appl.* 9, 271–290. doi: 10.1111/eva.12293

Benomar, L., Lamhamedi, M. S., Oeoin' S. Rainville, A., Lambert, M.-C., Margolis, H. A., Bousquet, J., et al. (2017). Thermal acclimation of photosynthesis and respiration of southern and northern white spruce seed sources tested along a regional climatic gradient indicates limited potential to cope with temperature warming. *Ann. Bot.* 121, 443–457. doi: 10.1093/aob/mcx174

Bunce, J. (2018). Three methods of estimating mesophyll conductance agree regarding its CO_2 sensitivity in the rubisco-limited C_i range. *Plants* 7, 62. doi: 10.3390/plants7030062

Dash, J. P., Watt, M. S., Pearse, G. D., Heaphy, M., and Dungey, H. S. (2017). Assessing very high resolution UAV imagery for monitoring forest health

during a simulated disease outbreak. *ISPRS J. Photogram. Remote Sens.* 131, 1–14. doi: 10.1016/j.isprsjprs.2017.07.007

Duursma, R. (2015). Plantecophys—an R package for analyzing and modelling leaf gas exchange data. *PLoS One*. doi: 10.1371/journal.pone.0143346

Furbank, R. T., and Tester, M. (2011). Phenomics—technologies to relieve the phenotyping bottleneck. *Trends Plant Sci.* 16, 635–644. doi: 10.1016/j.tplants.2011.09.005

Long, S. P., and Bernacchi, C. J. (2003). Gas exchange measurements, what can they tell us about the underlying limitations to photosynthesis? Procedures and sources of error. *J. Exp. Bot.* 54, 2393–2401. doi: 10.1093/jxb/erg262

Pilon, C., Snider, J. L., Sobolev, V., Chastain, D. R., Sorensen, R. B., Meeks, C. D., et al. (2018). Assessing stomatal and non-stomatal limitations to carbon assimilation under progressive drought in peanut (*Arachis hypogaea* L.). *J. Plant Physiol.* 231, 124–134. doi: 10.1016/j.jplph.2018.09.007

Pinheiro, J., Bates, D., DebRoy, S., Sarkar, D., and R Development Core Team. (2018). nlme: Linear and nonlinear mixed effects models. *R package version* 3.1-131. https://CRAN.R-project.org/package=nlme.

Rogers, A. (2014). The use and misuse of $V_{c,max}$ in Earth Systems Models. *Photosynth. Res.* 119, 15–29. doi: 10.1007/s11120-013-9818-1

Sendall, K. M., Reich, P. B., Zhao, C., Jihua, H., Wei, X., Stefanski, A., et al. (2015). Acclimation of photosynthetic temperature optima of temperate and boreal tree species in response to experimental forest warming. *Global Change Biol.* 21, 1342–1357. doi: 10.1111/gcb.12781

Stinziano, J. R., McDermitt, D. K., Lynch, D. J., Saathoff, A. J., Morgan, P. B., and Hanson, D. T. (2018). The rapid A/C_i response: a guide to best practices. *New Phytol.* 221: 625–627. doi: 10.1111/nph.15383

Stinziano, J. R., Morgan, P. B., Lynch, D. J., Saathoff, A. J., McDermitt, D. K., and Hanson, D. T. (2017). The rapid $A–C_i$ response: photosynthesis in the phenomic era. *Plant Cell Environ.* 40, 1256–1262. doi: 10.1111/pce.12911

Taylor, S. H., and Long, S. P. (2018). Phenotyping photosynthesis on the limit—a critical examination of RACiR. *New Phytol.* 221, 621–624. doi: 10.1111/nph.15382

Thompson, A. L., Thorp, K. R., Conley, M., Andrade-Sanchez, P., Heun, J. T., Dyer, J. M., et al. (2018). Deploying a proximal sensing cart to identify drought-adaptive traits in upland cotton for high-throughput phenotyping. *Front. Plant Sci.* 9, 507. doi: 10.3389/fpls.2018.00507

Conflict of Interest: The authors declare that the research was conducted in the absence of any commercial or financial relationships that could be construed as a potential conflict of interest.

frontiers in Plant Science

ORIGINAL RESEARCH
published: 06 December 2019
doi: 10.3389/fpls.2019.01605

De Novo Transcriptome Analysis of Durum Wheat Flag Leaves Provides New Insights Into the Regulatory Response to Elevated CO_2 and High Temperature

Rubén Vicente[1*†], *Anthony M. Bolger*[2], *Rafael Martínez-Carrasco*[1], *Pilar Pérez*[1], *Elena Gutiérrez*[1], *Björn Usadel*[2,3] *and Rosa Morcuende*[1*]

[1] Institute of Natural Resources and Agrobiology of Salamanca (IRNASA), Consejo Superior de Investigaciones Científicas (CSIC), Salamanca, Spain, [2] Institute for Biology 1, RWTH Aachen University, Aachen, Germany, [3] Institute of Bio- and Geosciences, IBG-2: Plant Sciences, Forschungszentrum Jülich, Jülich, Germany

Global warming is becoming a significant problem for food security, particularly in the Mediterranean basin. The use of molecular techniques to study gene-level responses to environmental changes in non-model organisms is increasing and may help to improve the mechanistic understanding of durum wheat response to elevated CO_2 and high temperature. With this purpose, we performed transcriptome RNA sequencing (RNA-Seq) analyses combined with physiological and biochemical studies in the flag leaf of plants grown in field chambers at ear emergence. Enhanced photosynthesis by elevated CO_2 was accompanied by an increase in biomass and starch and fructan content, and a decrease in N compounds, as chlorophyll, soluble proteins, and Rubisco content, in association with a decline of nitrate reductase and initial and total Rubisco activities. While high temperature led to a decline of chlorophyll, Rubisco activity, and protein content, the glucose content increased and starch decreased. Furthermore, elevated CO_2 induced several genes involved in mitochondrial electron transport, a few genes for photosynthesis and fructan synthesis, and most of the genes involved in secondary metabolism and gibberellin and jasmonate metabolism, whereas those related to light harvesting, N assimilation, and other hormone pathways were repressed. High temperature repressed genes for C, energy, N, lipid, secondary, and hormone metabolisms. Under the combined increases in atmospheric CO_2 and temperature, the transcript profile resembled that previously reported for high temperature, although elevated CO_2 partly alleviated the downregulation of primary and secondary metabolism genes. The results suggest that there was a reprogramming of primary and secondary metabolism under the future climatic scenario, leading to coordinated regulation of C-N metabolism towards C-rich metabolites at elevated CO_2 and a shift away from C-rich secondary metabolites at high temperature. Several candidate genes differentially expressed were identified, including protein kinases, receptor kinases, and transcription factors.

Keywords: climate change, elevated CO_2, high temperature, RNA sequencing, transcriptome, durum wheat

OPEN ACCESS

Edited by:
Alvaro Sanz-Saez, Auburn University, United States

Reviewed by:
Johann Martinez, University of California, Davis, United States
Ivan Jauregui, University of Liège, Belgium

****Correspondence:***
Rubén Vicente
vicenteperez.ruben@gmail.com
Rosa Morcuende
rosa.morcuende@irnasa.csic.es

[†]Present address:
Rubén Vicente
Max Planck Institute of Molecular Plant Physiology (MPIMP), Potsdam, Germany

Specialty section:
This article was submitted to Plant Abiotic Stress, a section of the journal Frontiers in Plant Science

Received: *09 September 2019*
Accepted: *14 November 2019*
Published: *06 December 2019*

Citation:
Vicente R, Bolger AM, Martínez-Carrasco R, Pérez P, Gutiérrez E, Usadel B and Morcuende R (2019) De Novo Transcriptome Analysis of Durum Wheat Flag Leaves Provides New Insights Into the Regulatory Response to Elevated CO_2 and High Temperature. Front. Plant Sci. 10:1605. doi: 10.3389/fpls.2019.01605

INTRODUCTION

Wheat is one of the most widely cultivated crop plants along the world and is basic for human nutrition in many areas. Although the hexaploid bread wheat accounts for most of the wheat production, the tetraploid durum wheat is a major crop in the Mediterranean basin, used for the production of traditional staple food. Improving wheat yield capacity is an important goal for future global food security under the challenge of global climate change. As atmospheric [CO_2] (AC) rises to somewhere in the range from 794 to 1,142 μmol mol^{-1} by the end of the 21st century, the global mean surface temperature is expected to increase, especially in the Mediterranean region, where it will be associated with water stress due to a reduction in rainfall (Habash et al., 2009; IPCC, 2013).

While a DNA array is available for bread wheat, quantitative reverse transcription-PCR (qRT-PCR) has been the most commonly used technique for transcript profiling of wheat grown under future climate scenario (Jauregui et al., 2015; Vicente et al., 2015a; Vicente et al., 2016). The development of next-generation high-throughput RNA sequencing technologies (RNA-Seq) provides new advantages for transcriptome analysis, such as higher sensitivity for genes expressed at extremely low or high level, more detailed gene expression profile, and no limitation by the lack of prior knowledge of the genome (Oshlack et al., 2010). RNA-Seq studies in wheat are rapidly increasing (Duan et al., 2012; Oono et al., 2013; IWGSC, 2014; Kumar et al., 2015; Pingault et al., 2015; Curci et al., 2017) thanks to the reconstruction of the whole transcriptome by using *de novo* assembly of short paired-end (PE) reads. This is particularly interesting for non-model organisms, such as durum wheat, due to the scarcity of sequences available in public databases. On the downside, the transcript data sets generated in RNA-Seq experiments are large and complex (Grabherr et al., 2011), needing bioinformatics knowledge and computation facilities to process the data.

Although plant biomass and yield frequently increase with elevated [CO_2] (EC) (Long et al., 2004; Aranjuelo et al., 2013; Vicente et al., 2015a), long-term exposure to EC often leads to a downregulation of photosynthetic capacity accompanied by a decline of Rubisco activity and amount (Pérez et al., 2005; del Pozo et al., 2007; Aranjuelo et al., 2011; Vicente et al., 2016). This decline can be accounted for by different mechanisms, including a carbohydrate sink limitation (Ainsworth and Rogers, 2007; Taub and Wang, 2008; Aranjuelo et al., 2011), due to faster CO_2 assimilation, that can repress photosynthetic genes (Moore et al., 1999; Long et al., 2004), or a lower plant N content caused either by restricted N uptake (del Pozo et al., 2007; Taub and Wang, 2008; Jauregui et al., 2016), the inhibition of N assimilation into proteins (Bloom et al., 2002; Bloom et al., 2010; Vicente et al., 2015a; Vicente et al., 2016), N dilution by accumulation of C-rich compounds (Taub and Wang, 2008), or some other unclear mechanisms (Taub and Wang, 2008; Vicente et al., 2016). In durum wheat grown in field chambers at anthesis, the decline of photosynthetic capacity and N compounds induced by EC is associated with a decrease in transcripts for genes involved in photosynthesis and N assimilation (Vicente et al., 2015a). In bread wheat, the decrease in Rubisco protein content and increase of inhibitors, rather than sugar-mediated gene repression, leads to acclimation to EC even under high N conditions (Pérez et al., 2005). In *Arabidopsis*, EC decreases transpiration, which could be related with the observed depletion of leaf N assimilation and mineral status (Jauregui et al., 2016). In addition, EC leads to an increase in transcripts for genes related to respiration, development, defense, signaling, and sugar content (Leakey et al., 2009; Fukayama et al., 2011; Markelz et al., 2014; Vicente et al., 2015a). In line with these observations, we have reported that EC leads to changes in protein content that enhance C storage and glycolysis (Aranjuelo et al., 2011). Nevertheless, significant disparity exists for the response to EC between plant species, genotypes, development stages, experimental setups, and CO_2 fumigation methods.

An increase in ambient temperature (AT) will negatively impact on global wheat grain production (Araus et al., 2002; Chauhan et al., 2011) with a predicted decrease of 6% for each °C increase in Earth's mean temperature (Asseng et al., 2015). Moderate high temperatures (HTs) frequently lead to an increase in photorespiration and an inhibition of photosynthesis (Salvucci and Crafts-Brandner, 2004), promotes early senescence, and is associated with smaller plants (Chauhan et al., 2011). Some studies focused on bread wheat transcript profiling at seedling (Qin et al., 2008; Chauhan et al., 2011) or flowering stage (Kumar et al., 2015) show that most of the heat-responsive genes encode transcription factors (TFs) and proteins involved in transcription, metabolic processes, and stress response, such as hormone, calcium, and sugar signaling, photosynthesis, carbohydrate metabolism, protein modification, and RNA metabolism.

Future enhancement of [CO_2] can partially compensate the adverse effect of HT (Araus et al., 2002; Habash et al., 2009), especially if other factors, as water stress and/or nutrient deficiencies, are not limiting plant growth and development. In field-grown wheat, Gutiérrez et al. (2009a) pointed that the photochemistry inhibition at HT was counteracted by EC, while Pérez et al. (2011) observed that the negative effect of EC and HT on Rubisco maximum carboxylation activity disappeared for the interaction of both treatments. In agreement with these studies, Chavan et al. (2019) found that EC alleviated heat stress effects on photosynthesis by increasing ribulose bisphosphate regeneration capacity and reducing photochemical damage in a high-yielding wheat cultivar grown in a glasshouse. In a field free air CO_2 enrichment facility, Fitzgerald et al. (2016) observed that EC stimulated bread wheat biomass and yield and, when combined with HT, buffered the negative effects of heat shocks on grain yield. In contrast, Benlloch-Gonzalez et al. (2014) showed that the positive effect of EC on shoot and root growth was reduced by HT in wheat. Furthermore, the interactive effects of the two factors in wheat negatively affected photosynthetic performance, respiration, N assimilation, and mineral content during grain filling (Jauregui et al., 2015) and repressed genes involved in photosynthesis, respiration, and N metabolism at anthesis (Vicente et al., 2015a). The discrepancies found in wheat

responses to EC × HT could likely be explained by the differences in the severity and the duration of the temperature rise, among other factors.

The aim of this work was to further the understanding of the molecular, biochemical, and physiological mechanisms underpinning the response to EC and moderately HT of durum wheat grown in the field in temperature-gradient chambers. The effect of extreme temperature events is out of the scope of this study. Given the importance of these environmental conditions on plant growth and metabolism, here we complement our previous study (Vicente et al., 2015a) to test the hypothesis that, besides primary C-N metabolism, other metabolic processes including cell expansion, hormone synthesis, and secondary metabolism, among others, may be associated with the adaptive mechanisms to these environmental factors, in particular at earlier developmental stages where a lower predominance of resource remobilization is expected as compared to anthesis. The plants were sampled at ear emergence, the start of the period when most of the carbohydrates in the grains are produced by photosynthesis or remobilized (Aranjuelo et al., 2011). We extend precedent qRT-PCR information, limited to genes related to primary C and N metabolism (Vicente et al., 2015a), with transcriptome-wide RNA-Seq analysis combined with functional data to better understand the crop behavior under changing climate conditions. The transcriptome response may improve the understanding of the molecular mechanisms of plant adaptation to EC and HT. Since the transcript changes may not result in parallel alterations in protein activity and metabolites, a complementary study of modifications in metabolites and enzyme activities can provide a more conclusive view.

MATERIALS AND METHODS

Plant Material and Growth Conditions

The field experiment was conducted in a clay–sand soil at the experimental fields of the Institute of Natural Resources and Agrobiology of Salamanca (IRNASA-CSIC), in Salamanca, Spain (40°95′ N, 5°5′ W, 800 m a.s.l.), under Mediterranean climate conditions. After adding 60 kg ha^{-1} each of P and K nutrients (as P_2O_5 and K_2O, respectively), durum wheat (*Triticum durum* Desf. cv. Regallo) seeds were sown at a rate of 200 kg ha^{-1} and 0.13 m row spacing on 29 October 2007. We chose cultivar Regallo (released in 1988) because it is a modern semi-dwarf durum wheat genotype with high yield, grain protein content, and adaptability to Mediterranean climate, widely commercialized in our region. N fertilization was applied by hand at 140 kg ha^{-1} as $Ca(NO_3)_2$ on 15 February 2008. This N supply was considered optimal based on previous experience from other experiments in the same location and soil. The crop was watered twice, sometimes once a week with a drip irrigation system, providing an amount of water nearly equivalent to the mean crop evapotranspiration [Allen et al., 2006; values for reference evapotranspiration (ET_o) and crop coefficient (K_c) of 3 mm day^{-1} and 1.15, respectively] (**Supplementary Figure 1**). Six temperature-gradient chambers (Pérez et al., 2005; Gutiérrez et al., 2009a; Gutiérrez et al., 2009b; Gutiérrez et al., 2013; Vicente et al., 2015a) were mounted over the crop on 27 February 2008. They were 9 m long, 2.2 m wide, and 1.7 m high with transparent walls and roof, divided into three modules separated by polycarbonate septa to reduce the mixing of air between modules due to convection. Three of them were kept at ambient [CO_2], 370 μmol mol^{-1}, while [CO_2] was increased to 700 μmol mol^{-1} in other three by injecting pure CO_2 at the two inlet fans of each chamber during the light hours, controlled by an infrared gas analyzer as described in Pérez et al. (2005) and Gutiérrez et al. (2009b). The temperatures at the extreme chamber modules were set at ambient and 4 °C warmer by using two inlet and one outlet fans at the required speed, in combination with fan heaters to create a temperature gradient between modules (Pérez et al., 2005; Gutiérrez et al., 2009b) (**Supplementary Figure 1**). Plants received a total of 255 mm from sowing to ear emergence (**Supplementary Figure 1**). Flag leaves were harvested on 7 May 2008 at ear emergence (Zadoks 59) and 2 days after this stage, respectively, in plants grown at ambient and high temperature; for simplicity, thereafter this stage will be referred to as ear emergence. The leaves were immediately frozen in liquid N and stored at −80°C for biochemical and molecular analyses. In summary, four treatments were considered in this study for further analysis: ambient CO_2 and temperature (AC-AT), ambient CO_2 and high temperature (AC-HT), elevated CO_2 and ambient temperature (EC-AT), and elevated CO_2 and high temperature (EC-HT). A schematic representation of the experimental design is detailed in **Figure 1**.

Physiological and Biochemical Parameters

Gas exchange in the central segment of the flag leaves was recorded between 3 and 8 h after the start of the photoperiod at the respective growth CO_2 concentration. Photosynthesis rate (A_n), stomatal conductance (g_s), transpiration (E), and intercellular CO_2 concentration (C_i) were measured at 300 ml min^{-1} air flow rate, 1,500 μmol m^{-2} s^{-1} irradiance, and 25°C temperature using the Peltier system in a 1.7 cm^2 window leaf chamber connected to a portable infrared gas analyzer CIRAS-2 (PP Systems, UK). The measurements were done when inlet [CO_2] was stable and after checking for leaks in the chamber. Shoots were collected to determine the dry weight of flag leaves and total shoot after drying in an oven at 60°C for 48 h. N concentration as a percentage of dry matter and the N content in flag leaves and shoots were determined as described by Vicente et al. (2015b). Briefly, dried samples were subjected to Kjeldhal digestion with H_2SO_4 using a Se catalyst and adjusting the pH to 3–4 using 1 M triethanolamine buffer (pH 7.2) and 5 M KOH. N, in the form of NH_4^+, was spectrophotometrically determined at 340 nm as the NADPH reduced during the conversion of NH_4^+ and 2-oxoglutarate into glutamate catalyzed by glutamate dehydrogenase (Ammonia Rapid kit, Megazyme, Ireland). After ethanol/water extraction, soluble sugars (glucose, fructose, sucrose, and fructans) and starch content were measured as mentioned in Morcuende et al. (2004). Firstly, glucose and fructose were measured spectrophotometrically in

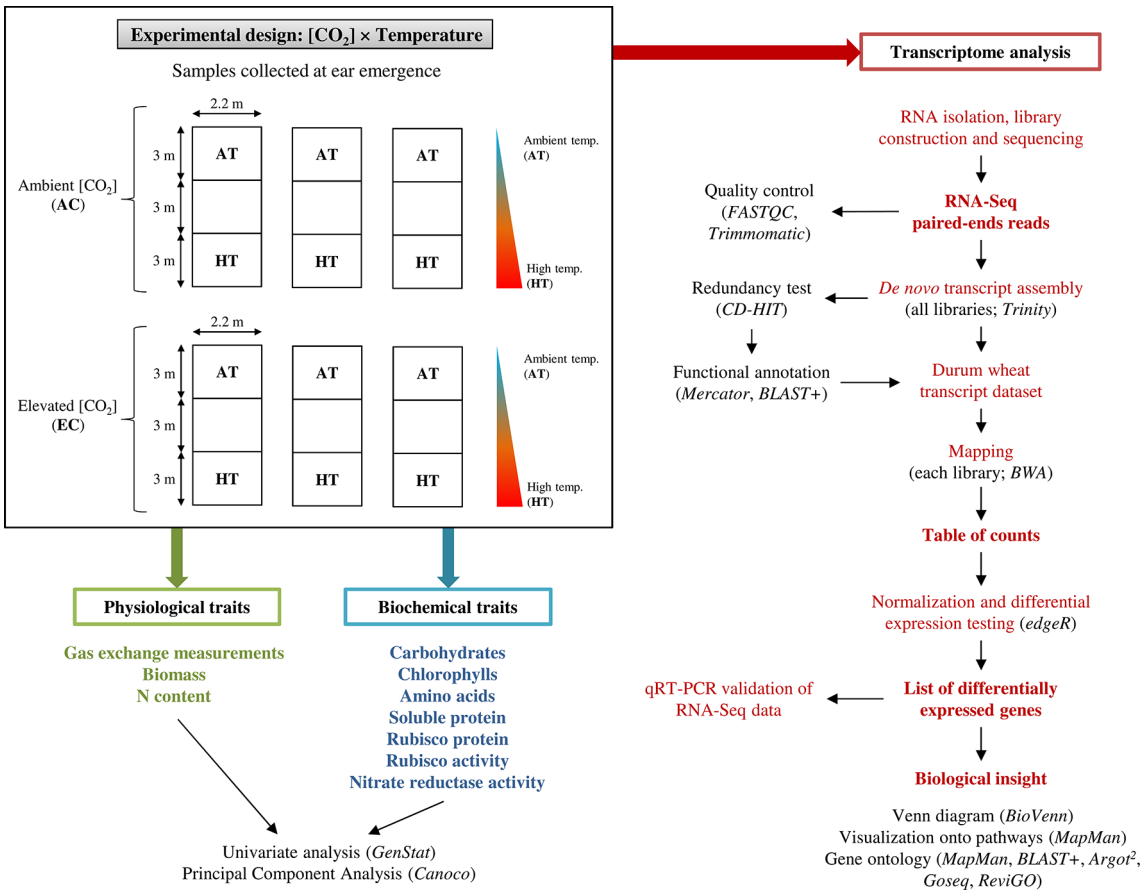

FIGURE 1 | Schematic representation of the experimental setup. Physiological, biochemical, and transcriptome analysis were performed to characterize the durum wheat responses to elevated [CO_2] and moderate high temperature in durum wheat grown in the temperature-gradient field chambers. RNA sequencing (RNA-Seq) analysis pipeline for the identification of differentially expressed transcripts is shown on right side.

the supernatant with an assay coupled to NADP reduction based on Jones et al. (1977). After incubating another aliquot with sucrase to metabolize the sucrose in the sample, the released glucose and fructose related with sucrose were determined. Later, in a third aliquot the content of fructans in the form of glucose and fructose were measured after their hydrolysis with fructanases. Finally, starch was measured in the insoluble residue from the extraction after incubation with amyloglucosidase and α-amylase at 37°C overnight. Then, starch was measured in the form of glucose as mentioned above. Chlorophyll (chl) was extracted in 80% acetone and assayed at 645 and 663 nm for the calculation of total chl according to Arnon (1949). Total amino acids content was measured in the ethanol/water extracts by the ninhydrin method (Hare, 1977) as described by Aranjuelo et al. (2011). Soluble proteins were extracted and determined spectrophotometrically according to Bradford (1976). Rubisco protein was separated by SDS-PAGE electrophoresis and the content determined by densitometry (Pérez et al., 2011). Initial and total Rubisco activities were measured using a cascade reaction involving several enzymes exactly as described in Pérez et al. (2011), where activity was at a stoichiometry of 1:2 equivalent to the NADH oxidation recorded at 340 nm. Rubisco activation state was calculated as the ratio between initial and total Rubisco activity. Maximal activity and activation state of nitrate reductase (NR) were assessed by the formation of NO_2^- in the absence or presence of 10 mM Mg^{2+} as described by Morcuende et al. (2004) based on the procedure described by Scheible et al. (1997).

RNA Isolation, cDNA Library Construction, Illumina Sequencing, and Quality Control Processing of Raw Data

Total RNA was prepared by grinding the flag leaves in liquid N and extracting RNA using the method described by Morcuende et al. (1998). Three biological replicates were used per treatment. RNA integrity/degradation was examined on 1.5% agarose gels (**Supplementary Figure 2**). RNA quality and concentration were assessed using NanoDrop ND-1000 spectrophotometer (Thermo Fisher Scientific, USA) and 2100 Bioanalyzer (Agilent Technologies, Santa Clara, CA) as shown in **Supplementary Table 1**. RIN^e (RNA integrity number equivalent) scores were

greater than 8.0 for all samples, as recommended by the manufacturer. Twelve cDNA libraries (one per sample) were generated by using Illumina TruSeq RNA Library Preparation Kit (Beckman Coulter Genomics, Beverly, USA). RNA sequencing was performed on each library to generate PE reads of length 100 nucleotides on two lanes of Illumina HiSeq 2000 (Beckman Coulter Genomics, Beverly, USA). Quality of raw data was verified by FastQC software (http://www.bioinformatics.babraham.ac.uk/projects/fastqc/). Adapters and contaminated sequences were removed, and low-quality bases from both ends of each read were trimmed at a Phred quality scores threshold of Q20 (< 1 error per 100 bp) from the raw data in FastQ format using PE mode of Trimmomatic (Bolger et al., 2014). **Figure 1** also contains an overview of the RNA-Seq analysis pipeline followed. Whole data set has been deposited in the European Nucleotide Archive with accession number PRJEB34302.

De Novo Assembly and Functional Annotation

All the quality-controlled PE reads from the 12 libraries were *de novo* assembled using Trinity (Grabherr et al., 2011), with a fixed *k*-mer size of 25, to generate a durum wheat transcript data set. Trinity has a good performance in wheat RNA-Seq experiments (Duan et al., 2012; Oono et al., 2013), and it was the most successful assembler after testing four different ones (Li et al., 2013). With a minimum *k*-mer coverage of 10 (minimum count of *k*-mers to be assembled), 196,843 contigs in 60,209 transcripts (unigenes/loci) were obtained. Transcript redundancy was tested using CD-HIT software with identity of 95%, although the number of redundant transcripts was negligible. Functional annotation of the durum wheat transcript data set was based on the large amount of public data for wheat and other plant species. Firstly, all transcripts were submitted to Mercator web tool (Lohse et al., 2014), which generated functional predictions by searching a variety of reference databases (TAIR release 10; SwissProt/UniProt Plant Proteins; TIGR5 rice proteins; clusters of orthologous eukaryotic genes database, KOG; and conserved domain database, CDD), using a BLAST cutoff of 40. Furthermore, a BLASTN/BLASTX search for all the transcripts against different databases (TAGI release 12 for bread wheat, TIGR release 1 and 2 for bread and durum wheat, *Brachypodium* genome v1.2 at PlantGDB, and rice genome release 7) was achieved using BLAST+ and an E-value cutoff of $1e^{-3}$ to improve transcript annotation.

Mapping of Reads to Durum Wheat Transcript Data Set, Normalization, and Identification of Differentially Expressed Transcripts

Quality-controlled PE reads for each sample were mapped back to the durum wheat transcript data set with the alignment program BWA (Li and Durbin, 2009), with the aim to find the location where each short read best matches the reference (Oshlack et al., 2010). The data were summarized in a table of counts, rows for transcripts, and columns for counts, which represent the total number of reads aligning to each non-redundant contig of the durum wheat transcript data set. Differential gene expression analysis across experimental conditions was performed using the R/Bioconductor package edgeR. The library sizes were computed from the column sums of the counts. Using the plants grown under ambient CO_2 and temperature as the control treatment, we focused on the EC-, HT- and EC × HT-responsive transcripts. We considered as differentially expressed (DE) transcripts the ones with a false discovery rate (FDR) < 0.05 and an induction or repression ratio ≥ two-fold.

Visualization of RNA-Seq Results and Functional Enrichment Analysis

Venn diagram analysis of DE transcripts was made in BioVenn (Hulsen et al., 2008). Visualization of metabolic pathways was performed using MapMan (Thimm et al., 2004). Previously, MapMan BINs (hierarchical functional categories assigned to certain biological processes) were assigned with Mercator to all input sequences with the aim to create a mapping file for MapMan (see section *De Novo Assembly and Functional Annotation*). For the transcripts incorporated to BIN 35.2 (unknown sequence) by Mercator, but annotated by BLAST+ using TAGI database, *Brachypodium*, and rice genomes, new BINs were assigned. A special BIN category (2.1.3) was created for the genes involved in fructan biosynthesis, due to its strong over-expression under EC in this study and in previous ones of our group (Vicente et al., 2015a; Vicente et al., 2016). Analysis of functional categories of the DE transcripts was performed based on the MapMan categories using the BINs assigned previously. Likewise, Gene Ontology (GO) terms provided by the GO project (http://www.geneontology.org/) were assigned to the DE transcripts based on the GO terms downloaded from the *Brachypodium distachyon* and rice genome annotation projects and UniProtKB database. GO terms for UniProtKB database were assigned after running Argot^2 tool using default parameters (Falda et al., 2012). The R/Bioconductor package GOseq was used to correct gene length bias. Only GO terms with corrected *P* values <0.05 were considered significantly enriched, and the results were visualized and summarized using a clustering algorithm with the web server ReviGO (Supek et al., 2011) with default parameters.

Validation of RNA-Seq Data by qRT-PCR

The validation of the RNA-Seq results and reverse transcription reactions were performed using qRT-PCR as described in Vicente et al. (2015a). Two technical replicates were analyzed for each one of the three biological replicates per treatment. The relative transcription levels were analyzed using the $2^{-\Delta\Delta Ct}$ method and compared with expression levels of RNA-Seq. The ADP-ribosylation factor was used as reference gene for qRT-PCR normalization (Vicente et al., 2015a; Vicente et al., 2016) and is listed in **Supplementary Table 2** together with the genes used for the validation.

Statistical Analysis

The experiment had three blocks with all the factorial combinations of two atmospheric [CO_2] (370 and 700 μmol mol^{-1}) and two temperatures (ambient and 4°C warmer). Treatment effects and interactions were determined through an analysis of variance (ANOVA) using GenStat software for physiological and biochemical parameters. When differences between treatments were significant (P <0.05), they were evaluated using the least significant difference test (*LSD*). As mentioned above, DE transcripts were considered significant with FDR <0.05 and a fold-change cutoff of 2 using edgeR. Multivariate statistical analysis of the physiological and biochemical data was performed using principal component analysis (PCA) with Canoco for Windows (Biometris, Plant Research International).

RESULTS

Physiological and Biochemical Responses to Elevated CO_2 and High Temperature

EC stimulated net photosynthetic rates (A_n) by 32% compared to AC at ear emergence (**Table 1**). This increase was greater in plants grown at AT than HT, although the CO_2 × temperature interaction did not reach statistical significance. EC led to a reduction of stomatal conductance (g_s) and transpiration (E), and an increase in intercellular [CO_2] (C_i), with greater C_i values at AT than HT. Shoot biomass was promoted by 17% by EC, while no differences in leaf dry weight were observed with an elevation of [CO_2] or temperature. The content of some carbohydrates was altered by EC, HT, or their interaction. Starch content increased by two-fold and glucose decreased by 25% under EC. In contrast, starch decreased by 70% and glucose increased by 60% at HT compared to AT. Furthermore, EC increased significantly fructan content, with larger content at AT relative to HT. Neither fructose nor sucrose contents were modified by growth conditions.

N concentration in leaves and shoots was consistently reduced by EC (16% and 21%, respectively), together with a decline of 17% in total shoot N content (**Table 1**). N-rich compounds were also affected by environmental conditions. Chl content was reduced by EC, HT, or the EC × HT interaction compared to AC and AT. Growth at EC caused a decrease in total soluble proteins (32%) and Rubisco content (36%), together with a decline (12%) of Rubisco as a percentage of soluble protein. HT also decreased significantly Rubisco content by 11%. Enzyme assays for key proteins of C (Rubisco) and N (NR) metabolism also revealed some changes caused by growth conditions. Similar to chl

TABLE 1 | Photosynthesis rate (A_n), stomatal conductance (g_s), transpiration (E), intercellular CO_2 concentration (C_i), dry weight (DW), N concentration, total N content (N_t), chlorophyll (chl), glucose, fructose, sucrose, fructan, starch, total amino acid, soluble and Rubisco protein contents, Rubisco as a percentage of soluble protein, initial and total Rubisco activities (Rbco act.), Rubisco activation state (Rbco %act.), maximal nitrate reductase (NR) activity, and activation (NR %act.) in durum wheat grown at ambient (AC, 370 μmol mol^{-1}) or elevated (EC, 700 μmol mol^{-1}) [CO_2] and ambient temperature (AT) or ambient + 4°C (HT).

		CO_2		Temperature		CO_2 × temperature			
Parameter	**Units**	**AC**	**EC**	**AT**	**HT**	**AC-AT**	**AC-HT**	**EC-AT**	**EC-HT**
A_n	μmol m^{-2} s^{-1}	**24.7 a**	**32.7 b**	29.9	27.5	25.3	24.1	34.6	30.9
g_s	mmol m^{-2} s^{-1}	**465 b**	**292 a**	371	386	419	511	323	262
E	mmol m^{-2} s^{-1}	**4.97 b**	**3.96 a**	4.31	4.62	4.56	5.38	4.06	3.85
C_i	μmol mol^{-1}	194	363	301	257	**183 a**	**204 a**	**417 c**	**308 b**
Leaf DW	g	0.131	0.141	0.141	0.131	0.130	0.131	0.152	0.130
Shoot DW	g	**2.40 a**	**2.80 b**	2.54	2.66	2.40	2.39	2.68	2.92
Glucose	μmol g FW^{-1}	**8.04 b**	**6.03 a**	**5.42 a**	**8.65 b**	5.96	10.13	4.88	7.17
Fructose	μmol g FW^{-1}	9.16	10.38	10.05	9.49	8.50	9.82	11.60	9.16
Sucrose	μmol g FW^{-1}	16.5	23.8	21.8	18.5	16.7	16.4	26.9	20.7
Fructans	μmol g FW^{-1}	19.0	135.3	95.9	58.5	**33.4 a**	**4.6 a**	**158.4 c**	**112.3 b**
Starch	μmol g FW^{-1}	**1.54 a**	**3.08 b**	**3.55 b**	**1.07 a**	2.24	0.84	4.86	1.31
Leaf %N	% dry weight	**3.89 b**	**3.26 a**	3.73	3.42	4.03	3.75	3.43	3.09
Shoot %N	% dry weight	**1.43 b**	**1.13 a**	1.34	1.22	1.52	1.33	1.16	1.10
Leaf N_t	mg N per organ	5.09	4.79	5.26	4.62	5.27	4.90	5.24	4.33
Shoot N_t	mg N per organ	**35.8 b**	29.7 a	33.1	32.4	36.2	35.5	30.0	29.4
Chl	mg g FW^{-1}	2.91	2.62	2.90	2.63	**3.27 b**	**2.56 a**	**2.53 a**	**2.71 a**
Amino acids	μmol g FW^{-1}	**20.1 b**	14.6 a	17.1	17.6	21.0	19.3	13.2	16.0
Soluble protein	mg g FW^{-1}	**33.6 b**	22.9 a	29.6	26.9	36.5	30.8	22.7	23.1
Rbco protein	mg g FW^{-1}	**19.7 b**	12.6 a	**17.1 b**	**15.3 a**	21.2	18.2	13.0	12.3
Rbco % sol. protein	%	**58.5 b**	51.4 a	55.1	54.7	58.7	58.2	51.6	51.3
Initial Rbco act.	μmol m^{-2} s^{-1}	43.4	29.4	42.9	29.8	**56.1 b**	**30.6 a**	**29.7 a**	**29.0 a**
Total Rbco act.	μmol m^{-2} s^{-1}	86.0	61.6	84.2	63.3	**105.1 b**	**66.9 a**	**63.4 a**	**59.7 a**
Rbco %act.	%	48.4	48.9	51.5	45.8	56.0	40.8	47.0	50.8
NR activity	μmol g^{-1} h^{-1}	**8.79 b**	**5.43 a**	7.81	6.41	9.76	7.83	5.87	4.99
NR %act.	%	57.5	80.3	79.6	58.2	**62.2 a**	**52.8 a**	**97.0 b**	**63.6 a**

Unless otherwise specified, the measurements were carried out on the flag leaf. Each main factor level is the mean of 12 replicates, and factor combinations are means of 6 replicates (half for gas exchange parameters). For each comparison of means, values with different letter are significantly different (P < 0.05) and marked in bold. No letters are added for the CO_2 × temperature combinations when the interaction is not significant or for the factor main effects when the interaction is significant.

content, initial and total Rubisco activities were remarkably reduced under EC, HT (45–48%), or the EC × HT interaction (36–43%; **Table 1**). NR activity was diminished by 38% under EC, while the activation state of the enzyme strongly increased by 56% compared to AC. This increase in the activation state under EC was not supported at HT.

The differences in physiological and biochemical traits between treatments were supported by PCA (**Figure 2**). There were variations caused by changes in air [CO_2] and temperature, represented by the first and second principal components, respectively, which were large for air [CO_2]. Most of the traits related to N content, N-rich compounds, and enzyme activities were concentrated in the same area, showing that the AC-AT control treatment reached the highest values. Warmer temperatures consistently decreased these traits and showed an increase in glucose content. Treatments under EC were clearly separated from those under AC, although differences due to changes in temperature were significantly reduced under EC relative to AC. Carbohydrates tended to increase under EC, especially fructans, starch, and sucrose at AT and fructose at HT. Growth at EC and AT promoted shoot biomass and the activation of NR enzyme.

Transcriptome Sequencing and *De Novo* Assembly

A total number of 395 million PE short-read sequences (77.2 Gb), were generated for the 12 libraries and used for downstream analysis, with an average of 65.9 million reads per sample (**Supplementary Table 3**). All reads were *de novo* assembled. An average of 88.21% reads was uniquely mapped per library (**Supplementary Table 3**). We obtained a durum wheat transcript data set of 60,209 transcripts. Functional annotation of this transcript data set was achieved by using Mercator tool (15,402 transcripts; 25.6% of the total), durum (4,994 transcripts; 8.3%), and bread (30,713 transcripts; 51.0%) wheat sequences available in TIGR, bread wheat sequences available in TAGI (24,558 transcripts; 40.8%), *Brachypodium* genome (protein sequences; 25,662 transcripts; 42.6%), and rice genome (protein sequences; 25,336 transcripts; 42.1%). Thus 38,869 transcripts were annotated by at least one database. Nonetheless, it is important to consider that some matches described a homologous locus/gene in other species without any annotation. The transcript levels of seven genes involved in primary metabolism were evaluated by qRT-PCR (**Supplementary Table 2**). The results of the relative expression of these genes under EC, HT, and its combination from qRT-PCR and RNA-Seq analysis were compared (**Supplementary Figure 3**). A similar pattern of changes were obtained from both techniques, which validates the RNA-Seq results.

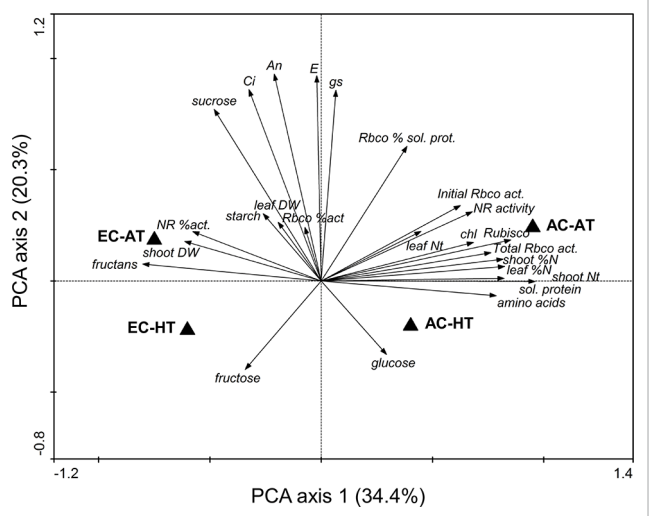

FIGURE 2 | Principal component analysis of the physiological and biochemical traits of durum wheat flag leaves in response to ambient (AC, 370 µmol mol^{-1}) or elevated (EC, 700 µmol mol^{-1}) [CO_2] and ambient temperature (AT) or ambient + 4°C (HT). Data analysis was carried out with the results included in **Table 1**.

Identification of Differentially Expressed Transcripts and Their Classification Using MapMan Categories

Based on FDR values, a total of 1,051 DE transcripts were detected in at least one treatment compared with the control treatment with AC and AT (**Figure 3A**). Venn diagrams exhibited an overlap of 419 DE transcripts between, at least, two treatments, while 223 of them were altered in all three treatment combinations relative to the control. A total of 27% and 29% of the DE transcripts were uniquely responsive to EC and HT, respectively, while only 4% was unique for EC × HT. Upregulation of 210, 19, and 36 genes, and downregulation of 465, 669, and 294 genes was detected under EC, HT, and EC × HT relative to control treatment, respectively (**Figure 3B**). A detailed summary of the DE transcripts is provided in **Supplementary Table 4**.

For the whole durum wheat transcriptome, we annotated 21,512 transcripts (35.7%) with MapMan BINs of known function, after running the Mercator web tool and using the BINs previously assigned to TAGI database and *Brachypodium* and rice genomes. Using these BINs, the DE transcripts were classified into 34 categories (**Table 2**), while 307, 319, and 146 transcripts differentially expressed, respectively, with EC, HT, and EC × HT were assigned to BIN 35 "no ontology/unknown". The results using the MapMan categories highlight that only a small proportion of genes related to primary and secondary metabolisms were up or downregulated (**Table 2**). Most of the genes that were DE belonged to categories such as stress, RNA and DNA metabolisms, miscellaneous enzyme families, protein and signaling. While several genes were upregulated under EC or the interaction EC × HT relative to control treatment, most of them were downregulated under HT.

Biological Insight Into Metabolic Pathways of the Differentially Expressed Transcripts

The MapMan BINs assigned to the transcripts allowed displaying gene expression results onto biological pathways using the MapMan application (**Figures 4–6**, **Supplementary Figure 4**). An overview of plant metabolism showed that

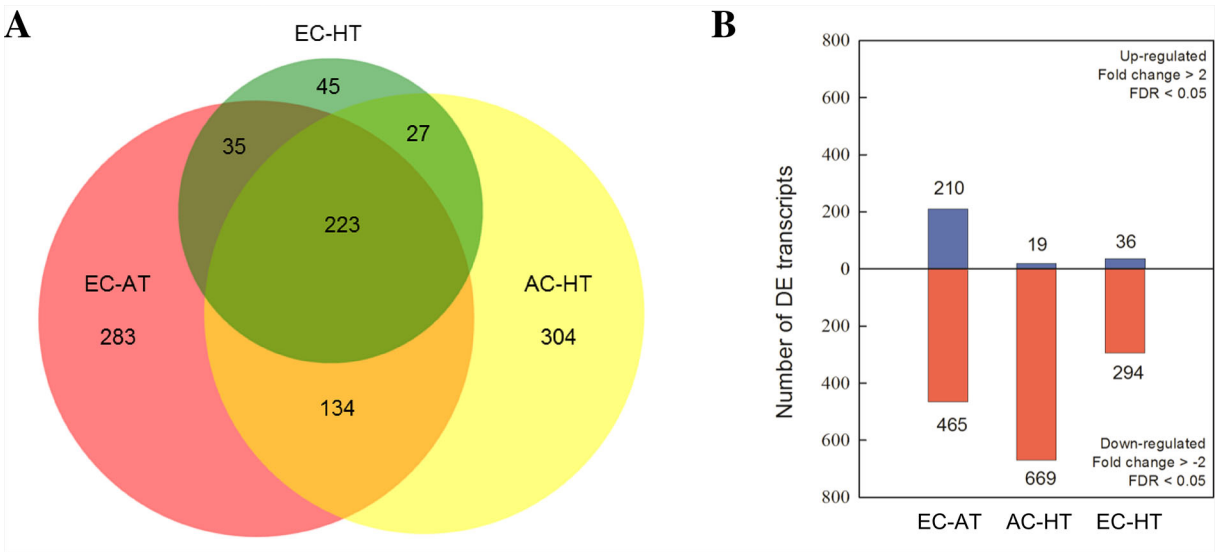

FIGURE 3 | (A) Venn diagram analysis of the differentially expressed (DE) transcripts and **(B)** number of DE transcripts which were up (blue) or downregulated (red) under ambient [CO_2] and high temperature (AC-HT), elevated [CO_2] and ambient temperature (EC-AT), or elevated [CO_2] and high temperature (EC-HT), relative to control treatment at ambient [CO_2] and temperature in durum wheat flag leaves.

TABLE 2 | Analysis of the differentially expressed (DE) transcripts based on the functional MapMan categories.

Bin code	Category	Elevated [CO_2] (EC-AT)			High temperature (AC-HT)			Elevated [CO_2] x high temperature (EC-HT)		
		Up	Down	Total	Up	Down	Total	Up	Down	Total
1	Photosynthesis	3	7	10	2	6	8	0	6	6
2	Major CHO metabolism	2	0	2	0	0	0	1	0	1
3	Minor CHO metabolism	1	3	4	0	4	4	1	3	4
4	Glycolysis	0	2	2	0	3	3	0	2	2
8	TCA cycle	0	0	0	0	1	1	0	0	0
9	Mitochondrial electron transport	5	1	6	0	1	1	0	1	1
10	Cell wall	1	2	3	0	6	6	1	0	1
11	Lipid metabolism	2	2	4	0	7	7	1	1	2
12	N metabolism	0	1	1	0	1	1	0	0	0
13	Amino acid metabolism	2	5	7	0	6	6	0	4	4
16	Secondary metabolism	11	5	16	0	15	15	1	3	4
17	Hormone metabolism	3	6	9	0	8	8	0	2	2
18	Co-factor and vitamin metabolism	0	0	0	0	1	1	0	0	0
19	Tetrapyrrole synthesis	1	0	1	0	0	0	0	0	0
20	Stress	12	77	89	0	81	81	0	44	44
21	Redox	1	1	2	0	3	3	0	0	0
23	Nucleotide metabolism	1	1	2	0	0	0	0	1	1
24	Biodegradation of xenobiotics	3	0	3	0	0	0	0	0	0
25	C1 metabolism	1	0	1	0	0	0	0	0	0
26	Miscellaneous enzyme families	10	15	25	1	28	29	5	7	12
27	RNA	16	16	32	0	29	29	5	12	17
28	DNA	4	12	16	2	17	19	3	9	12
29	Protein	18	28	46	1	50	51	3	19	22
30	Signaling	3	53	56	2	68	70	1	35	36
31	Cell	5	3	8	0	3	3	0	1	1
33	Development	5	1	6	1	7	8	1	1	2
34	Transport	11	6	17	0	15	15	3	7	10
35	Not assigned/unknown	89	218	307	10	309	319	10	136	146

The upregulated, downregulated, and total DE genes for each treatment relative to control treatment (ambient CO_2 and temperature) are shown.

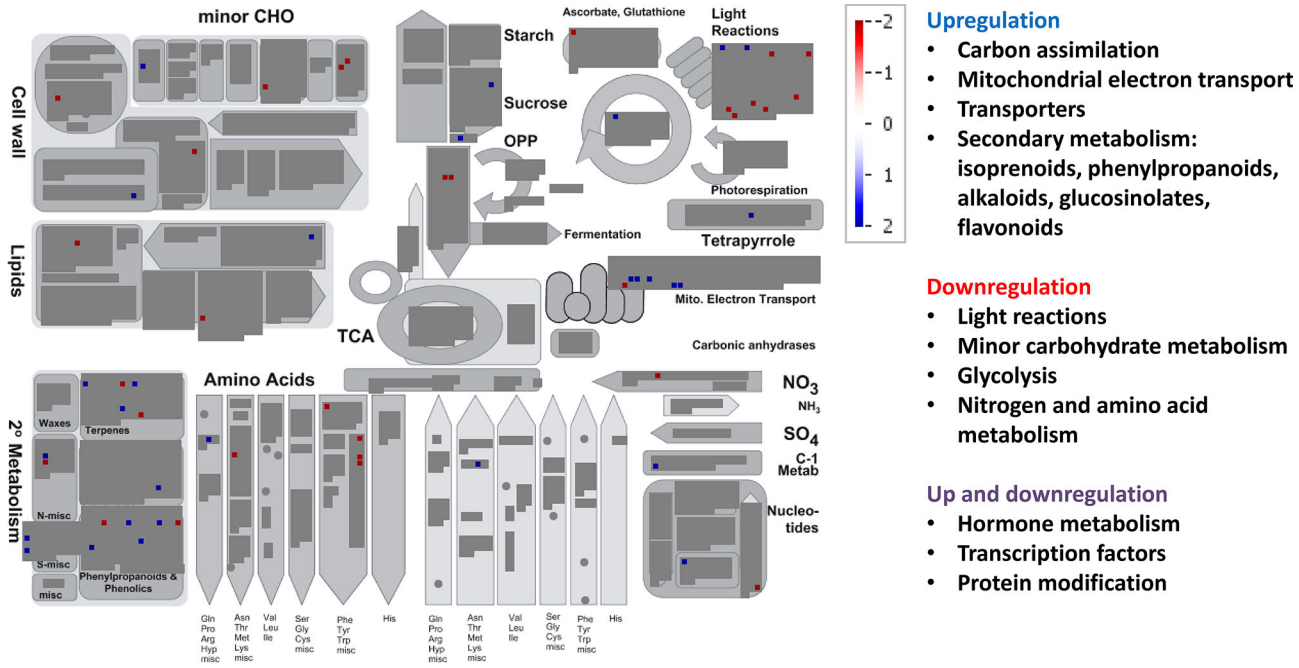

FIGURE 4 | Significant changes in transcript levels associated with metabolic pathways under elevated [CO_2] relative to the treatment under ambient [CO_2] and temperature. White indicates no change, blue upregulation, and red downregulation as shown in the color key for a log fold-change scale. The main pathways affected associated with primary and secondary metabolism are highlighted.

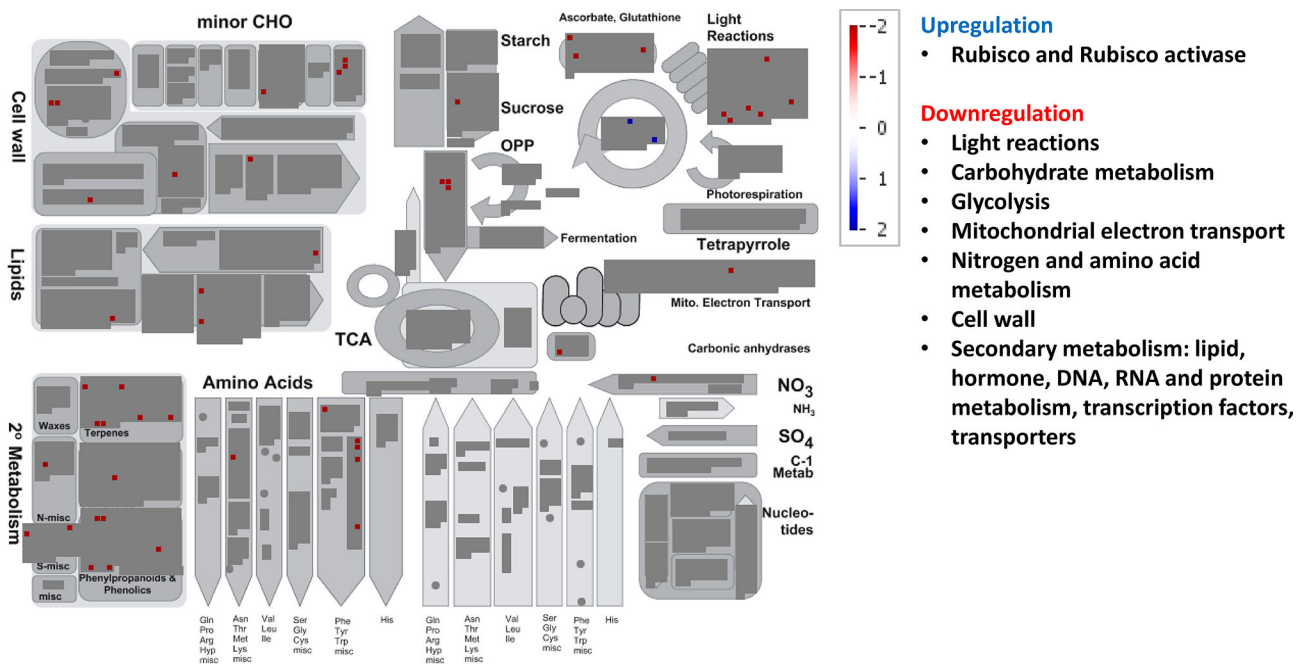

FIGURE 5 | Significant changes in transcript levels associated with metabolic pathways under high temperature relative to the treatment under ambient [CO_2] and temperature. White indicates no change, blue upregulation, and red downregulation as shown in the color key for a log fold-change scale. The main pathways affected associated with primary and secondary metabolism are highlighted.

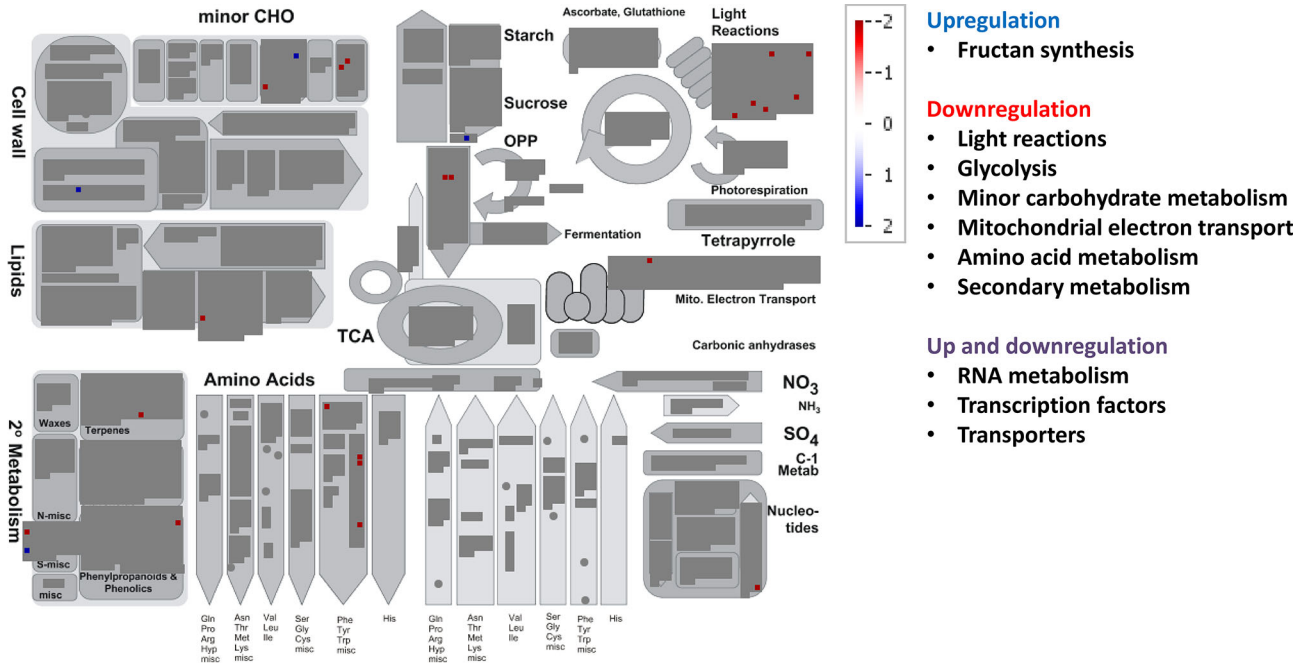

FIGURE 6 | Significant changes in transcript levels associated with metabolic pathways under the combination of elevated [CO_2] and high temperature relative to the treatment under ambient [CO_2] and temperature. White indicates no change, blue upregulation, and red downregulation as shown in the color key for a log fold-change scale. The main pathways affected associated with primary and secondary metabolism are highlighted.

EC increased the expression of several genes related to photosynthesis and carbohydrate metabolism relative to control treatment: two genes of light-harvesting complex II, CP12 (Calvin-Benson cycle), Mg protoporphyrin IX methyltransferase (tetrapyrrole synthesis), sucrose:fructan 6-fructosyltransferase (fructan synthesis), a vacuolar invertase, and a gene of raffinose synthase family protein (**Figure 4**, **Supplementary Figure 4**, **Supplementary Table 4**). However, seven genes from light harvesting (e.g. two photosystem II polypeptide subunits and several protein kinases) and three from minor carbohydrate metabolism (two involved in callose synthesis and one galactose mutarotase) were downregulated. EC also downregulated two genes of the cytosolic glyceraldehyde-3-phosphate dehydrogenase, involved in glycolysis pathway. EC strongly induced five of the six DE genes of mitochondrial electron transport (three cytochrome c oxidases and two ATP synthases). Although a gene involved in proline biosynthesis was upregulated, chiefly N metabolism was repressed by EC, as indicated by the downregulation of glutamate synthase, a gene of methionine synthesis, and four genes of the synthesis of aromatic amino acids (chorismate and tryptophan), and by the upregulation of one involved in the degradation of threonine. Most of the genes belonging to secondary metabolism were upregulated, including those involved in isoprenoid (e.g. carotenoids), phenylpropanoid (lignin), alkaloid, sulfur (glucosinolates), and flavonoid pathways. As for other plant functions, EC modified gene expression for hormone metabolism, inducing those related to gibberellins (DELLA protein) and jasmonates (12-oxophytodienoic acid reductase), and repressing those related to auxins, brassinosteroids, and ethylene (**Supplementary Table 4**). Eight of 11 genes related to RNA processing and transcription were downregulated, while the expression of 21 TFs from very diverse families was modified. Moreover, EC affected the expression of 46 genes involved in protein synthesis (mainly ribosomal proteins), posttranslational modification, and degradation (e.g. cysteine and serine proteases and ubiquitin). Regarding signaling functions, EC strongly reduced the transcript abundance of 53 out of 56 DE genes, including many receptor kinases (mainly leucine-rich repeat protein kinase family, DUF26 family of cysteine-rich receptor-like kinases, and cell wall–associated kinases) and other genes with unspecified functions. Transcript changes associated with transport revealed that, in general, EC induced the expression of transporters for amino acids (permease family protein), sulfate (transmembrane transporter), potassium (calcium-activated potassium channel), and peptides (proton-dependent oligopeptide transporters), as well as aquaporins (subfamily PIP) (**Supplementary Table 4**). EC repressed the expression of two porin genes and a plasma membrane ATP synthase, and modified the expression of genes encoding for several ABC and mitochondrial membrane transporters. Eighty-nine DE genes under EC were identified as stress-responsive genes, most of them downregulated relative to control treatment and lacking a good annotation. However, at variance with the other growth conditions, 12 stress-responsive genes were upregulated, mainly associated with heath shock proteins. The large enzyme families with more significant changes under EC were cytochrome P450 and oxidases (**Supplementary Table 4**).

Relative to control treatment, HT clearly repressed many metabolic pathways (**Figure 5**, **Supplementary Figure 4**). Thus, HT reduced the transcript abundance for genes involved in light reactions (diverse protein kinases associated with state transitions and a photosystem II polypeptide subunit), carbohydrate metabolism (galactose mutarotase and three enzymes involved in callose synthesis), glycolysis (3-phosphoglycerate kinase and two glyceraldehyde-3-phosphate dehydrogenases), mitochondrial electron transport (NADH dehydrogenase), cell wall (cellulose synthase, fasciclin-like arabinogalactan protein, leucine-rich repeat receptor protein kinase, glycoside hydrolase, and xyloglucan endotransglucosylase/hydrolase), lipid metabolism (several genes involved in fatty acid elongation, lipid transfer, and degradation), N and amino acid metabolisms (glutamate synthase and seven genes involved in the synthesis of methionine, chorismate, and tryptophan), and the glutathione–ascorbate cycle (**Figure 5**, **Supplementary Table 4**). Additionally, HT also repressed genes for secondary metabolism (related to non-mevalonate pathway, terpenoids, lignin, and other phenylpropanoids, alkaloids, glucosinolates, and flavonoids), a carbonic anhydrase, and an iron–sulfur enzyme related to NAD biosynthesis (quinolinate synthetase); and unexpectedly upregulated gene expression for ribulose-1,5-bisphosphate carboxylase oxygenase (Rubisco) large subunit and for Rubisco activase. All genes from hormone metabolism were also repressed by HT, such as those associated with abscisic acid, brassinosteroids, ethylene, gibberelins, and jasmonates. A total of 29 genes associated with RNA processing, transcription, binding, and regulation of transcription were downregulated, including TFs of the NAC, MYB, and WRKY families, auxin response factor, Constans-like zinc finger, and argonaute proteins, among others. Moreover, many genes involved in other regulation processes were downregulated, such as those related to DNA metabolism (DNA synthesis/chromatin structure and others with unspecified function), protein synthesis, posttranslational modification and degradation (similar to those altered under EC, but here all were downregulated), and signaling (leucine-rich repeat protein kinase family, DUF26 family of cysteine-rich receptor-like kinases, cell wall-associated kinases, LRK10 receptor-like protein kinases, and others associated with 14-3-3 proteins, phosphinositides, and light) (**Supplementary Table 4**). In transport category, we observed that HT repressed the expression of transporters for sugars (zinc induced facilitator), nitrate and ammonium (high affinity transporter members), peptides (proton-dependent oligopeptide transporters), as well as a plasma membrane ATP synthase, a cation efflux family protein, an ABC transporter, two porins, a cyclic nucleotide-gated ion channel, a mitochondrial substrate carrier family protein, and an aquaporin of TIP subfamily. Eighty-one DE genes corresponded to stress-responsive genes, all downregulated under HT relative to control treatment (**Supplementary Table 4**). Regarding changes in large enzyme families under HT, we highlight the downregulation of several members of cytochrome P450, UDP glucosyltransferases, oxidases, glutathione S-transferases, and GDSL-lipases, among others (**Supplementary Table 4**).

For the combined effects of EC and HT on gene expression, we observed lower number of total DE genes than under EC or HT (**Figure 3C**). EC × HT relative to control treatment decreased the expression of genes for light reactions (two photosystem II polypeptide subunits and some protein kinases associated with state transitions), minor carbohydrate metabolism (galactose mutarotase and two enzymes involved in callose synthesis), glycolysis (two glyceraldehyde 3-phosphate dehydrogenases), mitochondrial electron transport (NADPH:quinone oxidoreductase type 2), lipid degradation (glycerophosphodiester phosphodiesterase), amino acid metabolism (synthesis of chorismate and tryptophan), and secondary metabolism (related to terpenoids, phenylpropanoids, and synthesis of glucosinolates) (**Figure 6**, **Supplementary Figure 4**, **Supplementary Table 4**). In contrast, EC × HT upregulated the gene for sucrose:fructan 6-fructosyltransferase (fructan synthesis), aldose reductase (minor carbohydrate metabolism), xyloglucan endotransglucosylase (cell wall), fatty alcohol oxidase (lipid degradation), and another gene related to the degradation of glucosinolates. In the hormone metabolism, EC × HT only repressed two genes involved in the brassinosteroid signal transduction. The expression of genes for RNA metabolism were modified, with a general downregulation of those related to RNA transcription, binding, some TFs (basic helix-loop-helix and MYB families), an argonaute protein, and a DNA methyltransferases, while other TFs were upregulated (MADS box, MYB, and NAC families) (**Supplementary Table 4**). A few genes with unspecified function were downregulated in DNA metabolism, although some exonucleases and a helicase-like protein were overexpressed. Similar gene families related to protein synthesis, posttranslational modification and degradation, and signaling processes were downregulated under EC × HT relative to control as compared with HT, although the quantity was significantly lower. The transcript abundance of several transporters at the mitochondrial membrane and ABC transporters were altered (up and downregulated) under EC × HT, while those related with the transport of amino acids (amino acid–polyamine transporter), unspecified cations (organic cation/carnitine transporter), potassium (potassium ion transmembrane transporter), a plasma membrane ATP synthase, and a porin were downregulated. A total of 44 stress-responsive genes were downregulated, whereas a few genes of large enzyme families were modified by EC × HT: repression of two genes of cytochrome P450, three oxidases, and one alcohol dehydrogenase, and induction of two cytochrome P450 and two GDSL-lipases (**Supplementary Table 4**)

Functional Enrichment Analysis Using Gene Ontology Terms

To complement functional categories based on MapMan annotations, we evaluated the GO terms associated with the DE genes. A total of 387, 376, and 213 GO terms were related to durum wheat responses to EC, HT, and the EC × HT interaction, respectively (**Supplementary Table 4**). Attending to the GO terms with the highest occurrence under the different environmental growth conditions, we found that the top five high frequency GO terms for molecular function, cellular

component, and biological process were nearly the same for EC, HT, and EC × HT relative to control treatment. These GO terms were transferase activity, nucleotide binding, metal ion binding, oxidoreductase activity, and ATP binding for "molecular function"; cell, membrane, cytoplasm, integral component of membrane, and plasma membrane for "cellular component"; and cellular metabolic process, oxidation–reduction process, transmembrane transport, transcription, and regulation of transcription for "biological process." Therefore, the main differences between the growth conditions were found in many GO terms with low frequency (**Supplementary Table 5**).

DISCUSSION

Elevated CO_2 Enhances Photosynthesis and Shoot Biomass and Leads to Changes in Central C-N Metabolism That Are Accompanied by Marked Changes in the Expression of Genes Involved in Photosynthesis, Amino Acid Metabolism, and Respiration

Photosynthesis has long been recognized as sensitive to environmental conditions. In our study, the exposure to EC enhanced flag leaf photosynthesis in good agreement with the well-documented stimulation of CO_2 assimilation rate in response to CO_2 enrichment in C_3 plants (Long et al., 2004; Ainsworth and Rogers, 2007). Other widely observed response of plants to EC was a decrease in stomatal conductance (g_s) (Long et al., 2004). In FACE experiments, the lower g_s at EC did not appear to be caused by a significant change in stomatal density (Estiarte et al., 1994). Therefore, it is likely that changes in stomatal aperture rather than density determine the response of g_s to EC (Ainsworth and Rogers, 2007). Gene expression analysis showed an increase in transcript abundance for genes annotated as S-type anion channel SLAH3 (SLAC1 homologue 3) and calcium-activated potassium channel, which are components of the guard cell signaling network for stomatal closure in response to CO_2 (Laanemets et al., 2013) and could contribute to the g_s decrease. The greater shoot biomass accumulation was consistent with the increased photosynthetic rate at EC, as we have previously reported (Aranjuelo et al., 2011; Vicente et al., 2015a). Higher fructan and starch contents were also found in the flag leaves, which may be indicative of a sink limitation (Ainsworth et al., 2004). The fructan accumulation was associated with the induction of fructosyltransferases, as reported in rice (Fukayama et al., 2011) and wheat (Vicente et al., 2015a). The increase in photosynthesis caused by EC results in an increase in carbohydrate production, which may alter the C/N balance of wheat plants. Indeed, EC led to a decrease in the shoot N, on a weight and whole-organ basis, as well as the leaf N on a weight basis, suggesting that the plant N content of wheat plants decreased at EC (Taub and Wang, 2008; Aranjuelo et al., 2011), especially in leaf tissues (Seneweera et al., 2011; Gutiérrez et al., 2013; Vicente et al., 2015a). This decrease in N content could be associated with a limitation in N uptake or any other mechanism (del Pozo et al., 2007; Taub and Wang, 2008). Additionally, flag leaf NR activity was significantly decreased by EC. These results reflect that EC directly restrict leaf nitrate reduction, in agreement with other published works with wheat (Bloom et al., 2002; Bloom et al., 2010; Vicente et al., 2015a). However, higher (Vicente et al., 2016) or unaltered (Dier et al., 2017; Torralbo et al., 2019) NR activity in EC has been found. The decline with EC of foliar levels of most organic N compounds, such as Rubisco, amino acids, and soluble proteins, resembles previous findings (Bloom et al., 2002; Pérez et al., 2005; del Pozo et al., 2007; Gutiérrez et al., 2009a; Vicente et al., 2015a) and is consistent with an inhibition of N assimilation (Bloom et al., 2010). The fact that EC repressed the gene encoding glutamate synthase and genes linked to methionine and aromatic amino acid synthesis adds further support to a limitation in the assimilation of inorganic N into amino acids. A decline in foliar glutamine content, along with the increase in sucrose, could contribute to increase NR activation (Scheible et al., 1997; Morcuende et al., 1998). Interestingly, the approximately six-fold stronger induction of the proline synthesis enzyme delta-1-pyrroline-5-carboxylate synthetase by EC could lead to the accumulation of proline, which acts as a compatible osmolyte, protective agent for membranes and enzymes, scavenger of radicals, and/or transient storage form of organic N (Aswani et al., 2019).

The decrease in Rubisco amount, both in absolute terms and as a percentage of total soluble protein, could account for the lower Rubisco activity found in EC (Pérez et al., 2005), even though transcript levels for Rubisco large and small subunits were not altered. These findings indicate that gene transcription was not the only regulator of the enzyme. The maintenance of transcript abundance for Rubisco is consistent with our prior study in field-grown spring wheat at ear emergence (Pérez et al., 2005) and differs from the lower transcript levels found in durum wheat at anthesis (Vicente et al., 2015a), bread wheat (Nie et al., 1995), and rice (Fukayama et al., 2011; Seneweera et al., 2011). It therefore seems unlikely that sugar-mediated repression of Rubisco gene expression plays a dominant role in the loss in Rubisco protein found in our study (Moore et al., 1999), which presumably might be linked to a decrease in the leaf N status (Nakano et al., 1997; Pérez et al., 2005). The decrease in leaf glucose content could alleviate a possible carbohydrate repression of Rubisco gene expression (Moore et al., 1999). Although the foliar level of N compounds was lower under EC, the leaf chl content was not consistently decreased, possibly due to the increased transcripts for magnesium protoporphyrin IX methyltransferase (Alawady and Grimm, 2005). Likewise, two genes encoding light-harvesting complex (LHCII) were induced, whereas a set of genes encoding proteins involved in photosynthetic electron transport, including that encoding the photosystem II PsbR protein, were repressed (Vicente et al., 2015a), which may restrict the photosystem II functioning. Hence, it is tempting to speculate that a preferential decline of the photosystem proteins might be associated with a photo-oxidative damage, promoting proline accumulation to achieve

redox homeostasis and counterbalance the adverse effect of the formation of reactive oxygen species (ROS).

In spite of the repression of a couple of genes encoding the glycolytic enzyme cytosolic glyceraldehyde-3-phosphate dehydrogenase (Vicente et al., 2015a; Vicente et al., 2016), dark respiration rates can be enhanced (Leakey et al., 2009; Markelz et al., 2014) owing to the carbohydrate buildup at EC. This is in line with the observation that genes encoding proteins linked to mitochondrial electron transport chain and transport on the mitochondrial membrane were strongly induced. These included different subunits of the cytochrome c oxidase and mitochondrial ATPase, along with a dicarboxylate transporter. Therefore, our observations are consistent with an enhancement in the leaf respiratory rates to provide C skeletons, energy, and reducing power for N assimilation and other metabolic pathways to ensure maintenance of plant metabolism and growth. Further research is needed to measure dark respiration rate and its relation with the respiratory enzyme activities and the level of primary metabolites.

Elevated CO_2 Also Leads to Widespread Changes in the Expression of Genes for Secondary Metabolism, Hormones, and Transcriptional Regulators

CO_2 enrichment increased transcript levels for several genes linked to phenylpropanoid and isoprenoid biosynthetic pathways, e.g., a gene encoding 4-cuomarate CoA ligase 2 (4CL2), a key enzyme that provides the precursors for the synthesis of a large variety of secondary compounds, such as lignin, flavonoids, or phytoalexins (Stuible et al., 2000). Moreover, EC led to a decrease in transcript abundance for a cellulose synthase-like A protein that polymerizes the 1,4-β–linked backbone of mannans and glucomannans (Liepman and Cavalier, 2012), while increasing transcripts for a gene encoding an expansin-like A1 enzyme. This mediates the cell wall loosening that may contribute to cell wall expansion (Marowa et al., 2016). These data add support to the fact that the cell wall remodeling is vital for plant growth and leaf expansion at EC. Likewise, lignin accumulation may enhance the cell wall mechanical strength and protect against abiotic and biotic stresses (Liu et al., 2018). A large accumulation of secondary metabolites, including phenylpropanoids, alkaloids, glucosinolates, etc., has also been observed in plants exposed to elevated CO_2 (Ghasemzadeh et al., 2010; Klaiber et al., 2013). Similarly, our data at transcriptional level resemble previous work with nitrate deficient tobacco plants that showed a marked decrease in the aromatic amino acid content, together with the induction of genes for secondary metabolism, the accumulation of products of the phenylpropanoid pathway, and the lignification of the stem (Fritz et al., 2006). Overall, the results point to a shift away from N-rich compounds towards increased levels of C-rich metabolites by regulating the distribution of photosynthetic C and assimilation of N to aromatic amino acids and phenylpropanoid biosynthesis, along with the closely related lignin synthesis (Cong et al., 2013). Our finding provides evidence that the impairment of primary metabolism induced by EC may have marked consequences for secondary metabolism, as reported previously in other plant species (Ainsworth et al., 2006).

EC also increased transcripts for a gene encoding a member of DELLA proteins, which promote the expression of downstream negative components of the gibberellin-signaling pathway providing a direct feedback mechanism for regulating gibberellin homeostasis (Zentella et al., 2007). This phytohormone mainly regulates cell elongation as well as other events as flowering and pollen maturation (Davière and Achard, 2013). The upregulation of genes encoding members of the 12-oxo-phytodienoic acid reductase protein family suggests an induction of jasmonic acid synthesis, at variance with the repression found in other studies (Zavala et al., 2008). Genes linked to auxin and ethylene metabolism were repressed (Zavala et al., 2008; Córdoba et al., 2017), as well as others related to brassinosteroids, although an induction has been reported by Jiang et al. (2012). Taken together, these results indicate a complex regulatory hormone metabolism towards growth modulation and adaptation to EC.

In agreement with previous findings by Ainsworth et al. (2006), the gene expression for members of different TF families was found to be influenced by EC, including bHLH, DOF, GATA, NAC, MADS-box, Homeobox, and WRKY, most of them being upregulated. It has recently been reported that WRKY family specifically responded to N deficiency in durum wheat (Curci et al., 2017), suggesting that it might contribute to N stress tolerance. Therefore, we might hypothesize that the transcriptional response of those TFs at EC could be associated to a decrease in the leaf N status.

Interestingly, EC increased transcripts for a set of genes encoding heat shock proteins, mainly HSP70, which act as molecular chaperones protecting proteins from aggregation, contributing to maintenance of protein homeostasis, translocation, and degradation (Wang et al., 2004). This result suggests that EC presumably promotes protein turnover, concurrent with the induction of several genes assigned to protein synthesis/degradation, and posttranslational modifications. Heat shock proteins have also been implicated in regulation of oxidative stress (Wang et al., 2004). In line with this observation, several genes encoding proteins involved in ROS detoxification and protection from oxidative damage were upregulated, as glutathione-S-transferase and β-carotene hydroxylase (You and Chan, 2015). A few orthologues to cytochrome P450 family, which catalyze the oxidation of different compounds in plants and are major players in detoxification of pesticides and other pollutants (Morant et al., 2003), were also upregulated. It is important to highlight that developmental processes are tightly regulated by redox states (Foyer and Noctor, 2011). The proline accumulation could also be related with the control of redox balance, as mentioned above. These findings provide evidence of the activation of a complex network for maintaining redox homeostasis.

Additionally, the transcript levels for several ABC transporters, which are involved in transport of phytohormones, peptides, sugars, alkaloids, inorganic acids, lipids, etc. (Kang et al., 2011), were increased. The upregulation of a gene encoding for

oligopeptide transporter adds further support to the suggestion that protein turnover might occur in the flag leaf with subsequent transportation of N containing compounds, such as peptides. Consistent with this observation and the previous one, our data indicate that protein degradation in leaves is catalyzed by proteases through the proteasome ubiquitin system (Kurepa and Smalle, 2008). EC increased transcripts for a gene encoding a member of the UDP glucosyltransferase protein family. These mediate the transfer of sugars to a wide range of acceptor molecules, thus regulating certain properties such as their bioactivity, solubility, and transport within the cell and throughout the organism (Ross et al., 2001). A gene encoding a sulfate transporter was also induced. Taken together, these results reflect there were changes in cellular transport for maintenance of plant cellular homeostasis and growth in response to EC.

Finally, most of genes annotated as biotic or abiotic stress–related genes were strongly downregulated by EC. It may therefore be inferred that these plants were not subjected to significant stress conditions, in agreement with previous work of ourselves in barley (Córdoba et al., 2017) and of others in sugarcane (De Souza et al., 2008). A similar pattern of changes was also found in the expression of genes related to cellular functions as DNA synthesis and signaling (receptor kinases, sugar, and nutrients), in contrast with previous works (Ainsworth et al., 2006; Córdoba et al., 2017).

High Temperatures Do Not Affect Photosynthesis and Nitrate Reductase Activity, But Decrease the Starch Content and Transcript Levels for Primary and Secondary Metabolism-Related Genes as Well as Those Required for Other Cellular Processes

In our experiment with durum wheat, 4 °C higher than AT did not inhibit photosynthesis, in agreement with our earlier reports in spring (Gutiérrez et al., 2009a) and durum wheat at later growth stages (Vicente et al., 2015a), and consequently had no significant impact on shoot biomass. However, the Rubisco protein content and the activity of the enzyme were decreased (Vu et al., 1997; Pérez et al., 2005), whereas the transcript levels for the Rubisco large subunit were increased. This result differs from the lower transcripts found not only for the Rubisco large subunit (Vicente et al., 2015a), but also for the small subunit in wheat (Pérez et al., 2005; Vicente et al., 2015a) and soybean (Vu et al., 1997). Interestingly, HT increased transcripts for a gene encoding a Rubisco activase, in spite of the usual decrease in Rubisco activation state in many plant species (Salvucci and Crafts-Brandner, 2004). This increase in our experiment could contribute to the maintenance of the Rubisco activation state. Furthermore, HT led to a decline in the starch and fructan contents that was accompanied by an increase in glucose, which may originate from the degradation of the former. These data presumably reflect the stimulation of C mobilization into multiple metabolic pathways and/or other organs for growth rate adjustment at higher temperatures.

Furthermore, there was a decreasing trend in NR activity at HT that was accompanied by similar changes in leaf and shoot N, on a weight and whole-organ basis, whereas the amino acid content remained unaltered and the transcript levels for several amino acid metabolism and nitrate and ammonium transporter genes were decreased. These findings show that HT does not restrict nitrate reduction and further amino acid biosynthesis at ear emergence, in contrast with the decrease reported at later growth stages (Vicente et al., 2015a). The fact that the leaf glucose content increased with HT could contribute to the maintenance of NR activity (Morcuende et al., 1998). Along with these changes, HT led to a general decline of transcripts involved in photosynthesis, cell wall synthesis, C metabolism, glycolysis, TCA cycle, and respiration, in agreement with our previous work (Vicente et al., 2015a). Such decrease was also observed in genes related to secondary metabolism, in contrast to the upregulation found at EC, reflecting a shift away from C-rich secondary metabolites as a mechanism to adjust C requirements according to cellular needs at HT.

Intriguingly, the majority of genes potentially involved in regulation, as those for hormone metabolism, protein kinases and phosphatases, receptor kinases, TFs, etc., were repressed (Bita and Gerats, 2013). The repression of genes involved in cell growth found in our experiments, such as histones and DNA polymerases, has also been reported in other studies (Sakata and Higashitani, 2008). It is worth nothing that moderately warm temperatures can trigger ROS generation and induce oxidative stress responses. Several studies have shown that moderate oxidative stress downregulates the expression of various genes including TFs (Morel and Barouki, 1999). Overall, the results presented here at the transcriptional level suggest that prolonged exposure to moderately warm temperatures have little effect on gene expression as compared to short-term heat stress. Further studies are required to assess the effects of extreme temperature events, rather than a continuous 4°C temperature increase, on photosynthesis, N content, biomass, and gene expression.

The Transcriptional Response Induced by Elevated CO_2 Combined With High Temperature Resembles That Reported for High Temperature Alone, Although It Was Partially Alleviated by Elevated CO_2

In our study, wheat plants grown in EC and HT compared to those grown in AC and AT showed quite similar patterns of physiological and biochemical changes to plants exposed to EC as outlined above. Briefly, combined environmental factors led to a decrease in NR activity that was accompanied by a decline in leaf organic N compounds, including Rubisco protein, chl, and amino acids, whereas fructan content was increased in association with the upregulation of a gene encoding sucrose: fructan 6-fructosyltransferase, as in our prior study (Vicente et al., 2015a). The downregulation of genes linked to the shikimate pathway for the aromatic amino acids synthesis resembles previous findings in rice grown under low N (Xin et al., 2019) and is consistent with an inhibition of N assimilation and a decline in leaf N status.

Despite the repression of several genes involved in photosynthesis, C metabolism, glycolysis, and respiration under combined elevation of the factors studied, only a gene linked to phenylpropanoid and another linked to isoprenoid biosynthetic pathways were repressed, suggesting that possibly secondary metabolism is less sensitive to the effects of combined than separate elevation of these factors. Hence, it is possible that a proportion of excess C was diverted into secondary metabolism under HT and EC compared to HT alone. In addition, the transcript levels for a gene involved in glucosinolate degradation were increased. It is tempting to speculate that plants may catabolize glucosinolates to use the released sulfur to assist primary metabolism, such as protein synthesis in the leaf, allowing a readjustment to adverse conditions. Moreover, a gene encoding xyloglucan endotransglucosylase was induced, contrary to the repression observed at HT alone, which may contribute to cell wall loosening and elongation and the deposition of cellulose under combined factor elevation (Liu et al., 2007). Interestingly, most of the genes related to hormone metabolism remained unaltered compared to HT alone, except for the downregulation of two specific genes encoding brassinosteroids signaling proteins. This fact suggests that the hormonal response is translated into organ growth control (Wolters and Jurgens, 2009). Overall, the transcriptional response of plants to combined EC × HT was similar to, but weaker than, that reported for HT alone, indicating that it was partly attenuated by EC.

CONCLUSIONS

The increasing threat of global warming on agricultural production worldwide requires dissecting the mechanisms that regulate plant responses not only to EC or HT, but also to the interaction of both factors, in order to develop stress-tolerant crops. The transcriptome sequencing is a powerful tool for the identification of relevant metabolic processes and underlying molecular mechanisms in the response of durum wheat to climate change. Confirming the hypothesis of the present study, the use of an integrated approach combining physiological and biochemical traits along with the transcriptome response has reported evidences that the inhibition of N assimilation triggered by EC led to a C/N imbalance in the flag leaf that was accompanied by an induction of secondary metabolism as a mechanism to divert excess C from central metabolism. The reprograming of the mitochondrial electron transport pathway was consistent with increased coupling of respiration to ATP production. It also provides novel information with respect to genes involved in the activation of cell expansion and growth, maintenance of protein homeostasis, and ROS detoxification and protection from oxidative damage in response to EC. In turn, the repression of genes associated to secondary metabolism driven by HT point to a shift away from C-rich secondary metabolites as a mechanism to adjust C requirements for growth under such environmental cue. The biochemical and transcriptional response under combined EC × HT provides new insights into the complex coordination of central metabolism with other secondary metabolic pathways involving plant hormones, transcriptional regulators, etc., in plant acclimation. These findings support that the combination of environmental factors imposes a specific metabolic demand compared to EC or HT alone, demonstrating the ability of plants to respond to complex environmental conditions that may occur under field conditions. This study has identified a comprehensive set of genes involved in modulation of durum wheat responses to future climate change.

DATA AVAILABILITY STATEMENT

The datasets generated for this study can be found in the European Nucleotide Archive (accession number PRJEB34302).

AUTHOR CONTRIBUTIONS

RM-C, PP, and RM conceived and designed the experimental setup, while RV, AB, BU, and RM designed the RNA sequencing analysis. RM-C, PP, EG, and RM conducted most of the physiological and biochemical analyses, while RV and AB carried out the transcriptome analyses. All authors assisted in analyses of data and discussed the results. RV and RM drafted the manuscript, and all authors revised and contributed to writing the manuscript.

FUNDING

This research was supported by the Spanish National R&D&I Plan of the Ministry of Economy and Competitiveness [grants AGL2009-11987, AGL2013-41363-R (ERDF), and AGL2016-79589-R (ERDF)]. R. Vicente and E. Gutiérrez were the recipients of FPI fellowship from the Spanish Ministry of Economy and Competitiveness (BES-2010-031029) and I3P-European Fund fellowship, respectively.

ACKNOWLEDGMENTS

We are grateful to A.L. Verdejo and M.A. Boyero for technical support during physiological and biochemical analysis, and to the staff of the experimental farm of the IRNASA for technical assistance in crop husbandry. We also acknowledge support of the publication fee by the CSIC Open Access Publication Support Initiative through its Unit of Information Resources for Research (URICI).

SUPPLEMENTARY MATERIAL

The Supplementary Material for this article can be found online at: https://www.frontiersin.org/articles/10.3389/fpls.2019.01605/full#supplementary-material

REFERENCES

Ainsworth, E., and Rogers, A. (2007). The response of photosynthesis and stomatal conductance to rising [CO_2]: mechanisms and environmental interactions. *Plant Cell Environ.* 30, 258–270. doi: 10.1111/j.1365-3040.2007.01641.x

Ainsworth, E. A., Rogers, A., Nelson, R., and Long, S. P. (2004). Testing the "source-sink" hypothesis of down-regulation of photosynthesis in elevated [CO_2] in the field with single gene substitutions in *Glycine max*. *Agr For. Meteorol.* 122, 85–94. doi: 10.1016/j.agrformet.2003.09.002

Ainsworth, E. A., Rogers, A., Vodkin, L. O., Walter, A., and Schurr, U. (2006). The effects of elevated CO_2 concentration on soybean gene expression. An analysis of growing and mature leaves. *Plant Physiol.* 142, 135–147. doi: 10.1104/pp.106.086256

Alawady, A. E., and Grimm, B. (2005). Tobacco Mg protoporphyrin IX methyltransferase is involved in inverse activation of Mg porphyrin and protoheme synthesis. *Plant J.* 41, 282–290. doi: 10.1111/j.1365-313X.2004.02291.x

Allen, G., Pereira, L. S., Raes, D., and Smith, M. (2006). Evapotranspiración del cultivo. Guías para la determinación de los requerimientos de agua de los cultivos. Estudio FAO riego y drenaje no.56. Rome: Food and Agriculture Organization of the United Nations.

Aranjuelo, I., Cabrera-Bosquet, L., Morcuende, R., Avice, J. C., Nogués, S., Araus, J. L., et al. (2011). Does ear C sink strength contribute to overcoming photosynthetic acclimation of wheat plants exposed to elevated CO_2? *J. Exp. Bot.* 62, 3957–3969. doi: 10.1093/jxb/err095

Aranjuelo, I., Sanz-Sáez, Á., Jauregui, I., Irigoyen, J. J., Araus, J. L., Sánchez-Díaz, M., et al. (2013). Harvest index, a parameter conditioning responsiveness of wheat plants to elevated CO_2. *J. Exp. Bot.* 64, 1879–1892. doi: 10.1093/jxb/ert081

Araus, J. L., Slafer, G. A., Reynolds, M. P., and Royo, C. (2002). Plant breeding and drought in C_3 cereals: what should we breed for? *Ann. Bot.* 89, 925–940. doi: 10.1093/jxb/err095

Arnon, D. I. (1949). Copper enzymes in isolated chloroplasts. Polyphenoloxidase in *Beta vulgaris*. *Plant Physiol.* 24, 1–15. doi: 10.1104/pp.24.1.1

Asseng, S., Ewert, F., Martre, P., Rotter, R. P., Lobell, D. B., Cammarano, D., et al. (2015). Rising temperatures reduce global wheat production. *Nat. Clim. Change* 5, 143–147. doi: 10.1038/nclimate2470

Aswani, V., Rajsheel, P., Bapatla, R. B., Sunil, B., and Raghavendra, A. S. (2019). Oxidative stress induced in chloroplasts or mitochondria promotes proline accumulation in leaves of pea (*Pisum sativum*): another example of chloroplast-mitochondria interactions. *Protoplasma* 256, 449–457. doi: 10.1007/s00709-018-1306-1

Benlloch-Gonzalez, M., Bochicchio, R., Berger, J., Bramley, H., and Palta, J. A. (2014). High temperature reduces the positive effect of elevated CO_2 on wheat root system growth. *Field Crop Res.* 165, 71–79. doi: 10.1016/j.fcr.2014.04.008

Bita, C. E., and Gerats, T. (2013). Plant tolerance to high temperature in a changing environment: scientific fundamentals and production of heat stress-tolerant crops. *Front. Plant Sci.* 4, 273. doi: 10.3389/fpls.2013.00273

Bloom, A. J., Smart, D. R., Nguyen, D. T., Searles, P. S., Smart, D., Nguyen, D., et al. (2002). Nitrogen assimilation and growth of wheat under elevated carbon dioxide. *P. Natl. Acad. Sci. U.S.A.* 99, 1730–1735. doi: 10.1073/pnas.022627299

Bloom, A. J., Burger, M., Asensio, J. S. R., and Cousins, A. (2010). Carbon dioxide enrichment inhibits nitrate assimilation in wheat and Arabidopsis. *Science* 328, 899–903. doi: 10.1126/science.1186440

Bolger, A. M., Lohse, M., and Usadel, B. (2014). Trimmomatic: a flexible trimmer for Illumina sequence data. *Bioinformatics* 30, 2114–2120. doi: 10.1093/bioinformatics/btu170

Bradford, M. M. (1976). A rapid method for the quantification of microgram quantities of protein utilizaing the principle of protein-dye binding. *Anal. Biochem.* 72, 248–254. doi: 10.1016/0003-2697(76)90527-3

Córdoba, J., Pérez, P., Morcuende, R., Molina-Cano, J.-L., and Martinez-Carrasco, R. (2017). Acclimation to elevated CO_2 is improved by low Rubisco and carbohydrate content, and enhanced Rubisco transcripts in the G132 barley mutant. *Environ. Exp. Bot.* 137, 36–48. doi: 10.1016/j.envexpbot.2017.02.005

Chauhan, H., Khurana, N., Tyagi, A., Khurana, J., and Khurana, P. (2011). Identification and characterization of high temperature stress responsive genes in bread wheat (*Triticum aestivum* L.) and their regulation at various stages of development. *Plant Mol. Biol.* 75, 35–51. doi: 10.1007/s11103-010-9702-8

Chavan, S. G., Duursma, R. A., Tausz, M., and Ghannoum, O. (2019). Elevated CO_2 alleviates the negative impact of heat stress on wheat physiology but not on grain yield. *J. Exp. Bot.* 70, 6447–6459. doi: 10.1093/jxb/erz386

Cong, F., Diehl, B. G., Hill, J. L., Brown, N. R., and Tien, M. (2013). Covalent bond formation between amino acids and lignin: cross-coupling between proteins and lignin. *Phytochemistry* 96, 449–456. doi: 10.1016/j.phytochem.2013.09.012

Curci, P. L., Aiese Cigliano, R., Zuluaga, D. L., Janni, M., Sanseverino, W., and Sonnante, G. (2017). Transcriptomic response of durum wheat to nitrogen starvation. *Sci. Rep.* 7, 1176–1176. doi: 10.1038/s41598-017-01377-0

Davière, J.-M., and Achard, P. (2013). Gibberellin signaling in plants. *Development* 140, 1147. doi: 10.1242/dev.087650

De Souza, A. P., Gaspar, M., Da Silva, E. A., Ulian, E. C., Waclawovsky, A. J., Nishiyama, M. Y.Jr., et al. (2008). Elevated CO_2 increases photosynthesis, biomass and productivity, and modifies gene expression in sugarcane. *Plant Cell Environ.* 31, 1116–1127. doi: 10.1111/j.1365-3040.2008.01822.x

Del Pozo, A., Pérez, P., Gutiérrez, D., Alonso, A., Morcuende, R., and Martínez-Carrasco, R. (2007). Gas exchange acclimation to elevated CO_2 in upper-sunlit and lower-shaded canopy leaves in relation to nitrogen acquisition and partitioning in wheat grown in field chambers. *Environ. Exp. Bot.* 59, 371–380. doi: 10.1016/j.envexpbot.2006.04.009

Dier, M., Meinen, R., Erbs, M., Kollhorst, L., Baillie, C. K., Kaufholdt, D., et al. (2017). Effects of free air carbon dioxide enrichment (FACE) on nitrogen assimilation and growth of winter wheat under nitrate and ammonium fertilization. *Glob. Chang. Biol.* 24, 40–54. doi: 10.1111/gcb.13263

Duan, J., Xia, C., Zhao, G., Jia, J., and Kong, X. (2012). Optimizing de novo common wheat transcriptome assembly using short-read RNA-Seq data. *BMC Genomics* 13, 392. doi: 10.1186/1471-2164-13-392

Estiarte, M., Peñuelas, J., Kimball, B. A., Idso, S. B., Lamorte, R. L., Pinter, P. J., et al. (1994). Elevated CO_2 effects on stomatal density of wheat and sour orange trees. *J. Exp. Bot.* 45, 1665–1668. doi: 10.1093/jxb/45.11.1665

Falda, M., Toppo, S., Pescarolo, A., Lavezzo, E., Di Camillo, B., Facchinetti, A., et al. (2012). Argot2: a large scale function prediction tool relying on semantic similarity of weighted Gene Ontology terms. *BMC Bioinf.* 13, 1–9. doi: 10.1186/1471-2105-13-S4-S14

Fitzgerald, G. J., Tausz, M., O'Leary, G., Mollah, M. R., Tausz-Posch, S., Seneweera, S., et al. (2016). Elevated atmospheric [CO_2] can dramatically increase wheat yields in semi-arid environments and buffer against heat waves. *Glob. Change Biol.* 22, 2269–2284. doi: 10.1111/gcb.13263

Foyer, C. H., and Noctor, G. (2011). Ascorbate and glutathione: the heart of the redox hub. *Plant Physiol.* 155, 2–18. doi: 10.1104/pp.110.167569

Fritz, C., Palacios-Rojas, N., Feil, R., and Stitt, M. (2006). Regulation of secondary metabolism by the carbon-nitrogen status in tobacco: nitrate inhibits large sectors of phenylpropanoid metabolism. *Plant J.* 46, 533–548. doi: 10.1111/j.1365-313X.2006.02715.x

Fukayama, H., Sugino, M., Fukuda, T., Masumoto, C., Taniguchi, Y., Okada, M., et al. (2011). Gene expression profiling of rice grown in free air CO_2 enrichment (FACE) and elevated soil temperature. *Field Crop Res.* 121, 195–199. doi: 10.1016/j.fcr.2010.11.018

Ghasemzadeh, A., Jaafar, H. Z., and Rahmat, A. (2010). Elevated carbon dioxide increases contents of flavonoids and phenolic compounds, and antioxidant activities in Malaysian young ginger (*Zingiber officinale* Roscoe.) varieties. *Molecules* 15, 7907–7922. doi: 10.3390/molecules15117907

Grabherr, M. G., Haas, B. J., Yassour, M., Levin, J. Z., Thompson, D. A., Amit, I., et al. (2011). Full-length transcriptome assembly from RNA-Seq data without a reference genome. *Nat. Biotechnol.* 29, 644–652. doi: 10.1038/nbt.1883

Gutiérrez, D., Gutiérrez, E., Pérez, P., Morcuende, R., Verdejo, A. L., and Martínez-Carrasco, R. (2009a). Acclimation to future atmospheric CO_2 levels increases photochemical efficiency and mitigates photochemistry inhibition by warm temperatures in wheat under field chambers. *Physiol. Plant.* 137, 86–100. doi: 10.1111/j.1399-3054.2009.01256.x

Gutiérrez, E., Gutiérrez, D., Morcuende, R., Verdejo, A. L., and Kostadinova, S. (2009b). Changes in leaf morphology and composition with future increases in CO_2 and temperature revisited: wheat in field chambers. *Physiol. Plant.* 137, 86–100. doi: 10.1007/s00344-009-9102-y

Gutiérrez, D., Morcuende, R., Del Pozo, A., Martínez-Carrasco, R., and Pérez, P. (2013). Involvement of nitrogen and cytokinins in photosynthetic acclimation to elevated CO_2 of spring wheat. *J. Plant Physiol.* 170, 1337–1343. doi: 10.1016/j.jplph.2013.05.006

Habash, D. Z., Kehel, Z., and Nachit, M. (2009). Genomic approaches for designing durum wheat ready for climate change with a focus on drought. *J. Exp. Bot.* 60, 2805–2815. doi: 10.1093/jxb/erp211

Hare, P. E. (1977). Subnanomole-range amino acid analysis. *Methods Enzymol.* 47, 3–18. doi: 10.1016/0076-6879(77)47003-4

Hulsen, T., De Vlieg, J., and Alkema, W. (2008). BioVenn - a web application for the comparison and visualization of biological lists using area-proportional Venn diagrams. *BMC Genomics* 9, 488. doi: 10.1186/1471-2164-9-488

IPCC. (2013). *Climate change 2013: the physical science basis. Contribution of Working Group I to the Fifth Assessment Report of the Intergovernmental Panel on Climate Change* (New York, USA: Cambridge University Press).

IWGSC. (2014). A chromosome-based draft sequence of the hexaploid bread wheat (*Triticum aestivum*) genome. *Science* 345, 1251788. doi: 10.1126/science.1251788

Jauregui, I., Aroca, R., Garnica, M., Zamarreño, Á.M., García-Mina, J. M., Serret, D., et al. (2015). Nitrogen assimilation and transpiration: key processes conditioning responsiveness of wheat to elevated [CO_2] and temperature. *Physiol. Plant.* 155, 338–354. doi: 10.1111/ppl.12345

Jauregui, I., Aparicio-Tejo, P. M., Avila, C., Cañas, R., Sakalauskiené, S., and Aranjuelo, I. (2016). Root–shoot interactions explain the reduction of leaf mineral content in Arabidopsis plants grown under elevated [CO_2] conditions. *Physiol. Plant.* 158, 65–79. doi: 10.1111/ppl.12417

Jiang, Y. P., Cheng, F., Zhou, Y. H., Xia, X. J., Mao, W. H., Shi, K., et al. (2012). Hydrogen peroxide functions as a secondary messenger for brassinosteroids-induced CO_2 assimilation and carbohydrate metabolism in *Cucumis sativus*. *J. Zhejiang Univ. Sci. B.* 13, 811–823. doi: 10.1631/jzus.B120013

Jones, M. G. K., Outlaw, W. H., and Lowry, O. H. (1977). Enzymic assay of 10^{-7} to 10^{-14} moles of sucrose in plant tissues. *Plant Physiol.* 60, 379–383. doi: 10.1104/pp.60.3.379

Kang, J., Park, J., Choi, H., Burla, B., Kretzschmar, T., Lee, Y., et al. (2011). Plant ABC transporters. *The Arabidopsis Book*. 9, e0153–e0153. doi: 10.1199/tab.0153

Klaiber, J., Dorn, S., and Najar-Rodriguez, A. J. (2013). Acclimation to elevated CO_2 increases constitutive glucosinolate levels of Brassica plants and affects the performance of specialized herbivores from contrasting feeding guilds. *J. Chem. Ecol.* 39, 653–665. doi: 10.1007/s10886-013-0282-3

Kumar, R. R., Goswami, S., Sharma, S. K., Kala, Y. K., Rai, G. K., Mishra, D. C., et al. (2015). Harnessing next generation sequencing in climate change: RNA-seq analysis of heat stress-responsive genes in wheat (*Triticum aestivum* L.). *Omics* 19, 632–647. doi: 10.1089/omi.2015.0097

Kurepa, J., and Smalle, J. A. (2008). Structure, function and regulation of plant proteasomes. *Biochimie* 90, 324–335. doi: 10.1016/j.biochi.2007.07.019

Laanemets, K., Wang, Y.-F., Lindgren, O., Wu, J., Nishimura, N., Lee, S., et al. (2013). Mutations in the SLAC1 anion channel slow stomatal opening and severely reduce K^+ uptake channel activity via enhanced cytosolic [Ca^{2+}] and increased Ca^{2+} sensitivity of K^+ uptake channels. *New Phytol.* 197, 88–98. doi: 10.1111/nph.12008

Leakey, A. D. B., Xu, F., Gillespie, K. M., Mcgrath, J. M., Ainsworth, E. A., and Ort, D. R. (2009). Genomic basis for stimulated respiration by plants growing under elevated carbon dioxide. *P. Natl. Acad. Sci. U.S.A.* 106, 3597–3602. doi: 10.1073/pnas.0810955106

Li, H., and Durbin, R. (2009). Fast and accurate short read alignment with Burrows–Wheeler transform. *Bioinformatics* 25, 1754–1760. doi: 10.1093/bioinformatics/btp324

Li, H.-Z., Gao, X., Li, X.-Y., Chen, Q.-J., Dong, J., and Zhao, W.-C. (2013). Evaluation of assembly strategies using RNA-Seq data associated with grain development of wheat (*Triticum aestivum* L.). *PloS One* 8, e83530. doi: 10.1371/journal.pone.0083530

Liepman, A., and Cavalier, D. (2012). The CELLULOSE SYNTHASE-LIKE A and CELLULOSE SYNTHASE-LIKE C families: recent advances and future perspectives. *Front. Plant Sci.* 3, 109. doi: 10.3389/fpls.2012.00109

Liu, Y.-B., Lu, S.-M., Zhang, J.-F., Liu, S., and Lu, Y.-T. (2007). A xyloglucan endotransglucosylase/hydrolase involves in growth of primary root and alters the deposition of cellulose in Arabidopsis. *Planta* 226, 1547–1560. doi: 10.1007/s00425-007-0591-2

Liu, Q., Luo, L., and Zheng, L. (2018). Lignins: biosynthesis and biological functions in plants. *Int. J. Mol. Sci.* 19, 335. doi: 10.3390/ijms19020335

Lohse, M., Nagel, A., Herter, T., May, P., Schroda, M., Zrenner, R., et al. (2014). Mercator: a fast and simple web server for genome scale functional annotation of plant sequence data. *Plant Cell Environ.* 37, 1250–1258. doi: 10.1111/pce.12231

Long, S. P., Ainsworth, E. A., Rogers, A., and Ort, D. R. (2004). Rising atmospheric carbon dioxide: plants FACE the future. *Annu. Rev. Plant Biol.* 55, 591–628. doi: 10.1146/annurev.arplant.55.031903.141610

Markelz, R. J. C., Vosseller, L. N., and Leakey, A. D. B. (2014). Developmental stage specificity of transcriptional, biochemical and CO_2 efflux responses of leaf dark respiration to growth of *Arabidopsis thaliana* at elevated [CO_2]. *Plant Cell Environ.* 37, 2542–2552. doi: 10.1111/pce.12323

Marowa, P., Ding, A., and Kong, Y. (2016). Expansins: roles in plant growth and potential applications in crop improvement. *Plant Cell Rep.* 35, 949–965. doi: 10.1007/s00299-016-1948-4

Moore, B. D., Cheng, S. H., Sims, D., and Seemann, J. R. (1999). The biochemical and molecular basis for photosynthetic acclimation to elevated atmospheric CO_2. *Plant Cell Environ.* 22, 567–582. doi: 10.1046/j.1365-3040.1999.00432.x

Morant, M., Bak, S., Moller, B. L., and Werck-Reichhart, D. (2003). Plant cytochromes P450: tools for pharmacology, plant protection and phytoremediation. *Curr. Opin. Biotechnol.* 14, 151–162. doi: 10.1016/S0958-1669(03)00024-7

Morcuende, R., Krapp, A., Hurry, V., and Stitt, M. (1998). Sucrose-feeding leads to increased rates of nitrate assimilation, increased rates of alpha-oxoglutarate synthesis, and increased synthesis of a wide spectrum of amino acids in tobacco leaves. *Planta* 206, 394–409. doi: 10.1007/s004250050415

Morcuende, R., Kostadinova, S., Pérez, P., Martín Del Molino, I. M., and Martínez-Carrasco, R. (2004). Nitrate is a negative signal for fructan synthesis, and the fructosyltransferase-inducing trehalose inhibits nitrogen and carbon assimilation in excised barley leaves. *New Phytol.* 161, 749–759. doi: 10.1046/j.1469-8137.2004.00990.x

Morel, Y., and Barouki, R. (1999). Repression of gene expression by oxidative stress. *Biochem. J.* 342, 481–496. doi: 10.1042/bj3420481

Nakano, H., Makino, A., and Mae, T. (1997). The effect of elevated partial pressures of CO_2 on the relationship between photosynthetic capacity and N content in rice leaves. *Plant Physiol.* 115, 191–198. doi: 10.1104/pp.115.1.191

Nie, G. Y., Hendrix, D. L., Webber, A. N., Kimball, B. A., and Long, S. P. (1995). Increased accumulation of carbohydrates and decreased photosynthetic gene transcript levels in wheat grown at an elevated CO_2 concentration in the field. *Plant Physiol.* 108, 975–983. doi: 10.1104/pp.108.3.975

Oono, Y., Kobayashi, F., Kawahara, Y., Yazawa, T., Handa, H., Itoh, T., et al. (2013). Characterisation of the wheat (*Triticum aestivum* L.) transcriptome by *de novo* assembly for the discovery of phosphate starvation-responsive genes: gene expression in P_i-stressed wheat. *BMC Genomics* 14, 77. doi: 10.1186/1471-2164-14-77

Oshlack, A., Robinson, M., and Young, M. (2010). From RNA-seq reads to differential expression results. *Genome Biol.* 11, 220. doi: 10.1186/gb-2010-11-12-220

Pérez, P., Morcuende, R., Martín Del Molino, I. M., and Martínez-Carrasco, R. (2005). Diurnal changes of Rubisco in response to elevated CO_2, temperature and nitrogen in wheat grown under temperature gradient tunnels. *Environ. Exp. Bot.* 53, 13–27. doi: 10.1016/j.envexpbot.2004.02.008

Pérez, P., Alonso, A., Zita, G., Morcuende, R., and Martínez-Carrasco, R. (2011). Down-regulation of Rubisco activity under combined increases of CO_2 and temperature minimized by changes in Rubisco k_{cat} in wheat. *Plant Growth Regul.* 65, 439–447. doi: 10.1007/s10725-011-9613-y

Pingault, L., Choulet, F., Alberti, A., Glover, N., Wincker, P., Feuillet, C., et al. (2015). Deep transcriptome sequencing provides new insights into the structural and functional organization of the wheat genome. *Genome Biol.* 16, 29. doi: 10.1186/s13059-015-0601-9

Qin, D., Wu, H., Peng, H., Yao, Y., Ni, Z., Li, Z., et al. (2008). Heat stress-responsive transcriptome analysis in heat susceptible and tolerant wheat (*Triticum aestivum* L.) by using Wheat Genome Array. *BMC Genomics* 9, 432. doi: 10.1186/1471-2164-9-432

Ross, J., Li, Y., Lim, E., and Bowles, D. J. (2001). Higher plant glycosyltransferases. *Genome Biol.* 2, reviews3004.3001–3004.3006. doi: 10.1186/gb-2001-2-2-reviews3004

Sakata, T., and Higashitani, A. (2008). Male sterility accompanied with abnormal anther development in plants-genes and environmental stresses with special reference to high temperature injury. *Int. J. Plant Dev. Biol.* 2, 42–51.

Salvucci, M. E., and Crafts-Brandner, S. J. (2004). Inhibition of photosynthesis by heat stress: the activation state of Rubisco as a limiting factor in photosynthesis. *Physiol. Plant.* 120, 179–186. doi: 10.1111/j.0031-9317.2004.0173.x

Scheible, W. R., González-Fontes, A., Morcuende, R., Lauerer, M., Geiger, M., Glaab, J., et al. (1997). Tobacco mutants with a decreased number of functional *nia* genes compensate by modifying the diurnal regulation of transcription, post-translational modification and turnover of nitrate reductase. *Planta* 203, 304–319. doi: 10.1007/s004250050196

Seneweera, S., Makino, A., Hirotsu, N., Norton, R., and Suzuki, Y. (2011). New insight into photosynthetic acclimation to elevated CO_2: the role of leaf nitrogen and ribulose-1,5-bisphosphate carboxylase/oxygenase content in rice leaves. *Environ. Exp. Bot.* 71, 128–136. doi: 10.1016/j.envexpbot.2010.11.002

Stuible, H., Buttner, D., Ehlting, J., Hahlbrock, K., and Kombrink, E. (2000). Mutational analysis of 4-coumarate:CoA ligase identifies functionally important amino acids and verifies its close relationship to other adenylate-forming enzymes. *FEBS Lett.* 467, 117–122. doi: 10.1016/s0014-5793(00)01133-9

Supek, F., Bošnjak, M., Škunca, N., and Šmuc, T. (2011). REVIGO summarizes and visualizes long lists of gene ontology terms. *PloS One* 6, e21800. doi: 10.1371/journal.pone.0021800

Taub, D. R., and Wang, X. (2008). Why are nitrogen concentrations in plant tissues lower under elevated CO_2? A critical examination of the hypotheses. *J. Integr. Plant Biol.* 50, 1365–1374. doi: 10.1111/j.1744-7909.2008.00754.x

Thimm, O., Bläsing, O., Gibon, Y., Nagel, A., Meyer, S., Kruger, P., et al. (2004). MapMan: a user-driven tool to display genomics data sets onto diagrams of metabolic pathways and other biological processes. *Plant J.* 37, 914–939. doi: 10.1111/j.1365-313X.2004.02016.x

Torralbo, F., Vicente, R., Morcuende, R., González-Murua, C., and Aranjuelo, I. (2019). C and N metabolism in barley leaves and peduncles modulates responsiveness to changing CO_2. *J. Exp. Bot.* 70, 599–611. doi: 10.1093/jxb/ery380

Vicente, R., Pérez, P., Martínez-Carrasco, R., Usadel, B., Kostadinova, S., and Morcuende, R. (2015a). Quantitative RT-PCR platform to measure transcript levels of C and N metabolism-related genes in durum wheat: transcript profiles in elevated [CO_2] and high temperature at different nitrogen supplies. *Plant Cell Physiol.* 56, 1556–1573. doi: 10.1093/pcp/pcv079

Vicente, R., Pérez, P., Martínez-Carrasco, R., Gutiérrez, E., and Morcuende, R. (2015b). Nitrate supply and plant development influence nitrogen uptake and allocation under elevated CO_2 in durum wheat grown hydroponically. *Acta Physiol. Plant* 37, 114. doi: 10.1007/s11738-015-1867-y

Vicente, R., Pérez, P., Martínez-Carrasco, R., Feil, R., Lunn, J. E., Watanabe, M., et al. (2016). Metabolic and transcriptional analysis of durum wheat responses to elevated CO_2 at low and high nitrate supply. *Plant Cell Physiol.* 57, 2133–2146. doi: 10.1093/pcp/pcw131

Vu, J. C. V., Allen, L. H., Boote, K. J., and Bowes, G. (1997). Effects of elevated CO_2 and temperature on photosynthesis and Rubisco in rice and soybean. *Plant Cell Environ.* 20, 68–76. doi: 10.1046/j.1365-3040.1997.d01-10.x

Wang, W., Vinocur, B., Shoseyov, O., and Altman, A. (2004). Role of plant heat-shock proteins and molecular chaperones in the abiotic stress response. *Trends Plant Sci.* 9, 244–252. doi: 10.1016/j.tplants.2004.03.006

Wolters, H., and Jurgens, G. (2009). Survival of the flexible: hormonal growth control and adaptation in plant development. *Nat. Rev. Genet.* 10, 305–317. doi: 10.1038/nrg2558

Xin, W., Zhang, L., Zhang, W., Gao, J., Yi, J., Zhen, X., et al. (2019). An integrated analysis of the rice transcriptome and metabolome reveals differential regulation of carbon and nitrogen metabolism in response to nitrogen availability. *Int. J. Mol. Sci.* 20, 2349. doi: 10.3390/ijms20092349

You, J., and Chan, Z. (2015). ROS regulation during abiotic stress responses in crop plants. *Front. Plant Sci.* 6, 1092–1092. doi: 10.3389/fpls.2015.01092

Zavala, J. A., Casteel, C. L., Delucia, E. H., and Berenbaum, M. R. (2008). Anthropogenic increase in carbon dioxide compromises plant defense against invasive insects. *P. Natl. Acad. Sci. U.S.A.* 105, 5129. doi: 10.1073/pnas.0800568105

Zentella, R., Zhang, Z. L., Park, M., Thomas, S. G., Endo, A., Murase, K., et al. (2007). Global analysis of della direct targets in early gibberellin signaling in Arabidopsis. *Plant Cell* 19, 3037–3057. doi: 10.1105/tpc.107.054999

Conflict of Interest: The authors declare that the research was conducted in the absence of any commercial or financial relationships that could be construed as a potential conflict of interest.

frontiers in Plant Science

ORIGINAL RESEARCH
published: 21 January 2020
doi: 10.3389/fpls.2019.01637

Supplementary Calcium Restores Peanut (*Arachis hypogaea*) Growth and Photosynthetic Capacity Under Low Nocturnal Temperature

Qiaobo Song[1], Yifei Liu[1,2,3,4], Jiayin Pang[2,3], Jean Wan Hong Yong[4,5], Yinglong Chen[2,3], Chunming Bai[6], Clément Gille[4], Qingwen Shi[1], Di Wu[1], Xiaori Han[1], Tianlai Li[1], Kadambot H. M. Siddique[2] and Hans Lambers[2,4,7]*

[1] College of Land and Environment, National Key Engineering Laboratory for Efficient Utilization of Soil and Fertilizer Resources, Northeast China Plant Nutrition and Fertilization Scientific Observation and Research Station for Ministry of Agriculture and Rural Affairs, Key Laboratory of Protected Horticulture of Education Ministry and Liaoning Province, Shenyang Agricultural University, Shenyang, China, [2] The UWA Institute of Agriculture, The University of Western Australia, Perth, WA, Australia, [3] School of Agriculture and Environment, The University of Western Australia, Perth, WA, Australia, [4] School of Biological Sciences, The University of Western Australia, Perth, WA, Australia, [5] Department of Biosystems and Technology, Swedish University of Agricultural Sciences, Alnarp, Sweden, [6] Liaoning Academy of Agricultural Sciences, Shenyang, China, [7] College of Resources and Environmental Sciences, Key Laboratory of Plant-Soil Interactions, Ministry of Education, National Academy of Agriculture Green Development, China Agricultural University, Beijing, China

OPEN ACCESS

Edited by:
Alvaro Sanz-Saez, Auburn University, United States

Reviewed by:
Amy S. Verhoeven, University of St. Thomas, United States
Joel Reyes-Cabrera, Eastern New Mexico University, United States
Juan Liu, Henan Academy of Agricultural Sciences (HNAAS), China

***Correspondence:**
Yifei Liu
yifeiliu6@hotmail.com

Specialty section:
This article was submitted to Plant Abiotic Stress, a section of the journal Frontiers in Plant Science

Received: *12 August 2019*
Accepted: *20 November 2019*
Published: *21 January 2020*

Citation:
Song Q, Liu Y, Pang J, Yong JWH, Chen Y, Bai C, Gille C, Shi Q, Wu D, Han X, Li T, Siddique KHM and Lambers H (2020) Supplementary Calcium Restores Peanut (Arachis hypogaea) Growth and Photosynthetic Capacity Under Low Nocturnal Temperature. Front. Plant Sci. 10:1637. doi: 10.3389/fpls.2019.01637

Peanut (*Arachis hypogaea* L.) is a globally important oil crop, which often experiences poor growth and seedling necrosis under low nocturnal temperatures (LNT). This study assessed the effects of supplementary calcium (Ca^{2+}) and a calmodulin inhibitor on peanut growth and photosynthetic characteristics of plants exposed to LNT, followed by recovery at a higher temperature. We monitored key growth and photosynthetic parameters in a climate-controlled chamber in pots containing soil. LNT reduced peanut growth and dry matter accumulation, enhanced leaf nonstructural carbohydrates concentrations and non-photochemical quenching, decreased the electron transport rate, increased the transmembrane proton gradient, and decreased gas exchange rates. In peanuts subjected to LNT, foliar application of Ca^{2+} restored growth, dry matter production and leaf photosynthetic capacity. In particular, the foliar Ca^{2+} application restored temperature-dependent photosynthesis feedback inhibition due to improved growth/sink demand. Foliar sprays of a calmodulin inhibitor further deteriorated the effects of LNT which validated the protective role of Ca^{2+} in facilitating LNT tolerance of peanuts.

Keywords: peanut, low nocturnal temperature, growth, calcium, photosynthesis

INTRODUCTION

Arachis hypogaea L. (peanut or groundnut), originally from tropical South America (Bolivia and adjoining countries), is primarily grown in tropical and subtropical agro-climatic areas of Asia, Africa, Oceania, and the Americas. It is an important oil crop globally, providing the main source of edible oil and protein in many developing countries (Prasad et al., 2003; Bertioli et al., 2016).

Low-temperature stress, particularly low nocturnal temperature (LNT), is a major limiting factor curtailing productivity and limiting the cultivation distribution of peanuts (Wan, 2003). Tropical and subtropical plants are generally sensitive to chilling stress due to a lack of cold acclimation (Zhu et al., 2007; Liu et al., 2013; Hajihashemi et al., 2018). Low-temperature stress often negatively influences plant growth, development and photosynthetic carbon assimilation, especially during early growth. Low-temperature stress significantly reduced leaf area in rice (Zhou et al., 2018), maize (Wang et al., 2018), sunflower, sorghum (Tardieu et al., 1999) and Chinese crab apple seedlings (Li et al., 2017) and inhibited root growth and dry matter accumulation in maize (Mozafar and Oertli, 1990; Wang et al., 2018). In addition, low-temperature stress reduced the tillering rate and leaf expansion in rice (Huang et al., 2013; Liu et al., 2018) and induced rice spikelet sterility (Haque, 1988). The frequent and intense extreme climate environments of LNT stress followed by warm sunny days are common in temperate peanut-cultivating regions globally, particularly in north China (Wan, 2003). Peanut often experiences poor growth and seedling necrosis under LNT stress, which severely reduces peanut yield and seed quality (Bagnall et al., 1988; Wan 2003,; Liu et al., 2013).

Plants of tropical or subtropical origin are often susceptible to suboptimal, but non-freezing (chilling) temperature environments (Bauer et al., 1985; Damian and Donald, 2001; Zhu et al., 2007; Liu et al., 2013). LNT stress significantly reduces leaf growth and Chl a and Chl b concentrations in grapevine, which has a negative impact on photosynthesis (Bertamini et al., 2005). Photosynthesis is very sensitive to LNT stress (Allen et al., 2000; Yu et al., 2002; Zhang et al., 2014; Hajihashemi et al., 2018). LNT stress inhibits carbon fixation reactions and photosystem II (PSII) repair by suppressing *de novo* synthesis of the D1 protein and photoreaction center activity (Allakhverdiev and Murata, 2004; Murata et al., 2007; Liu et al., 2012). Temperature changes have a strong impact on photosynthetic reactions. When air temperature declined by 10°C, the activity of enzymes associated with carbon assimilation reduced by 50% (Yamori, 2016). The reduced consumption of NADPH results in the subsequent accumulation of reductants downstream of photosystem I (PSI) (Donald et al., 1996; Yamori and Shikanai, 2016). Furthermore, both PSI and PSII accelerate the production of reactive oxygen species under excess excitation energy which causes photoinhibition (Asada, 2006). Plants have a highly responsive regulatory system to prevent photodamage when subjected to chilling stress (Yamori, 2016). In addition to harnessing a non-photochemical quenching (NPQ) mechanism, which serves to dissipate excess excitation energy accumulated in PSII without causing adverse effects; cyclic electron flow (CEF) is another major photoprotection mechanism (Bukhov et al., 1999; Zhang et al., 2014).

Calcium, an essential element for plants, serves not only as a structural component in plant cells but also as a key signaling molecule involved in multiple signal-transduction pathways in its ionic form Ca^{2+} (White and Broadley, 2003; Tian et al., 2019). In particular, calcium has well-documented roles in mediating plant responses to abiotic and biotic stimuli (Cachorro et al., 1994; Skórzyńska-Polit et al., 1998; White and Broadley, 2003; Ding et al., 2018; He et al., 2018; Naeem et al., 2018; Patrick et al., 2018). Low-temperature stress often leads to an increase in free Ca^{2+} in plants, followed by cold-induced protein phosphorylation and the accumulation of the cold acclimation-specific genes that improve the adaptation of plants to cold stress (Monroy and Dhindsa, 1995). In addition, exogenous calcium improves the cold tolerance of plants through two ways: one is the maintenance of the cell membrane and cell wall structure, and an enhanced activity of protective enzymes; the other is the transfer of low-temperature signals which induce the expression of cold-tolerance genes (White and Broadley, 2003; Li et al., 2017). In response to chilling stress, the pre-treatment of exogenous Ca^{2+} significantly improved the physiological response including growth and photosynthesis in low-temperature sensitive plant species such as peanut (Liu et al., 2013), wheat (You et al., 2002), Chinese crab apple (Li et al., 2017) and tomato (Zhang et al., 2014). It is generally believed that plant cell wall, mitochondria and chloroplasts have enormous capacity to store Ca^{2+} (Hepler, 2005; Chen et al., 2015); moderate Ca^{2+} concentrations can sustain cell wall growth and membrane integrity as well as osmotic functioning (Poovaiah and Leopold, 1973; Hepler, 2005; Qu et al., 2012); mitochondrial NADH dehydrogenase activity is regulated by Ca^{2+} (Anderson and Cormier, 1978; Møller et al., 1981); furthermore, the Ca^{2+}/calmodulin is involved in the regulation of NAD kinase and photosynthesis (Jarrett et al., 1982; Rocha and Vothknecht, 2012). In our previous study, exogenous Ca^{2+} enhanced peanut photosynthate production under LNT stress (Liu et al., 2013); however, its underlying physiological mechanisms are largely unknown. Therefore, this study examined the effects of exogenous Ca^{2+} and a

Abbreviations: AL, Actinic light; ATP, Adenosine triphosphate; C_a, Atmospheric CO_2 concentration; C_i, Intercellular CO_2 concentration; CaM, Calmodulin; CEF, Cyclic electron flow; DoT, Days of LNT treatment; DoR, Days of normal temperature recovery; ETR(I), Relative electron transport rate in Photosystem I; ETR(II), Relative electron transport rate in Photosystem II; F, Fluorescence yield measured briefly before application of a saturation pulse; Fo, Minimal fluorescence yield of the dark-adapted sample with all PSII centers open; Fo', Minimal fluorescence yield of the illuminated sample with all PSII centers open; Fm, Maximal fluorescence yield of the dark-adapted sample with all PSII centers closed; Fm', Maximal fluorescence yield of the illuminated sample with all PSII centers closed; Fv/F, Maximal photochemistry efficiency in Photosystem II; FH1, Fenghua 1; g_s, Stomatal conductance; H, Plant height; LA, Leaf area; LNT, Low nocturnal temperature; Ls, Leaf stomatal limitation; NAD, Nicotinamide adenine dinucleotide; NADK, Nicotinamide adenine dinucleotide kinase; NADP, Oxidation form of nicotinamide adenine dinucleotide phosphate; NADPH, Nicotinamide adenine dinucleotide phosphate; NPQ, Non-photochemical quenching; PAR, Photosynthetically active radiation measured in μmol quanta m^{-2} s^{-1}; Pm, Maximal P700 signal'; Pm', Real-time P700 signal under light'; Pn, Net photosynthetic rate'; PPF, Photosynthetic photon flux density'; P_{red}, P700 reduction coefficient under light'; PSI, Photosystem I; PSII, Photosystem II; qE, The energy-dependent component of NPQ; RH, Relative humidity; TFP, Trifluoperazine; Tr, Transpiration rate; WUE, Water-use efficiency; Y(II) = ΦPSII, Actual quantum yield in PSII under light; Y(NO), Non-regulatory quantum yield in PSII under light; Y(NPQ), Regulatory quantum yield in PSII under light; Y(I) = ΦPSI, Actual quantum yield in PSI under light; Y(ND), Quantum yield of PSI non-photochemical energy dissipation due to donor-side limitation; Y(NA), Quantum yield of PSI non-photochemical energy dissipation due to acceptor-side limitation; △pH, Proton gradient; △ψ, Membrane potential.

calmodulin inhibitor, trifluoperazine (TFP, which have been extensively used to demonstrate calmodulin-mediated plant growth response), on the growth and photosynthetic function of peanut exposed to LNT and the following recovery from LNT stress.

MATERIALS AND METHODS

Plant Material and Experimental Design

Fenghua 1, the common high-yielding peanut cultivar in China, was used in this study. Uniform seeds of peanut were pre-germinated in a Petri dish for one day at 27°C and then planted in 32-cavity trays for 7 days before selecting 72 uniform peanut seedlings for transplantation into 72 pots (200 mm height, 260 mm diameter) filled with 4 kg of standard horticultural nutrient substrate (Changchun Xihe Agro-technology co. Ltd, Jilin, China). The pots were then placed in an artificial climate chamber (Conviron, Winnipeg, Canada), with a daytime temperature of 25°C and nocturnal temperature of 20°C at a relative humidity (RH) of 60 ± 5%. All plants received a 12 h daytime photoperiod at a photosynthetic photon flux density (PPFD) of 600 μmol quanta·m^{-2}·s^{-1} and a CO_2 concentration of 400 ± 5 μmol·mol^{-1}. After 3 days of acclimation, the pots were divided equally into four treatment groups: (1) CK (normal nocturnal temperature of 20°C/normal daytime temperature of 25°C + foliar spray of type 1 ultrapure water), (2) LNT (LNT of 10°C/normal daytime temperature of 25°C + foliar spray of type 1 ultrapure water), (3) LNT + Ca (LNT of 10°C/normal daytime temperature of 25°C + foliar spray of 15 mmol·L^{-1} $CaCl_2$) and (4) LNT + TFP (LNT of 10°C/normal daytime temperature of 25°C + foliar spray of 5 mmol·L^{-1} TFP). CK was defined as the normal temperature control group at normal nocturnal temperature (20°C), while the other groups were subjected to LNT (10°C) stress for 5 days (5 DoT, days of LNT treatment). After 5 days of LNT stress, the peanut seedlings from (2), (3), and (4) treatment groups mentioned above were recovered for another 5 days (5 DoR, days of normal temperature recovery) at a normal nocturnal temperature of 20°C and a normal daytime temperature of 25°C to simulate the common cold wave with LNT attack and recession in peanut production.

The optimal levels of exogenous Ca^{2+} (15 mmol·L^{-1} $CaCl_2$) and TFP (5 mmol·L^{-1} TFP), a calmodulin (CaM) inhibitor which disrupts the binding between Ca^{2+}/calmodulin and effector proteins, as well as the application technique, were established in a previous experiment (Liu et al., 2013). Leaves were sprayed carefully and evenly using moisture sprayers 3 days before the LNT stress (twice a day for 3 days). The LNT treatments were subjected to 12 h (from 18:00 to 6:00 h) LNT treatments at 10°C by transferring the peanut seedlings to an artificial climate chamber (Conviron, Winnipeg, Canada).

Plant Sampling and Measurements

Three peanut seedlings per treatment were sampled twice—after 5 days of LNT treatment (5 DoT, days of LNT treatment) and after another 5 days of recovery from LNT stress (5 DoR, days of normal temperature recovery) for the measurement of leaf area and photosynthetic pigments. Leaf area was measured using an LI-3000C (LI-COR Biosciences, Lincoln NE, USA). Chlorophyll a, chlorophyll b and carotenoid concentrations of the third youngest fully expanded leaves were determined using the spectrophotometer method (Lichtenthaler, 1987). Another six peanut seedlings from each treatment were sampled at 5 DoT and 5 DoR. All samples were oven-dried at 105°C for 30 min and then at 70°C to a constant weight. In addition, oven-dried leaflets from the third youngest fully expanded leaves of six peanut seedlings per treatment were pooled in three biological replicates and ground to a powder, and a total of three biological replicates/pools (six peanut seedlings) were used for carbohydrates measurements. Soluble sugars were extracted from approximately 100 mg of the oven-dried leaf powder with 80% (v/v) ethanol at 85°C and quantified using the microtiter method (Hendrix, 1993). Pellets containing starch were oven-dried overnight at 60°C. Starch in the pellet was first gelatinized by addition of 1 ml of 0.2 mol·l^{-1} KOH and incubated in a boiling water bath for 30 min (Rufty and Huber, 1983). After cooling, 0.2 ml of 1 mol·l^{-1} acetic acid was added, and the solution incubated with 2 ml acetate buffer (pH 4.6) containing amyloglucosidase (six units, Roche) at 55°C for 1 h. The reaction was terminated in a boiling water bath, and the resulting supernatant analyzed for glucose.

Leaf gas exchange was measured on the third youngest fully expanded leaves using an open system of gas exchange equipment (GFS-3000, Heinz Walz GmbH, Effeltrich, Germany) at 1, 3, and 5 DoT and 1, 3, and 5 DoR. During gas exchange measurements, the leaf cuvette temperature was set to 25°C and 60% RH. The CO_2 concentration was maintained at 400 μmol·mol^{-1}. An LED array provided a PPFD of 600 μmol quanta·m^{-2}·s^{-1}. The third youngest fully expanded leaf was kept in the chamber by ensuring the thermocouple touching it from the underside. Gas exchange parameters included net photosynthetic rate (Pn), stomatal conductance (g_s), atmospheric CO_2 concentration (C_a), transpiration rate (Tr), intercellular CO_2 concentration (C_i), water-use efficiency (WUE = Pn/Tr), and leaf stomatal limitation ($Ls = 1 - C_i/C_a$).

The software Dual-PAM v1.19 was used to control the Dual-PAM 100 measuring system (Heinz Walz, Effeltrich, Germany) and measure chlorophyll fluorescence and P700 parameters on the third youngest fully expanded leaf (*ca.* 1 cm^2); all steps were carried out in accordance with the standard protocols provided by the manufacturer (Heinz Walz, Effeltrich, Germany) and earlier research (Shi et al., 2019). The fluorescence slow-kinetics were measured after a dark adaptation of 30 min. The intensity of saturation pulse light (red light) and actinic light (red light) were set as 10,000 and 132 μmol quanta·m^{-2}·s^{-1}, respectively. Chlorophyll fluorescence parameters were calculated as follows: Fo and Fm are the minimum and maximum fluorescence yields of the dark-adjusted sample with all PSII center open and closed, respectively. Fo' and Fm' are the minimum and maximum fluorescence yield of the illuminated sample with some PSII center open and closed, respectively. F is the fluorescence yields measured briefly before applying a saturation pulse. Fv/Fm = (Fm – Fo)/Fm indicates the maximal/intrinsic photochemical efficiency of PSII (Kitajima and Butler, 1975). Y(II) = (Fm′– F)/Fm is the actual quantum

yield of PSII (Genty, 1989). Y(NO) = F/Fm is the non-regulated energy loss in PSII. Y(NO) represents the fraction of energy that is dissipated as heat and fluorescence, and high values of Y(NO) reflects the inability of the plant to protect itself against damage by excess excitation (Cailly et al., 1996; Klughammer and Schreiber, 2008). Y(NPQ) = 1 – Y(II) – Y(NO) is the regulatory quantum yield in PSII and represents the fraction of energy dissipated in the form of heat through the regulated photoprotective NPQ mechanism (Kramer et al., 2004). ETR (II) = PAR·Y(II)·0.84·0.5 is the relative electron transfer rate in PSII. PAR (μmol quanta·m^{-2}·s^{-1}) is photosynthetically active radiation (Genty, 1989; Schreiber et al., 1995).

The PSI photosynthetic parameters were measured using a Dual-PAM 100 device based on the P700 signal (absorption differences between 830 and 875 nm). The quantum yields of PSI were determined using the saturation pulse method (Klughammer and Schreiber, 1994). The P700 parameters were calculated as follows: Y(NA) = (Pm – Pm′)/Pm is the quantum yield of PSI non-photochemical energy dissipation due to the acceptor-side limitation. Y(ND) = 1 – $P700_{red}$ is the quantum yield of PSI non-photochemical energy dissipation due to the donor-side limitation (Cailly et al., 1996). Y(I) = 1 – Y(NA) – Y(ND) is the actual quantum yield in PSI under light (Klughammer and Schreiber, 1994; Klughammer and Schreiber, 2008). ETR(I) = PAR·Y(I)·0.84·0.5 is the relative electron transfer rate in PSI (Klughammer and Schreiber, 2008). Pm is the maximum oxidation state of PSI under far-red light (720 nm). Pm' is the maximum oxidation state of PSI under actinic light (420 nm). $P700_{red}$ is the P700 reduction parameter under the light. The CEF was estimated as CEF = ETR(I) – ETR(II). Similarly, Y(CEF)/Y (II) = [Y(I) – Y(II)]/Y(II) was calculated as the ratio of the quantum yield of CEF to Y(II) and later used to estimate cyclic electron transfer (Munekage et al., 2002; Yamori and Shikanai, 2016).

The dual-beam 550 nm to 515 nm difference signal (electrochromic shift) was monitored simultaneously using the P515/535 module of the Dual-PAM 100 (Klughammer and Schreiber, 2008; Zhang et al., 2014). Three independent peanut seedlings per treatment were selected at 5 DoT for the determination of the following indicators. After 1 h of dark acclimation, P515 changes induced by saturating single turnover flashes were recorded to evaluate thylakoid membrane integrity. After 10 min of pre-illumination at 600 μmol quanta·m^{-2}·s^{-1} and 4 min of dark acclimation, P515 changes induced by saturating single turnover flashes were recorded to evaluate ATP-synthase activity. Slow dark–light–dark induction transients of the 550 to 515 nm signals reflected changes in membrane potential (electrochromic pigment absorbance shift). Actinic light (AL; 600 μmol quanta·m^{-2}·s^{-1}) was turned on at 30 s and off at 330 s.

Statistical Analysis

Statistical analyses were carried out using one-way ANOVA in SPSS 19.0. A total of 72 uniform peanut seedlings were included in this study, which were allocated to four different treatments (i.e. 18 seedlings per treatment). Three out of the 18 peanut seedlings per treatment were used for the non-destructive measurement of leaf gas exchange, chlorophyll fluorescence and P700 parameters. The remaining peanut seedlings per treatment were used for the destructive sampling for peanut seedlings growth observation and photography as well as the measurement of leaf area, biomass accumulation, photosynthetic pigments concentrations, and carbohydrates. The results were presented as mean values and standard error of three biological replicates. Post-hoc LSD tests at $P = 0.05$ were performed to highlight the differences among the four treatments. The significant differences P-value is indicated as the *($P \leq 0.05$) and **($P \leq 0.01$), respectively, among the treatments.

RESULTS

Effect of Exogenous Calcium (Ca^{2+}) and a Calmodulin Inhibitor (TFP) on Peanut Growth After 5 Days of Low Nocturnal Temperature Stress Followed by 5 Days of Recovery

The LNT treatment significantly inhibited peanut growth, which did not recover after 5 days of recovery (**Figure 1**). Exogenous Ca^{2+} application (LNT + Ca) counteracted the LNT stress and benefited the recovery process. The calmodulin inhibitor (LNT + TFP) further reduced peanut growth and biomass when compared with LNT (**Figure 1**).

The LNT treatment significantly decreased leaf area in peanut. The LNT + Ca treatment had more leaf area than the LNT treatment, while the LNT + TFP treatment had less. LNT stress reduced dry matter accumulation in the roots, stems and leaves. The LNT + Ca treatment significantly increased root, stem and leaf dry weights, relative to LNT. The control (CK) had the highest chlorophyll a and b concentrations, followed by LNT + Ca and LNT, with the lowest in LNT + TFP. LNT stress significantly reduced the chlorophyll a and b concentrations while had no significant effect on the carotenoid level. LNT + Ca significantly enhanced the chlorophyll a and b concentrations in peanuts leaves. No significant difference in carotenoid concentration was observed among the four treatments at either 5 DoT or 5 DoR (**Table 1**).

Effect of Exogenous Calcium (Ca^{2+}) and a Calmodulin Inhibitor (TFP) on Soluble Sugar, Starch and Total Nonstructural Carbohydrates Concentrations of Peanut Leaves After 5 Days of Low Nocturnal Temperature Stress Followed by 5 Days of Recovery

The LNT treatment significantly increased the concentration of soluble sugars in leaves at 5 DoT (**Figure 2A**); the LNT + Ca treatment produced lower and the LNT + TFP treatment produced higher concentrations of soluble sugars than the LNT treatment. The CK treatment had the lowest concentrations of starch and total nonstructural carbohydrates at 5 DoT, followed by LNT + Ca and LNT, and LNT + TFP with the highest (**Figures 2B, C**). Soluble sugar, starch and total nonstructural carbohydrate concentrations did not differ between treatments at 5 DoR.

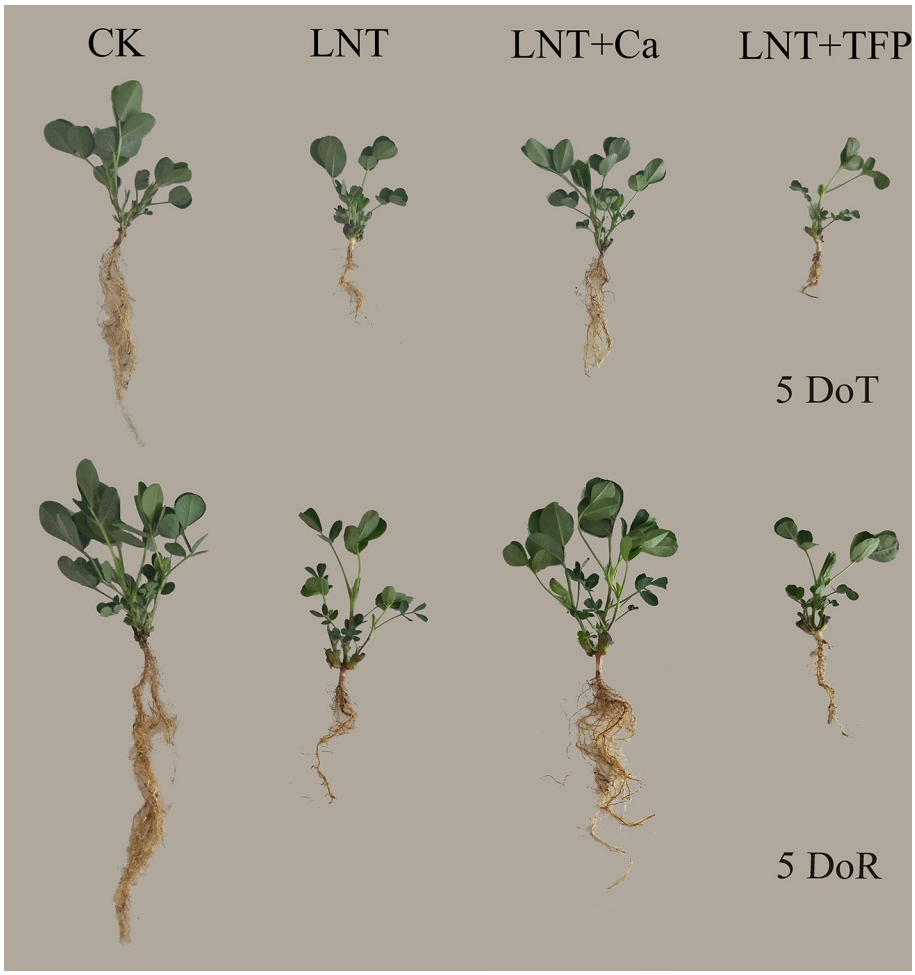

FIGURE 1 | Effect of exogenous calcium (Ca^{2+}) and a calmodulin inhibitor (TFP) on peanut growth after 5 days of low nocturnal temperature (LNT) (5 DoT) followed by 5 days of recovery (5 DoR). CK, normal nocturnal temperature of 20°C/normal daytime temperature of 25°C + foliar spray of type 1 ultrapure water; LNT, low nocturnal temperature of 10°C/normal daytime temperature of 25°C + foliar spray of type 1 ultrapure water; LNT + Ca, low nocturnal temperature of 10°C/normal daytime temperature of 25°C + foliar spray of 15 mmol·l^{-1} $CaCl_2$; LNT + TFP, low nocturnal temperature of 10°C/normal daytime temperature of 25°C + foliar spray of 5 mmol·l^{-1} TFP.

TABLE 1 | Effect of exogenous calcium (Ca^{2+}) and a calmodulin inhibitor (TFP) on peanut leaf area, dry matter and pigment concentrations (chlorophyll a and b, carotenoid) after 5 days low nocturnal temperature (LNT) (5 DoT) followed by 5 days of recovery (5 DoR).

Time	Treatments	Leaf area (cm^2)	Dry weight (mg) Root			Chlorophyll a concentration ($mg·g^{-1}$)	Chlorophyll b concentration ($mg·g^{-1}$)	Carotenoid concentration ($mg·g^{-1}$)
			Root	Stem	Leaf			
5 DoT	CK	52.7 ± 0.4a	215 ± 1a	527 ± 7a	480 ± 6a	1.56 ± 0.02a	0.81 ± 0.02a	0.24 ± 0.01a
	LNT	38.9 ± 0.8c	87 ± 3c	309 ± 8c	345 ± 5c	1.38 ± 0.01c	0.66 ± 0.01c	0.27 ± 0.02a
	LNT + Ca	46.5 ± 0.4b	147 ± 2b	401 ± 7b	410 ± 7b	1.47 ± 0.01b	0.73 ± 0.01b	0.26 ± 0.01a
	LNT + TFP	32.8 ± 0.2d	70 ± 3d	256 ± 7d	284 ± 8d	1.33 ± 0.01d	0.61 ± 0.02d	0.25 ± 0.01a
5 DoR	CK	79.8 ± 0.3a	360 ± 6a	932 ± 15a	784 ± 15a	1.79 ± 0.03a	0.93 ± 0.02a	0.28 ± 0.01a
	LNT	53.5 ± 0.8c	161 ± 3c	761 ± 10c	569 ± 15c	1.45 ± 0.01b	0.74 ± 0.02c	0.32 ± 0.01a
	LNT + Ca	65.7 ± 1.5b	207 ± 3b	836 ± 17b	644 ± 21b	1.72 ± 0.05a	0.87 ± 0.01b	0.29 ± 0.01a
	LNT + TFP	48.3 ± 1.3d	132 ± 1d	751 ± 8c	441 ± 20d	1.41 ± 0.01b	0.67 ± 0.01d	0.29 ± 0.02a

Values are means of three biological replicates ± SE (n = 3). Different letters (a, b, c, d) in the same column indicate significant differences among the treatments by LSD test (P ≤ 0.05).

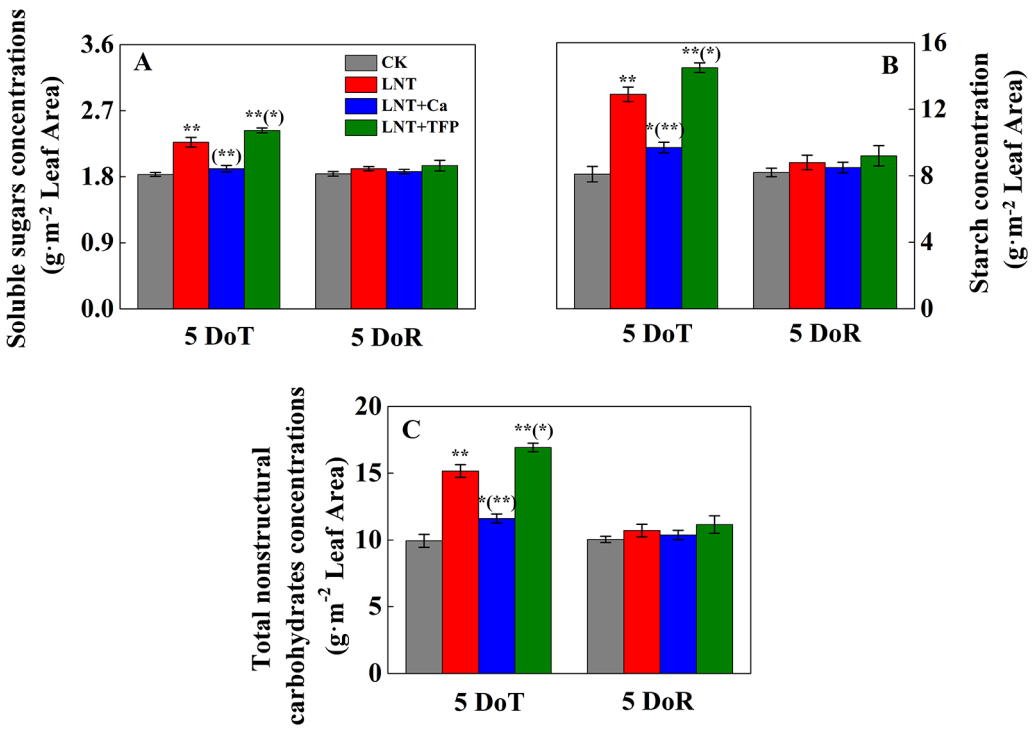

FIGURE 2 | Effect of exogenous calcium (Ca^{2+}) and a calmodulin inhibitor (TFP) on the concentration of soluble sugars **(A)**, starch **(B)** and total nonstructural carbohydrates **(C)** after 5 days of low nocturnal temperature (LNT) (5 DoT) followed by 5 days of recovery (5 DoR). Values are means of three biological replicates ± SE (n = 3). * and ** indicate significant differences at $P \leq 0.05$, and $P \leq 0.01$, respectively, among the treatments. The significance between the three treatments under LNT and CK at 5 DoT and 5 DoR was shown in parenthesis.

Effect of Exogenous Calcium (Ca^{2+}) and a Calmodulin Inhibitor (TFP) on Gas Exchange During 5 Days Low Nocturnal Temperature Stress Followed by 5 Days of Recovery

Leaf gas exchange parameters did not differ between treatments at 1 DoT, but CK and LNT differed at 3 and 5 DoT. The LNT treatment reduced Pn, g_s, Tr, and Ls (**Figure 3**) and increased C_i significantly. Compared with LNT, LNT + Ca significantly increased Pn, g_s, Tr, and Ls and decreased C_i while LNT + TFP significantly reduced Pn, g_s, Tr, and Ls, but increased C_i further. During the 5 days recovery at a normal nocturnal temperature, LNT-treated plants continued to increase Pn, g_s, Tr, and Ls and decrease C_i. The same pattern was observed for LNT + Ca but at a slightly lower level.

Effect of Exogenous Calcium (Ca^{2+}) and a Calmodulin Inhibitor (TFP) on Peanut Photosystem Activities During 5 Days of Low Nocturnal Temperature Stress Followed by 5 Days of Recovery

The maximum quantum yield of PSII (Fv/Fm) declined markedly under LNT stress (**Figure 4**). In particular, the Fv/Fm of the LNT + Ca treatment recovered fully by 5 DoR, it was significantly higher than that of LNT and LNT + TFP.

The LNT treatment decreased Y(II) significantly (**Figure 5A**). The actual quantum yield of PSII in LNT treatments declined significantly and dissipated excess energy by gradually increasing Y(NPQ), the regulatory quantum yield of PSII (**Figure 5B**). Y(II) tended to decrease gradually with the onset of LNT stress. The heat dissipation was not enough to dissipate the excess excitation energy in LNT treatments. Consequently, Y(NO) increased to a higher level (**Figure 5C**). During the 5 days recovery at a normal nocturnal temperature, Y(II) recovered gradually, while Y(NO) and Y(NPQ) decreased slowly. In general, the PSII self-repair process in the LNT + Ca treatment was significantly greater than that in the LNT and LNT + TFP treatments. LNT stress decreased Y(I) and increased Y(NA) (**Figures 5D, F**). At 1 DoT, Y(ND) did not differ between treatments (**Figure 5E**), increasing gradually during the LNT stress; by 5 DoT, the LNT + Ca treatment had higher Y(ND) than LNT and LNT + TFP (**Figure 5E**). At 5 DoT, the LNT + Ca treatment had significantly higher Y(I) and lower Y (NA) than LNT, while the LNT + TFP treatment had significantly higher Y(NA) and lower Y(I) than LNT. During the recovery, Y (ND) did not differ between treatments. It is noteworthy that Y (NA) and Y(I) in the LNT and LNT + TFP treatments were partially restored during the recovery, but not to the same levels as those in LNT + Ca and CK (**Figures 5D, F**).

The LNT treatment reduced ETR(II) and ETR(I) and enhanced CEF and Y(CEF)/Y(II) (**Figure 6**). Compared with

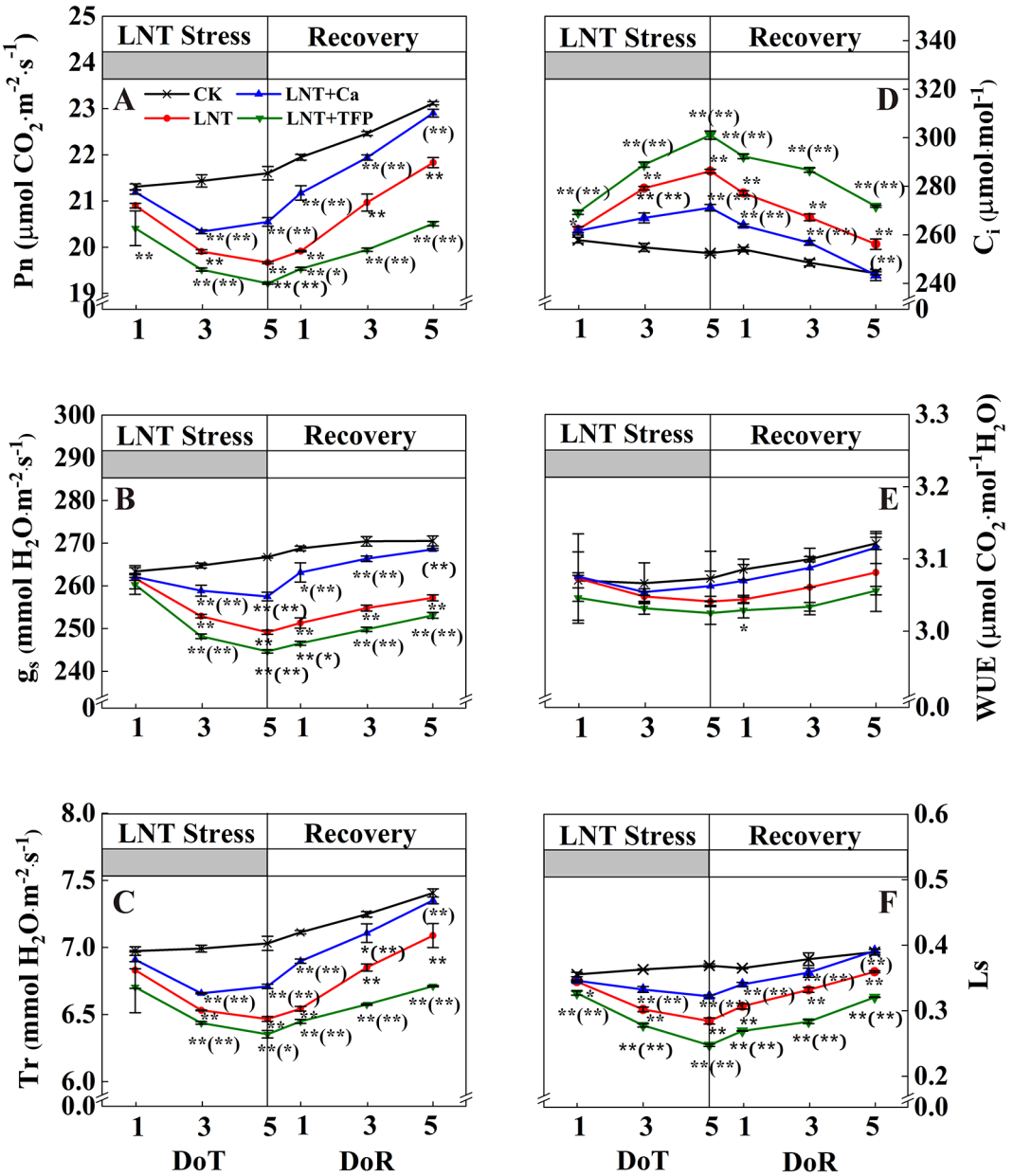

FIGURE 3 | Effect of exogenous calcium (Ca^{2+}) and a calmodulin inhibitor (TFP) on peanut gas exchange characteristics [net photosynthetic rate (Pn, **A**), stomatal conductance (g_s, **B**), transpiration rate (Tr, **C**), intercellular CO_2 concentration (C_i, **D**), water-use efficiency (WUE, **E**) and leaf stomatal limitation (Ls, **F**)] during 5 days of low nocturnal temperature (1, 3, and 5 DoT) followed by 5 days of recovery (1, 3 and 5 DoR). Values are means of three biological replicates ± SE (n = 3). * and ** indicate significant differences at $P \leq 0.05$, and $P \leq 0.01$, respectively, among the treatments. The significance between the three treatments under LNT and CK was shown in parenthesis.

LNT, LNT + Ca had higher ETR(II), ETR(I), CEF and Y(CEF)/Y (II), while LNT + TFP had lower ETR(II), ETR(I), CEF and Y (CEF)/Y(II). During the recovery, ETR(II) and ETR(I) of LNT and LNT + Ca treatments increased rapidly, while CEF and Y (CEF)/Y(II) decreased, more so in LNT + Ca. At 5 DoR, ETR(II) and ETR(I) of LNT + TFP had not recovered to the control level and were significantly lower than those of the other treatments.

Effect of Exogenous Calcium (Ca^{2+}) and a Calmodulin Inhibitor (TFP) on the Proton Motive Force, Thylakoid Membrane Integrity and ATP-Synthase Activity of Peanut Leaves After Low Nocturnal Temperature Stress

The LNT treatment significantly reduced thylakoid membrane integrity and ATPase activity, based on P515 signals

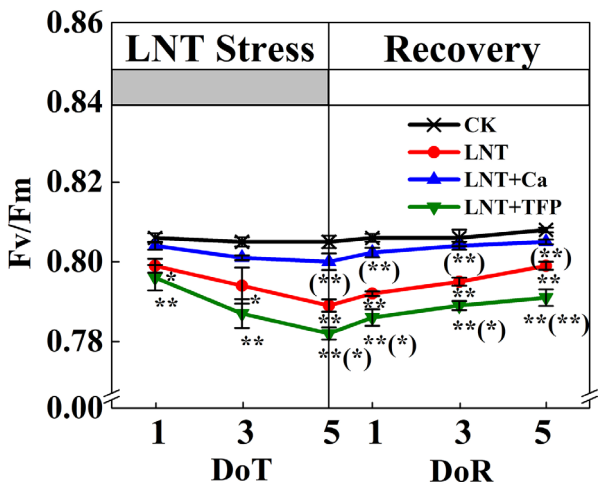

FIGURE 4 | Effect of exogenous calcium (Ca^{2+}) and a calmodulin inhibitor (TFP) on peanut maximum quantum yield of PSII (Fv/Fm) during 5 days of low nocturnal temperature (LNT) stress followed by 5 days of recovery. Values are means of three biological replicates ± SE (n = 3). * and ** indicate significant differences at $P \leq 0.05$, and $P \leq 0.01$, respectively, among the treatments. The significance between the three treatments under LNT and CK was shown in parenthesis.

(**Figures 7A, B**). The LNT + Ca treatment maintained thylakoid membrane integrity and ATPase activity in peanut leaves, while LNT + TFP further exacerbated thylakoid membrane damage. The LNT treatment also reduced thylakoid membrane potential ($\Delta\psi$) and increased transmembrane proton potential (ΔpH) (**Figures 7C, D**). Compared with LNT, LNT + Ca increased $\Delta\psi$ and decreased ΔpH markedly, while LNT + TFP had the opposite effect.

DISCUSSION

Effect of Low Nocturnal Temperature on Peanut Growth and Photosynthetic Capacity

We demonstrated that LNT stress significantly inhibited peanut growth, which could not be fully restored during the recovery period (**Figure 1**). Previous studies also showed that, below the peanut threshold temperature of 15°C, the leaves usually exhibit poor growth and necrotic injury in the field (Wan, 2003). Exposing peanuts to a dark chilling environment significantly inhibits seedling growth, with reduced leaf area and shoot and root dry matter accumulation (Solanke and Sharma, 2008; Dias et al., 2011; Hajihashemi et al., 2018). While leaf expansion rates generally vary with air temperature, low-temperature stress can reduce the rates of leaf initiation and expansion and final leaf area in sunflower, maize and sorghum (Tardieu et al., 1999). LNT stress also reduced leaf growth, the concentration of photosynthetic pigments and the shoot and root dry matter accumulation in tomato (Latef and He, 2011; Liu et al., 2011), and damaged leaf structure and growth in tobacco (Kasuga et al., 2004). In addition, our results showed that LNT stress increased soluble sugar, starch and total nonstructural carbohydrate concentrations in peanut leaves (**Figure 2**). The accumulation of leaf end-products (soluble sugars, starch) is important for balancing photosynthesis and the use of sugars for growth. In particular, there is a close two-way relationship between photosynthesis and growth, rather than a simple dependence of growth on photosynthesis. Carbohydrate synthesis occurs in photosynthetically active leaves (sources); sugars are then exported to support sinks (e.g., for leaf expansion, stem and root growth) (Adams et al., 2013; Cohu et al., 2014). Our results suggested that LNT stress directly inhibits peanut growth and source-to-sink sugar transport, and induces the accumulation of nonstructural carbohydrates in leaves (**Figure 2**), which is consistent with the previous findings in maize (Adams et al., 2013).

LNT stress significantly reduced photosynthetic activity in this study (**Figure 3**). Photosynthesis is the principal process of capturing light energy to form carbohydrates and is very sensitive to the low-temperature environment (Adams and Demmig-Adams, 2004; Stewart et al., 2016). Particularly, we found that the effects of LNT on peanut photosynthesis might be mainly due to reduced peanut growth and leaf expansion, and the export of nonstructural carbohydrates as we only exposed the peanuts to low-temperature during the nocturnal phase. Compared with the normal temperature control, transpiration and photosynthetic rates decreased in response to LNT stress, while intercellular CO_2 concentration increased (**Figure 3**) which is consistent with findings in maize (Zhu et al., 2010). Photosynthesis and transpiration are often tightly linked, as they both depend on stomatal conductance (Wong et al., 1979; Gago et al., 2016). Based on our results (**Figure 3**), LNT stress had a negative impact on photosynthesis in peanut leaves due to non-stomatal limitations, because C_i increased and Ls decreased. The results from the present study are consistent with previous studies on tomato and coffee tree (Bauer et al., 1985; Allen et al., 2000). The non-stomatal limitation was reported previously and attributed to a reduced rate of RuBP regeneration. There are three plausible reasons when RuBP regeneration becomes limiting under low-temperature environment: (i) limitation of the rate at which light-harvesting and electron transport produce ATP and NADPH; (ii) limitation of the rate at which the stromal bisphophatases regenerate RuBP in the photosynthetic carbon reduction cycle; or (iii) restriction of the rate at which end-product synthesis consumes triose-phosphates and regenerates inorganic phosphate (Pi) for photophosphorylation (Allen et al., 2000; Allen and Ort 2001; Usuda et al., 2006). Taken together, the non-stomatal limitation might be the dominant factor contributing to the down-regulation of photosynthesis under LNT stress.

Our study showed that LNT stress decreased Fv/Fm in peanut, based on chlorophyll fluorescence signal as subtle reflections of the primary reactions of photosynthesis (**Figure 4**). Other studies also suggest that LNT stress followed by warm sunny days with high light can induce severe photoinhibition in tomato and grapevine (Bertamini et al., 2006; Liu et al., 2012). In addition,

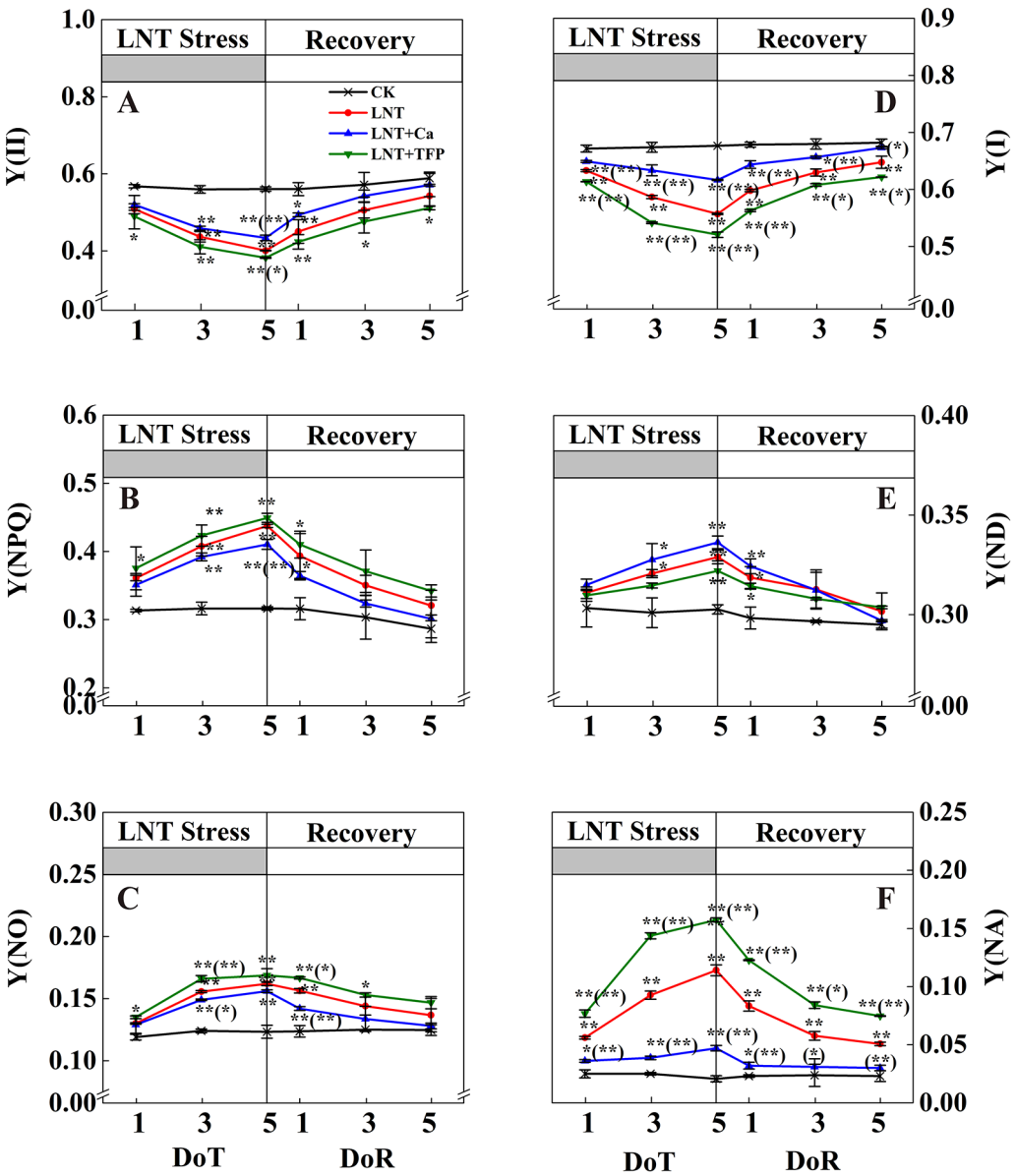

FIGURE 5 | Effect of exogenous calcium (Ca^{2+}) and a calmodulin inhibitor (TFP) on peanut photosystems parameters during 5 days of low nocturnal temperature (LNT) stress followed by 5 days of recovery. **(A)** Y(II): PSII photochemistry effective quantum yield; **(B)** Y(NPQ): PSII regulated energy dissipation quantum yield; **(C)** Y (NO): PSII non-regulated energy dissipation quantum yield; **(D)** Y(I): PSI photochemistry effective quantum yield; **(E)** Y(ND): PSI non-photochemical energy dissipation due to the donor-side limitation; **(F)** Y(NA): PSI non-photochemical energy dissipation due to the acceptor-side limitation. Values are means of three biological replicates ± SE (n = 3). * and ** indicate significant differences at $P \leq 0.05$, and $P \leq 0.01$, respectively, among the treatments. The significance between the three treatments under LNT and CK was shown in parenthesis.

chilling stress causes irreversible photoinhibition in leaves of other chilling-sensitive plants such as chickpea and cucumber (Sonoike, 1999; Turan and Ekmekçi, 2011). In particular, we found that the effects of LNT on peanut photosynthesis were mediated through sink feedback thereby down-regulating photosynthesis, but induced significant photoinhibition in peanuts leaves. Our interpretation was consistent with previous findings that insufficient sink activity and growth inhibition can lead to severe accumulation of foliar carbohydrates and leading to photoinhibition (Adams et al., 2013). Indeed, the low temperature can inhibit the activities of photosynthetic reaction centers, thus restricting the electron transport chain and carbon fixation rate (Kasuga et al., 2004; Baker, 2008). Our results also showed that thylakoid membranes integrity and ATPase activity decreased during LNT stress (**Figure 7**). LNT stress indirectly increased Y(NO)—the non-regulated energy loss in PSII—

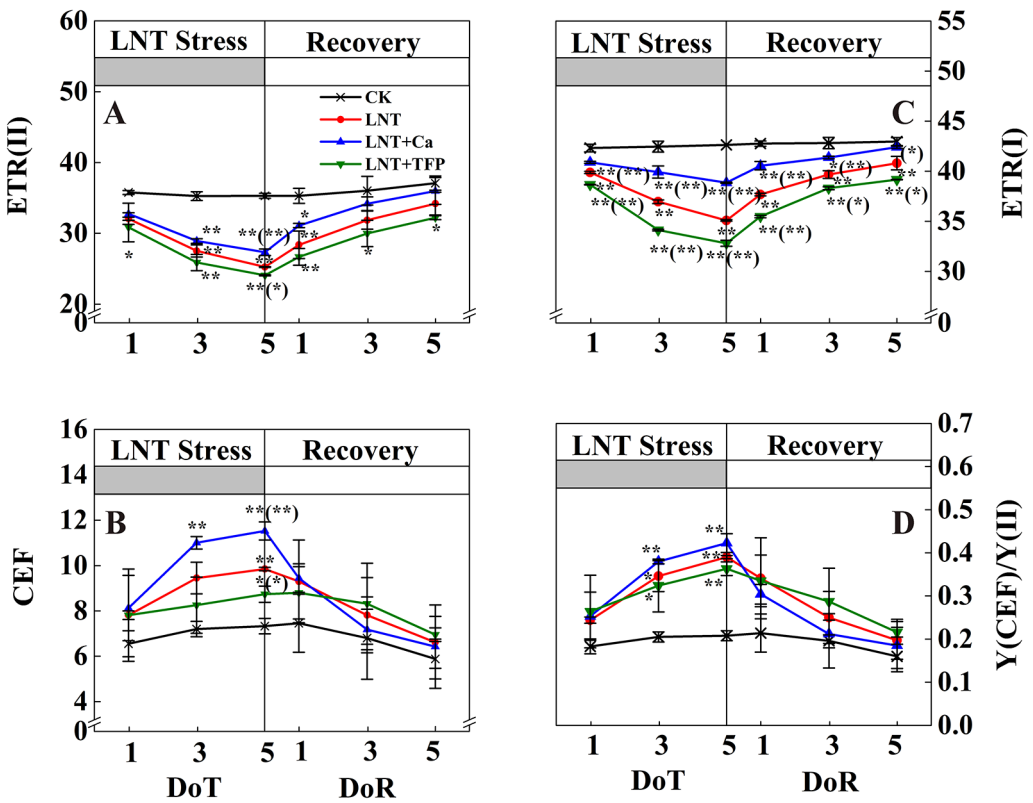

FIGURE 6 | Effect of exogenous calcium (Ca^{2+}) and a calmodulin inhibitor (TFP) on peanut photosynthetic electron transport during 5 days of low nocturnal temperature (LNT) stress followed by 5 days of recovery. **(A)** ETR(II): PSII photosynthetic electron transport rate; **(B)** CEF: cyclic electron flow around PSI; **(C)** ETR(I): PSI photosynthetic electron transport rate; **(D)** Y(CEF)/Y(II): the ratio of quantum yield of CEF to Y(II). Values are means of three biological replicates ± SE (n = 3). * and ** indicate significant differences at $P \leq 0.05$, and $P \leq 0.01$, respectively, among the treatments. The significance between the three treatments under LNT and CK was shown in parenthesis.

indicating the fraction of energy that was dissipated as heat and fluorescence; a high value of Y(NO) reflects the inability of the plant to protect itself against damage by excess excitation (**Figure 5**). It is also plausible that the PSII super-complexes were photodamaged during LNT stress. Both PSI and PSII are sensitive to excess light under chilling stress; PSII is easily inactivated by an excess of excitations and PSI more prone to potential photo-damage caused by excess electrons coming from PSII (Sonoike, 1996; Suorsa et al., 2012). Impairment of the photosynthetic electron transport chain from the donor side of PSII and up to the reduction of end-acceptors of PSI likely limits the production of reduction equivalents and alters the rate of carbon fixation (Song et al., 2018). In this study, the decline in linear electron transport and increase in cyclic electron transport lead to an increase in $P700^{+}$, thereby increasing Y(ND) accordingly (**Figures 5** and **6**). In addition, the low-temperature condition restricts the Calvin cycle, reducing the need for NADPH (Huang et al., 2012). In due course, NADPH accumulates downstream of PSI, altering the ATP/NADPH ratio and causing an over-reduction of the PSI acceptor side (Müller et al., 2001; Rumeau et al., 2007; Noctor et al., 2014).

Ca^{2+} Improved Peanut Growth and Photosynthetic Capacity During Low Nocturnal Temperature And Its Recovery

Our results showed that foliar application of Ca^{2+} enhanced leaf growth and dry matter accumulation of peanut roots, stems and leaves under LNT stress and improved the recovery (**Figure 1**). Previous studies have also shown that the pre-treatment of exogenous Ca^{2+} improves plant growth and photosynthesis, and enhances cold resistance (Brauer et al., 1990); for example, in peanut (Liu et al., 2013), wheat (You et al., 2002), Chinese crab apple (Li et al., 2017) and tomato (Zhang et al., 2014; Liu et al., 2015). High-yielding peanuts are a calcium-demanding oil crop, with calcium critical for peanut growth and development (Wan, 2003). The LNT + Ca treatment restored the concentration of chlorophyll a to a level similar to that in CK, while the concentration of chlorophyll b was lower than that in CK while higher than that in LNT. Peanut seedlings in the LNT + TFP treatment showed more severe growth inhibition and had lower levels of the main photosynthetic pigments (**Table 1**). Our results also indicated that exogenous Ca^{2+} relieved the excess accumulation of nonstructural

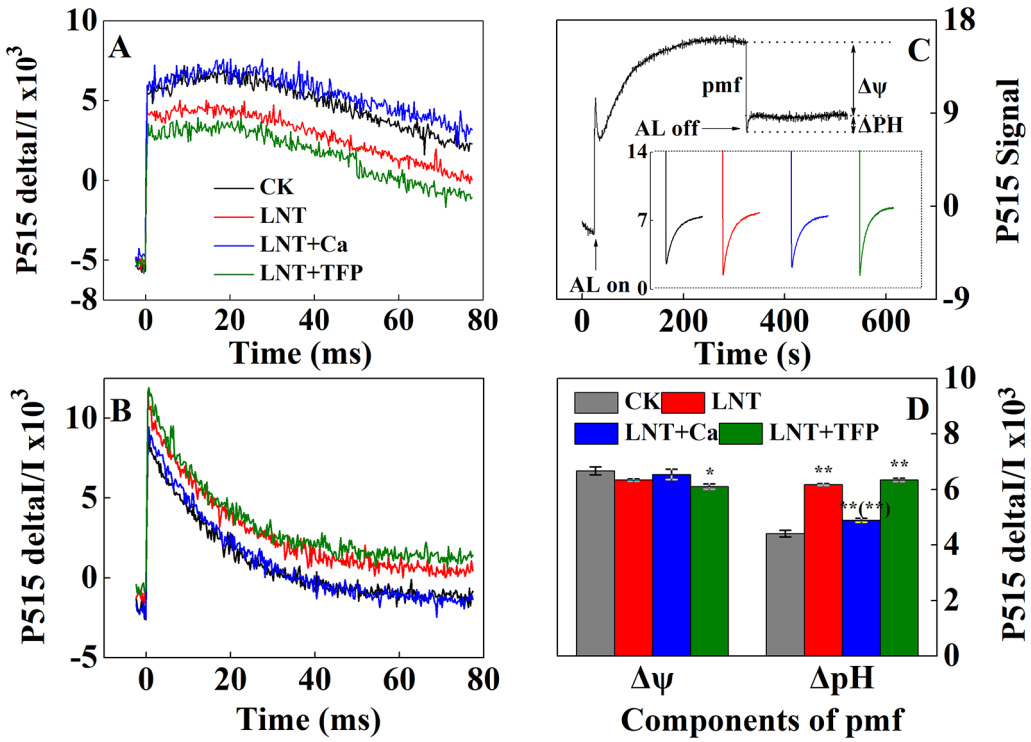

FIGURE 7 | Effect of exogenous calcium (Ca^{2+}) and a calmodulin inhibitor (TFP) on thylakoid membrane activity in peanut leaves after 5 days of low nocturnal temperature (LNT) stress. **(A)** Rapid kinetics of P515 induced by saturating single turnover flashes in peanut leaves after dark acclimation for 1 h; **(B)** Fast kinetics of P515 induced by saturating single turnover flashes in peanut leaves after pre-illumination for 10 min at 600 μmol photons·m^{-2}·s^{-1} followed by 4 min darkness; **(C)** Proton gradient (△pH) and **(D)** membrane potential (△ψ) by using the slow 'dark–light–dark' signal induction transients of 515 nm signal after fully dark-acclimated (12 h). Values are means of three biological replicates ± SE (n = 3). * and ** indicate significant differences at $P \leq 0.05$, and $P \leq 0.01$, respectively, among the treatments. The significance between the three treatments under LNT and CK at 5 DoT was shown in parenthesis.

carbohydrates (fructose, glucose, sucrose and starch) in peanut leaves under LNT stress (**Figure 2**). It is a well-established principle that plant growth and carbohydrate metabolism are closely linked since carbohydrates generated by photosynthesis are the primary source of building blocks and energy for the production and maintenance of biomass (Osorio et al., 2014). In particular, Ca^{2+}, involved in regulating carbohydrate metabolism of plants, can contribute to the regulation of sucrose synthesis, such as the inhibition of cytosolic Fru1, 6bisPase and the activation of SPS (Sucrose-Phosphate Synthase) as well as the turnover of PPi (Brauer et al., 1990; Eckardt, 2001; Lu et al., 2013). In addition, Ca^{2+} is an important component of several signal transduction pathways including sugar signaling (Ohto and Nakamura, 1995; Gounaris, 2001), and Ca^{2+} regulation has been implicated in phloem function (Eckardt, 2001). Furthermore, our results showed that supplementary Ca^{2+} indirectly ameliorated the decline of g_s and Tr and maintained C_i during LNT which prevented a major decline in Pn (**Figure 3**), which is in accordance with previous studies on *Arabidopsis* (Dong et al., 2013), cotton, tomato, and spinach (Joham, 1957; Brauer et al., 1990), where calcium improved the synthesis, phloem loading and translocation of photosynthetic carbohydrates (Joham, 1957; Eckardt, 2001; Lu et al., 2013). Taken together, exogenous Ca^{2+} application alleviated temperature-dependent photosynthesis feedback inhibition due to improved growth demand and reduced accumulation of nonstructural carbohydrates.

Exogenous Ca^{2+} can relieve photodamage as well as accelerating photosynthetic recovery in peanut leaves under LNT stress. The current study demonstrated that exogenous Ca^{2+} enhanced the PSII self-repairing process under LNT stress and during its recovery (**Figures 4** and **5**). Previous research has shown that the calcium-binding protein CAS is crucial for maintaining PSII activity, recovery, and turnover, as well as for driving high-light acclimation (Terashima et al., 2012). PSII is a multisubunit protein-pigment complex containing polypeptides, both intrinsic and extrinsic to the photosynthetic membrane. The extrinsic luminal protein PsbO can bind to calcium ions and stabilize the function of the oxygen-evolving complex (Heredia and Rivas, 2003; Sasi et al., 2018). In our study, exogenous Ca^{2+} decreased Y(NO) under LNT stress, whereas LNT and LNT + TFP increased Y(NO) indirectly (**Figure 5**). This suggests that the PSII reaction centers under the LNT and LNT + TFP treatments experienced severe photodamage. Conversely, the thylakoid lumen acidification (**Figure 7**) driven by CEF (**Figure 6**) with exogenous Ca^{2+} pretreatment under LNT

stress possibly promoted calcium binding to PsbO, which is important in the assembly and stabilization of PSII reaction center (Yi et al., 2005). Moreover, Ca^{2+} might affect the expression of LHC stress-related protein 3, which is crucial for qE, the energy-dependent component of NPQ (Terashima et al., 2012). However, CEF contributes to the pH gradient across the thylakoid membrane which is required for efficient qE. Foliar application of exogenous Ca^{2+} may also increase the binding of calmodulin to NADK2, which is known to modulate the NAD/NADP balance (Rocha and Vothknecht, 2012). Furthermore, our study showed that ATPase activity was promoted by exogenous Ca^{2+} under LNT stress (**Figure 7**). This finding is in accordance with previous studies on tomato under LNT stress (Zhang et al., 2014) and tobacco under high-temperature stress (Tan et al., 2011). Exogenous Ca^{2+} can also enhance the activities of several key enzymes in the Calvin cycle, which in turn boost cyclic electron transport and PSII reaction center activity (Terashima et al., 2012; Hochmal et al., 2015). Therefore, supplementary Ca^{2+} could indirectly reduce over-reduction damage on the PSI acceptor side of peanut leaves. The LNT + Ca treatment induced a rapid increase of CEF to minimize PSI photodamage (**Figures 5** and **6**). Therefore, exogenous Ca^{2+} could restore both PSII and PSI photodamage as well as accelerating the photosynthetic recovery in peanut leaves under LNT stress.

Our data showed that foliar application of a calmodulin inhibitor (trifluoperazine, TFP) exacerbated the inhibition of growth, dry matter accumulation and photosynthetic gas exchange in peanuts under LNT stress, with poor performance during the recovery stage (**Figures 1**–**5**, **Table 1**). The LNT + TFP treatment increased soluble sugar, starch and total nonstructural carbohydrate concentrations more than LNT (**Figure 2**). We found that LNT + TFP strongly reduced peanut photosynthetic capacity through its limitation on peanut growth, leaf expansion and nonstructural- carbohydrate export from leaves to support sink growth and development. TFP can enter plant cells through the cell membrane and prevent the formation of a Ca^{2+}–CaM complex, thus inhibiting Ca^{2+}–CaM effects (Hepler 2005,; Liu et al., 2013). It is plausible that the Ca^{2+}–CaM complex plays an important role in facilitating Ca^{2+} signal transduction to restore peanut growth and photosynthetic capacity under LNT stress. The specific molecular mechanism underpinning the Ca^{2+}–CaM complex–LNT stress interaction remains to be examined.

CONCLUSIONS

LNT decreased peanut growth and photosynthetic activity. The protective effects of foliar-applied calcium on peanut were mainly due to improved peanut growth and leaf expansion, and the export of nonstructural carbohydrates, secondarily increasing photochemical activity during exposure to LNT and its subsequent warm recovery. Therefore, exogenous Ca^{2+} restored temperature-dependent photosynthesis feedback inhibition by improving sink demand in peanut under LNT stress. In addition, TFP-treated peanut seedlings performed worst during LNT, which further confirmed the protective role of Ca^{2+} in LNT tolerance of peanut.

DATA AVAILABILITY STATEMENT

All datasets generated for this study are included in the article/supplementary material.

AUTHOR CONTRIBUTIONS

YL, TL, XH, and QBS designed the experiment. QBS, QWS, CB, DW, and XH conducted the experiment and collected data for preliminary analysis. YL, JP, CG, and YC further analyzed the data and prepared the manuscript. All authors reviewed and commented on the manuscript. HL, JP, JY, and KS revised the manuscript.

FUNDING

This research was funded by the Natural Science Foundation of China (project no. 31772391, 31301842, 31601627), the National Key Research and Development Plan (project no. 2018YFD0201206), the National Peanut Research System (project no. CARS-13- Nutrient Management).

ACKNOWLEDGMENTS

This study was carried out with support from the Sheng Jing Talents Project (Project No. RC170338), the China Scholarship Council (Project No. 201708210143).

REFERENCES

Adams, W. W., and Demmig-Adams, B. (2004). "Chlorophyll fluorescence as a tool to monitor plant response to the environment," in *Chlorophyll a Fluorescence: A Signature of Photosynthesis, Advances in Photosynthesis and Respiration*, vol. 19. Eds. G. C. Papageorgiou and Govindjee, (Dordrecht: Springer), 583–604.

Adams, W.W., III, Muller, O., Cohu, C. M., and Demmig-Adams, B. (2013). May photoinhibition be a consequence, rather than a cause, of limited plant production? *Photosynth. Res.* 117, 31–44. doi: 10.1007/s11120-013-9849-7

Allakhverdiev, S. I., and Murata, N. (2004). Environmental stress inhibits the synthesis *de novo* of proteins involved in the photodamage-repair cycle of Photosystem II in Synechocystis sp. PCC 6803. *Biochim. Biophys. Acta Bioenerg.* 1657, 23–32. doi: 10.1016/j.bbabio.2004.03.003

Allen, D. J., and Ort, D. R. (2001). Impact of chilling temperatures on photosynthesis in warm-climate plants. *Trends Plant Sci.* 6, 36–42. doi: 10.1016/S1360-1385(00)01808-2

Allen, D. J., Ratner, K., Giller, Y. E., Gussakovsky, E. E., Shahak, Y., and Ort, D. R. (2000). An overnight chill induces a delayed inhibition of photosynthesis at midday in mango *(Mangifera indica L.). J. Exp. Bot.* 51, 1893–1902. doi: 10.1093/jexbot/51.352.1893

Anderson, J. M., and Cormier, M. J. (1978). Calcium-dependent regulator of NAD kinase. *Biochem. Biophys. Res. Commun.* 84, 595–602. doi: 10.1016/0006-291X(78)90747-7

Asada, K. (2006). Production and scavenging of reactive oxygen species in chloroplasts and their functions. *Plant Physiol.* 141, 391–396. doi: 10.1104/pp.106.082040

Bagnall, D. J., King, R. W., and Farquhar, G. D. (1988). Temperature-dependent feedback inhibition of photosynthesis in peanut. *Planta* 175, 348–354. doi: 10.1007/BF00396340

Baker, N. R. (2008). Chlorophyll fluorescence: a probe of photosynthesis *in vivo*. *Annu. Rev. Plant Biol.* 59, 89–113. doi: 10.1146/annurev.arplant.59.032607.092759

Bauer, H., Wierer, R., Hatheway, W. H., and Larcher, W. (1985). Photosynthesis of *Coffea arabica* after chilling. *Physiol. Plant* 64, 449–454. doi: 10.1111/j.1399-3054.1985.tb08521.x

Bertamini, M., Muthuchelian, K., Rubinigg, M., Zorer, R., and Nedunchezhian, N. (2005). Low-night temperature (LNT) induced changes of photosynthesis in grapevine (*Vitis vinifera* L.) plants. *Plant Physiol. Bioch.* 43, 693–699. doi: 10.1016/j.plaphy.2005.06.001

Bertamini, M., Muthuchelian, K., Rubinigg, M., Zorer, R., Velasco, R., and Nedunchezhian, N. (2006). Low-night temperature increased the photoinhibition of photosynthesis in grapevine (*Vitis vinifera L.* cv. *Riesling*) leaves. *Environ. Exp. Bot.* 57, 25–31. doi: 10.1016/j.envexpbot.2005.04.002

Bertioli, D. J., Cannon, S. B., Froenicke, L., Huang, G., Farmer, A. D., Cannon, E. K. S., et al. (2016). The genome sequences of *Arachis duranensis* and *Arachis ipaensis*, the diploid ancestors of cultivated peanut. *Nat. Genet.* 48, 438–446. doi: 10.1038/ng.3517

Brauer, M., Sanders, D., and Stitt, M. (1990). Regulation of photosynthetic sucrose synthesis: a role for calcium? *Planta* 182, 236. doi: 10.1007/BF00197117

Bukhov, N. G., Wiese, C., Neimanis, S., and Heber, U. (1999). Heat sensitivity of chloroplasts and leaves: Leakage of protons from thylakoids and reversible activation of cyclic electron transport. *Photosynth. Res.* 59, 81–93. doi: 10.1023/a:1006149317411

Cachorro, P., Ortiz, A., and Antonio, C. (1994). Implications of calcium nutrition on the response of *Phaseolus vulgaris* L. @ to salinity. *Plant Soil* 159, 205–212. doi: 10.1007/bf00009282

Cailly, A., Rizzal, F., Genty, B., and Harbinson, J. (1996). Fate of excitation at PSII in leaves: the nonphotochemical side. in: Paper presented at the 10th FESPP Meeting, Florence, Italy.

Chen, J., Gutjahr, C., Bleckmann, A., and Dresselhaus, T. (2015). Calcium Signaling during Reproduction and *Biotrophic Fungal* Interactions in Plants. *Mol. Plant* 8, 595–611. doi: 10.1016/j.molp.2015.01.023

Cohu, C. M., Muller, O., Adams, W. W., and Demmig-Adams, B. (2014). Leaf anatomical and photosynthetic acclimation to cool temperature and hight light in two winter versus two summer annuals. *Physiol. Plant* 152, 164–173. doi: 10.1111/ppl.12154

Dias, P. M. B., Brunel-Muguet, S., Dürr, C., Huguet, T., Demilly, D., Wagner, M. H., et al. (2011). QTL analysis of seed germination and pre-emergence growth at extreme temperatures in *Medicago truncatula*. *Theor. Appl. Genet.* 122, 429–444. doi: 10.1007/s00122-010-1458-7

Ding, W., Clode, P., Clements, J., and Lambers, H. (2018). Sensitivity of different *Lupinus* species to calcium under a low phosphorus supply. *Plant Cell Environ.* 41, 1512–1523. doi: 10.1111/pce.13179

Donald, R. O., Charles, F. Y., and Iris, F. H. (1996). *Oxygenic photosynthesis: the light reactions* Vol. 4 (New York: Springer), 1–3. doi: 10.1007/0-306-48127-8

Dong, H. S., Myoung-Goo, C., Hyun, K. L., Misuk, C., Sang-Bong, C., Giltsu, C., et al. (2013). Calcium dependent sucrose uptake links sugar signaling to anthocyanin biosynthesis in *Arabidopsis*. *Biochem. Biophys. Res. Commun.* 2, 634–639. doi: 10.1016/j.bbrc.2012.11.100

Eckardt, N. A. (2001). A calcium-regulated gatekeeper in phloem sieve tubes. *Plant Cell* 13, 989–992. doi: 10.1105/tpc.13.5.989

Gago, J., Daloso, D. M., Figueroa, C. M., Flexas, J., Fernie, A. R., and Nikoloski, Z. (2016). Relationships of leaf net photosynthesis, stomatal conductance, and mesophyll conductance to primary plant metabolism: a multi-species meta-analysis approach. *Plant Physiol.* 171, 265–279. doi: 10.1104/pp.15.01660

Genty, B. (1989). The relationship between the quantum yield of photosynthetic electron transport and quenching of chlorophyll fluorescence. *Biochim. Biophys. Acta Gen. Subj.* 990, 87–92. doi: 10.1016/S0304-4165(89)80016-9

Gounaris, Y. (2001). A qualitative model for the mechanism of sugar accumulation in cold-stressed plant tissues. *Theory Biosci.* 120, 149–165. doi: 10.1007/s12064-001-0014-z

Hajihashemi, S., Noedoost, F., Geuns, J. M. C., Djalovic, I., and Siddique, K. H. M. (2018). Effect of cold stress on photosynthetic traits, carbohydrates, morphology, and anatomy in nine cultivars of *Stevia rebaudiana*. *Front. Plant Sci.* 9, 1430. doi: 10.3389/fpls.2018.01430

Haque, M. Z. (1988). Effect of nitrogen, phosphorus and potassium on spikelet sterility induced by low temperature at the reproductive stage of rice. *Plant Soil* 109, 31–36. doi: 10.1007/BF02197577

He, L. Z., Yu, L., Li, B., Du, N. S., and Guo, S. R. (2018). The effect of exogenous calcium on cucumber fruit quality, photosynthesis, chlorophyll fluorescence, and fast chlorophyll fluorescence during the fruiting period under hypoxic stress. *BMC Plant Biol.* 18, 180–190. doi: 10.1186/s12870-018-1393-3

Hendrix, D. L. (1993). Rapid extraction and analysis of nonstructural carbohydrates in plant tissues. *Crop Sci.* 33, 1306–1311. doi: 10.2135/cropsci1993.0011183X003300060037x

Hepler, P. K. (2005). Calcium: a central regulator of plant growth and development. *Plant Cell* 17, 2142–2155. doi: 10.1105/tpc.105.032508

Heredia, P., and Rivas, J. D. L. (2003). Calcium-dependent conformational change and thermal stability of the isolated PsbO protein detected by FTIR spectroscopy. *Biochemistry* 42, 11831–11838. doi: 10.1021/bi034582j

Hochmal, A. K., Schulze, S., Trompelt, K., and Hippler, M. (2015). Calcium-dependent regulation of photosynthesis. *Biochim. Biophys. Acta Bioenerg.* 1847, 993–1003. doi: 10.1016/j.bbabio.2015.02.010

Huang, W., Yang, S. J., Zhang, S. B., Zhang, S. B., Zhang, J. L., and Cao, K. F. (2012). Cyclic electron flow plays an important role in photoprotection for the resurrection plant *Paraboea rufescens* under drought stress. *Planta* 235, 819–828. doi: 10.1007/s00425-011-1544-3

Huang, M., Jiang, L., Zou, Y., and Zhang, W. X. (2013). On-farm assessment of effect of low temperature at seedling stage on early-season rice quality. *Field Crop Res.* 141, 63–68. doi: 10.1016/j.fcr.2012.10.019

Jarrett, H. W., Brown, C. J., Black, C. C., and Cormier, M. J. (1982). Evidence that calmodulin is in the chloroplast of peas and serves a regulatory role in photosynthesis. *J. Biol. Chem.* 257, 13795–13804. doi: 10.1016/0165-022X(82)90005-7

Joham, H. E. (1957). Carbohydrate distribution as affected by calcium deficiency in cotton. *Plant Physiol.* 32, 113–117. doi: 10.1104/pp.32.2.113

Kasuga, M., Miura, S., Shinozaki, K., and Yamaguchi-Shinozaki, K. (2004). A combination of the *Arabidopsis* DREB1A gene and stress-inducible *rd29A* promoter improved drought- and low-temperature stress tolerance in tobacco by gene transfer. *Plant Cell Physiol.* 45, 346–350. doi: 10.1093/pcp/pch037

Kitajima, M., and Butler, W. L. (1975). Quenching of chlorophyll fluorescence and primary photochemistry in chloroplasts by dibromothymoquinone. *Biochim. Biophys. Acta Bioenerg.* 376, 105–115. doi: 10.1016/0005-2728(75)90209-1

Klughammer, C., and Schreiber, U. (1994). An improved method, using saturating light pulses, for the determination of photosystem I quantum yield *via* $P700^+$-absorbance changes at 830 nm. *Planta* 192, 261–268. doi: 10.2307/23382564

Klughammer, C., and Schreiber, U. (2008). Saturation pulse method for assessment of energy conversion in PSI. *PAM Appl. Notes* 1, 11–14.

Kramer, D. M., Johnson, G., Kiirats, O., and Edwards, G. E. (2004). New fluorescence parameters for the determination of QA redox state and excitation energy fluxes. *Photosynth. Res.* 79, 209–218. doi: 10.1023/b:pres.0000015391.99477.0d

Latef, A. A. H. A., and He, C. (2011). *Arbuscular mycorrhizal* influence on growth, photosynthetic pigments, osmotic adjustment and oxidative stress in tomato plants subjected to low temperature stress. *Acta Physiol. Plant* 33, 1217–1225. doi: 10.1007/s11738-010-0650-3

Li, L., Su, H., Ma, H., and Lyu, D. (2017). Differential proteomic analysis reveals the effect of calcium on *Malus baccata* Borkh. leaves under temperature stress. *Int. J. Mol. Sci.* 18, 1755. doi: 10.3390/ijms18081755

Lichtenthaler, H. K. (1987). Chlorophylls and carotenoids: pigments of photosynthetic biomembranes. *Method. Enzymol.* 148, 350–382. doi: 10.1016/0076-6879(87)48036-1

Liu, Y. F., Li, T. L., Xu, T., Qi, M. F., and Xu, C. Q. (2011). Effect of low night temperature treatment and recovery on photosynthesis and the allocation absorbed light energy in tomato leaves. *J. Hortic. Sci. Biotech.* 86, 91–96. doi: 10.1080/14620316.2011.11512731

Liu, Y. F., Qi, M. F., and Li, T. L. (2012). Photosynthesis, photoinhibition, and antioxidant system in tomato leaves stressed by low night temperature and their subsequent recovery. *Plant Sci.* 196, 8–17. doi: 10.1016/j.plantsci.2012.07.005

Liu, Y. F., Han, X. R., Zhan, X. M., Yang, J. F., Wang, Y. Z., Song, Q. B., et al. (2013). Regulation of calcium on peanut photosynthesis under low night temperature stress. *J. Integr. Agric.* 12, 2172–2178. doi: 10.1016/S2095-3119(13)60411-6

Liu, Y. F., Zhang, G. X., Qi, M. F., and Li, T. L. (2015). Effects of calcium on photosynthesis, antioxidant system, and chloroplast ultrastructure in tomato leaves under low night temperature stress. *J. Plant Growth Regul.* 34, 263–273. doi: 10.1007/s00344-014-9462-9

Liu, Z. L., Tao, L. Y., Liu, T. T., Zhang, X. H., Wang, W., Song, J. M., et al. (2018). Nitrogen application after low-temperature exposure alleviates tiller decrease in rice. *Environ. Exp. Bot.* 158, 205–214. doi: 10.1016/j.envexpbot.2018.11.001

Lu, Y. Q., Liu, H. P., Wang, Y., Zhang, X. Z., and Han, Z. H. (2013). Synergistic roles of leaf boron and calcium during the growing season in affecting sugar and starch accumulation in ripening apple fruit. *Acta Physiol. Plant* 35, 2483–2492. doi: 10.1007/s11738-013-1283-0

Møller, I. M., Johnston, S. P., and Palmer, J. M. (1981). A specific role for Ca^{2+} in the oxidation of exogenous NADH by Jerusalem-artichoke (*Helianthus tuberosus*) mitochondria. *Biochemistry* 194, 487–495. doi: 10.1042/bj1940487

Müller, P., Li, X. P., and Niyogi, K. K. (2001). Non-photochemical quenching. A response to excess light energy. *Plant Physiol.* 125, 1558–1566. doi: 10.2307/42797

Monroy, A. F., and Dhindsa, R. S. (1995). Low-temperature signal transduction: Induction of cold acclimation-specific genes of alfalfa by calcium at 25 degrees °C. *Plant Cell* 7, 321–331. doi: 10.1105/tpc.7.3.321

Mozafar, A., and Oertli, J. J. (1990). Multiple stress and growth of barley: effect of salinity and temperature shock. *Plant Soil* 128, 153–160. doi: 10.1007/bf00011104

Munekage, Y., Hojo, M., Meurer, J., Endo, T., Tasaka, M., and Shikanai, T. (2002). PGR5 is involved in cyclic electron flow around photosystem I and is essential for photoprotection in *Arabidopsis*. *Cell* 110, 361–371. doi: 10.1016/s0092-8674(02)00867-x

Murata, N., Takahashi, S., Nishiyama, Y., and Allakhverdiev, S. I. (2007). Photoinhibition of photosystem II under environmental stress. *Biochim. Biophys. Acta Bioenerg.* 1767, 414–421. doi: 10.1016/j.bbabio.2006.11.019

Naeem, M., Naeem, M. S., Ahmad, R., Ihsan, M. Z., Ashraf, M. Y., Hussain, Y., et al. (2018). Foliar calcium spray confers drought stress tolerance in maize *via* modulation of plant growth, water relations, proline content and hydrogen peroxide activity. *Arch. Agron. Soil Sci.* 64, 116–131. doi: 10.1080/03650340.2017.1327713

Noctor, G., Mhamdi, A., and Foyer, C. H. (2014). The roles of reactive oxygen metabolism in drought: not so cut and dried. *Plant Physiol.* 164, 1636–1648. doi: 10.1104/pp.113.233478

Ohto, M., and Nakamura, K. (1995). Sugar-induced increase of calcium-dependent protein kinases associated with the plasma membrane in leaf tissues of tobacco. *Plant Physiol.* 109, 973–981. doi: 10.1104/pp.109.3.973

Osorio, S., Ruan, Y. L., and Fernie, A. R. (2014). An update on source-to-sink carbon partitioning in tomato. *Front. Plant Sci.* 5, 516. doi: 10.3389/fpls.2014.00516

Patrick, E. H., Peta, L. C., Rafael, S. O., and Lambers, H. (2018). *Proteaceae* from phosphorus-impoverished habitats preferentially allocate phosphorus to photosynthetic cells: An adaptation improving phosphorus-use efficiency. *Plant Cell Environ.* 41, 605–619. doi: 10.1111/pce.13124

Poovaiah, B. W., and Leopold, A. C. (1973). Deferral of leaf senescence with calcium. *Plant Physiol.* 52, 236–239. doi: 10.1104/pp.52.3.236

Prasad, P. V. V., Boote, K. J., Allen, L., and Thomas, J. M. G. (2003). Super-optimal temperatures are detrimental to peanut (*Arachis hypogaea* L.) reproductive processes and yield at both ambient and elevated carbon dioxide. *Global Change Biol.* 9, 1775–1787. doi: 10.1046/j.1365-2486.2003.00708.x

Qu, C., Liu, C., Gong, X., Li, C., Hong, M., Wang, L., et al. (2012). Impairment of maize seedling photosynthesis caused by a combination of potassium deficiency and salt stress. *Environ. Exp. Bot.* 75, 134–141. doi: 10.1016/j.envexpbot.2011.08.019

Rocha, A., and Vothknecht, U. (2012). The role of calcium in the chloroplasts-an intriguing and unresolved puzzle. *Protoplasma* 249, 957–966. doi: 10.1007/s00709-011-0373-3

Rufty, T. W., and Huber, S. C. (1983). Changes in starch formation and activities of sucrose phosphate synthase and cytoplasmic fructose-1,6-bisphosphatase in response to source-sink alterations. *Plant Physiol.* 72, 474–480. doi: 10.2307/4268053

Rumeau, D., Peltier, G., and Cournac, L. (2007). Chlororespiration and cyclic electron flow around PSI during photosynthesis and plant stress response. *Plant Cell Environ.* 30, 1041–1051. doi: 10.1111/j.1365-3040.2007.01675.x

Sasi, S., Venkatesh, J., Daneshi, R. F., and Gururani, M. A. (2018). Photosystem II extrinsic proteins and their putative role in abiotic stress tolerance in higher plants. *Plants* 7, 100. doi: 10.3390/plants7040100

Schreiber, U., Bilger, W., and Neubauer, C. (1995). "Chlorophyll fluorescence as a non-intrusive indicator for rapid assessment of *in vivo* photosynthesis," in *Ecophysiology of Photosynthesis*. Ed. M. M. Caldwell (Berlin: Springer), 49–70.

Shi, Q. W., Pang, J. Y., Yong, J. W. H., Bai, C. M., Pereira, C. G., Song, Q. B., et al. (2019). Phosphorus-fertilisation has differential effects on leaf growth and photosynthetic capacity of *Arachis hypogaea* L. *Plant Soil*. doi: 10.1007/s11104-019-04041-w

Skórzyńska-Polit, E., Tukendorf, A., Selstam, E., and Baszyński, T. (1998). Calcium modifies Cd effect on runner bean plants. *Environ. Exp. Bot.* 40, 275–286. doi: 10.1016/s0098-8472(98)00045-8

Solanke, A. U., and Sharma, A. K. (2008). Signal transduction during cold stress in plants. *Physiol. Mol. Biol. Plant* 14, 69–79. doi: 10.1007/s12298-008-0006-2

Song, H., Li, Y. B., Zhou, L., Xu, Z. Z., and Zhou, G. S. (2018). Maize leaf functional responses to drought episode and rewatering. *Agr. For. Meteorol.* 249, 57–70. doi: 10.1016/j.agrformet.2017.11.023

Sonoike, K. (1996). Photoinhibition of photosystem I: its physiological significance in the chilling sensitivity of plants. *Plant Cell Physiol.* 37, 239–247. doi: 10.1093/oxfordjournals.pcp.a028938

Sonoike, K. (1999). The different roles of chilling temperatures in the photoinhibition of photosystem I and photosystem II. *J. Photochem. Photobio. B.* 48, 136–141. doi: 10.1016/s1011-1344(99)00030-5

Stewart, J. J, Demmig-Adams, B., Cohu, C. M., Wenzl, C. A., Muller, O., and Adams, W. W. (2016). Growth temperature impact on leaf form and function in Arabidopsis thaliana ecotypes from northern and southern Europe. *Plant Cell Environ.* 39, 1549–1558. doi: 10.1111/pce.12720

Suorsa, M., Järvi, S., Grieco, M., Nurmi, M., Pietrzykowska, M., Rantala,, et al. (2012). PROTON GRADIENT REGULATION5 is essential for proper acclimation of *arabidopsis* photosystem I to naturally and artificially fluctuating light conditions. *Plant Cell.* 24, 2934–2948. doi: 10.1105/tpc.112.097162

Tan, W., Meng, Q. W., Brestic, M., Olsovska, K., and Yang, X. (2011). Photosynthesis is improved by exogenous calcium in heat-stressed tobacco plants. *J. Plant Physiol.* 168, 2063–2071. doi: 10.1016/j.jplph.2011.06.009

Tardieu, F., Granier, C., and Muller, B. (1999). Modelling leaf expansion in a fluctuating environment: are changes in specific leaf area a consequence of changes in expansion rate? *New Phytol.* 143, 33–43. doi: 10.1046/j.1469-8137.1999.00433.x

Terashima, M., Petroutsos, D., Hüdig, M., Tolstygina, I., Trompelt, K., Gäbelein, P., et al. (2012). Calcium-dependent regulation of cyclic photosynthetic electron transfer by a CAS, ANR1, and PGRL1 complex. *PNAS* 109, 17717–17722. doi: 10.1073/pnas.1207118109

Tian, W., Hou, C. C., Ren, Z. J., Wang, C., Zhao, F. G., Dahlbeck, D., et al. (2019). A calmodulin-gated calcium channel links pathogen patterns to plant immunity. *Nature* 7767, 131–151. doi: 10.1038/s41586-019-1413-y

Turan, Ö., and Ekmekçi, Y. (2011). Activities of photosystem II and antioxidant enzymes in chickpea (*Cicer arietinum L.*) cultivars exposed to chilling temperatures. *Acta Physiol. Plant* 33, 67–78. doi: 10.1007/s11738-010-0517-7

Usuda, H., Ku, M. S. B., and Edwards, G. E. (2006). Influence of light intensity during growth on photosynthesis and activity of several key photosynthetic enzymes in a C4 plant (*Zea mays*). *Physiol. Plant* 63, 65–70. doi: 10.1111/j.1399-3054.1985.tb02819.x

Wan, S. B. (2003). *Peanut cultivation in China* (Shanghai: Shanghai Science and Technology Press).

Wang, Y., Li, J., Gu, W. R., Zhang, Q., Tian, L. X., Guo, S., et al. (2018). Exogenous application of 5-aminolevulinic acid improves low-temperature stress tolerance of maize seedlings. *Crop Pasture Sci.* 69, 587–593. doi: 10.1071/CP17401

White, P. J., and Broadley, M. R. (2003). Calcium in Plants. *Ann. Bot.* 92, 487–511. doi: 10.1093/aob/mcg164

Wong, S. C., Cowan, I. R., and Farquhar, G. D. (1979). Stomatal conductance correlates with photosynthetic capacity. *Nature* 282, 424–426. doi: 10.1038/282424a0

Yamori, W., and Shikanai, T. (2016). Physiological functions of cyclic electron transport around photosystem I in sustaining photosynthesis and plant

growth. *Annu. Rev. Plant Biol.* 67, 81–106. doi: 10.1146/annurev-arplant-043015-112002

Yamori, W. (2016). Photosynthetic response to fluctuating environments and photoprotective strategies under abiotic stress. *J. Plant Res.* 129, 379–395. doi: 10.1007/s10265-016-0816-1

Yi, X., McChargue, M., Laborde, S., Frankel, L. K., and Bricker, T. M. (2005). The manganese-stabilizing protein is required for photosystem II assembly/stability and photoautotrophy in higher plants. *J. Biol. Chem.* 280, 16170–16174. doi: 10.1074/jbc.M501550200

You, J. H., Lu, J. H., and Yang, W. J. (2002). Effects of Ca^{2+} on photosynthesis and related physiological indexes of wheat seedlings under low temperature stress. *Acta Agron. Sinica.* 168, 693–696. doi: 10.1006/jfls.2001.0409

Yu, L. H., Guo, H. L., Xu, X. D., and Feng, B. (2002). Effect of the photosynthesis inhibitor DCMU on chlorophyll synthesis in heterotrophic cyanobacteria. *Acta Hydrobiol. Sinica.* 1, 102–104. doi: ssswxb.ihb.ac.cn/EN/Y2002/V/I1/102

Zhang, G. X., Liu, Y. F., Ni, Y., Meng, Z., Lu, T., and Li, T. (2014). Exogenous calcium alleviates low night temperature stress on the photosynthetic apparatus of tomato leaves. *PloS One* 9, 1–12. doi: 10.1371/journal.pone.0097322

Zhou, Y. J., Li, X. X., Cao, J., Li, Y., Huang, J. L., and Peng, S. B. (2018). High nitrogen input reduces yield loss from low temperature during the seedling stage in early-season rice. *Field Crop Res.* 228, 68–75. doi: 10.1016/j.fcr.2018.08.018

Zhu, J., Dong, C. H., and Zhu, J. K. (2007). Interplay between cold-responsive gene regulation, metabolism and RNA processing during plant cold acclimation. *Curr. Opin. Plant Biol.* 10, 290–295. doi: 10.1016/j.pbi.2007.04.010

Zhu, X. C., Song, F. B., and Xu, H. W. (2010). *Arbuscular mycorrhizae* improves low temperature stress in maize *via* alterations in host water status and photosynthesis. *Plant Soil* 331, 129–137. doi: 10.1007/s11104-009-0239-z

Conflict of Interest: The authors declare that the research was conducted in the absence of any commercial or financial relationships that could be construed as a potential conflict of interest.

frontiers in Plant Science

ORIGINAL RESEARCH
published: 07 February 2020
doi: 10.3389/fpls.2020.00026

Response of Photosynthesis to High Growth Temperature Was Not Related to Leaf Anatomy Plasticity in Rice (*Oryza sativa* L.)

Desheng Yang[1], *Shaobing Peng*[1,2] *and Fei Wang*[1,3]*

[1] *MARA Key Laboratory of Crop Ecophysiology and Farming System in the Middle Reaches of the Yangtze River, College of Plant Science and Technology, Huazhong Agricultural University, Wuhan, China,* [2] *National Key Laboratory of Crop Genetic Improvement, Huazhong Agricultural University, Wuhan, China,* [3] *Hubei Collaborative Innovation Center for Grain Industry, Yangtze University, Jingzhou, China*

Photosynthesis is highly sensitive to high temperature stress, and with the rising global temperature, it is meaningful to investigate the response of photosynthesis to growth temperature and its relationship with leaf anatomy plasticity. We planted 21 cultivars including eight *indica* cultivars, eight *japonica* cultivars, and five *javanica* cultivars in pot experiments under high growth temperature (HT, 38/28°C, day/night) and control treatment (CK, 30/28°C, day/night). Photosynthetic rate (*A*), stomatal conductance (g_s), transpiration rate (*E*), stomatal density (SD), vein density (VD), minor vein area (SVA), and major vein area (LVA) were measured after 30 treatment days. Results showed HT significantly increased *A*, g_s, and *E*, while significantly decreased SD and LVA. There was no significant difference in *A* among the three subspecies both under CK and HT, while the *javanica* subspecies had higher g_s, *E*, SVA, and LVA under HT, and the *indica* cultivars had higher VD and SD both under CK and HT. The *javanica* subspecies had higher relative value (HT/CK) of *A*, g_s, and *E*, while difference was not observed in the relative value of SD, VD, and LVA among the three subspecies. The relative value of *A* was positively related to that of g_s, while the latter was not correlated with the relative value of SD, VD, SVA, and LVA. Overall, the results suggested the increase of *A* and g_s at HT was not attributed to leaf anatomy plasticity in respect of stomata and vein under HT.

Keywords: rice, photosynthesis, leaf anatomy, stomata, vein

OPEN ACCESS

Edited by:
Marouane Baslam, Niigata University, Japan

Reviewed by:
Shubin Zhang, Xishuangbanna Tropical Botanical Garden, China
Fernando Torralbo, University of Missouri, United States

***Correspondence:**
Fei Wang
fwang@mail.hzau.edu.cn

Specialty section:
This article was submitted to Plant Abiotic Stress, a section of the journal Frontiers in Plant Science

Received: *09 August 2019*
Accepted: *13 January 2020*
Published: *07 February 2020*

Citation:
Yang D, Peng S and Wang F (2020) Response of Photosynthesis to High Growth Temperature Was Not Related to Leaf Anatomy Plasticity in Rice (Oryza sativa L.). Front. Plant Sci. 11:26. doi: 10.3389/fpls.2020.00026

HIGHLIGHTS

1. High growth temperature (HT) significantly affected rice leaf photosynthetic rate (*A*), stomatal conductance (g_s), transpiration rate (*E*), stomatal density (SD), and major vein area (LVA).
2. The *javanica* subspecies had higher g_s, *E*, and LVA under HT, and possessed higher heat resistance than *indica* and *japonica* subspecies.
3. Across different cultivars, the response of *A* and g_s to HT were not related to leaf anatomy plasticity such as stomatal and vein anatomy.

INTRODUCTION

Rice is a stable food for more than half of the global population (Khush, 2013). China is the top rice producer in the world, accounting for almost 30% of the global rice production (Tang et al., 2014). However, after a remarkable 86% increase in cereal production from 1980 to 2005, recent crop yield growth in China has been slow (Huang and Rozelle, 2015). Further improvement of crop yield potential through crop improvement is the best way to increase the grain yield (Peng, 2014). Yield potential of grain crop is defined as the grain yield obtained under optimum conditions without pests, diseases, weeds, and other stresses (Evans and Fischer, 1999). It is determined by the following factors, i.e. the total incident solar radiation on the land throughout the growing season, the light interception efficiency of plant canopy, the photosynthetic conversion efficiency of leaves and the harvest index (Monteith, 1977). Over the past few decades, the yield potential has been successfully achieved through increasing the light interception efficiency and harvest index, there is limited scope for further improvement when they reach 0.9 and 0.6, respectively (Beadle and Long, 1985; Hay, 1995). Therefore, it is more effective to increase crop yield by increasing photosynthetic capacity, which is known as the new 'green revolution' (Zhu et al., 2010; Long et al., 2015).

Global warming represents a continual challenge for agricultural production and food security. For example, each 1° C increase in growing season temperature can result in up to 17% decrease in corn and soybean yield (Lobell and Asner, 2003), and a 10% decrease in rice yield (Peng et al., 2004). The mean surface air temperature has increased globally by ∼1°C in the last 100 years and will further increase by 1 to 4°C in this century (Zhao et al., 2017). Nevertheless, photosynthesis is highly sensitive to high temperature stress and is often inhibited before other cell functions are impaired (Berry and Bjorkman, 1980). Photosynthesis usually peaks at ~30°C in rice plants, and CO_2 assimilation may decrease significantly after suffering a heat stress (Yamori et al., 2011; Xiong et al., 2017). Mathur et al. (2014) concluded that high temperature stress mainly inhibited various redox and metabolic reactions taking place in Photosystem II, Photosystem I, Cytochrome complex, and Rubisco, eventually resulting in a decrease in photosynthetic rate (A). Huang et al. (2017) indicated that Rubisco activity, regeneration capacity of RuBP, rate of electron transport, and CO_2 diffusion capacity are sensitive to temperature and negatively impacted by high temperature stress.

Under high temperature conditions, plants exhibit short-term avoidance or acclimation mechanisms such as transpirational cooling, stomatal closure, and so on (Mathur et al., 2014). This means a close relationship exist between CO_2 delivery and water transportation in a leaf. Stomata, through which CO_2 and water vapor diffuse into and out of the leaf, are involved in the regulation and control of photosynthesis and transpiration responses (Farquhar and Sharkey, 1982; Jones, 1998). Stomatal density (SD) and size are leaf anatomical traits contributing to build the leaf g_s to gas diffusion (Franks et al., 2010). Under high temperature, stomata closure is another reason for impaired photosynthesis that affects the intercellular CO_2 (Hasanuzzaman et al., 2013). The leaf venation system as water transport channel in vascular plants plays an important role in maintaining adequate E (Sack and Holbrook, 2006; Tholen et al., 2012). An increased VD may facilitate a higher photosynthetic capacity by allowing for more efficient photosynthate export from mesophyll cells (Amiard et al., 2005).

Rice is cultivated under a wide range of climatic conditions. *Indica* rice and *japonica* rice are two subspecies with different genotypic background that evolved from different temperature environment. *Indica* rice has stronger heat tolerance and is more suitable for high temperature environment than *japonica* rice (Weng and Chen, 1987). *Javanica* rice (tropical *japonica*) mainly distributes in tropical mountains of Indonesia, Malay Peninsula, the Philippines, e.g. which has strong resistance to abiotic stresses (Xiao and Yuan, 2009). Zhao et al. (2013) proposed that maintaining a higher level of photosynthesis and osmoregulation substance was the physiological basis for heat tolerance in *javanica* rice. Leaves have evolved in different environments showing great variation in morphology and anatomy, and investigating relationships between leaf anatomy and photosynthetic features can lead to the identification of structural features for enhancing crop productivity and improve our understanding of plant evolution and adaptation (Evans, 1998).

At present, there have been many studies about the effect of temperature treatment on photosynthesis, and the relationship between leaf anatomies and photosynthesis. However, the difference in response of A to HT among different subspecies (*indica*, *japonica,* and *javanica* rice) is still obscure. Exploring the natural genotypic variation in leaf anatomy plasticity in relation to photosynthesis at HT will facilitate rice genetic improvement especially under future climate conditions. Therefore, the objectives of the present study were to determine the contribution of g_s to photosynthetic acclimation to HT for the three subspecies in rice, and examine its relationship with leaf plasticity.

MATERIALS AND METHODS

Site Description and Growth Conditions

Pot experiments were conducted in controlled-growth chamber at the Huazhong Agricultural University, Wuhan city, Hubei province, China (114.37°E, 30.48°N) in 2017. In the chamber (Model GR48, Conviron, Controlled Environments Limited, Winnipeg, MB, Canada), the air temperature was set to 30/28° C (day/night, the control treatment) and 38/28°C (day/night, the high temperature treatment), with a relative humidity of 75%, photosynthetic photon flux density (PPFD) of 1,500 μmol m^{-2} s^{-1} and a light/dark regime of 12/12 h. Eleven-liter plastic pots were filled with 10.0 kg air-dried, pulverized, and well-mixed soil taken from the top 25 cm layer of a field located at the Experimental Station in the campus. The soil used in this study was a clay loam with a pH of 7.1, organic matter of 6.7g kg^{-1}, Olsen-P of 6.27 mg kg^{-1}, exchangeable K of 129 mg kg^{-1}, and total N of 0.063%.

Experimental Design and Crop Management

Twenty-one rice cultivars were used in present study, including eight *indica* cultivars: Shenglixian (SLX), Huangguaxian (HGX), Zhenzhuai (ZZA), Ezhong2 (EZ2), Guichao2 (GC2), Huanghuazhan (HHZ), Yliangyou900 (YLY900), and Yangliangyou6 (YLY6), eight *japonica* cultivars: Guihuaqiu (GHQ), Guihuahuang (GHH), Xudao2 (XD2), Yanjing2 (YJ2), Zhendao88 (ZD88), Huaidao5 (HD5), Huaidao9 (HD9), and Lianjing7 (LJ7), and five *javanica* cultivars: PEMBE (J-1), TREMBESE (J-2), ASE BOLONG KAMANDI (J-3), PADI SEGUTUK (J-4), and BULUH BAWU (J-5) (**Table S1**). Particularly, the eight *indica* cultivars and eight *japonica* cultivars we used were historical cultivars from 1940s to present in China. Pre-germinated seeds were sown in a nursery plates on 27 August and transplanted to pots on 11 September with a density of three hills per pot and two seedlings per hill. Each cultivar was planted in six pots with three replicates. Equal pots were transferred to two growth chambers with different temperature treatments on 20 September. Other managements: 0.8 and 0.6 g N as urea per pot were applied at 1 d before transplanting and 7 d after transplanting, respectively; 1.5 g P as monocalcium phosphate and 1.5 g K as potassium chloride per pot were applied at 1d before transplanting. Three to 5 cm of standing water was kept in the pots throughout the experiment. Weeds were removed manually. Pests and diseases were controlled by chemicals two to three times. The measurements were conducted at the maximal tillering stage, on 20 October.

Measurement of Leaf Gas Exchange

Gas exchange measurements were conducted at 30 days after treatment (or 53 days after sowing at tillering stage) from 09:00 h to 16:00 h on the newest fully expanded leaves using a portable photosynthesis system (LI-6400XT; LI-COR Inc., Lincoln, NE, USA) with a 6400-40 leaf chamber. In the leaf chamber, the PPFD was maintained at 1,500 μmol m^{-2} s^{-1}, the leaf-to-air vapor pressure deficit (VPD) was 1.5 to 2.0 kPa, and the CO_2 concentration was adjusted to 400 μmol mol^{-1} using a CO_2 mixer. The block temperature during the measurement was set to the same as the growth condition temperature. After equilibration to a steady state, the gas exchange parameters including net photosynthesis rate (A), g_s, and E were recorded.

Measurement of Leaf Anatomy

After measuring the photosynthetic parameters, the middle part of the corresponding leaf blade was sampled. Half of it was stored in a distilled water to measure the leaf SD and VD. The other half of the leaf was cut into slices broadwise for determination of leaf vascular bundle anatomies, including SVA and major vein area (LVA). Specifically, the inverted fluorescence microscope (U-TVO.5XC; Olympus, Tokyo, Japan) was used to observe and photograph the leaf vein, stomata, and vein anatomies. The number of leaf stomata and vein, as well as the length and width of major vein and minor vein in each photograph were manually measured using ImageJ (Wayne Rasband/NIH, Bethesda, MD, USA). The leaf stomata density and VD were calculated by the formula: no./actual area, and the SVA and major vein area were calculated by the formula: $\pi * ((\text{length} + \text{width})/4)^2$.

Statistical Analysis

Two-way analysis of variance (ANOVA) was used to assess the effects of high temperature and subspecies on each parameter using Statistix 9 software (Analytical Software, Tallahassee, Florida, USA). Linear regression analysis was performed to test the correlations between g_s and A, SD and g_s, and VD and vein area using SigmaPlot 12.5 (Systat Software Inc., California, USA).

RESULTS

Photosynthetic Rate, Stomatal Conductance, Transpiration Rate, and Intrinsic Water Use Efficiency (WUEi)

Temperature (T) significantly affected the A, but subspecies (S) had no significant effect on A (**Figure 1A**). Compared with the control treatment (CK), HT increased A by 23% averagely across all cultivars. There were no significant differences in A among the three subspecies both at high temperature and CK treatments. Stomatal conductance (g_s) and E were significantly affected by temperature and subspecies (**Figures 1B, C**). HT increased g_s and E by a mean value of 35% and 162%, respectively. *Japonica* cultivars had significantly higher g_s than *indica* and *javanica* cultivars at CK, however, *javanica* cultivars had significantly higher g_s than *indica* cultivars at HT treatment (**Figure 1B**). There was no significant difference in E among the three subspecies at CK, while E of *javanica* cultivars was significantly higher than that of *japonica* cultivars and *indica* cultivars had the lowest value (**Figure 1C**). At CK, *indica* and *javanica* cultivars had the similar WUEi higher than *japonica* cultivars, while WUEi of *indica* cultivars was significantly higher than that of *japonica* and *javanica* cultivars at HT (**Figure 1D**).

Different response of A to HT was observed among *indica*, *japonica*, and *javanica* subspecies (**Figure 2A**). Compared to that at CK, the increment of A of *indica*, *japonica*, and *javanica* subspecies at HT were 23%, 18% and 29% on average, respectively. The response of A to HT varied significantly among the *indica* cultivars with the relative value of A ranging from 0.95 to 1.87, while the responses of A to high temperature in *japonica* cultivars were consistent. Similar results in the response to HT between the three subspecies were observed for g_s and E (**Figures 2B, C**). For WUEi, only *javanica* cultivars showed a reduction in WUEi under HT in comparison with CK (**Figure 2D**).

Stomatal Density, Vein Density, and Vein Area

Temperature significantly affected SD and major vein area (LVA), while no differences were observed in VD and SVA between HT and CK (**Figure 3**). Compared to CK, HT decreased SD and LVA by a mean value of 7% and 8.9%, respectively (**Figures 3A, D**). At both CK and HT, *indica* cultivars had significantly higher SD than *japonica* and *javanica* cultivars on average, moreover, the genotypic variation was also larger within *indica* cultivars

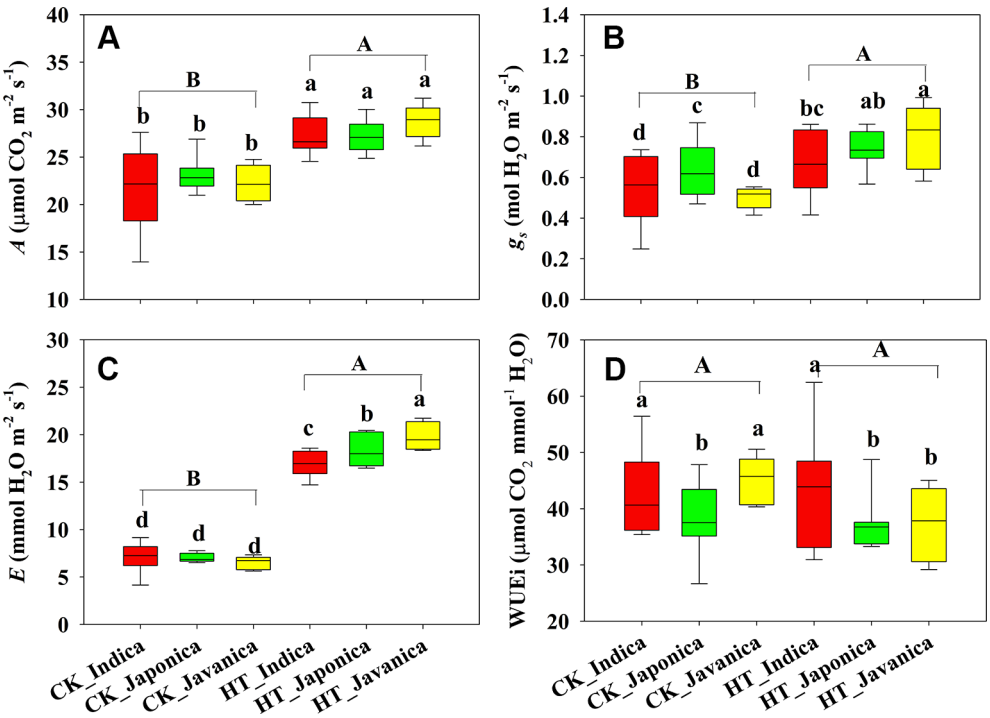

FIGURE 1 | Light saturated photosynthetic rate (*A*, **A**), stomatal conductance (g_s, **B**), transpiration rate (*E*, **C**), and intrinsic water use efficiency (WUEi, **D**) for the three rice (*Oryza sativa* L.) subspecies at high growth temperature (HT) and control (CK) treatments. Different lowercase and uppercase letters indicate significant differences between subspecies means and temperature treatments, respectively ($p < 0.05$). The outer box edges represent the 25th and 75th percentiles, the error bars are the 5th and 95th percentiles, and the line within the box represents the mean values. For each cultivar, three flag leaves were measured (one leaf per plant), and the three values were averaged as one biological replicate. n (the biological replicates) was 8, 8, and 5 for the indica, japonica, and javanica cultivars, respectively.

(**Figure 3A**). Similar results were observed for the VD (**Figure 3B**). There were no significant differences in SD and VD between the *japonica* and *javanica* cultivars (**Figures 3A, B**). *Javanica* cultivars had the largest vein area, which were significantly higher than that of *indica* cultivars in minor vein (**Figure 3C**) and that of *indica* and *japonica* cultivars in major vein (**Figure 3D**).

There were no significant differences in the response of SD, VD, and major vein area to HT (**Figures 4A, B, D**). *Japonica* cultivars had higher relative value of SVA than *javanica* cultivars (**Figure 4C**). Large variations were observed for all the leaf anatomy parameters within each subspecies, for example the relative value of SD ranged from 0.75 to 1.03 for the *indica* cultivars (**Figure 4**).

Correlations Between Vein Density and Vein Area, g_s and *A*, Stomatal Density, and G_s

Significantly negative correlations between VD and SVA, as well as between VD and major vein area were observed both under CK and HT (**Figures 5A, B**). Stomatal density significantly correlated with VD at CK ($R^2 = 0.15$), but not at HT treatment (**Figure 5C**). *A* was positively related to g_s both under CK and HT (**Figure 6A**), but the correlation coefficient under CK was much larger than that under HT ($R^2 = 0.63$ and 0.19), which was due to the integral higher g_s under HT. Nevertheless, g_s was not related to SD both under CK and HT (**Figure 6B**). The responses of *A* and *E* to HT were significantly correlated to the response of g_s to HT ($R^2 = 0.45$ and 0.62, **Figure 7**).

DISCUSSION

Photosynthetic Acclimation to High Growth Temperature

In present study, HT significantly increased *A* of all cultivars except two *indica* cultivars, EZ2 and GC2 (**Figure 1** and **Figure S1**). Among the three subspecies, *javanica* (the tropical *japonica*) is closer to *japonica* at the genomic level (Wang et al., 2018). This was also manifested by the similar leaf anatomy of the two subspecies (**Figure 3**). However, *javanica* subspecies possessed higher heat resistance than *indica* and *japonica* subspecies in respect of the photosynthetic physiology, for example the response of *A*, g_s, and *E* to high temperature (**Figure 2**). This is possible because *javanica* cultivars mainly distributes in tropical mountains with strong resistance to abiotic stresses (Xiao and Yuan, 2009). *Javanica* cultivars could maintain a higher level of photosynthesis and osmoregulation substance under HT (Zhao et al., 2013).

The thermal response curve of *A* usually peaks between 25 and 30°C in C_3 photosynthetic species (Sage and Kubien, 2007;

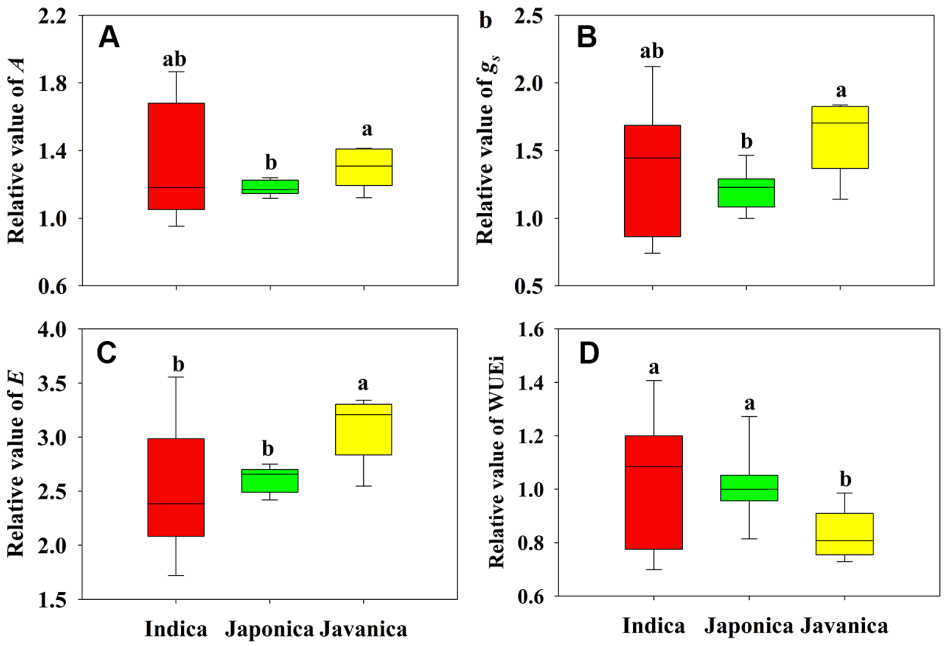

FIGURE 2 | Relative value (HT/CK) of light saturated photosynthetic rate (*A*, **A**), stomatal conductance (g_s, **B**), and transpiration rate (*E*, **C**), and intrinsic water use efficiency (WUEi, **D**) for the three rice (*Oryza sativa* L.) subspecies. Different lowercase letters indicate significant differences between subspecies means ($p < 0.05$). The outer box edges represent the 25th and 75th percentiles, the error bars are the 5th and 95th percentiles, and the line within the box represents the mean values. For each cultivar, three flag leaves were measured (one leaf per plant), and the three values were averaged as one biological replicate. n (the biological replicates) was 8, 8, and 5 for the indica, japonica, and javanica cultivars, respectively.

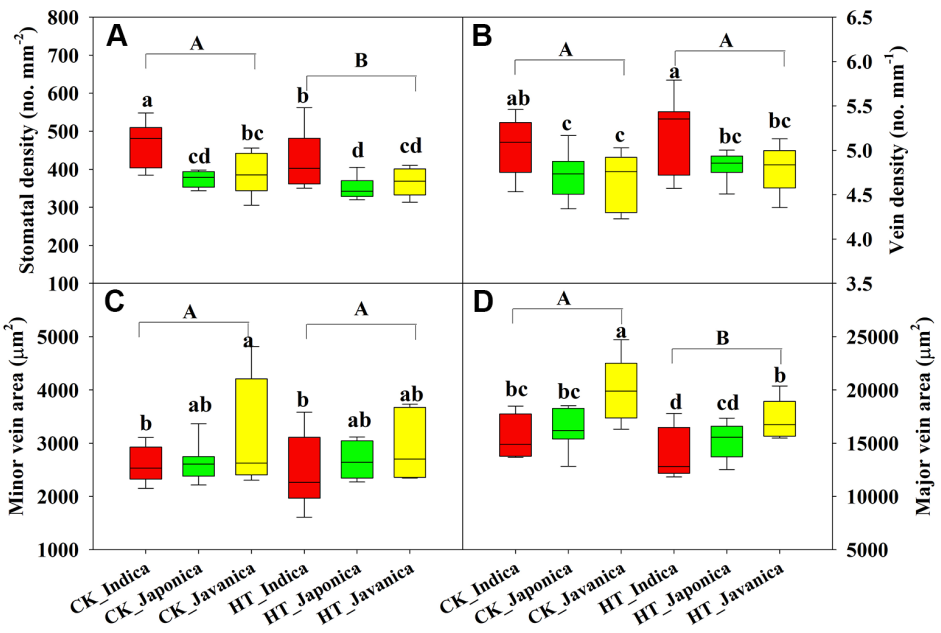

FIGURE 3 | Stomatal density **(A)**, vein density **(B)**, and vein area of minor **(C)**, and major **(D)** veins for the three rice (*Oryza sativa* L.) subspecies at high growth temperature (HT) and control (CK) treatments. Different lowercase and uppercase letters indicate significant differences between subspecies means and temperature treatments, respectively ($p < 0.05$). The outer box edges represent the 25th and 75th percentiles, the error bars are the 5th and 95th percentiles, and the line within the box represents the mean values. For each cultivar, three flag leaves were measured (one leaf per plant), and the three values were averaged as one biological replicate. n (the biological replicates) was 8, 8, and 5 for the indica, japonica, and javanica cultivars, respectively.

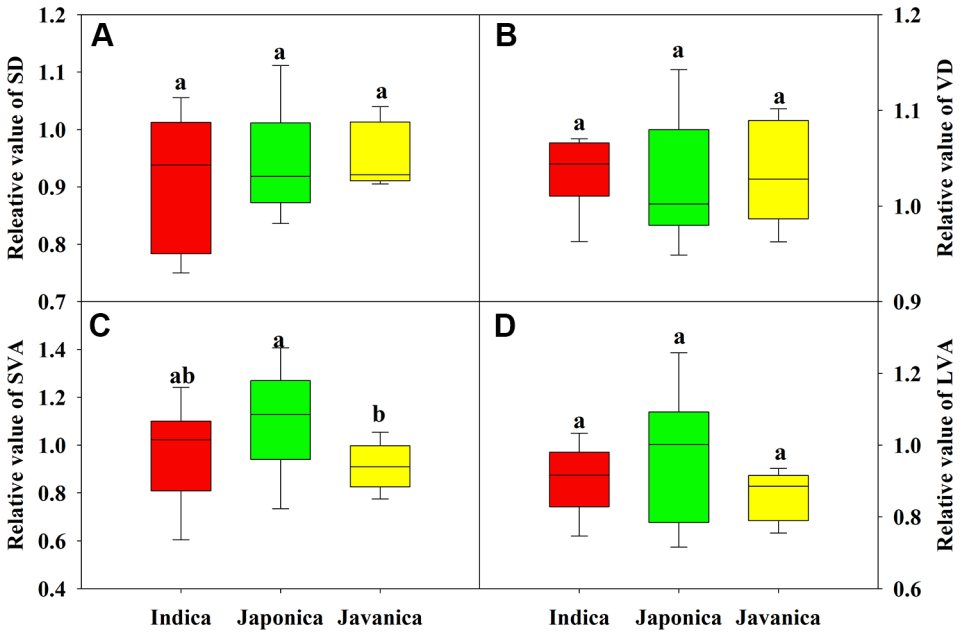

FIGURE 4 | Relative value (HT/CK) of stomatal density (SD, **A**), vein density (VD, **B**), and vein area of minor **(C)** and major **(D)** veins for the three rice (*Oryza sativa* L.) subspecies. Different lowercase letters indicate significant differences between subspecies means ($p < 0.05$). The outer box edges represent the 25th and 75th percentiles, the error bars are the 5th and 95th percentiles, and the line within the box represents the mean values. For each cultivar, three flag leaves were measured (one leaf per plant), and the three values were averaged as one biological replicate. n (the biological replicates) was 8, 8, and 5 for the indica, japonica, and javanica cultivars, respectively.

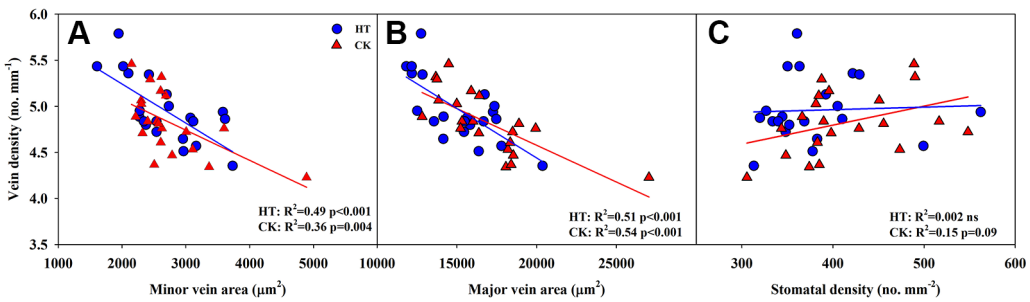

FIGURE 5 | Correlations between vein density (VD) and vein area of minor vein (SVA, **A**) and major vein (LVA, **B**), and between VD and stomatal density (SD, **C**) at high growth temperature (HT) and control (CK) treatments for the three rice (*Oryza sativa* L.) subspecies.

Yamori et al., 2014; Xiong et al., 2017), although some C_3 species can maintain high *A* at temperatures as high as 45°C (e.g. Lawson et al., 2014). Two main biochemical hypotheses have been put forward to explain why *A* decreases above the optimum temperature: Rubisco activase heat lability and electron transport declines (Dusenge et al., 2019). It is notable that tissues that develop after a shift in temperature often show greater acclimation to that new temperature than those that developed prior to the change in temperature (i.e. "long-term" > "short-term"; e.g. Campbell et al., 2007). Many studies have shown that the response of *A* to temperature depends on the temperature experienced by the plant over longer time periods, a response termed temperature acclimation (Berry and Bjorkman, 1980; Hikosaka et al., 2006; Way and Yamori, 2014; Yamori et al., 2014). For example, Way and Yamori (2014) found that about half of the 103 species in their database had increased *A* in response to warming. Within C_3 species, annual herbaceous plants (*A* of high temperature/low temperature, 1.31 ± 0.07) show greater *A* temperature response than evergreen woody plants (0.99 ± 0.03), deciduous woody plants (1.19 ± 0.12), and perennial herbaceous plants (1.03 ± 0.07, Yamori et al., 2014). In present study, rice plants were treated at HT for one month, and

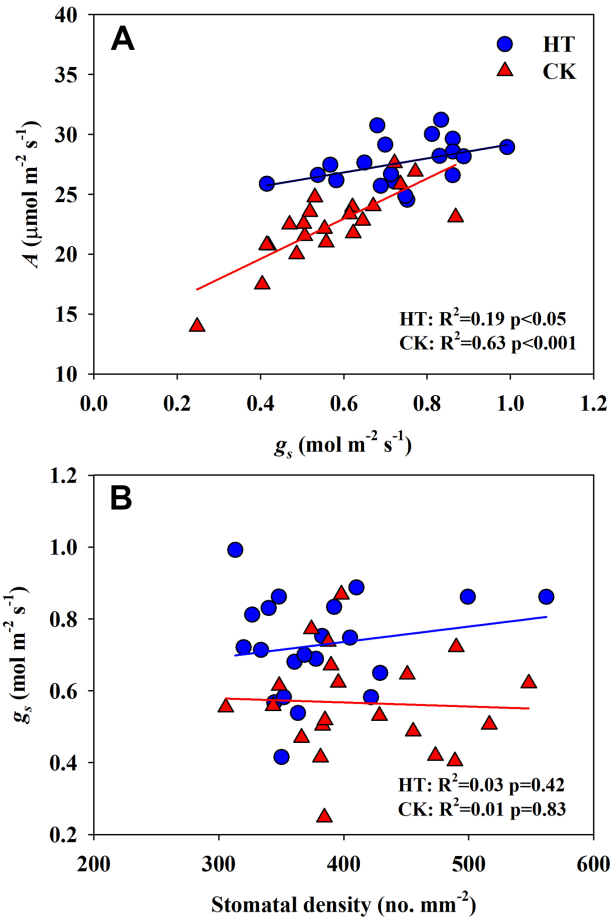

FIGURE 6 | Correlations between light saturated photosynthetic rate **(A)** and stomatal conductance (g_s), and between stomatal conductance (g_s) **(B)** and stomatal density (SD) at high growth temperature (HT) and control (CK) treatments for the three rice (*Oryza sativa* L.) subspecies.

A at high temperature treatment was higher than that at control treatment by 23.7% on average.

Physiological Mechanisms Underlying the Temperature Acclimation

The physiological mechanisms underlying photosynthetic acclimation of *A* to warmer temperatures have been extensively investigated (Sage and Kubien, 2007; Yamori et al., 2014). Proton leakiness of the thylakoid membrane has been frequently proposed as a problem at high temperatures, since it could lead to the impairment of the coupling of ATP synthesis to electron transport. Increases in cyclic electron flow around PSI at high temperature can compensate for thylakoid leakiness, allowing ATP synthesis to continue (Bukhov et al., 2000; Yamori et al., 2014). In many plant species, the Rubisco activation state decreases at short-term high temperature due to the insufficient activity of Rubisco activase, however, in plants adapted to HT, a different isoform of Rubisco activase that confers heat stability can be produced by some species, including spinach, cotton, and wheat (Yamori et al., 2014). Moreover, expression of heat-shock proteins (HSPs)/chaperones at high temperature contributes to the temperature acclimation through their effects in protein folding and assembly, stabilization of proteins and membranes, and for cellular homeostasis at high temperature (Barua et al., 2003).

Under high temperature, transpirational cooling is also an important acclimation mechanism in plants (Crawford et al., 2012; Mathur et al., 2014). Heat stress may be somewhat mitigated if transpiration-mediated cooling can be maintained, for example, rice can remain productive in air temperatures of 40°C if humidity remains low (Jagadish et al., 2014). In Blueberry, the thermal tolerant cultivars could improve their heat dispersing efficiency through regulating stomatal traits (Hao et al., 2019). In present study, the *E* of all cultivars was significantly increased under high temperature. The increase in *A* and *E* at HT was mainly related to the significantly increased g_s (**Figures 6** and **7A**).

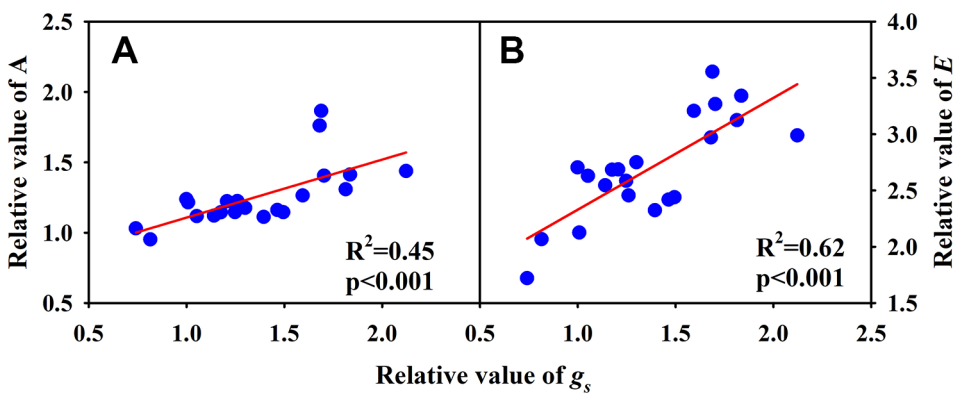

FIGURE 7 | Correlations between the relative value of light saturated photosynthetic rate **(A)** and the relative value of stomatal conductance (g_s), and between the relative value of transpiration rate **(B)** and conductance (g_s) and the relative value of g_s for the three rice (*Oryza sativa* L.) subspecies.

Anatomical Mechanisms Underlying the Temperature Acclimation

Photosynthetic acclimation to long-term high temperature may be partly due to the structural changes in leaf tissues (Sage and Kubien, 2007; Yamori et al., 2014). In higher plants, water from the stem enters the petiole and moves through xylem in different vein orders, then exits into the bundle sheath and moves through mesophyll tissue before evaporating into the intercellular airspace and diffusing through stomata (Xiong et al., 2016). Stomatal density, leaf vein systems include VD and vascular bundle features, were strongly correlated with the hydraulic conductivity and maximum *A* (Brodribb et al., 2007). In present study, there was no significant difference in the response of SD, VD, and vein area to high temperature between the three subspecies (**Figure 4**), however, significant genotypic variation was found within each subspecies (**Figure S2**). High temperature significantly reduced SD and SVA (**Figures 3A, D**). This was consistent with previous studies in the model species *Arabidopsis thaliana* and Scots pine (*Pinus sylvestris* L.) (Luomala et al., 2005; Vile et al., 2012). Crawford et al. (2012) illustrated that increased stomatal spacing by lowering SD, may facilitate evaporative cooling in high temperature conditions, through increasing the inter−stomatal space available for vapor diffusion. However, some other studies found significant increase in SD at high temperature in soybean (Jumrani et al., 2017) and rice (Caine et al., 2018). Therefore, more studies are needed to examine the plasticity of other leaf structures in response to high temperature and its effects on photosynthetic physiology.

CONCLUSION

The current study revealed rice leaf photosynthetic physiology exhibited high temperature acclimation, and the *javanica* subspecies possessed higher heat resistance than *indica* and *japonica* subspecies. Large genotypic variation in response of *A*, g_s, *E*, and other leaf anatomies to HT as well as correlation analysis showed the response of *A* and g_s among different cultivars to HT was not related to the plasticity of leaf anatomy (mainly the stomatal and vein structure).

DATA AVAILABILITY STATEMENT

All datasets generated for this study are included in the article/ **Supplementary Material**.

AUTHOR CONTRIBUTIONS

FW conceived and designed the research. DY conducted the experiments and collected the data, DY and FW analyzed the data and wrote the paper. FW and SP commented and revised the paper

FUNDING

This work was supported by the Program of National Natural Science Foundation of China (No. 31501255), the National Key Research and Development Program of China (No. 2017YFD0301401-3).

ACKNOWLEDGMENTS

We thank Guanjun Huang, Lilian Wu, Zhuang Xiong and Miao Ye for their technological support.

SUPPLEMENTARY MATERIAL

The Supplementary Material for this article can be found online at: https://www.frontiersin.org/articles/10.3389/fpls.2020.00026/full#supplementary-material

REFERENCES

Amiard, V., Mueh, K. E., Demmig-Adams, B., Ebbert, V., Turgeon, R., and Adams, W. W. (2005). Anatomical and photosynthetic acclimation to the light environment in species with differing mechanisms of phloem loading. *Proc. Natl. Acad. Sci. U.S.A.* 102, 12968–12973. doi: 10.1073/pnas.0503784102

Barua, D., Downs, C. A., and Heckathorn, S. A. (2003). Variation in chloroplast small heat-shock protein function is a major determinant of variation in thermotolerance of photosynthetic electron transport among ecotypes of *chenopodium album*. *Funct. Plant Biol.* 30, 1071–1079. doi: 10.1071/FP03106

Beadle, C. L., and Long, S. P. (1985). Photosynthesis — Is it limiting to biomass production? *Biomass* 8, 119–168. doi: 10.1016/0144-4565(85)90022-8

Berry, J., and Bjorkman, O. (1980). Photosynthetic response and adaptation to temperature in higher plants. *Annu. Rev. Plant Physiol.* 31, 491–543. doi: 10.1146/annurev.pp.31.060180.002423

Brodribb, T. J., Feild, T. S., and Jordan, G. J. (2007). Leaf maximum photosynthetic rate and venation are linked by hydraulics. *Plant Physiol.* 144, 1890–1898. doi: 10.1104/pp.107.101352

Bukhov, N. G., Samson, G., and Carpentier, R. (2000). Nonphotosynthetic reduction of the intersystem electron transport chain of chloroplasts following heat stress: steady-state rate. *Photochem. Photobiol.* 72, 351–357. doi: 10.1562/0031-8655(2000)0720351NROTIE2.0.CO2

Caine, R. S., Yin, X., Sloan, J., Harrison, E. L., Mohammed, U., Fulton, T., et al. (2018). Rice with reduced stomatal density conserves water and has improved drought tolerance under future climate conditions. *New Phytol.* 221, 371–384. doi: 10.1111/nph.15344

Campbell, C., Atkinson, L., Zaragoza-Castells, J., Lundmark, M., Atkin, O., and Hurry, V. (2007). Acclimation of photosynthesis and respiration is asynchronous in response to changes in temperature regardless of plant functional group. *New Phytol.* 176, 375–389. doi: 10.1111/j.1469-8137.2007.02183.x

Crawford, A. J., McLachlan, D. H., Hetherington, A. M., and Franklin, K. A. (2012). High temperature exposure increases plant cooling capacity. *Curr. Biol.* 22, R396–R397. doi: 10.1016/j.cub.2012.03.044

Dusenge, M. E., Duarte, A. G., and Way, D. A. (2019). Plant carbon metabolism and climate change: elevated CO_2 and temperature impacts on photosynthesis, photorespiration and respiration. *New Phytol.* 221, 32–49. doi: 10.1111/nph.15283

Evans, L. T., and Fischer, R. A. (1999). Yield potential: its definition, measurement, and significance. *Crop Sci.* 39, 1544–1551. doi: 10.2135/cropsci1999.3961544x

Evans, L. T. (1998). Crop evolution, adaptation and yield. *Photosynthetica* 34, 56–56. doi: 10.1023/A:1006889901899

Farquhar, G. D., and Sharkey, T. D. (1982). Stomatal conductance and photosynthesis. *Annu. Rev. Plant Physiol.* 33, 317–345. doi: 10.1146/annurev.pp.33.060182.001533

Franks, P. J., Drake, P. L., and Beerling, D. J. (2010). Plasticity in maximum stomatal conductance constrained by negative correlation between stomatal size and density: an analysis using *eucalyptus globulus*. *Plant Cell Environ.* 32, 1737–1748. doi: 10.1111/j.1365-3040.2009.002031.x

Hao, L., Guo, L., Li, R., Cheng, Y., Huang, L., Zhou, H., et al. (2019). Responses of photosynthesis to high temperature stress associated with changes in leaf structure and biochemistry of blueberry (Vaccinium corymbosum L.). *Sci. Hortic* 246, 251–264. doi: 10.1016/j.scienta.2018.11.007

Hasanuzzaman, M., Nahar, K., Alam, M., Roychowdhury, R., and Fujita, M. (2013). Physiological, biochemical, and molecular mechanisms of heat stress tolerance in plants. *Int. J. Mol. Sci.* 14, 9643–9684. doi: 10.3390/ijms14059643

Hay, R. K. M. (1995). Harvest index: a review of its use in plant breeding and crop physiology. *Ann. Appl. Biol.* 126, 197–216. doi: 10.1111/j.1744-7348.1995.tb05015.x

Hikosaka, K., Ishikawa, K., Borjigidai, A., Muller, O., and Onoda, Y. (2006). Temperature acclimation of photosynthesis: mechanisms involved in the changes in temperature dependence of photosynthetic rate. *J. Exp. Bot.* 57, 291–302. doi: 10.1093/jxb/erj049

Huang, J., and Rozelle, S. (2015). Agricultural development, nutrition, and the policies behind china's success. *Asian. J. Agric. Dev.* 7, 93–126. doi: 10.22004/ag.econ.199084

Huang, G., Zhang, Q., Wei, X., Peng, S., and Li, Y. (2017). Nitrogen can alleviate the inhibition of photosynthesis caused by high temperature stress under both steady-state and flecked irradiance. *Front. Plant Sci.* 8, 945. doi: 10.3389/fpls.2017.00945

Jagadish, S. V. K., Murty, M. V. R., and Quick, W. P. (2014). Rice responses to rising temperatures–challenges, perspectives and future directions. *Plant Cell Environ.* 38, 1686–1698. doi: 10.1111/pce.12430

Jones, H. G. (1998). Stomatal control of photosynthesis and transpiration. *J. Exp. Bot.* 49, 387–398. doi: 10.1093/jexbot/49.suppl_1.387

Jumrani, K., Bhatia, V. S., and Pandey, G. P. (2017). Impact of elevated temperatures on specific leaf weight, stomatal density, photosynthesis and chlorophyll fluorescence in soybean. *Photosynth. Res.* 131, 333–350. doi: 10.1007/s11120-016-0326-y

Khush, G. S. (2013). Strategies for increasing the yield potential of cereals: case of rice as an example. *Plant Breed.* 132, 433–436. doi: 10.1111/pbr.1991

Lawson, T., Davey, P. A., Yates, S. A., Bechtold, U., Baeshen, M., Baeshen, N., et al. (2014). C_3 photosynthesis in the desert plant Rhazya stricta is fully functional at high temperatures and light intensities. *New Phytol.* 201 (3), 862–873.

Lobell, D. B., and Asner, G. P. (2003). Climate and management contributions to recent trends in US agricultural yields. *Science* 299, 1032–1032. 1078475. doi: 10.1126/science

Long, S. P., Marshall-Colon, A., and Zhu, X. (2015). Meeting the global food demand of the future by engineering crop photosynthesis and yield potential. *Cell* 161, 56–66. doi: 10.1016/j.cell.2015.03.019

Luomala, E. M., Laitinen, K., Sutinen, S., Kellomaki, S., and Vapaavuori, E. (2005). Stomatal density, anatomy and nutrient concentrations of Scots pine needles are affected by elevated CO_2 and temperature. *Plant Cell Environ.* 28, 733–749. doi: 10.1111/j.1365-3040.2005.01319.x

Mathur, S., Agrawal, D., and Jajoo, A. (2014). Photosynthesis: response to high temperature stress. *J. Photochem. Photobiol. B.* 137, 116–126. doi: 10.1016/j.jphotobiol.2014.01.010

Monteith, J. L. (1977). Climate and the efficiency of crop production in Britain. *Phil. Trans. R. Soc. London B* 281, 277–294. doi: 10.1098/rstb.1977.0140

Peng, S., Huang, J., Sheehy, J. E., Laza, R. C., Visperas, R. M., Zhong, X., et al. (2004). Rice yields decline with higher night temperature from global warming. *Proc. Natl. Acad. Sci. U.S.A.* 101, 9971–9975. doi: 10.1073/pnas.0403720101

Peng, S. (2014). Reflection on China's rice production strategies during the transition period. *Sci. Sin. Vitae.* 44, 845–850. doi: 10.1360/052014-98

Sack, L., and Holbrook, N. M. (2006). Leaf hydraulics. *Annu. Rev. Plant Biol.* 57, 361–381. doi: 10.1146/annurev.arplant.56.032604.144141

Sage, R. F., and Kubien, D. S. (2007). The temperature response of C_3 and C_4 photosynthesis. *Plant Cell Environ.* 30, 1086–1106. doi: 10.1111/j.1365-3040.2007.01682.x

Tang, H., Pang, J., Zhang, G., Takigawa, M., Liu, G., Zhu, J., et al. (2014). Mapping ozone risks for rice in china for years 2000 and 2020 with flux-based and exposure-based doses. *Atmos. Environ.* 86, 74–83. doi: 10.1016/j.atmosenv.2013.11.078

Tholen, D., Boom, C., and Zhu, X. (2012). Opinion: prospects for improving photosynthesis by altering leaf anatomy. *Plant Sci.* 197, 92–101. doi: 10.1016/j.plantsci.2012.09.005

Vile, D., Pervent, M., Belluau, M., Vasseur, F., Bresson, J., Muller, B., et al. (2012). *Arabidopsis* growth under prolonged high temperature and water deficit: independent or interactive effects? *Plant Cell Environ.* 35, 702–718. doi: 10.1111/j.1365-3040.2011.02445.x

Wang, W., Mauleon, R., Hu, Z., Chebotarov, D., Tai, S., Wu, Z., et al. (2018). Genomic variation in 3,010 diverse accessions of Asian cultivated rice. *Nature* 557, 43–49. doi: 10.1038/s41586-018-0063-9

Way, D. A., and Yamori, W. (2014). Thermal acclimation of photosynthesis: on the importance of adjusting our definitions and accounting for thermal acclimation of respiration. *Photosynth. Res.* 119, 89–100. doi: 10.1007/s11120-013-9873-7

Weng, J., and Chen, C. (1987). Differences between indica and japonica rice varieties in CO_2 exchange rates in response to leaf nitrogen and temperature. *Photosynth. Res.* 14, 171–178. doi: 10.1007/BF00032321

Xiao, G., and Yuan, L. (2009). *Studies on Javanica Rice and Heterosis of Inter-subspecific Hybrids* (Beijing: Science Press). (in Chinese).

Xiong, D., Flexas, J., Yu, T., Peng, S., and Huang, J. (2016). Leaf anatomy mediates coordination of leaf hydraulic conductance and mesophyll conductance to CO_2 in Oryza. *New Phytol.* 213, 572–583. doi: 10.1111/nph.14186

Xiong, D., Ling, X., Huang, J., and Peng, S. (2017). Meta-analysis and dose-response analysis of high temperature effects on rice yield and quality. *Environ. Exp. Bot.* 141, 1–9. doi: 10.1016/j.envexpbot.2017.06.007

Yamori, W., Nagai, T., and Makino, A. (2011). The rate-limiting step for CO_2 assimilation at different temperatures is influenced by the leaf nitrogen content in several C_3 crop species. *Plant Cell. Environ.* 34, 764–777. doi: 10.1111/j.1365-3040.2011.02280.x

Yamori, W., Hikosaka, K., and Way, D. A. (2014). Temperature response of photosynthesis in C_3, C_4, and CAM plants: temperature acclimation and temperature adaptation. *Photosynth. Res.* 119, 101–117. doi: 10.1007/s11120-013-9874-6

Zhao, S., Yu, J., and Xiao, G. (2013). Effects of high temperature stress on the photosynthesis and osmoregulation substances of flag leaves in *Oryza stavia* L. ssp. *javanica*. *Ecol. Environ. Sci.* 22, 110–115. (in Chinese with English abstract). doi: 10.16258/j.cnki.1674-5906.2013.01.022

Zhao, C., Liu, B., Piao, S., Wang, X., Lobell, D. B., Huang, Y., et al. (2017). Temperature increase reduces global yields of major crops in four independent estimates. *PNAS* 114, 9326–9331. doi: 10.1073/pnas.1701762114

Zhu, X., Long, S. P., and Ort, D. R. (2010). Improving photosynthetic efficiency for greater yield. *Annu. Rev. Plant Biol.* 61, 235–261. doi: 10.1146/annurev-arplant-042809-112206

Conflict of Interest: The authors declare that the research was conducted in the absence of any commercial or financial relationships that could be construed as a potential conflict of interest.

frontiers in Plant Science

ORIGINAL RESEARCH
published: 28 February 2020
doi: 10.3389/fpls.2020.00043

Interactional Effects of Climate Change Factors on the Water Status, Photosynthetic Rate, and Metabolic Regulation in Peach

Sergio Jiménez[1,2†], *Masoud Fattahi*[1,3†], *Khaoula Bedis*[1], *Shirin Nasrolahpour-moghadam*[1,3], *Juan José Irigoyen*[4] *and Yolanda Gogorcena*[1*]

[1] Laboratory of Genomics, Genetics and Breeding of Fruit Trees and Grapevine, Department of Pomology, Estación Experimental de Aula Dei-Consejo Superior de Investigaciones Científicas, Zaragoza, Spain, [2] Bayer AG, Crop Science Division, Research and Development, Environmental Science Field Solutions, Monheim, Germany, [3] Department of Agriculture, Shahrekord University, Shahrekord, Iran, [4] Departamento de Biología Ambiental, Grupo de Fisiología del Estrés en Plantas, Unidad Asociada al CSIC (EEAD, Zaragoza e ICVV, Logroño), Facultad de Ciencias, Universidad de Navarra, Pamplona, Spain

OPEN ACCESS

Edited by:
Marouane Baslam,
Niigata University, Japan

Reviewed by:
Sergio González Nebauer,
Universitat Politècnica de València, Spain
Francisco M. Del Amor,
Instituto Murciano de Investigación y Desarrollo Agrario y Alimentario, Spain

***Correspondence:**
Yolanda Gogorcena
aoiz@eead.csic.es

[†]These authors have contributed equally to this work

Specialty section:
This article was submitted to Plant Abiotic Stress, a section of the journal Frontiers in Plant Science

Received: 03 October 2019
Accepted: 14 January 2020
Published: 28 February 2020

Citation:
Jiménez S, Fattahi M, Bedis K, Nasrolahpour-moghadam S, Irigoyen JJ and Gogorcena Y (2020) Interactional Effects of Climate Change Factors on the Water Status, Photosynthetic Rate, and Metabolic Regulation in Peach. Front. Plant Sci. 11:43. doi: 10.3389/fpls.2020.00043

Environmental stress factors caused by climate change affect plant growth and crop production, and pose a growing threat to sustainable agriculture, especially for tree crops. In this context, we sought to investigate the responses to climate change of two *Prunus* rootstocks (GF677 and Adesoto) budded with Catherina peach cultivar. Plants were grown in 15 L pots in temperature gradient greenhouses for an 18 days acclimation period after which six treatments were applied: [CO_2 levels (400 versus 700 μmol mol^{-1}), temperature (ambient versus ambient + 4°C), and water availability (well irrigated versus drought)]. After 23 days, the effects of stress were evaluated as changes in physiological and biochemical traits, including expression of relevant genes. Stem water potential decreased under drought stress in plants grafted on GF677 and Adesoto rootstocks; however, elevated CO_2 and temperature affected plant water content differently in both combinations. The photosynthetic rate of plants grafted on GF677 increased under high CO_2, but decreased under high temperature and drought conditions. The photosynthetic rates of plants grafted onto Adesoto were only affected by drought treatment. Furthermore, in GF677–Catherina plants, elevated CO_2 alleviated the effect of drought, whereas in those grafted onto Adesoto, the same condition produced acclimation in the rate. Stomatal conductance decreased under high CO_2 and drought stress in both grafted rootstocks, and the combination of these conditions improved water-use efficiency. Changes in the sugar content in scion leaves and roots were significantly different under the stress conditions in both combinations. Meanwhile, the expression of most of the assessed genes was significantly affected by treatment. Regarding genotypes, GF677 rootstock showed more changes at the molecular and transcriptomic level than did Adesoto rootstock. A coordinated shift was found between the physiological status and the transcriptomic responses. This study revealed adaptive responses to climate change at the physiological, metabolic, and transcriptomic levels in two *Prunus* rootstocks

budded with 'Catherina'. Overall, these results demonstrate the resilient capacity and plasticity of these contrasting genotypes, which can be further used to combat ongoing climate changes and support sustainable peach production.

Keywords: *Prunus* rootstocks, elevated CO_2, warming, drought, osmotic potential, water-use efficiency, soluble sugars, gene expression

INTRODUCTION

Peach is the third most important temperate fruit tree species of the Rosaceae family, behind apples and pears (FAOSTAT, 2018; http://faostat.fao.org), with China being the largest producer (14.3 million tons), followed by European countries (Spain, Italy, and Greece) and the United States. In 2017, world growth area and production were 1.52 million hectares and 24.7 million tons, respectively. Peach is grown in temperate areas and it is routinely grafted on rootstocks for adaption to different soil and climate conditions. Predictions for new climate scenarios, which include an increase in temperature, alterations in rainfall patterns, and increasing frequency of extreme climate events, are likely to negatively affect global agriculture, especially in Mediterranean regions (IPCC, 2014; FAO, 2016; IPCC, 2018). This concern is especially relevant for peach trees because warming temperatures will impact negatively flowering and production (Gogorcena et al., 2020). In this situation, it is still more critical to choose the correct rootstock–scion combination to cope with the effects of climate change.

In the last century, climate change (high CO_2 concentration and temperature, and limited availability of water) has become a major concern for the scientists. According to long-term warming trends since pre-industrial times, temperatures are estimated to have increased by 0.1 to 0.3°C per decade across the world (IPCC, 2014; IPCC, 2018) and the mean global temperature is expected to increase by 1.5°C between 2030 and 2052 if it continues to rise at the current rate (IPCC, 2018). Atmospheric CO_2 concentrations have risen at an accelerated pace since the start of the industrial revolution. For the one thousand years prior to the industrial revolution, CO_2 levels were stable at about 280 μmol mol^{-1}. Nowadays, this concentration is approximately 53% higher at 414 μmol mol^{-1} (NOAA Mauna Loa Atmospheric Baseline Observatory, 2019). By the end of this century, it is predicted to reach 700 μmol mol^{-1} (Long et al., 2004; Ainsworth et al., 2008; Salazar-Parra et al., 2018). To cope with such catastrophic climate change, plants need to develop a width spectrum of physiological, biochemical, and molecular programs to rapidly sense change and adapt. In this context, understanding how peach may respond and adapt to future increases in CO_2 concentration, temperature, and drought is critical for the agricultural fruit sector.

Previous studies have shown that elevated CO_2 concentrations stimulate photosynthetic carbon gain and net primary production (Leakey et al., 2009; Medina et al., 2016; Afzal et al., 2018). However, in long-term experiments, it has been reported that the initial stimulation of photosynthesis decreases due to acclimation of photosynthetic capacity (Leakey et al., 2009; Aranjuelo et al., 2011; Salazar-Parra et al., 2015; Medina et al., 2016), and that environmental or genetic factors predispose plants to greater or lesser variation (reviewed in Arp, 1991; Leakey et al., 2009 and references therein; Medina et al., 2016). Moreover, elevated CO_2 improves nitrogen-use efficiency and decreases water use in leaves (Medina et al., 2016). Furthermore, elevated CO_2 stimulates leaf dark respiration *via* a transcriptional reprogramming of metabolism in soybean, but not in other species (Leakey et al., 2009).

It is well accepted that water scarcity will dramatically increase due to climate change and will become a major problem for crop production by limiting the growth and productivity of many crop species. Water limitation in the near future has resulted in strong interest in drought tolerance afforded by rootstocks (Serra et al., 2014), which enable the scion to grow and bear fruit. Plant responses to water limitation are usually monitored through select morphological and physiological traits (Jiménez et al., 2013; Santana-Veira et al., 2016; Fathi et al., 2017; Afzal et al., 2018). Drought inhibits the growth and development of plants, directly affecting the photosynthetic process, resulting in physiological limitations and transcriptional responses that may cause severe decreases in plant yield (Jiménez et al., 2013; Nakashima et al., 2014; Ksouri et al., 2016). Under these stress conditions, there are physiological changes such as reduction of net photosynthesis, and decreases in stomatal conductance and internal CO_2 concentrations (Jones, 2007; Cattivelli et al., 2008; Lovisolo et al., 2010). The decrease of stomatal conductance may lead to the reduction of transpiration and water losses as well as to overproduction of reactive oxygen species (ROS) and activation of antioxidant enzymes (Gogorcena et al., 1995; Salazar-Parra et al., 2012; Haider et al., 2017). The accumulation of metabolites such as soluble carbohydrates and proline in leaves and roots of *Prunus* (Jiménez et al., 2013; Haider et al., 2018), carbohydrates and proline in leaves of pearl millet (Fabbrin et al., 2015), and carbohydrates in citrus rootstocks (Pedroso et al., 2014; Santana-Veira et al., 2016) have all been reported previously as a consequence of drought stress.

Plant responses to elevated CO_2 in combination with drought stress and/or temperature increases have been widely studied in different plant species, such as wheat (Erice et al., 2014; Medina et al., 2016), grapevines (Kizildeniz et al., 2015; Salazar-Parra et al., 2015; Martínez-Lüscher et al., 2016; Kizildeniz et al., 2018), alfalfa, soybean, and other plant species (Aranjuelo et al., 2005; Aranjuelo et al., 2006; Baslam et al., 2014; Gray and Brady, 2016 and references therein; Irigoyen et al., 2014; Kelly et al., 2016).

These earlier studies have found that responses are genotype-dependent; however, conflicting experimental results make it difficult to draw general conclusions (Kelly et al., 2016). Some studies have shown positive effects of elevated CO_2 on water stress tolerance in some wheat and grapevine genotypes, but these effects were not universal. In wheat, elevated CO_2 promoted plant growth and mitigated the deleterious effect of drought on biomass decreases (Medina et al., 2016). In grapevines, a protective effect of CO_2 independent of temperature was found concerning oxidative damage (Salazar-Parra et al., 2015) and plant growth (Kizildeniz et al., 2015). However, in bread wheat genotypes, the effect of CO_2 and drought interacted to cause oxidative stress (Bencze et al., 2014), and in other woody species, such as American sycamore, sweet gum, and sugar maple, it negatively affected growth (Gray and Brady, 2016). Other changes under elevated CO_2 and drought stress have been described, such as a decrease in Rubisco content and activity, changes in amino acids and N content, and an increase in carbohydrates in wheat (Aranjuelo et al., 2011), as well as increases in sugar and changes in organic acids and anthocyanin content in grape berries (Kizildeniz et al., 2015).

In fruit plant breeding, rootstocks have been shown to play an important role in drought tolerance by adjusting the water supply to the demands of shoot transpiration. In fact, rootstocks are considered to confer drought and heat tolerance to the scion (Iacono et al., 1998; Meggio et al., 2014; Serra et al., 2014). Morphological and physiological changes were observed in *Prunus* rootstocks subjected to water deprivation (Solari et al., 2006; Jiménez et al., 2013). Apart from these changes, water-stressed plants may accumulate proline and raffinose in leaves and roots to protect membranes and enzymes, and to deal with the deleterious effects of drought-induced oxidative stress (Jiménez et al., 2013). Proline content in roots and leaves, sorbitol in leaves, and raffinose in roots were all found to be associated with increases in water-use efficiency (Jiménez et al., 2013). Moreover, at the transcriptional level, changes in gene expression were consistently found to support the accumulation of these metabolites in root and leaf tissues in *Prunus* (Jiménez et al., 2013) and in grapevines (Haider et al., 2017).

As mentioned above, agriculture productivity is strongly affected by drought, temperature increases, and other forms of climate changes (FAO, 2016; Afzal et al., 2018). In the future, plants will not experience individual climate change factors, but will be exposed to several interacting environmental effects at the same time (Gray and Brady, 2016). Plant responses to elevated CO_2, temperature, and drought are genotype-dependent (Kizildeniz et al., 2015; Medina et al., 2016; Kizildeniz et al., 2018) and the interactive effects of environmental conditions and genotypic influences cannot be anticipated by studying the effect of each individual climate change factor. For this reason, to investigate plant responses where CO_2 concentration, temperature, and water availability can be modulated simultaneously, gradient temperature greenhouses are needed to enable comparisons of current climate with future predictions (Morales et al., 2014). Previous investigations in these facilities have been carried out by a number of authors for different herbaceous plant species (Sanz-Sáez et al., 2012; Sanz-Sáez et al., 2013; Fabbrin et al., 2015) and grapevines (Kizildeniz et al., 2015; Salazar-Parra et al., 2015; Martínez-Lüscher et al., 2016; Kizildeniz et al., 2018; Salazar-Parra et al., 2018), but never for *Prunus* spp and never taking into consideration rootstock plasticity.

The aim of the present work is to investigate the physiological, biochemical, and molecular responses of two contrasting *Prunus* rootstocks (GF677 and Adesoto) budded with Catherina peach cultivar to climate change-induced stresses (elevated CO_2, elevated temperature, and water deficit). Understanding how rootstocks with different genetic background modulate the response of peach trees under stress conditions and disentangle the underlying molecular mechanisms will be very helpful to develop resilient rootstocks in future breeding programs.

MATERIALS AND METHODS

Plant Material and Experimental Conditions

Micropropagated GF677 (*Prunus dulcis* Miller × *P. persica* L. Batsch) and Adesoto (*P. insititia* L.) rootstock plants were grown for two weeks in 300 cm^3 pots containing a peat substrate, then they were micrografted with variety Catherina (*P. persica* L. Batsch). Plants were transferred to 15 L containers with a medium of 1:1 sand-peat substrate (TKS-1, Floragard, Oldenburg, Germany) and 2 g kg^{-1} osmocote 14-13-13 (The Scotts Company LLC, Marsyville, OH, USA). Plants were grown for two months in an experimental greenhouse in Zaragoza, Spain (41°43′N, 0°48′W) under normal day light conditions (14 h light/10 h dark photoperiod) with mean day and night temperatures and humidity of 24 and 18°C, and 51 and 67%, respectively. Plants were divided randomly into eight groups (20 plants per group) and were transferred to four greenhouses and grown at the University of Navarra (Pamplona, Spain, 42°48′N, 1°40′W). All temperature gradient greenhouses (TGGs) have been designed in a modular way to have a temperature gradient (ambient to + 4°C) and CO_2 gassed inside to reach the desired CO_2 concentration. Treatments were a combination of two CO_2 levels (ambient, approximately 400 ppm and elevated, 700 ppm), two temperature regimes (ambient temperature and ambient + 4° C) for 18 d, a period that used for acclimation. Then plants were subjected to two regimes of irrigation. Well-watered plants were maintained at around 80% of the substrate field capacity. In the water-deficit treatment, plants were watered daily with the 80% of the evapotranspirated water (Jiménez et al., 2013). Then, in each greenhouse, plants were irrigated and partially irrigated for 23 d. Soil water sensors (Watermark soil moisture sensor, Spectrum Technologies Inc., IL, USA) were placed into the pots and used for irrigation control. Stems (leaves and main shoot) and roots were harvested at 23 d, weighed (fresh weight, FW), and then oven-dried (dry weight, DW) at 80°C for 48 h. For all treatments, specific leaf area (SLA) was measured and chlorophyll (Chl) concentration per unit leaf area was estimated using a SPAD 502 meter (Minolta Co., Osaka, Japan). Samples from plants submitted to ambient and elevated CO_2, ambient and elevated

temperature, and control and drought stress for 23 d were randomly collected. Root and leaf tissues from each treatment-plant (four biological replicates) were rinsed in distilled water, immediately frozen in liquid nitrogen and stored at -80°C until their use for the molecular determinations.

Water Status

A single mature leaf (fifth expanded leaf) of each of the four replicate plants was assayed for stem water potential (Ψstem) at day 23 of the experiment. Leaves were enclosed in aluminum foil-covered plastic envelopes to stop transpiration and allow equilibration with Ψstem 30 min before measurement. Midday Ψstem were measured using a Schölander-type pressure chamber (PMS instrument, Corvallis, OR, USA). After measurements, leaves were wrapped in aluminum foil, frozen in liquid nitrogen, and stored in plastic bags at -20°C (García-Sánchez et al., 2007). After thawing, osmotic potential (Ψπ) was measured with a Psychrometer Tru PSi SC10X (Decagon Devices, Inc., Pullman, WA, USA).

Leaf relative water content (RWC) was measured on a mature leaf (sixth expanded leaf) of the four replicate plants. Leaves were immediately weighed to obtain a leaf FW and petioles were submerged into water overnight in the dark. Fully hydrated leaves were reweighed to obtain turgid weight (TW) and dried at 80°C for 24 h to obtain DW. RWC was calculated as 100×(FW-DW)/(TW-DW) according to Morgan (Morgan, 1984).

Photosynthetic Parameters

Photosynthetic rate (A_N), stomatal conductance (g_s), intercellular CO_2 concentration (*C*i), and transpiration rate (*E*) were measured after 23 d using a portable photosynthesis system (LI-6400XT, Licor, Inc., Lincoln, NE, USA). Measurements were conducted between 10:00 and 12:00 (GMT) in the same leaves used for Ψstem determinations (n = 4). Parameters were measured with saturating light (1400 μmol m^{-2} s^{-1} provided by an external light source), 400 μmol mol^{-1} CO_2 and 30.5°C (average leaf temperature during measurements). Water-use efficiency (WUE) or instantaneous water-use efficiency was calculated as the ratio between the photosynthetic rate and stomatal conductance (A_N/g_s).

Osmotic-Regulating Compounds: Soluble Sugars and Proline

Leaf and root soluble sugar content was determined by high-performance liquid chromatography (HPLC). Plant tissue (n = 4) was ground to a fine powder in a pre-cooled mortar with liquid nitrogen. Polar compounds from ~0.1 g FW were extracted into aqueous ethanol at 80°C, in three steps, each lasting 20 min (step 1: 0.75 ml of 80% ethanol; steps 2 and 3: 0.75 ml of 50% ethanol). The mixture of each step was centrifuged for 10 min at 4800*g* and slurries were pooled (Moing et al., 2004). The ethanol was allowed to evaporate in a speed-vac and dry extracts were solubilized in 1 ml double-distilled water. Soluble sugars were purified using ion exchange resins (Bio-Rad AG 1-X4 Resin 200-400 chloride form, Bio-Rad AG 50W-X8 Resin 200-400 mesh hydrogen form, Bio-Rad, Hercules, CA, USA). Samples were concentrated to 0.2 ml, filtered and 20 μl was injected and analyzed by HPLC, using a Ca-column (Aminex HPX-87C 300 mm × 7.8 mm column Bio-Rad) flushed with 0.6 ml min^{-1} double-distilled water at 85°C with a refractive index detector (Waters 2410) (Milford, MA, USA). Concentrations of the main sugars (fructose, glucose, raffinose, sorbitol, sucrose, and xylose) were calculated for each sample, using mannitol as an internal standard. Sugar quantification was carried out with Empower Login software from Waters, using commercial standards (Panreac Química S.A. Barcelona, Spain). The amounts of soluble sugars were reported as mg g^{-1} DW.

Leaf and root proline were determined using the methodology described previously (Bates et al., 1973; Ábrahám et al., 2010). Plant tissue (n = 4) was ground to a fine powder in a pre-cooled mortar with liquid nitrogen. About 0.1 g of FW per sample was homogenized with 3% sulfosalicylic acid (Panreac Química S.A.) and the supernatant was reacted with ninhydrine (Sigma-Aldrich, St. Louis, MO, USA). The absorbance was read at 520 nm and the free proline concentration was calculated from a calibration curve using proline as a standard (Sigma-Aldrich). Free proline content was reported as mg g^{-1} DW.

RNA Isolation and RT-qPCR

Frozen plant tissue (four biological replicates) was ground to a fine powder in a pre-cooled mortar with liquid nitrogen and subsequently total RNA was isolated from ~100 mg of FW following the protocol of Meisel et al. (2005) with some modifications. After DNase I treatment (Thermo Scientific, Waltham, MA, USA) to eliminate possible genomic DNA contamination, 2 μg of total RNA were reverse transcribed using an oligo-(dT) 18 as a primer with RevertAid H Minus first-strand cDNA synthesis system (Thermo Scientific). Samples from cDNA synthesis were used to evaluate the expression of genes involved in sorbitol metabolism and raffinose and proline synthesis. These included sorbitol dehydrogenase (*SDH*), sorbitol-6-phosphate dehydrogenase (*S6PDH*), raffinose synthase (*SIP1*), Δ-1-pyrrolyne-carboxylate synthase (*P5CS*), Δ-1-pyrrolyne-carboxylate reductase (*P5CR*), and ornithine aminotransferase (*OAT*), which encodes an enzyme that synthesizes a precursor for proline biosynthesis. Also, phosphatidylinositol 4,5-bisphosphate (*PIP2*), which plays a role in membrane transport, dehydration responsive element binding protein (*DREB2*), ABA responsive element binding protein (*AREB2*), and the homeodomain-leucine zipper protein (*HAT22*) genes were assayed (**Supplementary Table 1**). Gene sequences were identified by Blastn against the "Peach Genome v1.0 predicted transcripts" database in GDR (http://www.rosaceae.org) with an *E*-value of $>1 \times 10^{-5}$. Finally, gene-specific primers were designed using Primer3Plus (Untergasser et al., 2007). Real-time qPCR was carried out using the Kapa SYBR Fast Maxter Mix (Kapa Biosystems, Cambridge, MA, USA) on a Applied Biosystem 7500 Real Time PCR (Life Technologies, Carlsbad, CA, USA) as described previously (Ksouri et al., 2016). Fluorescence values were baseline-corrected and averaged efficiencies for each gene and

quantification cycle (Cq) values were calculated using LinRegPCR program (Ruijter et al., 2009). Gene expression was determined with the gene expression Cq difference (GED) formula (Schefe et al., 2006) using *Actin 2* as an internal reference gene. Gene expression levels were normalized relative to the values of the drought-tolerant GF677 under control conditions (Jiménez et al., 2013; Ksouri et al., 2016). Normalized data allowed for the comparison of the magnitude of gene expression both across treatments and genotypes.

Statistical Analysis

Data were evaluated by three-way (2 CO_2 × 2 temperature × 2 water regimes) analysis of variance (ANOVA) for each genotype-tissue with SPSS 25.0.0 (Inc., Chicago, IL, USA). Previously, data were normalized and evaluated by Levene's homoscedasticity test and transformed if necessary. The main treatment parameters (CO_2, temperature, and drought) were evaluated alone and as interactions. For simplicity in figures, only two-level interactions (CO_2 × T^e) or triple (CO_2 × T^e × drought) were labeled. When treatment interaction terms were significant ($P \leq 0.05$), means were separated using Duncan's multiple range test at $P \leq 0.05$. Means of two samples were compared using a Student t-test. Regression analysis was carried out by Pearson's correlation.

RESULTS

Effect of Climate Change on Biomass, Water Status and Physiological Traits

Biomass

After 23 d of treatment, elevated CO_2 and drought modified biomass in plants grafted on both genotypes whereas temperature did not affect plant growth. High CO_2 concentrations increased leaf and root DW only in grafted GF677 plants, but decreased shoot/root DW ratio in both genotypes (**Table 1**). In GF677–Catherina plants, elevated CO_2 decreased specific leaf area, while drought decreased the shoot/root ratio and increased SPAD values. Drought decreased leaf DW in both genotypes and, as a consequence, the shoot/root ratio also decreased.

TABLE 1 | Leaf and root dry weight (DW), shoot-to-root ratio, specific leaf area (SLA), and SPAD in control and stressed *Prunus* rootstocks (GF677 and Adesoto) budded with var. Catherina, after 23 days of treatment.

GF677		Leaf DW (g)	Root DW (g)	Shoot/Root DW ratio	SLA (cm^2 g^{-1} DW)	SPAD
Principal Effects						
CO_2	CO_2 Amb	4.8 b	3.0 b	3.3 a	166 a	44
	CO_2 Elev	6.3 a	4.9 a	2.7 b	145 b	44
Temperature	T^e Amb	5.0	3.7	2.9	150	45
	T^e Amb+4°C	6.0	4.3	3.2	160	44
Irrigation	Control	6.6 a	4.3	3.4	159	43 b
	Drought	4.4 b	3.6	2.7	151	46 a
Signification						
CO_2		*	**	*	***	ns
T^e		ns	ns	ns	ns	ns
Irrigation		**	ns	*	ns	***
Adesoto						
Principal Effects						
CO_2	CO_2 Amb	4.1	2.9	3.0 a	157	43
	CO_2 Elev	3.6	3.5	2.4 b	147	42
Temperature	T^e Amb	3.6	3.1	2.5	146	42
	T^e Amb+4°C	4.1	3.2	3.0	158	42
Irrigation	Control	4.7 a	3.2	3.0 a	155	42
	Drought	3.0 b	3.2	2.4 b	149	42
Signification						
CO_2		ns	ns	*	ns	ns
T^e		ns	ns	ns	ns	ns
Irrigation		***	ns	*	ns	ns

*Three-way ANOVA was performed for linear model, on raw data. Significance: *P ≤ 0.05, **P ≤ 0.01, ***P ≤ 0.001 and ns indicates not significant. Comparison means by Duncan's test (P ≤ 0.05) were shown for the significant interaction among treatments. Different letters indicate significant differences among data within the same factor. Amb, Ambient; Elev, Elevated; T^e, Temperature.*

These data were presented at the conference of the Spanish Society of Plant Physiology (Fattahi et al., 2019).

Stem Water and Osmotic Potentials

Drought stress reduced stem water and osmotic potentials in Catherina cv. grafted on both rootstocks, GF677 and Adesoto ($P \leq 0.001$). The Ψstem in Catherina cv. grafted on Adesoto was also affected by the CO_2 concentration and temperature ($P \leq 0.001$) (**Figure 1A**). The osmotic potential, Ψπ, was significantly diminished by elevated CO_2 and affected by temperature ($P \leq 0.001$) in plants grafted on both rootstocks (**Figure 1B**). Elevated CO_2 in plants grafted on Adesoto and elevated temperature in those grafted on GF677 increased stem water and osmotic potentials, respectively.

Photosynthetic Response and Gas Exchange

The photosynthetic rate (A_N) of plants grafted on GF677 increased under elevated CO_2, but decreased with high temperature and drought (**Figure 2**). However, when plants were grafted onto Adesoto rootstock, the photosynthetic rate decreased only under drought stress condition. Stomatal conductance (g_s) of grafted plants on GF677 and Adesoto rootstocks decreased with elevated CO_2 concentration and drought stress (**Figure 2**), while transpiration rate (E) decreased only under drought stress condition. Elevated temperature did not affect the Adesoto rootstock.

In both genotypes, the climate change-like conditions, except for elevated temperature in Adesoto, improved the WUE (**Figure 2**).

Interactive effects among treatments were found for both grafted GF677 and Adesoto rootstocks, between CO_2 and temperature (A_N in Adesoto, and g_s in both genoypes, **Figure 2**), between CO_2 and drought (A_N, E in GF677, and g_s in both genotypes), and between temperature and drought (E and WUE in both genotypes). A triple interaction was found only in Adesoto–Catherina for transpiration rate (E, **Figure 2**). Interaction between elevated temperature and drought resulted in a higher WUE in drought stressed plants in both genotypes.

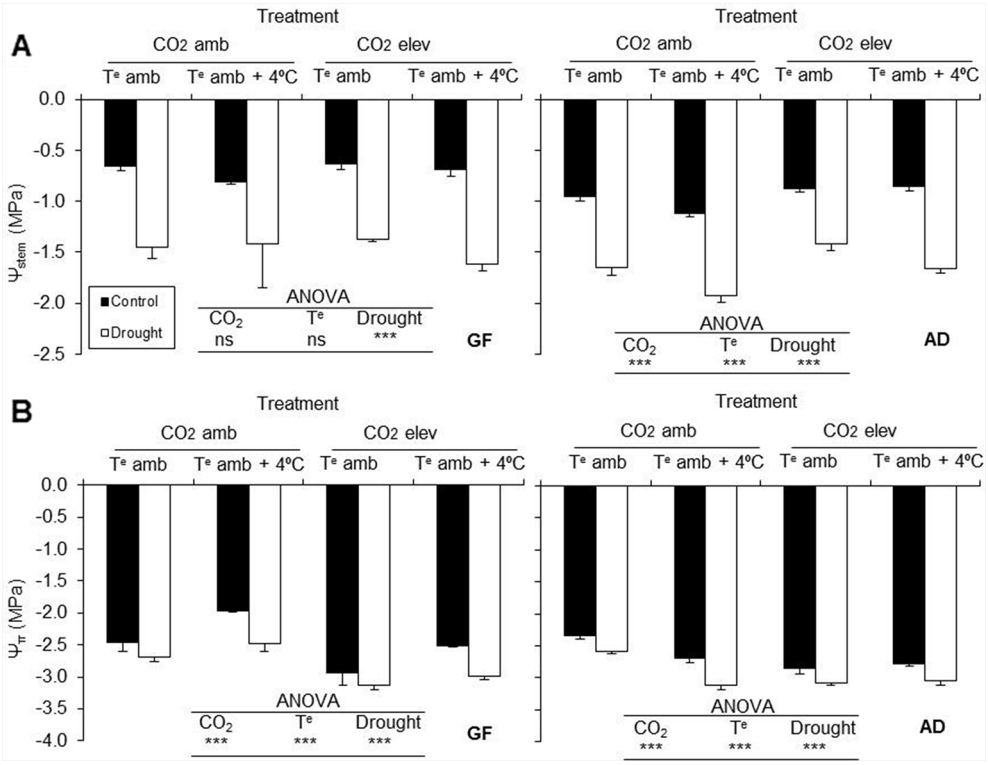

FIGURE 1 | (A) Stem water potential (Ψstem) and **(B)** osmotic potential (Ψπ) in peach plants (variety Catherina) grafted on GF677 (GF) and Adesoto (AD) and subjected to ambient (amb CO_2) and high (CO_2 elev) CO_2, ambient (T^e amb) and high (T^e amb + 4°C) temperature, and control irrigation and drought for 23 days. Vertical bars indicate the standard error (n = 4). Significant differences: *** $P \leq 0.001$ and ns: non-significant.

Effect of Climate Change on Soluble Carbohydrates and Proline Content

The biochemical responses involving sugars and proline content in roots and leaves of 'Catherina' grafted on both rootstocks (GF677 and Adesoto) subjected to stresses associated with climate change for 23 d are shown in **Tables 2** and **3**. In roots, elevated CO_2 increased the concentration of glucose and total sugars in both rootstocks, xylose in GF677, and fructose in Adesoto (**Table 2**). In this study, we noticed that the content of sorbitol and total sugars increased in response to high temperature, but only in roots of Adesoto (**Table 2B**). In roots, under drought stress condition, raffinose and proline concentration increased in GF677, sorbitol decreased in GF677, but increased in Adesoto rootstock, and fructose decreased in Adesoto (**Table 2**). The interactive effects between treatments also significantly increased the concentration of sugars (**Supplementary Tables 2** and **3**). In GF677 rootstock, the interaction between elevated temperature and irrigation increased root raffinose and xylose concentration. In contrast, in Adesoto rootstock, the interaction between elevated CO_2 and irrigation increased root glucose content.

Concerning leaves of 'Catherina' grafted on GF677, elevated CO_2 significantly increased the concentration of all sugars except xylose, while leaves of 'Catherina' grafted on Adesoto rootstock showed increases only for sucrose (**Table 3**). Elevated temperature affected only leaves of the GF677–Catherina combination, increasing the content of glucose and decreasing the content of sucrose and proline. Drought had the same effects for sucrose, xylose, and proline in leaves of both combinations. Under drought stress, sucrose decreased, while xylose and proline increased. Furthermore, in the GF677–Catherina combination, this stress condition led to decreased fructose and increased sorbitol content. Interactive effects of CO_2 with irrigation in GF677–Catherina led to increases in leaf sorbitol and proline, but in Adesoto–Catherina, the triple interaction (CO_2 × temperature × drought) seemed to maintain the levels of sucrose, sorbitol, and total sugars (**Supplementary Tables 4** and **5**).

Correlations Between the Physiological Traits, Soluble Sugars, and Proline Content

Pearson correlation analysis was conducted between the physiological traits and content of biochemical compounds after 23 d of climate change-like conditions. Osmotic potential (Ψ_Π) was negatively correlated with different sugar concentration depending on the tissue and genotype studied. In GF677–Catherina leaves, the content of sucrose, TSS, and

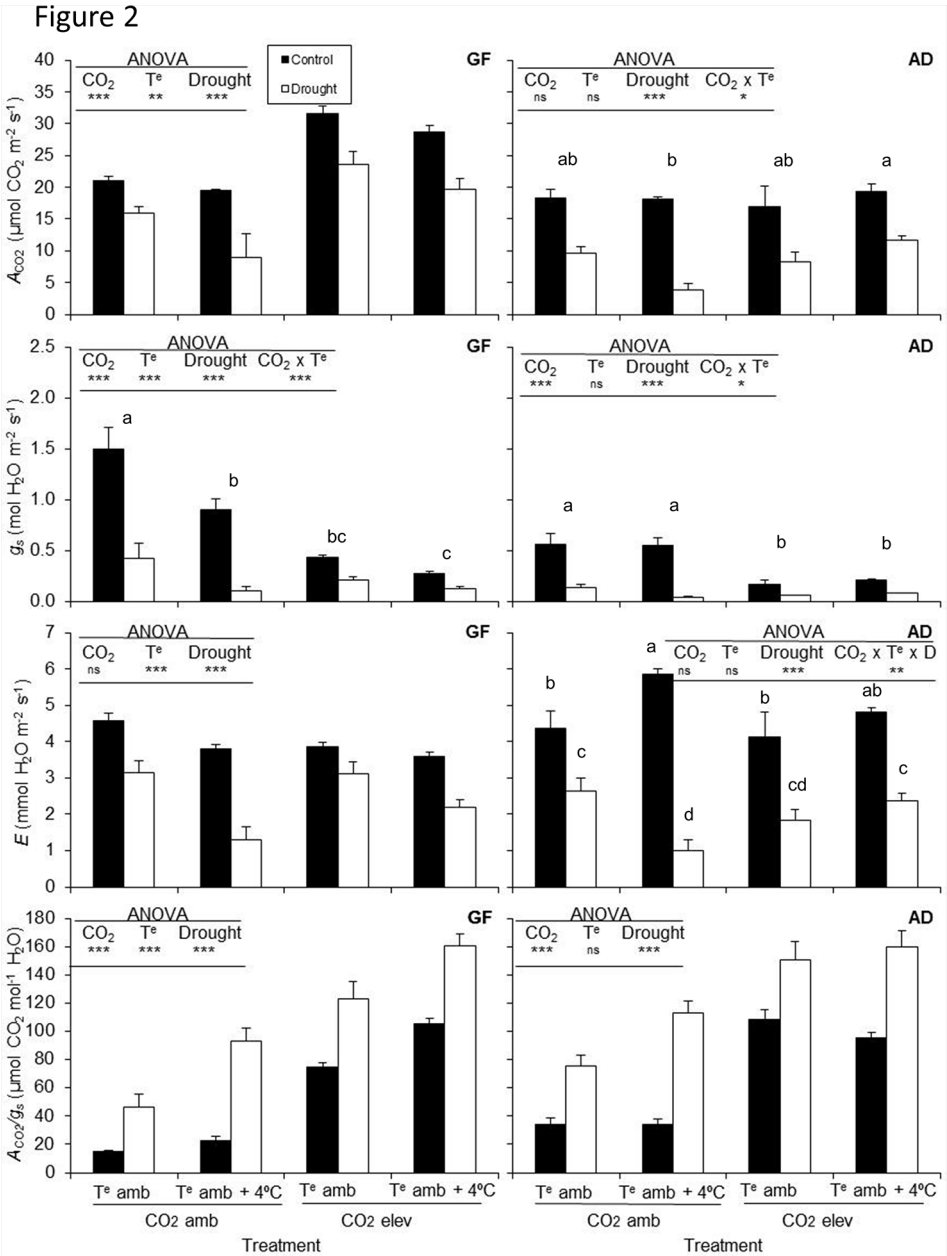

FIGURE 2 | Photosynthetic rate (A_N), stomatal conductance (g_s), transpiration rate (E), and water-use efficiency (A_N/g_s) in peach plants (variety Catherina) grafted on GF677 (GF) and Adesoto (AD) and subjected to ambient (CO_2 amb) and high (CO_2 elev) CO_2, ambient (T^e amb) and high (T^e amb + 4°C) temperature, and irrigation control (C), and drought (D) for 23 days. Vertical bars indicate the standard error (n = 4). Significant differences: * $P \leq 0.05$, ** $P \leq 0.01$, *** $P \leq 0.001$ and ns: non-significant. For the significant double ($CO_2 \times T^e$) and triple ($CO_2 \times T^e \times D$) interactions, differences among means are shown with different letters (Duncan's test, $P < 0.05$).

proline was negatively correlated with osmotic potential. In the Adesoto–Catherina combination, the content of xylose in leaves, sorbitol and TSS in roots, and proline in both tissues showed negative correlation with osmotic potential. Photosynthetic rate in leaves of 'Catherina' grafted on GF677 and Adesoto were positively correlated with sucrose and proline. Positive correlations were also detected between WUE and content of sorbitol (0.521**, 0.534**), TSS (0.515**, 0.503**), and proline (0.461**, 0.474**) in leaves of GF677–Catherina and roots of Adesoto, respectively. Also in roots of plants grafted on GF677, WUE was positively correlated with TSS (0.543**) and proline (0.612***). The content of xylose in leaves of Adesoto–Catherina, and raffinose in roots of GF677, were negatively correlated with most of the physiological parameters except for WUE (**Table 4**).

TABLE 2 | Root soluble sugars and proline (mg g^{-1} DW) concentration (n=4) in ambient (amb CO_2) and high (CO_2 elev) CO_2, ambient (T^e amb) and high (T^e amb + 4°C) temperature, and control irrigation and drought-stressed GF677 (A) and Adesoto (B) *Prunus* rootstocks budded with cv. Catherina, after 23 days of treatment.

Roots		Fructose	Glucose	Raffinose	Sucrose	Sorbitol	Xylose	Total sugars	Proline
				A) GF677					
Principal Effects									
CO_2	CO_2 Amb	4.5	11.9 b	1,3	17.6	14.2	0.6 b	50.1 b	1.0
	CO_2 Elev	5.4	20.0 a	1,2	21.0	13.7	1.0 a	62.2 a	1.3
T^e	T^e Amb	4.4	14.6	1,2	20.5	13.6	0.9	55.1	1.0
	T^e Amb+4°C	5.6	17.5	1,3	18.2	14.2	0.8	57.5	1.4
Irrigation	Control	4.7	14.6	0.9 b	18.3	16.2 a	0.8	55.5	0.7 b
	Drought	5.3	17.4	1.6 a	20.3	11.7 b	0.8	57.1	1.7 a
Signification									
CO_2		ns	***	ns	ns	ns	**	**	ns
T^e		ns	ns	ns	ns	ns	ns	ns	ns
Irrigation		ns	ns	**	ns	***	ns	ns	***
$CO_2 \times T^e$		ns	ns	ns	ns	ns	ns	ns	ns
$CO_2 \times$ Irrigation		ns	ns	ns	ns	ns	ns	ns	ns
$T^e \times$ Irrigation		ns	ns	**	ns	ns	*	ns	ns
$CO_2 \times T^e \times$ Irrigation		ns	ns	ns	ns	ns	ns	ns	ns
				B) Adesoto					
Principal Effects									
CO_2	CO_2 Amb	4.7 b	18.7 b	0.6	26.3	18.6	0.9	70.5 b	0.9
	CO_2 Elev	5.8 a	23.6 a	0.7	30.5	20.3	1.1	82.7 a	1.0
T^e	T^e Amb	5.0	21.4	0.7	27.4	15.3 b	0.9	71.3 b	0.9
	T^e Amb+4°C	5.4	21.0	0.7	29.5	23.3 a	1.1	81.4 a	1.0
Irrigation	Control	5.9 a	19.7	0.6	30.7	14.2 b	1.1	72.6	0.9
	Drought	4.6 b	22.6	0.8	26.4	24.4 a	1.0	80.2	1.0
Signification									
CO_2		**	*	ns	ns	ns	ns	*	ns
T^e		ns	ns	ns	ns	***	ns	*	ns
Irrigation		**	ns	ns	ns	***	ns	ns	ns
$CO_2 \times T^e$		ns	ns	ns	ns	ns	ns	ns	ns
$CO_2 \times$ Irrigation		ns	**	ns	ns	ns	ns	ns	ns
$T^e \times$ Irrigation		ns	ns	ns	ns	ns	ns	ns	ns
$CO_2 \times T^e \times$ Irrigation		ns	ns	ns	ns	ns	ns	ns	ns

*Three-way ANOVA was performed for linear model, on raw data. Significance: *P ≤ 0.05, **P ≤ 0.01, ***P ≤ 0.001 and ns indicates not significant. Comparison means by Duncan's test (P ≤ 0.05) were shown for the significant interaction among treatments. Different letters indicate significant differences among data within the same factor. Amb, Ambient; Elev, Elevated; T^e, Temperature.*

Effect of Climate Change on Transcriptional Responses

After 23 d of growth under climate change conditions, samples from roots and scion leaves of 'Catherina' budded on GF677 and Adesoto rootstocks were collected to study the transcriptomic responses. The transcript levels were evaluated by RT-qPCR for nine and seven genes, in roots and leaves, respectively. We focused on the significant changes under stress conditions concerning relative gene expression (RNorm) in both tissues and rootstocks (**Tables 5** and **6**).

For roots of GF677 rootstock (**Table 5A**), we found that the CO_2 treatment significantly decreased the transcript level of raffinose synthase (*SIP1*), which encodes an enzyme involved in raffinose biosynthesis. The temperature treatment strongly affected the expression of genes related to sugar and proline metabolism, as well as other genes associated with the drought stress responses. We observed decrease expression of sorbitol dehydrogenase (*SDH*) and sorbitol-6-phosphate dehydrogenase (*S6PDH*), key enzymes of sorbitol catabolism and biosynthesis, respectively. Elevated temperature also decreased the expression of Δ-1-pyrrolyne-carboxylate synthase (*P5CS*), dehydration responsive element binding protein 2 (*DREB2*), ABA responsive element binding protein (*AREB2*), and homeodomain-leucine zipper protein (*HAT22*). Finally, water deficit in roots of GF677 also diminished the expression of *SDH* while the normalized expression of *S6PDH,* Δ-1-pyrrolyne-carboxylate synthase (*P5CS*), and Δ-1-pyrrolyne-carboxylate reductase (*P5CR*) was upregulated (**Table 5A**). These results were consistent with the

TABLE 3 | Scion leaf soluble sugars and proline (mg g^{-1} DW) concentration (n = 4) in ambient (amb CO_2) and high (CO_2 elev) CO_2, ambient (T^e amb) and high (T^e amb + 4°C) temperature, and control irrigation and drought-stressed GF677 (A) and Adesoto (B) *Prunus* rootstocks budded with cv. Catherina, after 23 days of treatment.

Leaves		Fructose	Glucose	Raffinose	Sucrose	Sorbitol	Xylose	Total sugars	Proline
A) GF677									
Principal Effects									
CO_2	CO_2 Amb	8.4 b	11.1 b	0.3 b	40.2 b	80.6 b	1.2	142.1 b	1.7 b
	CO_2 Elev	10.3 a	14.2 a	0.4 a	60.5 a	90.9 a	1.3	177.3 a	3.1 a
T^e	T^e Amb	9.7	11.4 b	0.4	54.6 a	83.0	1.2	160.2	2.9 a
	T^e Amb+4°C	8.9	13.9 a	0.4	46.1 b	88.5	1.3	159.5	2.0 b
Irrigation	Control	10.2 a	12.1	0.4	53.4 a	79.4 b	1.1 b	157.7	2.2 b
	Drought	8.4 b	13.1	0.4	47.3 b	92.1 a	1.4 a	163.4	2.6 a
Signification									
CO_2		**	**	**	***	*	ns	***	***
T^e		ns	*	ns	**	ns	ns	ns	***
Irrigation		**	ns	ns	*	*	**	ns	*
$CO_2 \times T^e$		ns	ns	ns	ns	ns	ns	ns	ns
$CO_2 \times$ Irrigation		ns	ns	ns	ns	*	ns	ns	**
$T^e \times$ Irrigation		ns	ns	ns	ns	ns	ns	ns	ns
$CO_2 \times T^e \times$ Irrigation		ns	ns	ns	ns	ns	ns	ns	ns
B) Adesoto									
Principal Effects									
CO_2	CO_2 Amb	9.1	15.9	1.0	39.0 b	91.1	1.4	157.2	2.6
	CO_2 Elev	9.2	16.6	0.4	47.2 a	86.2	1.4	161.3	2.6
T^e	T^e Amb	9.6	15.9	0.4	46.2	85.3	1.4	158.1	2.8
	T^e Amb+4°C	8.8	16.6	0.9	40.5	91.0	1.4	159.4	2.4
Irrigation	Control	9.2	17.7	0.4	51.5 a	89.3	1.2 b	169.3	1.9 b
	Drought	9.2	15.0	1.0	35.5 b	87.4	1.6 a	149.1	3.2 a
Signification									
CO_2		ns	ns	ns	*	ns	ns	ns	ns
T^e		ns	ns	ns	ns	ns	ns	ns	ns
Irrigation		ns	ns	ns	***	ns	***	ns	***
$CO_2 \times T^e$		ns	ns	ns	ns	ns	ns	ns	ns
$CO_2 \times$ Irrigation		ns	ns	ns	ns	ns	ns	ns	ns
$T^e \times$ Irrigation		ns	ns	ns	ns	ns	ns	ns	ns
$CO_2 \times T^e \times$ Irrigation		ns	ns	ns	*	*	ns	*	ns

*Three-way ANOVA was performed for linear model, on raw data. Significance: *P ≤ 0.05, **P ≤ 0.01, ***P ≤ 0.001 and ns indicates not significant. Comparison means by Duncan's test (P ≤ 0.05) were shown for the significant interaction among treatments. Different letters indicate significant differences among data within the same factor. Amb, Ambient; Elev, Elevated; T^e, Temperature.*

increase in proline content in roots of GF677 under drought stress (**Table 2A**). In roots of the Adesoto rootstock, only four genes were affected by the climate change-like conditions (**Table 5B**). Elevated CO_2 significantly increased the transcript levels of *S6PDH* and *AREB2*, while drought condition downregulated the expression of *SDH*. The interactive effect of CO_2 and irrigation modified *PIP2* gene expression, but without a clear trend (**Supplementary Tables 6** and **7**). It is important to note that under drought stress, gene regulation of sorbitol metabolism (downregulated catabolism) was consistent with the increase in sorbitol content in roots of Adesoto (**Table 2B**).

Our results showed that in 'Catherina' scion leaves, elevated CO_2 downregulated *HAT22* when budded either on GF677 or Adesoto (**Table 6**). When 'Catherina' was grafted on GF677, drought stress significantly enhanced the expression of *S6PDH, SIP1*, and *HAT22* (**Table 6A**, **Supplementary Table 8**). When 'Catherina' was grafted on Adesoto, elevated CO_2 and temperature, as well as its interaction, significantly enhanced the expression of *SDH* in scion leaves (**Table 6B**, **Supplementary Table 9**). The transcript level of *P5CR* decreased in the same rootstock with elevated CO_2 and drought stress treatments, but the double and triple interactions did not follow the same trend (**Table 6B**, **Supplementary Table 9**). Regarding the ornithine aminotransferase (*OAT*) gene, which encodes an enzyme that synthesizes a precursor for proline biosynthesis, significant differences in its expression were found only when plants were grafted on Adesoto in the triple interaction, but without a clear trend (**Supplementary Table 9**). Interestingly, under drought stress conditions, gene regulation related to sorbitol metabolism was consistent with the increase in sorbitol content in scion leaves of GF677 (**Table 3A**). Furthermore, the lack of accumulation of sorbitol in scion leaves of Adesoto under elevated CO_2 and temperature may be due to the upregulation of its catabolism (*SDH*).

In summary, gene regulation under climate change conditions was divers and depended on the stress, tissue, and genotype (**Supplementary Table 10**). Concerning tissues, in roots nine different genes associated with specific treatments were modified; eight were affected in GF677, and four in Adesoto. In leaves, five genes were differently expressed on cv. Catherina budded on each rootstock, GF677 or Adesoto. Concerning genotypes, GF677 rootstock showed differences in the expression of 13 genes in both tissues, with roots (eight

TABLE 4 | Pearson correlations between the physiological traits and biochemical content in leaves and roots of 'Catherina' plants grafted on GF677 and Adesoto rootstocks and subjected to climate change conditions for 23 days (n = 32).

Rootstock			**Leaves**				**Rootstock**			**Roots**			
GF677	**Fructose**	**Sucrose**	**Xylose**	**Sorbitol**	**TSS**	**Proline**	**GF677**	**Fructose**	**Glucose**	**Raffinose**	**Sorbitol**	**TSS**	**Proline**
Ψ_{stem}	0.474**									-0.494**	0.524**		-0.585***
$\Psi\pi$		-0.483**			-0.507**	-0.666***							
RWC	0.507***	0.402*								-0.505**	0.547***		0.583***
A_N	0.553**	0.679***				0.424*							-0.367*
g_s				-0.501**					0.457*		0.431*		-0.394*
E				0.493**						-0.488**			0.584***
WUE				0.521**	0.515**	0.461**			0.727***		-0.379*	0.543**	0.612***
Adesoto			**Leaves**				**Adesoto**			**Roots**			
Ψ_{stem}		-0.716***	-0.642***			-0.533**		0.519**			-0.681***		
$\Psi\pi$			-0.460**			-0.391*					-0.589***	-0.507**	-0.507**
RWC													
A_N		0.610***	-0.529**			0.586***		0.601***			-0.422*		
g_s			-0.455**			-0.508**					-0.429*		-0.443*
E		0.576***	-0.549***			0.589***		0.504**			-0.447*		
WUE			0.449*								0.534**	0.503**	0.474**

Significance level: P ≤ 0.05 (*); P ≤ 0.01 (**) and P ≤ 0.001 (***); Ψstem, stem water potential; Ψπ, osmotic potential; RWC, relative water content; A_N, photosynthesis; g_s, conductance; E, transpiration; WUE, water use efficiency (A_N /g_s), TSS, total soluble sugars.

genes) being more affected than scion leaves (five genes). Adesoto rootstock was less affected and only nine genes were modified, four genes in roots and five in scion leaves, respectively. Finally, concerning stresses, in plants grafted on GF677 rootstock, elevated CO_2 significantly modified the expression of only two genes, one in each organ tissue, while elevated temperature affected six genes (all in roots), and as a response to the irrigation treatment, seven genes (four in roots, three in leaves) were differentially expressed. Concerning plants grafted on Adesoto rootstock, CO_2 treatment altered the expression of five genes (two in roots and three in scion leaves), while elevated temperature (in scion leaves) and irrigation (in roots and scion leaves) modified the expression of only one gene. Elevated temperature did not affect gene expression in leaves of 'Catherina' grafted on GF677 or roots of Adesoto rootstock. The triple interaction between CO_2, temperature, and irrigation affected only one gene (*SIP1*) in 'Catherina' grafted on GF677 rootstock (in leaf tissue) and three genes in the Adesoto–Catherina combination (*S6PDH* in roots, and *P5CR* and *OAT* in scion leaves). The double interaction between treatments involved transcriptome variations mainly in leaf tissues.

DISCUSSION

Effect of Climate Change-Like Conditions (Elevated CO_2 and Temperature, and Low Irrigation) on Growth and Physiological Status

The decrease in shoot/root DW ratio under elevated CO_2 and drought suggests that root growth is more stimulated than the aerial part, which was also reported in other plant species (Madhu and Hatfeld, 2013; Medina et al., 2016), although these changes depend on interactions between genotype and environment (Medina et al., 2016). Temperature did not affect biomass as was reported in other plant species (Gray and Brady, 2016). Drought decreased leaf DW and shoot/root ratio in both genotypes, which is in accordance with previous studies in grapevine and wheat (Kizildeniz et al., 2015; Medina et al., 2016) and in *Prunus* genotypes (Jiménez et al., 2013). Under water deficit, investment in root growth over leaf growth has the benefit of reducing the aerial part avoiding water loss *via* transpiration (Gray and Brady, 2016). This effect was more evident in plants grafted on the GF677 rootstock that also had increased SPAD values as a consequence of the chlorophyll accumulation. Elevated CO_2 alone or in combination with elevated temperature attenuated the negative effect of drought on plant growth in both rootstocks (Fattahi et al., 2019), as was reported previously for elevated CO_2 in drought-stressed grapevine plants (Kizildeniz et al., 2015) and in waterlogged cherry rootstocks (Pérez-Jiménez et al., 2018). In the future, climate change conditions may alleviate drought effects in *Prunus* species, as has been reported for other trees (Kelly et al., 2016).

The photosynthetic rates of plants grafted on GF677 were higher with elevated CO_2, but lower with elevated temperature and drought stress. However, the photosynthetic rates of plants grafted on Adesoto decreased only under drought stress conditions. Previous work has shown that elevated CO_2 can lead to increases in photosynthetic rates in some plant species, but often involve acclimation process that limit yield and production of biomass. Under such conditions, we found in plants grafted on GF677 an increase in photosynthesis and biomass, while those grafted on Adesoto showed not

TABLE 5 | Gene expression (Rnorm values) in root tissue (n = 4) under ambient (amb CO_2) and high (CO_2 elev) CO_2, ambient (T^e amb) and high (T^e amb + 4°C) temperature, and control irrigation and drought-stressed GF677 (A) and Adesoto (B) *Prunus* rootstocks budded with cv. Catherina, after 23 days of treatment.

Roots		*SDH*	*S6PDH*	*SIP1*	*P5CS*	*P5CR*	*PIP2*	*DREB2*	*AREB2*	*HAT22*
A) GF677										
Principal Effects										
CO_2	CO_2 Amb	9.5	0.03	1.1 a	0.5	1.8	0.1	0.4	0.2	1.4
	CO_2 Elev	9.1	0.01	0.9 b	0.7	2.1	0.1	0.3	0.2	1.7
T^e	T^e Amb	13.3 a	0.03 a	1.2	0.7 a	2.2	0.1	0.5 a	0.2 a	2.1 a
	T^e Amb+4°C	5.3 b	0.01 b	0.7	0.5 b	1.7	0.1	0.2 b	0.1 b	1.0 b
Irrigation	Control	14.5 a	0.01 b	0.6	0.3 b	1.6 b	0.1	0.4	0.2	1.7
	Drought	4.02 b	0.03 a	1.4	0.9 a	2.3 a	0.1	0.4	0.2	1.3
Signification										
CO_2		ns	ns	*	ns	ns	ns	ns	ns	ns
T^e		***	**	ns	*	ns	ns	*	***	***
Irrigation		***	**	ns	***	*	ns	ns	ns	ns
$CO_2 \times T^e$		ns	*	ns	ns	ns	ns	ns	ns	ns
$CO_2 \times$ Irrigation		ns	ns	*	ns	ns	ns	ns	*	ns
$T^e \times$ Irrigation		***	*	ns	ns	ns	ns	ns	ns	ns
$CO_2 \times T^e \times$ Irrigation		ns	ns	ns	ns	ns	ns	ns	ns	ns
B) Adesoto										
Principal Effects										
CO_2	CO_2 Amb	7.8	0.004 b	0.5	0.4	1.2	0.11	0.6	0.14 b	1.3
	CO_2 Elev	10.8	0.034 a	0.9	0.8	1.9	0.11	0.7	0.22 a	1.8
T^e	T^e Amb	10.0	0.005	0.7	0.5	1.4	0.12	0.8	0.17	1.6
	T^e Amb+4°C	8.6	0.032	0.7	0.7	1.8	0.10	0.5	0.19	1.5
Irrigation	Control	12.8 a	0.006	0.6	0.4	1.6	0.12	0.6	0.18	1.2
	Drought	5.8 b	0.032	0.9	0.7	1.5	0.10	0.6	0.17	1.9
Signification										
CO_2		ns	**	ns	ns	ns	ns	ns	*	ns
T^e		ns	ns	ns	ns	ns	ns	ns	ns	ns
Irrigation		**	ns	ns	ns	ns	ns	ns	ns	ns
$CO_2 \times T^e$		ns	ns	ns	ns	ns	ns	ns	ns	ns
$CO_2 \times$ Irrigation		ns	ns	ns	ns	ns	**	ns	ns	ns
$T^e \times$ Irrigation		ns	ns	ns	ns	ns	ns	ns	ns	ns
$CO_2 \times T^e \times$ Irrigation		ns	*	ns	ns	ns	ns	ns	ns	ns

*Three-way ANOVA was performed for lineal model on raw data. Significance: *P ≤ 0.05, **P ≤ 0.01, ***P ≤ 0.001 and ns indicates not significant. Comparison means by Duncan's test (P ≤ 0.05) were shown for the significant interaction among treatments. Different letters indicate significant differences among data within the same factor. Amb, Ambient; Elev, Elevated; T^e, Temperature.*

significant changes. After 23 d of exposure to elevated CO_2, plants grafted on Adesoto rootstock showed acclimation effects irrespective of the temperature and drought stress conditions, as shown in grapevines (Leibar et al., 2015). Leakey et al. (2009) described genetic factors that predispose plants to a greater acclimation of photosynthesis and mentioned the importance of an unbalance in sink capacity leading to increases in foliar carbohydrates. Apparently, this is not the case in the *Prunus* rootstocks studied herein, because photosynthetic acclimation was not associated with carbohydrate accumulation in scion leaves of GF677 or Adesoto (see sugars leaf/root ratio as fold change in stress compare to control, **Figure S1**). Differences expressed in a logarithmic basis often allow for easier comparison of preferential compound accumulation in leaves or roots. A positive value [Log_2 (Stress/Control) > 1] indicates a preferential accumulation in scion leaves under stress conditions. On the contrary, a negative value [Log_2 (Stress/Control) < 1] indicates preferential accumulation in roots under stress conditions. We found that in GF677–Catherina plants, elevated CO_2 led to increased leaf biomass, decreased SLA, and accumulation of carbohydrates in roots and scion leaves did not provoke acclimation. Similarly, a lack of such acclimation was found in other species as *Populus* trees that export photosynthates during the day and accumulate the overflow as starch to avoid acclimation, which acts to maintain A_N at elevated CO_2 (Scarascia-Mugnozza et al., 2006).

High temperature and drought are frequently co-occurring stresses and they have a substantial impact on the performance and vitality of plants (Afzal et al., 2018). However, at the physiological level, temperature only affected plants grafted on GF677. In these conditions, plants of GF677 showed significantly decreased photosynthesis rates, reduced stomatal conductance, and decreased transpirational water loss, compared to control plants, as reported for grapevine (Leibar et al., 2015). Under drought stress conditions plants grafted on *Prunus* rootstocks showed a significant decrease in stem and osmotic potentials, photosynthetic rate (A_N), stomatal conductance (g_s), and transpiration rate, which is in agreement with previous studies

TABLE 6 | Gene expression (Rnorm values) in leaf tissue (n = 4) under ambient (amb CO_2) and high (CO_2 elev) CO_2, ambient (T^e amb) and high (T^e amb + 4°C) temperature, and control irrigation and drought-stressed GF677 (A) and Adesoto (B) *Prunus* rootstocks budded with cv. Catherina, after 23 days of treatment.

Leaves		*SDH*	*S6PDH*	*SIP1*	*P5CS*	*P5CR*	*OAT*	*HAT22*
A) GF677								
Principal Effects								
CO_2	CO_2 Amb	0.3	161.3	5.2	5.5	10.3	32.2	8.3 a
	CO_2 Elev	0.1	178.2	3.0	4.7	5.8	24.3	5.0 b
T^e	T^e Amb	0.3	219.0	3.9	5.5	6.8	25.5	6.9
	T^e Amb+4°C	0.1	120.5	4.4	4.7	9.3	30.9	6.4
Irrigation	Control	0.2	106.7 b	2.4 b	4.6	10.3	24.6	5.2 b
	Drought	0.2	232.8 a	5.8 a	5.7	5.9	31.9	8.2 a
Signification								
CO_2		ns	ns	ns	ns	ns	ns	**
T^e		ns	ns	ns	ns	ns	ns	ns
Irrigation		ns	*	**	ns	ns	ns	*
$CO_2 \times T^e$		ns	ns	*	*	**	ns	ns
$CO_2 \times$ Irrigation		ns	ns	ns	ns	*	ns	*
$T^e \times$ Irrigation		ns	ns	ns	ns	*	ns	ns
$CO_2 \times T^e \times$ Irrigation		ns	ns	*	ns	ns	ns	ns
B) Adesoto								
Principal Effects								
CO_2	CO_2 Amb	0.009 b	44.1	0.8	0.9	1.9 a	9.8	2.6 a
	CO_2 Elev	0.036 a	34.3	0.5	0.8	1.2 b	7.7	1.6 b
T^e	T^e Amb	0.009 b	46.9	0.7	0.8	1.5	8.1	1.9
	T^e Amb+4°C	0.036 a	31.5	0.6	0.9	1.7	9.3	2.3
Irrigation	Control	0.027	31.7	0.5	0.9	2.2 a	9.0	1.9
	Drought	0.018	46.7	0.9	0.7	1.0 b	8.4	2.3
Signification								
CO_2		*	ns	ns	ns	*	ns	*
T^e		*	ns	ns	ns	ns	ns	ns
Irrigation		ns	ns	ns	ns	**	ns	ns
$CO_2 \times T^e$		*	ns	ns	*	ns	ns	ns
$CO_2 \times$ Irrigation		ns	ns	ns	ns	ns	ns	ns
$T^e \times$ Irrigation		ns	ns	ns	ns	*	ns	ns
$CO_2 \times T^e \times$ Irrigation		ns	ns	ns	ns	*	*	ns

*Three-way ANOVA was performed for lineal model on raw data. Significance: *P ≤ 0.05, **P ≤ 0.01 and ns indicates not significant. Comparison means by Duncan's test (P≤0.05) were shown for the significant interaction among treatments. Different letters indicate significant differences among data within the same factor. Amb, Ambient, Elev, Elevated; T^e, Temperature.*

(Mellisho et al., 2011; Jiménez et al., 2013; Pedroso et al., 2014; Ksouri et al., 2016; Haider et al., 2018). Stomatal closure is one of the earliest responses to water deficiency adopted by plants as a water saving strategy (Long et al., 2006; Serra et al., 2014; Nakhforoosh et al., 2015; Vicente et al., 2015; Pazzagli et al., 2016) to decrease evaporative water loss and maintain a water balance.

In plants grafted on both rootstocks, the combination of climate change-like stress conditions improved water-use efficiency (A_N/g_s) (**Figure 2**) except for temperature in Adesoto–Catherina. Also, in both genotypes, the increase in atmospheric CO_2 concentration, alone or combined with drought, decreased stomatal conductance and resulted in increases in WUE, as reported for grapevine (Leibar et al., 2015). On the contrary, Centritto and coworkers (Centritto et al., 1999) observed neither reduction of stomatal conductance nor changes in WUE in response to elevated CO_2 in droughted cherry plantlets. In this study, elevated CO_2 ameliorated the drought-induced decrease in photosynthesis only in plants grafted on GF677.

Metabolic Rearrangements and Transcriptional Regulation in Response to Climate Change-Like Conditions (Elevated CO_2 and Temperature, and Low Irrigation)

Plant growth depends on assimilation of carbohydrates, which are accumulated and mobilized in the form of soluble sugars under stress conditions (Fabbrin et al., 2015; Sami et al., 2016). In this experiment, changes in sugar content in scion leaves and roots under climate stress conditions are summarized as fold changes [FC = log(2) (Stress/control)] in **Figure S2**. Changes (increase or decrease are positive or negative values, respectively) were different between genotypes and among treatments and are related to the biomass changes found in each genotype and tissue combination. The increase in total sugars in roots and leaves in plants grafted on GF677 was consistent with the increase in dry weight in both tissues under elevated CO_2 (**Figure S2**, **Table 1**). In the same way, increases in fructose, glucose, and total sugars in roots of Adesoto were consistent with the increase in root growth (decrease of shoot/root DW ratio, **Table 1**). It has been established that metabolic adjustments in response to

unfavorable conditions are dynamic and multifaceted and not only depend on the type and strength of the stress, but also on the cultivar and the plant species (Krasensky and Jonak, 2012). In this study, elevated CO_2 led to an increase in sugars in scion leaves and in roots in GF677 (**Figure S2**). However, only fructose, raffinose, sucrose, and sorbitol accumulated (**Figure S1**) more in scion leaves than in roots. Interestingly, in Adesoto soluble sugar concentration, except for sucrose, increased mainly in roots (**Figure S2**) and accumulated there (**Figure S1**) being this tissue the main sink. In both genotypes, under elevated CO_2, independently of acclimation, the increase and accumulation of sucrose in leaves did not limit photosynthesis neither in plants grafted on GF677 nor Adesoto, which was supported by the positive correlation between sucrose and A_N. Furthermore, the increase in proline and its accumulation in leaves of GF677–Catherina plants under elevated CO_2 may be linked to the role of proline as a ROS scavenger protecting the photosynthetic apparatus from oxidative damage.

Accumulation of particular osmolytes (soluble sugars and/or proline) has been observed in different plant species under stress conditions (Krasensky and Jonak, 2012; Baslam et al., 2014; Fabbrin et al., 2015; Yu et al., 2015; Haider et al., 2017; Pérez-Jiménez et al., 2018) and is thought to help maintain osmolarity. Higher accumulation of compatible solutes may contribute to drought tolerance by protecting the photosynthetic apparatus (Krasensky and Jonak, 2012; Jiménez et al., 2013) and maintaining osmotic homeostasis (Jiménez et al., 2013). In particular, the increases in sorbitol in leaves, raffinose in roots, and proline in both tissues were related to a decrease in osmotic potential and an increase in WUE in *Prunus* rootstocks (Jiménez et al., 2013). In this study, comparable results were found in GF677 grown under drought stress (increases in raffinose and proline in roots, and sorbitol, xylose, and proline in scion leaves). In the GF677 rootstock under drought stress, sugars accumulated in the same organs, but proline was allocated preferentially in roots. In Adesoto, sorbitol, xylose, and proline increased (**Figure S2**) and accumulated (**Figure S1**) under drought stress condition in the same organs, in roots (sorbitol) and in scion leaves (xylose and proline). These changes were also consistent with the negative correlations found between the content of sugar and proline in scion leaves and roots versus stem water and osmotic potentials, indicating a role in maintaining water status in plants grafted on GF677 and Adesoto rootstocks (**Table 4**). We suggest that the accumulation of sorbitol, xylose, and proline in different plant tissues may increase the tolerance of *Prunus* trees to progressive drought stress (**Figure S1**). According to our results, we suggest that proline may act as an osmolyte in roots of GF677 and as a ROS scavenger in leaves of Adesoto–Catherina (partially in GF677) to protect each from oxidative damage (Krasensky and Jonak, 2012). In this regard, each genotype has the capacity to accumulate active solutes as osmolytes and the ability to maintain its own strategy to increase WUE.

Sorbitol is a major end product of photosynthesis that under moderate drought conditions, is preferentially synthesized over sucrose (Escobar-Gutiérrez et al., 1998), which is in agreement with the significant increases in sorbitol content we observed in scion leaves and roots and the decreased sucrose levels in scion leaves in the drought-tolerant GF677. On the contrary, in Adesoto, another pattern was found for sorbitol, which increased only in roots and preferentially accumulated along with sucrose in roots (**Figures S1** and **S2**). Several studies on *Prunus* rootstocks confirmed that sorbitol content in scion leaves (Ranney et al., 1991; Haider et al., 2018) and in roots (Ranney et al., 1991) were enhanced resulting in active osmotic adjustment and decreased osmotic potential, which increased plant resistance to drought stress (Arndt et al., 2000; Krasensky and Jonak, 2012). Apparently, scion leaf sorbitol in GF677–Catherina did not result in osmotic adjustment, while root sorbitol in Adesoto rootstock negatively correlated with osmotic potential (**Table 4**). Functions of sorbitol—other than osmotic adjustment—such as translocation and storage of carbon, cryoprotection, and prevention of reactive oxygen species, have been described previously (Lo Bianco et al., 2000). The osmotic adjustment of sorbitol in roots may influence shoot/root partitioning patterns and root growth, and may indirectly control plant growth in responses to water deficit (Turner, 1986). We may speculate that the allocation of sorbitol in roots of Adesoto may be a stimulus to increase the photosynthetic rate and evade or reduce the acclimation process.

In order to shed light on the complex regulatory networks of all changes at the molecular level caused by climate change-like stress conditions, we followed the expression of genes that regulate sugar and proline metabolism. Sorbitol levels were determined by the balance between biosynthesis and catabolism. Sorbitol is synthesized by S6PDH (sorbitol-6-phosphate dehydrogenase) in source leaves, translocated through phloem, and catabolized by SDH in fruit (Suzuki and Dandekar, 2014) and other sink organs. As a result of drought stress, the increase in sorbitol content in scion leaves of GF677 was consistent with the upregulation of *S6PDH* as found previously in peach leaves (Sakanishi et al., 1998). However under climate change-like stress conditions, *SDH* transcript levels were not correlated with sorbitol content, suggesting that other factors have significant regulatory effects, as other authors have pointed out under control conditions (Wu et al., 2010). Likewise, the enhanced expression of *SIP1* in scion leaves of GF677 under drought stress did not provide evidence supporting a role of raffinose in stress tolerance as was reported in *Prunus* rootstocks (Jiménez et al., 2013) or in Arabidopsis plants (Krasensky and Jonak, 2012).

Proline is biosynthesized in plants through two successive reductions catalyzed by 1-pyrroline-5-carboxylate synthetase and pyrroline-5-carboxylate reductase (Verbruggen and Hermans, 2008). In the present study, the significant increases in *P5CS* and *P5CR* under drought stress were accompanied by higher proline content in roots of the tolerant rootstock GF677 as it was found in *P5CS* in GF677 and Cadaman rootstocks (Jiménez et al., 2013). However, in leaves of 'Catherina' grafted on Adesoto, we found the opposite. *P5CR* was downregulated while proline content increased under drought stress without evidences that confirmed the synthesis of proline precursor through the ornithine alternative pathway (Miller et al., 2009).

The apparent inconsistency for the downregulation of *P5CR* under elevated CO_2 and drought treatments and the increase of proline in scion leaves of Adesoto could be explained by gene regulation linked to the interaction. In line with the contrasting results found in both genotypes in this study, Szabados and Savoure (2010) reported that the correlation between proline content and abiotic stress in plants is not always positive and may be genotype-dependent.

Finally, to better establish differences among stresses and to understand the regulation of the physiological and molecular responses found among the genotypes, we explored gene expression of stress-inducible and -responsive genes. It has been described that many stress-inducible genes are enriched in motifs that are binding targets of transcription factors (drought or ABA-regulated genes) (Huang et al., 2008). Numerous gene families and transcription factors (TFs) are implicated in the defense responses to stress in plants through regulation of metabolites levels. *DREB2*, which encodes a DRE/CRT-binding protein, activates the expression of genes related to osmoprotectant and antioxidant biosynthesis and whose expression is rapidly induced by osmotic stress (Song et al., 2014). However, our results are in contrast with the upregulation found under high temperature in poplar (Song et al., 2014) and under drought stress in peach leaves (Haider et al., 2018). In our experimental conditions, the lack of activation of *DREB2* could be due to elevated temperature or drought stress in *Prunus* rootstocks not related to oxidative damage as found in Arabidopsis (Hwang et al., 2012). Furthermore, *AREB* encodes a major TF involved in abiotic stress responses in Arabidopsis (Fujita et al., 2013; Nakashima et al., 2014). Overexpression of *AREB1* in rice and soybean improved drought tolerance (Oh et al., 2005), while overexpression of *AREB2* in apple led to increased sugar accumulation (Ma et al., 2017). In our study, the downregulation of *AREB* in roots of GF677 under elevated temperature may be linked to the lack of significant accumulation of sugars in this organ. On the contrary, upregulation of *AREB* in roots of Adesoto under elevated CO_2 treatment may be linked to the accumulation of total sugars (**Figure S1**). Finally, the homeodomain-leucine zipper (HD-ZPII) gene (*HAT22)* was upregulated in scion leaves of GF677 under drought stress conditions, as was found previously in cotton plants as a response to drought stress (Hou et al., 2018) and in Arabidopsis in response to ABA treatment and drought (Liu et al., 2016). It has been reported that the dehydration-responsive homeodomain-leucine zipper gene family (HD-Zips) show modulated expression in response to dehydration in leaves and roots (Deng et al., 2002), supporting the role of HD-Zips in regulatory pathways that lead to desiccation tolerance. Results found in plants grafted on GF677 may be in agreement with the model proposed in Arabidopsis (Liu et al., 2016) concerning the role of *HAT22/ABIG1* TF. In this combination, drought may act through ABA to increase *HAT22* transcription to limit shoot growth and promote leaf senescence. In contrast, in Adesoto–Catherina the response concerning shoot growth and senescence was less evident.

Taken into account all these transcriptomic changes, it underscores the difficulty in understanding the global context of multi-stress responses. The broad number of genes that are differentially modified under environmental stress conditions reveals the complex regulatory network of TFs controlling plant responses at the morphological, physiological, and molecular level.

CONCLUSION

Climate change will alter future plant growth conditions and, in this scenario, knowledge of the plasticity of *Prunus* rootstocks will be critical for peach production. Elevated CO_2, elevated temperature, and drought stress were applied to simulate future climate conditions and to compare two contrasting *Prunus* rootstocks for 'Catherina' peach at the physiological, molecular, and transcriptomic level. This study revealed that the impact of climate change was not uniform for *Prunus* species and the responses depend on the genetic background and the performance of the genotypes facing the stress in a specific manner.

In response to stress, morphological and physiological changes were accompanied by molecular and transcriptomic changes in a coordinated manner, but depending on the rootstock. Elevated CO_2 increased photosynthetic rates in plants grafted on GF677, while in plants grafted in Adesoto, acclimation was observed. At the molecular level, metabolite content was affected by climate change-like stress factors such that soluble sugars and proline were partitioned in different shoot:root patterns depending on the stress and the genotype. Under elevated CO_2, osmoprotectants accumulated in leaves of GF677–Catherina, while in Adesoto–Catherina these metabolites accumulated mainly in roots. The metabolic adjustments developed in response to stress involved pathways controlling levels of sugar and proline that were highly coordinated and regulated at the transcriptomic level (*SDH*, *S6PDH*, *SIP1*, *P5CR*, and *P5CS*) in both tissues and genotypes.

Stress tolerance is a complex trait that is controlled by multiple genes. GF677–grafted plants showed more changes than those grafted on Adesoto, scion leaves were more affected than roots, although some responses were quite similar for both genotypes and varied depending on the stress and the affected tissue. We conclude that both peach rootstocks may be tolerant to climate change, but the strategies employed by each genotype in response to stress are different and are associated with the genetic background.

GF677 is a tolerant rootstock that utilizes a range of machinery to maintain good performance, and control plant growth and senescence under stress. At elevated CO_2, plants increase A_N, and as a consequence, the rootstock needs to control oxidative stress and plant growth. This genotype increased proline content in scion leaves as a ROS scavenger and downregulated *HAT22* to avoid senescence and increase leaf growth, to create a better balance with root growth. At elevated temperature, no significant changes were found in growth, but all transcriptomic changes were in roots to control root growth and senescence *via* downregulation of genes (*AREB2* to reduce the accumulation of sugars and *HAT22* to restrict growth and senescence). Under drought stress, this rootstock controls leaf

growth *via* the upregulation of *HAT22*, which may result in a decrease in aerial growth in favor of root growth to improve water uptake. Adesoto is a resilient rootstock suitable to grow under climate change stress conditions. Under elevated CO_2, this rootstock is able to control photosynthesis, growth, and sugar biosynthesis. It is also insensitive to elevated temperature, and under drought stress, maintains water status through metabolic balance among tissues. In scion leaves, *HAT22* was downregulated maintaining growth of the aerial part. In roots, *AREB2* was upregulated to promote accumulation of sugars and indirectly stimulate photosynthesis. This study confirms the importance of rootstocks in sensing stress, regulating of scion growth, and conferring tolerance to the variety. This work establishes a basis for developing screening methods that may enable early selection of woody tree species adapted to new environmental scenarios.

DATA AVAILABILITY STATEMENT

All datasets generated for this study are included in the article/ **Supplementary Material**.

AUTHOR CONTRIBUTIONS

SJ and YG devised the study objectives and designed the experiment. SJ carried out the experiment, conducted the statistical analysis and drafted the manuscript. MF contributed to the writing of the paper, to the statistical analysis and figure preparation. KB conducted the expression analysis work. SN-m contributed to the writing. JJI helped with the experimental facilities and physiological measures and supervised the manuscript. YG conceived the experiment, wrote and edited the paper and helped with the statistical analysis. All authors read and approved the manuscript.

FUNDING

This work was partly funded by the Spanish Ministry of Economy and Competitiveness grants AGL2014-52063R, AGL2017-83358-R (MCIU/AEI/FEDER/UE); and the Government of Aragón with grants A44, A09_17R and La Caixa-GA-0007/2010 which were co-financed with FEDER funds. MF and SN-M were recipients of Iranian fellowships. SJ was supported by JAE-Doc-CSIC contract co-funded by ESF. KB received a Master's fellowship awarded by the CIHEAM-IAMZ.

ACKNOWLEDGMENTS

We thank M. Sánchez-Díaz and the Universidad de Navarra for allowing us to use the apparatus and all the TGGs facilities. We also thank V. Barja, D. Gutiérrez, J. Dridi, A. Urdiain, J. Montenegro for the excellent technical assistance and J. Pinochet (Agromillora Iberia S.L.) and M.A. Moreno (EEAD-CSIC) for providing the plant material.

SUPPLEMENTARY MATERIAL

The Supplementary Material for this article can be found online at: https://www.frontiersin.org/articles/10.3389/fpls.2020.00043/full#supplementary-material

REFERENCES

Ábrahám, E., Hourton-Cabassa, C., Erdei, L., and Szabados, L. (2010). Methods for determination of proline in plants. *Methods Mol. Biol.* 639, 317–331. doi: 10.1007/978-1-60761-702-0_20

Afzal, M., Shabbir, G., Ilyas, M., Jan, S.S.A., and Jan, S. A. (2018). Impact of climate change on crop adaptation: current challenges and future perspectives. *Pure Appl. Biol.* 7, 965–972. doi: 10.19045/bspab.2018.700115

Ainsworth, E. A., Leakey, A. D. B., Ort, D. R., and Long, S. P. (2008). FACE-ing the facts: inconsistencies and interdependence among field, chamber and modeling studies of elevated CO_2 impacts on crop yield and food supply. *New Phytol.* 179, 5–9. doi: 10.1111/j.1469-8137.2008.02500.x

Aranjuelo, I., Irigoyen, J. J., Perez, P., Martinez-Carrasco, R., and Sanchez-Díaz, M. (2005). The use of temperature gradient tunnels for studying the combined effect of CO_2, temperature and water availability in N_2 fixing alfalfa plants. *Ann. Appl. Biol.* 146, 51–60. doi: 10.1111/j.1744-7348.2005.04074.x

Aranjuelo, I., Irigoyen, J. J., Perez, P., Martinez-Carrasco, R., and Sanchez-Diaz, M. (2006). Response of nodulated alfalfa to water supply, temperature and elevated CO_2: Productivity and water relations. *Environ. Exp. Bot.* 55, 130–141. doi: 10.1016/j.envexpbot.2004.10.007

Aranjuelo, I., Cabrera-Bosquet, L., Morcuende, R., Avice, J. C., Nogués, S., Araus, J. L., et al. (2011). Does ear C sink strength contribute to overcoming photosynthetic acclimation of wheat plants exposed to elevated CO_2? *J. Exp. Bot.* 62, 3957–3969. doi: 10.1093/jxb/err095

Arndt, S. K., Wanek, W., Clifford, S. C., and Popp, M. (2000). Contrasting adaptations to drought stress in field-grown *Ziziphus mauritiana* and *Prunus persica* trees: water relations, osmotic adjustment and carbon isotope composition. *Aust. J. Grape Wine Res.* 27, 985–996. doi: 10.1071/PP00022

Arp, W. (1991). Effects of source–sink relations on photosynthetic acclimation to elevated CO_2. *Plant Cell Environ.* 14, 869–875. doi: 10.1111/j.1365-3040.1991.tb01450.x

Baslam, M., Antolín, M. C., Gogorcena, Y., Muñoz, F., and Goicoechea, N. (2014). Changes in alfalfa forage quality and stem carbohydrates induced by arbuscular mycorrhizal fungi and elevated atmospheric CO_2. *Ann. Appl. Biol.* 164, 190–199. doi: 10.1111/aab.12092

Bates, L. S., Waldren, R. P., and Teare, I. D. (1973). Rapid determination of free proline for water-stress studies. *Plant Soil* 39, 205–207. doi: 10.1007/BF00018060

Bencze, S., Bamberger, Z., Janda, T., Balla, K., Varga, B., Bedö, Z., et al. (2014). Physiological response of wheat varieties to elevated atmospheric CO_2 and low water supply levels. *Photosynthetica* 52, 71–82. doi: 10.1007/s11099-014-0008-y

Cattivelli, L., Rizza, F., Badeck, F., Mazzucotelli, E., Mastrangelo, A. M., Francia, E., et al. (2008). Drought tolerance improvement in crop plants : an integrated view from breeding to genomics. *Field Crops Res.* 105, 1–14. doi: 10.1016/j.fcr.2007.07.004

Centritto, M., Lee, H., and Jarvis, P. (1999). Interactive effects of elevated [CO_2] and drought on cherry (*Prunus avium*) seedlings. *New Phytol.* 141, 129–140. doi: 10.1046/j.1469-8137.1999.00327.x

Deng, X., Phillips, J., Meijer, A. H., Salamini, F., and Bartels, D. (2002). Characterization of five novel dehydration-responsive homeodomain leucine zipper genes from the resurrection plant *Craterostigma plantagineum*. *Plant Mol. Biol.* 49, 601–610. doi: 10.1023/A:1015501205303

Erice, G., Sanz-Sáez, A., Urdiain, A., Araus, J. L., Irigoyen, J. J., and Aranjuelo, I. (2014). Harvest index combined with impaired N availability constrains the responsiveness of durum wheat to elevated CO_2 concentration and terminal water stress. *Funct. Plant Biol.* 41, 1138–1147. doi: 10.1071/FP14045

Escobar-Gutiérrez, A., Zipperlin, B., Carbonne, F., Moing, A., and Gaudillere, J. (1998). Photosynthesis, carbon partitioning and metabolite content during drought stress in peach seedlings. *Aust. J. Plant Physiol.* 25, 197–205. doi: 10.1071/PP97121

Fabbrin, E. G., Gogorcena, Y., Mogor, A. F., Garmendia, I., and Goicoechea, N. (2015). Pearl millet growth and biochemical alterations determined by mycorrhizal inoculation, water availability and atmospheric CO_2 concentration. *Crop Pasture Sci.* 66, 831–840. doi: 10.1071/CP14089

FAO (2016). *The State of Food and Agriculture: Climate Change, Agriculture and Food Security* (Rome: Food and Agriculture Organization of the United Nations).

Fathi, H., Amiri, M. E., Imani, A., Hajilou, J., and Nikbakht, J. (2017). Response of almond genotypes/cultivars grafted on GN15 "Garnem" rootstock in deficit-irrigation stress conditions. *J. Nuts* 8, 123–135. doi: 10.22034/jon.2017.536243

Fattahi, M., Jiménez, S., Nasrolahpour-moghadam, S., Irigoyen, J., and Gogorcena, Y. (2019). "Effects of climate change on peach grafted into two contrasting *Prunus* spp. rootstocks," in *XXIII of the Spanish Society of Plant Physiology* (Pamplona (Spain): Spanish Society of Plant Physiology), 89.

Fujita, Y., Yoshida, T., and Yamaguchi-Shinozaki, K. (2013). Pivotal role of the AREB/ABF-SnRK2 pathway in ABRE-mediated transcription in response to osmotic stress in plants. *Physiol. Plant* 147, 15–27. doi: 10.1111/j.1399-3054.2012.01635.x

García-Sánchez, F., Syvertsen, J. P., Gimeno, V., Botía, P., and Perez-Perez, J. G. (2007). Responses to flooding and drought stress by two citrus rootstock seedlings with different water-use efficiency. *Physiol. Plant* 130, 532–542. doi: 10.1111/j.1399-3054.2007.00925.x

Gogorcena, Y., Iturbe-Ormaetxe, I., Escuredo, P. R., and Becana, M. (1995). Antioxidant defenses against activated oxygen in pea nodules subjected to water stress. *Plant Physiol.* 108, 753–759. doi: 10.1104/pp.108.2.753

Gogorcena, Y., Sánchez, G., Moreno, S., Pérez, S., and Ksouri, N. (2020). "Genomic-based breeding for climate-smart peach varieties," in *Genome designing of climate fruit crops*. Ed. Ch. Kole (Cham, Switzerland AG: Springer Nature). 291–351. doi: 10.1007/978-3-319-97946-5_9

Gray, S. B., and Brady, S. M. (2016). Plant developmental responses to climate change. *Dev. Biol.* 419, 64–77. doi: 10.1016/j.ydbio.2016.07.023

Haider, M. S., Zhang, C., Kurjogi, M. M., Pervaiz, T., Zheng, T., Zhang, C., et al. (2017). Insights into grapevine defense response against drought as revealed by biochemical, physiological and RNA-Seq analysis. *Sci. Rep.* 7, 1–15. doi: 10.1038/s41598-017-13464-3

Haider, M. S., Kurjogi, M. M., Khalil-ur-Rehman, M., Pervez, T., Songtao, J., Fiaz, M., et al. (2018). Drought stress revealed physiological, biochemical and gene-expressional variations in 'Yoshihime' peach (*Prunus persica* L) cultivar. *J. Plant Interact.* 13, 83–90. doi: 10.1080/17429145.2018.1432772

Hou, S., Zhu, G., Li, Y., Li, W., Fu, J., Niu, E., et al. (2018). Genome-wide association studies reveal genetic variation and candidate genes of drought stress related traits in cotton (*Gossypium hirsutum* L.). *Front. Plant Sci.* 9, 1–15. doi: 10.3389/fpls.2018.01276

Huang, D., Wu, W., Abrams, S. R., and Cutler, A. J. (2008). The relationship of drought-related gene expression in *Arabidopsis thaliana* to hormonal and environmental factors. *J. Exp. Bot.* 59, 2991–3007. doi: 10.1093/jxb/ern155

Hwang, J., Lim, C., Chen, H., Je, J., Song, C., and Lim, C. (2012). Overexpression of Arabidopsis dehydration-responsive element-binding protein 2C confers tolerance to oxidative stress. *Mol. Cells* 33, 135–140. doi: 10.1007/s10059-012-2188-2

Iacono, F., Buccella, A., and Peterlunger, E. (1998). Water stress and rootstock influence on leaf gas exchange of grafted and ungrafted grapevines. *Sci. Hortic. (Amsterdam).* 75, 27–39. doi: 10.1016/S0304-4238(98)00113-7

IPCC (2014). "Climate Change 2014 Synthesis Report," in *Contribution of Working Groups I, II and III to the Fifth Assessment Report of the Intergovernmental Panel on Climate Change*. Eds. R. K. Pachauri and L. A. Meyer Geneva (Switzerland: Intergovernmental Panel on Climate Change (IPCC)).

IPCC (2018). "Global warming of 1.5°C," in *An IPCC Special Report on the impacts of global warming of 1.5°C above pre-industrial levels and related global greenhouse gas emission pathways, in the context of strengthening the global response to the threat of climate change, sustainable development.* Intergovernmental Panel on Climate Change (IPCC). T. W. V. Masson-Delmotte, P. Zhai, H. O. PörtnerV. Masson-Delmotte, P. Zhai, H. O. Pörtner, D. Roberts, J. Skea, P. R. Shukla, A. Pirani, W. Moufouma-Okia, C. Péan, R. Pidcock, S. Connors, J. B. R. Matthews, Y. Chen, X. Zhou, M. I. Gomis, E. Lonnoy and T. Maycock

Irigoyen, J. J., Goicoechea, N., Antolín, M. C., Pascual, I., Sánchez-Díaz, M., Aguirreolea, J., et al. (2014). Growth, photosynthetic acclimation and yield quality in legumes under climate change simulations : an updated survey. *Plant Sci.* 226, 22–29. doi: 10.1016/j.plantsci.2014.05.008

Jiménez, S., Dridi, J., Gutiérrez, D., Moret, D., Irigoyen, J. J., Moreno, M. A., et al. (2013). Physiological, biochemical and molecular responses in four *Prunus* rootstocks submitted to drought stress. *Tree Physiol.* 33, 1061–1075. doi: 10.1093/treephys/tpt074

Jones, H. G. (2007). Monitoring plant and soil water status: Established and novel methods revisited and their relevance to studies of drought tolerance. *J. Exp. Bot.* 58, 119–130. doi: 10.1093/jxb/erl118

Kelly, J. W. G., Duursma, R. A., Atwell, B. J., Tissue, D. T., and Medlyn, B. E. (2016). Drought × CO_2 interactions in trees: a test of the low-intercellular CO_2 concentration (Ci) mechanism. *New Phytol.* 209, 1600–1612. doi: 10.1111/nph.13715

Kizildeniz, T., Mekni, I., Santesteban, H., Pascual, I., Morales, F., and Irigoyen, J. J. (2015). Effects of climate change including elevated CO_2 concentration, temperature and water deficit on growth, water status, and yield quality of grapevine (*Vitis vinifera* L.) cultivars. *Agric. Water Manage.* 159, 155–164. doi: 10.1016/j.agwat.2015.06.015

Kizildeniz, T., Pascual, I., Irigoyen, J. J., and Morales, F. (2018). Using fruit-bearing cuttings of grapevine and temperature gradient greenhouses to evaluate effects of climate change (elevated CO_2 and temperature, and water deficit) on the cv. red and white Tempranillo. Yield and must quality in three consecutive growin. *Agric. Water Manage.* 202, 299–310. doi: 10.1016/j.agwat.2017.12.001

Krasensky, J., and Jonak, C. (2012). Drought, salt, and temperature stress-induced metabolic rearrangements and regulatory networks. *J. Exp. Bot.* 63, 1593–1608. doi: 10.1093/jxb/err460

Ksouri, N., Jiménez, S., Wells, C. E., Contreras-Moreira, B., and Gogorcena, Y. (2016). Transcriptional responses in root and leaf of *Prunus persica* under drought stress using RNA sequencing. *Front. Plant Sci.* 7, 1715. doi: 10.3389/fpls.2016.01715

Leakey, A. D. B., Ainsworth, E. A., Bernacchi, C. J., Rogers, A., Long, S. P., and Ort, D. R. (2009). Elevated CO_2 effects on plant carbon, nitrogen, and water relations: Six important lessons from FACE. *J. Exp. Bot.* 60, 2859–2876. doi: 10.1093/jxb/erp096

Leibar, U., Aizpurua, A., Unamunzaga, O., Pascual, I., and Morales, F. (2015). How will climate change influence grapevine cv. Tempranillo photosynthesis under different soil textures? *Photosynth. Res.* 124, 199–215. doi: 10.1007/s11120-015-0120-2

Liu, T., Longhurst, A. D., Talavera-Rauh, F., Hokin, S. A., and Barton, M. K. (2016). The Arabidopsis transcription factor ABIG1 relays ABA signaled growth inhibition and drought induced senescence. *Elife* 5, 1–19. doi: 10.7554/eLife.13768

Lo Bianco, R., Rieger, M., and Sung, S. J. S. (2000). Effect of drought on sorbitol and sucrose metabolism in sinks and sources of peach. *Physiol. Plant* 108, 71–78. doi: 10.1034/j.1399-3054.2000.108001071.x

Long, S. P., Ainsworth, E. A., Rogers, A., and Ort, D. R. (2004). Rising atmospheric carbon dioxide: Plants FACE the future. *Annu. Rev. Plant Biol.* 55, 591–628. doi: 10.1146/annurev.arplant.55.031903.141610

Long, S. P., Ainsworth, E. A., Leakey, A. D. B., Nösberger, J., and Ort, D. R. (2006). Food for thought: lower-than-expected crop yield stimulation with rising CO_2 concentrations. *Science* (80-.), 1918–1921. doi: 10.1126/science.1114722

Lovisolo, C., Perrone, I., Carra, A., Ferrandino, A., Flexas, J., Medrano, H., et al. (2010). Drought-induced changes in development and function of grapevine (*Vitis* spp.) organs and in their hydraulic and non-hydraulic interactions at the whole-plant level: a physiological and molecular update. *Funct. Plant Biol.* 37, 98. doi: 10.1071/FP09191

Ma, Q. J., Sun, M. H., Lu, J., Liu, Y. J., Hu, D. G., and Hao, Y. J. (2017). Transcription factor AREB2 is involved in soluble sugar accumulation by activating sugar transporter and amylase genes. *Plant Physiol.* 174, 2348–2362. doi: 10.1104/pp.17.00502

Madhu, M., and Hatfeld, J. L. (2013). Dynamics of plant root growth under increased atmospheric carbon dioxide. *Agron. J.* 105, 657–669. doi: 10.2134/agronj2013.0018

Martínez-Lüscher, J., Kizildeniz, T., Vučetić, V., Dai, Z., Luedeling, E., van Leeuwen, C., et al. (2016). Sensitivity of grapevine phenology to water availability, temperature and CO_2 concentration. *Front. Environ. Sci.* 4, 48. doi: 10.3389/fenvs.2016.00048

Medina, S., Vicente, R., Amador, A., and Araus, J. L. (2016). Interactive effects of elevated [CO_2] and water stress on physiological traits and gene expression during vegetative growth in four durum wheat genotypes. *Front. Plant Sci.* 7, 1–17. doi: 10.3389/fpls.2016.01738

Meggio, F., Prinsi, B., Negri, A., Simone di Lorenzo, G., Lucchini, G., Pitacco, A., et al. (2014). Biochemical and physiological responses of two grapevine rootstock genotypes to drought and salt treatments. *Aust. J. Grape Wine Res.* 20, 310–323. doi: 10.1111/ajgw.12071

Meisel, L., Fonseca, B., Gonzalez, S., Baeza-Yates, R., Cambiazo, V., Campos, R., et al. (2005). A rapid and efficient method for purifying high quality total RNA from peaches (*Prunus persica*) for functional genomics analyses. *Biol. Res.* 38, 83–88. doi: 10.4067/S0716-97602005000100010

Mellisho, C. D., Cruz, Z. N., Conejero, W., Ortuno, M. F., and Rodríguez, P. (2011). Mechanisms for drought resistance in early maturing cvar Flordastar peach trees. *J. Agric. Sci.* 149, 609–616. doi: 10.1017/S0021859611000141

Miller, G., Honig, A., Stein, H., Suzuki, N., Mittler, R., and Zilberstein, A. (2009). Unraveling delta1-pyrroline-5- carboxylate-proline cycle in plants by uncoupled expression of proline oxidation enzymes. *J. Biol. Chem.* 284, 26482–26492. doi: 10.1074/jbc.M109.009340

Moing, A., Maucourt, M., Renaud, C., Gaudillère, M., Brouquisse, R., Lebouteiller, B., et al. (2004). Quantitative metabolic profiling by 1-dimensional 1H-NMR analyses: application to plant genetics and functional genomics. *Funct. Plant Biol.* 31, 889–902. doi: 10.1071/FP04066

Morales, F., Pascual, I., Sánchez-Díaz, M., Aguirreolea, J., Irigoyen, J. J., Goicoechea, N., et al. (2014). Methodological advances: Using greenhouses to simulate climate change scenarios. *Plant Sci.* 226, 30–40. doi: 10.1016/j.plantsci.2014.03.018

Morgan, J. (1984). Osmoregulation and water stress in higher plants. *Annu. Rev. Plant Physiol.* 35, 299–319. doi: 10.1146/annurev.pp.35.060184.001503

Nakashima, K., Yamaguchi-Shinozaki, K., and Shinozaki, K. (2014). The transcriptional regulatory network in the drought response and its crosstalk in abiotic stress responses including drought, cold, and heat. *Front. Plant Sci.* 5, 1–7. doi: 10.3389/fpls.2014.00170

Nakhforoosh, A., Grausgruber, H., Kaul, H. P., and Bodner, G. (2015). Dissection of drought response of modern and underutilized wheat varieties according to passioura's yield-water framework. *Front. Plant Sci.* 6, 1–13. doi: 10.3389/fpls.2015.00570

NOAA Mauna Loa Atmospheric Baseline Observatory (2019). Carbon dioxide levels hit record peak in May. Available at: https://research.noaa.gov/article/ArtMID/587/ArticleID/2461/Carbon-dioxide-levels-hit-record-peak-in-May.

Oh, S.-J., Song, S. I., Kim, Y. S., Jang, H.-J., Kim, S. Y., Kim, M., et al. (2005). Arabidopsis CBF3/DREB1A and ABF3 in transgenic rice increased tolerance to abiotic stress without stunting growth. *Plant Physiol.* 138, 341–351. doi: 10.1104/pp.104.059147

Pérez-Jiménez, M., Hernández-Munuera, M., Piñero, M. C., López-Ortega, G., and del Amor, F. M. (2018). Are commercial sweet cherry rootstocks adapted to climate change? Short-term waterlogging and CO_2 effects on sweet cherry cv. 'Burlat.'. *Plant Cell Environ.* 41, 908–918. doi: 10.1111/pce.12920

Pazzagli, P. T., Weiner, J., and Liu, F. (2016). Effects of CO_2 elevation and irrigation regimes on leaf gas exchange, plant water relations, and water use efficiency of two tomato cultivars. *Agric. Water Manage.* 169, 26–33. doi: 10.1016/j.agwat.2016.02.015

Pedroso, F. K. J. V., Prudente, D. A., Bueno, A. C. R., Machado, E. C., and Ribeiro, R. V. (2014). Drought tolerance in citrus trees is enhanced by rootstock-dependent changes in root growth and carbohydrate availability. *Environ. Exp. Bot.* 101, 26–35. doi: 10.1016/j.envexpbot.2013.12.024

Ranney, T. G., Bassuk, N. L., and Whitlow, T. H. (1991). Osmotic adjustment and solute constituents in leaves and roots of water-stressed cherry (*Prunus*) trees. *J. Am. Soc Hortic. Sci.* 116, 684–688. doi: 10.21273/JASHS.116.4.684

Ruijter, J. M., Ramakers, C., Hoogaars, W. M. H., Karlen, Y., Bakker, O., Van den Hoff, M. J. B., et al. (2009). Amplification efficiency: linking baseline and bias in the analysis of quantitative PCR data. *Nucleic Acids Res.* 37, e45. doi: 10.1093/nar/gkp045

Sakanishi, K., Kanayama, Y., Mori, H., Yamada, K., and Yamaki, S. (1998). Expression of the gene for NADH-dependent sorbitol-6-phosphate dehydrogenase in peach leave of various developmental stages. *Plant Cell Physiol.* 39, 1372–1374. doi: 10.1093/oxfordjournals.pcp.a029344

Salazar-Parra, C., Aguirreolea, J., Sánchez-Díaz, M., Irigoyen, J. J., and Morales, F. (2012). Climate change (elevated CO_2, elevated temperature and moderate drought) triggers the antioxidant enzymes' response of grapevine cv. Tempranillo, avoiding oxidative damage. *Physiol. Plant* 144, 99–110. doi: 10.1111/j.1399-3054.2011.01524.x

Salazar-Parra, C., Aranjuelo, I., Pascual, I., Erice, G., Sanz-Sáez, Á., Aguirreolea, J., et al. (2015). Carbon balance, partitioning and photosynthetic acclimation in fruit-bearing grapevine (*Vitis vinifera* L. cv. Tempranillo) grown under simulated climate change (elevated CO_2, elevated temperature and moderate drought) scenarios in temperature gradient greenhouse. *J. Plant Physiol.* 174, 97–109. doi: 10.1016/j.jplph.2014.10.009

Salazar-Parra, C., Aranjuelo, I., Pascual, I., Aguirreolea, J., Sánchez-Díaz, M., Irigoyen, J. J., et al. (2018). Is vegetative area, photosynthesis, or grape C uploading involved in the climate change-related grape sugar/anthocyanin decoupling in Tempranillo? *Photosynth. Res.* 138, 115–128. doi: 10.1007/s11120-018-0552-6

Sami, F., Yusuf, M., Faizan, M., Faraz, A., and Hayat, S. (2016). Role of sugars under abiotic stress. *Plant Physiol. Biochem.* 109, 54–61. doi: 10.1016/j.plaphy.2016.09.005

Santana-Veira, D. D. S., Freschi, L., Aragão, L., Henrique, D., Moraes, S., De Neves, D. M., et al. (2016). Survival strategies of citrus rootstocks subjected to drought. *Sci. Rep.* 6, 1–12. doi: 10.1038/srep38775

Sanz-Sáez, Á., Erice, G., Aguirreolea, J., Irigoyen, J. J., and Sánchez-Díaz, M. (2012). Alfalfa yield under elevated CO_2 and temperature depends on the *Sinorhizobium* strain and growth season. *Environ. Exp. Bot.* 77, 267–273. doi: 10.1016/j.envexpbot.2011.11.017

Sanz-Sáez, Á., Erice, G., Aranjuelo, I., Aroca, R., Ruíz-Lozano, J. M., Aguirreolea, J., et al. (2013). Photosynthetic and molecular markers of CO_2-mediated photosynthetic downregulation in nodulated alfalfa. *J. Integr. Plant Biol.* 55, 721–734. doi: 10.1111/jipb.12047

Scarascia-Mugnozza, G., Calfapietra, C., Ceulemans, R., Gielen, B., Cotrufo, M., De Angelis, P., et al. (2006). "Responses to elevated [CO_2] of a short rotation, multispecies poplar plantation: the POPFACE/EUROFACE experiment," in *Managed ecosystems and CO_2: case studies, processes and perspectives. Ecological Studies 187*. Eds. S. Long, R. Norby, M. Stitt, G. Hendrey and H. Blum (Berlin, Heidelberg, Germany: Springer-Verlag), 173–195. doi: 10.1007/3-540-31237-4_10

Schefe, J. H., Lehmann, K. E., Buschmann, I. R., Unger, T., and Funke-Kaiser, H. (2006). Quantitative real-time RT-PCR data analysis: Current concepts and the novel "gene expression's CT difference" formula. *J. Mol. Med.* 84, 901–910. doi: 10.1007/s00109-006-0097-6

Serra, I., Strever, A., Myburgh, P. A., and Deloire, A. (2014). Review: The interaction between rootstocks and cultivars (*Vitis vinifera* L.) to enhance drought tolerance in grapevine. *Aust. J. Grape Wine Res.* 20, 1–14. doi: 10.1111/ajgw.12054

Solari, L. I., Johnson, S., and Dejong, T. M. (2006). Hydraulic conductance characteristics of peach (*Prunus persica*) trees on different rootstocks are related to biomass production and distribution. *Tree Physiol.* 26, 1343–1350. doi: 10.1093/treephys/26.10.1343

Song, Y., Chen, Q., Ci, D., Shao, X., and Zhang, D. (2014). Effects of high temperature on photosynthesis and related gene expression in poplar. *BMC Plant Biol.* 14, 111. doi: 10.1186/1471-2229-14-111

Suzuki, Y., and Dandekar, A. M. (2014). Sucrose induces expression of the sorbitol-6-phosphate dehydrogenase gene in source leaves of loquat. *Physiol. Plant* 150, 355–362. doi: 10.1111/ppl.12106

Szabados, L., and Savoure, A. (2010). Proline: a multifunctional amino acid. *Trends Plant Sci.* 15, 89–97. doi: 10.1016/j.tplants.2009.11.009

Turner, N. (1986). Adaptation to water deficits: a changing perspective. *Aust. J. Plant Physiol.* 13, 175–190. doi: 10.1071/PP9860175

Untergasser, A., Nijveen, H., Rao, X., Bisseling, T., Geurts, R., and Leunissen, J. A. M. (2007). Primer3Plus, an enhanced web interface to Primer3. *Nucleic Acids Res.* 35, 71–74. doi: 10.1093/nar/gkm306

Verbruggen, N., and Hermans, C. (2008). Proline accumulation in plants: a review. *Amino Acids* 35, 753–759. doi: 10.1007/s00726-008-0061-6

Vicente, R., Pérez, P., Martínez-Carrasco, R., Usadel, B., Kostadinova, S., and Morcuende, R. (2015). Quantitative RT-PCR platform to measure transcript levels of C and N metabolism-related genes in durum wheat: transcript profiles in elevated [CO_2] and high temperature at different nitrogen supplies. *Plant Cell Physiol.* 56, 1556–1573. doi: 10.1093/pcp/pcv079

Wu, B. H., Li, S. H., Nosarzewski, M., and Archbold, D. D. (2010). Sorbitol dehydrogenase gene expression and enzyme activity in apple: Tissue specificity during bud development and response to rootstock vigor and growth manipulation. *J. Am. Soc Hortic. Sci.* 135, 379–387. doi: 10.21273/JASHS.135.4.379

Yu, J., Sun, L., Fan, N., Yang, Z., and Huang, B. (2015). Physiological factors involved in positive effects of elevated carbon dioxide concentration on Bermuda grass tolerance to salinity stress. *Environ. Exp. Bot.* 115, 20–27. doi: 10.1016/j.envexpbot.2015.02.003

Conflict of Interest: Author SJ was employed by company Bayer AG, though the research was conducted before his employment at the company, in the absence of any conflict of interest.

The remaining authors declare that the research was conducted in the absence of any commercial or financial relationships that could be construed as a potential conflict of interest.

frontiers in Plant Science

ORIGINAL RESEARCH
published: 06 March 2020
doi: 10.3389/fpls.2020.00153

Characterization of Photosynthetic Phenotypes and Chloroplast Ultrastructural Changes of Soybean (*Glycine max*) in Response to Elevated Air Temperatures

Matthew T. Herritt[1] *and Felix B. Fritschi*[2*]

[1] US Arid Land Agricultural Research Center, United States Department of Agriculture, Agricultural Research Service, Maricopa, AZ, United States, [2] Division of Plant Science, University of Missouri, Columbia, MO, United States

OPEN ACCESS

Edited by:
Iker Aranjuelo, Superior Council of Scientific Investigations, Spain

Reviewed by:
Fumihiko Sato, Kyoto University, Japan
Raquel Esteban, University of the Basque Country, Spain

***Correspondence:**
Felix B. Fritschi
fritschif@missouri.edu

Specialty section:
This article was submitted to Plant Abiotic Stress, a section of the journal Frontiers in Plant Science

Received: *01 October 2019*
Accepted: *31 January 2020*
Published: *06 March 2020*

Citation:
Herritt MT and Fritschi FB (2020) Characterization of Photosynthetic Phenotypes and Chloroplast Ultrastructural Changes of Soybean (Glycine max) in Response to Elevated Air Temperatures. Front. Plant Sci. 11:153. doi: 10.3389/fpls.2020.00153

Heat stress negatively affects photosynthesis in crop plants. Chlorophyll fluorescence provides information about the efficiency of the light-dependent reactions of photosynthesis and can be measured non-destructively and rapidly. Four soybean (*Glycine max*) genotypes were grown in controlled environments at 28/20°C (control), followed by imposition of control, 38/28°C, and 45/28°C day/night temperature regimes for 7 days. Coordinated chlorophyll fluorescence, gas exchange, and chloroplast ultrastructure measurements were conducted over the course of the 7-day temperature treatments and revealed contrasting responses among the different genotypes. Although generally similar, the extent of the impact of elevated temperatures on net photosynthesis differed among genotypes. Despite dramatic effects on photosynthetic light reactions, net photosynthetic rates were not reduced by exposure to 45°C on the 1st day of treatment imposition. Temporal dynamics of light reaction characteristics over the course of the 7-day heat-wave simulation revealed distinct responses among the genotypes. Similarly, chloroplast ultrastructure examination identified contrasting responses of DT97-4290 and PI603166, particularly with respect to starch characteristics. These changes were positively associated with differences in the percent area of chloroplasts that were occupied by starch grains. Elevated temperature increased number and size of starch grains on the 1st day of DT97-4290 which was coordinated with increased minimum chlorophyll fluorescence (F_0) and reduced leaf net CO_2 assimilation (A). Whereas on the 7th day the elevated temperature treatment showed reduced numbers and sizes of starch grains in chloroplasts and was coordinated with similar levels of F_0 and A to the control treatment. Unlike starch dynamics of PI603166 which elevated temperature had little effect on. The genotypic differences in photosynthetic and chloroplast ultrastructure responses to elevated temperatures identified here are of interest for the development of more tolerant soybean cultivars and to facilitate the dissection of molecular mechanisms underpinning heat stress tolerance of soybean photosynthesis.

Keywords: chlorophyll fluorescence, gas exchange, transmission electron microscopy, heat stress, soybean

INTRODUCTION

Plants have the ability to cool their leaves below that of the air temperature. In areas like the US Southwest, leaf temperatures of plants can be up to 10°C cooler than air temperatures (Idso et al., 1982). However, in conditions where leaf cooling cannot keep pace with increasing air temperatures, elevated leaf temperatures can lead to reductions in photosynthesis (Fischer et al., 1998). Reduction of net photosynthesis with increased temperatures have been observed for numerous species, including tomato (*Lycopersicon esculentum*) (Abdelmageed and Gruda, 2009), cotton (*Gossypium barbadense* L.) (Carmo-Silva et al., 2012), wheat (*Triticum aestivum* L.) (Hassan, 2006), and soybean [*Glycine max* (L.) Merr.] (Vu et al., 1997). The impacts of elevated temperature on photosynthesis have primarily been attributed to inactivation of Rubisco mediated by effects on Rubisco activase stability (Crafts-Brandner and Salvucci, 2000; Sharkey et al., 2001; Salvucci and Crafts-Brandner, 2004; Kurek et al., 2007) and photosynthetic electron transport (Yamane et al., 1997; Zhang et al., 2010).

The light-dependent reactions of photosynthesis allow plants to harvest and convert light energy into chemical energy, including ATP and NADPH for use in carbon fixation reactions. Central to the light-dependent reactions are photosystems I and II (PS1 and PS2). The photosystems are the central hubs where the energy from absorbed light is used to excite electrons. Electrons originate from water and are transported from PS2 *via* mobile electron carriers and cytochrome b6f to PS1. The photosystems, cytochrome b6f and the mobile electron carriers as well as the bulk of the accessory proteins involved with the light-dependent reactions are located either within or near the thylakoid membrane (Maxwell and Johnson, 2000; Friso et al., 2004).

The location of the light-dependent reactions in and around the thylakoid membrane is critical for photosynthesis. The thylakoid membrane serves several roles for the light-dependent reactions, including maintenance of the proton gradient that is used for ATP production (Alberts et al., 2002). The interaction between the thylakoid membrane and the photosystems is also crucial for the light dependent reactions of photosynthesis (Loll et al., 2007). To balance the production of ATP and NADPH, the two photosystems are spatially separated in the thylakoid membrane (Albertsson, 2001). The separation of the photosystems leads to stacking of the thylakoid membranes rich in PS2 through electrochemical and protein-protein interactions (Andersson et al., 2003; Chow et al., 2005). The stacked thylakoid, grana, allow for regions that are concentrated with PS2 complexes and some PS1 complexes. The rest of the thylakoid that does not form into grana contains many more PS1and ATP synthases than grana. This separation of complexes and the organization of the thylakoid membrane allows for efficient NADPH production within the grana and ATP production primarily in the non-appressed regions (Kirchhoff et al., 2013). Grana stacking is often associated with efficient light-dependent reactions (Jenny et al., 2003). When grana stacking is interfered with under heat stress, the efficiency of the light reactions is reduced (Xu et al., 2006). Damage to the D1 protein of PS2 reduces the efficiency of NADPH production and this damage can disrupt the forces responsible for stacking (Fristedt et al., 2009). The full OJIP traits from the experiment can be found in **Supplementary Table 1**.

The critical role of chloroplast ultrastructure for the light-dependent reactions, warrants detailed investigations to assess changes that may occur because of heat stress. Indeed, previous investigations into the effects of heat stress have included analyses of chloroplast ultrastructure. Zhang et al. (2010) determined that increased air temperatures induced chloroplast swelling in *Arabidopsis*. This swelling was coordinated with increased non-photochemical quenching (NPQ). Chloroplast swelling has also been linked to increased chloroplastic pH and grana destacking (Semenova, 2002). Chloroplast ultrastructure changes have also been observed in response to potassium deficiency (Zhao et al., 2001), arsenic (Li et al., 2006), salt stress (Fidalgo et al., 2004), nitrogen fertilization (Bondada and Syvertsen, 2003), drought (Vassileva et al., 2012), and heat (Vani et al., 2001; Xu et al., 2006; Zhang et al., 2010). Genotypic variation in chlorophyll a/b ratios has been reported for soybean, but structural or functional implications were not investigated (Fritschi and Ray, 2007). Surprisingly, to date, no investigations of genotypic differences in chloroplast ultrastructure have been reported for soybean.

The primary route for energy from absorbed light is its use for the light-dependent reactions of photosynthesis. Excess energy can be dissipated as heat, NPQ, and as light in the form of fluorescence. Chlorophyll fluorescence can be evaluated rapidly and nondestructively, and can be used to provide information on the efficiency of the light-dependent reactions (Maxwell and Johnson, 2000). The vast body of work that exists about chlorophyll fluorescence and its relationship to the light-dependent reactions has allowed calculations that reflect the state of various processes of the light-dependent reactions. Thus, chlorophyll fluorescence measurements have significantly enhanced our understanding of the effects of abiotic stresses on the biochemical steps of the light-dependent reactions of photosynthesis (Strasser and Strasser, 1995). Chlorophyll fluorescence measurements have been used to assess the effects of abiotic stress factors on the light-dependent reactions, including the effects of nitrogen deficiency (Congming and Jianhua, 2000; Huang et al., 2004), salt stress (Misra et al., 2001; Woo et al., 2008), and heat stress (Schreiber and Berry, 1977; Briantais et al., 1996; Zhou et al., 2018). Damage to PS2 caused by elevated temperature can be observed as increases in minimum fluorescence (Briantais et al., 1996) and reduced grana stacking (Yamamoto et al., 2008). Damage to PS2 can lead to destacking of the grana and alter ATP and NADPH production ratios. Reductions in NADPH caused by damage to PS2 can limit the availability of reducing power for Rubisco and thus change both CO_2 assimilation and Rubisco activase repair and synthesis (Murata et al., 2007). Although potentially valuable to devise strategies to improve soybean heat tolerance, detailed physiological studies about light-dependent reaction responses of soybean to heat stress are lacking.

This study was conducted to determine the effects of elevated temperatures on chloroplast ultrastructure, chlorophyll fluorescence, and gas exchange of soybean. To this end, four genotypes were grown in growth chambers and three temperature regimes were imposed for 7 days after initial growth in uniform conditions. The effects of the different temperature regimes on chloroplast

ultrastructure, chlorophyll fluorescence, and gas exchange were assessed. The study provides novel information about the effects of high temperatures on the structure and function of soybean chloroplasts which may be used for crop improvement efforts and for studies aimed at further dissection of heat stress tolerance mechanisms in soybean.

MATERIALS AND METHODS

Genotypes and Growth Conditions

Four soybean genotypes were selected for inclusion in this experiment based on the characterization of 120 diverse maturity group (MG) IV soybean genotypes. Briefly, the soybean genotypes were grown under control conditions (28°C) in a greenhouse until at least the 4th leaf stage after which they were exposed to elevated air temperature (> 40°C) on three non-consecutive days. Chlorophyll fluorescence measurements were conducted on each day of elevated air temperature. Two genotypes from this experiment were selected for inefficient (PI603166) and efficient (PI398226) photosynthetic parameters in elevated air temperature based on rankings of more than 20 chlorophyll fluorescence phenotypes. PI603166 was ranked in the bottom 5% whereas PI398226 was ranked in the top 5% based on chlorophyll fluorescence measurements. The remaining two genotypes, DS25-1 (tolerant) and DT97-4290 (sensitive), were included in the greenhouse screening and in the present study because they differ in germinability of seeds that developed under elevated temperature (Smith, 2017). Hereafter, genotypes will be referred to as PI-26, PI-66, DS25, and DT97 for PI398226, PI603166, DS25-1, and DT97-4290, respectively. Five seeds of each genotype were sown approximately 2.5 cm deep in each of six pots (12.7 cm × 12.7 cm × 30.5 cm) filled with top soil (Ri-Mor Mulch and Landscape, Columbia, MO, USA) placed in one of two PGR15 growth chambers (Controlled Environments Ltd, Winnipeg, MB, Canada). After plants had their 1st unrolled trifoliate (V1; Fehr et al., 1971) pots were thinned to a single plant, aiming for uniform height and vegetative stage across pots. Growth chamber conditions were set to 14 h of light (1,000 μmol m^{-2} s^{-1} PAR) and 28°C and 50% relative humidity during the light hours (6 am to 8 pm) and 22°C and 75% relative humidity in the dark. Temperatures were increased from 22 to 28°C 1 h after lights were turned on and returned to 22 from 28°C 1 h after lights were turned off. Plants were grown for three additional weeks until they reached four fully expanded trifoliate leaves. At that time, three temperature treatments were initiated, namely 28, 38, and 45°C maximum air temperatures which were imposed as follows: For the control treatment (28°C), the temperature regime was maintained the same as for initial growth. For elevated air temperature treatments, the temperature was increased gradually from 28°C at 7:00 am to reach 38 or 45°C by 9:00 am and held at these temperatures until 1:00 pm. Then the temperature was reduced from 38 or 45°C to 28°C from 1:00 pm to 3:00 pm and maintained at 28°C until 8:00 pm. Elevated temperatures that occur during the growing season often come in the form of heat waves that generally last a few to several days. Therefore, temperature treatments were imposed over the course of 7 days, at which point the experiments were terminated.

Each temperature regime was imposed in two separate experiments, once in each of the two growth chambers that were used for this study. Chlorophyll fluorescence measurements and gas exchange measurements were collected both times while samples for microscopy were collected in one of the two experiments. For each experiment, the four genotypes were grown in six replications arranged as a completely randomized design.

Chlorophyll Fluorescence and Net Photosynthesis Measurements

Chlorophyll fluorescence was measured every day during the 7 days of temperature treatment imposition, starting at 10:00 am (1 h after reaching maximum temperature in the 38 and 45°C treatments) and finishing at approximately 10:30 am. Leaf clips were attached to the center leaflet of the 2nd fully expanded trifoliate leaf for 20 min of dark adaptation. Chlorophyll fluorescence measurements were obtained using the OJIP protocol of a Fluorpen Z995-PAR (Qubit systems INC, Kinston Ontario, Canada). Due to the number of phenotypes, time points and treatments, only a subset of phenotypes (F_0, F_M, F_V/F_M, and ABS/RC) and time points (days 1, 3, 5, and 7) that simplified but captured the differences and similarities observed in chlorophyll fluorescence, were selected to be presented here.

The same leaves that were measured for chlorophyll fluorescence were also used for net photosynthesis measurements with a portable photosynthesis system (LI-6400XT, LI-COR, Lincoln, NE, USA). The conditions in the measurement chamber were controlled at ambient CO_2 level (380 μmol mol^{-1}), leaf block temperature was set to match the air temperature of the respective treatment (28, 35, or 45°C), and photosynthetically active radiation was set to 1,000 μmol m^{-2} s^{-1} to match the light intensity in the growth chamber. Gas exchange and leaf temperatures were measured in each replication on the 1st, 3rd, 5th, and 7th day of temperature treatment starting at approximately 10:30 am (~1.5 h after reaching maximum temperature in the 35 and 45°C treatments).

Chloroplast Ultrastructure Assessment

Tissue samples for chloroplast ultrastructure analysis were obtained on the 1st and 7th day of the 28 and 45°C treatments from genotypes DT97 and PI-66 at approximately 12:30 pm after leaf gas exchange measurement before temperatures began changing. These two genotypes and the 28 and 45°C temperature treatments were selected for examination of chloroplast ultrastructure based on the chlorophyll fluorescence measurements conducted during the greenhouse screening. One leaf disk (1 mm diameter) was collected from the area of the center leaflet of the 2nd fully expanded leaf that was used for chlorophyll fluorescence measurements and was immediately placed into primary fixative (5% glutaraldehyde). Samples were post fixed in osmium tetroxide (OsO_4) and dehydrated in increasing concentrations of ethanol. Samples were embedded in Spurr's epoxy and ultrathin sections were cut using a microtome set to 60 nm for the 28°C treatment and to 80 nm for the 45°C treatments (due to impaired integrity of the

sections at 60 nm). All samples were post stained with Reynold's Lead Citrate. Sections were viewed with a JEOL JEM-1400 transmission electron microscope (JEOL Ltd. Akishima, Tokyo, Japan). Images of chloroplasts were obtained at ×7,000 magnification. Multiple images were collected per chloroplast and were stitched to form one image of each chloroplast at ×7,000 using MS paint (Microsoft Corporation, Redmond, WA, USA). ImageJ (Schneider et al., 2012) was used to measure ultrastructural traits of chloroplasts using the 1 μm scale bar of the electron microscopic images to scale pixels. Twenty-five chloroplasts from each of the two temperature treatments and genotypes were analyzed for total grana number, total grana area, average grana area, total number of starch grains, total starch grain area, average starch grain area, chloroplast area, percent grana area, and percent starch grain area. To assess total grana number per chloroplast, each granum was counted for each of the chloroplasts and totaled. Total grana area was assessed by measuring the area of all grana by tracing lines around each grana of all chloroplasts and then summing the areas. Average grana area was calculated by dividing the total grana area by the number of grana for each chloroplast. Total number of starch grains was assessed by counting the number of starch grains present in each chloroplast. Total starch grain area was measured by tracing edges of starch grains and then adding all the areas together. Average starch grain area was calculated by dividing the total area of starch grains by the number of starch grains for each chloroplast. Chloroplast area was measured by tracing the outside of each chloroplast. Percent grana area was calculated by dividing the total grana area by the chloroplast area and multiplying by 100. Percent starch grain area was calculated by dividing the total starch grain area by chloroplast area and multiplying by 100.

Statistical Analysis

Statistical analyses were performed with SAS 9.4 (SAS institute Inc. 2004). Repeated measures analysis was performed by PROC MIXED with genotype by treatment by experiment nested within sample as the repeated measure and the model genotype, day of treatment, temperature treatment, and experiment as main effects and including the respective interaction effects for chlorophyll fluorescence and gas exchange data. While significant differences were found between repeat experiments for some phenotypes, data trends across days of treatments were the same. Therefore, statistical analysis and data presentation were considered together. Analysis of variance for chloroplast ultrastructure was performed with PROC GLM by genotype with temperature treatment, day of treatment, replication, and respective interaction effects included in the model. Pair-wise Tukey analysis was used to identify differences between treatments by genotype and day of treatment for the chloroplast ultrastructure.

RESULTS

Effects of Temperature Treatments on Gas Exchange

Leaf net photosynthesis (A) was measured between 1.5 and 4 h after air temperatures in the growth chambers reached their respective treatment maxima on the 1st, 3rd, 5th, and 7th day of temperature treatments (**Figure 1** and **Table 1**). In the 45°C treatment, A was greatest on the 1st day of treatment and declined over the course of the 7-day treatment period in all four genotypes (**Figure 1**). In contrast, A in the control treatment (28°C) was more stable over the course of the 7 days, decreasing slightly in DT97 or increasing somewhat in DS25, PI-26, and PI-66. While A at 45 and 28°C did not differ on the 1st day in PI-66, it was lower at 45°C on the 7thday. In contrast, A did not differ between 45 and 28°C in DT97, on the 1st or 7th days. Leaf net photosynthesis (A) of PI-26 at 28°C was lower than in the other three genotypes and started out lowest with 28 and 45°C treatments on the 1st day but did not differ from 38 and 45°C treatments on the 7th day. In general, A in the 38°C treatment was high in the beginning or even increased slightly early on and declined only after the 3rd or 5th day of treatment.

In general, stomatal conductance (g_s) followed similar temporal patterns for the different temperature treatments as the responses of A (**Figure 1**). Stomatal conductance was lowest and more stable across the 7 days in the control treatment compared to the 38 and 45°C treatments. In the 45°C treatment g_s decreased from the 1st to 7th day in all genotypes. In contrast, at 38°C, g_s of all genotypes increased sharply from the 1st to the 3rd day of treatment, followed by a steady decline over the course of the remaining days with DS25 and PI-66. On average across the 7-day treatment period, g_s at 28°C was lower in PI-26 than in the other three genotypes which had similar g_s. This lower gs of PI-26 was consistent with the lower A observed for PI-26 in the control treatment.

Internal CO_2 concentration (C_i) in the 28 and 38°C treatments followed a similar temporal pattern as g_s across the 7-days for all genotypes (**Figure 1** and **Table 1**). However, C_i in the 45°C treatment was more stable than g_s and A did not exhibit a pronounced decline over the course of the heat treatment. In fact, in PI-66, a small increase in C_i occurred with the 45°C treatment over the course of the heat treatment period.

Treatments strongly influenced leaf temperatures of all genotypes (**Figure 1**). Leaf temperatures were relatively stable across the 7 days in the 28°C treatment in DT97, DS25, and PI-66. However, a small decline (1.2°C decrease) of leaf temperature from the 1st to 7th day was observed for PI-26 in the 28°C treatment. In the 38 and 45°C treatments, leaf temperatures of PI-26 (maximum difference among days ~1.3°C) and PI-66 (maximum difference among days <0.9°C) were relatively stable. While leaf temperatures in the 38°C of DT97 increased from the 3rd to 5th day, and a steady increase of leaf temperature with the 45°C treatment. A small decrease in leaf temperature on the 3rd day of 38°C was observed with DS25 followed by increasing leaf temperatures on the 5th and 7th days.

Temperature Treatment Influences on Chlorophyll Fluorescence

Minimum fluorescence (F_0) provides information on the status of PS2 which is critical for the overall efficiency of the light reactions. Analysis of F_0 by treatment across all 7 days revealed that F_0 increased in all genotypes when exposed to 45°C as

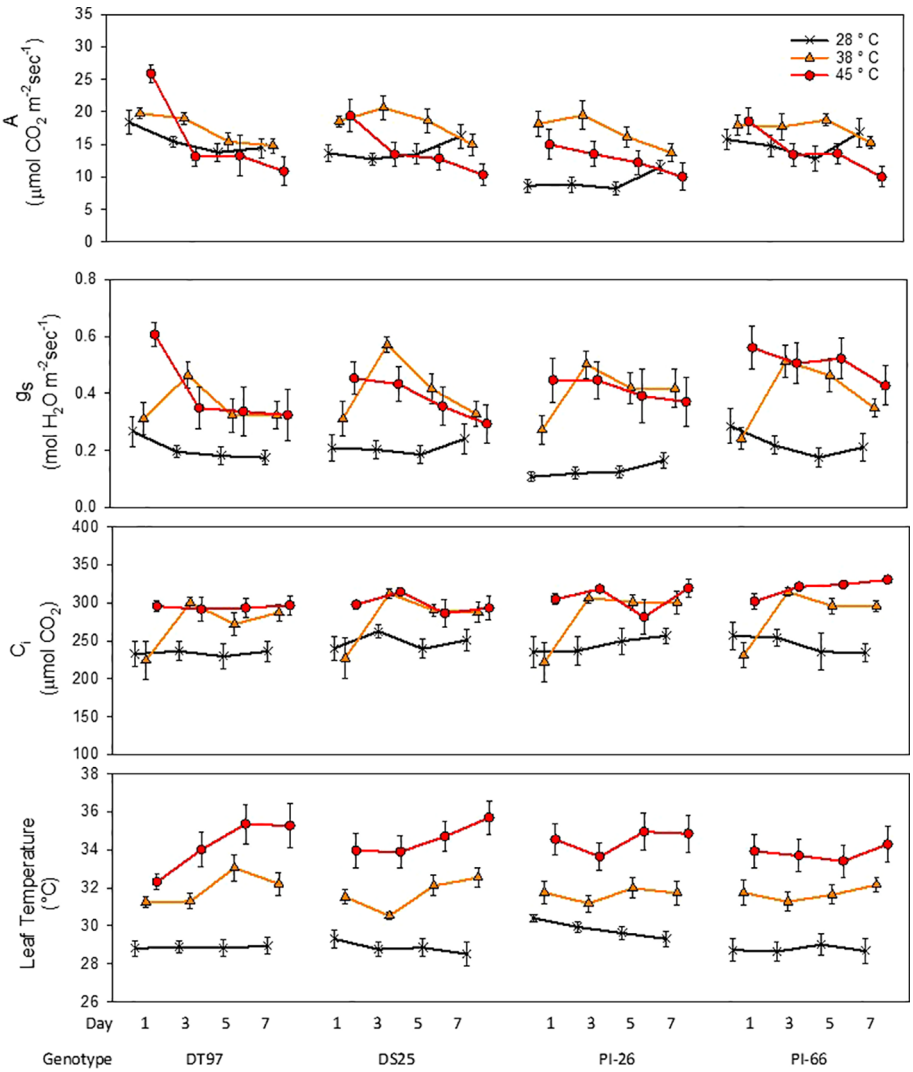

FIGURE 1 | Responses of photosynthetic rate (A), stomatal conductance (g_s), internal CO_2 (C_i), and leaf temperature of four soybean genotypes to the imposition of maximum day time temperatures of 28, 38, and 45°C over the course of 7 days. Measurements were taken from the uppermost middle trifoliate leaves 2 h after air temperatures reached the indicated temperature on days 1, 3, 5, and 7. Symbols represent mean values (N = 12) and whiskers indicate standard error.

compared to the 28°C treatment (**Figure 2**). In DT97, PI-26, and PI-66, F_0 at 38°C was lower than at 45°C and higher than in the 28°C treatment, whereas, in DT97, F_0 at 38°C was similar to the 28°C treatment. Temporal analysis of F_0 indicated that F_0 was higher at 45°C than at 28°C throughout the 7-day heat treatment in DT97 and PI-66, while in DS25 and PI-26, it was higher on all but the last day of measurements (**Figure 3** and **Table 2**). In the 38°C treatment, F_0 tended to be intermediate in PI-26 and PI-66 or similar to the 45°C treatment in DS25 for much of the 7-day treatment period or similar to the 28°C treatment in DT97. The temporal pattern of F_0 in the different temperature treatments generally were similar within a genotype, except for a dramatic drop on the 7th day in PI-26 grown at 45°C.

The capacity for energy utilization by the light-dependent reactions can be assessed with maximum fluorescence (F_M). Across the 7 days of treatment, maximum fluorescence of DT97, PI-26, and PI-66 in the 45°C treatment was lower than in the 28 and 38°C treatments (**Figure 2**). However, the F_M of DS25 was lower in the 28 and 45°C treatments than the 38°C treatment. Maximum fluorescence was relatively consistent throughout the 7-day period in the 28 and 38°C treatments in DT97 and PI-66 (**Figure 3**). In the 45°C treatment, F_M generally varied more and was greater on the 7th day compared to the 28 and 45°C treatments in PI-26. While F_M at 45°C was maximal on the 7th day in DT97, F_M maxima occurred on day 5 in DS25 and PI-26, and in PI-66 a sharp increase was observed from day 1 to day 3 after which it remained steady.

Photochemical efficiency (F_V/F_M) is a measure of the maximum photosystem II efficiency. In general, F_V/F_M declined with increasing temperature in all four genotypes

TABLE 1 | Statistical groupings from **Figure 1** for photosynthetic rate (A), stomatal conductance (g_s), internal CO_2 (Ci) and leaf temperature.

Genotype	A	28	38	45	g_s	28	38	45
DT97	1st day	AB	B	A	1st day	B	B	A
	3rd day	B	A	AB	3rd day	B	A	A
	5th day	A	A	A	5th day	B	A	AB
	7th day	A	A	A	7th day	B	A	A
DS25	1st day	B	AB	A	1st day	B	AB	A
	3rd day	B	A	AB	3rd day	B	A	A
	5th day	AB	A	B	5th day	B	A	AB
	7th day	A	A	B	7th day	B	A	AB
PI-26	1st day	C	A	B	1st day	B	A	A
	3rd day	C	A	B	3rd day	B	A	A
	5th day	B	A	AB	5th day	B	A	A
	7th day	A	A	A	7th day	B	A	A
PI-66	1st day	A	A	A	1st day	B	B	A
	3rd day	AB	A	B	3rd day	B	B	A
	5th day	B	A	B	5th day	B	B	A
	7th day	A	AB	B	7th day	B	AB	A
	Ci	**28**	**38**	**45**	**LTemp**	**28**	**38**	**45**
DT97	1st day	AB	B	A	1st day	B	A	A
	3rd day	B	A	A	3rd day	B	AB	A
	5th day	A	A	A	5th day	C	B	A
	7th day	B	A	A	7th day	C	B	A
DS25	1st day	A	A	A	1st day	B	A	A
	3rd day	A	A	A	3rd day	C	B	A
	5th day	A	A	A	5th day	C	B	A
	7th day	B	A	AB	7th day	C	B	A
PI-26	1st day	B	B	A	1st day	B	A	A
	3rd day	B	B	A	3rd day	B	A	A
	5th day	A	A	A	5th day	C	B	A
	7th day	B	A	A	7th day	C	B	A
PI-66	1st day	B	AB	A	1st day	B	A	A
	3rd day	B	A	A	3rd day	C	B	A
	5th day	B	AB	A	5th day	B	A	A
	7th day	B	A	A	7th day	B	A	A

Same letter represents temperature treatments that were grouped together based on differences of least square means.

(**Figure 2**). In PI-26 and PI-66 the decrease in F_V/F_M was significant between every temperature regime, whereas in DT97, F_V/F_M was lower at 45°C than at both 28 and 38°C, which were not different from each other. On average, across all days and compared with F_V/F_M at 28°C, F_V/F_M at 45°C was reduced by 10.3, 5.39, 8.53, and 7.86%, in DT97, DS25, PI-26, and PI-66, respectively. Over the course of the 7-day treatments, a considerable increase in F_V/F_M was observed for all genotypes at 45°C whereas it increased only slightly or was relatively stable at 28 and 38°C. In DT97, DS25, and PI-66, increases in F_V/F_M from the 1st to the 3rd day were observed at 45°C, but no change was found after that. In contrast, a more gradual increase in F_V/F_M from 1st to 7th day was observed in PI-26 in 45°C treatment. The F_V/F_M in 45°C recovered from 85.5% of the control (28°C) on day 1 to 90.6% of the control on the 7th day in DT97, and from 90.1 to 93.9%, 87.3 to 94.1%, and 87.6 to 93.3% in DS25, PI-26, and PI-66, respectively.

The absorption per reaction center (ABS/RC) represents the total number of photons absorbed by chlorophyll molecules in proportion to the total number of active reaction centers. Across all measurement days, all genotypes showed an increase in ABS/RC with increasing temperature (**Figure 2**). Over the course of the 7 days, ABS/RC in the 28 and 38°C treatments were relatively stable and differed little between these two treatments (**Figure 3** and **Table 2**). On the other hand, ABS/RC at 45°C was greater than that at 28°C in all genotypes and on all measurement days. On the 1st day, ABS/RC at 45°C was dramatically greater than at 38°C in all genotypes. However, by the 7th day ABS/RC had declined in the 45°C treatment such that differences between 38 and 48°C were not significant anymore in DS25, PI-26, and PI-66.

Effects of Heat Stress on Chloroplast Ultrastructure

Chloroplast ultrastructure was examined in leaf tissues sampled after gas exchange measurements on the 1st and 7th days from DT97 and PI-66 plants grown at 28 and 45°C. Representative transmission electron micrographs depicted in **Figure 4** illustrate genotype differences at both 28 and 45°C as well as heat treatment effects on both genotypes. Quantitative assessment of chloroplast characteristics based on transmission electron microscopy (TEM) images revealed that the responses to 7 days of 28 or 45°C differed between genotypes for chloroplast area, percent starch grain area per chloroplast, starch area per chloroplast, and average area per granum (**Figure 5**). On the 1stday, the chloroplast area was greater at 45°C than at 28°C in DT97 but similar in PI-66. On the 1st day at 45°C, the number of starch grains and grana per chloroplast were greater than at 28°C in DT97. In contrast, no treatment effect on starch grain and grana numbers per chloroplast were found in PI-66 after the 1st day. Both percent grana area per chloroplast as well as grana area per chloroplast was greater at 45°C than at 28°C in DT97 on the 1st day but did not differ on the 7th day. In PI-66, no differences in the percent grana area per chloroplast were observed on either day, but the grana area per chloroplast was larger at 45°C than 28°C on the 1st day and smaller at 45°C than at 28°C on the 7th day. As can be seen in **Figures 4** and **5**, the starch area per chloroplast was greater in the heat stress treatment on the 1st day for DT97 but smaller than in the control by the 7th day. In contrast, the starch area per chloroplast in PI-66 was not affected by temperature on the 1st or 7th day. However, the percent starch area per chloroplast was increased in PI-66 but decreased in DT97 in the 45°C compared to the 28°C treatment on the 7th day. Overall, the starch was much less in DT97 than PI-66, and this was associated with smaller starch grains of DT97 than PI-66. In response to 45°C compared to 28°C, DT97 exhibited larger starch grains on the 1st day, but smaller starch grains on the 7th day. Unlike in DT97, the size of individual starch grains was not influenced by the temperature treatment in PI-66. These results for average starch grain area paralleled those observed for the starch area per chloroplast.

DISCUSSION

Temperature Treatment Effects on Leaf Temperatures and Gas Exchange Parameters

For the 7 days of temperature treatment imposition, air temperatures in the growth chambers were ramped up from 22°C (night time) over

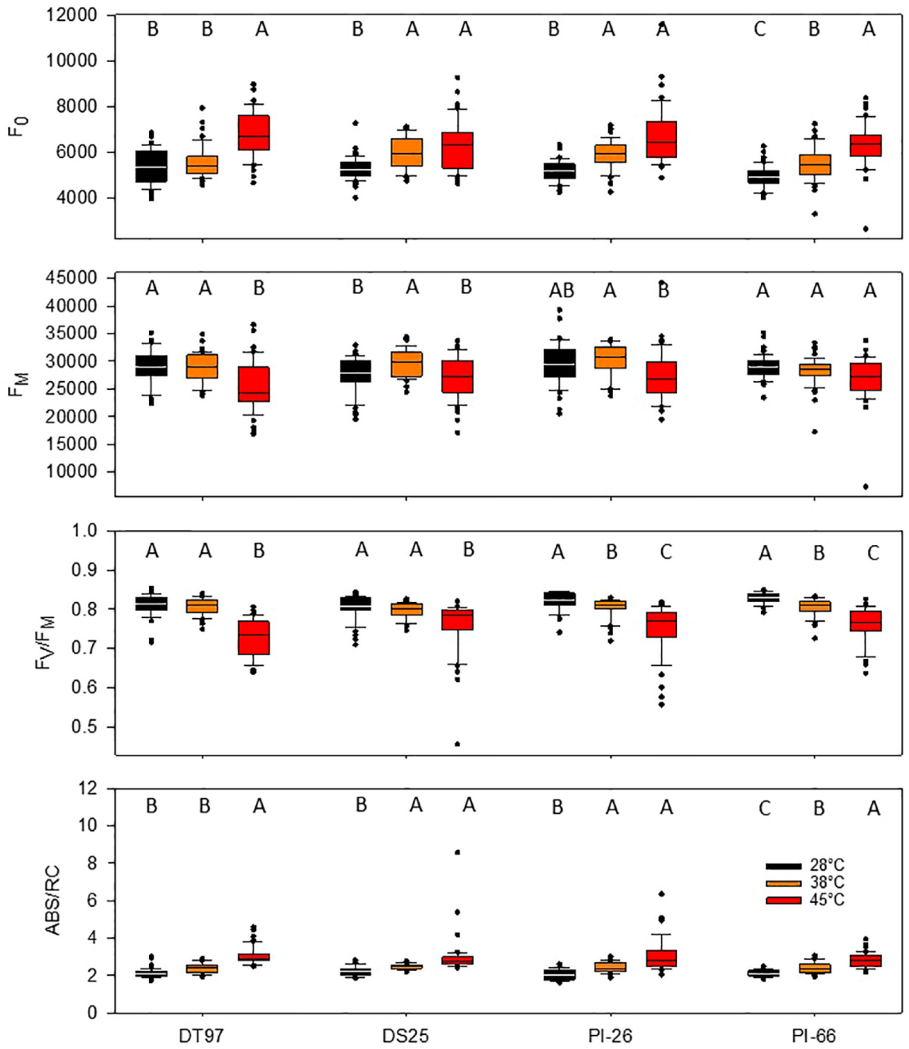

FIGURE 2 | Minimum fluorescence (F_0), maximum fluorescence (F_M), maximum photochemical efficiency (F_V/F_M), and absorption per reaction center (ABS/RC) of four soybean genotypes exposed to maximum day time temperatures of 28, 38, and 45°C over the course of 7 days. Data represents chlorophyll fluorescence measurements on the center leaflet of the upper-most fully expanded leaf after 1 h of temperature treatment on days 1, 3, 5, and 7 from two independent growth chamber experiments for each temperature treatment (N = 48). Lines within boxes represent the median and top and bottom of whiskers represent the 1st and 3rd quartiles respectively. Circles represent outlier data one and a half times the 1st and 3rd quartiles. Letters indicate similar treatments of phenotypes within genotype based on Tukey pairwise analysis.

the course of 2 h to reach maximum daytime temperatures of 28 (control), 38, or 45°C by 9 am. These maximum temperatures were maintained for 4 h after which air temperatures were gradually reduced to the control temperature for the remaining time of the 14-h photoperiod, and then to night time temperature. Because plants were well-watered throughout the experiments, the imposition of these air temperature treatments, coupled with the control of relative humidity at 50% during the photoperiod, allowed for significant transpirational cooling which resulted in average leaf temperatures of 29.1, 31.9, and 34.5°C in the 28, 38, and 45°C treatments, respectively (**Figure 1**). Thus, the responses of gas exchange, chlorophyll fluorescence, and chloroplast ultrastructure of the genotypes to the three temperature treatments should be considered in the context of leaf temperatures and not only with respect to air temperatures.

In general, net photosynthetic rates observed in this study (18 μmol m^{-2} s^{-1}—average across all genotypes) on the 1st day of 28°C were comparable with those documented by others for growth chamber experiments at the same or similar temperature. For instance, Djanaguiraman et al. (2011) reported net photosynthetic rates of ~22 μmol m^{-2} s^{-1} for soybean genotype K 03-2897 grown at 28°C, and Ziska and Bunce (1995) reported ~12 μmol m^{-2} s^{-1} 18 days after emergence for the cultivar Clark grown at 25°C. Djanaguiraman et al. (2011) also exposed K 03-2897 to 38°C, and on the 2nd and 6th day measured net photosynthetic rates of ~20 and 17 μmol m^{-2} s^{-1},

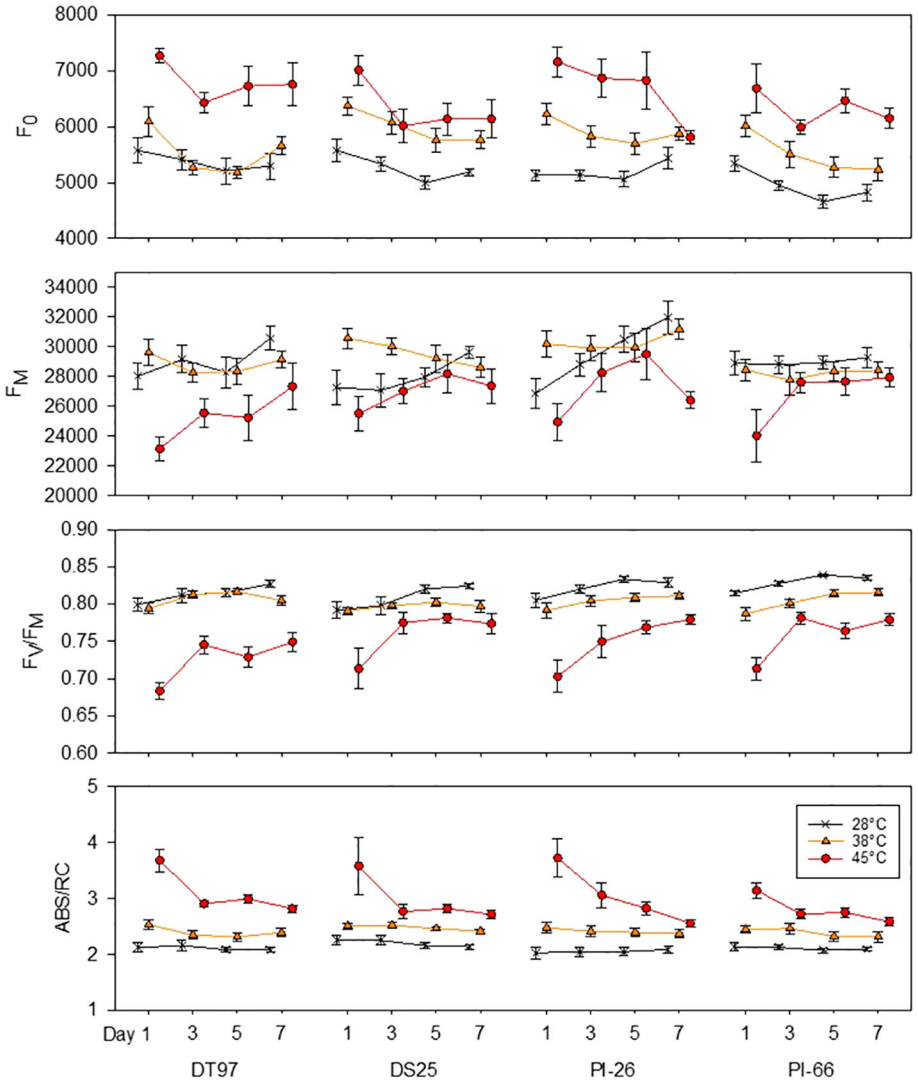

FIGURE 3 | Responses of minimum fluorescence (F_0), maximum fluorescence (F_M), maximum photochemical efficiency (F_V/F_M), and absorption per reaction center (ABS/RC) of four soybean genotypes to the imposition of maximum day time temperatures of 28, 38, and 45°C over the course of 7 days. Measurements weretaken from the middle leafleft of the uppermost fully expanded leaf between one and two hours after air temperatures reached the indicated temperature on days 1, 3, 5, and 7. Symbols represent mean values (N = 12) and whiskers indicate standard error.

respectively. These values were similar to the net photosynthetic rates obtained in the present study on day 3 (~19 μmol m^{-2} s^{-1}) and 7th day (~17 μmol m^{-2} s^{-1}), but were considerably lower than those normally observed under well-watered field conditions which generally are above 25 μmol m^{-2} s^{-1} (Haile and Higley, 2003; He et al., 2016; Yao et al., 2017; Sakowska et al., 2018). A decline of net photosynthesis is commonly observed in crops in response to increased temperatures. Reduced net photosynthesis in response to elevated temperatures has been shown for cotton (*Gossypium* spp.) (Salvucci and Crafts-Brandner, 2004) and soybean (Harley et al., 1985; Djanaguiraman et al., 2011). At elevated day/night temperatures of 48/28°C, photosynthesis in greenhouse-grown soybean was reduced from 24.9 μmol m^{-2} s^{-1} at 28/22°C day/night temperatures to 16.0 μmol m^{-2} s^{-1} (Jumrani et al., 2017). Similarly, soybean exposed to multiple short term (4 day) heat waves reduced photosynthetic rate of field grown soybean from ~36 μmol m^{-2} s^{-1} to ~20 μmol m^{-2} s^{-1} on the 1st day of the 3rd heat wave (Siebers et al., 2015). Similar to these studies, net photosynthesis was at elevated temperature. On average, across the 7-day treatment, net photosynthetic rates were greater (17.5 μmol m^{-2} s^{-1}) at 38°C than at 45°C (14.0 μmol m^{-2} s^{-1}) and 28°C (13.3 μmol m^{-2} s^{-1}). However, these average values mask distinct temporal responses among the three treatments as well as differences among the genotypes.

At 45°C a significant decline in net photosynthesis was observed over the course of the 7 days of treatment. On the 1st day of treatment, net photosynthesis at 45°C was greater than 28°C in

TABLE 2 | Statistical groupings for traits from **Figure 3**.

Genotype	F_0	28	38	45	F_M	28	38	45
DT97	1st day	B	B	A	1st day	A	A	B
	3rd day	B	B	A	3rd day	A	A	B
	5th day	B	B	A	5th day	A	A	B
	7th day	B	B	A	7th day	A	AB	B
DS25	1st day	C	B	A	1st day	B	A	B
	3rd day	B	A	A	3rd day	B	A	B
	5th day	B	A	A	5th day	A	A	A
	7th day	B	AB	A	7th day	A	AB	B
PI-26	1st day	C	B	A	1st day	B	A	B
	3rd day	C	B	A	3rd day	A	A	A
	5th day	C	B	A	5th day	A	A	A
	7th day	A	A	A	7th day	A	A	B
PI-66	1st day	C	B	A	1st day	A	A	B
	3rd day	B	AB	A	3rd day	A	A	A
	5th day	C	B	A	5th day	A	A	A
	7th day	B	B	A	7th day	A	A	A
	F_V/F_M	**28**	**38**	**45**	**ABS/RC**	**28**	**38**	**45**
DT97	1st day	A	A	B	1st day	C	B	A
	3rd day	A	A	B	3rd day	B	B	A
	5th day	A	A	B	5th day	B	B	A
	7th day	A	A	B	7th day	B	B	A
DS25	1st day	A	A	B	1st day	B	B	A
	3rd day	A	A	A	3rd day	B	AB	A
	5th day	A	AB	B	5th day	B	B	A
	7th day	A	B	B	7th day	B	AB	A
PI-26	1st day	A	A	B	1st day	C	B	A
	3rd day	A	A	B	3rd day	C	B	A
	5th day	A	A	B	5th day	C	B	A
	7th day	A	A	B	7th day	B	AB	A
PI-66	1st day	A	B	C	1st day	B	B	A
	3rd day	A	B	B	3rd day	B	A	A
	5th day	A	A	B	5th day	B	B	A
	7th day	A	A	B	7th day	B	AB	A

Same letter represents temperature treatments that were grouped together based on differences of least square means.

DS25 and PI-26, but the decline was dramatic just as found for the other two genotypes. Similarly, while initially greater at 38°C than at 28°C in DS25 and PI-26, net photosynthesis at 38°C declined after 3 or 5 days and was not different from that in 28°C in any of the genotypes on 7th day. Declines in photosynthesis with exposure to elevated temperatures (starting around 35°C) over the course of several days have been reported for other crop species (Crafts-Brandner and Salvucci, 2002; Salvucci and Crafts-Brandner, 2004). These findings may explain the high net photosynthetic rates and the initial lack of response observed in the 38°C treatment in the present study as plants were able to maintain leaf temperatures at approximately 31°C. Thus, transpirational cooling allowed soybean plants to maintain leaf temperatures in the range of 27–37°C when grown at 38°C air temperature, which resulted in similar or greater net photosynthetic rates than when grown at 28°C and leaf temperatures in the range of 25–32°C. Additionally, it is important to note that gas exchange measurements were conducted starting approximately 1.5 h after maximum temperatures were reached. Thus, it appears that, in conjunction with the transpirational cooling, the duration of exposure to 45°C on day 1 was not long enough to significantly impair net photosynthesis and that these soybean genotypes have the ability to tolerate exposures to such high air temperatures in the short term.

The response of stomatal conductance (g_s) in the 38°C treatment differed from that in 45°C treatment such that g_s on the 1st day was much greater at 45°C than at 28°C but similar to that at 28°C in the 38°C treatment. However, g_s increased dramatically from day 1 to day 3 in the 38°C treatment, to levels similar or greater than those observed in the 45°C treatment in all genotypes. This strong response suggests that day 1 exposure to 38°C preconditioned subsequent stomatal regulation. Similar responses of g_s to increased temperature have been shown at an even shorter time scale of under one hour (Hamerlynck and Knapp, 1996). It is likely that the dramatic response in g_s already occurred by day 2 of the treatment, but that remains to be shown.

Despite the low light environment, the photosynthetic rate of genotype PI-66 on the 7th day of the 45°C treatment was reduced compared to the 28 and 38°C treatments and was in concurrence with the accumulation of starch in chloroplasts as shown by TEM. Conversely, the lower starch accumulation by DT97 on the 7th day of the 45°C treatment compared to the control was associated with similar levels of photosynthetic rate between the 28 and 45°C treatments. Because of the importance of feedback mechanisms in photosynthetic regulation, determination of the effects of heat stress on the expression of photosynthetic genes and enzyme activities are important to advance mechanistic understanding of heat stress effects on photosynthesis in soybean.

Chlorophyll Fluorescence Responses to Elevated Temperature Stress

Chlorophyll fluorescence measurements have been used broadly to elucidate the effects of abiotic stress factors on photosynthetic light reactions. In the present study, chlorophyll fluorescence measurements were made on the 1st, 3rd, 5th, and 7th day of 7-day heat wave simulation treatments with maximum air temperatures of 38 and 45°C compared to a 28°C control treatment. Measurements of F_0, F_M, F_V/F_M, and ABS/RC revealed significant temperature treatment effects in all four soybean genotypes either throughout the heat stress period or at one of the four measurement days (**Figure 2** and **Figure 3**). On average across the duration of the heat wave, F_0 was significantly greater in all four genotypes when they were exposed to 45°C compared to 28°C air temperatures, and in all genotypes but DT97, $F_0$was also greater in the 38°C treatment than in the control (**Figure 2**). Temporal F_0 dynamics illustrated in **Figure 3** and **Table 1** indicate differences among genotypes in acclimation over the course of the heat wave. Among the four genotypes, F_0 in the 45°C treatment reached control levels only for PI-26 and only by 7th day. It is well known that F_0 increases in response to elevated temperature (Briantais et al., 1996; Yamane et al., 1997). Increases of F_0 have been shown previously to occur in soybean in response to high light (Hong and Xu, 1999). Previous investigations of chlorophyll fluorescence in soybean in response to various abiotic stresses primarily reported on F_V/F_M (Kao et al., 2003; Van Heerden et al., 2004; Ohashi et al., 2006). Increased F_0 is caused by photoinhibitory damage to photosystem II (PS2) which has been shown to occur at elevated temperatures (Yamane et al., 1997).

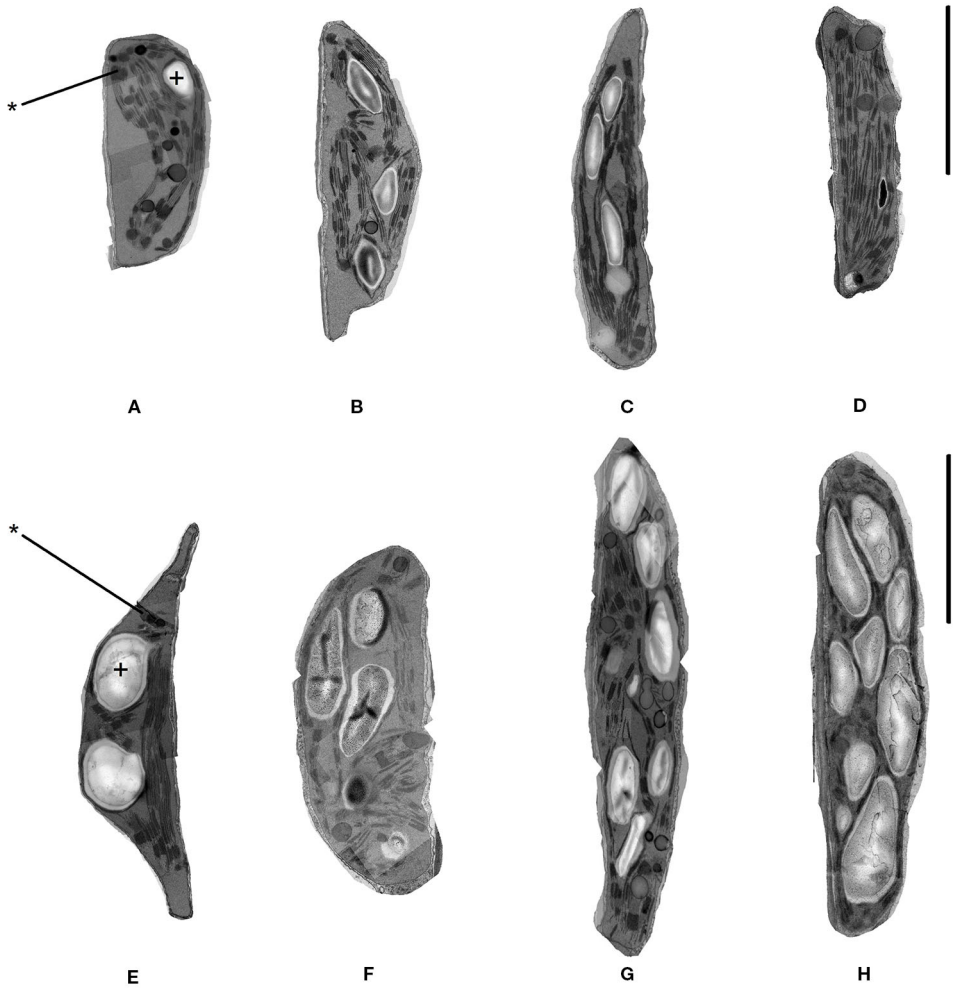

FIGURE 4 | Representative transmission electron microscope images of chloroplasts in upper-most fully expanded trifoliate leaves from DT97 **(A–D)** and PI-66 **(E–H)**. Images were acquired from samples collected on the 1st day of 28°C treatment **(A, E)**, 7th day of 28°C treatment **(B, F)**, 1st day of 45°C treatment **(C, G)**, and 7th day of 45°C treatment **(D, H)**. Black bars represent 1.0 μm. Starch grains and grana are identified with + and *, respectively.

Impairment of PS2 occurs through oxidative damage to the D1 protein and subsequent removal and replacement of D1 are essential to maintaining efficient light-dependent reactions (Aro et al., 1993). Photoinhibition is influenced by the repair capacity of PS2, light harvesting antenna size, (Tyystjarvi et al., 1992), cyclic electron flow (Takahashi et al., 2009), NPQ (Niyogi et al., 1998), and D1 protein turn over (Aro et al., 1993). Indeed, cyclic electron flow (Bukhov and Carpentier, 2000; Egorova and Bukhov, 2002), NPQ (Sinsawat et al., 2004; Zhang et al., 2010), and D1 protein turn over (Yoshioka et al., 2006) have been shown to increase at elevated temperatures. Thus, it is possible that the higher temperature required to produce a response of F_0 with DT97 to a temperature increase was due to increased repair capacity, and/or NPQ. This response of F_0 in DT97 was paralleled by reduced net photosynthetic rates of the 38°C treatment that were similar to the 28°C treatment and on the 5th and 7th day the 45°C treatment had similar A to the 28 and 38°C treatments. Additional physiological studies will be needed to determine how DT97 is responding to increased temperature with respect to photoinhibition and implications for CO_2 assimilation.

Maximum fluorescence (F_M) is related with the donor side capacity of PS2, and has been shown to decrease in response to heat stress (Pospíšil et al., 1998; Mathur et al., 2011). Thus, the reduced F_M observed in this study, particularly early during heat stress imposition (**Figure 3**), is consistent with previous reports and a reduction of donor side capacity of PS2. The overall response of DT97 was similar to that of F_0 in that an increase in temperature from 28 to 38°C did not have a profound effect, while a substantial impact was observed in response to the 45°C treatment. In contrast, unlike F_0, an increase in temperature from 28 to 38°C did not have any effects on F_M in DT97, PI-26, and PI-66 and only an increase in temperature to 45°C lead to significant reductions in F_M. In DS25, on average across days, an increase in temperature from 28 to 38°C lead

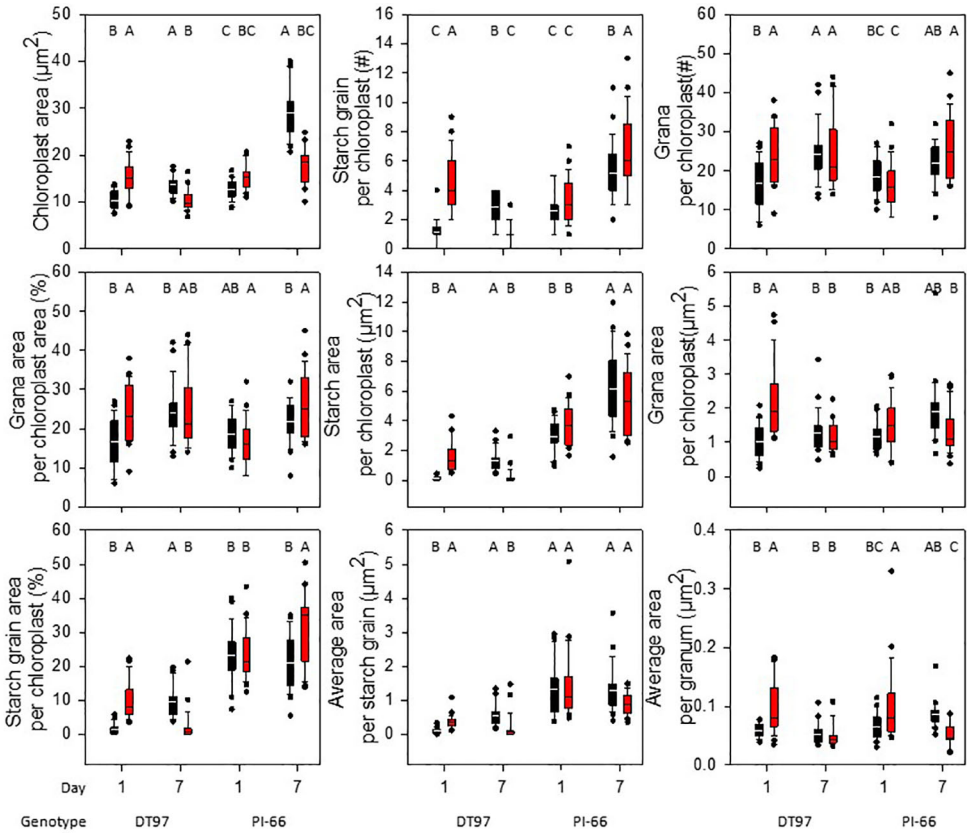

FIGURE 5 | Chloroplast ultrastructure characteristics in upper-most fully expanded leaves of DT97 and PI-66 from the 1st and 7th day of 28 and 45°C temperature treatments. Traits were assessed on transmission electron microscopy images of 25 chloroplasts for each time point and temperature treatment of both genotypes (N = 25). Lines within boxes represent the median and top and bottom of whiskers represent the 1st and 3rd quartiles respectively. Circles represent outlier data one and a half times the 1st and 3rd quartiles. Letters indicate similar treatments of phenotypes within genotype based on Tukey pairwise analysis.

to an increase in F_M, but no difference was observed at 45°C compared to 28°C. The increase of F_M in DS25 was due to high F_M levels on the 1st and 3rd day and a return to the level of the 28°C treatment by the 5th day. Temporal dynamics of F_M were more varied among the genotypes compared to F_0. The F_M of PI-66 in the 45°C treatment rapidly recovered (by the 3rd day) to the levels observed at 28°C, but F_M in DT97 recovered more slowly, never completely reaching those in the 28°C treatment. Overall, the temporal responses of F_M and F_0 in the four genotypes indicate genotypic variation in the effects of high temperatures on the factors driving F_0 compared to those underlying F_M. Petkova et al. (2007), suggested that decreases in F_M observed in common bean cultivars (*Phaseolus vulgaris* L.) exposed to 42°C temperatures were due to an increase in NPQ. This suggestion seems to hold true for PI-66 given the observed responses of F_0 and F_M to increased temperature. That is, F_M was relatively stable over the temperature treatments and was contrasted by increased F_0. Thus, the capacity for protection against photoinhibition associated with NPQ may be reduced with PI-66 resulting in photoinhibition and increased F_0. In the short term this reduced protection of PI-66 yielded similar photosynthetic rates between the 28 and 45°C treatments. However, on the 7th day net photosynthetic rate at 45°C was lower than at 28 and 38°C. Reduced NPQ may have allowed more energy to be used by PI-66 in the 3rd and 5th days, while eventually causing increased damage resulting in reduced CO_2 assimilation on 7th day. Measurements of NPQ in PI-66 exposed to different temperatures will be needed to ascertain if NPQ is not responding to increased temperature in this genotype and how this relates to net photosynthesis.

Only DT97 and DS25 were able to maintain similar levels of F_V/F_M in 38 and 28°C treatments (**Figure 2**). Genotypes PI-26 and PI-66 both exhibited reductions in F_V/F_M in response to a temperature increase from 28 to 38°C. All genotypes exhibited reductions in F_V/F_M with an increase in temperature from 38 to 45°C. Camejo et al. (2005), reported that the F_V/F_M of wild tomato genotypes were similar under control (28°C) and heat (45°C) conditions while the increased temperature resulted in lower F_V/F_M in a cultivar. Both F_V/F_M and F_0 are reliable indicators of photoinhibition due to heat stress (Gamon and Pearcy, 1989), as well as of high light (Ogren and Sjostrom, 1990), water stress (Epron et al., 1992), and low temperature (Groom and Baker, 1992). Thus, compared to the other two genotypes which exhibited reductions in F_V/F_M in response to a

temperature increase from 28 to 38°C, it appears that DT97 and DS25 can adapt to a 10°C increase. This was also supported by the net photosynthetic rates of DT97 which were similar at 45 and 28°C. Given the wealth of knowledge surrounding F_V/F_M and the F_V/F_M results for DT97 and DS25 documented here, soybean heat stress research and breeding may benefit from these two genotypes. To this end, DT97 may be of particular interest due to its ability to maintain lower levels of photoinhibition at higher temperatures compared to the other genotypes.

Absorption per reaction center (ABS/RC) represents the photon flux per reaction center. Overall, ABS/RC of all four genotypes increased with temperature. Temporal dynamics of ABS/RC at 45°C revealed rapid return to control or near-control levels in all genotypes except PI-26. The ABS/RC of PI-26 remained elevated compared to the other treatments until the 7th day when the level of the 45°C treatment was similar to the 38°C but not the 28°C treatment. Absorption per reaction center is strongly driven, by the number of active reaction centers. Increases of ABS/RC have been shown to occur in soybean exposed to elevated temperatures (De Ronde et al., 2004), high salt stress in salt-stressed wheat (*T. aestivum*) (Mehta et al., 2010), and in nitrogen deficient corn and tomato (Kalaji et al., 2014). In contrast, ABS/RC was reduced in drought-stressed rice (Redillas et al., 2011). De Ronde et al. (2004), attributed the observed increase in ABS/RC in response to heat stress in soybean to fewer active reaction centers. Although increased ABS/RC in response to higher temperatures was expected (De Ronde et al., 2004), it is unknown whether it was due to fewer active reaction centers. In contrast, the temporal response of ABS/RC in PI-26 was unexpected as there are no studies which report temporal responses of ABS/RC. Differences in repair dynamics of PS2 in PI-26 compared to the other three genotypes may have resulted in slower, more gradual recovery of ABS/RC over the course of the 7-day treatment. Additional studies will be required to determine if the observed temporal responses are due to antenna size, active reactions centers, or other factors. Genotypes with contrasting responses such as DS25 and PI-66 should be suitable for future studies aimed at elucidating the mechanisms underpinning the different temporal responses in ABS/RC and their relevance with respect to improvement of soybean heat tolerance.

At this time, it is unclear whether the rapid return of F_V/F_M and ABS/RC observed in DS25 or the slower recovery or acclimation observed for PI-26 is more advantageous for soybeans exposed to high temperatures. Information on F_V/F_M dynamics over the course of several days of heat stress from other species is limited and does not provide much insight in that regard and no reports on temporal responses of ABS/RC at this time could be found. Liu and Huang (2000) reported F_V/F_M from two varieties of creeping bentgrass that were exposed to control (22°C) and elevated temperature (35°C) treatments for 56 days. Temporal dynamics of F_V/F_M from creeping bentgrass varieties showed steady decline to ~.5 at the end of the 56 day elevated temperature treatment while control levels remained unchanged (Liu and Huang, 2000). Differences in the temporal responses of soybean light-dependent reactions to high temperatures may be of interest as the ability to respond flexibly to perturbations in the environment was evolutionarily programmed into the photosynthesis of plants with the fast and slow component of NPQ (Krause and Weis, 1991). These components allow photoprotection to respond on different timescales (Nilkens et al., 2010), which may be critical for plant fitness as well as crop productivity (Kromdijk et al., 2016). Indeed, enhancing relaxation kinetics of NPQ by increasing expression of violaxanthin de-epoxidase, zeaxanthin epoxidase, and PS2 subunit S which increased biomass accumulation of transgenic tobacco (*Nicotiana tabacum*) (Kromdijk et al., 2016). Thus, a better understanding of the mechanisms that determine temporal dynamics of stress responses may lead to the identification of promising targets for soybean stress tolerance improvement.

Effects of High Temperature Stress on Chloroplast Ultrastructure

Information about the impact of heat stress on chloroplast ultrastructure in soybean is largely lacking. Although Djanaguiraman et al. (2011) indicated that heat stress affected soybean chloroplast ultrastructure, including size, number, reduced grana stacking, they did not quantify the effects. Thus, to better understand the impact of heat stress on chloroplast ultrastructure as well as the relationship between ultrastructure and photosynthetic gas exchange and light reactions, chloroplast ultrastructure was assessed in DT97 and PI-66 plants exposed to the control day-time high air temperature of 28°C and the 45°C heat stress treatment for 1 day or for 7 days. The impact of heat stress was particularly pronounced on day 1 in DT97, whereas PI-66 showed little or no ultrastructure changes after 1 day of treatment (**Figure 4** and **Figure 5** and **Table 2**). In DT97, significant increases in chloroplast area (1.5×), percent grana area (1.5×), percent starch area (7.3×), total number of starch grains (3.8×), total starch area (12.1×), average area per starch grain (4.1×), total number of grana (1.4×), total grana area (1.2×), and average area per granum (1.7×) were measured. In contrast, no differences in any of these parameters, except for a 1.5-fold increase in the average area per granum, were observed in PI-66 in response to 1 day in the 45°C treatment. Given that, after 7 days of treatment, net photosynthetic rate of DT97 was more similar between the 45 and 28°C treatments than that of PI-66, the extensive chloroplast ultrastructural responses observed on day 1 in DT97 did not appear to have been detrimental to acclimation. The lack of differences between 28 and 45°C treatments on 7th day in the measured grana characteristics in DT97 and the reduction in total grana area and average area per granum in PI-66, suggest a greater sensitivity of PI-66 than DT97 to several days of high temperature stress in regard to these characteristics. The increases in all grana phenotypes on the 1st day of 45°C in DT97 was associated with greater F_0, and lower F_M and F_V/F_M values than in the 28°C treatment. Interestingly, while the grana characteristics of PI-66 were unchanged on the 1st day of 45°C F_0, F_M and F_V/F_M values responded in the same manner as in DT97 (**Figures 3**, **5**). In contrast, starch grain number, area, and relative area per chloroplast were reduced in DT97 but not in PI-66 after 7 days of exposure to 45°C day-time elevated temperatures. These

reduced levels of starch in DT97 were associated with net photosynthetic rates that did not differ between 45 and 28°C treatments, whereas net photosynthetic rates in PI-66 at 45°C were lower than at 28°C. These contrasting responses are consistent with differential sensitivity and acclimation ability of the two genotypes.

Zhang et al. (2010), reported swelling of chloroplasts in *Arabidopsis thaliana* leaves in response to 30 min of 40°C exposure, but did not report on differences in starch grain area or the effect of an extended heat stress treatment. However, their representative images had visibly more starch grain area after heat stress. The changes in starch abundance is noteworthy as starch dynamics of chloroplasts are indicative of carbon-use efficiency and can lead to limitations in growth (Ainsworth and Bush, 2011). Increases in soluble sugars can have profound effects on photosynthesis. Feedback mechanisms exist in which expression of photosynthetic genes are down regulated and starch synthesis related gene expression is increased in response to increased sugars (Sheen, 1990). Possible issues caused by heat stress may lead to decreased triose transport out of the chloroplast and/or increased sugar production which leads to metabolic feedback inhibition of photosynthesis. Given that net photosynthetic rate was maintained relative to the control treatment, the reduction of starch area in DT97 observed on the 7th day of 45°C heat stress may be the result of increased sugar transport. Greater carbon export appears to be the likely reason for the reduced starch area in DT97 chloroplasts. The distinct effects of high temperature imposition on grana and starch characteristics of the two genotypes, highlight the need for further physiological and molecular characterization to elucidate the mechanisms involved in the regulation of thylakoid membrane and starch dynamics in heat stressed soybean.

CONCLUSION

Exposure of soybean genotypes to elevated air temperatures for a 7-day period strongly influenced gas exchange, chlorophyll fluorescence, and chloroplast ultrastructure. Although general responses in gas exchange and chlorophyll fluorescence were similar, genotypic differences in the temporal dynamics over the course of the 7-day heat treatment were observed for numerous traits. Chloroplast ultrastructure analyses in two genotypes revealed contrasting phenotypes in chloroplast, grana, and starch characteristics in response to high temperature stress. While F_V/F_M was dramatically reduced in response to high temperature stress in all genotypes on the 3rd day, net photosynthetic rates were increased or not affected. The dramatic effect of 45°C on the light reactions on day 1 of the treatment was associated with increased starch and grana areas. Genotypic differences in chloroplast starch characteristics between DT97 and PI-66 were particularly pronounced on 7th day of the heat treatment while net photosynthetic rates were similar between the two genotypes. The reasons underlying the contrasting responses in starch dynamics between these two genotypes are unclear but are likely due to differences in sugar transport and/or starch synthesis or turnover.

The present study provides much needed baseline information on the effects of high temperature on soybean chloroplast ultrastructure, and identified genotypes differing in the temporal characteristics of light reaction adaptation to a 7-day heat-wave simulation. Additional physiological and genetic studies are required to determine the mechanisms underlying the different responses among genotypes and the implications associated with these responses relative to heat tolerance, and to identify strategies to breed soybean for future climates.

DATA AVAILABILITY STATEMENT

The datasets generated for this study are available on request to the corresponding author.

AUTHOR CONTRIBUTIONS

MH planned, conducted, analyzed and provided initial manuscript draft. FF planned and provided critical review of manuscript.

FUNDING

This work was partially funded by United Soybean Board project 2504.

ACKNOWLEDGMENTS

The authors would like to acknowledge the Electron Microscopy Core Facility at the University of Missouri for their help with creating high quality images for quantitative analysis of chloroplast ultrastructure.

SUPPLEMENTARY MATERIAL

The Supplementary Material for this article can be found online at: https://www.frontiersin.org/articles/10.3389/fpls.2020.00153/full#supplementary-material

REFERENCES

Abdelmageed, A. H. A., and Gruda, N. (2009). Influence of high temperatures on gas exchange rate and growth of eight tomato cultivars under controlled heat stress conditions. *Eur. J. Hortic. Sci.* 74 (4), 152–159.

Ainsworth, E. A., and Bush, D. R. (2011). Carbohydrate export from the leaf: a highly regulated process and target to enhance photosynthesis and productivity. *Plant Physiol.* 155 (1), 64–69. doi: 10.1104/pp.110.167684

Alberts, B., Johnson, A., Lewis, J., Raff, M., Roberts, K., and Walter, P. (2002). *Molecular Biology of the Cell* (New York: Garland Publishing).

Albertsson, P. (2001). A quantitative model of the domain structure of the photosynthetic membrane. *Trends Plant Sci.* 6 (8), 349–358. doi: 10.1016/s1360-1385(01)02021-0

Andersson, J., Wentworth, M., Walters, R., Howard, C., Ruban, A., Horton, P., et al. (2003). Absence of the Lhcb1 and Lhcb2 proteins of the light-harvesting complex of photosystem II–effects on photosynthesis, grana stacking and fitness. *Plant J.* 35 (3), 350–361. doi: 10.1046/j.1365-313X.2003.01811.x

Aro, E. M., Virgin, I., and Andersson, B. (1993). Photoinhibition of Photosystem II. Inactivation, protein damage and turnover. *Biochim. Biophys. Acta* 1143 (2), 113–134. doi: 10.1016/0005-2728(93)90134-2

Bondada, B. R., and Syvertsen, J. P. (2003). Leaf chlorophyll, net gas exchange and chloroplast ultrastructure in citrus leaves of different nitrogen status. *Tree Physiol.* 23 (8), 553–559. doi: 10.1093/treephys/23.8.553

Briantais, J. M., Dacosta, J., Goulas, Y., Ducruet, J. M., and Moya, I. (1996). Heat stress induces in leaves an increase of the minimum level of chlorophyll fluorescence, Fo: a time-resolved analysis. *Photosynth. Res.* 48 (1-2), 189–196. doi: 10.1007/BF00041008

Bukhov, N. G., and Carpentier, R. (2000). Heterogeneity of photosystem II reaction centers as influenced by heat treatment of barley leaves. *Physiol. Plant.* 110 (2), 279–285. doi: 10.1034/j.1399-3054.2000.110219.x

Camejo, D., Rodriguez, P., Morales, M. A., Dell'Amico, J. M., Torrecillas, A., and Alarcon, J. J. (2005). High temperature effects on photosynthetic activity of two tomato cultivars with different heat susceptibility. *J. Plant Physiol.* 162 (3), 281–289. doi: 10.1016/j.jplph.2004.07.014

Carmo-Silva, A. E., Gore, M. A., Andrade-Sanchez, P., French, A. N., Hunsaker, D. J., and Salvucci, M. E. (2012). Decreased CO2 availability and inactivation of Rubisco limit photosynthesis in cotton plants under heat and drought stress in the field. *Environ. Exp. Bot.* 83, 1–11. doi: 10.1016/j.envexpbot.2012.04.001

Chow, W. S., Kim, E. H., Horton, P., and Anderson, J. M. (2005). Granal stacking of thylakoid membranes in higher plant chloroplasts: the physicochemical forces at work and the functional consequences that ensue. *Photochem. Photobiol. Sci.* 4 (12), 1081–1090. doi: 10.1039/b507310n

Congming, L., and Jianhua, Z. (2000). Photosynthetic CO2 assimilation, chlorophyll fluorescence and photoinhibition as affected by nitrogen deficiency in maize plants. *Plant Sci. (Limerick)* 151 (2), 135–143. doi: 10.1016/S0168-9452(99)00207-1

Crafts-Brandner, S. J., and Salvucci, M. E. (2000). Rubisco activase constrains the photosynthetic potential of leaves at high temperature and CO2. *Proc. Natl. Acad. Sci.* 97 (24), 13430–13435. doi: 10.1073/pnas.230451497

Crafts-Brandner, S. J., and Salvucci, M. E. (2002). Sensitivity of photosynthesis in a C4 plant, maize, to heat stress. *Plant Physiol.* 129 (4), 1773–1780. doi: 10.1104/pp.002170

De Ronde, J. A., Cress, W. A., Kruger, G. H., Strasser, R. J., and Van Staden, J. (2004). Photosynthetic response of transgenic soybean plants, containing an Arabidopsis P5CR gene, during heat and drought stress. *J. Plant Physiol.* 161 (11), 1211–1224. doi: 10.1016/j.jplph.2004.01.014

Djanaguiraman, M., Prasad, P. V., Boyle, D., and Schapaugh, W. (2011). High-temperature stress and soybean leaves: leaf anatomy and photosynthesis. *Crop Sci.* 51 (5), 2125–2131. doi: 10.2135/cropsci2010.10.0571

Egorova, E. A., and Bukhov, N. G. (2002). Effect of elevated temperatures on the activity of alternative pathways of photosynthetic electron transport in intact barley and maize leaves. *Russian J. Plant Physiol.* 49 (5), 575–584. doi: 10.1023/A:1020268313852

Epron, D., Dreyer, E., and Breda, N. (1992). Photosynthesis of oak trees [Quercus petraea (Matt.) Liebl.] during drought under field conditions: diurnal course of net CO2 assimilation and photochemical efficiency of photosystem II. *Plant Cell Environ.* 15 (7), 809–820. doi: 10.1111/j.1365-3040.1992.tb02148.x

Fehr, W., Caviness, C., Burmood, D., and Pennington, J. (1971). Stage of development descriptions for soybeans, Glycine Max (L.) Merrill 1. *Crop Sci.* 11 (6), 929–931. doi: 10.2135/cropsci1971.0011183X001100060051x

Fidalgo, F., Santos, A., Santos, I., and Salema, R. (2004). Effects of long-term salt stress on antioxidant defence systems, leaf water relations and chloroplast ultrastructure of potato plants. *Ann. Appl. Biol.* 145 (2), 185–192. doi: 10.1111/j.1744-7348.2004.tb00374.x

Fischer, R. A., Rees, D., Sayre, K. D., Lu, Z. M., Condon, A. G., and Saavedra, A. L. (1998). Wheat yield progress associated with higher stomatal conductance and photosynthetic rate, and cooler canopies. *Crop Sci.* 38, 1467–1475. doi: 10.2135/cropsci1998.0011183X003800060011x

Friso, G., Giacomelli, L., Ytterberg, A. J., Peltier, J. B., Rudella, A., Sun, Q., et al. (2004). In-depth analysis of the thylakoid membrane proteome of Arabidopsis thaliana chloroplasts: new proteins, new functions, and a plastid proteome database. *Plant Cell* 16 (2), 478–499. doi: 10.1105/tpc.017814

Fristedt, R., Willig, A., Granath, P., Crevecoeur, M., Rochaix, J. D., and Vener, A. V. (2009). Phosphorylation of photosystem II controls functional macroscopic folding of photosynthetic membranes in Arabidopsis. *Plant Cell* 21 (12), 3950–3964. doi: 10.1105/tpc.109.069435

Fritschi, F., and Ray, J. (2007). Soybean leaf nitrogen, chlorophyll content, and chlorophyll a/b ratio. *Photosynthetica* 45 (1), 92–98. doi: 10.1007/s11099-007-0014-4

Gamon, J., and Pearcy, R. (1989). Leaf movement, stress avoidance and photosynthesis in Vitis californica. *Oecologia* 79 (4), 475–481. doi: 10.1007/BF00378664

Groom, Q. J., and Baker, N. R. (1992). Analysis of light-induced depressions of photosynthesis in leaves of a wheat crop during the winter. *Plant Physiol.* 100 (3), 1217–1223. doi: 10.1104/pp.100.3.1217

Haile, F. J., and Higley, L. G. (2003). Changes in soybean gas-exchange after moisture stress and spider mite injury. *Environ. Entomol.* 32 (3), 433–440. doi: 10.1603/0046-225X-32.3.433

Hamerlynck, E., and Knapp, A. K. (1996). Photosynthetic and stomatal responses to high temperature and light in two oaks at the western limit of their range. *Tree Physiol.* 16 (6), 557–565. doi: 10.1093/treephys/16.6.557

Harley, P., Weber, J., and Gates, D. M. (1985). Interactive effects of light, leaf temperature, CO 2 and O 2 on photosynthesis in soybean. *Planta* 165 (2), 249–263. doi: 10.1007/BF00395048

Hassan, I. (2006). Effects of water stress and high temperature on gas exchange and chlorophyll fluorescence in Triticum aestivum L. *Photosynthetica* 44 (2), 312–315. doi: 10.1007/s11099-006-0024-7

He, Y., Chen, Y., Yu, C. L., Lu, K. X., Jiang, Q. S., Fu, J. L., et al. (2016). Photosynthesis and yield traits in different soybean lines in response to salt stress. *Photosynthetica* 54 (4), 630–635. doi: 10.1007/s11099-016-0217-7

Hong, S.-S., and Xu, D.-Q. (1999). Light-induced increase in initial chlorophyll fluorescence Fo level and the reversible inactivation of PS II reaction centers in soybean leaves. *Photosynth. Res.* 61 (3), 269–280. doi: 10.1023/A:1006357203466

Huang, Z. A., Jiang, D. A., Yang, Y., Sun, J. W., and Jin, S. H. (2004). Effects of nitrogen deficiency on gas exchange, chlorophyll fluorescence, and antioxidant enzymes in leaves of rice plants. *Photosynthetica* 42 (3), 357–364. doi: 10.1023/B:PHOT.0000046153.08935.4c

Idso, R. J., Reginato, J. W., and Radin, (1982). Leaf diffusion resistance and photosynthesis in cotton as related to a foliage temperature based plant water stress index. *Agric. Meteoro.* 27 (1–2), 27–34. doi: 10.1016/0002-1571(82)90016-4

Jenny, A., Mark, W., Robin, G., Caroline, A., Alexander, V., Peter, H., et al. (2003). Absence of the Lhcb1 and Lhcb2 proteins of the light-harvesting complex of photosystem II–effects on photosynthesis, grana stacking and fitness. *Plant J.* 35 (3), 350–361. doi: 10.1046/j.1365-313X.2003.01811.x

Jumrani, K., Bhatia, V. S., and Pandey, G. P. (2017). Impact of elevated temperatures on specific leaf weight, stomatal density, photosynthesis and chlorophyll fluorescence in soybean. *Photosynth. Res.* 131 (3), 333–350. doi: 10.1007/s11120-016-0326-y

Kalaji, H. M., Oukarroum, A., Alexandrov, V., Kouzmanova, M., Brestic, M., Zivcak, M., et al. (2014). Identification of nutrient deficiency in maize and tomato plants by *in vivo* chlorophyll a fluorescence measurements. *Plant Physiol. Biochem.* 81, 16–25. doi: 10.1016/j.plaphy.2014.03.029

Kao, W.-Y., Tsai, T.-T., and Shih, C.-N. (2003). Photosynthetic gas exchange and chlorophyll a fluorescence of three wild soybean species in response to NaCl treatments. *Photosynthetica* 41 (3), 415–419. doi: 10.1023/B:PHOT.0000015466.22288.23

Kirchhoff, H., Sharpe, R. M., Herbstova, M., Yarbrough, R., and Edwards, G. E. (2013). Differential mobility of pigment-protein complexes in granal and agranal thylakoid membranes of C(3) and C(4) plants. *Plant Physiol.* 161 (1), 497–507. doi: 10.1104/pp.112.207548

Krause, G., and Weis, E. (1991). Chlorophyll fluorescence and photosynthesis: the basics. *Annu. Rev. Plant Biol.* 42 (1), 313–349. doi: 10.1146/annurev.pp.42.060191.001525

Kromdijk, J., Glowacka, K., Leonelli, L., Gabilly, S. T., Iwai, M., Niyogi, K. K., et al. (2016). Improving photosynthesis and crop productivity by accelerating recovery from photoprotection. *Science* 354 (6314), 857–861. doi: 10.1126/science.aai8878

Kurek, I., Chang, T. K., Bertain, S. M., Madrigal, A., Liu, L., Lassner, M. W., et al. (2007). Enhanced thermostability of Arabidopsis rubisco activase improves photosynthesis and growth rates under moderate heat stress. *Plant Cell* 19 (10), 3230–3241. doi: 10.1105/tpc.107.054171

Li, W. X., Chen, T. B., Huang, Z. C., Lei, M., and Liao, X. Y. (2006). Effect of arsenic on chloroplast ultrastructure and calcium distribution in arsenic hyperaccumulator Pteris vittata L. *Chemosphere* 62 (5), 803–809. doi: 10.1016/j.chemosphere.2005.04.055

Liu, X., and Huang, B. (2000). Heat stress injury in relation to membrane lipid peroxidation in creeping bentgrass. *Crop Sci.* 40 (2), 503–510. doi: 10.2135/cropsci2000.402503x

Loll, B., Kern, J., Saenger, W., Zouni, A., and Biesiadka, J. (2007). Lipids in photosystem II: interactions with protein and cofactors. *Biochim. Biophys. Acta* 1767 (6), 509–519. doi: 10.1016/j.bbabio.2006.12.009

Mathur, S., Jajoo, A., Mehta, P., and Bharti, S. (2011). Analysis of elevated temperature-induced inhibition of photosystem II using chlorophyll a fluorescence induction kinetics in wheat leaves (Triticum aestivum). *Plant Biol.* 13 (1), 1–6. doi: 10.1111/j.1438-8677.2009.00319.x

Maxwell, K., and Johnson, G. N. (2000). Chlorophyll fluorescence—a practical guide. *J. Exp. Bot.* 51 (345), 659–668. doi: 10.1093/jexbot/51.345.659

Mehta, P., Jajoo, A., Mathur, S., and Bharti, S. (2010). Chlorophyll a fluorescence study revealing effects of high salt stress on Photosystem II in wheat leaves. *Plant Physiol. Biochem.* 48 (1), 16–20. doi: 10.1016/j.plaphy.2009.10.006

Misra, A. N., Srivastava, A., and Strasser, R. J. (2001). Utilization of fast chlorophyll a fluorescence technique in assessing the salt/ion sensitivity of mung bean and Brassica seedlings. *J. Plant Physiol.* 158 (9), 1173–1181. doi: 10.1078/S0176-1617(04)70144-3

Murata, N., Takahashi, S., Nishiyama, Y., and Allakhverdiev, S. I. (2007). Photoinhibition of photosystem II under environmental stress. *Biochim. Biophys. Acta* 1767 (6), 414–421. doi: 10.1016/j.bbabio.2006.11.019

Nilkens, M., Kress, E., Lambrev, P., Miloslavina, Y., Muller, M., Holzwarth, A. R., et al. (2010). Identification of a slowly inducible zeaxanthin-dependent component of non-photochemical quenching of chlorophyll fluorescence generated under steady-state conditions in Arabidopsis. *Biochim. Biophys. Acta* 1797 (4), 466–475. doi: 10.1016/j.bbabio.2010.01.001

Niyogi, K. K., Grossman, A. R., and Bjorkman, O. (1998). Arabidopsis mutants define a central role for the xanthophyll cycle in the regulation of photosynthetic energy conversion. *Plant Cell* 10 (7), 1121–1134. doi: 10.1105/tpc.10.7.1121

Ogren, E., and Sjostrom, M. (1990). Estimation of the effect of photoinhibition on the carbon gain in leaves of a willow canopy. *Planta* 181 (4), 560–567. doi: 10.1007/BF00193011

Ohashi, Y., Nakayama, N., Saneoka, H., and Fujita, K. (2006). Effects of drought stress on photosynthetic gas exchange, chlorophyll fluorescence and stem diameter of soybean plants. *Biol. Plant.* 50 (1), 138–141. doi: 10.1007/s10535-005-0089-3

Petkova, V., Denev, I. D., Cholakov, D., and Porjazov, I. (2007). Field screening for heat tolerant common bean cultivars (Phaseolus vulgaris L.) by measuring of chlorophyll fluorescence induction parameters. *Sci. Hortic.* 111 (2), 101–106. doi: 10.1016/j.scienta.2006.10.005

Pospíšil, P., Skotnica, J., and Nauš, J. (1998). Low and high temperature dependence of minimum F0 and maximum FM chlorophyll fluorescence *in vivo*. *Biochim. Biophys. Acta (BBA)-Bioenergetics* 1363 (2), 95–99. doi: 10.1016/S0005-2728(97)00095-9

Redillas, M. C., Strasser, R. J., Jeong, J. S., Kim, Y. S., and Kim, J.-K. (2011). The use of JIP test to evaluate drought-tolerance of transgenic rice overexpressing OsNAC10. *Plant Biotechnol. Rep.* 5 (2), 169–175. doi: 10.1007/s11816-011-0170-7

Sakowska, K., Alberti, G., Genesio, L., Peressotti, A., Delle Vedove, G., Gianelle, D., et al. (2018). Leaf and canopy photosynthesis of a chlorophyll deficient soybean mutant. *Plant Cell Environ.* 41 (6), 1427–1437. doi: 10.1111/pce.13180

Salvucci, M. E., and Crafts-Brandner, S. J. (2004). Inhibition of photosynthesis by heat stress: the activation state of Rubisco as a limiting factor in photosynthesis. *Physiol. Plant.* 120 (2), 179–186. doi: 10.1111/j.0031-9317.2004.0173.x

Schneider, C. A., Rasband, W. S., and Eliceiri, K. W. (2012). NIH Image to ImageJ: 25 years of image analysis. *Nat. Methods* 9 (7), 671–675. doi: 10.1038/nmeth.2089

Schreiber, U., and Berry, J. A. (1977). Heat-induced changes of chlorophyll fluorescence in intact leaves correlated with damage of the photosynthetic apparatus. *Planta* 136 (3), 233–238. doi: 10.1007/BF00385990

Semenova, G. A. (2002). The thylakoid membrane in a wide pH range. *J. Plant Physiol.* 159 (6), 613–625. doi: 10.1078/0176-1617-0632

Sharkey, T. D., Badger, M. R., von Caemmerer, S., and Andrews, T. J. (2001). Increased heat sensitivity of photosynthesis in tobacco plants with reduced Rubisco activase. *Photosynth. Res.* 67 (1-2), 147–156. doi: 10.1023/A:1010633823747

Sheen, J. (1990). Metabolic repression of transcription in higher plants. *Plant Cell* 2 (10), 1027–1038. doi: 10.1105/tpc.2.10.1027

Siebers, M. H., Yendrek, C. R., Drag, D., Locke, A. M., Rios Acosta, L., Leakey, A. D., et al. (2015). Heat waves imposed during early pod development in soybean (G lycine max) cause significant yield loss despite a rapid recovery from oxidative stress. *Global Change Biol.* 21 (8), 3114–3125. doi: 10.1111/gcb.12935

Sinsawat, V., Leipner, J., Stamp, P., and Fracheboud, Y. (2004). Effect of heat stress on the photosynthetic apparatus in maize (Zea mays L.) grown at control or high temperature. *Environ. Exp. Bot.* 52 (2), 123–129. doi: 10.1016/j.envexpbot.2004.01.010

Smith, J. R. (2017). Soybean germplasm line DS25-1 with heat tolerance and competitive yield under heat stress. *USDA-ARS*.

Strasser, B., and Strasser, R. (1995). Measuring fast fluorescence transients to address environmental questions: the JIP-test. *Photosynth.: Light to Biosphere* 5, 977–980. doi: 10.1007/978-94-009-0173-5_1142

Takahashi, S., Milward, S. E., Fan, D.-Y., Chow, W. S., and Badger, M. R. (2009). How does cyclic electron flow alleviate photoinhibition in Arabidopsis? *Plant Physiol.* 149 (3), 1560–1567. doi: 10.1104/pp.108.134122

Tyystjarvi, E., Aliyrkko, K., Kettunen, R., and Aro, E. M. (1992). Slow degradation of the D1 protein is related to the susceptibility of low-light-grown pumpkin plants to photoinhibition. *Plant Physiol.* 100 (3), 1310–1317. doi: 10.1104/pp.100.3.1310

Van Heerden, P. D., Strasser, R. J., and Krüger, G. H. (2004). Reduction of dark chilling stress in N2-fixing soybean by nitrate as indicated by chlorophyll a fluorescence kinetics. *Physiol. Plant.* 121 (2), 239–249. doi: 10.1111/j.0031-9317.2004.0312.x

Vani, B., Saradhi, P. P., and Mohanty, P. (2001). Alteration in chloroplast structure and thylakoid membrane composition due to *in vivo* heat treatment of rice seedlings: correlation with the functional changes. *J. Plant Physiol.* 158 (5), 583–592. doi: 10.1078/0176-1617-00260

Vassileva, V., Demirevska, K., Simova-Stoilova, L., Petrova, T., Tsenov, N., and Feller, U. (2012). Long-term field drought affects leaf protein pattern and chloroplast ultrastructure of winter wheat in a cultivar-specific manner. *J. Agron. Crop Sci.* 198 (2), 104–117. doi: 10.1111/j.1439-037X.2011.00492.x

Vu, J., Allen, L.Jr., Boote, K., and Bowes, G. (1997). Effects of elevated CO2 and temperature on photosynthesis and Rubisco in rice and soybean. *Plant Cell Environ.* 20 (1), 68–76. doi: 10.1046/j.1365-3040.1997.d01-10.x

Woo, N. S., Badger, M. R., and Pogson, B. J. (2008). A rapid, non-invasive procedure for quantitative assessment of drought survival using chlorophyll fluorescence. *Plant Methods* 4 (1), 27. doi: 10.1186/1746-4811-4-27

Xu, S., Li, J. L., Zhang, X. Q., Wei, H., and Cui, L. J. (2006). Effects of heat acclimation pretreatment on changes of membrane lipid peroxidation, antioxidant metabolites, and ultrastructure of chloroplasts in two cool-season turfgrass species under heat stress. *Environ. Exp. Bot.* 56 (3), 274–285. doi: 10.1016/j.envexpbot.2005.03.002

Yamamoto, Y., Aminaka, R., Yoshioka, M., Khatoon, M., Komayama, K., Takenaka, D., et al. (2008). Quality control of photosystem II: impact of light and heat stresses. *Photosynth. Res.* 98 (1-3), 589–608. doi: 10.1007/s11120-008-9372-4

Yamane, Y., Kashino, Y., Koike, H., and Satoh, K. (1997). Increases in the fluorescence of Fo level and reversible inhibition of photosystem II reaction center by high-temperature treatments in higher plants. *Photosynth. Res.* 52, 57–64. doi: 10.1023/A:1005884717655

Yao, X. D., Li, C. H., Li, S. Y., Zhu, Q., Zhang, H. J., Wang, H. Y., et al. (2017). Effect of shade on leaf photosynthetic capacity, light-intercepting, electron transfer and energy distribution of soybeans. *Plant Growth Regul.* 83 (3), 409–416. doi: 10.1007/s10725-017-0307-y

Yoshioka, M., Uchida, S., Mori, H., Komayama, K., Ohira, S., Morita, N., et al. (2006). Quality control of photosystem II cleavage of reaction center D1 protein in spinach thylakoids by FtsH protease under moderate heat stress. *J. Biol. Chem.* 281 (31), 21660–21669. doi: 10.1074/jbc.M602896200

Zhang, R., Wise, R. R., Struck, K. R., and Sharkey, T. D. (2010). Moderate heat stress of Arabidopsis thaliana leaves causes chloroplast swelling and plastoglobule formation. *Photosynth. Res.* 105 (2), 123–134. doi: 10.1007/s11120-010-9572-6

Zhao, D. L., Oosterhuis, D. M., and Bednarz, C. W. (2001). Influence of potassium deficiency on photosynthesis, chlorophyll content, and chloroplast ultrastructure of cotton plants. *Photosynthetica* 39 (1), 103–109. doi: 10.1023/A:1012404204910

Zhou, R., Hyldgaard, B., Yu, X. Q., Rosenqvist, E., Ugarte, R. M., Yu, S. X., et al. (2018). Phenotyping of faba beans (Vicia faba L.) under cold and heat stresses using chlorophyll fluorescence. *Euphytica* 214 (4), 68. doi: 10.1007/s10681-018-2154-y

Ziska, L. H., and Bunce, J. A. (1995). Growth and photosynthetic response of three soybean cultivars to simultaneous increases in growth temperature and CO2. *Physiol. Plant.* 94 (4), 575–584. doi: 10.1111/j.1399-3054.1995.tb00970.x

Conflict of Interest: The authors declare that the research was conducted in the absence of any commercial or financial relationships that could be construed as a potential conflict of interest.

frontiers in Plant Science

REVIEW
published: 24 March 2020
doi: 10.3389/fpls.2020.00268

Photosynthetic Acclimation to Fluctuating Irradiance in Plants

Alejandro Morales[1,2,3†] *and Elias Kaiser*[4*†]

[1] Centre for Crop Systems Analysis, Plant Science Group, Wageningen University and Research, Wageningen, Netherlands, [2] Plant Ecophysiology, Institute of Environmental Biology, Utrecht University, Utrecht, Netherlands, [3] Molecular Plant Physiology, Institute of Environmental Biology, Utrecht University, Utrecht, Netherlands, [4] Horticulture and Product Physiology, Plant Science Group, Wageningen University and Research, Wageningen, Netherlands

Unlike the short-term responses of photosynthesis to fluctuating irradiance, the long-term response (i.e., acclimation) at the chloroplast, leaf, and plant level has received less attention so far. The ability of plants to acclimate to irradiance fluctuations and the speed at which this acclimation occurs are potential limitations to plant growth under field conditions, and therefore this process deserves closer study. In the first section of this review, we look at the sources of natural irradiance fluctuations, their effects on short-term photosynthesis, and the interaction of these effects with circadian rhythms. This is followed by an overview of the mechanisms that are involved in acclimation to fluctuating (or changes of) irradiance. We highlight the chain of events leading to acclimation: retrograde signaling, systemic acquired acclimation (SAA), gene transcription, and changes in protein abundance. We also review how fluctuating irradiance is applied in experiments and highlight the fact that they are significantly slower than natural fluctuations in the field, although the technology to achieve realistic fluctuations exists. Finally, we review published data on the effects of growing plants under fluctuating irradiance on different plant traits, across studies, spatial scales, and species. We show that, when plants are grown under fluctuating irradiance, the chlorophyll a/b ratio and plant biomass decrease, specific leaf area increases, and photosynthetic capacity as well as root/shoot ratio are, on average, unaffected.

Keywords: fluctuating light, acclimation, dynamic photosynthesis, gene transcription, signaling

OPEN ACCESS

Edited by:
Iker Aranjuelo,
Institute of Agrobiotechnology,
The Superior Council of Scientific Investigations, Spain

Reviewed by:
Lea Hallik,
University of Tartu, Estonia
Thomas Pfannschmidt,
Leibniz University Hannover, Germany

***Correspondence:**
Elias Kaiser
elias.kaiser@wur.nl

†These authors have contributed equally to this work

Specialty section:
This article was submitted to Plant Abiotic Stress, a section of the journal Frontiers in Plant Science

Received: *29 October 2019*
Accepted: *20 February 2020*
Published: *24 March 2020*

Citation:
Morales A and Kaiser E (2020) Photosynthetic Acclimation to Fluctuating Irradiance in Plants. Front. Plant Sci. 11:268. doi: 10.3389/fpls.2020.00268

INTRODUCTION

Fluctuations in irradiance are ubiquitous in nature, and they impact photosynthesis, water use, and plant growth. Ever since the realization that short-term (seconds-minutes) responses of photosynthesis to these fluctuations were under genetic control (Cruz et al., 2016) and that the speed of these responses could be improved by exploiting natural genetic variation (Qu et al., 2016; Soleh et al., 2017; Salter et al., 2019) or gene editing techniques to increase growth in the field (Kromdijk et al., 2016), research interest in this topic has been immense, as exemplified by the reviews published on it in recent years (Lawson and Blatt, 2014; Kaiser et al., 2015, 2018b, 2019; Armbruster et al., 2017; Slattery et al., 2018; Burgess et al., 2019; Simkin et al., 2019; Tanaka et al., 2019). Given this interest, it is surprising that the long-term response to irradiance fluctuations, i.e., photosynthetic acclimation (in the scale of days), has received relatively limited attention. For example, to our knowledge this is the first review to emphasize the long-term acclimation of plants to fluctuating irradiance. Importantly, enhancing the capacity to optimally acclimate to irradiance

fluctuations and the speed at which acclimation happens could be another approach to improving plant growth in the field.

The most extensive work on acclimation to fluctuating irradiance was recently performed by Lawson and co-workers, who found that *Arabidopsis thaliana* plants acclimated to fluctuating irradiance showed reductions in biomass, leaf thickness, photosynthetic capacity, and concentrations of thylakoid proteins (Vialet-Chabrand et al., 2017) as well as changes in stomatal kinetics (Matthews et al., 2018). While these results highlight the importance of photosynthetic acclimation to irradiance fluctuations for photosynthesis and the plant, these responses may vary across species, frequency of fluctuation, and other environmental factors as yet unidentified, for which a broader analysis is needed.

In this review, we summarize the state-of-the-art on (i) the causes and characteristics of natural irradiance fluctuations which should be used to design better fluctuating irradiance protocols in the lab, (ii) the mechanisms of acclimation from which genetic improvements may be attempted, and (iii) an overview of studies published so far on long-term effects of fluctuating irradiance on plant growth: we review the methodology used in these studies (with emphasis on how fluctuations in irradiance were achieved) and provide an overview of effects of fluctuating irradiance on different plant traits, across studies, spatial scales, and species.

NATURAL IRRADIANCE FLUCTUATIONS AND CIRCADIAN RHYTHMS AFFECT DYNAMIC PHOTOSYNTHESIS

Changes in Natural Irradiance

Irradiance projected onto the Earth's surface varies during the day and season (**Figure 1**) mainly due to changes in the solar incident angle and changes in atmospheric transmissivity due to clouds and aerosols (Wald, 2018). Seasonal variability in irradiance increases with latitude due to larger variations in daylength and average solar incident angle, but synoptic weather patterns also introduce significant variation in atmospheric transmissivity (Parding et al., 2016). Generally, the variability in irradiance decreases with the timescale of integration (Perez et al., 2016).

Accurate empirical and mechanistic models for diurnal and seasonal solar radiation under clear skies exist (Ruiz-Arias and Gueymard, 2018), but predicting the effect of clouds on irradiance fluctuations remains challenging. For a given location, these effects can follow statistical trends, allowing the use of predictive models at the seasonal (Kafka and Miller, 2019) and daily timescales (Wang et al., 2016). Additionally, recent modeling efforts allow for simulating dynamic diurnal cloud formation and effects of these clouds on the spatial and temporal distribution of surface irradiance (Sikma et al., 2018).

Much of the recent research on variability in irradiance is driven by the needs of the solar energy sector (Victoria and Andresen, 2019), and plant science could benefit from that knowledge. For example, in a partially cloudy sky, the movement of clouds can cause strong fluctuations superimposed on the diurnal temporal pattern (cloudflecks; **Figure 1**). Understanding the distribution of cloudfleck duration and irradiance reduction is important, as it affects the response of photosynthesis, even if the total irradiance remains the same (Kaiser et al., 2016; Morales et al., 2018a). However, to our knowledge, very few studies have quantified the characteristics of cloudflecks from the perspective of photosynthesis (Knapp and Smith, 1988; Kaiser et al., 2018b).

The fluctuations in irradiance will also depend on the spatial scale under consideration. Whereas the models and studies cited above focus on understanding irradiance on the surface of the Earth based on data from irradiance sensors, photosynthesis occurs in chloroplasts within the leaves. Gaps in the canopy that expose leaves to the sun and which depend on plant architecture and/or movements of plants by wind introduce additional fluctuations in the irradiance incident on that leaf (Kaiser et al., 2018b), known as sunflecks (**Figure 1**). Partial exposure to the sun may also result in fluctuations due to the penumbra effect (Smith et al., 1989). Additionally, simulations of irradiance distribution within the leaf using a ray-tracing approach suggest that fluctuations may be enhanced at the chloroplast level, due to the heterogeneity of the light environment within leaves (Xiao et al., 2016), but an experimental confirmation of such an enhancement is currently lacking.

The duration and amplitude of sunflecks depends on wind speed (Tang et al., 1988; Roden, 2003), canopy structure (Peressotti et al., 2001; Kaiser et al., 2018b), plant biomechanical properties (Burgess et al., 2016, 2019), and position within the canopy (Pearcy et al., 1990). These fluctuations may be simulated with detailed 3D reconstructions of canopies coupled with physically based ray tracing algorithms, but challenges remain in the realistic simulation and measurement of plant movements by wind (Burgess et al., 2016; Retkute et al., 2018; Gibbs et al., 2019). The statistical properties of sunflecks were reviewed by Kaiser et al. (2018b) showing that sunflecks are generally short (<2 s).

Depending on the source responsible for the fluctuation in irradiance, there will also be a fluctuation in the spectral composition of the irradiance. Small changes in the spectrum will occur in cloudflecks due to differences in spectra of clouds, sun, and sky, but larger changes are associated with sunflecks due to the optical properties of leaves (Endler, 1993). A leaf under green shade is exposed to a higher relative proportion of green and far red (>700 nm) irradiance compared to direct exposure to the sky or direct solar irradiance. Thus, the transition from low to high irradiance during a sunfleck will also result in a rapid change in the red:far red ratio (R/FR) and in the proportion of green irradiance.

Short-Term Responses of Photosynthesis to Irradiance Changes

The dynamic response of leaf photosynthesis to sunflecks and cloudflecks (the "short-term response" of photosynthesis) is determined by the dynamic regulation of enzyme and electron transport activities, metabolite buffering, CO_2 diffusion, light harvesting capacity, non-photochemical quenching, and chloroplast movements (Kaiser et al., 2015, 2018b, 2019). While these responses are well characterized at the leaf level for C3 species (Morales et al., 2018a,b), less is known about the responses

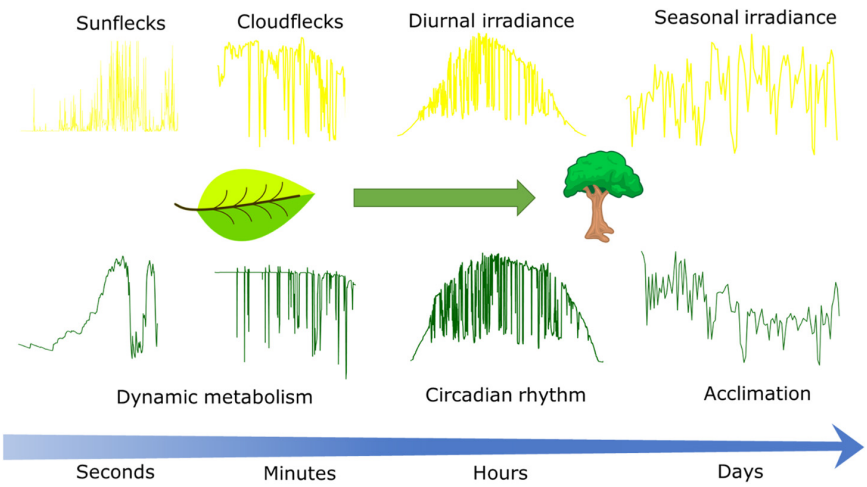

FIGURE 1 | Conceptual scheme describing the time scales at which irradiance fluctuates in the field **(Upper)** and responses of CO_2 assimilation to these fluctuations **(Lower)**. Leaf CO_2 assimilation in response to sunflecks and cloudflecks as driven by dynamic metabolism was simulated with the dynamic photosynthesis model by Morales et al. (2018a). Canopy CO_2 assimilation in response to diurnal and seasonal weather was simulated with the sun-shade canopy photosynthesis model by De Pury and Farquhar (1997) and happens at the timescales at which circadian rhythms (hours) and the effects of acclimation (days) are relevant. Time series of irradiance from weather station in Wageningen, Netherlands, except for the sunflecks time series that was measured by the authors with a portable light sensor placed beneath a durum wheat canopy during a clear summer day in Wageningen.

in C4 and CAM plants (Kaiser et al., 2018b). The short-term response of photosynthesis to fluctuating irradiance is known to be modulated by air temperature, humidity, soil salinity, CO_2 concentration, and far red irradiance (Kono et al., 2019), but significant knowledge gaps remain (Kaiser et al., 2015; Zhang et al., 2018).

Circadian Rhythms

Circadian rhythms in photosynthesis (Hennessey et al., 1993; Dodd et al., 2004; Resco de Dios et al., 2016) may contribute 15–25% of the diurnal variation across species and environments (Resco de Dios and Gessler, 2018). Also, in the evening, stomata opened faster and closed more slowly in response to increases and decreases in irradiance, respectively, regardless of the light regime (constant, sinusoidal, or fluctuating) that the plants were grown under (Matthews et al., 2018). Circadian rhythms have also been observed at the levels of photosynthetic metabolites (Fredeen et al., 1991) and sugars (Graf et al., 2010), and circadian rhythms in photosynthetic products may be partially responsible for driving circadian rhythms in gene expression (Dodd et al., 2015; Haydon and Webb, 2016).

ACCLIMATION UNDER FLUCTUATING IRRADIANCE: SIGNALING, GENE EXPRESSION, PROTEIN ABUNDANCE, AND KINETICS

In this review, we follow Smith and Dukes (2013) who define acclimation as "a physiological, structural, or biochemical adjustment by an individual plant in response to an environmental stimulus that is manifested as alterations in the short-term response function of a physiological process". Therefore, we consider as part of acclimation of photosynthesis to fluctuating irradiance any reversible physiological process or irreversible developmental process that affects the short-term response of photosynthesis to fluctuating irradiance. This definition is in agreement with recent literature on acclimation to irradiance (Athanasiou et al., 2010; Dietz, 2015; Vialet-Chabrand et al., 2017; Yin et al., 2019), though we acknowledge that some studies on acclimation may only focus on reversible physiological processes (Walters, 2005; Caliandro et al., 2013; Miller et al., 2017; Albanese et al., 2018).

Types of Acclimation

The short-term response of leaf photosynthesis varies over time, both diurnally and seasonally (**Figure 1**). Diurnal changes are driven by changes in environmental factors and circadian rhythms (Resco de Dios and Gessler, 2018). There are two types of acclimatory processes in leaves: (i) developmental acclimation during leaf development, which determines anatomical and biochemical traits and (ii) dynamic (physiological) acclimation after the leaf is fully expanded, whereby leaf N in pigments and proteins and biochemical composition of the chloroplasts (i.e., the relative amounts of pigments and proteins involved in photosynthesis) may change further (Athanasiou et al., 2010). In *Chenopodium album*, developmental acclimation of a growing leaf responded to the irradiance incident on mature, fully expanded leaves (Yano and Terashima, 2001). The same phenomenon was observed in *Glycine max* (Wu et al., 2018), *Phaseolus vulgaris* (Murakami et al., 2014), *Helianthus annuus* (Yamazaki and Shinomiya, 2013), *Sorghum bicolor* (Jiang et al., 2011), and Arabidopsis (Munekage et al., 2015). When mature leaves where shaded and growing leaves exposed to high irradiance, the leaf traits (i.e., leaf thickness, stomatal density, total N) reflected the irradiance level on

mature leaves, whereas biochemical composition and chloroplast ultrastructure responded to irradiance absorbed by the growing leaf (Yano and Terashima, 2001; Jiang et al., 2011; Yamazaki and Shinomiya, 2013). This suggests different mechanisms, whereby developmental acclimation may be regulated by long distance signals (Munekage et al., 2015), while dynamic acclimation and changes in chloroplast composition are controlled locally, most likely by retrograde signaling from the chloroplast.

Chloroplast Retrograde Signaling and Gene Expression

Periods of high irradiance enable higher rates of electron and proton transport and CO_2 fixation, but also cause photooxidative stress. Multiple signaling components arising in the chloroplast, such as the plastoquinone redox state, photosynthetic metabolites, reactive oxygen species (ROS), sugars, and hormones, act on multiple time scales in pathways that trigger changes in chloroplast (Mullet, 1993; Pfannschmidt et al., 1999) and in nuclear gene expression, the latter through chloroplast to nucleus (i.e., retrograde) signaling. These changes in expression lead to subsequent changes in protein abundance that are associated with dynamic acclimation to fluctuating irradiance (Dietz, 2015; Chan et al., 2016). In the first seconds after an increase in irradiance, faster linear electron transport increases the concentrations of plastoquinol and reduced thioredoxin, Calvin Bassham Benson (CBB) cycle metabolites (Vogel et al., 2014) and glutathione (Choudhury et al., 2018b), which may participate in retrograde signaling. During these first seconds, singlet oxygen ($^1O_2$) is produced in the photosystem II reaction center and, although it is unlikely to diffuse out of the cytosol, it can reduce β-carotene to β-cyclocitral, which may trigger changes in nuclear gene expression (Matsubara et al., 2016). Within minutes, hydrogen peroxide (H_2O_2) levels increase due to the activity of superoxide dismutase (Mubarakshina et al., 2010; Choudhury et al., 2018a); H_2O_2 can then diffuse into the cytosol and interact with several nuclear gene expression mediators (Pfalz et al., 2012). Also, in the minute to hour domain, levels of the phytohormones abscisic acid (ABA; Galvez-Valdivieso et al., 2009), jasmonic acid, and its precursor oxophytodienoic acid, as well as that of methylerythritol cyclodiphosphate, rise (Alsharafa et al., 2014). Sugars, salicylic acid, auxin, and gibberellic acid are to respond last, with their concentrations rising hours after an irradiance was increased. For more comprehensive reviews, the reader is referred to Dietz (2015) and Chan et al. (2016).

Systemic Acquired Acclimation

Upon abiotic stress (including high irradiance), signals not only flow from chloroplasts to the nucleus inside the same cell, but also from exposed (target) leaves to non-exposed (systemic) plant organs, in a process termed SAA (Mittler and Blumwald, 2015). Signals triggering SAA include ROS waves (Gechev et al., 2006), calcium waves, hydraulic waves, electric signals, and ABA (Mittler and Blumwald, 2015), and the calcium, ROS, and electric wave are likely linked to propagate and reinforce one another (Gilroy et al., 2016). A large range of metabolites increased in systemic tissues within 1–12 min of high irradiance (1500 μmol m^{-2} s^{-1}) exposure of a target leaf in Arabidopsis (Choudhury et al., 2018a), triggering changes in several thousand gene transcripts in the systemic leaf within minutes (Zandalinas et al., 2019). Systemic signals such as H_2O_2, either directly applied or triggered through high light stress, have been shown to make target leaves more resistant to subsequent stress (Karpinski et al., 1999), including pathogen attacks (Karpinski et al., 2013). Clearly, both local and global signaling and gene expression respond rapidly and massively to high irradiance stress, to prepare the plant for future stresses.

Light Signaling Under Fluctuating Irradiance: A Role for Photoreceptors?

Photoreceptors such as phytochromes could be another signaling system for sunflecks. For example, phytochrome B is known to sense neighboring plants through the red:far red ratio, and to trigger subsequent shade avoidance responses which strongly impact on plant morphology (Ballaré and Pierik, 2017). Exposure to FR typically increases whole-plant irradiance capture (increased stem and leaf elongation), tends to decrease leaf photosynthetic capacity (e.g., Ji et al., 2019), and may affect the distribution of canopy-wide irradiance fluctuations.

Rapid transitions between shade and full sunlight in the field do not only change the irradiance a plant is exposed to, but also R/FR, thereby impinging on the phytochrome photostationary state. Indeed, 2 h high-irradiance periods in the field, during which irradiance increased 10- to 30-fold and R/FR increased 10-fold, reduced the shade avoidance reactions (hypocotyl elongation) in Arabidopsis WT, but not in *phyAphyB* double mutants (Sellaro et al., 2011). A subsequent study (Sellaro et al., 2019) modeled the kinetics of phytochrome B conversion between its active and inactive forms, and predicted responses in hypocotyl growth to R/FR experiments, suggesting that the concentrations of active and inactive forms of phytochrome B are affected by fluctuations in irradiance. Interestingly, their experimental data (Figure 3A in Sellaro et al., 2019) suggested that nuclear phytochrome B abundance increases with irradiance. Additionally, Franklin et al. (2007) showed synergistic regulation of hypocotyl elongation in response to different red irradiances by phytochromes A and B, suggesting that these photoreceptors do not only respond to changes in light quality, but also quantity. These results hint that phytochromes do not only act as sensors of light spectrum and temperature (Jung et al., 2016; Legris et al., 2016), but that they may additionally be responsive to changes in irradiance alone.

In addition to shade avoidance responses, high R/FR will result in an imbalance between the two photosystems responsible for light capture in photosynthesis due to their different spectra of absorbance. In the short term, this imbalance can be compensated for by state transitions that will transfer pigments between photosystems but in the long term it will result in acclimation of the photosynthetic apparatus through changes in the stoichiometry of protein complexes and pigments (Walters and Horton, 1995; Dietzel et al., 2008). However, this experimental evidence was acquired under constant irradiance

conditions during daytime and, to our knowledge, the effect of R/FR on photosynthetic acclimation under fluctuating irradiance has not been studied yet.

Gene Expression

Nuclear gene expression reacts to irradiance in a highly dynamic way: hundreds of transcripts change within seconds-minutes after increases (Suzuki et al., 2015) and decreases (Crisp et al., 2017) in irradiance, suggesting that under a naturally fluctuating irradiance, gene expression will also be strongly affected. Indeed, a recent ground-breaking study (Schneider et al., 2019) has demonstrated the impact of fluctuating irradiance on gene expression in Arabidopsis. Short and strong light pulses, applied repeatedly for 3 d, caused a differential expression (DE) of ∼4000 genes, 75% of which were upregulated. Chloroplast components were mostly found among upregulated genes whereas genes encoding for ribosomes, the Golgi apparatus, and cell wall components were more strongly downregulated. Half of the genes that were upregulated in young leaves were also upregulated in leaves inoculated with *Pseudomonas syringae*, suggesting that exposure to fluctuating irradiance may prime plants for biotic stress. Large effects of time of day and leaf developmental stage were observed: for example, many genes encoding for light harvesting complex proteins were downregulated in young leaves in the evening whereas a large number of genes involved in photosynthesis, photoprotection, and photorespiration were specifically upregulated in old leaves, but only in the evening. Gene expression seems to be coordinated by circadian rhythms, as explained above.

Of all 4000 DE genes, only 46 were shared between all samples, i.e. in young and mature leaves and at both times of sampling (morning and evening). These central genes included genes for components of light harvesting (LHCB7), CBB enzymes (sedoheptulose-1,7-bisphosphatase, fructose-1,6-bisphosphate, and CP12), the photorespiratory pathway and ROS metabolism (glycolate oxidase, catalase), CO_2 interconversion (beta carbonic anhydrase), sucrose transport (sucrose-phosphate synthase C), photooxidative stress responses (activity of BC1 complex kinases, fatty acid desaturases, vitamin 6 biosynthesis, and glutathione peroxidase), and photoreceptor interacting factors involved in photomorphogenesis (blue light inhibitor of cryptochromes 1, HY5-homolog, B-box domain 17 protein).

The molecular response to fluctuating irradiance goes far beyond that of photooxidative stress: the data by Schneider et al. (2019) suggested that processes regulating plant growth are affected on many levels, and that the expression of the respective genes is further under strong circadian and developmental control. However, altered gene expression does not necessarily equate altered protein abundance. Also, changes in protein contents, enabling effective acclimation, may take several more days to take effect (Athanasiou et al., 2010).

Protein Abundance and Canopy-Wide N Distribution

Information on changes in protein abundance due to acclimation to fluctuating irradiance is scarce. For Arabidopsis exposed to lightflecks for 7 d, Caliandro et al. (2013) found that chlorophylls decreased, carotenoids remained unchanged, and the PsbS protein (involved in non-photochemical quenching) increased. However, since Caliandro et al. (2013) only looked at these proteins, it is not clear whether other proteins may be affected by irradiance fluctuations, too. Some ideas may be derived from proteomics studies of high light acclimation (Miller et al., 2017) 100–400 μmol m^{-2} s^{-1} for 7 d, Arabidopsis) and growth of *Pisum sativum* at 30, 150, and 750 μmol m^{-2} s^{-1} (Albanese et al., 2018). In Miller et al. (2017), dynamic high irradiance acclimation entailed a strong increase in most proteins (1284 out of 1993 proteins increased, 14 decreased). In the chloroplast electron transport chain, high irradiance caused a reorganization (but not an increase) in both photosystems, as well as increases in the abundance of cytochrome b_6f complex proteins, plastocyanin, the ferredoxin $NADP^+$ reductase, and several ATP synthase subunits (Miller et al., 2017; Albanese et al., 2018). Further, there were increases in PsbS and the violaxanthin de-epoxidase (Miller et al., 2017). Downstream of the electron transport chain, CBB enzymes were increased in abundance (on average by 50%), as were nearly all enzymes belonging to starch and sucrose metabolism (Miller et al., 2017).

After a leaf is fully expanded, further dynamic acclimation may occur, but this is constrained by leaf anatomy (Oguchi et al., 2005) and N distribution in the canopy (Kull, 2002). Redistribution of N within canopies results in vertical profiles of total leaf N and photosynthetic capacity that theoretically should approximate average irradiance profiles (Hikosaka et al., 2016), as this would maximize canopy photosynthesis for a given set of environmental conditions and total canopy N content (Field, 1983; Farquhar, 1989). However, canopies often display shallower profiles, indicating supraoptimal amounts of N and photosynthetic capacity in the lower leaves of a canopy (Anten, 2016; Hikosaka et al., 2016). This behavior can be explained in evolutionary terms, either because the species being analyzed evolved in a different environment (e.g., crops in intensive agriculture) or because the fitness functions driving natural selection are more complex than the instantaneous rate of canopy photosynthesis (Anten, 2016). Nevertheless, considering irradiance fluctuations provides novel insights into the analysis of acclimation at the canopy level with the use of optimization algorithms.

Retkute et al. (2015) suggested that the leaf optimal photosynthetic capacity under fluctuating irradiance depends on the frequency and amplitude of fluctuations for the same average irradiance, resulting in sub-optimal photosynthetic acclimation in wheat canopies (Townsend et al., 2018). Mott and Woodrow (2000) explored the optimal partitioning of N between Rubisco and Rubisco activase, suggesting that the optimal partitioning between the two is highly dependent on the duration of the fluctuations (shorter durations meaning a higher ratio of Rubisco activase to Rubisco).

A general issue with these model-based analyses is that they tend to oversimplify the dynamic responses of photosynthesis by using a single rate constant, thereby assuming a single limiting mechanism. However, the different mechanisms limiting dynamic responses of photosynthesis are characterized by

different rate constants and their relative importance depends on the frequency of fluctuations (Morales et al., 2018a). Although detailed dynamic models of C3 photosynthesis exist (Zhu et al., 2013; Morales et al., 2018a,b), no comprehensive optimization analysis of photosynthesis under fluctuating irradiance has been published thus far.

Genetic Diversity of Acclimation

There is genetic diversity in dynamic acclimation to a change in irradiance (Athanasiou et al., 2010; Rooijen et al., 2015), but this remains unexplored with regards to fluctuating irradiance. The ability to undergo dynamic acclimation in Arabidopsis has been linked to the glucose-6-phosphate/phosphate translocator across the chloroplast envelope (Athanasiou et al., 2010; Dyson et al., 2015; Miller et al., 2017) and loss-of-function mutants in this gene had significantly lower fitness when grown under fluctuating irradiance (Athanasiou et al., 2010). The increase in activity of this transporter in response to an increase in irradiance could result in the import of glucose-6-phosphate into the chloroplast, which would stabilize photosynthetic metabolism during acclimation (Weise et al., 2019) but it is still unclear why its expression is required for dynamic acclimation to occur.

Dynamic Acclimation May Never Reach a Steady State

Dynamic acclimation in response to a change in irradiance can take days to take place (Athanasiou et al., 2010; Rooijen et al., 2015). Since fluctuations in irradiance are faster, even at the seasonal level, it is possible that plants never reach full acclimation and remain in an intermediate, dynamic equilibrium state. This equilibrium state would depend on the speed of dynamic acclimation and the degree of linearity in the response of plant traits to changes in irradiance. These dynamics have been captured in simulation models either (i) by implementing a goal-seeking behavior that calculates steady-state acclimation from optimization theory (Yin et al., 2019) or (ii) by simulating protein turnover dynamically (Thornley, 1998; Kull and Kruijt, 1999; Barillot et al., 2016; Pao et al., 2019a). Experimental evidence exists that coordination across leaves may be achieved through cytokinins carried by the transpiration stream (Pons et al., 2001), as transpiration will vary according to the irradiance profile. This mechanism has been included in a recent mechanistic model of wheat incorporating plant carbon and N balances, but has not yet been validated experimentally (Barillot et al., 2016).

EXPERIMENTATION ON ACCLIMATION TO FLUCTUATING IRRADIANCE: METHODOLOGY AND SUMMARIZED RESULTS

Methodology

In several groundbreaking pioneer studies, relatively simple experiments were used to test the effects of various molecular players on plant growth and fitness under fluctuating irradiance: Mutants lacking components of energy quenching (*npq1*, *npq4*) and state transitions (*stn7*) showed reductions in fitness (i.e., number of seeds produced) and/or biomass relative to the wild-type, when grown under fluctuating light (Kühlheim et al., 2002; Bellafiore et al., 2005; Kühlheim and Jansson, 2005; Frenkel et al., 2007; Wagner et al., 2008). Fluctuating light was supplied naturally, in the field (Kühlheim et al., 2002; Kühlheim and Jansson, 2005; Frenkel et al., 2007) and/or in controlled climate chamber experiments (Kühlheim et al., 2002; Bellafiore et al., 2005; Wagner et al., 2008). In none of these cases was a control treatment with constant light used in which the average intensity and spectrum were identical to that of the fluctuating light treatment; given that these experiments were aimed at characterizing the (relatively strong) effects of specific and well-characterized mutations on FL acclimation, this approach can be justified. However, if an experiment is to accurately quantify the (sometimes small) effects of irradiance fluctuations on wild-type plants, it requires a control where irradiance is constant throughout the photoperiod, and whose average intensity and spectrum are the same as that of the treatment(s) containing irradiance fluctuations. Also, the experimenter needs to be in full control of intensity, timing, and frequency of the irradiance fluctuations. From these requirements it follows that such experiments must be done under controlled growth conditions and in the absence of natural background irradiance (i.e., not in the field or greenhouse). Several such experiments have been performed (Watling et al., 1997; Leakey et al., 2002; Kubásek et al., 2013; Cruz et al., 2016; Annunziata et al., 2017, 2018; Vialet-Chabrand et al., 2017; Kaiser et al., 2018a; Matthews et al., 2018) and some of their results are analyzed below.

Most fluctuating irradiance regimes have been achieved by modulating intensity of an artificial light source in plant growth chambers or cabinets (Watling et al., 1997; Kubásek et al., 2013; Cruz et al., 2016; Annunziata et al., 2017, 2018; Vialet-Chabrand et al., 2017; Matthews et al., 2018). However, other methods have been employed, including moving light sources over the plants (Zheng et al., 2006; Blom and Zheng, 2009; Kaiser et al., 2018a) and rotating shading discs that transiently block the light sources (Leakey et al., 2002). Shading discs are perhaps logistically more complex to implement, but they can be used to alter the spectrum of the artificial light at the same time as the irradiance (although, to our knowledge, they have not been used with that purpose). The use of moving light sources differs from the rest, as it introduces changes in the angle of incidence of the irradiance in addition to fluctuations in the irradiance level.

The fluctuations in irradiance employed in these experiments can be classified into two categories: (i) experiments that focused on diurnal variation of irradiance and (ii) experiments that focused on rapid, repeated fluctuations (denoted as lightflecks, to distinguish between the natural fluctuations such as sunflecks and cloudflecks). The diurnal variation of irradiance has been approximated with a sinusoidal pattern (half the period of a sine wave) where the maximum occurs in the middle of the photoperiod (Cruz et al., 2016; Annunziata et al., 2017, 2018; Matthews et al., 2018). Rapid fluctuations were most often implemented by adding periods of high irradiance

on top of a constant, low irradiance, background (Watling et al., 1997; Leakey et al., 2002) or on top of a sinuosidal pattern (Cruz et al., 2016; Matthews et al., 2018). Exceptions include experiments based on moving light sources (Kaiser et al., 2018a) and experiments that mimic time series of irradiance measured outdoors (Vialet-Chabrand et al., 2017; Matthews et al., 2018).

For studies that focused on rapid fluctuations, the shortest duration for a lightfleck was 20 s (Kaiser et al., 2018a) while most studies used lightflecks of ≥180 s. As discussed above, a typical duration for a sunfleck is <2 s (Kaiser et al., 2018b), meaning that these experiments have not used the correct timescale if the objective was to study the response of plants to the most frequently occurring sunflecks. Also, lightflecks in these experiments resemble cloudflecks rather than sunflecks, in the sense that the fluctuations are applied to the light source itself, rather than as a result of change in incident angle, gaps in the canopy or wind-induced plant movements.

Summary of Observed Responses to Fluctuating Irradiance

To explore whether plant traits at the various integration levels respond in a similar manner across species, we compiled published data on some of the most frequently measured traits, i.e. the chlorophyll a/b ratio (chloroplast level), specific leaf area (SLA, $cm^2\ g^{-1}$), light saturated net photosynthesis rate (A_{max}; leaf level), root/shoot ratio, and plant biomass. For this analysis, we focused on studies with (near-) identical average irradiance and spectrum between treatments, such that the effect may be caused by irradiance pattern alone, i.e., constant (C) vs. fluctuating irradiance (F). Using this criterium allowed us to include 43 data sets from six studies (**Supplementary Table S1**; Watling et al., 1997; Leakey et al., 2002; Grieco et al., 2012; Kubásek et al., 2013; Vialet-Chabrand et al., 2017; Kaiser et al., 2018a). Unfortunately, many studies were excluded from this analysis as they either (i) did not contain a constant irradiance treatment, (ii) did not ensure that average irradiance between treatments was identical, or (iii) measured traits that were not reported in a sufficient number of other studies to allow for a cross-study comparison. Data were analyzed correcting for variability of individual data sets and number of biological replicates, and relative effects of fluctuating light were then expressed as $(F-C)/C$, where F and C denote the average trait value under fluctuating and constant irradiance, respectively.

Chlorophyll a/b ratio was significantly lower, on average by 7%, in leaves grown under lightflecks (**Figure 2**; n = 4). These results suggest a relative increase of light harvesting (associated with Chl b) over reaction center complexes in photosystem II (associated with Chl a) in leaves under fluctuating irradiance, which is typically observed in shade-acclimated leaves (Schöttler and Tóth, 2014; Albanese et al., 2018). However, our numbers are based on only four studies, three of which were conducted on Arabidopsis. The reduction in Chl a/b ratio may be species specific. Indeed, in the study using *Shorea leprosula* instead of Arabidopsis, Chl a/b was unaffected (Leakey et al., 2002).

Specific leaf area was 12% higher in lightfleck acclimated leaves (**Figure 2**, n = 8), implying that the formation of leaves with a reduced biomass per area under fluctuating irradiance was a generic response, which again is reminiscent of shade acclimation (Evans and Poorter, 2001).

Photosynthetic capacity, here expressed as light-saturated CO_2 assimilation (A_{max}), was not generally affected by fluctuating irradiance (**Figure 2**, n = 10). These lightfleck effects may be species-specific: when grown under identical treatments, A_{max} in petunia (*Petunia* × *hybrida*) and tomato (*Solanum lycopersicum*) increased significantly under fluctuating irradiance, while in chrysanthemum (*Chrysanthemum morifolium*) it did not (Blom and Zheng, 2009). Given the large differences between species in high irradiance acclimation capacity (Murchie and Horton, 1997), this result may be unsurprising. Nevertheless, these data are in contrast to a modeling study by Retkute et al. (2015) which indicated that the optimal plant response to fluctuating irradiance was to increase A_{max}. These results may also be in disagreement with a recent commentary by Pao et al. (2019b), who suggested that photosynthetic capacity (expressed as maximum electron transport and carboxylation rates, J_{max} and V_{cmax}, respectively) is reduced in leaves under fluctuating irradiance; this analysis was based on a non-linear relationship between irradiance and protein synthesis rate, using data from a previous modeling study validated with measurements on *Cucumis sativa* (grown under constant irradiance) as reference (Pao et al., 2019a). The reasoning by Pao et al. (2019b) is that leaves under fluctuating irradiance experience a relatively longer time close to the saturating end of this relationship compared to leaves under lower, uniform light. We did not find a sufficient number of datasets on J_{max} or V_{cmax} in studies on lightfleck acclimation to draw robust conclusions, but assuming that a reduction in J_{max} and V_{cmax} would coincide with a reduction A_{max}, we can at least conclude that it is unlikely that J_{max} and V_{cmax} will generally decrease under fluctuating irradiance.

There was a tendency for a decrease in the root/shoot ratio under fluctuating irradiance, but this was not significant (**Figure 2**, n = 9). Similarly to A_{max}, this trait seemed to be under strong genetic control, as under identical treatments wheat (*Triticum aestivum*), *Setaria macrostachya*, and *Amaranthus caudatus* showed strong (37–52%) decreases in the root/shoot ratio under fluctuating irradiance, whereas *Celosia argentea* showed no response (Kubásek et al., 2013).

Plant biomass was significantly reduced under fluctuating irradiance, by 32%, although there was large variability around the mean (**Figure 2**; n = 12). At first glance, this reduction may seem obvious, given that (a) photosynthesis reacts non-instantaneously to an increase in irradiance due to photosynthetic induction and thereby has a lower time-integrated CO_2 assimilation compared to the steady state (Kaiser et al., 2015, 2018b) and (b) due to the saturating, non-linear response of steady-state leaf photosynthesis to irradiance, fluctuating irradiance treatments typically expose the leaf to a larger fraction of high irradiance that is used with a lower quantum efficiency compared to the uniform, low irradiance

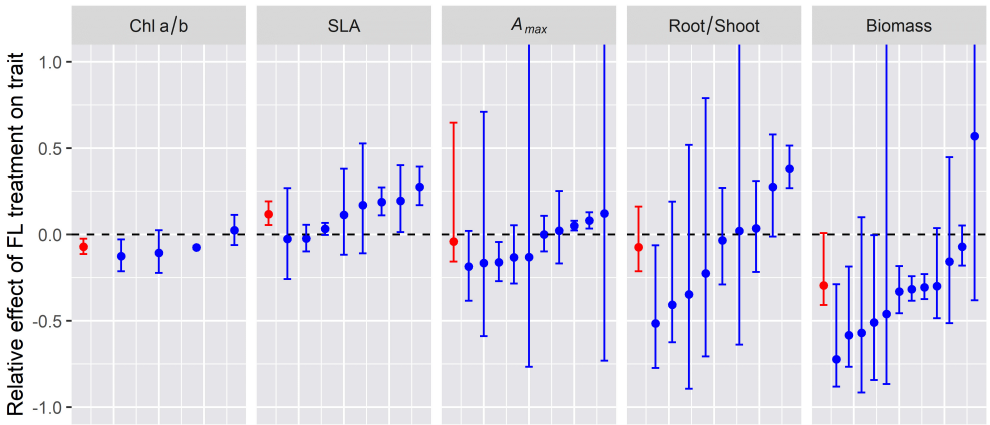

FIGURE 2 | Relative effect of fluctuating irradiance (FL) treatment on plan traits for the different experiments reviewed (blue symbols and error bars) and the average relative effect across experiments (red symbol and error bars). Error bars indicate 95% confidence intervals (i.e., the 2.5 and 97.5% of the distribution of relative effect) whereas symbols indicate the median relative effect.

controls. However, it is noteworthy that as with A_{max} and the root/shoot ratio, different species in the same experiment displayed very different plant biomass responses to fluctuating irradiance: while biomass was significantly reduced (−21%) in tomato under fluctuating irradiance, in chrysanthemum, petunia and rose (*Rosa* × *hybrida*) it was unaffected (Blom and Zheng, 2009). These results hint at the possibility that acclimation to fluctuating irradiance may counteract the negative effects of fluctuating irradiance on biomass, and that the capacity for this compensatory acclimation may be species dependent and could therefore be used as a breeding target.

Some of the reported effects of fluctuating light on treatments coincide with the effects expected from a low irradiance treatment (i.e., acclimation to low irradiance) including higher SLA and lower chlorophyll a/b ratio (**Figure 2**), but A_{max} did not change or even increased (unlike acclimation to low irradiance when it would always decrease). Therefore, acclimation to fluctuating light seems to differ from acclimation to low irradiance although some traits may respond similarly.

The experiments reviewed maintained the same average irradiance in the constant and fluctuating light treatments. This means that plants under fluctuating light were being exposed to lower irradiance than in the control during part of the daytime. However, the fraction of the daytime when this was the case varied across studies (**Supplementary Table S1**) from approximately 50% (Vialet-Chabrand et al., 2017) to >83% (Watling et al., 1997; Kaiser et al., 2018a). There was a weak negative correlation (−0.33) between A_{max} and the fraction of the daytime where irradiance was lower (**Supplementary Table S1**), but stronger correlations for chlorophyll a/b ratio and SLA (0.64 and −0.65, respectively). This means that, across the different experiments, a longer exposure to lower irradiance resulted in a smaller effect of fluctuating irradiance on chlorophyll a/b ratio and SLA but a stronger effect on A_{max}. This trend further reinforces the hypothesis that the changes observed in the different traits are not due to acclimation to the low irradiance periods of the fluctuating light treatment.

Although these data suggest that acclimation to fluctuating irradiance is distinct from acclimation to low irradiance, the experiments reviewed used different plant species, average irradiance levels, and dynamic patterns of oscillations, so confounding effects cannot be discarded. We suggest that future experiments on fluctuating irradiance include (when relevant) a second control where plants are grown at a constant, low irradiance level equal to the prevailing background irradiance of the fluctuating treatment, to further clarify the role of low irradiance in acclimation to fluctuating irradiance.

OUTLOOK

The data summarized here suggest that acclimation to fluctuating irradiance resembles that of shade acclimation for some traits. However, we are still lacking (insights from) studies that expose plants to several combinations of lightfleck timing, frequency, amplitude, and absolute intensity, to fully understand what the drivers for acclimation of a given trait are. Such studies should also account for the genetic variation that exists for the capacity to change a given trait during acclimation. Further, we emphasize once more the need for experimental setups that ensure that the average irradiance (and spectrum) between treatments is identical and that a treatment with constant irradiance is included. Recent advances in LED technology (Pattison et al., 2018) that allow for accurate and rapid modulation of intensity, as well as for emulating the natural light spectra, are instrumental to advancement of this field of research. Finally, many studies, e.g., those cited on retrograde signaling, SAA, and gene transcription were conducted under relatively extreme conditions: plants were grown under a very low irradiance (2–5% of full sunlight) and then were exposed to 50–100% of full sunlight to trigger a change. The molecular responses in these studies were indeed intriguingly rapid and massive, but these may be weaker in field-grown plants that are acclimated to a stronger, and more fluctuating, irradiance.

AUTHOR CONTRIBUTIONS

All authors listed have made a substantial, direct and intellectual contribution to the work, and approved it for publication.

FUNDING

While writing this review, AM was funded by the Netherlands Organisation for Scientific Research (Project Numbers 867.15.031 and 867.15.032). EK was funded by the 4TU Programme "PLANTENNA: Botanic sensor networks, towards an Internet of Plants."

SUPPLEMENTARY MATERIAL

The Supplementary Material for this article can be found online at: https://www.frontiersin.org/articles/10.3389/fpls.2020.00268/full#supplementary-material

REFERENCES

Albanese, P., Manfredi, M., Re, A., Marengo, E., Saracco, G., and Pagliano, C. (2018). Thylakoid proteome modulation in pea plants grown at different irradiances: quantitative proteomic profiling in a non-model organism aided by transcriptomic data integration. *Plant J.* 96, 786–800. doi: 10.1111/tpj.14068

Alsharafa, K., Vogel, M. O., Oelze, M. L., Moore, M., Stingl, N., König, K., et al. (2014). Kinetics of retrograde signalling initiation in the high light response of *Arabidopsis thaliana*. *Philos. Trans. R. Soc. B Biol. Sci.* 369, 1–9. doi: 10.1098/rstb.2013.0424

Annunziata, M. G., Apelt, F., Carillo, P., Krause, U., Feil, R., Koehl, K., et al. (2018). Response of *Arabidopsis* primary metabolism and circadian clock to low night temperature in a natural light environment. *J. Exp. Bot.* 69, 4881–4895. doi: 10.1093/jxb/ery276

Annunziata, M. G., Apelt, F., Carillo, P., Krause, U., Feil, R., Mengin, V., et al. (2017). Getting back to nature: a reality check for experiments in controlled environments. *J. Exp. Bot.* 68, 4463–4477. doi: 10.1093/jxb/erx220

Anten, N. P. R. (2016). "Optimization and game theory in canopy models," in *Canopy Photosynthesis: From Basics to Applications*, eds K. Hikosaka, Ü Niinemets, and N. P. R. Anten (Dordrecht: Springer), 355–378.

Armbruster, U., Correa Galvis, V., Kunz, H. H., and Strand, D. D. (2017). The regulation of the chloroplast proton motive force plays a key role for photosynthesis in fluctuating light. *Curr. Opin. Plant Biol.* 37, 56–62. doi: 10.1016/j.pbi.2017.03.012

Athanasiou, K., Dyson, B. C., Webster, R. E., and Johnson, G. N. (2010). Dynamic acclimation of photosynthesis increases plant fitness in changing environments. *Plant Physiol.* 152, 366–373. doi: 10.1104/pp.109.149351

Ballaré, C. L., and Pierik, R. (2017). The shade-avoidance syndrome: multiple signals and ecological consequences. *Plant Cell Environ.* 40, 2530–2543. doi: 10.1111/pce.12914

Barillot, R., Chambon, C., and Andrieu, B. (2016). CN-Wheat, a functional-structural model of carbon and nitrogen metabolism in wheat culms after anthesis. II. Model evaluation. *Ann. Bot.* 118, 1015–1031. doi: 10.1093/aob/mcw143

Bellafiore, S., Barneche, F., Peltier, G., and Rochaix, J.-D. (2005). State transitions and light adaptation require chloroplast thylakoid protein kinase STN7. *Nature* 433, 892–895. doi: 10.1038/nature03286

Blom, T. J., and Zheng, Y. (2009). The response of plant growth and leaf gas exchange to the speed of lamp movement in a greenhouse. *Sci. Hortic.* 119, 188–192. doi: 10.1016/j.scienta.2008.07.014

Burgess, A. J., Gibbs, J. A., and Murchie, E. H. (2019). A canopy conundrum: can wind-induced movement help to increase crop productivity by relieving photosynthetic limitations? *J. Exp. Bot.* 70, 2371–2380. doi: 10.1093/jxb/ery424

Burgess, A. J., Retkute, R., Preston, S. P., Jensen, O. E., Pound, M. P., Pridmore, T. P., et al. (2016). The 4-dimensional plant: effects of wind-induced canopy movement on light fluctuations and photosynthesis. *Front. Plant Sci.* 7:1392. doi: 10.3389/fpls.2016.01392

Caliandro, R., Nagel, K. A., Kastenholz, B., Bassi, R., Li, Z., Niyogi, K. K., et al. (2013). Effects of altered α- and β-branch carotenoid biosynthesis on photoprotection and whole-plant acclimation of *Arabidopsis* to photo-oxidative stress. *Plant Cell Environ.* 36, 438–453. doi: 10.1111/j.1365-3040.2012.02586.x

Chan, K. X., Phua, S. Y., Crisp, P., McQuinn, R., and Pogson, B. J. (2016). Learning the languages of the chloroplast: retrograde signaling and beyond. *Annu. Rev. Plant Biol.* 67, 25–53. doi: 10.1146/annurev-arplant-043015-111854

Choudhury, F. K., Devireddy, A. R., Azad, R. K., Shulaev, V., and Mittler, R. (2018a). Local and systemic metabolic responses during light-induced rapid systemic signaling. *Plant Physiol.* 178, 1461–1472. doi: 10.1104/pp.18.01031

Choudhury, F. K., Devireddy, A. R., Azad, R. K., Shulaev, V., and Mittler, R. (2018b). Rapid accumulation of glutathione during light stress in *Arabidopsis*. *Plant Cell Physiol.* 59, 1817–1826. doi: 10.1093/pcp/pcy101

Crisp, P. A., Ganguly, D. R., Smith, A. B., Murray, K. D., Estavillo, G. M., Searle, I., et al. (2017). Rapid recovery gene downregulation during excess-light stress and recovery in *Arabidopsis*. *Plant Cell* 29, 1836–1863. doi: 10.1105/tpc.16.00828

Cruz, J. A., Savage, L. J., Zegarac, R., Hall, C. C., Satoh-Cruz, M., Davis, G. A., et al. (2016). Dynamic environmental photosynthetic imaging reveals emergent phenotypes. *Cell Syst.* 2, 365–377. doi: 10.1016/j.cels.2016.06.001

De Pury, D. G. G., and Farquhar, G. D. (1997). Simple scaling of photosynthesis from leaves to canopies without the errors of big-leaf models. *Plant Cell Environ.* 20, 537–557. doi: 10.1111/j.1365-3040.1997.00094.x

Dietz, K. J. (2015). Efficient high light acclimation involves rapid processes at multiple mechanistic levels. *J. Exp. Bot.* 66, 2401–2414. doi: 10.1093/jxb/eru505

Dietzel, L., Brautigam, K., and Pfannschmidt, T. (2008). Photosynthetic acclimation: state transitions and adjustment of photosystem stoichiometry – functional relationships between short-term and long-term light quality acclimation in plants. *FEBS J.* 275, 1080–1088. doi: 10.1111/j.1742-4658.2008.06264.x

Dodd, A. N., Belbin, F. E., Frank, A., and Webb, A. A. R. (2015). Interactions between circadian clocks and photosynthesis for the temporal and spatial coordination of metabolism. *Front. Plant Sci.* 6:245. doi: 10.3389/fpls.2015.00245

Dodd, A. N., Parkinson, K., and Webb, A. A. R. (2004). Independent circadian regulation of assimilation and stomatal conductance in the ztl-1 mutant of *Arabidopsis*. *New Phytol.* 162, 63–70. doi: 10.1111/j.1469-8137.2004.01005.x

Dyson, B. C., Allwood, J. W., Feil, R., Xu, Y., Miller, M., Bowsher, C. G., et al. (2015). Acclimation of metabolism to light in *Arabidopsis thaliana*: the glucose 6-phosphate/phosphate translocator GPT2 directs metabolic acclimation. *Plant Cell Environ.* 38, 1404–1417. doi: 10.1111/pce.12495

Endler, J. A. (1993). The color of light in forests and its implications. *Ecol. Monogr.* 63, 1–27. doi: 10.2307/2937121

Evans, J. R., and Poorter, H. (2001). Photosynthetic acclimation of plants to growth irradiance: the relative importance of specific leaf area and nitrogen partitioning in maximizing carbon gain. *Plant Cell Environ.* 24, 755–767. doi: 10.1046/j.1365-3040.2001.00724.x

Farquhar, G. D. (1989). Models of integrated photosynthesis of cells and leaves. *Philos. Trans. R. Soc. B Biol. Sci.* 323, 357–367. doi: 10.1098/rstb.1989.0016

Field, C. (1983). Allocating leaf nitrogen for the maximization of carbon gain: leaf age as a control on the allocation program. *Oecologia* 56, 341–347. doi: 10.1007/BF00379710

Franklin, K. A., Allen, T., and Whitelam, G. C. (2007). Phytochrome A is an irradiance-dependent red light sensor. *Plant J.* 50, 108–117. doi: 10.1111/j.1365-313X.2007.03036.x

Fredeen, A. L., Hennessey, T. L., and Field, C. B. (1991). Biochemical correlates of the circadian rhythm in photosynthesis in Phaseolus vulgaris. *Plant Physiol.* 97, 415–419. doi: 10.1104/pp.97.1.415

Frenkel, M., Bellafiore, S., Rochaix, J.-D., and Jansson, S. (2007). Hierarchy amongst photosynthetic acclimation responses for plant fitness. *Physiol. Plant.* 129, 455–459. doi: 10.1111/j.1399-3054.2006.00831.x

Galvez-Valdivieso, G., Fryer, M. J., Lawson, T., Slattery, K., Truman, W., Smirnoff, N., et al. (2009). The high light response in *Arabidopsis* involves ABA signaling between vascular and bundle sheath cells. *Plant Cell.* 21, 2143–2162. doi: 10.1105/tpc.108.061507

Gechev, T. S., Breusegem, F., Van Stone, J. M., Denev, I., and Laloi, C. (2006). Reactive oxygen species as signals that modulate plant stress responses and programmed cell death. *Bioassays* 28, 1091–1101. doi: 10.1002/bies.20493

Gibbs, J. A., Burgess, A. J., Pound, M. P., Pridmore, T. P., and Murchie, E. H. (2019). Recovering wind-induced plant motion in dense field environments via deep learning and multiple object tracking. *Plant Physiol.* 181, 28–42. doi: 10.1104/pp.19.00141

Gilroy, S., Bialasek, M., Suzuki, N., Górecka, M., Devireddy, A. R., Karpinski, S., et al. (2016). ROS, calcium, and electric signals: key mediators of rapid systemic signaling in plants. *Plant Physiol.* 171, 1606–1615. doi: 10.1104/pp.16.00434

Graf, A., Schlereth, A., Stitt, M., and Smith, A. M. (2010). Circadian control of carbohydrate availability for growth in *Arabidopsis* plants at night. *Proc. Natl. Acad. Sci. U.S.A.* 107, 9458–9463. doi: 10.1073/pnas.0914299107

Grieco, M., Tikkanen, M., Paakkarinen, V., Kangasjärvi, S., and Aro, E. M. (2012). Steady-state phosphorylation of light-harvesting complex II proteins preserves photosystem I under fluctuating white light. *Plant Physiol.* 160, 1896–1910. doi: 10.1104/pp.112.206466

Haydon, M. J., and Webb, A. A. R. (2016). Assessing the impact of photosynthetic sugars on the *Arabidopsis* circadian clock. *Methods Mol. Biol.* 1398, 133–140. doi: 10.1007/978-1-4939-3356-3_10

Hennessey, T. L., Freeden, A. L., and Field, C. B. (1993). Environmental effects on circadian rhythms in photosynthesis and stomatal opening. *Planta* 189, 369–376. doi: 10.1007/BF00194433

Hikosaka, K., Anten, N. P. R., Borjigidai, A., Kamiyama, C., Sakai, H., Hasegawa, T., et al. (2016). A meta-analysis of leaf nitrogen distribution within plant canopies. *Ann. Bot.* 118, 239–247. doi: 10.1093/aob/mcw099

Ji, Y., Ouzounis, T., Courbier, S., Kaiser, E., Nguyen, P. T., Schouten, H. J., et al. (2019). Far-red radiation increases dry mass partitioning to fruits but reduces Botrytis cinerea resistance in tomato. *Environ. Exp. Bot.* 168:103889. doi: 10.1016/j.envexpbot.2019.103889

Jiang, C. D., Wang, X., Gao, H. Y., Shi, L., and Chow, W. S. (2011). Systemic regulation of leaf anatomical structure, photosynthetic performance, and high-light tolerance in sorghum. *Plant Physiol.* 155, 1416–1424. doi: 10.1104/pp.111.172213

Jung, J. H., Domijan, M., Klose, C., Biswas, S., Ezer, D., Gao, M., et al. (2016). Phytochromes function as thermosensors in *Arabidopsis*. *Science* 354, 886–889. doi: 10.1126/science.aaf6005

Kafka, J. L., and Miller, M. A. (2019). A climatology of solar irradiance and its controls across the United States: implications for solar panel orientation. *Renew. Energy* 135, 897–907. doi: 10.1016/j.renene.2018.12.057

Kaiser, E., Galvis, V. C., and Armbruster, U. (2019). Efficient photosynthesis in dynamic light environments: a chloroplast' s perspective. *Biochem. J.* 476, 2725–2741. doi: 10.1042/BCJ20190134

Kaiser, E., Matsubara, S., Harbinson, J., Heuvelink, E., and Marcelis, L. F. M. (2018a). Acclimation of photosynthesis to lightflecks in tomato leaves: interaction with progressive shading in a growing canopy. *Physiol. Plant.* 162, 506–517. doi: 10.1111/ppl.12668

Kaiser, E., Morales, A., and Harbinson, J. (2018b). Fluctuating light takes crop photosynthesis on a rollercoaster ride. *Plant Physiol.* 176, 977–989. doi: 10.1104/pp.17.01250

Kaiser, E., Morales, A., Harbinson, J., Heuvelink, E., Prinzenberg, A. E., and Marcelis, L. F. M. (2016). Metabolic and diffusional limitations of photosynthesis in fluctuating irradiance in *Arabidopsis thaliana*. *Sci. Rep.* 6:31252. doi: 10.1038/srep31252

Kaiser, E., Morales, A., Harbinson, J., Kromdijk, J., Heuvelink, E., and Marcelis, L. F. M. (2015). Dynamic photosynthesis in different environmental conditions. *J. Exp. Bot.* 66, 2415–2426. doi: 10.1093/jxb/eru406

Karpinski, S., Reynolds, H., Karpinska, B., Wingsle, G., Creissen, G., and Mullineaux, P. (1999). Systemic signaling and acclimation in response to excess excitation energy in *Arabidopsis*. *Science* 284, 654–658.

Karpinski, S., Szechynska-Hebda, M., Wituszynska, W., and Burdiak, P. (2013). Light acclimation, retrograde signalling, cell death and immune defences in plants. *Plant Cell Environ.* 36, 736–744. doi: 10.1111/pce.12018

Knapp, A. K., and Smith, W. K. (1988). Effect of water stress on stomatal and photosynthetic responses in subalpine plants to cloud patterns. *Am. J. Bot.* 75, 851–858. doi: 10.1002/j.1537-2197.1988.tb13508.x

Kono, M., Kawaguchi, H., Mizusawa, N., Yamori, W., Suzuki, Y., and Terashima, I. (2019). Far-Red light accelerates photosynthesis in the low-light phases of fluctuating light. *Plant Cell Physiol.* 61, 192–202. doi: 10.1093/pcp/pcz191

Kromdijk, J., Glowacka, K., Leonelli, L., Gabilly, S. T., Iwai, M., Niyogi, K. K., et al. (2016). Improving photosynthesis and crop productivity by accelerating recovery from photoprotection. *Science* 354, 857–861. doi: 10.1126/science.aai8878

Kubásek, J., Urban, O., and Šantrůček, J. (2013). C4 plants use fluctuating light less efficiently than do C3 plants: a study of growth, photosynthesis and carbon isotope discrimination. *Physiol. Plant* 149, 528–539. doi: 10.1111/ppl.12057

Kühlheim, C., Agren, J., and Jansson, S. (2002). Rapid regulation of light harvesting and plant fitness in the field. *Science* 297, 91–94.

Kühlheim, C., and Jansson, S. (2005). What leads to reduced fitness in non-photochemical quenching mutants? *Physiol. Plant.* 125, 202–211. doi: 10.1111/j.1399-3054.2005.00547.x

Kull, O. (2002). Acclimation of photosynthesis in canopies: models and limitations. *Oecologia* 133, 267–279. doi: 10.1007/s00442-002-1042-1

Kull, O., and Kruijt, B. (1999). Acclimation of photosynthesis to light: a mechanistic approach. *Funct. Ecol.* 13, 24–36. doi: 10.1046/j.1365-2435.1999.00292.x

Lawson, T., and Blatt, M. R. (2014). Stomatal size, speed, and responsiveness impact on photosynthesis and water use efficiency. *Plant Physiol.* 164, 1556–1570. doi: 10.1104/pp.114.237107

Leakey, A. D. B., Press, M. C., Scholes, J. D., and Watling, J. R. (2002). Relative enhancement of photosynthesis and growth at elevated CO2 is greater under sunflecks than uniform irradiance in a tropical rain forest tree seedling. *Plant Cell Environ.* 25, 1701–1714. doi: 10.1046/j.1365-3040.2002.00944.x

Legris, M., Klose, C., Burgie, E. S., Rojas, C. C., Neme, M., Hiltbrunner, A., et al. (2016). Phytochrome B integrates light and temperature signals in *Arabidopsis*. *Science* 354, 897–900. doi: 10.1126/science.aaf5656

Matsubara, S., Schneider, T., and Maurino, V. G. (2016). Dissecting long-term adjustments of photoprotective and photo-oxidative stress acclimation occurring in dynamic light environments. *Front. Plant Sci.* 7:1690. doi: 10.3389/fpls.2016.01690

Matthews, J. S. A., Vialet-Chabrand, S., and Lawson, T. (2018). Acclimation to fluctuating light impacts the rapidity of response and diurnal rhythm of stomatal conductance. *Plant Physiol.* 176, 1939–1951. doi: 10.1104/pp.17.01809

Miller, M. A. E., O'Cualain, R., Selley, J., Knight, D., Karim, M. F., Hubbard, S. J., et al. (2017). Dynamic acclimation to high light in *Arabidopsis thaliana* involves widespread reengineering of the leaf proteome. *Front. Plant Sci.* 8:1239. doi: 10.3389/fpls.2017.01239

Mittler, R., and Blumwald, E. (2015). The roles of ROS and ABA in systemic acquired acclimation. *Plant Cell* 27, 64–70. doi: 10.1105/tpc.114.133090

Morales, A., Kaiser, E., Yin, X., Harbinson, J., Molenaar, J., Driever, S. M., et al. (2018a). Dynamic modelling of limitations on improving leaf CO<inf>2</inf>assimilation under fluctuating irradiance. *Plant Cell Environ.* 41, 589–604. doi: 10.1111/pce.13119

Morales, A., Yin, X., Harbinson, J., Driever, S. M., Molenaar, J., Kramer, D. M., et al. (2018b). In silico analysis of the regulation of the photosynthetic electron transport chain in C3 plants. *Plant Physiol.* 176, 1247–1261. doi: 10.1104/pp.17.00779

Mott, K. A., and Woodrow, I. E. (2000). Modelling the role of Rubisco activase in limiting non-steady-state photosynthesis. *J. Exp. Bot.* 51, 399–406. doi: 10.1093/jexbot/51.suppl_1.399

Mubarakshina, M. M., Ivanov, B. N., Naydov, I. A., Hillier, W., Badger, M. R., and Krieger-Liszkay, A. (2010). Production and diffusion of chloroplastic H2O2 and its implication to signalling. *J. Exp. Bot.* 61, 3577–3587. doi: 10.1093/jxb/erq171

Mullet, J. E. (1993). Dynamic regulation of chloroplast transcription. *Plant Physiol.* 103, 309–313. doi: 10.1104/pp.103.2.309

Munekage, Y. N., Inoue, S., Yoneda, Y., and Yokota, A. (2015). Distinct palisade tissue development processes promoted by leaf autonomous signalling and long-distance signalling in *Arabidopsis thaliana*. *Plant Cell Environ.* 38, 1116–1126. doi: 10.1111/pce.12466

Murakami, K., Matsuda, R., and Fujiwara, K. (2014). Light-induced systemic regulation of photosynthesis in primary and trifoliate leaves of Phaseolus

vulgaris: effects of photosynthetic photon flux density (PPFD) versus spectrum. *Plant Biol.* 16, 16–21. doi: 10.1111/plb.12055

Murchie, E. H., and Horton, P. (1997). Acclimation of photosynthesis to irradiance and spectral quality in British plant species: chlorophyll content, photosynthetic capacity and habitat preference. *Plant Cell Environ.* 20, 438–448. doi: 10.1046/j.1365-3040.1997.d01-95.x

Oguchi, R., Hikosaka, K., and Hirose, T. (2005). Leaf anatomy as a constraint for photosynthetic acclimation: differential responses in leaf anatomy to increasing growth irradiance among three deciduous trees. *Plant Cell Environ.* 28, 916–927. doi: 10.1111/j.1365-3040.2005.01344.x

Pao, Y. C., Chen, T. W., Moualeu-Ngangue, D. P., and Stützel, H. (2019a). Environmental triggers for photosynthetic protein turnover determine the optimal nitrogen distribution and partitioning in the canopy. *J. Exp. Bot.* 70, 2419–2433. doi: 10.1093/jxb/ery308

Pao, Y.-C., Stützel, H., and Chen, T.-W. (2019b). A mechanistic view of the reduction in photosynthetic protein abundance under diurnal light fluctuation. *J. Exp. Bot.* 70, 3705–3708. doi: 10.1093/jxb/erz164

Parding, K. M., Liepert, B. G., Hinkelman, L. M., and Ackerman, T. P. (2016). Influence of synoptic weather patterns on solar irradiance variability in Northern Europe. *J. Clim.* 29, 4229–4250. doi: 10.1175/JCLI-D-15-0476.1

Pattison, P. M., Tsao, J. Y., Brainard, G. C., and Bugbee, B. (2018). LEDs for photons, physiology and food. *Nature* 563, 493–500. doi: 10.1038/s41586-018-0706-x

Pearcy, R. W., Roden, J. S., and Gamon, J. A. (1990). Sunfleck dynamics in relation to canopy structure in a soybean (*Glycine max* (L.) Merr.) canopy. *Agric. For. Meteorol.* 52, 359–372. doi: 10.1016/0168-1923(90)90092-K

Peressotti, A., Marchiol, L., and Zerbi, G. (2001). Photosynthetic photon fluc density and sunfleck regime within canopies of wheat, sunflower and maize in different wind conditions. *Ital. J. Agron.* 4, 87–92.

Perez, R., David, M., Hoff, T. E., Jamaly, M., Kivalov, S., Kleissl, J., et al. (2016). Spatial and temporal variability of solar energy. *Found. Trends Renew. Energy* 1, 1–44. doi: 10.1561/2700000006

Pfalz, J., Liebers, M., Hirth, M., Grübler, B., Holtzegel, U., Schröter, Y., et al. (2012). Environmental control of plant nuclear gene expression by chloroplast redox signals. *Front. Plant Sci.* 3:257. doi: 10.3389/fpls.2012.00257

Pfannschmidt, T., Nilsson, A., and Allen, J. F. (1999). Photosynthetic control of chloroplast gene expression. *Nature* 397, 625–628. doi: 10.1038/17624

Pons, T. L., Jordi, W., and Kuiper, D. (2001). Acclimation of plants to light gradients in leaf canopies: evidence for a possible role for cytokinins transported in the transpiration stream. *J. Exp. Bot.* 52, 1563–1574. doi: 10.1093/jexbot/52.360.1563

Qu, M., Hamdani, S., Li, W., Wang, S., Tang, J., Chen, Z., et al. (2016). Rapid stomatal response to fluctuating light: an under-explored mechanism to improve drought tolerance in rice. *Funct. Plant Biol.* 43, 727–738. doi: 10.1071/FP15348

Resco de Dios, V., and Gessler, A. (2018). Circadian regulation of photosynthesis and transpiration from genes to ecosystems. *Environ. Exp. Bot.* 152, 37–48. doi: 10.1016/j.envexpbot.2017.09.010

Resco de Dios, V., Gessler, A., Ferrio, J. P., Alday, J. G., Bahn, M., Del Castillo, J., et al. (2016). Circadian rhythms have significant effects on leaf-to-canopy scale gas exchange under field conditions. *Gigascience* 5:43. doi: 10.1186/s13742-016-0149-y

Retkute, R., Smith-Unna, S. E., Smith, R. W., Burgess, A. J., Jensen, O. E., Johnson, G. N., et al. (2015). Exploiting heterogeneous environments: does photosynthetic acclimation optimize carbon gain in fluctuating light? *J. Exp. Bot.* 66, 2437–2447. doi: 10.1093/jxb/erv055

Retkute, R., Townsend, A. J., Murchie, E. H., Jensen, O. E., and Preston, S. P. (2018). Three-dimensional plant architecture and sunlit-shaded patterns: a stochastic model of light dynamics in canopies. *Ann. Bot.* 122, 291–302. doi: 10.1093/aob/mcy067

Roden, J. S. (2003). Modeling the light interception and carbon gain of individual fluttering aspen (*Populus tremuloides* Michx) leaves. *Trees* 17, 117–126. doi: 10.1007/s00468-002-0213-3

Rooijen, R., Van Aarts, M. G. M., and Harbinson, J. (2015). Natural genetic variation for acclimation of photosynthetic light use efficiency to growth irradiance in *Arabidopsis*. *Plant Physiol.* 167, 1412–1429. doi: 10.1104/pp.114.252239

Ruiz-Arias, J. A., and Gueymard, C. A. (2018). Worldwide inter-comparison of clear-sky solar radiation models: consensus- based review of direct and global irradiance components simulated at the earth surface. *Sol. Energy* 168, 10–29. doi: 10.1016/j.solener.2018.02.008

Salter, W. T., Merchant, A. M., Richards, R. A., Trethowan, R., and Buckley, T. N. (2019). Rate of photosynthetic induction in fluctuating light varies widely among genotypes of wheat. *J. Exp. Bot.* 70, 2787–2796. doi: 10.1093/jxb/erz100

Schneider, T., Bolger, A., Zeier, J., Preiskowski, S., Benes, V., Trenkamp, S., et al. (2019). Fluctuating light interacts with time of day and leaf development stage to reprogram gene expression. *Plant Physiol.* 179, 1632–1657. doi: 10.1104/pp.18.01443

Schöttler, M. A., and Tóth, S. Z. (2014). Photosynthetic complex stoichiometry dynamics in higher plants: environmental acclimation and photosynthetic flux control. *Front. Plant Sci.* 5:188. doi: 10.3389/fpls.2014.00188

Sellaro, R., Smith, R. W., Legris, M., Fleck, C., and Casal, J. J. (2019). Phytochrome B dynamics departs from photoequilibrium in the field. *Plant Cell Environ.* 42, 606–617. doi: 10.1111/pce.13445

Sellaro, R., Yanovsky, M. J., and Casal, J. J. (2011). Repression of shade-avoidance reactions by sunfleck induction of HY5 expression in *Arabidopsis*. *Plant J.* 68, 919–928. doi: 10.1111/j.1365-313X.2011.04745.x

Sikma, M., Ouwersloot, H. G., Pedruzo-Bagazgoitia, X., and Van Heerwaarden, C. C. (2018). Interactions between vegetation, atmospheric turbulence and clouds under a wide range of background wind conditions. *Agric. For. Meteorol.* 255, 31–43. doi: 10.1016/j.agrformet.2017.07.001

Simkin, A. J., López-Calcagno, P. E., and Raines, C. A. (2019). Feeding the world: Improving photosynthetic efficiency for sustainable crop production. *J. Exp. Bot.* 70, 1119–1140. doi: 10.1093/jxb/ery445

Slattery, R. A., Walker, B. J., Weber, A. P. M., and Ort, D. R. (2018). The impacts of fluctuating light on crop performance. *Plant Physiol.* 176, 990–1003. doi: 10.1104/pp.17.01234

Smith, N. G., and Dukes, J. S. (2013). Plant respiration and photosynthesis in global-scale models: incorporating acclimation to temperature and CO2. *Glob. Chang. Biol.* 19, 45–63. doi: 10.1111/j.1365-2486.2012.02797.x

Smith, W. K., Knapp, A. K., and Reiners, W. A. (1989). Penumbral effects on sunlight penetration in plant communities. *Ecology* 70, 1603–1609. doi: 10.2307/1938093

Soleh, M. A., Tanaka, Y., Kim, S. Y., Huber, S. C., Sakoda, K., and Shiraiwa, T. (2017). Identification of large variation in the photosynthetic induction response among 37 soybean [Glycine max (L.) Merr.] genotypes that is not correlated with steady-state photosynthetic capacity. *Photosynth. Res.* 131, 305–315. doi: 10.1007/s11120-016-0323-321

Suzuki, N., Devireddy, A. R., Inupakutika, M. A., Baxter, A., Miller, G., Song, L., et al. (2015). Ultra-fast alterations in mRNA levels uncover multiple players in light stress acclimation in plants. *Plant J.* 84, 760–772. doi: 10.1111/tpj.13039

Tanaka, Y., Adachi, S., and Yamori, W. (2019). Natural genetic variation of the photosynthetic induction response to fluctuating light environment. *Curr. Opin. Plant Biol.* 49, 52–59. doi: 10.1016/j.pbi.2019.04.010

Tang, Y. H., Washitani, I., Tsuchiya, T., and Iwaki, H. (1988). Fluctuation of photosynthetic photon flux density within a Miscanthus sinensis canopy. *Ecol. Res.* 3, 253–266. doi: 10.1007/BF02348584

Thornley, J. H. M. (1998). Dynamic model of leaf photosynthesis with acclimation to light and nitrogen. *Ann. Bot.* 81, 421–430. doi: 10.1006/anbo.1997.0575

Townsend, A. J., Retkute, R., Chinnathambi, K., Randall, J. W. P., Foulkes, J., Carmo-Silva, E., et al. (2018). Suboptimal acclimation of photosynthesis to light in wheat Canopies. *Plant Physiol.* 176, 1233–1246. doi: 10.1104/pp.17.01213

Vialet-Chabrand, S., Matthews, J. S. A., Simkin, A. J., Raines, C. A., and Lawson, T. (2017). Importance of fluctuations in light on plant photosynthetic acclimation. *Plant Physiol.* 173, 2163–2179. doi: 10.1104/pp.16.01767

Victoria, M., and Andresen, G. B. (2019). Using validated reanalysis data to investigate the impact of the PV system configurations at high penetration levels in European countries. *Prog. Photovoltaics Res. Appl.* 27, 576–592. doi: 10.1002/pip.3126

Vogel, M. O., Moore, M., König, K., Pecher, P., Alsharafa, K., Lee, J., et al. (2014). Fast retrograde signaling in response to high light involves metabolite export, mitogen-activated protein KINASE6, and AP2/ERF transcription factors in *Arabidopsis*. *Plant Cell* 26, 1151–1165. doi: 10.1105/tpc.113.121061

Wagner, R., Dietzel, L., Brautigam, K., Fischer, W., and Pfannschmidt, T. (2008). The long-term response to fluctuating light quality is an important and distinct

light acclimation mechanism that supports survival of *Arabidopsis thaliana* under low light conditions. *Planta* 228, 573–587. doi: 10.1007/s00425-008-0760-y

Wald, L. (2018). *Basics in Solar Radiation at Earth Surface*. Paris: PSL Research University.

Walters, R. G. (2005). Towards an understanding of photosynthetic acclimation. *J. Exp. Bot.* 56, 435–447. doi: 10.1093/jxb/eri060

Walters, R. G., and Horton, P. (1995). Acclimation of *Arabidopsis thaliana* to the light environment: changes in photosynthetic function. *Planta* 197, 306–312.

Wang, L., Kisi, O., Zounemat-Kermani, M., Ariel, G. A., Zhu, Z., and Gong, W. (2016). Solar radiation prediction using different techniques: model evaluation and comparison. *Renew. Sustain. Energy Rev.* 61, 384–397. doi: 10.1016/j.rser.2016.04.024

Watling, J. R., Ball, M. C., and Woodrow, I. E. (1997). The utilization of lightflecks for growth in four australian rain-forest species. *Funct. Ecol.* 11, 231–239. doi: 10.1046/j.1365-2435.1997.00073.x

Weise, S. E., Liu, T., Childs, K. L., Preiser, A. L., Katulski, H. M., Perrin-Porzondek, C., et al. (2019). Transcriptional regulation of the glucose-6-phosphate/phosphate translocator 2 is related to carbon exchange across the chloroplast envelope. *Front. Plant Sci.* 10:827. doi: 10.3389/fpls.2019.00827

Wu, Y., Gong, W., Wang, Y., Yong, T., Yang, F., Liu, W., et al. (2018). Leaf area and photosynthesis of newly emerged trifoliolate leaves are regulated by mature leaves in soybean. *J. Plant Res.* 131, 671–680. doi: 10.1007/s10265-018-1027-8

Xiao, Y., Tholen, D., and Zhu, X. G. (2016). The influence of leaf anatomy on the internal light environment and photosynthetic electron transport rate: exploration with a new leaf ray tracing model. *J. Exp. Bot.* 67, 6021–6035. doi: 10.1093/jxb/erw359

Yamazaki, J., and Shinomiya, Y. (2013). Effect of partial shading on the photosynthetic apparatus and photosystem stoichiometry in sunflower leaves. *Photosynthetica* 51, 3–12. doi: 10.1007/s11099-012-0073-z

Yano, S., and Terashima, I. (2001). Separate localization of light signal perception for sun or shade type chloroplast and palisade tissue differentiation in Chenopodium album. *Plant Cell Physiol.* 42, 1303–1310. doi: 10.1093/pcp/pce183

Yin, X., Schapendonk, A. H. C. M., and Struik, P. C. (2019). Exploring the optimum nitrogen partitioning to predict the acclimation of C3 leaf photosynthesis to varying growth conditions. *J. Exp. Bot.* 70, 2435–2447. doi: 10.1093/jxb/ery277

Zandalinas, S. I., Sengupta, S., Burks, D., Azad, R. K., and Mittler, R. (2019). Identification and characterization of a core set of ROS wave-associated transcripts involved in the systemic acquired acclimation response of *Arabidopsis* to excess light. *Plant J.* 98, 126–141. doi: 10.1111/tpj.14205

Zhang, Y., Kaiser, E., Zhang, Y., Yang, Q., and Li, T. (2018). Short-term salt stress strongly affects dynamic photosynthesis, but not steady-state photosynthesis, in tomato (*Solanum lycopersicum*). *Environ. Exp. Bot.* 149, 109–119. doi: 10.1016/j.envexpbot.2018.02.014

Zheng, Y., Blom, T., and Dixon, M. (2006). Moving lamps increase leaf photosynthetic capacity but not the growth of potted gerbera. *Sci. Hortic.* 107, 380–385. doi: 10.1016/j.scienta.2005.09.004

Zhu, X. G., Wang, Y., Ort, D. R., and Long, S. P. (2013). e-photosynthesis: a comprehensive dynamic mechanistic model of C3 photosynthesis: from light capture to sucrose synthesis. *Plant Cell Environ.* 36, 1711–1727. doi: 10.1111/pce.12025

Conflict of Interest: The authors declare that the research was conducted in the absence of any commercial or financial relationships that could be construed as a potential conflict of interest.

frontiers in Plant Science

ORIGINAL RESEARCH
published: 21 April 2020
doi: 10.3389/fpls.2020.00345

The Pyruvate-Phosphate Dikinase (C_4-*SmPPDK*) Gene From *Suaeda monoica* Enhances Photosynthesis, Carbon Assimilation, and Abiotic Stress Tolerance in a C_3 Plant Under Elevated CO_2 Conditions

*Sonam Yadav, Mangal Singh Rathore and Avinash Mishra**

Division of Applied Phycology and Biotechnology, CSIR-Central Salt and Marine Chemicals Research Institute, Bhavnagar, India

OPEN ACCESS

Edited by:
Marouane Baslam, Niigata University, Japan

Reviewed by:
Petronia Carillo, University of Campania Luigi Vanvitelli, Italy
Parvaiz Ahmad, Sri Pratap College Srinagar, India

***Correspondence:**
Avinash Mishra
avinash@csmcri.res.in; avinashmishra11@rediffmail.com; avinashmishra.csmcri@gmail.com

Specialty section:
This article was submitted to Plant Abiotic Stress, a section of the journal Frontiers in Plant Science

Received: *09 December 2019*
Accepted: *09 March 2020*
Published: *21 April 2020*

Citation:
Yadav S, Rathore MS and Mishra A (2020) The Pyruvate-Phosphate Dikinase (C_4-SmPPDK) Gene From Suaeda monoica Enhances Photosynthesis, Carbon Assimilation, and Abiotic Stress Tolerance in a C_3 Plant Under Elevated CO_2 Conditions. Front. Plant Sci. 11:345. doi: 10.3389/fpls.2020.00345

A pyruvate-phosphate dikinase (C_4-*PPDK*) gene was cloned from *Suaeda monoica*, which had a single-cell C_4 photosynthesis pathway without Kranz anatomy and was functionally validated in a C_3 model plant under different abiotic stress conditions in an ambient and elevated CO_2 environment. Overexpression of *SmPPDK* promoted growth of C_3 transgenic plants, enhancing their photosynthesis (CO_2 assimilation) by lowering photorespiration under stress conditions. Transgenic plants also showed an improved physiological status, with higher relative water content (RWC), membrane integrity, concentration of glycine betaine, total soluble sugars, free amino acids, polyphenols and antioxidant activity, and lower electrolyte leakage, lipid peroxidation, free radical accumulation, and generation of reactive oxygen species (ROS), compared to control plants. Moreover, *SmPPDK* transgenic plants exhibited earlier flowering and higher dry biomass compared to controls. These results suggested that the C_4-*PPDK* gene was appropriate for improvement of carbon assimilation, and it also played an important role in adaption to salinity and severe drought-induced stress. More intriguingly, an elevated CO_2 environment alleviated the adverse effects of abiotic stress, particularly caused by drought through coordination of osmoprotectants and antioxidant defense systems. The molecular, physiological, metabolic, and biochemical indicators ameliorated the overall performance of model C_3 plants overexpressing the C_4-*PPDK* gene in an elevated CO_2 environment, by lowering photorespiration metabolic processes, however, further studies are needed to confirm its precise role in C_3 plants as protection against future climate change.

Keywords: abiotic stress, C_4 photosynthesis, carbon sequestration, halophyte, salinity, transgenic

INTRODUCTION

Global climate changes such as increasing temperature, atmospheric CO_2 concentration and salinization, and altered precipitation are among the primary constraints on crop improvement, including biomass production and yield (Dhir, 2018). In addition, the increasing demands in feeding a fast growing population also impose pressure to enhance the productivity and quality

of current crops under limited resources. Global climate changes result in desertification and salinization, with >6% of global land area and >30% of irrigated farmland being salt affected (FAO, 2011). Global CO_2 concentrations have increased from a preindustrial level of 285 μmol mol^{-1} to the current level of 384 μmol mol^{-1}, and they have been predicted to reach 936 μmol mol^{-1} by the year 2100, with an increase in global atmospheric temperature of about 6.4°C (IPCC, 2014). These stresses will likely affect the productivity of plants, influencing the sequestration and assimilation of atmospheric CO_2 through photosynthesis.

Various studies on elevated CO_2 concentrations have shown a close relationship between improvements to photosynthesis and increases in yield and total biomass of plants (Kellner et al., 2019; Pastore et al., 2019). Therefore, this provides an attractive approach to enhancing yield by increasing photosynthesis of a particular crop species (Zhang et al., 2014; Yadav et al., 2018). Among the three categories of photosynthesis in carbon-assimilating plants, productivity and biomass of C_4 plants are not limited by atmospheric CO_2; therefore, they are considered the most efficient CO_2 sequestrators. C_4 photosynthesis inhibits the oxygenation reaction and acts as a CO_2 pump, increasing the intracellular CO_2/O_2 ratio at the active site of ribulose bisphosphate carboxylase/oxygenase (Rubisco) (Hatch, 1987; Sage, 2004). It has been well documented that C_3 plants lose about 50% of total available CO_2 to photorespiration compared to C_4 plants. In addition, C_4 photosynthesis has an advantage over that of C_3 plants, exhibiting a higher assimilation efficiency and yield of biomass under different abiotic stress conditions, including drought, high temperature, and high light intensity, by improving water and nitrogen use efficiency (Hatch, 1987; Sage and Pearcy, 2000). Enzymes involved in the C_4 assimilation pathway could also play a significant role in tolerance to abiotic and biotic stress (Ku et al., 2000; Gu et al., 2013). Enhancing photosynthesis efficiency in C_3 plants using an enzyme from the C_4 pathway could provide an alternative approach for improving productivity, biomass, and yield (Yadav and Mishra, 2019). Genera *Suaeda* and *Bienertia* have broken the dual-cell paradigm that Kranz anatomy is essential for C_4 carbon assimilation (Freitag and Stichler, 2002; Voznesenskaya et al., 2002; Akhani et al., 2005).

Suaeda species belong to the family Amaranthaceae and have a unique approach to C_4 carbon assimilation within a single chlorenchyma cell (Voznesenskaya et al., 2002, 2004), in which chloroplasts are dimorphic. A single-cell process is the most common in the nicotinamide adenine dinucleotide phosphate-dependent malic enzyme (NADP-ME) subtype of C_4 photosynthesis species, where the chloroplasts of mesophyll cells have well-developed grana, while the chloroplasts of bundle sheath lack grana. However, single-cell C_4 photosynthesis is not repressed by O_2, under low CO_2 concentration, and carbon isotope values are the same as for the Kranz type of the C_4 plant (Voznesenskaya et al., 2002, 2004). Likewise, single-cell C_4 plants contain dimorphic polarized chloroplasts, with a key enzyme, pyruvate phosphate dikinase (PPDK) located at the distal end of the chloroplast, while Rubisco is at the proximal end, effectively following the same differentiation as the Kranz type of anatomy (Dengler and Nelson, 1999; Sheen, 1999). As such, engineering of a single-cell C_4 organization into C_3 crops might provide an alternative approach to achieving Kranz type C_4 carbon assimilation without the need to establish a dual-cell system.

PPDK (EC 2.7.9.1) is nuclear encoded, abundantly present in the chloroplasts of mesophyll cells, an important rate-limiting enzyme of the C_4 pathway (Edwards et al., 1985; Hatch, 1987), and is regulated by light-dependent gene expression (Sheen and Bogorad, 1987). It catalyzes the interconversion of pyruvate to phosphoenolpyruvate (PEP), the acceptor of atmospheric CO_2 in C_4 plants, and C_4 photosynthesis rate is correlated (r = 0.96) with the activity of PPDK (Edwards et al., 1985). Its structural and functional properties have been studied in the bacterium *Clostridium symbiosum* (Chastain et al., 2011). The phylogenetic distribution of PPDK is confined to selected groups of bacteria, archaea, protozoa, lower fungi, and green plants (Liapounova et al., 2006; Slamovits and Keeling, 2006). C_4 PPDK is highly homologous to C_3 PPDK (Agarie et al., 1997), with the regions and residues involved in catalysis also being highly conserved among bacteria (Fißlthaler et al., 1995). PPDK can also contribute to the conversion of NADH to NADPH, which is an essential coenzyme of antioxidant enzymes, and is also involved in nitrogen assimilation and synthesis of fatty acids and osmotically active compounds (Doubnerová and Ryšlavá, 2011). PPDK is critically involved during early seedling growth and seed development in both C_3 and C_4 plants (Chastain et al., 2006; Yu et al., 2016; Chang et al., 2017). In *Arabidopsis thaliana*, PPDK is overexpressed during leaf senescence by significantly accelerating nitrogen remobilization from leaves (Taylor et al., 2010; Wang et al., 2019). PPDK also plays a key role in host stress defense mechanisms, as it is induced by various abiotic stresses, such as drought, salinity, heavy metals, submergence, low oxygen and cold (Doubnerová and Ryšlavá, 2011; Hýsková et al., 2014; Wang et al., 2018), and biotic stress, including viral infection (Spoustová et al., 2015). In nonphotosynthetic parts of the plant, PPDK plays a significant role in the maintenance of pH and rejuvenation of citric acid intermediates, which are involved in the synthesis of amino acids (Hýsková et al., 2014). PPDK homologs have been reported from bacteria and unicellular parasitic protists, such as *Giardia lamblia*, *Trichomonas vaginalis*, and *Entamoeba histolytica*, however, they have not been found in insects or vertebrates. As such, PPDK is a potential target for antiparasitic and antimicrobial drugs, as well as C_4-specific herbicides (Minges and Groth, 2017).

The advantages of a C_4-based physiology are observed during stress triggered by high temperatures, drought, salinity, and elevated CO_2 levels. PPDK is detected in C_3 plants (Chastain et al., 2008), however, its role is undefined. Consequently, the integration of the C_4 *PPDK* gene into C_3 plants could be a promising approach to relegate photorespiration, resulting in the improvement of photosynthetic efficiency of C_3 plants under climatic stress (Yadav and Mishra, 2020). In this current study, a gene that encoded PPDK was successfully introduced and

expressed in a C_3 plant (Ku et al., 2000; Fukayama et al., 2001; Gu et al., 2013).

Our previous studies suggested that halophytes were a potential resource for stress tolerance genes (Jha et al., 2011; Chaturvedi et al., 2012, 2014; Joshi et al., 2013; Singh et al., 2014b; Udawat et al., 2014, 2016; Tiwari et al., 2015) and promoters (Tiwari et al., 2014, 2016, 2019; Singh et al., 2016) that improved photosynthesis (Patel et al., 2015; Jha et al., 2019) and also provide abiotic stress tolerance (Singh et al., 2014a; Pandey et al., 2016; Mishra and Tanna, 2017; Udawat et al., 2017). Notably, the single-cell *PPDK* gene of *Suaeda* spp. was induced under elevated CO_2 conditions (Yadav et al., 2018). In the current study, a C_4 photosynthetic *PPDK* gene was isolated from the C_4 halophyte *Suaeda monoica* and was functionally validated by being introduced into a C_3 model plant, tobacco. The effects of overexpression of *SmPPDK* were studied on the phenotype, photosynthetic efficiency, and yield of transgenic tobacco plants. In addition, the synergetic effect of elevated CO_2 stress along with other abiotic stress conditions was studied on morphology, physiology, metabolites, and the biochemical status of transgenic lines, compared to ambient conditions and wild-type (WT) plants.

MATERIALS AND METHODS

Cloning and *in silico* Analysis of *SmPPDK* Gene

The *PPDK* gene was isolated by rapid amplification of complementary DNA (cDNA) ends (RACE) techniques, using different combinations of primers and PCR conditions (**Supplementary Table S1**). A full-length *PPDK* gene was cloned, sequenced (at M/s Macrogen, South Korea), and submitted to the National Center for Biotechnology information (NCBI) (accession no. MK704410).

Genome Organization of *SmPPDK* Gene

Genomic DNA was isolated from *S. monoica* leaves using the *N*-cetyl-*N*,*N*,*N*-trimethyl ammonium bromide (CTAB) method, and the *PPDK* gene was amplified with gene-specific primers (**Supplementary Table S1**). Amplicons were purified, cloned, and sequenced (M/s Macrogen, South Korea). Introns and exons were analyzed using available online tools (NCBI).

Genetic Transformation of *SmPPDK* Gene

The full-length coding sequence (CDS) of *SmPPDK* gene was amplified from cDNA using gene-specific primers containing *Kpn*I and *Xba*I restriction sites at the 5′- and 3′-ends, respectively (**Supplementary Table S1**), and was cloned into *pCAMBIA1301* through an intermediary plant expression vector pRT101. The resulting vector, *pCAMBIA1301:SmPPDK* was mobilized into *Agrobacterium tumefaciens* strain EHA104 and transformed to tobacco (*Nicotiana tabacum* cv. Petit Havana) plants by the standard leaf disk cocultivation method (Horsch et al., 1985). Leaf disks were cocultivated for 72 h and then transferred into direct shooting medium, followed by shoot elongation medium. Subsequently, they were transferred to rooting medium supplemented with 20 mg/L hygromycin. Rooted plants were acclimatized in soil and then transferred to a greenhouse.

Putative T0 and T1 transgenic lines were screened by germination of seeds on Murashige and Skoog (MS) medium supplemented with hygromycin (20 mg/L). Insertion of the transgene was confirmed by polymerase chain reaction (PCR) amplification using gene-specific (GSP) and vector-specific primers (**Supplementary Table S1**). In addition, β-glucuronidase (GUS) activity was determined in transgenic lines, along with WT and vector-control (VC) plants, using a GUS staining kit (Sigma, United States).

Analysis of T1 Transgenic Tobacco Plants

Seed Germination Assay and Growth Parameter Analysis

Seeds of *SmPPDK* transgenic lines (L1, L20, L32, L33, and L40) were surface sterilized, and they germinated on MS media supplemented with hygromycin (20 mg/L), whereas seeds of WT (tobacco plants cv. Petit Havana) and VC (tobacco plants transformed with vector *pCAMBIA1301*) plants only germinated on MS basal medium without hygromycin. In addition, surface-sterilized seeds (transgenic lines, VC, and WT) were also germinated on MS medium supplemented with 200 mM NaCl, 300 mM mannitol, and two different concentrations of sucrose (1 and 2%) at 25 ± 2°C with a light cycle of 12 h light and 12 h dark. Germination assays were performed in three replicates, with each replicate containing 20 seeds. The rate of emergence/seed germination and mean germination time (MGT) were calculated (Pandey et al., 2015).

One-week-old equally sized plants, including positive T1 transgenic, VC, and WT seedlings, were arranged on MS media supplemented with 200 mM NaCl, 300 mM mannitol, and sucrose (1 or 2%) and incubated for 21 days for growth parameter (root length, shoot length, fresh weight, and dry weight) studies. In addition, uniformly sized seedlings were transferred into 1/2 strength Hoagland medium (Hoagland and Arnon, 1950) and allowed to grow at 25 ± 2°C for 45 days under a 12-/12-h light/dark cycle. Experiments were designed in two sets. In the first set, transgenic plants along with WT and VC plants were studied for stress (salinity and drought) tolerance at ambient CO_2 (400 ppm) concentrations. Acclimatized plants were subjected to 200 mM NaCl or 10% polyethylene glycol (PEG) treatment in a hydroponic culture system for 24 h. For the second set of experiments, all plants (T1, VC, and WT) were first acclimatized at an elevated CO_2 (900 ppm) concentration and then subjected to the stress treatments described above for 24 h in a hydroponic culture system. Subsequently, samples were harvested and processed for physiological, biochemical, and molecular analysis, with all physio-biochemical parameters of transgenic lines being compared with control plants (WT and VC). In addition, the performance of plants was compared under ambient and elevated CO_2 stress conditions.

Measurement of Leaf Gas Exchange Parameter

Transgenic lines, along with WT and VC plants, treated and untreated, were grown in a plant growth chamber (Percival Scientific, United States), with the fourth youngest fully expanded leaves being used to measure photosynthetic parameters, such as net photosynthetic rate (Pn), stomatal conductance (Gs), electron transport rate (ETR), internal CO_2 concentration (Ci), transpiration rate, and VpdL, using a portable photosynthesis system (LI-COR Biosciences Inc., Nebraska). Water use efficiency (WUE) of photosynthesis was calculated (Schulte et al., 2003). Photosynthesis-related measurements were started at 9:00 AM under the following condition: photosynthetically active radiation (PAR), 1,000 μmol m^{-2} s^{-1} photosynthesis photon flux density (PPFD); relative humidity (RH), 55–60%; leaf chamber temperature, 25°C; leaf chamber area, 2 cm; CO_2 flowrate, 300 μm; and reference CO_2 concentration, 400 μmol mol^{-1} for ambient CO_2 and 900 μmol mol^{-1} for elevated CO_2.

Measurement of Chlorophyll Fluorescence and Fluorescence Induction Curves

Plants were kept under actinic light (1,000 μmol^{-2} s^{-1}) for 1 min, at which point photochemical quenching (qP) and quantum efficiency of photosystem II (ϕPSII) were recorded. The light-adapted chlorophyll fluorescence parameters were calculated as follows:

$$\text{Photochemical quenching (qP)} = \frac{(Fm' - Fs)}{(Fm' - Fo')}$$

$$\text{Actual photochemical efficiency of PSII}(\phi\text{PSII}) = \frac{(Fm' - Fs)}{Fm'}$$

Where Fm′ is the maximum fluorescence in light-adapted plant, Fs is the steady state of fluorescence for light-adapted plant, and Fo′ is the initial fluorescence in light-adapted plant.

The dark-adapted maximum photochemical efficiency of PSII (Fv/Fm) was recorded on the same fourth fully expanded leaves using the following equation:

$$\text{Photosynthesis efficiency (PSII)}\ \frac{Fv}{Fm} = \frac{Fm - Fo}{Fm}$$

The dark-adapted fluorescence transient induction curve (based on OJIP curve) was recorded using a chlorophyll analyzer (Handy PEA, Hansatech Co., United Kingdom), and the resulting OJIP curve was analyzed (Strasser and Strasser, 1995). The first (O), second (J), third (I), and fourth (P) phases were recorded with fluorescence intensities at 0.02, 0.3, 2, and 30 ms, respectively.

Measurement of Photosynthetic Pigments

About 100 mg fresh weight (FW) of leaves (control and treated plants) was homogenized in 1 ml chilled *N*,*N*-dimethylformamide (DMF) for 2–3 h in the dark. Absorbance was measured at 665, 647, and 461 nm using a UV–visible spectrophotometer (SpectramaxPlus 384, Molecular Devices, United States). Total chlorophyll (a + b), chlorophyll a (Chl a), chlorophyll b (Chl b), and carotenoids were calculated as per following equation (Inskeep and Bloom, 1985; Chamovitz et al., 1993):

$$\text{Chl a} = 12.70(A_{665}) - 2.79(A_{647})$$

$$\text{Chl b} = 20.70(A_{647}) - 4.62(A_{665})$$

$$\text{Total Chl(a + b)} = 17.90(A_{647}) + 8.08(A_{665})$$

$$\text{Carotenoids} = [A_{461} - (0.046 \times A_{665})] \times 4$$

Measurement of Relative Water Contain

The weight of fresh leaves of equal size about 2 cm (from control and treated plants) was recorded (FW); leaves were immersed in deionized water at room temperature for overnight (16 h). Samples were dried at room temperature (by keeping on blotting papers), and turgid weight (TW) was recorded; after that, samples were dried at 65°C (in an oven) for 48 h, and dry weight (DW) was calculated. The relative water content (RWC) was calculated as percentage by following equation:

$$\text{Relative water contain (RWC)\%} = \left(\frac{FW - DW}{TW - DW}\right) \times 100$$

Measurement of Electrolyte Leakage and Membrane Stability Index

Fresh leaf samples of control and treated plants were washed with deionized water to remove surface-staking electrolytes. Simultaneously, leaves were cut into equal size and immersed into 10 ml of deionized water in closed vials and incubated in gentle shaking at room temperature for 4 h. Electrical conductivity was recorded (L_t) with a conductivity meter (Seven Easy, Mettler Toledo AG8603, Switzerland), and after that, sample vials were incubated at 99°C for 20 min and cooled at room temperature, and final electrical conductivity (L_0) was recorded (Lutts et al., 1996).

For membrane stability index (MSI), fresh leaf samples were washed thoroughly with deionized water, and then, the experiment was conducted into two sets. In one set, leaves were immersed in 10 ml of deionized water and incubated at 40°C for 30 min. In another set, leavers were immersed in 10 ml of water and incubated at 99°C for 10 min. Electrical conductivity was measured for both the sets of vials (Sairam, 1994). The percentage of electrolyte leakage and MSI were calculated using the following equation:

$$\text{Electrolyte leakage(EL)} = \left(\frac{L_t}{L_0}\right) \times 100$$

$$\text{Membrane stability iindex(MSI)} = 100 \times 1 - \left(\frac{L_1}{L_2}\right)$$

Quantification of PPDK Enzyme and Activity Assay

About 500 mg of fresh leaf samples of control and treated plants was homogenized with 2 ml of extraction buffer [50 mM HEPES–KOH and 10 mM of dithiothreitol (DTT); pH 7.5] for the extraction of PPDK enzyme (Yadav et al., 2018). The enzyme was quantified (Bradford, 1976), and the activity was measured at 340 nm in the forward direction by coupling the production of PEP to NADH via PEPC and malate dehydrogenase (MDH)

(Alla and Hassan, 2012). Briefly, a reaction mixture containing 25 mM HEPES–KOH (pH 8.0), 8 mM $MgSO_4$, 10 mM DTT, 10 mM $NaHCO_3$, 2 mM pyruvate, 5 mM $(NH_4)_2SO_4$, 1 mM glucose-6-phosphate, 1 mM ATP, 2.5 mM KPO_4, 0.2 mM NADH, 0.5 U PEPC, and 2 U MDH was prepared. The activity of PPDK was started by adding 0.2 ml of crude enzyme extract in 1 ml freshly prepared reaction mixture, allowed to react at 25°C, and absorbance was read at 340 nm (ε = 6,221 μl μmol^{-1} cm^{-1}). The PPDK specific activity was expressed as nanomoles of enzyme per gram of FW, and enzyme activity was expressed as kat (the release of 1 mol of NAD s^{-1}) mg^{-1} protein.

Measurement of Malondialdehyde and Hydrogen Peroxide Contents

About 500 mg of fresh leaf samples was extracted with 1 ml of ice-cold 0.1% of trichloroacetic acid (TCA) reagent followed by centrifugation at 10,000 *g* for 10 min at 4°C, and the supernatant (extract) was collected for malondialdehyde (MDA) and hydrogen peroxide content. Lipid peroxidation was studied by estimating MDA content (Hodges et al., 1999). Extracts were divided into two sets: first, 0.5 ml of the extract was mixed with 2 ml of TBA (0.65% *w*/*v*, in 20% TCA); second, 0.5 ml of the extract was mixed with 20% TCA. Samples were incubated at 95°C for 30 min and, after cooling, centrifuged at 10,000 *g* for 5 min. The absorbance was measured at 440, 532, and 600 nm, respectively, and MDA content was quantified using the following equation:

$$A = (Abs_{532+TBA} - Abs_{600+TBA}) - (Abs_{532-TBA} - Abs_{600-TBA})$$

$$B = (Abs_{440+TBA} - Abs_{600-TBA}) \times 0.0571$$

$$MDA(nmolg^{-1}) = \frac{\left[\left(\frac{A-B}{157000}\right) \times 10^6\right]}{\text{Weight of tissue in gram}}$$

For the estimation of hydrogen peroxide (H_2O_2) content, 0.25 ml of the extract was mixed with reaction buffer [0.25 mM $FeSO_4$, 0.25 mM $(NH_4)_2SO_4$, 25 mM H_2SO_4, 1.25 mM xylenol orange, and 1 mM sorbitol], followed by incubation at room temperature for 30 min. The absorbance was measured at 560 nm to quantified hydrogen peroxide content with a known concentration of H_2O_2, which was used as a standard (He et al., 2000).

Quantification of Glycine Betaine

Glycine betaine (GB), a quaternary ammonium compound, was quantified with some modifications (Grieve and Grattan, 1983). Glycine betaine was extracted from 1,000 mg of leaves in 20 ml of deionized H_2O (for 24 h at 25°C). Extracts were filtered, diluted 1:1 with 2 N H_2SO_4, and incubated for 1 h at ice. Subsequently, 200 μl of freshly prepared cold KI–I_2 (15.7 g of iodine and 20 g of KI in 100 ml of H_2O) was added in the sample and incubated 15–20 min and then centrifuged at 10,000 *g* for 10 min at 4°C. After that, periodide crystals were separated from an acid medium, dissolved in 3 ml of 1,2-dichloroethane, and incubated for 2.5 h in dark. Simultaneously, a standard curve was prepared with glycine betaine (100 μg/ml), and absorbance was recorded at 365 nm.

Measurement of Antioxidant Enzyme Activity

About 500 mg of the leaf samples was used for the extraction of protein. Samples were homogenized in 2 ml of extraction buffer, containing 50 mM potassium phosphate buffer (pH 7.0), 1 mM EDTA, 0.05% (*w*/*v*) Triton X-100, 5% (*w*/*v*) polyvinylpolypyrrolidone (PVPP), 1 mM phenylmethylsulfonyl fluoride (PMSF), and 2 mM DTT. The extracted protein was quantified (Bradford, 1976) and further used for the estimation of catalase (CAT), ascorbate peroxidase (APX), superoxide dismutase (SOD), and glutathione reductase (GR) activities.

Catalase (1.11.1.6) activity was quantified by observing the disappearance of H_2O_2 (Miyagawa et al., 2000). The activity of catalase was started by adding 20 μg of enzyme extract in 3 ml of the reaction mixture that contained 50 mM of phosphate buffer (pH 7.0) and 10 mM of H_2O_2. The absorbance was measured at 240 nm for every 30 s up to 3 min in a UV–visible spectrophotometer (Molecular Devices, United States). The change in absorbance at 240 nm was recorded, and activity of CAT was measured using ϕ = 43.6 mM^{-1} cm^{-1} as extinction coefficient and expressed as U/mg (Patterson et al., 1984).

Ascorbate peroxidase (APX: EC 1.11.1.11) was estimated by observing the oxidation of ascorbate (Nakano and Asada, 1981). The activity of APX in the reaction was started by adding 40–60 μg of enzyme extract in 3 ml of reaction mixture containing 50 mM phosphate buffer (pH 7.0), 0.5 mM ascorbic acid, and 0.1 mM H_2O_2, and absorbance was recorded at 290 nm for 2 min to determine the specific activity of APX (ϕ = 2.8 mM^{-1} cm^{-1}).

For glutathione reductase (GR: EC 1.8.1.7) activity, 50 μl of the enzyme extract was added in the reaction mixture containing 50 mM of phosphate buffer (pH 7.5), 1 mM EDTA, 1 mM glutathione oxidized (GSSG), 0.75 mM 5,5-dithio-bis-(2-nitrobenzoic acid) (DTNB), and 0.1 mM NADPH. Absorbance was recorded at 412 nm for 2 min, and specific activity was estimated (ε = 26.6 mM^{-1} cm^{-1}).

For the measurement of SOD activity, the inhibition of photochemical reduction in nitro-blue tetrazolium (NBT) was used (Beyer and Fridovich, 1987). For the enzyme assay, 3 ml of reaction mixture containing 50 mM phosphate buffer (pH 7.8), 9.9 mM L-methionine, 58 μM NBT, 0.025% Triton-X, and 2.4 μM riboflavin was prepared. Simultaneously, 0.1 ml of the enzyme extract was added into the reaction mixture and allowed to react for 10 min at an illuminated light along with blank (containing reaction mix without enzyme extract). The reaction was stopped by incubating the sample (and blank) in the dark for 15 min. The amount of enzyme required for 50% inhibition of the photochemical reduction in NBT was recorded at 560 nm and represented as 1 U of SOD activity.

Measurements of Total Sugar, Reducing Sugar, Starch, Free Amino Acid, and Polyphenol Content

About 1,000 mg of leaves was extracted in 80% ethanol. The extract was reacted with 2 ml of anthrone reagent (0.2% *w*/*v* anthrone in 95% of H_2SO_4) for total sugar and 3 ml of freshly prepared 3,5-dinitrosalicylic acid (DNS) reagent for reducing sugar estimation, respectively. Subsequently, samples were incubated at a boiling water bath for 5 min and cooled at room temperature, and the absorbance was measured at 630 and

540 nm, respectively. For starch estimation, the left pellet was digested with 52% of perchloric acid and centrifuged at 10,000 *g* for 10 min. The digested product was reacted with 3 ml of anthrone reagent, incubated at a boiling water bath for 10 min, and the absorbance was recorded at 630 nm (Ghose, 1987). For estimation of free amino acid and polyphenol, about 0.2 ml of plant extracts was reacted with Ninhydrin reagent (Sugano et al., 1975) and Folin–Ciocalteu (FC) reagent (Chandler and Dodds, 1983), respectively. The reaction mixture was incubated at a boiling water bath, and absorbance was measured at 540 and 650 nm for free amino acid and polyphenol, respectively. Known concentration of glucose, glycine, and catechol were used as a standard for the estimation of sugars (including starch), amino acids, and polyphenol, respectively.

Gene Expression Analysis

Total RNA was isolated from transgenic lines, WT and VC plants (Chomczynski and Sacchi, 1987), converted to cDNA using reverse transcriptase according to the manufacturer's (Promega, United States) instructions. Primer *NtActine* was used as an internal reference to normalize the gene expression of selected genes studied by real-time quantitative PCR (**Supplementary Table S1**). Differential transcript expression was studied for key genes involved in the metabolism of reactive oxygen species (ROS) (*NtCAT*, *NtAPX*, *NtGR*, and *NtSOD*), and photorespiration [hydroxypyruvate reductase (NtHPR) and glycolate oxidase (*NtGO*)]. The real-time quantitative PCR (RT-qPCR) was performed in a CFX 96TM Real-Time system (Bio-Rad, United States) with 1× SYBR green PCR reaction mix (**Supplementary Table S1**). The relative expression of the transcript ($2^{-\Delta\Delta Ct}$) was compared with the corresponding control (Livak and Schmittgen, 2001).

Analysis of Metabolites

Total metabolites were extracted from transgenic lines, WT, and VC plants and analyzed by gas chromatography–mass spectrometry (Lisec et al., 2006). Leaf samples (1,000 mg) were made fine powder using liquid N_2 and extracted with 100% ethanol (ice cold). Simultaneously, 30 μl of adonitol (0.2 mg/ml) was added as an internal reference, vortexed for 20 s, incubated at 70°C, after which it was sonicated for 10 min at room temperature. Samples were centrifuged at 10,000 *g* for 10 min, clear supernatant was collected, 325 μl chloroform was added, followed by addition of 700 μl of water; samples were mixed thoroughly and centrifuged at 10,000 *g* for 5 min. The aqueous phase was collected and dried in a vacuum concentrator. About 60 μl of methoxyamine pyridine was added and incubated at 37°C for 2 h. Finally, 130 μl of *N*-methyl-*N*-(trimethylsilyl) trifluoroacetamide (MSTFA) was added, incubated for 30 min at 37°C, and used for the gas chromatography–mass spectrometry (GC-MS) analysis (GC-2010 Plus Shimadzu, Model GCMS TQ8040). The chromatographic parameters were as follows: column, RTX-5MS (diphenyl dimethyl polysiloxane, 30.0 m × 0.25 mm); injection, split injection; injection volume, 1 μl; split ratio, 50.0; and temperature, 250°C (Tanna et al., 2018). The initial temperature was 80°C with a hold time of 2 min; after that, temperature was raised up to 315°C with a rate of 10°C/min and held for 15 min (Tanna et al., 2019). As a carrier, helium gas was used with a flowrate of 2 ml/min, and the total processing time was 40–50 min. Mass spectra were recorded, metabolites were identified by matching peaks with available NIST library, and concentration was measured with respect to internal reference peak area and expressed as μg/g FW.

In situ Localization of Peroxide (H_2O_2) and Superoxide Radicals (O_2^-)

In situ analysis of peroxide and superoxide radicals were analyzed by histochemical staining with 3,3-diaminobenzidine (DAB) and NBT, respectively (Shi et al., 2010). Both DAB and NBT staining solutions were prepared with a concentration of 1 mg/ml in 10 mM phosphate buffer (pH 3.8 for DAB and pH 7.8 for NBT). Same age of leaves, harvested from transgenic lines, WT, and VC were immersed in their corresponding staining solutions and incubated for 2 h in the dark at room temperature. Later on, they were exposed to light until the brown and blue color visualized on the leaf surface. The staining solutions were removed, samples were bleached with aqueous ethanol (70%), and photographs were taken.

Statistical Analysis

All experiments were performed in triplicate, and each replicate contained 15 plants. Data were given as mean ± standard error (SE), and statistical significance was determined by analysis of variance (ANOVA), using Tukey's honestly significant difference (HSD) test. Significant differences were considered at $p < 0.05$ and designated by different letters. Correlation and multivariate analyses were performed using Pearson's correlation matrix, regression analysis, and principal component analysis, using SYSTAT and Sigma Plot software.

RESULTS

Genomic Organization and Genetic Transformation of the *PPDK* Gene

A 4,434 bp *PPDK* gene sequence, obtained from genomic DNA of *S. monoica*, comprised six introns flanked by seven exons (**Supplementary Figure S1**). A full-length cDNA (2,862 bp) of the *SmPPDK* gene (**Supplementary Figure S2**) was cloned in *pCAMBIA1301* under the control of the cauliflower mosaic virus (CaMV) 35S promoter (*pCAMBIA1301:SmPPDK*) (**Figure 1A**) and transformed to tobacco, resulting in 50 transgenic lines (T0) being obtained. The presence of the transgene (*PPDK*, *hptII*, and *uidA*) was confirmed in T0-transgenic lines by PCR amplification, using gene-specific primers (**Supplementary Table S1**). In addition, T0 transgenic seedlings and controls [wild-type (WT) and vector control (VC)] were subjected to histochemical GUS assays. Based on molecular confirmation by PCR and histochemical GUS assays, five transgenic lines L1, L20, L32, L33, and L40 were selected for further analysis. For these, T1 transgenic lines were further confirmed by histochemical GUS assay (**Figure 1B**) and PCR (**Figure 1C**), in comparison with the controls. Semiquantitative reverse

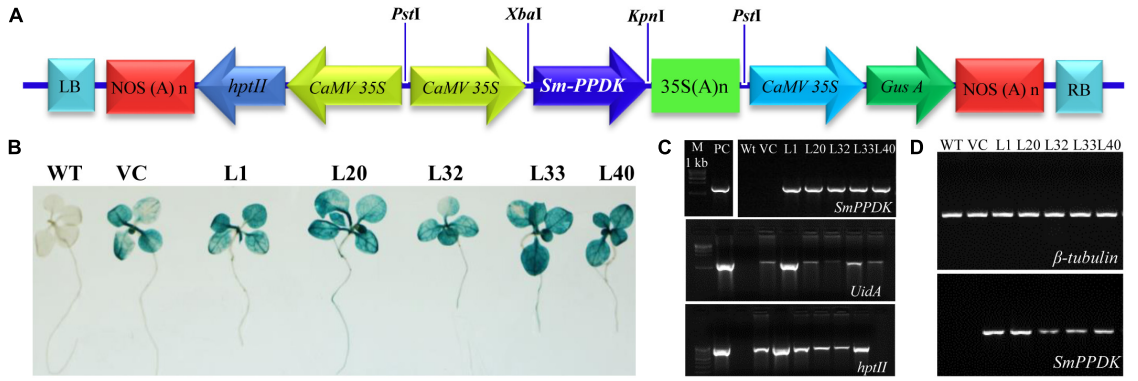

FIGURE 1 | Vector construct and conformation of transgene in transgenic lines. Gene construct: **(A)** *pCAMBIA1301:SmPPDK*, **(B)** histochemical β-glucuronidase (GUS) assay of selected transgenic lines, **(C)** molecular confirmation of transgenic lines by PCR, and **(D)** semiquantitative reverse transcriptase PCR.

transcriptase PCR, in which β-*tubulin* was used as an internal reference gene for normalization, demonstrated that there was overexpression of the *SmPPDK* gene in selected T1 transgenic lines (**Figure 1D**). Quantitative real-time-based analysis confirmed that all transgenic lines (L1, L20, L32, L33, and L40) contained a single integration event (**Supplementary Figure S3**). Scanning electron microscopy (field emission) of leaves of transgenic and control plants confirmed that overexpression of *SmPPDK* did not affect the ultrastructure of mesophyll cells (**Supplementary Figure S4**).

Overexpression of the *SmPPDK* Gene Improved Seed Germination and Seedling Growth Under Stress Conditions

Transgenic seed showed significantly higher germination (mean germination time and seed germination rate) compared to WT and VC seeds under different stress conditions (**Supplementary Figures S5, S6**). They also took less time to germinate (higher seed germination rate) under different abiotic stress conditions, compared to WT and VC seeds. Similarly, improved growth (**Supplementary Figure S7**), including increased fresh weight, dry weight, shoot length, and root length (**Supplementary Figure S8**), and morphological changes (**Supplementary Figure S9**) were observed in transgenic seedlings under different abiotic stress conditions, compared to WT and VC plants.

SmPPDK Overexpressing Transgenic Lines Showed Improved Photosynthesis and Physiology Under Different Abiotic Stress Conditions at Ambient and Elevated CO_2 Level

A cumulative principal component analyses revealed a complex biplot comprised of seven observations (WT, VC, and transgenic lines, L1, L20, L32, L33, and L40) and 114 variables (**Supplementary Figure S10**). Principal components analysis (PCA) and heat map showed the differential physiological and biochemical response of transgenic lines (L1, L20, L32, L33, and L40) and control plants (WT and VC) under normal and stress conditions (**Supplementary Figures S10, S11**).

CO_2 Assimilation Indicators

Net photosynthesis rate (Pn) of transgenic lines (16–24 μmol CO_2 m^{-2} s^{-1}) was higher than that of control (WT and VC) plants (12–17 μmol CO_2 m^{-2} s^{-1}) under control and stress conditions at ambient CO_2 levels. Although Pn of all plants (transgenic lines along with WT and VC) significantly lowered under elevated CO_2 conditions; the level of decrease was less for the transgenic lines and was still higher (14–23 μmol CO_2 m^{-2} s^{-1}) compared to control (WT and VC) plants (3–12 μmol CO_2 m^{-2} s^{-1}) under control and stress conditions (**Figure 2A**). Under ambient CO_2 conditions, no significant difference in stomatal conductance (Gr; 0.1–0.2 mmol H_2O m^{-2} s^{-1}) was observed between transgenic lines and control plants (WT and VC), whereas under NaCl and drought stress, transgenic lines showed higher stomatal conductance (0.02–0.8 and 0.01–0.08 mmol H_2O m^{-2} s^{-1}, respectively) than WT and VC plants (0.01–0.05 mmol H_2O m^{-2} s^{-1}). At elevated CO_2 levels, stomatal conductance significantly decreased under control conditions compared to ambient CO_2, however, transgenic lines maintained a higher level of conductance under control and stress conditions (0.02–0.1 mmol H_2O m^{-2} s^{-1}) than that of WT and VC plants (0.005–0.05 mmol H_2O m^{-2} s^{-1}) (**Figure 2B**). At ambient CO_2 levels, the vapor pressure difference between leaf intercellular air spaces and the atmosphere (VpdL) was significantly higher in transgenic lines (1.3–1.8 kPa) compared to WT and VC plants (1.2–1.6 kPa), under control and stress conditions. Under elevated CO_2 levels, VpdL decreased in control and stress conditions, however, no significant difference was observed between transgenic lines and control (WT and VC) plants (**Figure 2C**). The trend of photosynthetic electron transport rate (ETR) complemented that of photosynthetic rate and was similar in both controlled and stressed plants under ambient and elevated CO_2 conditions (**Figure 3A**). At ambient CO_2 levels, the transpiration rate (Tr) was higher in all plants (transgenic lines along with WT and VC) under control

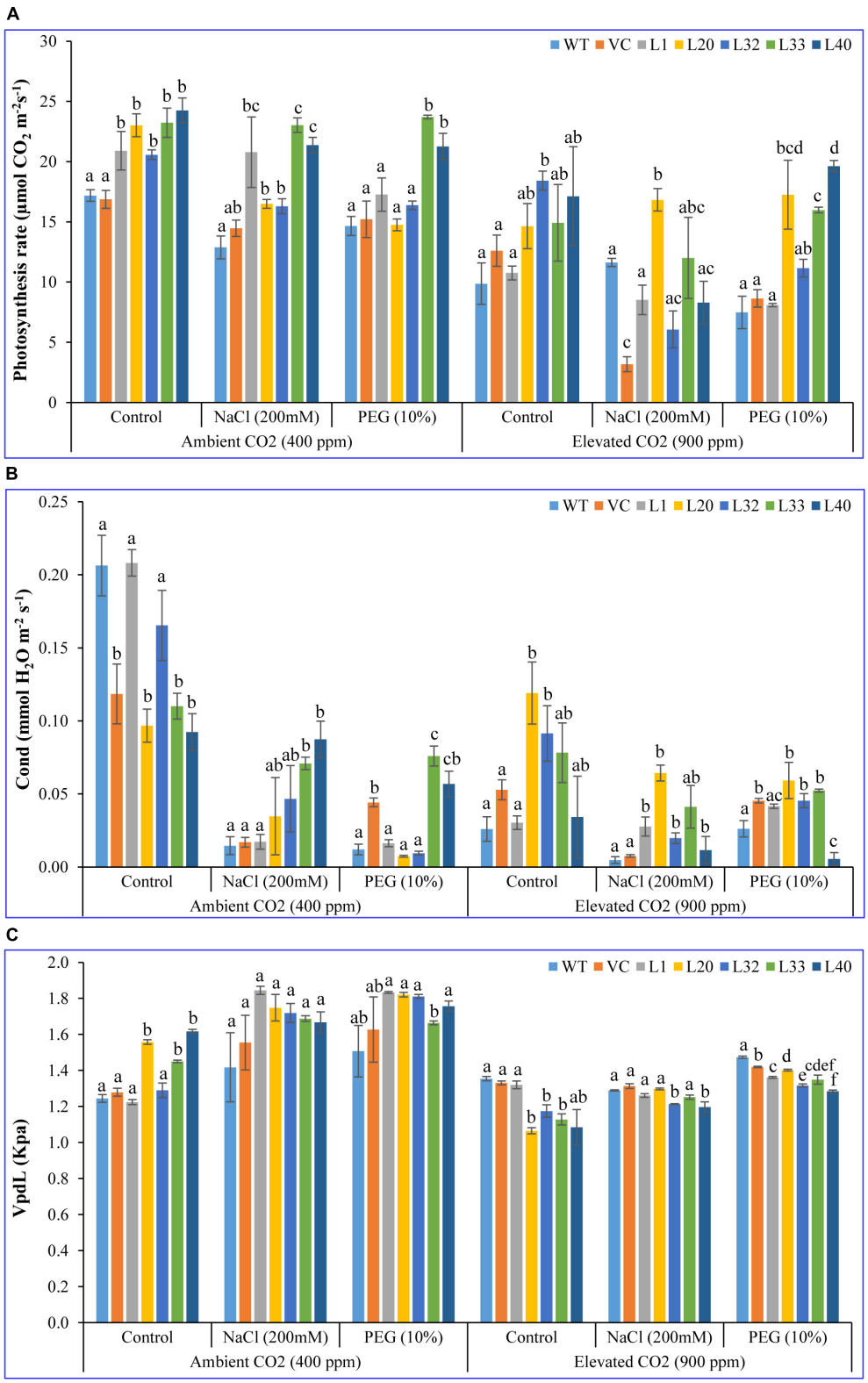

FIGURE 2 | Analysis of the photosynthesis parameters (net photosynthesis, stomatal conductance, and VpdL) of transgenic lines. **(A)** Net photosynthesis, **(B)** stomatal conductance, and **(C)** VpdL of T1 transgenic lines (L1, L20, L32, L33, and L40), wild type (WT), and vector control (VC) were analyzed under salinity (200 mM NaCl) and osmotic [10% polyethylene glycol (PEG)] stress condition grown in ambient and elevated CO_2 environment. Bars represent means ± SE, and values with different letters are significant at $P < 0.05$.

conditions (1.5–2.5 mmol H_2O m^{-2} s^{-1}), compared to elevated CO_2 conditions (0.4–1.5 mmol H_2O m^{-2} s^{-1}), and no significant difference was noticed between transgenic lines and control (WT and VC) plants (**Figure 3B**), although, under elevated CO_2 levels, transgenic lines showed a higher Tr in control and drought stress conditions than that of WT and VC plants. In addition, WUE of photosynthesis was higher in transgenic lines under salt (15–77) and drought (19–109) stress at ambient CO_2 levels, compared to WT (12) and VC (20–63) plants (**Figure 3C**). However, at elevated CO_2 levels, WUE decreased in all plants, however, the degree of decline was lower in transgenic lines than that of control (WT and VC) plants. Overall, these results indicated that tobacco transgenic for *SmPPDK* had better photosynthesis characteristics than WT and VC plants, under both ambient and elevated CO_2 stress conditions.

Chlorophyll a Fluorescence Parameters and Fluorescence Induction Curve

The pattern of ϕPSII and qP was found to be quite similar in all plants (transgenic lines and control, WT, and VC) under both ambient and elevated CO_2 levels. At ambient CO_2 levels, no significant difference was observed between transgenic and control plants, under both control and stress (salinity and drought) treatments. By contrast, at elevated CO_2 levels, transgenic lines showed a higher ϕPSII and qP than WT and VC plants under control and stress conditions (**Figure 4**). Consequently, the maximal quantum yield of PSII (Fv/Fm) did not show a significant difference between plants under ambient CO_2 levels for control and salt stress conditions, although under drought stress conditions, transgenic lines showed a higher Fv/Fm, as compared to WT and VC. However, under elevated CO_2 stress conditions, transgenic lines exhibited a higher Fv/Fm compared to WT and VC plants (**Figure 4**). Overall, transgenic lines showed higher values for chlorophyll fluorescence parameters under elevated CO_2 stress conditions than WT and VC plants. These results suggested that, under stress, the transgenic lines underwent a slight photoinhibition, however, higher photochemical efficiency was still maintained under drought stress at ambient and elevated CO_2 levels.

The OJIP curve represented a polyphasic fluorescence transient curve, which gave an indication of PSII efficiency under stress conditions (**Supplementary Figure S12**). The curve for the transgenic lines overlapped with that of WT and VC plants at ambient CO_2 levels under control and salt treatment, whereas Fm values were higher in transgenic lines than in WT and VC plants. However, under drought treatment, the OJIP curves of the transgenic lines were significantly changed from those of WT and VC plants. Similarly, under elevated CO_2 levels, no significant changes were noticed. Differences were observed under salt and drought stress treatments, however, the impact on the OJIP curve of transgenic lines was lower than that of WT and VC plants. Compared to control plants, changes observed in the initial fluorescence (Fo) of transgenic lines were comparatively insignificant, however, the maximum fluorescence (Fm) significantly decreased in the WT and VC plants (**Supplementary Figure S12**). The values of Fm were related to the antenna complex, its structure, function, and energy dissipation. These observations suggested that elevated CO_2 levels could cause less damage to PSII antenna complexes under salt or drought stress in transgenic lines, compared to corresponding control (WT and VC) plants.

Physiological Characteristics

Change in the RWC of studied plants (transgenic lines, WT, and VC) was insignificant at ambient CO_2 levels, under control and stress conditions. By contrast, there was a distinct difference for transgenic lines under drought stress at elevated CO_2 levels (**Figure 5A**). MSI was considerably higher in transgenic lines (62–93%) than WT and VC plants (51–75%) at both ambient and elevated CO_2 levels, under control and stress conditions (**Figure 5B**). In addition, EL was significantly lower in transgenic lines (8.5–18.5) compared to WT and VC plants (13–21) at elevated CO_2 levels, under control and stressed conditions, whereas EL was higher at ambient CO_2 compared to that at elevated CO_2 levels under both control and stress conditions (**Figure 5C**). At ambient CO_2 levels, transgenic lines showed higher chlorophyll content under stress compared to WT and VC plants. Elevated CO_2 levels resulted in significantly higher chlorophyll content in transgenic lines, compared to WT and VC plants, under control and stress treatments (**Supplementary Figure S13**). By contrast, transgenic lines did not show any significant difference in carotenoid content at ambient and elevated CO_2 levels under control and stress conditions (**Supplementary Figure S13**). All these observations suggested that transgenic plants showed an improved physiological status under stress conditions compared to control (WT and VC) plants.

SmPPDK Activity in Transgenic Plants Under Different Stress Conditions and Elevated CO_2

The maximum PPDK activity was measured in the L40 transgenic line, which was 3.5-fold higher than that of WT plants under control conditions at ambient CO_2 levels. Similarly, L20 showed 3.8-fold higher activity under salinity stress at ambient CO_2 levels. PPDK activity was more pronounced under drought stress conditions in ambient CO_2, being 4.1-fold higher than for WT plants. By contrast, PPDK activity was found to be higher at elevated CO_2 levels under both control and stress conditions. At elevated CO_2 levels, the L32 line showed about a 10-fold higher activity under control conditions, while L20 showed a maximum of a 2.2-fold increase under salt stress. Under drought stress, L40 showed a maximum 25-fold higher activity of PPDK compared to the control (WT and VC) plants (**Supplementary Figure S14**). All these observations indicated that the transgenic lines had higher *Sm*PPDK enzyme activity under abiotic stress in elevated CO_2 conditions.

SmPPDK transcript expression showed a maximum of about 5-fold higher levels in L1 and L33 under NaCl stress conditions, followed by a 3-fold upregulation for L20, whereas a maximum of 6-fold higher expression was noted in L33, followed by a 4.5-fold upregulation for L20 under drought stress, compared to control (unstressed) conditions in an ambient

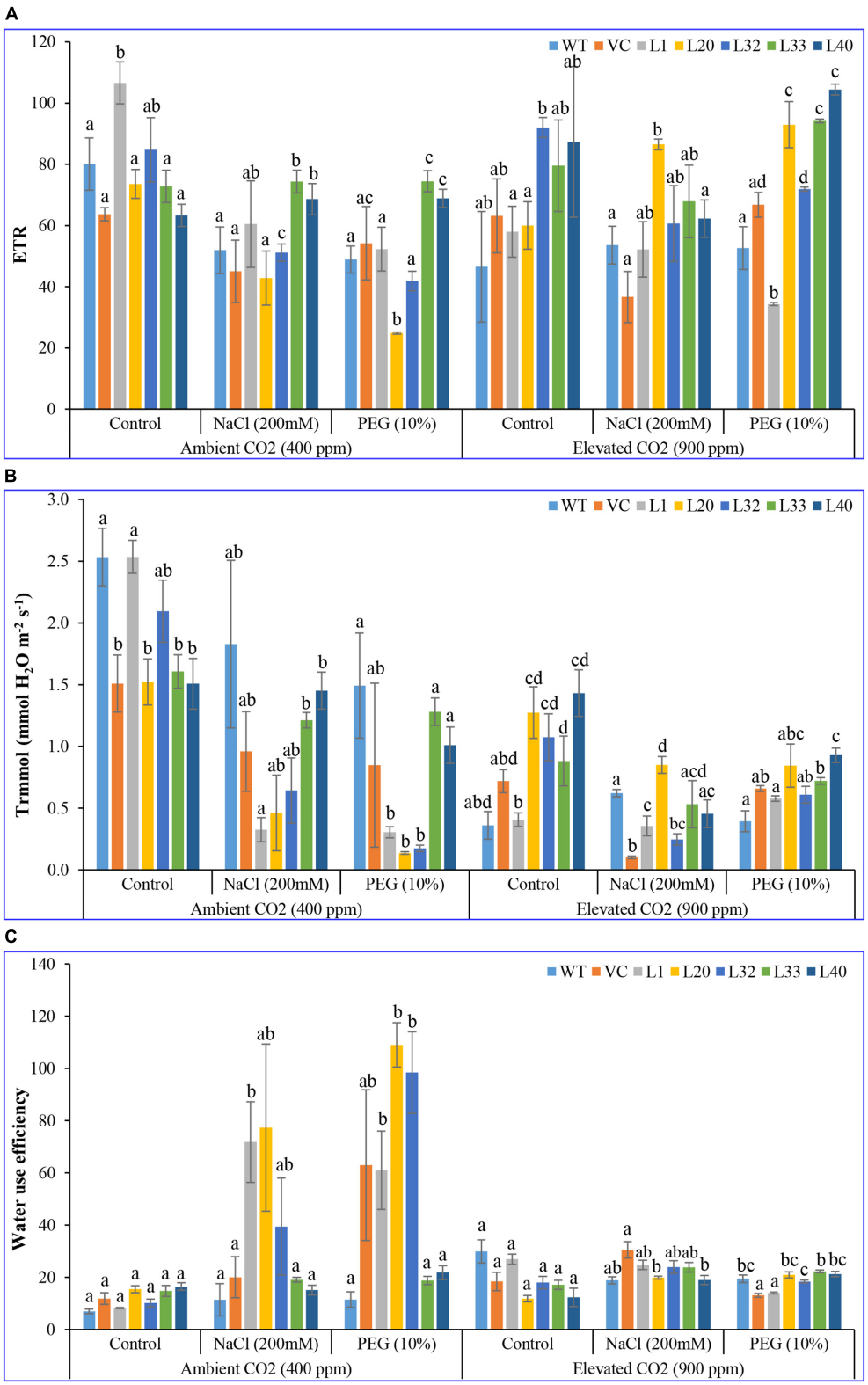

FIGURE 3 | Analysis of the photosynthesis parameters (electron transport rate, transpiration rate, and water use efficiency) of transgenic lines. **(A)** Electron transport rate, **(B)** transpiration rate, and **(C)** water use efficiency of T1 transgenic lines (L1, L20, L32, L33, and L40), wild type (WT), and vector control (VC) were analyzed under salinity (200 mM NaCl) and osmotic [10% polyethylene glycol (PEG)] stress condition grown in ambient and elevated CO_2 environment. Bars represent means ± SE, and values with different letters are significant at $P < 0.05$.

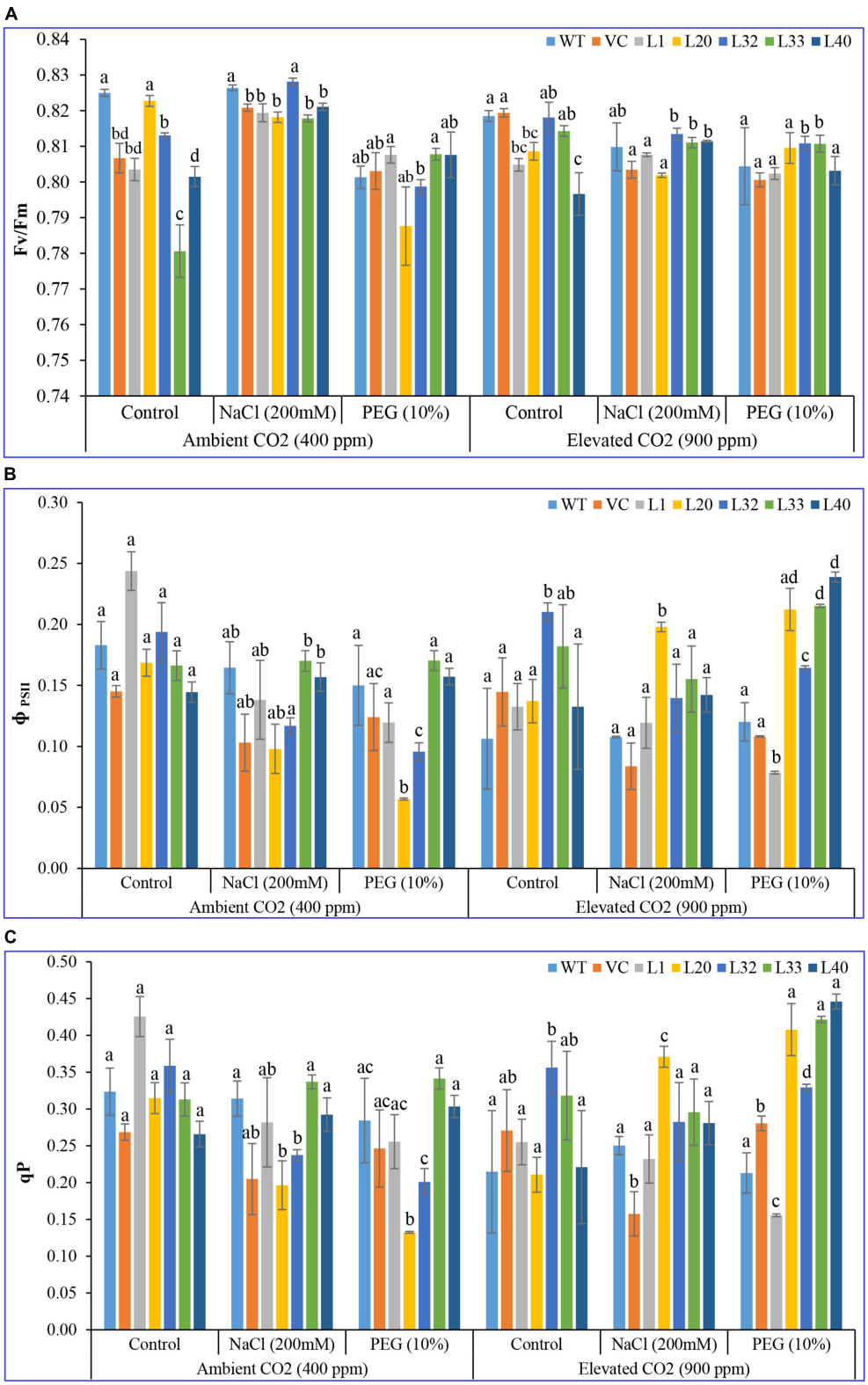

FIGURE 4 | Analysis of the photosynthesis parameters (Fv/Fm, ϕPSII, and photochemical quenching) of transgenic lines. The maximum photochemical efficiency of **(A)** PSII–Fv/Fm, **(B)** the actual photochemical efficiency of PSII–ϕPSII, and **(C)** photochemical quenching of T1 transgenic lines (L1, L20, L32, L33, and L40), wild type (WT), and vector control (VC) were analyzed under salinity (200 mM NaCl) and osmotic [10% polyethylene glycol (PEG)] stress condition grown in ambient and elevated CO_2 environment. Bars represent means ± SE, and values with different letters are significant at $P < 0.05$.

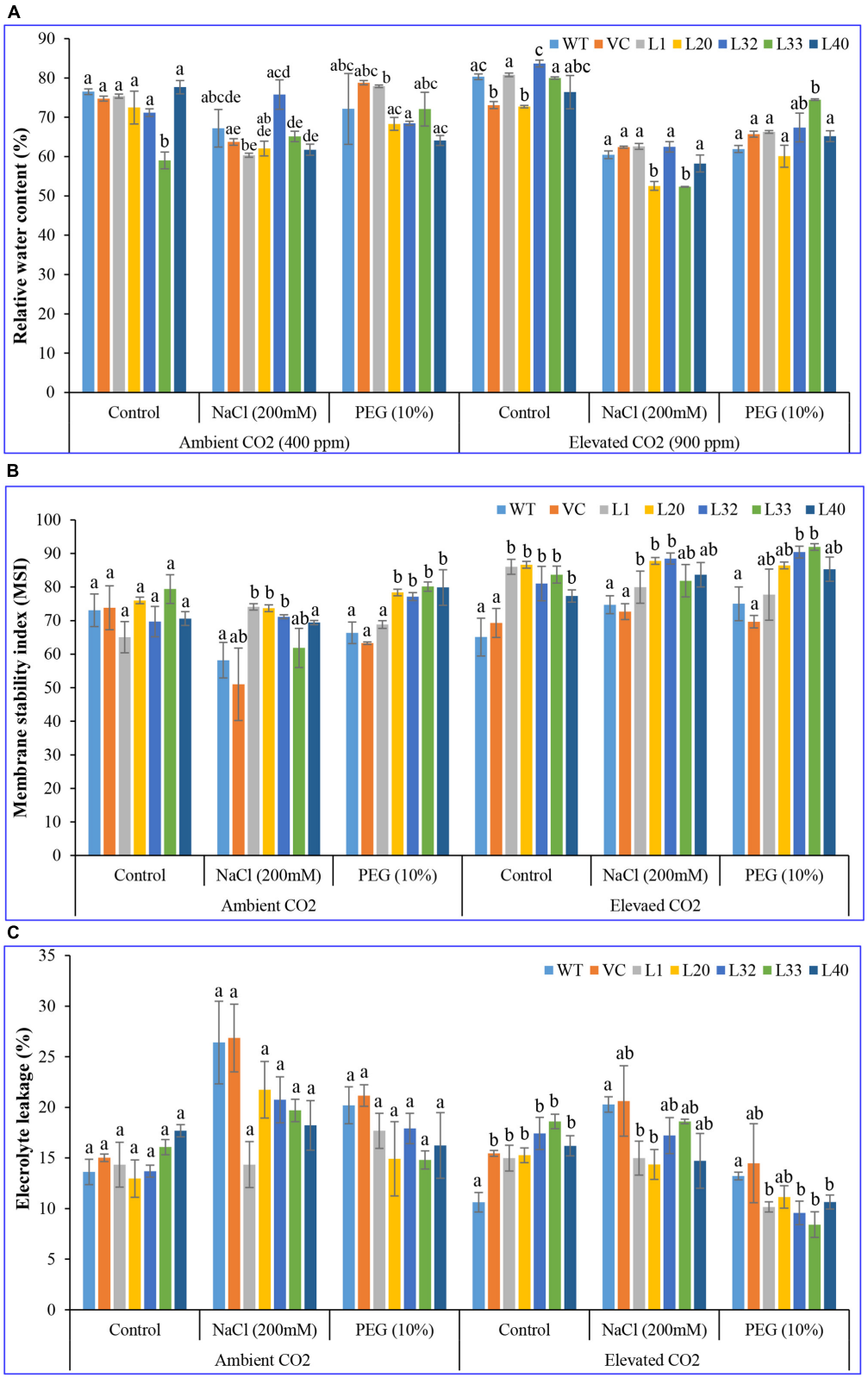

FIGURE 5 | Analysis of the physiological status of transgenic lines. **(A)** Relative water content, **(B)** membrane stability index, and **(C)** electrolyte leakage of wild type (WT), vector control (VC), and T1 transgenic lines (L1, L20, L32, L33, and L40) were measured under salinity (200 mM NaCl) and osmotic [10% polyethylene glycol (PEG)] stress condition grown in ambient and elevated CO_2 environment. Bars represent means ± SE, and values with different letters are significant at $P < 0.05$.

CO_2 environment. Similarly, transgenic line L32 showed a maximum of 4- and 7.5-fold increase in expression under NaCl and drought stress conditions, respectively, in an elevated CO_2 environment, followed by an increase shown by transgenic line L1 (**Supplementary Figure S14**).

Overexpression of *SmPPDK* Protected Plants From Abiotic Stress-Induced Reactive Oxygen Species Damage

Reactive oxygen species (ROS), such as superoxide radical (O_2^-) and hydrogen peroxide (H_2O_2), often accumulated when plants were senescing or facing different abiotic stresses. However, some enzymatic antioxidant defense mechanisms could act to protect plants against impairment due to oxidative stress. When plants were subjected to abiotic stress, a large amount of ROS accumulated with the antioxidant system not able to compensate; this situation was often indicated by elevated lipid peroxidation (measured by MDA content) and reduced levels of antioxidant enzymes.

For both ambient and elevated CO_2 levels, most of the transgenic lines had a lower MDA content, under stress conditions, compared to WT and VC plants (**Figure 6A**). The accumulation of ROS in transgenic lines was considerably lower than for WT and VC plants under salt and drought stress at both ambient and elevated CO_2 conditions. Under elevated CO_2, the MDA content decreased in all samples for control and stress treatments, however, the MDA content of transgenic lines was significantly lower than in WT plants.

For ambient CO_2 levels, no significant difference was observed in H_2O_2 content for transgenic lines under salt stress, compared to that for control plants, however, under drought stress, L32, L33, and L40 lines accumulated a significantly higher amount of H_2O_2 compared to WT and VC plants. By contrast, at elevated CO_2 levels, transgenic lines had a lower level of H_2O_2 compared to WT and VC plants, under control and salt stress conditions, whereas under drought stress, all transgenic lines accumulated significantly higher H_2O_2 contents (**Figure 6B**). These results showing a lower level of MDA and a higher level of H_2O_2 in transgenic lines indicated that overexpression of the *SmPPDK* gene ameliorated abiotic-stress-induced ROS damage under elevated CO_2 conditions, with it being more distinct in transgenic lines under drought stress at elevated CO_2 levels.

GB acted as an osmoprotectant under a stressful environment, in ambient CO_2 conditions, being significantly increased under stress in all transgenic lines compared to the control plants. However, under salt stress, L32 showed a higher glycine content, whereas under drought stress, L20, L33, and L40 lines had significantly higher glycine betaine as compared to WT and VC plants. Similarly, at elevated CO_2 conditions, transgenic lines accumulated a higher amount of glycine betaine as compared to WT and VC plants under control and stress conditions (**Figure 6C**). In addition, increased glycine betaine content was more pronounced in transgenic lines under drought stress at both ambient and elevated CO_2 conditions.

In situ, higher localization of superoxide free radicals (O_2^-) and peroxide (H_2O_2) was observed in the leaves of control plants (WT and VC) compared to that of transgenic lines, under stress conditions at ambient and elevated CO_2 levels. Similarly, higher accumulations were also found in elevated CO_2 conditions compared to ambient CO_2 levels under different stress treatments (**Figure 7**).

Overexpression of the *SmPPDK* Gene Enhanced an Antioxidant Defense System Under Adverse Stress Conditions

High activity of CAT was observed in transgenic plants under stress in both ambient and elevated CO_2 conditions, as compared to WT and VC plants, although it was significantly more pronounced under drought stress at elevated CO_2 levels (**Figure 8A**). Similarly, high APX activity was detected in all stress-treated plants, and the activity increased significantly in the drought-treated transgenic plants under elevated CO_2 conditions, compared to WT and VC plants (**Figure 8B**). The activity of SOD was significantly higher in the transgenic lines under salt and drought stress in ambient CO_2 conditions, as compared to that in WT and VC plants. By contrast, transgenic lines showed significantly lower activity of SOD under control and stress treatments at elevated CO_2 condition as compared to WT and VC plants (**Figure 8C**). All transgenic lines showed significantly higher activity of GR under stress conditions in both ambient and elevated CO_2 environments compared to WT and VC plants (**Figure 8D**).

Transcript expression analysis of ROS scavenging enzyme-encoding genes from tobacco, e.g., catalase (*NtCAT*), ascorbate peroxidase (*NtAPX*), superoxide dismutase (*NtSOD*), and glutathione reductase (*NtGR*), was performed (**Supplementary Figure S15**). The transcript level of *NtCAT* decreased in all plants under elevated CO_2 conditions compared to the control. Transgenic lines L20 and L40 showed about a 3.5-fold upregulation of this transcript under drought stress in ambient CO_2. The transcript for *NtAPX* increased 2–3-fold under stress at ambient CO_2 levels. However, at elevated CO_2 levels, its expression decreased on drought treatment, although it was slightly increased under salt stress (1.5–2-fold). By contrast, in elevated CO_2 condition, the transgenic line L33 showed a 5- and 3-fold upregulation of the transcript for *NtAPX* under salt and drought stress, respectively Both *NtSOD* and *NtGR* genes were marginally upregulated (1.2–2-fold) in the transgenic under stress conditions in both ambient and elevated CO_2 environments, except for line L40, which showed a 7- and 3-fold upregulation of the *NtGR* gene under salt and drought stress, respectively, in ambient CO_2 conditions.

Overexpression of the *SmPPDK* Gene Mitigated the Effect of Abiotic Stress Under Elevated CO_2 by Lowering the Photorespiration Rate in Transgenic Lines

Photorespiration was considered the second most imperative metabolism in plants. However, it increased under stress conditions, such as drought and salinity, leading to H_2O_2

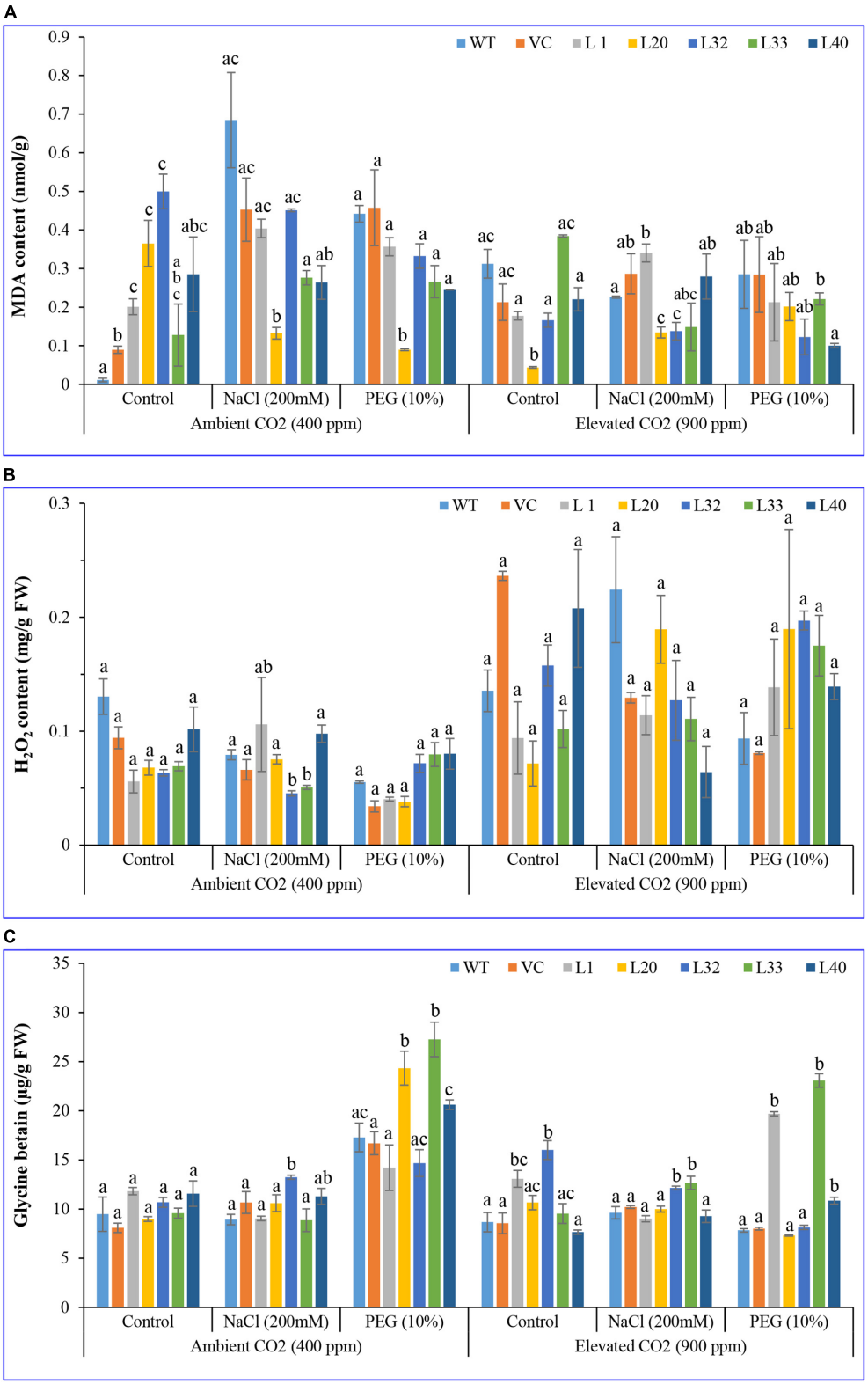

FIGURE 6 | Biochemical analysis of transgenic lines. Estimation of **(A)** lipid peroxidation–malondialdehyde, **(B)** hydrogen peroxide, and **(C)** glycine betaine contents of wild type (WT), vector control (VC), and T1 transgenic lines (L1, L20, L32, L33, and L40) were measured under salinity (200 mM NaCl) and osmotic [10% polyethylene glycol (PEG)] stress condition grown in ambient and elevated CO_2 environment. Bars represent means ± SE, and values with different letters are significant at $P < 0.05$.

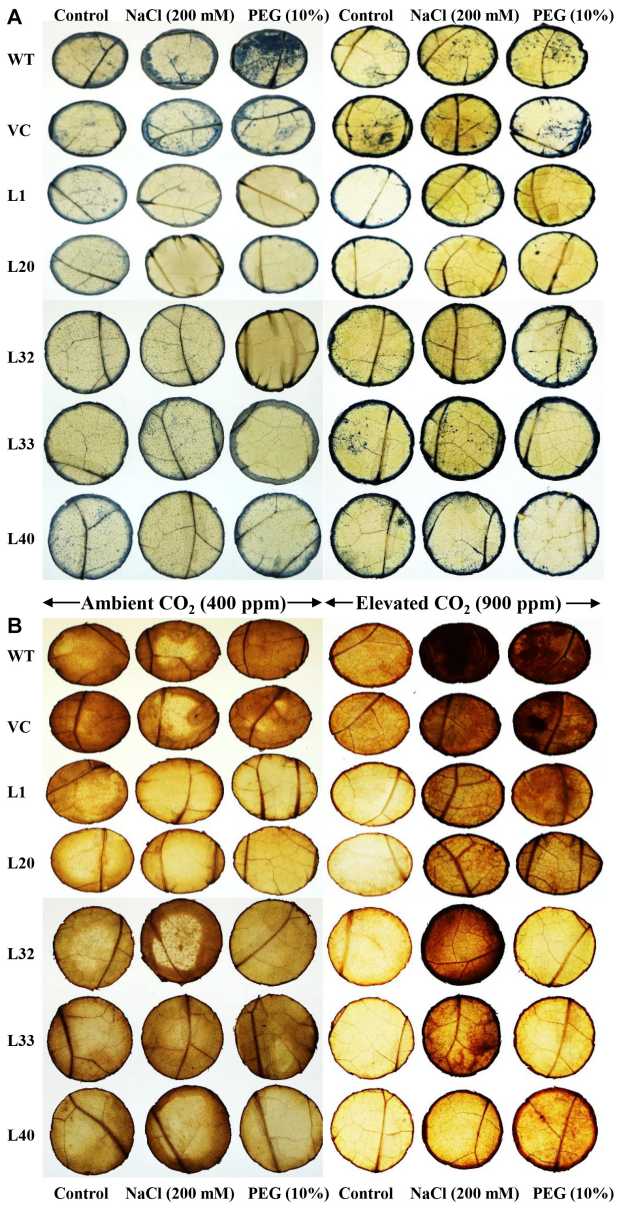

FIGURE 7 | *In vivo* localization of free radicals. Localization of **(A)** superoxide free (O_2^-) radicals and **(B)** hydrogen peroxide (H_2O_2) in the leaves of wild type (WT), vector control (VC), and T1 transgenic lines (L1, L20, L32, L33, and L40) under salinity (200 mM NaCl) and osmotic [10% polyethylene glycol (PEG)] stress condition grown in ambient and elevated CO_2 environment.

production in plant cells. The Gly/Ser ratio, one of the primary indicators of photorespiration, was significantly higher in selected transgenic plants and WT plants under ambient CO_2 conditions compared to plants grown under stress (**Supplementary Figure S16A**). By contrast, the ratio was lower in transgenic lines grown under an elevated CO_2 environment compared to WT plants. Photorespiration-associated genes from tobacco, *NtHPR* and *NtGO*, were differentially expressed under different stress conditions. In an ambient CO_2 environment, the *NtHPR* gene was downregulated in transgenic lines under salt and drought stress conditions, compared to WT and VC plants (**Supplementary Figure S16B**). Similarly, at elevated CO_2 levels, expression of *NtHPR* gene was higher in control plants compared to transgenic lines under stress conditions. By contrast, the *NtGO* gene was considerably upregulated in an elevated CO_2 environment compared to ambient CO_2 conditions (**Supplementary Figure S16C**). In ambient CO_2 conditions, *NtGO* gene was downregulated in transgenic lines under salt (except L1) and drought (except L1 and L20) stress, whereas in elevated CO_2 conditions, the *NtGO* gene was upregulated in all stress conditions except for L40 under NaCl.

SmPPDK Transgenic Lines Accumulated Sugars, Polyphenols, and Free Amino Acids Under Abiotic Stress Conditions

In ambient and elevated CO_2 conditions, total soluble sugar and reducing sugar were found to be significantly higher in transgenic lines under control conditions compared to WT and VC plants, however, this effect was more pronounced at elevated CO_2 levels (**Supplementary Figure S17**). However, at ambient CO_2 levels under salt stress, no significant difference in total sugar and reducing sugar contents were noticed among transgenic lines and WT and VC plants. By contrast, in an elevated CO_2 state, transgenic lines accumulated a significantly higher amount of total sugar and reducing sugar under salt and drought stress, compared with WT and VC plants. The starch content increased considerably in L20 and L32 under control conditions, whereas it was reduced under salt and drought stress at ambient CO_2 levels (**Supplementary Figure S17**). Under drought stress, L1 and L40 accumulated about a 12- and 5-fold higher starch content, respectively, compared to WT plants. By contrast, under elevated CO_2 conditions, all transgenic lines accumulated high starch contents (**Supplementary Figure S17**).

Free amino acid (FAA) content showed no distinction among transgenic lines and WT and VC plants under control and NaCl stress conditions at ambient CO_2 levels. However, it increased considerably under drought stress in transgenic lines compared to WT and VC plants. By contrast, at elevated CO_2 levels, FAA content was significantly increased in transgenic lines under control, NaCl, and drought stress conditions compared with WT and VC plants (**Supplementary Figure S18**). Transgenic lines showed high polyphenol contents compared to control plants, however, they did not change significantly under stress conditions (**Supplementary Figure S18**). Overall, the results suggested that the transgenic lines accumulated a higher amount of sugars, FAA, and polyphenols to protect the host plant under stress conditions.

Analysis of Metabolites

In total, 43 and 33 metabolites were detected in plants grown in ambient and elevated CO_2 environments, respectively (**Supplementary Tables S2, S3**). Out of these, 25 metabolites were common to both conditions, 18 were unique to ambient conditions, while 8 metabolites were accumulated exclusively under elevated CO_2 levels. Metabolites were differentially accumulated in plants (WT, and transgenic lines L20 and L40)

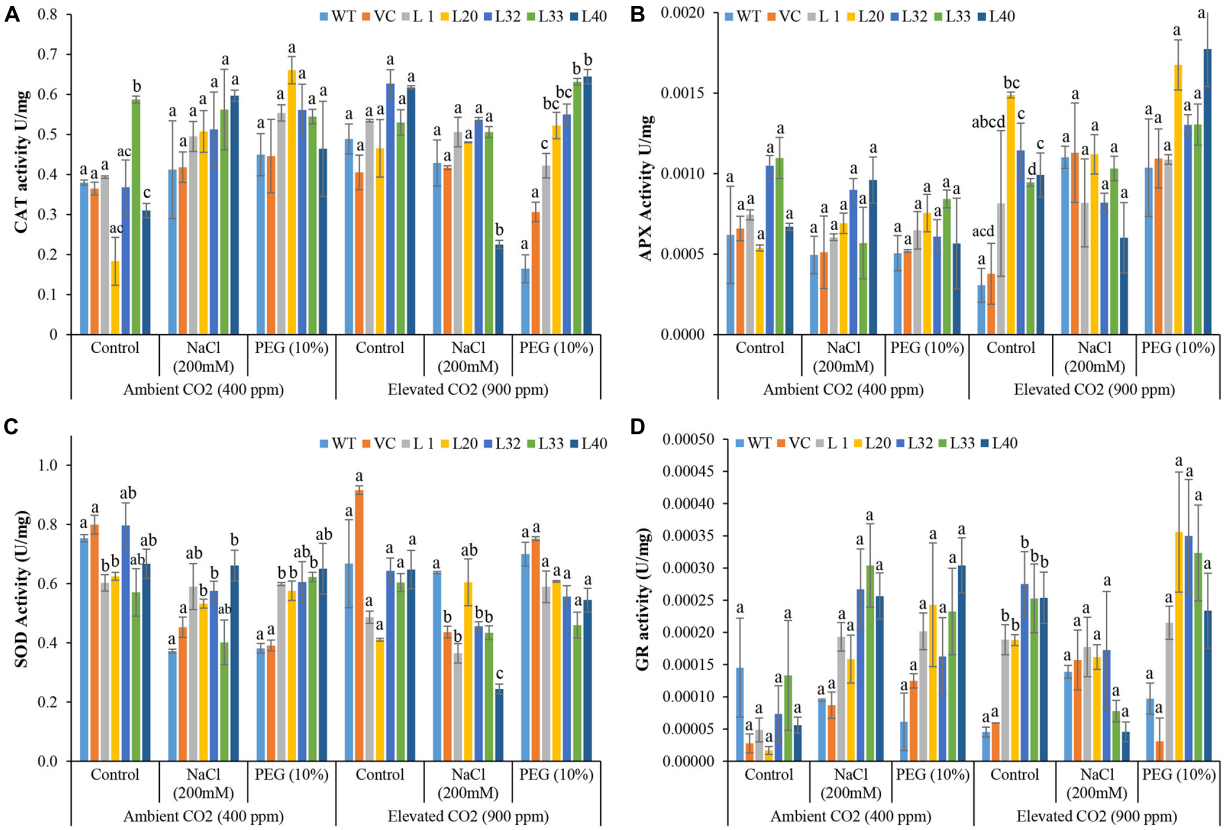

FIGURE 8 | Analysis of reactive oxygen species (ROS) scavenging enzymes activity in transgenic lines. Estimation of **(A)** catalase, **(B)** ascorbate peroxidase, **(C)** superoxide dismutase, and **(D)** glutathione reductase activities in wild type (WT), vector control (VC), and T1 transgenic lines (L1, L20, L32, L33, and L40) were measured under salinity (200 mM NaCl) and osmotic [10% polyethylene glycol (PEG)] stress condition grown in ambient and elevated CO_2 environment. Bars represent means ± SE, and values with different letters are significant at $P < 0.05$.

under different stress conditions (salt and drought) in both ambient and elevated CO_2 environments.

The metabolites commonly identified in WT and transgenic plants under ambient CO_2 and control and stress conditions were 11 amino acids, 10 sugars, 6 organic acids, 3 sugar acids, 4 fatty acids, and 5 miscellaneous metabolites (**Supplementary Table S2**). The metabolites commonly identified in WT and transgenic plants under elevated CO_2 (900 ppm) and control and stress conditions were 19 amino acids, 7 sugars, 1 sugar acid and 1 sugar alcohol, 4 organic acids, 1 fatty acid, 1 amine, and 2 miscellaneous metabolites (**Supplementary Table S3**). Out of 19 amino acids, only 6 amino acids, adenine, L-leucine, L-lysine, L-tryptophan, L-valine, and β-alanine, were differentially expressed in WT and transgenic lines under elevated CO_2 levels in control and stress conditions, however, not at ambient CO_2 levels in control and stress conditions. The concentration of asparagine was higher in transgenic lines under elevated CO_2 and control and stress conditions, as compared to WT plants, and was also increased under ambient CO_2 stress conditions. L-Proline was one of the most important indicators of drought stress, acting as an osmoprotectant to mitigate damage in plants under stress conditions. However, level of L-proline in *SmPPDK* transgenic lines were decreased under salt and drought stress in both ambient and elevated CO_2 as compared to WT and control conditions. By contrast, accumulation of L-aspartic acid was increased under salt stress but downregulated under drought stress in transgenic lines at ambient CO_2 levels; whereas, in elevated CO_2 conditions, the opposite situation occurred, with L-aspartic acid being upregulated in transgenic lines under drought stress, compared to WT plants. Some important photorespiration metabolites, including glycine, serine, L-glutamic acid, and L-glutamine, were downregulated in transgenic lines under stress conditions at ambient CO_2 levels, relative to WT plants, however, their expression was not significantly altered under elevated CO_2 and control and stress conditions. Important sugar metabolites, such as fructose, galactose, and glucose, were differentially expressed in WT and transgenic lines. There was a considerably higher accumulation of sugar in transgenic lines in control conditions but downregulation under stress conditions at both ambient and elevated CO_2 levels, as compared to WT plants. In some important Kreb's cycle intermediates, such as citric acid, 2-ketoglutaric acid, and malic acid, accumulation showed considerably higher accumulation in transgenic lines under ambient CO_2 but were downregulated at elevated CO_2 levels, compared to WT plants.

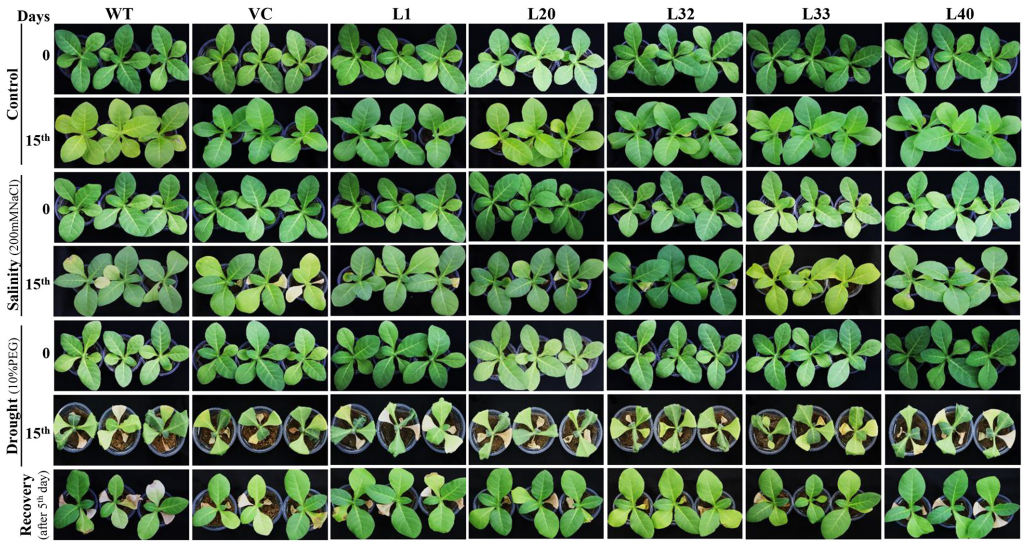

FIGURE 9 | Comparative plant growth studies under salt and osmotic stress. Morphological studies of wild type (WT), vector control (VC), and T1 transgenic lines (L1, L20, L32, L33, and L40) under salinity (200 mM NaCl) and osmotic [10% polyethylene glycol (PEG)] stress condition.

Overexpression of *SmPPDK* Improved Plant Performance Without Affecting Yield

One-week-old seedlings (transgenic and control plants) were transferred to a soil-filled pot and allowed to grow under normal growth conditions for 30 days. After being subjected to salt and drought stress treatments for a further 15 days, plant growth was documented and compared to control plants (**Figure 9**) and those treated under control conditions. Transgenic plants were only marginally affected or actually grew better under stress conditions compared to WT and VC plants. In addition, drought-treated plants recovered after the fifth day of restarting irrigation, with transgenic lines recovering faster than WT and VC plants. Transgenic and control (WT and VC) plants were also grown under normal greenhouse conditions and allowed to complete their life cycle (**Supplementary Figure S19**). No differences were found in vegetative performance between plants (**Supplementary Table S4**), however, comparatively delayed flowering was observed in WT and VC (control) plants (**Supplementary Figure S19**), with flowering time of transgenic lines being considerably shorter. In addition, L1 and L40 gave a significantly higher number of pods per plant than WT and VC plants. Even so, all transgenic lines displayed higher plant dry weight compared to that of WT and VC plants. Overall, these observations confirmed that integration of the C_4-specific *PPDK* gene into C_3 tobacco plants improved plant morphology, growth characteristics, and plant performance, without imposing any adverse effects.

DISCUSSION

An approach for increasing crop yield and photosynthetic efficiency in current climate conditions involves the ectopic expression of C_4 genes in existing C_3 crops. C_4 plants have advantages under different climatic and environmental conditions, such as high salinity, drought, higher temperatures, and nitrogen or CO_2 limitation, with these plants having a higher affinity for CO_2. The overexpression of C_4 PPDK, on its own or in combination with other C_4 enzymes, has been performed in a number of C_3 crops, with some of the transgenic plants showing greater biomass, while others exhibited alterations in photosynthetic efficiency (Yadav and Mishra, 2020).

In this current study, a C_4-specific *PPDK* gene was cloned from single-celled *S. monoica*, and integrated into a C_3 modal plant tobacco genome under the control of the CaMV35S constitutive promoter, using *Agrobacterium*-mediated genetic transformation (**Figure 1** and **Supplementary Figure S2**). Previously, introgression of the maize *PPDK* gene increased photosynthesis efficiency and yield of transgenic lines by enhancing PPDK activity in leaves (Fukayama et al., 2001). The *SmPPDK* gene comprised of seven exons and six introns in the transgenic lines (**Supplementary Figure S1**), and overexpression *SmPPDK* cDNA resulted in increased plant biomass, vegetative growth, and sugar content (including total sugar, reducing sugar, and starch) under different stress conditions (**Supplementary Figures S5–S9, S17**). The *PPDK* gene played an important role in sugar metabolism, as transgenic plants grew efficiently under sugar deficiency (caused by stress) compared to WT and VC plants.

Photosynthesis is a primary metabolic process in the production of biomass, however, it is sensitive to different abiotic stresses. We observed a decrease in the rate of photosynthesis at elevated CO_2 levels and under abiotic stresses (salt and drought), however, this decrease was lower in transgenic lines compared to WT and VC plants (**Figure 2**). Commonly, photosynthesis increases under elevated CO_2 condition due to greater availability of carbon triggering higher Rubisco

activity. Higher photosynthesis increases the amount of reserve carbohydrates in leaves, and this downregulates the expression of photosynthetic gene, thereby decreasing the photosynthesis (Cheng et al., 1998). It is a type of feedback inhibition in which photosynthesis decreases under long-term elevated CO_2 exposure (Thompson et al., 2017).

Interestingly, the reduction in photosynthesis rate was found to be linked with transpiration under elevated CO_2 conditions. In transgenic plants, increased total chlorophyll content was estimated due to high activity of C_4 *Sm*PPDK, which improved photosynthetic efficiency (**Supplementary Figures S13, S14**). The integration of the transgene maintained the chlorophyll fluorescence efficiency without affecting the electron transport chain, under different abiotic stress conditions (**Figures 2–4** and **Supplementary Figure S12**). In addition, PSII utilized the most energy by chlorophyll for photosynthesis, and it was considered a useful indicator to measure the effects of abiotic stress on plants (Maxwell and Johnson, 2000). Chlorophyll "a" fluorescence efficiency was also correlated with the content of total chlorophyll in leaves, and interestingly, transgenic lines showed increased chlorophyll content with higher chlorophyll "a" fluorescence efficiency. Fv/Fm ratio is a widely used parameter for measuring the status of PSII under stress conditions. *SmPPDK* transgenic plants did not show a significant change in Fv/Fm ratio, compared to WT and VC plants, under stress conditions in ambient CO_2 condition, but performed better under stress at elevated CO_2 levels (Zhao et al., 2007). Overall, the pattern of chlorophyll fluorescence suggested that a high Fv/Fm ratio under salt and drought stress at both ambient and elevated CO_2 levels indicated higher photosynthesis and maximum quantum efficiency of PSII centers in transgenic plants. This resulted in an increase in biomass, CO_2 assimilation, and yield in transgenic lines compared to WT and VC plants under adverse climate conditions (**Supplementary Table S4**). In a previous study, similar results were also obtained when the maize C_4 *PPDK* gene was overexpressed in rice, with transgenic lines having larger panicles and greater yield compared to WT plants (Wang et al., 2004). There are several reports confirming that ectopic expression of a C_4-specific *PPDK* gene in C_3 plants has synergistic effects on photosynthesis (Ding et al., 2013; Zhang et al., 2014). Photosynthesis efficiency was also found to be positively correlated with stomatal conductance and internal CO_2 concentrations (Ku et al., 2000).

Chlorophyll–fluorescence transient curve (OJIP) have been extensively used to study PSII activity (Yusuf et al., 2010), and those in the current study (**Supplementary Figure S12**) suggested that salt and drought stress were major constraints on PSII activity in the host plant. In addition, the expression of the exogenous *SmPPDK* gene alleviated damage to the PSII system and thus maintained photosynthetic electron transportation under adverse conditions. As such, *SmPPDK* transgenic tobacco plants maintained a comparatively high photochemical efficiency. Transgenic lines also maintained relatively higher water content under drought stress in elevated CO_2 conditions compared to WT and VC plants (**Figure 5**). Improved RWC could also be correlated with an increase in stomatal conductance, and this was directly regulated by different C_4 enzymes of organic acid metabolism, which modulate stomatal conductance by influencing guard cells (Lawson et al., 2018).

Transgenic lines had higher *Sm*PPDK activity compared to WT and VC plants, and the increment was greater under elevated CO_2 conditions (**Supplementary Figure S14**). We previously reported that the activity of PPDK enzyme increased under elevated CO_2 conditions in *Suaeda* spp. (Yadav et al., 2018). PPDK, involved in C_4 photosynthesis, was more resistant to abiotic stress and elevated CO_2 levels, ameliorating the adverse effects of induced stress. Previously, about a 5-fold increase in PPDK activity was estimated for transgenic lines compared to untransformed controls (Jiao et al., 2002). Enzymes, which are involved in C_4 carbon assimilation, are known to accumulate in leaves under different abiotic stress conditions (Fißlthaler et al., 1995). These enzymes play a crucial role in plant responses to drought by minimizing the production of ROS and stabilizing membrane lipid peroxidation (Jiao et al., 2002; Gu et al., 2013). Similar results were observed in the current study, with a lower accumulation of MDA (i.e., lower lipid peroxidation) and H_2O_2 in transgenic lines under stress and elevated CO_2 condition compared to WT and VC plants, which accounted for the improved tolerance of plants overexpressing the C_4-specific *SmPPDK* gene (**Figures 6**, **7**). Furthermore, lower production and localization of superoxide and peroxide free radicals were observed in transgenic lines compared to WT and VC plants. This suggested the *SmPPDK* gene mitigated oxidative stress by ROS scavenging activity.

Elevated CO_2 reduces H_2O_2 accumulation by lowering the photorespiration rate, mitigating oxidative stress, and also by inducing protective mechanisms for the photosynthetic apparatus. However, improvements in photosynthesis efficiency due to enrichment of CO_2 might also enhance the activity of antioxidant enzymes, leading to lower production of ROS (Zinta et al., 2014). The Gly/Ser ratio is an important parameter, which provides evidence that photorespiration is suppressed under elevated CO_2 conditions (Kebeish et al., 2007). Transgenic lines showed reduced Gly/Ser ratios under stress conditions, with this ratio being considerably decreased under elevated CO_2 stress conditions (**Supplementary Figure S16**). A decrease in Gly/Ser ratio was similarly observed in *A. thaliana* under elevated CO_2 conditions, which was correlated with a lowering of photorespiration (Kebeish et al., 2007).

It has been well established that plants accumulate high levels of ROS under different stresses, and commonly, antioxidant systems are not adequate, a situation characteristically indicated by lipid peroxidation and low activity of antioxidant enzymes (Gill and Tuteja, 2010; Alexander et al., 2019). Elevated CO_2 increased the level of antioxidants, including polyphenols, ascorbate, alkaloids, and the activity of some antioxidant enzymes (SOD, CAT, GR, and APX), which improve the antioxidant defense mechanisms and reduce ROS generation (Zinta et al., 2014). In the current study, *SmPPDK* transgenic lines showed high antioxidant activities under stress conditions, facilitating efficient survival under adverse conditions (**Figure 8**). Osmoprotectants such as glycine betaine, different sugars, FAAs, and polyphenols are considered essential biochemical stress markers for determining the response of plants to osmotic stress

(Ksouri et al., 2007). The overexpressing *SmPPDK* transgenic lines accumulated high glycine betaine, total sugar, reducing sugars, polyphenols, and FAAs, with these accumulations increasing under elevated CO_2 conditions (**Figure 6** and **Supplementary Figures S17, S18**). In general, accumulation of polyphenols and different sugars help protect plants against ROS (Ksouri et al., 2007). These compounds accumulate to conserve the osmotic equilibrium across the membranes under osmotic stress conditions. Glycine betaine is mainly found in chloroplasts and plays an important role in the protection of thylakoid membranes, thus conserving photosynthetic activity. In addition, at higher salinity, it protects PSII, membranes, and Rubisco from osmotic stress (Jagendorf and Takabe, 2001). Under salt and drought stress conditions, glycine betaine and the antioxidant defense system have been shown to have a protective effect in wheat and suspension cultures of tobacco BY2 cells (Raza et al., 2007).

Wang et al. (2009) validated the two main ROS detoxifying enzymes, CAT and APX. In the current study, the activities of these enzymes were elevated in *SmPPDK* transgenic lines exposed to salinity, as compared to control plants. Furthermore, *SmPPDK* transgenic lines could detoxify ROS more efficiently; therefore, they showed tolerance under stress. Transcript expression analysis (**Supplementary Figure S15**) showed that in ambient CO_2, *NtCAT,* and *NtAPX* were upregulated in transgenic lines under both NaCl and drought stress. By contrast, elevated CO_2 resulted in downregulation of *NtCAT* expression in transgenic lines under stress conditions, as compared to ambient CO_2. Likewise, *NtAPX* and *NtSOD* were also induced in all transgenic plants under elevated CO_2 as compared to control plants. At elevated CO_2 levels, *NtGR* was also upregulated significantly under both salt and drought stresses, relative to WT plants under the control conditions.

The different types and quantities of metabolites, as final products of cell regulation mechanisms, can be assayed to measure the direct response of biological systems to any environmental or genetic change (Patel et al., 2016). They are involved in various functions such as osmotic alterations, antioxidant protection, and signal transduction (Fiehn, 2002). Secondary metabolites play a key role in defense under stress condition (Tanna and Mishra, 2018). Plants produce different metabolites in response to abiotic stress and accumulate organic acids, sugars, polyamines, amino acids, and lipids (Guy et al., 2008). In this current present study, we examined the synthesis of metabolites as a prospective mechanism for improving photosynthesis and for stress tolerance in tobacco transformed with the *SmPPDK* gene. Accumulation of sugar alcohols mitigated the damage caused by stress and provided tolerance. *Salicornia brachia*, an extreme halophyte, accumulates a number of metabolites as a protective mechanism under salt and drought stress conditions (Mishra et al., 2015).

Under elevated CO_2 conditions, the CO_2/O_2 ratio increased at sites of photoreduction in leaves due to a higher CO_2 concentration gradient. Consequentially, the rate of photorespiration and formation of ROS decreased due to an increase in NADPH consumption. Pn and carbon supply is also increased, which leads to an enhanced WUE for photosynthesis (Morgan et al., 2011). All these effects minimize the oxidative stress, and further energy could be used for energy-dependent stress mitigation mechanisms, such as the production of osmolytes and antioxidants (Drake et al., 1997).

Overexpression of individual genes in different species is currently one of the more common practices in molecular biolog, however, it is a complicated process and is controlled by many different factors, such as transcriptional and posttranscriptional modifications, integration site, and transgene copy number (Ma et al., 2011). Although these factors will cause various phenotypic and biochemical changes, their exact mechanisms are still unknown. This was the first report of a C_4-specific *PPDK* gene from single-celled *S. monoica* improving photosynthesis performance under salt and drought stress conditions at ambient and elevated CO_2 levels. In this study, we observed that transgenic lines showed earlier flowering than control plants due to increases in carbon assimilation efficiency by decreasing the rate of photorespiration. Furthermore, transgenic plants were shown to produce a higher number of leaves per plant by increasing soluble sugar. Overall, *SmPPDK* transgenic lines also performed better in control field conditions (**Supplementary Table S5**) completing their life cycle earlier and with higher biomass than WT and VC plants. We hypothesized that reduction in photorespiration and ROS production in transgenic lines by improved antioxidant defense systems, enhanced photosynthesis performance of C_3 transgenic tobacco lines under salt and drought stress conditions, at ambient and elevated CO_2 levels, however, further molecular studies will be required to support this hypothesis.

DATA AVAILABILITY STATEMENT

The datasets generated for this study can be found in the MK704410.

AUTHOR CONTRIBUTIONS

AM: conceptualization and designing. SY: conduct of the experiments. SY and MR: data acquisition. SY and AM: analysis and interpretation, and drafting of the manuscript.

ACKNOWLEDGMENTS

CSIR-Young Scientist (YSP-02/2016-17) and SERB-DST (EMR/2016/000538) projects are thankfully acknowledged. Dr. Manish Kumar Patel is thankfully acknowledged for his support in GC-MS experiment. Thanks to Prof. Bhavanath Jha for securing initial funds to support this research. CSIR-CSMCRI Communication No. is 052/2019.

SUPPLEMENTARY MATERIAL

The Supplementary Material for this article can be found online at: https://www.frontiersin.org/articles/10.3389/fpls.2020.00345/full#supplementary-material

REFERENCES

Agarie, S., Kai, M., Takatsuji, H., and Ueno, O. (1997). Expression of C3 and C4 photosynthetic characteristics in the amphibious plant *Eleocharis vivipara*: structure and analysis of the expression of isogenes for pyruvate, orthophosphate dikinase. *Plant Mol. Biol.* 34, 363–369. doi: 10.1023/a:1005897118660

Akhani, H., Barroca, J., Koteeva, N., Voznesenskaya, E., Franceschi, V., Edwards, G., et al. (2005). *Bienertia sinuspersici* (Chenopodiaceae): a new species from Southwest Asia and discovery of a third terrestrial C4 plant without Kranz anatomy. *Syst. Bot.* 30, 290–301. doi: 10.1600/0363644054223684

Alexander, A., Singh, V. K., Mishra, A., and Jha, B. (2019). Plant growth promoting rhizobacterium *Stenotrophomonas* maltophilia BJ01 augments endurance against N2 starvation by modulating physiology and biochemical activities of *Arachis hypogea*. *PLoS One* 14:e0222405. doi: 10.1371/journal.pone.0222405

Alla, M. M. N., and Hassan, N. M. (2012). A possible role for C4 photosynthetic enzymes in tolerance of Zea mays to NaCl. *Protoplasma* 249, 1109–1117. doi: 10.1007/s00709-011-0356-4

Beyer, W. F. Jr., and Fridovich, I. (1987). Assaying for superoxide dismutase activity: some large consequences of minor changes in conditions. *Anal. Biochem.* 161, 559–566. doi: 10.1016/0003-2697(87)90489-1

Bradford, M. M. (1976). A rapid and sensitive method for the quantitation of microgram quantities of protein utilizing the principle of protein-dye binding. *Anal. Biochem.* 72, 248–254. doi: 10.1006/abio.1976.9999

Chamovitz, D., Sandmann, G., and Hirschberg, J. (1993). Molecular and biochemical characterization of herbicide-resistant mutants of cyanobacteria reveals that phytoene desaturation is a rate-limiting step in carotenoid biosynthesis. *J. Biol. Chem.* 268, 17348–17353.

Chandler, S. F., and Dodds, J. H. (1983). The effect of phosphate, nitrogen and sucrose on the production of phenolics and solasodine in callus cultures of *Solanum laciniatum*. *Plant Cell Rep.* 2, 205–208. doi: 10.1007/BF00270105

Chang, T. S., Liu, C. W., Lin, Y. L., Li, C. Y., Wang, A. Z., Chien, M. W., et al. (2017). Mapping and comparative proteomic analysis of the starch biosynthetic pathway in rice by 2D PAGE/MS. *Plant Mol. Biol.* 95, 333–343. doi: 10.1007/s11103-017-0652-2

Chastain, C. J., Failing, C. J., Manandhar, L., Zimmerman, M. A., Lakner, M. M., and Nguyen, T. H. (2011). Functional evolution of C4 pyruvate, orthophosphate dikinase. *J. Exp. Bot.* 62, 3083–3091. doi: 10.1093/jxb/err058

Chastain, C. J., Heck, J. W., Colquhoun, T. A., Voge, D. G., and Gu, X. Y. (2006). Posttranslational regulation of pyruvate, orthophosphate dikinase in developing rice (*Oryza sativa*) seeds. *Planta* 224:924. doi: 10.1007/s00425-006-0259-3

Chastain, C. J., Xu, W., Parsley, K., Sarath, G., Hibberd, J. M., and Chollet, R. (2008). The pyruvate, orthophosphate dikinase regulatory proteins of *Arabidopsis* possess a novel, unprecedented Ser/Thr protein kinase primary structure. *Plant J.* 53, 854–863. doi: 10.1111/j.1365-313X.2007.03366.x

Chaturvedi, A. K., Mishra, A., Tiwari, V., and Jha, B. (2012). Cloning and transcript analysis of type 2 metallothionein gene (SbMT-2) from extreme halophyte *Salicornia brachiata* and its heterologous expression in *E. coli*. *Gene* 499, 280–287. doi: 10.1016/j.gene.2012.03.001

Chaturvedi, A. K., Patel, M. K., Mishra, A., Tiwari, V., and Jha, B. (2014). The SbMT-2 gene from a halophyte confers abiotic stress tolerance and modulates ROS scavenging in transgenic tobacco. *PLoS One* 9:e111379. doi: 10.1371/journal.pone.0111379

Cheng, S. H., Moore, B. D., and Seemann, J. R. (1998). Effects of short- and long-term elevated CO2 on the expression of ribulose-1,5-bisphosphate carboxylase/oxygenase genes and carbohydrate accumulation in leaves of *Arabidopsis thaliana* (L.) Heynh. *Plant Physiol.* 116, 715–723. doi: 10.1104/pp.116.2.715

Chomczynski, P., and Sacchi, N. (1987). Single-step method of RNA isolation by acid guanidinium thiocyanate-phenol-chloroform extraction. *Anal. Biochem.* 162, 156–159. doi: 10.1006/abio.1987.9999

Dengler, N. G., and Nelson, T. (1999). "Leaf structure and development in C4 plants," in *C4 Plant Biology*, eds R. F. Sage, and R. K. Monson, (San Diego, CA: Academic Press), 133–172. doi: 10.1016/b978-012614440-6/50006-9

Dhir, B. (2018). "Crop productivity in changing climate," in *Sustainable Agriculture Reviews 27*, ed. E. Lichtfouse, (Cham: Springer), 213–241. doi: 10.1007/978-3-319-75190-0_8

Ding, Z. S., Huang, S. H., Zhou, B. Y., Sun, X. F., and Zhao, M. (2013). Over-expression of phosphoenolpyruvate carboxylase cDNA from C4 millet (Seteria italica) increase rice photosynthesis and yield under upland condition but not in wetland fields. *Plant Biotechnol. Rep.* 7, 155–163. doi: 10.1007/s11816-012-0244-1

Doubnerová, V., and Ryšlavá, H. (2011). What can enzymes of C4 photosynthesis do for C3 plants under stress? *Plant Sci.* 180, 575–583. doi: 10.1016/j.plantsci.2010.12.005

Drake, B. G., Gonzàlez-Meler, M. A., and Long, S. P. (1997). More efficient plants: a consequence of rising atmospheric CO2? *Annu. Rev. Plant Physiol. Plant Mol. Biol.* 48, 609–639. doi: 10.1146/annurev.arplant.48.1.609

Edwards, G. E., Nakamoto, H., Burnell, J. N., and Hatch, M. D. (1985). Pyruvate, Pi dikinase and NADP-malate dehydrogenase in C4 photosynthesis: properties and mechanism of light/dark regulation. *Annu. Rev. Plant Physiol.* 36, 255–286. doi: 10.1146/annurev.pp.36.060185.001351

FAO, (2011). *Land and Plant Nutrition Management Service*. Available online at: http://www.fao.org/land-water/en/ (accessed March 09, 2019).

Fiehn, O. (2002). Metabolomics–the link between genotypes and phenotypes. *Plant Mol. Biol.* 48, 155–171. doi: 10.1023/A:1013713905833

Fißlthaler, B., Meyer, G., Bohnert, H. J., and Schmitt, J. M. (1995). Age-dependent induction of pyruvate, orthophosphate dikinase in *Mesembryanthemum crystallinum* L. *Planta* 196, 492–500.

Freitag, H., and Stichler, W. (2002). *Bienertia cycloptera* Bunge ex Boiss, *Chenopodiaceae*, another C4 Plant without Kranz tissues. *Plant Biol.* 4, 121–132. doi: 10.1055/s-2002-20444

Fukayama, H., Tsuchida, H., Agarie, S., Nomura, M., Onodera, H., Ono, K., et al. (2001). Significant accumulation of C4-specific pyruvate, orthophosphate dikinase in a C3 plant, rice. *Plant Physiol.* 127, 1136–1146. doi: 10.1104/pp.010641

Ghose, T. K. (1987). Measurement of cellulase activities. *Pure Appl. Chem.* 59, 257–268. doi: 10.1351/pac198759020257

Gill, S. S., and Tuteja, N. (2010). Reactive oxygen species and antioxidant machinery in abiotic stress tolerance in crop plants. *Plant Physiol. Biochem.* 48, 909–930. doi: 10.1016/j.plaphy.2010.08.016

Grieve, C. M., and Grattan, S. R. (1983). Rapid assay for determination of water soluble quaternary ammonium compounds. *Plant Soil* 70, 303–307. doi: 10.1007/BF02374789

Gu, J. F., Qiu, M., and Yang, J. C. (2013). Enhanced tolerance to drought in transgenic rice plants overexpressing C4 photosynthesis enzymes. *Crop J.* 1, 105–114. doi: 10.1016/j.cj.2013.10.002

Guy, C., Kaplan, F., Kopka, J., Selbig, J., and Hincha, D. K. (2008). Metabolomics of temperature stress. *Physiol. Plant.* 132, 220–235. doi: 10.1111/j.1399-3054.2007.00999.x

Hatch, M. D. (1987). C4 photosynthesis: a unique elend of modified biochemistry, anatomy and ultrastructure. *Biochim. Biophys. Acta. Bioenerg.* 895, 81–106. doi: 10.1016/s0304-4173(87)80009-5

He, Z., Wang, Z. Y., Li, J., Zhu, Q., Lamb, C., Ronald, P., et al. (2000). Perception of brassinosteroids by the extracellular domain of the receptor kinase BRI1. *Science* 288, 2360–2363. doi: 10.1126/science.288.5475.2360

Hoagland, D. R., and Arnon, D. I. (1950). The water-culture method for growing plants without soil. *Calif. Agric. Exp. Stn.* 347, 1–32.

Hodges, D. M., DeLong, J. M., Forney, C. F., and Prange, R. K. (1999). Improving the thiobarbituric acid-reactive-substances assay for estimating lipid peroxidation in plant tissues containing anthocyanin and other interfering compounds. *Planta* 207, 604–611. doi: 10.1007/s004250050524

Horsch, R. B., Fry, J. E., Hoffmann, N. L., Eichholtz, D., Rogers, S. A., and Fraley, R. T. (1985). A simple and general method for transferring genes into plants. *Science* 227, 1229–1231. doi: 10.1126/science.227.4691.1229

Hýsková, V. D., Miedzińska, L., Dobrá, J., Vankova, R., and Ryšlavá, H. (2014). Phosphoenolpyruvate carboxylase, NADP-malic enzyme, and pyruvate, phosphate dikinase are involved in the acclimation of *Nicotiana tabacum* L. to drought stress. *J. Plant Physiol.* 171, 19–25. doi: 10.1016/j.jplph.2013.10.017

Inskeep, W. P., and Bloom, P. R. (1985). Extinction coefficients of chlorophyll a and b in N, N-dimethylformamide and 80% acetone. *Plant Physiol.* 77, 483–485. doi: 10.1104/pp.77.2.483

IPCC, (2014). *Climate Change 2014: Synthesis Report. Contribution of Working Groups I, II and III to the Fifth Assessment Report of the Intergovernmental Panel on Climate Change*. Cambridge: Cambridge University Press.

Jagendorf, A. T., and Takabe, T. (2001). Inducers of glycine betaine synthesis in barley. *Plant Physiol.* 127, 1827–1835. doi: 10.1104/pp.010392

Jha, B., Sharma, A., and Mishra, A. (2011). Expression of SbGSTU (tau class glutathione S-transferase) gene isolated from *Salicornia brachiata* in tobacco for salt tolerance. *Mol. Biol. Rep.* 38, 4823–4832. doi: 10.1007/s11033-010-0625-x

Jha, R. K., Patel, J., Mishra, A., and Jha, B. (2019). "Introgression of halophytic salt stress-responsive genes for developing stress tolerance in crop plants," in *Halophytes and Climate Change: Adaptive Mechanisms and Potential Uses*, eds M. Hasanuzzaman, S. Shabala, and M. Fujita, (Wallingford: CABI), 288–299. doi: 10.1079/9781786394330.0275

Jiao, D., Huang, X., Li, X., Chi, W., Kuang, T., Zhang, Q., et al. (2002). Photosynthetic characteristics and tolerance to photo-oxidation of transgenic rice expressing C4 photosynthesis enzymes. *Photosynth. Res.* 72, 85–93. doi: 10.1023/A:1016062117373

Joshi, M., Jha, A., Mishra, A., and Jha, B. (2013). Developing transgenic Jatropha using the SbNHX1 gene from an extreme halophyte for cultivation in saline wasteland. *PLoS One* 8:e71136. doi: 10.1371/journal.pone.0071136

Kebeish, R., Niessen, M., Thiruveedhi, K., Bari, R., Hirsch, H. J., Rosenkranz, R., et al. (2007). Chloroplastic photorespiratory bypass increases photosynthesis and biomass production in *Arabidopsis thaliana*. *Nat. Biotechnol.* 25, 593–599. doi: 10.1038/nbt1299

Kellner, J., Houska, T., Manderscheid, R., Weigel, H. J., Breuer, L., and Kraft, P. (2019). Response of maize biomass and soil water fluxes on elevated CO2 and drought–from field experiments to process−based simulations. *Glob. Chang. Boil.* 25, 2947–2957. doi: 10.1111/gcb.14723

Ksouri, R., Megdiche, W., Debez, A., Falleh, H., Grignon, C., and Abdelly, C. (2007). Salinity effects on polyphenol content and antioxidant activities in leaves of the halophyte *Cakile maritima*. *Plant Physiol. Biochem.* 45, 244–249. doi: 10.1016/j.plaphy.2007.02.001

Ku, M. S. B., Cho, D., Ranade, U., Hsu, T. P., Li, X., Jiao, D. M., et al. (2000). Photosynthetic performance of transgenic rice plants overexpressing maize C4 photosynthesis enzymes. *Stud. Plant Sci.* 7, 193–204. doi: 10.1016/S0928-3420(00)80015-4

Lawson, T., Terashima, I., Fujita, T., and Wang, Y. (2018). "Coordination between photosynthesis and stomatal behavior," in *The Leaf: a Platform for Performing Photosynthesis*, eds I. I. I. W. Adams, and I. Terashima, (Cham: Springer), 141–161. doi: 10.1007/978-3-319-93594-2_6

Liapounova, N. A., Hampl, V., Gordon, P. M., Sensen, C. W., Gedamu, L., and Dacks, J. B. (2006). Reconstructing the mosaic glycolytic pathway of the anaerobic eukaryote Monocercomonoides. *Eukaryot. Cell.* 5, 2138–2146. doi: 10.1128/EC.00258-06

Lisec, J., Schauer, N., Kopka, J., Willmitzer, L., and Fernie, A. R. (2006). Gas chromatography mass spectrometry-based metabolite profiling in plants. *Nature Protoc.* 1, 387–396. doi: 10.1038/nprot.2006.59

Livak, K. J., and Schmittgen, T. D. (2001). Analysis of relative gene expression data using real-time quantitative PCR and the 2-ΔΔCt method. *Methods* 25, 402–408. doi: 10.1006/meth.2001.1262

Lutts, S., Kinet, J. M., and Bouharmont, J. (1996). NaCl-induced senescence in leaves of rice (*Oryza sativa* L.) cultivars differing in salinity resistance. *Ann. Bot.* 78, 389–398. doi: 10.1006/anbo.1996.0134

Ma, X., Feng, D. S., Wang, H. G., Li, X. F., and Kong, L. R. (2011). Cloning and expression analysis of wheat cytokinin oxidase/dehydrogenase gene TaCKX3. *Plant Mol. Biol. Rep.* 29, 98–105. doi: 10.1007/s11105-010-0209-x

Maxwell, K., and Johnson, G. N. (2000). Chlorophyll fluorescence- a practical guide. *J. Exp. Bot.* 51, 659–668. doi: 10.1093/jxb/51.345.659

Minges, A., and Groth, G. (2017). Small-molecule inhibition of pyruvate phosphate dikinase targeting the nucleotide binding site. *PLoS One* 12:e0181139. doi: 10.1371/journal.pone.0181139

Mishra, A., Patel, M. K., and Jha, B. (2015). Non-targeted metabolomics and scavenging activity of reactive oxygen species reveal the potential of *Salicornia brachiata* as a functional food. *J. Funct. Foods.* 13, 21–31. doi: 10.1016/j.jff.2014.12.027

Mishra, A., and Tanna, B. (2017). Halophytes: potential resources for salt stress tolerance genes and promoters. *Front. Plant Sci.* 8:829. doi: 10.3389/fpls.2017.00829

Miyagawa, Y., Tamoi, M., and Shigeoka, S. (2000). Evaluation of the defense system in chloroplasts to photooxidative stress caused by paraquat using transgenic tobacco plants expressing catalase from *Escherichia coli*. *Plant Cell Physiol.* 41, 311–320. doi: 10.1093/pcp/41.3.311

Morgan, J. A., LeCain, D. R., Pendall, E., Blumenthal, D. M., Kimball, B. A., Carrillo, Y., et al. (2011). C4 grasses prosper as carbon dioxide eliminates desiccation in warmed semi-arid grassland. *Nature* 476, 202–205. doi: 10.1038/nature10274

Nakano, Y., and Asada, K. (1981). Hydrogen peroxide is scavenged by ascorbate-specific peroxidase in spinach chloroplasts. *Plant Cell Physiol.* 22, 867–880. doi: 10.1093/oxfordjournals.pcp.a076232

Pandey, S., Patel, M. K., Mishra, A., and Jha, B. (2015). Physio-biochemical composition and untargeted metabolomics of cumin (*Cuminum cyminum* L.) make it promising functional food and help in mitigating salinity stress. *PLoS One* 10:e0144469. doi: 10.1371/journal.pone.0144469

Pandey, S., Patel, M. K., Mishra, A., and Jha, B. (2016). In planta transformed cumin (*Cuminum cyminum* L.) plants, overexpressing the SbNHX1 gene showed enhanced salt endurance. *PLoS One* 11:e0159349. doi: 10.1371/journal.pone.0159349

Pastore, M. A., Lee, T. D., Hobbie, S. E., and Reich, P. B. (2019). Strong photosynthetic acclimation and enhanced water−use efficiency in grassland functional groups persist over 21 years of CO2 enrichment, independent of nitrogen supply. *Glob. Chang. Biol.* 25, 3031–3044. doi: 10.1111/gcb.14714

Patel, M. K., Joshi, M., Mishra, A., and Jha, B. (2015). Ectopic expression of SbNHX1 gene in transgenic castor (*Ricinus communis* L.) enhances salt stress by modulating physiological process. *Plant Cell Tiss. Organ Cult.* 122, 477–490. doi: 10.1007/s11240-015-0785-4

Patel, M. K., Mishra, A., and Jha, B. (2016). "Untargeted metabolomics of halophytes," in *Marine Omics: Principles and Applications*, ed. S. Kim, (Boca Raton, FL: CRC Press), 309–325. doi: 10.1201/9781315372303-18

Patterson, B. D., Payne, L. A., Chen, Y. Z., and Graham, D. (1984). An inhibitor of catalase induced by cold in chilling-sensitive plants. *Plant Physiol.* 76, 1014–1018. doi: 10.1104/pp.76.4.1014

Raza, S. H., Athar, H. R., Ashraf, M., and Hameed, A. (2007). Glycine betaine-induced modulation of antioxidant enzymes activities and ion accumulation in two wheat cultivars differing in salt tolerance. *Environ. Exp. Bot.* 60, 368–376. doi: 10.1016/j.envexpbot.2006.12.009

Sage, R. F. (2004). The evolution of C4 photosynthesis. *New Phytol.* 161, 341–370. doi: 10.1111/j.1469-8137.2004.00974.x

Sage, R. F., and Pearcy, R. W. (2000). "The physiological ecology of c4 photosynthesis," in *Photosynthesis. Advances in Photosynthesis and Respiration*, eds R. C. Leegood, T. D. Sharkey, and S. von Caemmerer, (Dordrecht: Springer), 497–532. doi: 10.1007/0-306-48137-5_21

Sairam, R. K. (1994). Effects of homobrassinolide application on plant metabolism and grain yield under irrigated and moisture-stress conditions of two wheat varieties. *Plant Growth Regul.* 14, 173–181. doi: 10.1007/BF00025220

Schulte, M., Offer, C., and Hansen, U. (2003). Induction of CO2-gas exchange and electron transport: comparison of dynamic and steady-state responses in *Fagus sylvatica* leaves. *Trees* 17, 153–163. doi: 10.1007/s00468-002-0219-x

Sheen, J. (1999). C4 gene expression. *Annu. Rev. Plant Physiol. Plant Mol. Biol.* 50, 187–217. doi: 10.1146/annurev.arplant.50.1.187

Sheen, J. Y., and Bogorad, L. (1987). Regulation of levels of nuclear transcripts for C4 photosynthesis in bundle sheath and mesophyll cells of maize leaves. *Plant Mol. Biol.* 8, 227–238. doi: 10.1007/BF00015031

Shi, J., Fu, X. Z., Peng, T., Huang, X. S., Fan, Q. J., and Liu, J. H. (2010). Spermine pretreatment confers dehydration tolerance of citrus in vitro plants via modulation of antioxidative capacity and stomatal response. *Tree Physiol.* 30, 914–922. doi: 10.1093/treephys/tpq030

Singh, N., Mishra, A., and Jha, B. (2014b). Over-expression of the peroxisomal ascorbate peroxidase (SbpAPX) gene cloned from halophyte *Salicornia brachiata* confers salt and drought stress tolerance in transgenic tobacco. *Mar. Biotechnol.* 16, 321–332. doi: 10.1007/s10126-013-9548-6

Singh, N., Mishra, A., and Jha, B. (2014a). Ectopic over-expression of peroxisomal ascorbate peroxidase (SbpAPX) gene confers salt stress tolerance in transgenic peanut (*Arachis hypogaea*). *Gene* 547, 119–125. doi: 10.1016/j.gene.2014.06.037

Singh, V. K., Mishra, A., Haque, I., and Jha, B. (2016). A novel transcription factor-like gene SbSDR1 acts as a molecular switch and confers salt and osmotic endurance to transgenic tobacco. *Sci. Rep.* 6:31686. doi: 10.1038/srep31686

Slamovits, C. H., and Keeling, P. J. (2006). Pyruvate-phosphate dikinase of oxymonads and parabasalia and the evolution of pyrophosphate-dependent glycolysis in anaerobic eukaryotes. *Eukaryot. Cell* 5, 148–154. doi: 10.1128/EC.5.1.148-154.2006

Spoustová, P., Hýsková, V., Müller, K., Schnablová, R., Ryšlavá, H., Čeřovská, N., et al. (2015). Tobacco susceptibility to potato virus YNTN infection is affected by grafting and endogenous cytokinin content. *Plant Sci.* 235, 25–36. doi: 10.1016/j.plantsci.2015.02.017

Strasser, B. J., and Strasser, R. J. (1995). "Measuring fast fluorescence transients to address environmental questions: the JIP-test," in *Photosynthesis: From Light to Biosphere*, ed. P. Mathis, (Dordrecht: Kluwer Academic Publishers), 977–980.

Sugano, N., Tanaka, T., Yamamoto, E., and Nishi, A. (1975). Behaviour of phenylalanine ammonia-lyase in carrot cells in suspension cultures. *Phytochemistry* 14, 2435–2436. doi: 10.1016/0031-9422(75)80359-1

Tanna, B., Brahmbhatt, H. R., and Mishra, A. (2019). Phenolic, flavonoid, and amino acid compositions reveal that selected tropical seaweeds have the potential to be functional food ingredients. *J. Food Process. Pres.* 43:e14266. doi: 10.1111/jfpp.14266

Tanna, B., Choudhary, B., and Mishra, A. (2018). Metabolite profiling, antioxidant, scavenging and anti-proliferative activities of selected tropical green seaweeds reveal the nutraceutical potential of *Caulerpa* spp. *Algal Res.* 36, 96–105. doi: 10.1016/j.algal.2018.10.019

Tanna, B., and Mishra, A. (2018). "Metabolomics of seaweeds: tools and techniques," in *Plant Metabolites and Regulation Under Environmental Stress*, eds P. Ahmad, M. A. Ahanger, V. P. Singh, D. K. Tripathi, P. Alam, and M. N. Alyemeni, (Cambridge, MA: Academic Press), 37–52. doi: 10.1016/B978-0-12-812689-9.00002-9

Taylor, L., Nunes−Nesi, A., Parsley, K., Leiss, A., Leach, G., Coates, S., et al. (2010). Cytosolic pyruvate, orthophosphate dikinase functions in nitrogen remobilization during leaf senescence and limits individual seed growth and nitrogen content. *Plant J.* 62, 641–652. doi: 10.1111/j.1365-313X.2010.04179.x

Thompson, M., Gamage, D., Hirotsu, N., Martin, A., and Seneweera, S. (2017). Effects of elevated carbon dioxide on photosynthesis and carbon partitioning: a perspective on root sugar sensing and hormonal crosstalk. *Front. Physiol.* 8:578. doi: 10.3389/fphys.2017.00578

Tiwari, V., Chaturvedi, A. K., Mishra, A., and Jha, B. (2014). The transcriptional regulatory mechanism of the peroxisomal ascorbate peroxidase (pAPX) gene cloned from an extreme halophyte, *Salicornia brachiata*. *Plant Cell Physiol.* 55, 201–217. doi: 10.1093/pcp/pct172

Tiwari, V., Chaturvedi, A. K., Mishra, A., and Jha, B. (2015). Introgression of the SbASR-1 gene cloned from a halophyte *Salicornia brachiata* enhances salinity and drought endurance in transgenic groundnut (*Arachis hypogaea*) and acts as a transcription factor. *PLoS One* 10:e0135541. doi: 10.1371/journal.pone.0131567

Tiwari, V., Patel, M. K., Chaturvedi, A. K., Mishra, A., and Jha, B. (2016). Functional characterization of the tau class Glutathione-S-Transferases gene (SbGSTU) promoter of *Salicornia brachiata* under salinity and osmotic stress. *PLoS One* 11:e0148494. doi: 10.1371/journal.pone.0148494

Tiwari, V., Patel, M. K., Chaturvedi, A. K., Mishra, A., and Jha, B. (2019). Cloning and functional characterization of the Na+/H+ antiporter (NHX1) gene promoter from an extreme halophyte *Salicornia brachiata*. *Gene* 683, 233–242. doi: 10.1016/j.gene.2018.10.039

Udawat, P., Jha, R. K., Mishra, A., and Jha, B. (2017). Overexpression of a plasma membrane-localized SbSRP-like protein enhances salinity and osmotic stress tolerance in transgenic tobacco. *Front. Plant Sci.* 8:582. doi: 10.3389/fpls.2017.00582

Udawat, P., Jha, R. K., Sinha, D., Mishra, A., and Jha, B. (2016). Overexpression of a cytosolic abiotic stress responsive universal stress protein (SbUSP) mitigates salt and osmotic stress in transgenic tobacco plants. *Front. Plant Sci.* 7:518. doi: 10.3389/fpls.2016.00518

Udawat, P., Mishra, A., and Jha, B. (2014). Heterologous expression of an uncharacterized universal stress protein gene (SbUSP) from the extreme halophyte, *Salicornia brachiata*, which confers salt and osmotic tolerance to *E. coli*. *Gene* 536, 163–170. doi: 10.1016/j.gene.2013.11.020

Voznesenskaya, E. V., Franceschi, V. R., and Edwards, G. E. (2004). Light−dependent development of single cell C4 photosynthesis in cotyledons of *Borszczowia aralocaspica* (Chenopodiaceae) during transformation from a storage to a photosynthetic organ. *Ann. Bot.* 93, 177–187. doi: 10.1093/aob/mch026

Voznesenskaya, E. V., Franceschi, V. R., Kiirats, O., Artyusheva, E. G., Freitag, H., and Edwards, G. E. (2002). Proof of C4 photosynthesis without Kranz anatomy in *Bienertia cycloptera* (Chenopodiaceae). *Plant J.* 31, 649–662. doi: 10.1046/j.1365-313x.2002.01385.x

Wang, D., Chi, W., Wang, S., Jiao, D., Wu, S., Li, X., et al. (2004). Characteristics of transgenic rice overexpressing maize photosynthetic enzymes for breeding two-line hybrid rice. *Acta Agron. Sin.* 30, 248–252.

Wang, H., Liu, C., Ma, P. A., Lu, C., Li, K., and Wang, W. (2018). Functional characterization of cytosolic pyruvate phosphate dikinase gene (MecyPPDK) and promoter (MecyPPDKP) of cassava in response to abiotic stress in transgenic tobacco. *Crop Sci.* 58, 2002–2009. doi: 10.2135/cropsci2018.03.0204

Wang, W. B., Kim, Y. H., Lee, H. S., Kim, K. Y., Deng, X. P., and Kwak, S. S. (2009). Analysis of antioxidant enzyme activity during germination of alfalfa under salt and drought stresses. *Plant Physiol. Biochem.* 47, 570–577. doi: 10.1016/j.plaphy.2009.02.009

Wang, X., Gao, J., Gao, S., Song, Y., Yang, Z., and Kuai, B. (2019). The H3K27me3 demethylase REF6 promotes leaf senescence through directly activating major senescence regulatory and functional genes in *Arabidopsis*. *PLoS Genet.* 15:e1008068. doi: 10.1371/journal.pgen.1008068

Yadav, S., and Mishra, A. (2019). "Introgression of C4 pathway gene (s) in C3 plants to improve photosynthetic carbon assimilation for crop improvement: a biotechnological approach," in *Photosynthesis, Productivity and Environmental Stress*, eds P. Ahmad, M. A. Ahanger, M. N. Alyemeni, and P. Alam, (Hoboken, NJ: John Wiley Blackwell), 267–281. doi: 10.1002/9781119501800.ch13

Yadav, S., and Mishra, A. (2020). Ectopic expression of C4 photosynthetic pathway genes improves carbon assimilation and alleviate stress tolerance for future climate change. *Physiol. Mol. Biol. Plants* 26, 195–209. doi: 10.1007/s12298-019-00751-8

Yadav, S., Mishra, A., and Jha, B. (2018). Elevated CO2 leads to carbon sequestration by modulating C4 photosynthesis pathway enzyme (PPDK) in *Suaeda monoica* and *S. fruticosa*. *J Photochem. Photobiol. B* 178, 310–315. doi: 10.1016/j.jphotobiol.2017.11.022

Yu, T., Li, G., Dong, S., Liu, P., Zhang, J., and Zhao, B. (2016). Proteomic analysis of maize grain development using iTRAQ reveals temporal programs of diverse metabolic processes. *BMC Plant Biol.* 16:241. doi: 10.1186/s12870-016-0878-1

Yusuf, M. A., Kumar, D., Rajwanshi, R., Strasser, R. J., Tsimilli-Michael, M., and Sarin, N. B. (2010). Overexpression of γ-tocopherol methyl transferase gene in transgenic Brassica juncea plants alleviates abiotic stress: physiological and chlorophyll a fluorescence measurements. *Biochim. Biophys. Acta* 1797, 1428–1438. doi: 10.1016/j.bbabio.2010.02.002

Zhang, H., Xu, W., Wang, H., Hu, L., Li, Y., Qi, X., et al. (2014). Pyramiding expression of maize genes encoding phosphoenolpyruvate carboxylase (PEPC) and pyruvate orthophosphate dikinase (PPDK) synergistically improve the photosynthetic characteristics of transgenic wheat. *Protoplasma* 251, 1163–1173. doi: 10.1007/s00709-014-0624-1

Zhao, G. Q., Ma, B. L., and Ren, C. Z. (2007). Growth, gas exchange, chlorophyll fluorescence, and ion content of naked oat in response to salinity. *Crop Sci.* 47, 123–131. doi: 10.2135/cropsci2006.06.0371

Zinta, G., AbdElgawad, H., Domagalska, M. A., Vergauwen, L., Knapen, D., Nijs, I., et al. (2014). Physiological, biochemical, and genome−wide transcriptional analysis reveals that elevated CO2 mitigates the impact of combined heat wave and drought stress in *Arabidopsis thaliana* at multiple organizational levels. *Glob. Chang. Biol.* 20, 3670–3685. doi: 10.1111/gcb.12626

Conflict of Interest: The authors declare that the research was conducted in the absence of any commercial or financial relationships that could be construed as a potential conflict of interest.

frontiers in Plant Science

ORIGINAL RESEARCH
published: 29 May 2020
doi: 10.3389/fpls.2020.00481

Low Salinity Improves Photosynthetic Performance in *Panicum antidotale* Under Drought Stress

Tabassum Hussain[1,2], Hans-Werner Koyro[3], Wensheng Zhang[1], Xiaotong Liu[1], Bilquees Gul[2] and Xiaojing Liu[1]**

[1] Center for Agricultural Resources Research, Institute of Genetics and Developmental Biology, Chinese Academy of Sciences, Shijiazhuang, China, [2] Dr. Muhammad Ajmal Khan Institute of Sustainable Halophyte Utilization, University of Karachi, Karachi, Pakistan, [3] Institute of Plant Ecology, Justus Liebig University Giessen, Giessen, Germany

OPEN ACCESS

Edited by:
Iker Aranjuelo, Institute of Agrobiotechnology, Superior Council of Scientific Investigations, Spain

Reviewed by:
Jiyi Zhang, BASF, United States
Luisa C. Carvalho, Higher Institute of Agronomy, University of Lisbon, Portugal

***Correspondence:**
Tabassum Hussain
thussain@uok.edu.pk
Xiaojing Liu
xjliu@sjziam.ac.cn

Specialty section:
This article was submitted to Plant Abiotic Stress, a section of the journal Frontiers in Plant Science

Received: *07 December 2019*
Accepted: *31 March 2020*
Published: *29 May 2020*

Citation:
Hussain T, Koyro H-W, Zhang W, Liu X, Gul B and Liu X (2020) Low Salinity Improves Photosynthetic Performance in Panicum antidotale Under Drought Stress. Front. Plant Sci. 11:481. doi: 10.3389/fpls.2020.00481

Salinity and drought are two often simultaneously occurring abiotic stresses that limit the production of food crops worldwide. This study aimed to distinguish between the separate and combined impacts of drought and salinity on the plant response. *Panicum antidotale* was cultivated in a greenhouse under the following growth conditions: control, 100 mM NaCl (100) and 300 mM NaCl (300) salinity, drought (D; 30% irrigation), and two combinations of salinity and drought (100 + D and 300 + D). The growth response was as follows: 0 ≈ 100 > 100 + D > > D ≈ 300 ≈ 300 + D. Growth correlated directly with photosynthesis. The net photosynthesis, stomatal conductance, intercellular CO_2, transpiration, ribulose 1,5-bisphosphate carboxylase (Rubisco), ribulose 1,5-bisphosphate (RuBP) regeneration, and triose phosphate utilization protein (e.g., phosphoenolpyruvate carboxylase) were highest in the control and declined most at 300 + D, while 100 + D performed significantly better as compared to drought. Maximum and actual photosystem II (PSII) efficiencies, along with photochemical quenching during light harvesting, resemble the plant growth and contemporary CO_2/H_2O gas exchange parameters in the given treatments. Plant improves water use efficiency under salt and drought treatments, which reflects the high water conservation ability of *Panicum*. Our findings indicate that the combination of low salinity with drought was able to minimize the deleterious effects of drought alone on growth, chlorophyll content, cell integrity, photosynthesis, leaf water potential, and water deficit. This synergetic effect demonstrates the positive role of Na^+ and Cl^- in carbon assimilation and osmotic adjustment. In contrast, the combination of high salinity and drought enforced the negative response of plants in comparison to single stress, demonstrating the antagonistic impact of water availability and ion toxicity.

Keywords: water deficit, salt resistance, combined stress, photosynthesis, halophyte, stomatal and biochemical limitations

INTRODUCTION

The rapid change in global climate threatens plant growth and productivity worldwide. These changes are seriously abrupt and can be present in combinations at any given time (Qadir et al., 2014). Alterations in abiotic factors like water, salinity, temperature, soil composition, irradiance, ultraviolet radiations, nutrients, flooding, etc., are some of the examples of such changes. Tremendous efforts had been made to address the impacts of each of these abiotic stressors on plant growth (Argus et al., 2015; Hatfield and Prueger, 2015; Liu et al., 2017; Negrao et al., 2017). However, the number of studies to unravel the combined effect of multiple stress factors on plants' productivity are very few (Mittler, 2006; Zandalinas et al., 2018). The combination of the different stresses causes either a positive (synergetic) or negative (antagonistic) influence on plant performance when studied at the levels of morphology, biochemistry, and physiology (see the review of Zandalinas et al., 2018 and other references within). The interaction of water deficit (drought) and salinity is a common co-occurring constraint (Hu and Schmidhalter, 2005) that has been paid less attention to. The increase in dry lands is often linked to inappropriate irrigation with saline water resources. Thus, a progressive and consecutive development of drought and salinity stress decreases the availability of cultivable land (Abdelraheem et al., 2019). This alarming situation should be resolved at the earliest. For this, a detailed understanding of the interactions of both stressors on plant growth needs to be undertaken.

Soil salinity imposes ionic (ion toxicity and imbalance) and osmotic stress (water deficiency) by lowering the soil water potential. Low values of soil matric potential (due to excessive salts) also cause water deficit, a primary physiological constraint for plant growth (Duarte et al., 2013). However, the contribution of these factors varies according to the type of soil. Excessive Na^+ and Cl^- hinder vital physiological and biochemical mechanisms (e.g., CO_2 assimilation). Halophytes are defined as species adapted to perpetually saline conditions. Salinity can even stimulate their growth by the accumulation of Na^+ and Cl^-, i.e., cheap osmotica (Cheeseman, 2015). Such physiological mechanisms are well established in the literature (Muchate et al., 2016). In contrast, there exist a few studies on the combined effect of salinity and drought, and that, too, are on glycophytes, the plants of a non-saline environment, where reduction in plant biomass is a common finding (Ahmed et al., 2013). Xero-halophytes, the plants capable of thriving both salinity and drought stress, seem a more promising focus for such studies. Gaining such knowledge will assist in their utilization for phytoremediation and in the development of xero-halophytic crops, i.e., crops with improved tolerance to drought and salinity stresses. The latter task can be achieved by following a simple breeding procedure between a crop species and a related stress-tolerant species (Cheeseman, 2015). This is a long-desired goal considered in the context of problems such as increasing desertification, salinization of agricultural land, increasing misuse of saline irrigation, and decreasing acreage (Abdelraheem et al., 2019).

Plant biomass production and net photosynthesis are correlated (Flexas et al., 2012b). The latter is a non-invasive indicator of non-optimal environmental conditions for plant growth. Net photosynthesis rate, under stress conditions, decreases due to stomatal and non-stomatal limitations, such as ribulose 1,5-bisphosphate carboxylase (Rubisco) enzyme activity, regeneration of ribulose 1,5-bisphosphate (RuBP), triose phosphate utilization, electron transport rate, the efficiency of photosystem II (PSII), etc. (Chaves et al., 2009; Chen et al., 2015). A large number of studies had been conducted to elucidate photosynthesis-limiting steps during stress conditions (such as salinity and drought) (Chen et al., 2015; Wang et al., 2017; Bellasio et al., 2018).

Stomatal closure appears as a first major response due to salinity (osmotic effect) that ultimately limits CO_2 assimilation. Nevertheless, this is not the case for every halophyte as the efficiency of PSII (F_v/F_m and ΦPS2), electron transportation rate (ETR), and other biochemical factors also play a role in limiting photosynthesis (Wang et al., 2017). Accumulated Na^+ and Cl^- directly inhibit the activity of the Rubisco enzyme (Koyro et al., 2013; Galmés et al., 2017). The maximum and actual quantum efficiency of PSII was decreased in some plant species, while others are capable of resisting this reduction under stress (Koyro et al., 2013; Asrar et al., 2017). Reduction in ETR slows down the photochemical reactions, but it also protects the cell from electron leakage due to the damage in photosynthetic pigments (Tezara et al., 1999). Likewise, non-photochemical quenching (NPQ) enhances the photoprotective mechanism when a plant cannot properly channel the incident light energy to photochemistry. Thus, this competition between NPQ and photochemistry lowers the use of available light energy into photosynthesis. NPQ benefits plants when a decrease in gaseous exchange (due to closed stomata) reduces carbon fixation (Calvin cycle) and light energy becomes excessive to its utilization in light reactions. The rate-limiting factors of photosynthesis under salinity have been discussed in detail. A very few studies have focused on water deficit experiments while quantifying these limiting factors (Tezara et al., 1999; Galmés et al., 2017).

The closure of the stomata limits carbon uptake; however, it reduces the loss of water. Thus, plants maintain tissue osmotic conditions under stress (i.e., salt and drought). Such advantage becomes more apparent in the case of plants with C_4 (i.e., an efficient) carbon fixation mechanism. These plants achieve high water use efficiency and are competitively better than plants possessing the C_3 mechanism, a common carbon fixation pathway. In this study, we hypothesized whether the combination of salinity with a water deficit condition in the C_4 plant *Panicum antidotale* minimizes the impact of stress due to its advantageous C-fixing mechanism and high water use efficiency. The reason for selecting this test species is its wide and natural distribution in plant-deprived lands (e.g., water deficit, saline, high temperature, etc.). Also, it is often regarded for its potential as an alternate crop (Ashraf, 2003; Ahmad et al., 2009; Khan et al., 2009; Hussain et al., 2015). These observations provoked our interest to determine its adaptation mechanisms in response to a combination of stress factors as the combined effect of salt and drought stress on the photosynthetic capacity of plants has not been investigated

earlier, to the best of our knowledge. We designed this study to quantify the photosynthetic responses of *P. antidotale* in response to the combined stress of salinity and water deficit, i.e., conditions comparable to its natural environment. The specific objectives of the studies were to: (1) correlate photosynthetic responses with growth and water relations and (2) distinguish the stomatal and non-stomatal limitations of photosynthesis.

MATERIALS AND METHODS

Plant Culture and Stress Treatments

Seeds were collected from natural mono-stand populations from the coast of Karachi, Pakistan, and were surface sterilized with 1% sodium hypochlorite for 1 min. Seeds were allowed to germinate in a growth chamber (25°C/14°C and 14/10-h day/night regimes) in perlite. Equal-sized three-leaf stage seedlings were transplanted to a greenhouse (28°C/16°C ± 2 and 14/10 h day/night regimes, 40–60% humidity, 600 ± 45 μmol photon m^{-2} s^{-1} light) in pots (15 × 22 cm, three plants/pot and three pots for each treatment) containing about 4 kg quartz sand (1–2 mm diameter) and irrigated with half-strength Hoagland's nutrient solution (Epstein, 1972). Stress treatments were introduced after 2 weeks of seedling establishment. Plants were subjected to the following treatments: control (CK), salinity with 100 and 300 mM NaCl (S), drought (D), and a combination of salinity and drought (S + D). The drought-treated pots were irrigated 30% (by volume) of solution as compared to the control pots (i.e., irrigated with maximum field capacity), while in the case of the S + D treatment, 100 mM + nutrient solution (100 + D) and 300 mM + nutrient solution (300 + D) with the same volume as in the drought treatment. The salinity and drought treatments were introduced in steps: 50 mM NaCl in the morning and evening, and drought was achieved after 4–5 days in all drought treatments. The NaCl concentrations and drought conditions were maintained daily by a gravimetric approach and nutrient solutions were replaced every 3 days to avoid nutrient deficiencies. The pots' positions were replaced randomly in the greenhouse to minimize block effects.

Plant Biomass

Three plants from three pots were harvested after 4 weeks of stress treatments, and fresh weight was recorded immediately while dry weight was measured after drying at 70°C in an oven until a constant weight was achieved (>48 h).

Water Relations

Leaf water content (WC) was calculated by subtracting the leaf dry weight from the fresh weight and expressing it as percent of fresh weight. The relative water content (RWC) was estimated by the method of Sharp et al. (1990). Leaf discs (more than eight) of 1 cm diameter (avoiding the margins and midrib) were cut and fresh weight (FW) was recorded. Five milliliters of deionized water was poured on these discs overnight at 4°C and then turgid weight (TW) was determined. Leaf discs were dried at 65°C for ∼48 h and, subsequently, dry weight (DW) was measured and the relative water content [RWC = (FW − DW)/(TW − DW) × 100] was calculated. Leaf water potential was determined at predawn by a dew point potential meter (WP4 dew point potentiometer, Decagon Devices, Pullman, NE, United States). Therefore, leaf samples were cut into sample pieces (∼1–2 mm diameter discs) to cover the 40 mm cup of the WP4 dew point potentiometer. The water potential (ψ_w) was expressed in megapascals.

Photosynthesis Measurements

Gas exchange and chlorophyll fluorescence measurements were performed on the first fully expanded (third and fourth) leaf by using an infrared gas analyzer, IRGA (LI6400XT, LI-COR Biosciences, Lincoln, NE, United States), equipped with red–blue LED chamber (2 cm^2 area; 6400-40, LI-COR Biosciences). The light response curve (P_n–PAR, photosynthetic active radiation), CO_2 response curve (P_n–C_i), and chlorophyll fluorescence were measured on three different plants (each from a different pot) on each treatment. All measurements were performed from 0830 to 1500 h.

Light Response Curves

Photosynthesis light response curves (P_n–PAR) were measured after leaf acclimation at 2,000 μmol photon m^{-2} s^{-1} for about 40–50 min to stabilize stomatal conductance at C_{atm} 400 μmol CO_2 m^{-2} s^{-1} with a flow rate of 300 μmol s^{-1} and humidity was about 40–65%. A stepwise decrease of the photosynthetic photon flux density (PPFD) from 2,000 to 0 μmol photon m^{-2} s^{-1} was carried. Measurements were taken at each light step after about 7–10 min, at a steady and stabilized response of the leaf. In accordance with Schulte et al. (2003), a non-linear exponential function was applied to the light response curve.

$$f(x) = a - \exp[b(-x)]c \tag{1}$$

where $f(x)$ is the net carbon assimilation and x the incident PPFD on leaf. The coefficients (a), (b), and (c) were calculated by Newton's least-square method. Coefficient (a) represents the maximum carbon flux at the saturated light, while dark respiration (R_d) was estimated as the [(a) − (c)]. The saturation irradiance (I_s), light compensation point (I_c), and apparent quantum yield of CO_2 assimilation (Φ_{CO2}) were calculated using the following equations:

$$I_s = \ln\left(0.1.\frac{a}{c}\right).(-\frac{1}{b}) \tag{2}$$

$$I_c = \ln\left(\frac{a}{c}\right).(-\frac{1}{b}) \tag{3}$$

$$\Phi_{CO2} = \exp\exp\left[b\,(-\mathrm{Ic})\right]cb \tag{4}$$

At saturated PPFD, the net photosynthesis rate (P_n), stomatal conductance (g_s), intercellular CO_2 (C_i), transpiration (E), intrinsic water use efficiency (WUEi: P_n/g_s), ETR/P_{ngross} (P_{gross} = P_n + dark respiration), and C_i/C_{atm} were also recorded at saturated PPFD of three different plants in each treatment.

Photosynthesis CO_2 Response Curves

The CO_2 response curves were measured at light saturation at 1,500 μmol photon m^{-2} s^{-1} PPFD at a temperature of 28°C,

60% humidity, 1.0–1.5 kPa vapor pressure deficit (VPD), and 300 μmol s^{-1} flow rate by the LED chamber (2 cm^2 area; 6400-40, LI-COR Biosciences). Leaves were acclimated for 40–50 min to achieve a constant net photosynthesis and stomatal conductance at a C_{atm} of 400 μmol CO_2 m^{-2} s^{-1} before the induction of the CO_2 response curve. A series of C_{atm} ranging from 1,500 to 0 μmol CO_2 m^{-2} s^{-1} (400, 300, 200, 100, 50, 0, 400, 400, 600, 1,000, and 1,500) was adjusted until a stable reading of the net photosynthesis, intercellular CO_2, and stomatal conductance (about 7 min at each change) for constructing the photosynthesis CO_2 response curves on the three different plants of each treatment. According to Von Caemmerer (2000), we estimated Rubisco carboxylase activity (V_{cmax}) and RuBP regeneration in terms of J_{max}.

Chlorophyll Fluorescence and Chlorophyll Content

Chlorophyll *a* fluorescence was measured simultaneously with the P_n–C_i response curves by using the same LED chamber (2 cm^2 area; 6400-40, LI-COR Biosciences). About 30-min dark-adapted leaves were used for the minimal fluorescence (F_o) at 0.5 μmol photon m^{-2} s^{-1}, while the maximum fluorescence (F_m) was recorded after applying a light saturating pulse (>8,000 μmol photons m^{-2} s^{-1} for 0.8 s). The maximum quantum efficiency of PSII reaction centers ($F_v/F_m = F_m - F_o/F_m$) was calculated (Kitajima and Butler, 1975). The leaf was adapted to saturated light for about 40–50 min and then steady-state fluorescence (F_s) and the maximum quantum efficiency of PSII of the light-adapted leaf (F'_m) were recorded. The quantum efficiency of PSII (ΦPS2), non-photochemical quenching (NPQ), and photochemical quenching (qP) were determined using the following equations (Genty et al., 1989; Kooten and Snel, 1990):

$$\Phi PS2 = \frac{F'_m - F_s}{F'_m} \quad (5)$$

$$NPQ = \frac{F_m}{F'_m} - 1 \quad (6)$$

$$qP = \frac{F'_m - F_s}{F'_m - F'_o} \quad (7)$$

ΦPS2 represents the electron transport in PSII of the photosynthesis per absorbed photon. The electron transport rate (ETR) was also calculated as:

$$ETR = \Phi PS2.PPFD.0.5.0.87 \quad (8)$$

where 0.5 is the assumption of equal distribution of incident light between PSI and PSII and 0.87 indicates the leaf light absorbance.

The chlorophyll content of leaves was measured with a SPAD 502 chlorophyll meter without causing damage to plants on the same leaf, which has been selected for gas exchange measurements. A minimum of 15 readings were performed on one leaf and the data expressed as the mean of three different plant leaves.

Photosynthetic Proteins

Fully matured leaves were taken from the plant and immediately frozen in liquid nitrogen. About 0.1 g of ground leaves was vortexed in an extraction buffer (125 mM Tris–HCl, pH 6.8, containing 4% SDS, 10% mercaptoethanol, 20% glycerol, and 0.004% bromophenol blue) and heated at 95°C for 10 min. Proteins were separated by 10% SDS-PAGE for phosphoenolpyruvate carboxylase (PEPC), Rubisco, and glycine decarboxylase complex (GDC). The proteins were then transferred to a nitrocellulose membrane and immunoblotted (n = 3) with primary antibodies, PEPC and GDC H-subunits (1:1,000), purchased from PhytoLab (catalog numbers PHY0048 and PHY0655S). The band intensities were quantified with ImageJ 1.52 software (NIH, United States). Band intensities of the control treatments were assumed to be 100%, and upregulation and downregulation were expressed accordingly after using β-actin protein as the standard to calculate proteins in each sample.

Analyses of Limitation in CO_2 Assimilation and Stomatal Morphometry

Separation of the quantitative limitation analysis approach at saturating light was used. Disentangling the limitations of the net photosynthesis due to stomata (L_S) and non-stomata (L_{SN}) was estimated by the following expressions:

$$L_S = \frac{P'''_n - P''_n}{P'''_n} * 100 \quad (9)$$

$$L_{SN} = \frac{P''_n - P'_n}{P'''_n} * 100 \quad (10)$$

where P'_n is the net photosynthesis rate at ambient conditions in the greenhouse, P''_n is the P_n at C_{atm} = 400 μmol CO_2 m^{-2} s^{-1}, while P'''_n is the P_n at C_i = C_{atm} = 400 μmol CO_2 m^{-2} s^{-1} (Farquhar and Sharkey, 1982; Bellasio et al., 2018).

Stomatal morphometric analyses were conducted with the peel-off method. Transparent nail polish was used to prepare slides (n = 3). The number of stomata, area of the guard cells (stomatal area), the roundness of the stomata, and the area of the stomatal aperture were estimated in the given area by using ImageJ 1.52 software (NIH, United States).

Carbon Isotope Discrimination and Bundle Sheath Leakiness

The leaves used for photosynthesis measurements (third and fourth from the top) were dried and ground in a ball mill (MM200, Retch, Germany). The triplicate of 2 mg samples was packed into a tin capsule for ^{13}C isotope determination using a mass spectrometer (IRMS IsoPrime 100 Elementar, a vario PYRO cube, Elementar, Germany). The following formula was used to calculate $\delta^{13}C$ (Kubásek et al., 2007):

$$\delta^{13}C = \left(\frac{R_p}{R_s} - 1\right) * 1,000 \quad (11)$$

where R_p is the $^{13}C/^{12}C$ obtained from a mass spectrometer in plant samples and R_s is a reference value of $^{13}C/^{12}C$ in standard V-PDB (Vienna Pee Dee Belemnite); all values were expressed as per mil of dry weight. Carbon isotope discrimination ($\Delta^{13}C$) in

the leaves was calculated from plant $\delta^{13}C$ values (δ_p) and air $\delta^{13}C$ values (δ_a) with the following formula (Farquhar et al., 1989):

$$\Delta^{13}C = \frac{\delta_a - \delta_p}{1 + \frac{\delta_p}{1{,}000}} \quad (12)$$

Bundle sheath leakiness (φ) was estimated according to Farquhar (1983) with the following expression:

$$\varphi = \frac{\left[\Delta^{13}C - a + \frac{(a-b_4)C_i}{C_{atm}}\right]}{\left[\frac{(b_3-s)C_i}{C_{atm}}\right]} \quad (13)$$

where a, b_3, b_4, and s are isotopic discrimination constants; a (4.4‰) is CO_2 in air diffusivity through the stomata, b_3 (29‰) is the carboxylation of Rubisco, b_4 (−5.7‰) is the HCO_3^- dissolution and fractionation of phosphoenolpyruvate (PEP) carboxylation, and s (1.8‰) is the leakage of CO_2 from the bundle sheath to mesophyll cells.

Statistical Analyses

The experiment was repeated twice in similar conditions of greenhouse and the data presented here as the mean ± SE ($n = 3$) for all parameters. Two-way analysis of variance (ANOVA) was performed to study differences in treatments, while a *post hoc* test (Bonferroni) was also calculated to examine the significant difference ($P < 0.05$) among the means of each treatment. Linear regressions were carried out between P_n vs. (L_S, L_{NS}, $\Delta^{13}C$, and φ), $\Delta^{13}C$ vs. (ψ_w, C_i/C_{atm}, WUEi, and φ), φ vs. (ψ_w, C_i/C_{atm}, and WUEi), g_s vs. (L_S and WUEi), L_S vs. WUEi, V_{cmax} vs. L_{NS}, and ΦPS2 vs. Φ_{CO2} at various PPFDs in all treatments. These are shown as **Supplementary Material**.

RESULTS

Plant Biomass and Water Relations

Salinity, drought, and a combination of both (S + D) affected the biomass of *P. antidotale* significantly ($P < 0.001$; **Figure 1**). Plant biomass did not only decline under individual treatments of high salinity and drought but also at 300 + D in comparison to the control treatment. Interestingly, combined treatment (100 + D, $P < 0.001$) led to a higher growth (significant differences in various parameters: dry weight, water content, and relative water content) than did drought alone. The water potential (negative values in megapascals) of leaves also showed a similar trend, with the exception of the 100 + D treatment, where it was similar to the control and 100 mM NaCl-treated plants.

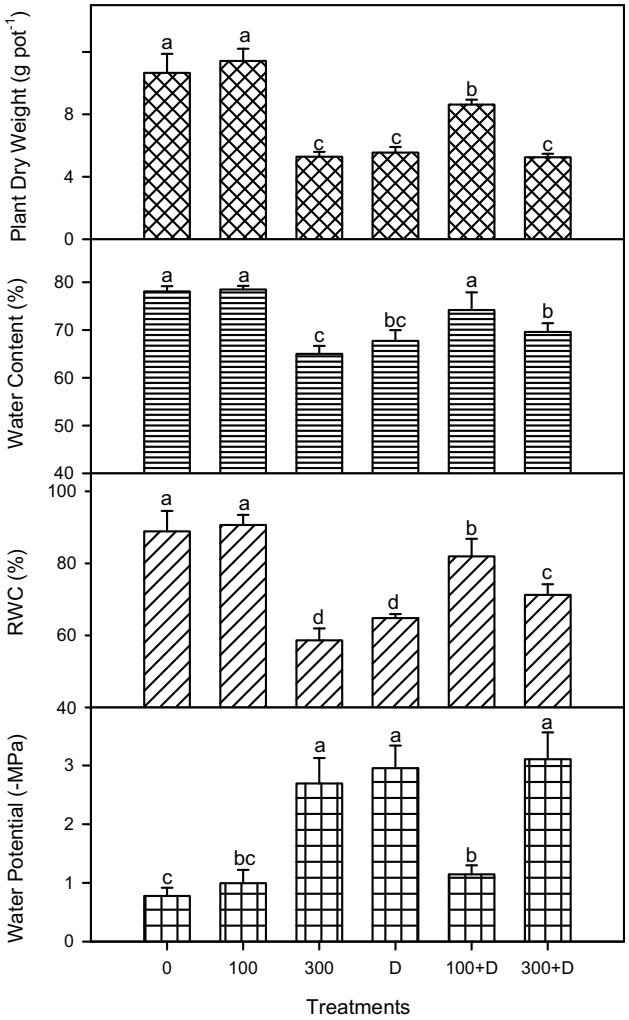

FIGURE 1 | | Plant biomass and water relations under salinity, drought, and a combination of both treatments. Mean ± SE ($n = 3$) of plant dry weight (in grams per pot), leaf water content (percent of fresh weight), relative water content (*RWC*, in percent), and leaf water potential (in megapascals) for treatments of 0, 100, and 300 mM NaCl, drought (D), and a combination of salinity and drought [100 and 300 mM NaCl + drought (100 + D and 300 + D, respectively)]. *Different letters* denote, after Bonferroni *post hoc* test, significant difference ($P < 0.05$).

H_2O_2/CO_2 Gas Exchange Parameters at Saturated Light

The P_n declined under provided stress treatments of either salt and drought alone or a combination of both ($P < 0.001$; **Table 1**). The maximum P_n was recorded under 100 mM NaCl treatment (statistically insignificant when compared to the control) and the lowest value was observed under 300 + D treatment. High salinity severely decreased the values of P_n when added to drought conditions, whereas low salinity enhanced the values when combined with drought (i.e., 100 + D). The other parameters of gaseous exchange, g_s, C_i, and E are also well correlated with P_n and with each other. The light response curves revealed CO_2 saturation of the control and low-salinity-treated plants at a PPFD of 2,000 μmol photon m^{-2} s^{-1} while that of drought (alone)-treated plants at irradiance below 600 μmol photon m^{-2} s^{-1}. The addition of salinity (both moderate and high) to drought conditions improved the saturation irradiance of the plants compared to that in response to drought alone (see I_s data; **Table 1**). The CO_2 compensation point (I_c), the quantum efficiency of CO_2 (Φ_{CO2}), and dark respiration were also significantly affected by the applied treatments, while ETR/P_{ngross}

TABLE 1 | CO_2/H_2O gas exchange responses under salinity, drought, and the combination of both.

Gas exchange	Treatments					
	0	100	300	D	100 + D	300 + D
P_n (μmol m^{-2} s^{-1})	22.71*a* ± 0.82	23.19*a* ± 0.83	12.78*c* ± 0.31	10.64*c* ± 0.49	17.61*b* ± 0.52	8.20*d* ± 0.20
g_s (mol m^{-2} s^{-1})	0.149*a* ± 0.012	0.122*b* ± 0.010	0.074*d* ± 0.003	0.044*e* ± 0.003	0.109*c* ± 0.009	0.039*e* ± 0.001
C_i (μmol m^{-2} s^{-1})	235*a* ± 18.43	175*b* ± 6.03	107*d* ± 4.76	98*e* ± 6.65	151*c* ± 3.76	62*f* ± 4.22
E (mol m^{-2} s^{-1})	3.71*a* ± 0.059	2.78*b* ± 0.014	1.50*c* ± 0.053	1.29*d* ± 0.017	2.81*b* ± 0.008	0.78*e* ± 0.012
WUEi (P_n/g_s)	155*bc* ± 18	193*b* ± 18	171*bc* ± 5	245*a* ± 22	164*c* ± 16	212*a* ± 7
ETR/P_{ngross} (unitless)	4.61*b* ± 0.21	4.78*b* ± 0.06	6.79*a* ± 0.81	4.67*b* ± 0.07	4.45*b* ± 0.13	4.28*b* ± 0.13
C_i/C_{atm} (unitless)	0.59*a* ± 0.046	0.44*b* ± 0.015	0.27*d* ± 0.012	0.49*b* ± 0.017	0.38*c* ± 0.009	0.16*e* ± 0.011
R_d (μmol m^{-2} s^{-1})	−0.65*b* ± 0.07	−0.61*b* ± 0.01	−0.36*a* ± 0.06	−0.92*c* ± 0.08	−1.76*e* ± 0.08	−1.46*d* ± 0.05
I_S (μmol m^{-2} s^{-1})	2, 050*a* ± 100	2, 015*a* ± 44	1, 296*c* ± 55	542*d* ± 47	1, 809*b* ± 100	1, 020*c* ± 77
I_C (μmol m^{-2} s^{-1})	56.65*a* ± 3.22	47.68*b* ± 2.23	37.26*c* ± 5.22	20.71*d* ± 6.23	49.74*b* ± 5.23	35.15*c* ± 3.23
Φ_{CO2} (mol CO_2 μmol^{-1})	0.017*a* ± 0.000	0.018*a* ± 0.000	0.012*c* ± 0.001	0.009*d* ± 0.001	0.014*b* ± 0.000	0.008*d* ± 0.000
V_{cmax} (μmol m^{-2} s^{-1})	72.68*b* ± 5.93	78.49*a* ± 7.67	36.86*d* ± 3.93	24.20*e* ± 2.31	57.88*c* ± 5.35	14.84*f* ± 1.91
J_{max} (μmol m^{-2} s^{-1})	72.51*b* ± 8.24	78.94*a* ± 8.68	36.03*d* ± 4.91	24.49*e* ± 3.91	57.89*c* ± 2.00	15.16*f* ± 1.03

The values of net photosynthesis (P_n), stomatal conductance (g_s), intercellular CO_2 (C_i), transpiration rate (E), water use efficiency (WUEi), ETR/P_{ngross}, C_i-to-CO_2 in air ratio (C_i/C_a), dark respiration (R_d), saturation light (I_s), CO_2 compensation point (I_c), apparent quantum yield of CO_2 assimilation (Φ_{CO2}), Rubisco carboxylase activity (V_{cmax}), and RuBP regeneration (J_{max}) are the mean of three replicates ± SE. Different letters express differences between treatments after Bonferroni post hoc test ($P < 0.05$). 0, 100, and 300 are millimolar concentrations of NaCl treatments, D is drought, and 100 + D and 300 + D are combinations of drought with 100 and 300 mM NaCl, respectively.

increased only in 300 mM NaCl. The highest intrinsic water use efficiency (WUEi) was recorded for drought alone (D) and 300 + D-treated plants.

The CO_2 response curves (**Figure 2**) were used to determine various photosynthetic parameters (**Table 1**). The V_{cmax} and J_{max} were unaffected at 100 mM NaCl, but significantly reduced in response to other treatments (300 mM NaCl, D, 100 + D, and 300 + D) when compared to the control. The combination of drought and low salinity enhanced V_{cmax} and J_{max} about 50% in comparison to drought only, but these values were still lower than 100 mM NaCl. The highest reduction was observed with the 300 + D treatment, where these parameters were about one-fifth of the values of the control.

Immunoblots of PEPC, Rubisco, and GDC contents in leaf tissues revealed significant changes under the treatments provided (**Figure 3**). The protein content increased in response to 100 mM NaCl, but decreased at 300 mM NaCl. A combination of high salinity and drought caused a severe reduction in their contents as compared to salt and drought alone.

Carbon Isotope Discrimination and Stomatal and Non-stomatal Limitations During Photosynthesis

Carbon isotope ($\delta^{13}C$) in leaf tissues was significantly reduced under high salinity, and a further reduction was recorded at drought and 300 + D treatments, in contrast to control plants. A similar trend was observed in leaf ^{13}C isotope discrimination ($\Delta^{13}C$) among all treatments, while bundle sheath leakiness (φ) of CO_2 was the highest in the 300 + D treatment (**Figure 4**). **Figure 5** shows the quantitative contribution of photosynthetic limitations in response to the applied treatments. Stomatal limitation (L_S) contributed about 25–30% at salinity (300 mM NaCl) and combination of salinity and drought (300 + D), while L_S was significantly higher at drought treatment (about 35%). The non-stomatal limitation (L_{NS}) appears to be a major limiting factor of photosynthesis in response to the combination of salinity and drought (300 + D), although it accounted for at least 30% of limitation at 300 mM NaCl and drought treatment as well.

The stomatal morphometric estimation showed a decreasing trend of stomatal area and aperture in salt, drought, and the combination of both, whereas the number of stomata was mainly decreased with the introduction of the drought condition. The 100 + D treatment showed increased values of these parameters as compared to drought alone (**Figure 6**).

Chlorophyll *a* Fluorescence Parameters and Chlorophyll (SPAD)

Chlorophyll *a* fluorescence was measured simultaneously with the gas exchange parameters on the similar leaf in all the aforementioned treatments (**Figure 7**). The maximum and apparent quantum efficiency of PSII (F_v/F_m and ΦPS2) remained unaffected under saline treatment (both low and high salinity), but with about 15 and 10% reductions in F_v/F_m, and 3.9- and 4.3-fold reductions in ΦPS2 were recorded under drought and 300 + D treatments, respectively, when compared to the control. These parameters were a little improved in response to not only 100 mM NaCl but also to 100 + D. In comparison to the control, photochemical quenching (qP) and ETR were reduced at salinity, drought, and the combination of both. The reduction in qP were about 31, 85, and 60% at 300 mM NaCl, drought, and 300 + D, respectively, while the reduction in ETR was more pronounced at the 300 + D treatment. The magnitude of heat dissipation (NPQ, non-photochemical quenching) increased by 20% at drought and 300 + D treatments when compared to the control. These aforementioned parameters of chlorophyll fluorescence had a better response at 100 + D when compared to drought treatment

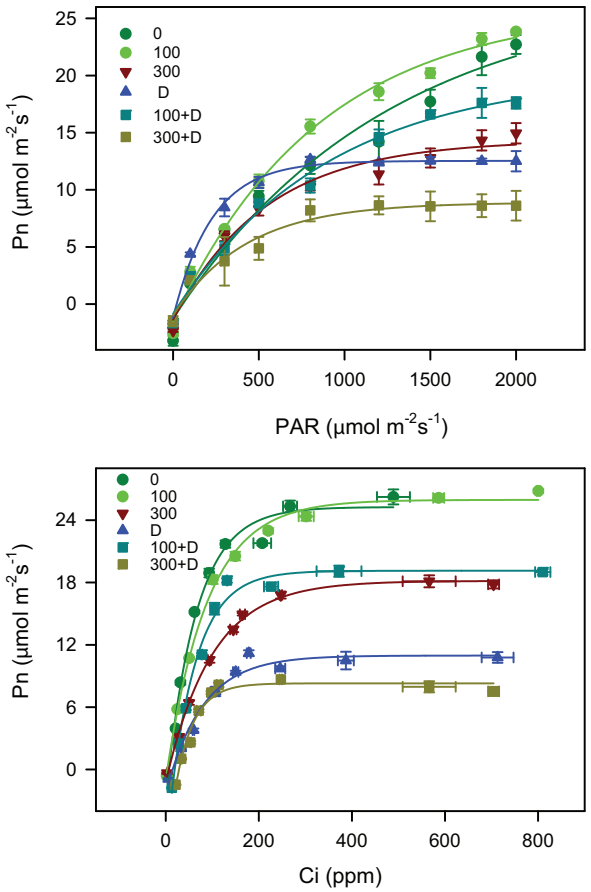

FIGURE 2 | Light response curve (P_n–PAR) and carbon response curve (P_nn–C_i) measurements under salinity, drought, and a combination of both treatments. P_n–PAR curve represents the response of net photosynthesis in the range of 0–2000 µmol m^{-2} s^{-1} photosynthetic active radiation (PAR) and P_n–C_i curve indicates the capacity of net photosynthesis under various intercellular CO_2 concentrations (in micromoles per square meter per second) when CO_2 in the air (C_{atm}) is in the range of 0–1,500 µmol m^{-2} s^{-1}. Values shown are the mean ± SE (n = 3) under all treatments, as described in **Figure 1**.

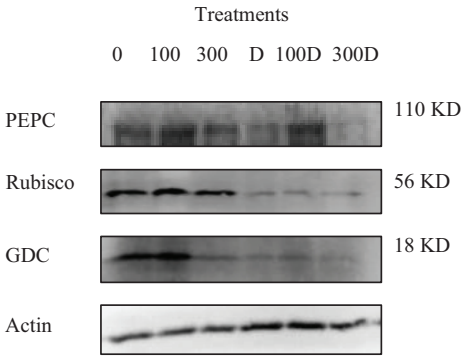

	Treatments					
	0	**100**	**300**	**D**	**100+D**	**300+D**
PEPC	100b	141a	63c	34d	119a	19e
Rubisco	100b	133a	78c	34d	45d	24e
GDC	100b	167a	44c	29d	40c	19e

FIGURE 3 | Variations of photosynthetic protein expressions. Immunoblots of phosphoenolpyruvate carboxylase (PEPC), ribulose 1-5, bisphosphate carboxylase/oxygenase (Rubisco), and glycine decarboxylase (GDC) expressed changes in the protein expressions under treatments of 0, 100, and 300 mM NaCl, drought (D), and a combination of salinity with drought [100 and 300 mM NaCl + drought (100 + D and 300 + D respectively)]. *Different letters* denote, after Bonferroni *post hoc* test, significant difference ($P < 0.05$).

alone. In addition, SPAD values representing the chlorophyll content in the leaves also reveal a similar pattern, i.e., reduced content at high salinity, drought, and a combination of both.

Correlation Between Various Parameters

The linear regressions were carried out between various parameters at salt, drought, and a combination of both treatments (**Supplementary Material**). The r^2-values showed a strong correlation under all the treatments tested. The decline in net photosynthesis was well correlated ($P < 0.001$) with the various parameters (**Supplementary Figure S1**), and similarly the water potential was significantly correlated ($P < 0.01$) with the carbon isotope data (**Supplementary Figure S1**). WUEi was also correlated with L_s ($P < 0.001$, $r^2 = 0.51$), g_s ($P = 0.07$, $r^2 = 0.60$), and φ ($P = 0.1$, $r^2 = 0.48$). The r^2-values were low (∼0.2–0.3) with $\Delta^{13}C$ and φ, while a high correlation was observed between $\Delta^{13}C$ and φ ($P < 0.001$, $r^2 = 0.99$). The reduction in stomatal conductance (g_s) was well correlated ($r^2 = 0.71$) with stomatal limitation of photosynthesis.

DISCUSSION

Salinity and water deficit conditions often coexist in nature, particularly in arid and semi-arid areas of the world. The purpose of this study was to determine the individual and combined effects of these stressors, with special emphasis on the photosynthesis performance of *Panicum antidotale*. A combined stress of low salinity and drought (100 + D) benefited the plants. However, high salinity combined with drought (300 + D) negatively affected several physiological processes.

Synergetic Relationship Between Salinity and Water Deficit Condition

The synergetic effects of salinity and drought were observed at both 100 + D and 300 + D treatments (**Figure 1**). Similar effects have been reported for the halophyte *Zygophyllum xanthoxylum* (Ma et al., 2012) and some cultivars of barley (Ahmed et al., 2013). Although the plant growth was not stimulated by low salinity, as reported for other monocotyledon halophytes (Flowers and Colmer, 2008; Koyro et al., 2013; Hussain et al., 2015), a combination of low salinity and drought

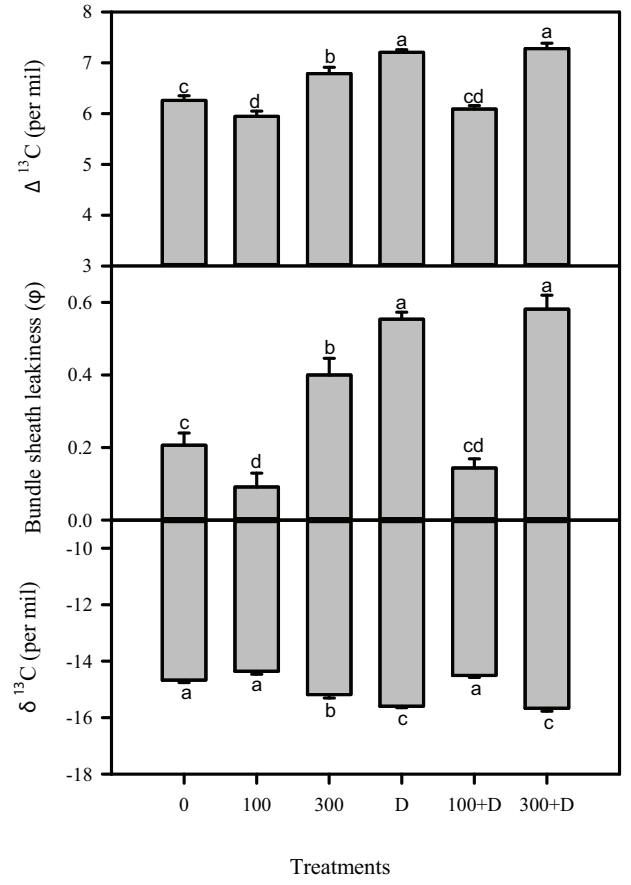

FIGURE 4 | Measurement of carbon isotope in the leaf of *Panicum antidotale* under salinity, drought, and a combination of both treatments. Carbon isotope discrimination in the leaf ($\Delta^{13}C$), bundle sheath leakiness (φ), and carbon isotope in leaf ($\delta^{13}C$) showed variations under treatments of 0, 100, and 300 mM NaCl, drought (D), and a combination of salinity with drought [100 and 300 mM NaCl + drought (100 + D and 300 + D, respectively)]. *Different letters* denote, after Bonferroni *post hoc* test, significant difference ($P < 0.05$).

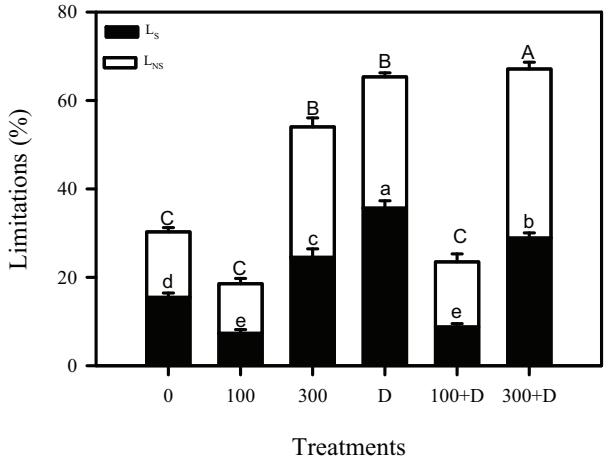

FIGURE 5 | Contribution of limitation in photosynthesis estimation. *Dark* and *white bars* represent stomatal limitation (L_S) and non-stomatal limitation (L_{NS}), respectively, in the leaf of *Panicum antidotale* under treatments of 0, 100, and 300 mM NaCl, drought (D), and a combination of salinity with drought [100 and 300 mM NaCl + drought (100 + D and 300 + D, respectively)]. *Different letters* denote, after Bonferroni *post hoc* test, significant difference ($P < 0.05$).

(100 + D treatment) enhanced plant biomass in contrast to drought treatment alone. Thus, the role of the uptake of Na^+ and Cl^- ions, i.e., cheap osmotica, in reducing the drastic effects of water deficit conditions can be presumed. This assumption is further evidenced by the high values of the relative water content (RWC) and water content (WC) in this treatment (**Figure 1**). On the other hand, high salinity combined with drought (300 + D) did not cause any further decrease in plant biomass when compared to both (high salinity and drought) treatments alone. This response is antagonistic to that recorded at the 100 + D treatment, i.e., reduction in biomass.

Photosynthetic Adaptation Under Salinity, Drought, and Combined Stress Conditions

Measurements of CO_2/H_2O in our test species clearly indicated the different responses under single (salinity or drought) and combined stresses (**Table 1**). Low salinity coupled with drought (100 + D) buffered the negative impact of drought on gaseous exchange. However, alone (100 mM NaCl), it did not cause any significant increase in net photosynthesis. We, therefore, assume that the hazardous impacts of drought conditions on photosynthetic performance can be lessened by combining drought stress and moderate salinity. This can be explained as enhanced activities of certain enzymes of the C_4 cycle by chloride ions (Guo et al., 2018). Analyses of the PEP carboxylase expression also validated this hypothesis. The accumulated ions contribute to osmotic adjustment (Flowers and Colmer, 2008) by allowing plants to uptake water (i.e., RWC) when very little water is available in the medium. The uptake of water in such a stressful environment facilitates stomatal conductance (g_s), which ensures CO_2 influx to the photosynthesizing cells (Flowers and Colmer, 2008; Ma et al., 2012; Hussain et al., 2015).

A further increase in salinity led to an antagonistic plant response. The plants could not cope with the combined stress treatment (300 + D), probably because of the excessive intake of ions, as an effort to adjust osmotically, causing ion toxicity or imbalance. Thus, the closure of the stomata (low g_s and stomatal aperture) (**Table 1** and **Figure 6**), as a strategy to conserve plant water, resulted in lower values of intercellular CO_2 (C_i) and C fixation, as explained in Ashraf (2003) and Asrar et al. (2017). Net photosynthesis and gaseous exchange were significantly decreased in these plants compared to high salinity and drought alone. On the contrary, C_i remained unchanged in a number of C_4 species under drought or salinity (Koyro et al., 2013; Asrar et al., 2017). This variation may be due to the different experimental setup, non-stomatal limitations such as CO_2 leakage (see below), species specificity, and/or different tolerance limits under various stresses.

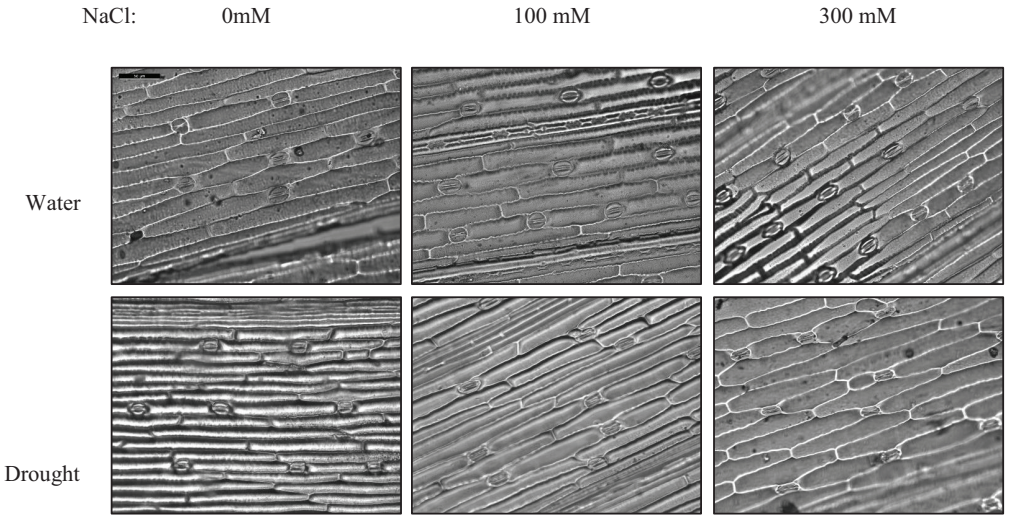

Treatments	Number of stomata (# / cm^2)		Stomatal area (μm^2)		Roundness of stomata (μm)		Stomatal aperture (μm^2)	
0	13.50a	±0.50	388.67b	±4.18	0.88a	±0.05	91.25a	±8.34
100	13.57a	±0.30	427.33a	±29.55	0.89a	±0.03	105.25a	±3.17
300	12.63ab	±0.63	249.00c	±6.56	0.60c	±0.06	71.67b	±7.69
D	8.68c	±0.34	208.67d	±24.74	0.71b	±0.04	39.00d	±3.21
100+D	11.02b	±0.58	232.33dc	±5.04	0.60c	±0.01	49.93c	±1.46
300+D	9.19c	±0.19	200.00d	±22.55	0.45d	±0.01	36.67d	±1.20

FIGURE 6 | Stomatal morphometric characteristics of *Panicum antidotale*. Changes in the number of stomata, stomatal area, roundness of stomata, and area of the stomatal aperture for treatments of 0, 100, and 300 mM NaCl, drought (D), and a combination of salinity with drought [100 and 300 mM NaCl + drought (100 + D and 300 + D, respectively)] are shown. *Different letters* denote, after Bonferroni *post hoc* test, significant difference ($P < 0.05$).

C_4 plants are equipped with a competitively better photosynthetic machinery, i.e., the presence of PEP carboxylase in mesophyll cells. This enzyme is highly efficient in fixing carbon even when the concentration of C_i becomes low due to stomatal closure (Way et al., 2014). Thus, the plants are benefited with minimal loss of water and improved photosynthesis as compared to C_3 plants. Our results clearly indicate that the stomatal limitation (L_S) in *Panicum* is an adaptive strategy to conserve water by reducing transpirational rates and improving WUEi (**Table 1**), particularly in response to drought and 300 + D treatments. This may be an advantageous effect, but at the cost of low carbon assimilation, similar to other C_4 plants (Ashraf, 2003; Galmés et al., 2017).

Diffusional resistance or leakiness of CO_2 into bundle sheath cells affects photosynthesis in drought- and/or salinity-treated C_4 plants (Farquhar and Sharkey, 1982; Farquhar, 1983; Ellsworth and Cousins, 2016). An enhanced leakage of CO_2, in drought treatment and combined stress (300 + D), decreased the efficiency of the C_4 carbon-concentrating mechanism, which is evidenced by the reduced expression of PEP carboxylase (**Figure 3**). Such findings have been previously discussed (Cernusak et al., 2013; Tomás et al., 2013; Kromdijk et al., 2014). In contrast to the control (no salinity and no drought) plants, low values of bundle sheath leakiness (φ) and a high expression of PEP carboxylase in plants treated with 100 mM NaCl and combined stress (100 + D) demonstrate the beneficial effects of these treatments on the C_4 cycle, probably due to the intact leaf anatomy (e.g., Kranz anatomy). The high values of carbon isotopes in these plants represent no restriction to the carboxylation activity of Rubisco, hence the higher net photosynthesis and less photorespiration (Leisner et al., 2010; Moinuddin et al., 2017). Besides, regression analyses showed an inverse correlation of $\Delta^{13}C$ with P_n ($r^2 = 0.87$, $P < 0.01$; **Supplementary Figure S1**). Hence, we conclude that moderate salinity (100 mM NaCl) improves C_4 photosynthesis and alleviates the negative impact of drought (Leisner et al., 2010; Moinuddin et al., 2017). However, the reduced content of Rubisco at 100 + D limited photosynthesis in these plants. The negative

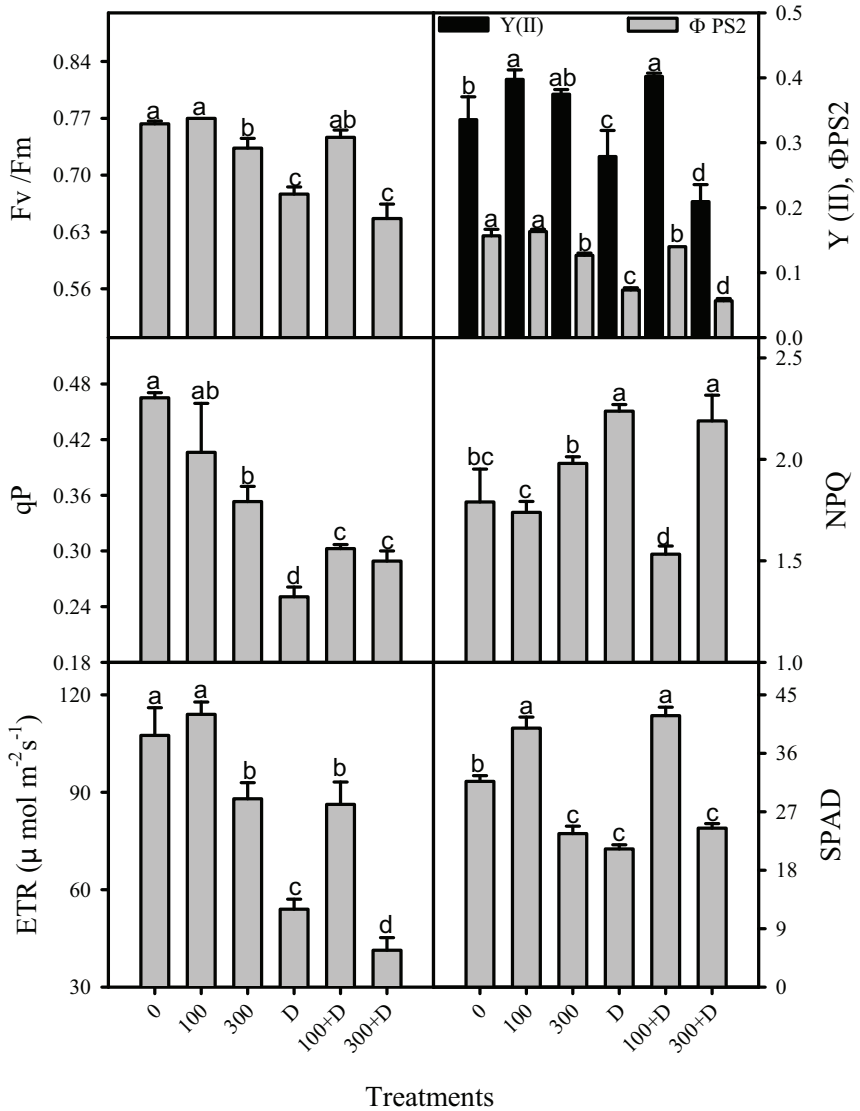

FIGURE 7 | Responses of chlorophyll *a* fluorescence in the leaf of *Panicum antidotale* under salinity, drought, and a combination of both treatments. The mean ± SE (n = 3), maximum quantum efficiency of PS2 (F_v/F_m), apparent quantum efficiency of PS2 (ΦPS2, YII), photochemical quenching (qP), non-photochemical quenching (NPQ), electron transport rate (ETR), and chlorophyll (SPAD) for treatments of 0, 100, and 300 mM NaCl, drought (D), and a combination of salinity with drought [100 and 300 mM NaCl + drought (100 + D and 300 + D, respectively)] are shown. *Different letters* denote, after Bonferroni *post hoc* test, significant difference ($P < 0.05$).

impact of high salinity and drought treatments on the content of Rubisco was discussed earlier by Koyro et al. (2013), and we recorded a severe reduction in its content by combining both stresses (**Figure 3**). The content of carbon isotopes is considered a reliable indicator of the water use efficiency in C_4 plants (Cernusak et al., 2013; Caemmerer et al., 2014; Kromdijk et al., 2014; Ellsworth and Cousins, 2016). Accordingly, the regression analysis illustrated a direct relationship (r^2 = 0.48, P = 0.05) between $\Delta^{13}C$ and WUEi in this study.

Biochemical processes, in addition to stomatal limitations, also affect CO_2 assimilation (Von Caemmerer, 2000; Long and Bernacchi, 2003). An enhanced carboxylation rate of Rubisco (V_{cmax}), the continuous supply of RuBP (i.e., higher J_{max}), and carbon utilization for sucrose and starch synthesis (Φ_{CO2}) at 100 mM NaCl kept the photosynthetic rates comparable to plants of the control (i.e., no stress) treatment (**Table 1**). Combining moderate salinity with drought (100 + D) caused a slight decrease in these biochemical processes. On the other hand, the stressful effects of high salinity and drought treatments were visible, with significant reductions of V_{cmax}, J_{max}, and Φ_{CO2}, which led to a decline in P_n and plant biomass. These biochemical limitations were even more pronounced when the plants were exposed to combined stresses, i.e., 300 + D, indicating impairment in the light-independent phase of photosynthesis. The reason behind such a finding may be either the downregulated activity of enzymes of the Calvin cycle or the reduced supply of products

of the light-dependent phase (i.e., ATP and NADPH). Also, the toxic effects of accumulated ions such as Na^+ and Cl^- on photosynthesis cannot be neglected (Pérez-López et al., 2012; Asrar et al., 2017; Galmés et al., 2017). These assertions are further strengthened by the expression analysis of a large subunit of Rubisco (**Figure 3**) and the regression analysis between P_n and non-stomatal limitation (L_{NS}) ($r^2 = 0.93$, $P < 0.001$) (**Supplementary Figure S1**). The photosynthetic performance of *Panicum* has been limited due to stomata (L_S) (Ashraf, 2003) and other biochemical limitations (Koyro et al., 2013) under salinity, and it has been confirmed by the estimation of the contributions of L_{NS} and L_S (**Figure 5**). Nevertheless, more limiting factors of photosynthesis (such as light and mesophyll conductance) need to unravel from a set of complicated calculations, particularly for C_4 plants. Nevertheless, photochemical reactions of photosynthesis are discussed (see below) by measurement of the chlorophyll fluorescence.

Light-Harvesting and Chlorophyll Variations Under Salinity, Drought, and Combined Stress Conditions

The electron transfer during light reactions of photosynthesis provides energy for the synthesis of NADPH and ATP. These products are vital for the carbon assimilation reactions. Chlorophyll fluorescence and chlorophyll content were used as non-invasive indicators to determine impairment (if any) in light reactions of photosynthesis (Genty et al., 1989; Baker, 2008). The comparatively low values of F_v/F_m (the maximal photochemical efficiency) in response to drought, high salinity, and a combination of both (**Figure 7**) indicate severe damage to the PSII reaction centers (Farquhar et al., 1989; Duarte et al., 2013; Chen et al., 2016), which is further evidenced by the decrease in the actual efficiency of photosystem II, i.e., Y(II) and ΦPSII. Similar findings exist for several Mediterranean species under water deficit conditions (Oxborough and Baker, 1997; Bellot et al., 2004; Flexas et al., 2012a). The reduction in the electron transport rate of the plants treated with drought, 300 mM NaCl, and 300 + D corresponded to their low stomatal conductance and suggested a reduction in light-harvesting capacity. It prevents the otherwise inevitable photo-oxidative stress, excess generation of reactive oxygen species (ROS), and membrane lipid peroxidation (Dalal and Tripathy, 2018). This assumption is further supported by the decreased contents of photosynthetic pigments (e.g., chlorophyll). Thus, the capacity to fix light energy decreases (Manaa et al., 2019) and plants are light-saturated at low values of irradiance (*I*s; **Table 1**). The findings of this study indicate a strict check and balance between P_n and the light-harvesting and photoprotection capacity of *Panicum*.

Non-photochemical quenching (NPQ) serves as a photoprotective mechanism to prevent photo-oxidative stress in plants (Külheim et al., 2002). The observed increase in NPQ in response to drought, high salinity, and a combination of both (300 + D) demonstrates the dissipation of excessive energy *via* the xanthophyll cycle. Such a regulation of unutilized light energy in light reactions minimizes the chance of injury to the thylakoid membrane that can, otherwise, be caused by overly produced ROS, particularly when the biochemical and photochemical reactions are disrupted (Bellot et al., 2004; Koyro et al., 2013; Manaa et al., 2019). The low risk of ROS (e.g., O_2^-, ^-OH, and H_2O_2) toxicity is also reflected by the adjusted ETR (as discussed above) and the low ETR/P_{ngross} ratio in plants. Further, the low expression of GDC under high salinity, drought, and their combination (300 + D), reveals an unregulated carbon flow between photosynthesis and photorespiration, which may also lead to developing a balance between respiratory metabolites (e.g., glycine) and increased cellular mole ratios of CO_2/O_2 (Timm et al., 2018; Giuliani et al., 2019). In contrast, *Panicum* treated with low salinity (alone and in combination with drought) efficiently regulated photochemical reactions, i.e., Y(II), ΦPSII, qP, ETR, and, therefore, net photosynthesis.

CONCLUSION

This study demonstrates that an addition of 100 mM NaCl to dry soil (100 + D) minimized the deleterious effects of water deficit on the biomass and photosynthetic performance of *P. antidotale*. This is due to the positive effects of low-salinity treatment on the photochemical reactions by stimulating photosynthetic pigments and PSII efficiency (YII) to harvest light energy for the efficient synthesis of ATP and NADPH. Increases in stomatal area, enzymes involved in bioenergetics (PEP carboxylase, Rubisco, and glycine carboxylase), and the biochemical reactions [i.e., the carboxylation rate of Rubisco (V_{cmax}) and RuBP regeneration (J_{max})] contributed to an overall higher CO_2 assimilation in these plants. Combining low salinity with drought (100 + D) lowered the CO_2 leakage, enriching CO_2 in the bundle sheath cells to allow maximum carboxylase activities of Rubisco. However, it was the reduction in the content of Rubisco that limited the photosynthetic performance in these plants (100 + D). In contrast, the combination of high salinity (300 mM NaCl) and drought had a severe impact on the photosynthetic performance (P_n) than both the stresses alone. Although high salinity lessened the damaging effect of drought on stomatal limitations (number of stomata and stomatal conductance) photochemical (PSII efficiency, ETR) and biochemical (V_{cmax} and J_{max}) reactions, non-stomatal limitations, mainly the metabolic enzymes (PEP carboxylase, Rubisco, and glycine carboxylase), were significantly enhanced in the combination of these stresses (300 + D). The risk of photo-oxidative stress in these plants was lowered by limiting the light-harvesting capacity. Plant biomass (i.e., FW) was even improved due to better management of the plant water status (RWC and WUEi), demonstrating a beneficial effect of the osmotic component at such a high salinity.

The shown comparative study of the individual and combined effects of salinity and drought conditions on *Panicum* opens new doors for a better understanding of plant responses in their natural environment, where multiple environmental constraints are present simultaneously. Nevertheless, the type of soil in different habitats of plant may vary and, therefore, the impact of

soil properties on setting particular stress conditions must be kept into account while analyzing large fields.

DATA AVAILABILITY STATEMENT

The datasets generated for this study are available on request to the corresponding author.

AUTHOR CONTRIBUTIONS

TH and XJL conceived the idea. TH executed the experiments and drafted the manuscript. XTL helped out in conducting immunoblot experiments. H-WK reviewed the manuscript critically and checked the calculations. WZ contributed to setting up the experiment. BG improved the manuscript and idea.

FUNDING

This study was funded by the Chinese Academy of Sciences (Grant No. KFZD-SW-112).

SUPPLEMENTARY MATERIAL

The Supplementary Material for this article can be found online at: https://www.frontiersin.org/articles/10.3389/fpls.2020.00481/full#supplementary-material

REFERENCES

Abdelraheem, A., Esmaeili, N., O'connell, M., and Zhang, J. (2019). Progress and perspective on drought and salt stress tolerance in cotton. *Indus. Crops Products* 130, 118–129.

Ahmad, M. S. A., Ali, Q., Ashraf, M., Haider, M. Z., and Abbas, Q. (2009). Involvement of polyamines, abscisic acid and anti-oxidative enzymes in adaptation of Blue Panicgrass (*Panicum antidotale* Retz.) to saline environments. *Environ. Exp. Bot.* 66, 409–417.

Ahmed, I. M., Dai, H., Zheng, W., Cao, F., Zhang, G., Sun, D., et al. (2013). Genotypic differences in physiological characteristics in the tolerance to drought and salinity combined stress between Tibetan wild and cultivated barley. *Plant Physiol. Biochem.* 63, 49–60. doi: 10.1016/j.plaphy.2012.11.004

Argus, R., Colmer, T. D., and Grierson, P. F. (2015). Early physiological flood tolerance is followed by slow post-flooding root recovery in the dryland riparian tree *Eucalyptus camaldulensis* subsp. refulgens. *Plant Cell Environ.* 38, 1189–1199. doi: 10.1111/pce.12473

Ashraf, M. (2003). Relationships between leaf gas exchange characteristics and growth of differently adapted populations of Blue panicgrass (*Panicum antidotale* Retz.) under salinity or waterlogging. *Plant Sci.* 165, 69–75.

Asrar, H., Hussain, T., Hadi, S. M. S., Gul, B., Nielsen, B. L., and Khan, M. A. (2017). Salinity induced changes in light harvesting and carbon assimilating complexes of *Desmostachya bipinnata* (L.) Staph. *Environ. Exp. Bot.* 135, 86–95.

Baker, N. R. (2008). Chlorophyll fluorescence: a probe of photosynthesis in vivo. *Annu. Rev. Plant Biol.* 59, 89–113. doi: 10.1146/annurev.arplant.59.032607.092759

Bellasio, C., Quirk, J., and Beerling, D. J. (2018). Stomatal and non-stomatal limitations in savanna trees and C4 grasses grown at low, ambient and high atmospheric CO2. *Plant Sci.* 274, 181–192. doi: 10.1016/j.plantsci.2018.05.028

Bellot, J., Maestre, F. T., and Hernández, N. (2004). Spatio-temporal dynamics of chlorophyll fluorescence in a semi-arid Mediterranean shrubland. *J. Arid Environ.* 58, 295–308.

Caemmerer, S. V., Ghannoum, O., Pengelly, J. J. L., and Cousins, A. B. (2014). Carbon isotope discrimination as a tool to explore C4 photosynthesis. *J. Exp. Bot.* 65, 3459–3470. doi: 10.1093/jxb/eru127

Cernusak, L. A., Ubierna, N., Winter, K., Holtum, J. A. M., Marshall, J. D., and Farquhar, G. D. (2013). Environmental and physiological determinants of carbon isotope discrimination in terrestrial plants. *New Phytologist* 200, 950–965. doi: 10.1111/nph.12423

Chaves, M. M., Flexas, J., and Pinheiro, C. (2009). Photosynthesis under drought and salt stress: regulation mechanisms from whole plant to cell. *Ann. Bot.* 103, 551–560. doi: 10.1093/aob/mcn125

Cheeseman, J. M. (2015). The evolution of halophytes, glycophytes and crops, and its implications for food security under saline conditions. *New Phytol.* 206, 557–570. doi: 10.1111/nph.13217

Chen, T., Kahlen, K., and Stutzel, H. (2015). Disentangling the contributions of osmotic and ionic effects of salinity on stomatal, mesophyll, biochemical and light limitations to photosynthesis. *Plant Cell Environ.* 38, 1528–1542. doi: 10.1111/pce.12504

Chen, Y.-E., Liu, W.-J., Su, Y.-Q., Cui, J.-M., Zhang, Z.-W., Yuan, M., et al. (2016). Different response of photosystem II to short and long-term drought stress in *Arabidopsis thaliana*. *Physiol. Plant* 158, 225–235. doi: 10.1111/ppl.12438

Dalal, V. K., and Tripathy, B. C. (2018). Water-stress induced downsizing of light-harvesting antenna complex protects developing rice seedlings from photo-oxidative damage. *Sci. Rep.* 8:5955. doi: 10.1038/s41598-017-14419-4

Duarte, B., Santos, D., Marques, J., and Caçador, I. (2013). Ecophysiological adaptations of two halophytes to salt stress: photosynthesis, PS II photochemistry and anti-oxidant feedback–implications for resilience in climate change. *Plant Physiol. Biochem.* 67, 178–188. doi: 10.1016/j.plaphy.2013.03.004

Ellsworth, P. Z., and Cousins, A. B. (2016). Carbon isotopes and water use efficiency in C4 plants. *Curr. Opin. Plant Biol.* 31, 155–161. doi: 10.1016/j.pbi.2016.04.006

Epstein, E. (1972). *Mineral Nutrition of Plants: Principles and Perspectives*. New York: John Wiley and Sons.

Farquhar, G. D. (1983). On the nature of carbon isotope discrimination in C4 species. *Aust. J. Plant Physiol.* 10, 205–226.

Farquhar, G. D., Ehleringer, J. R., and Hubick, K. T. (1989). Carbon isotope discrimination and photosynthesis. *Annu. Rev. Plant Biol.* 40, 503–537.

Farquhar, G. D., and Sharkey, T. D. (1982). Stomatal conductance and photosynthesis. *Annu. Rev. Plant Biol.* 33, 317–345.

Flexas, J., Barbour, M. M., Brendel, O., Cabrera, H. M., Carriquí, M., Díaz-Espejo, A., et al. (2012a). Mesophyll diffusion conductance to CO2: an unappreciated central player in photosynthesis. *Plant Sci.* 193-194, 70–84. doi: 10.1016/j.plantsci.2012.05.009

Flexas, J., Gallé, A., Galmés, J., Ribas-Carbo, M., and Medrano, H. (2012b). "The response of photosynthesis to soil water stress," in *Plant Responses to Drought Stress: From Morphological to Molecular Features*, ed. R. Aroca, (Berlin: Springer Berlin Heidelberg), 129–144.

Flowers, T. J., and Colmer, T. D. (2008). Salinity tolerance in halophytes. *New Phytol.* 179, 945–963.

Galmés, J., Molins, A., Flexas, J., and Conesa, M. A. (2017). Coordination between leaf CO2 diffusion and Rubisco properties allows maximizing photosynthetic efficiency in Limonium species. *Plant Cell Environ.* 40, 2081–2094. doi: 10.1111/pce.13004

Genty, B., Briantais, J. M., and Baker, N. R. (1989). The relationship between the quantum yield of photosynthetic electron transport and quenching of chlorophyll fluorescence. *Biochim. Biophys. Acta* 990, 87–92.

Giuliani, R., Karki, S., Covshoff, S., Lin, H.-C., Coe, R. A., Koteyeva, N. K., et al. (2019). Knockdown of glycine decarboxylase complex alters photorespiratory carbon isotope fractionation in *Oryza sativa* leaves. *J. Exp. Bot.* 70, 2773–2786. doi: 10.1093/jxb/erz083

Guo, Z., He, J., and Barry, B. A. (2018). Calcium, conformational selection, and redox-active tyrosine YZ in the photosynthetic oxygen-evolving cluster. *Proc. Natl. Acad. Sci. U.S.A.* 115, 5658–5663. doi: 10.1073/pnas.1800758115

Hatfield, J. L., and Prueger, J. H. (2015). Temperature extremes: effect on plant growth and development. *Weather Clim. Extremes* 10, 4–10.

Hu, Y., and Schmidhalter, U. (2005). Drought and salinity: A comparison of their effects on mineral nutrition of plants. *J. Plant Nutr. Soil Sci.* 168, 541–549.

Hussain, T., Koyro, H.-W., Huchzermeyer, B., and Khan, M. A. (2015). Eco-physiological adaptations of *Panicum antidotale* to hyperosmotic salinity: Water and ion relations and anti-oxidant feedback. *Flora Morphol. Distribut. Funct. Ecol. Plants* 212, 30–37.

Khan, M. A., Ansari, R., Ali, H., Gul, B., and Nielsen, B. L. (2009). Panicum turgidum, a potentially sustainable cattle feed alternative to maize for saline areas. *Agricult. Ecosyst. Environ.* 129, 542–546.

Kitajima, M., and Butler, W. (1975). Quenching of chlorophyll fluorescence and primary photochemistry in chloroplasts by dibromothymoquinone. *Biochim. Biophys. Acta* 376, 105–115. doi: 10.1016/0005-2728(75)90209-1

Kooten, O., and Snel, J. F. H. (1990). The use of chlorophyll fluorescence nomenclature in plant stress physiology. *Photosynthesis Res.* 25, 147–150. doi: 10.1007/BF00033156

Koyro, H.-W., Hussain, T., Huchzermeyer, B., and Khan, M. A. (2013). Photosynthetic and growth responses of a perennial halophytic grass Panicum turgidum to increasing NaCl concentrations. *Environ. Exp. Bot.* 91, 22–29.

Kromdijk, J., Ubierna, N., Cousins, A. B., and Griffiths, H. (2014). Bundle-sheath leakiness in C4 photosynthesis: a careful balancing act between CO2 concentration and assimilation. *J. Exp. Bot.* 65, 3443–3457. doi: 10.1093/jxb/eru157

Kubásek, J., Šetlík, J., Dwyer, S., and Šantruček, J. (2007). Light and growth temperature alter carbon isotope discrimination and estimated bundle sheath leakiness in C4 grasses and dicots. *Photosynthesis Res.* 91:47. doi: 10.1007/s11120-007-9136-6

Külheim, C., Ågren, J., and Jansson, S. (2002). Rapid regulation of light harvesting and plant fitness in the field. *Science* 297, 91–93. doi: 10.1126/science.1072359

Leisner, C. P., Cousins, A. B., Offermann, S., Okita, T. W., and Edwards, G. E. (2010). The effects of salinity on photosynthesis and growth of the single-cell C4 species *Bienertia sinuspersici* (Chenopodiaceae). *Photosynthesis Res.* 106, 201–214. doi: 10.1007/s11120-010-9595-z

Liu, H., Sun, G. W., Dong, L., Yang, L. Q., Yu, S. N., Zhang, S., et al. (2017). Physiological and molecular responses to drought and salinity in soybean. *Biol. Plant.* 61, 557–564.

Long, S., and Bernacchi, C. (2003). Gas exchange measurements, what can they tell us about the underlying limitations to photosynthesis? Procedures and sources of error. *J. Exp. Bot.* 54, 2393–2401. doi: 10.1093/jxb/erg262

Ma, Q., Yue, L., Zhang, J., Wu, G., Bao, A., and Wang, S. (2012). Sodium chloride improves photosynthesis and water status in the succulent xerophyte *Zygophyllum xanthoxylum*. *Tree Physiol.* 32, 4–13. doi: 10.1093/treephys/tpr098

Manaa, A., Goussi, R., Derbali, W., Cantamessa, S., Abdelly, C., and Barbato, R. (2019). Salinity tolerance of quinoa (*Chenopodium quinoa* Willd) as assessed by chloroplast ultrastructure and photosynthetic performance. *Environ. Exp. Bot.* 162, 103–114.

Mittler, R. (2006). Abiotic stress, the field environment and stress combination. *Trends Plant Sci.* 11, 15–19. doi: 10.1016/j.tplants.2005.11.002

Moinuddin, M., Gulzar, S., Hameed, A., Gul, B., Ajmal Khan, M., and Edwards, G. E. (2017). Differences in photosynthetic syndromes of four halophytic marsh grasses in Pakistan. *Photosynthesis Res.* 131, 51–64. doi: 10.1007/s11120-016-0296-0

Muchate, N. S., Nikalje, G. C., Rajurkar, N. S., Suprasanna, P., and Nikam, T. D. (2016). Plant salt stress: adaptive responses, tolerance mechanism and bioengineering for salt tolerance. *Bot. Rev.* 82, 371–406. doi: 10.3389/fpls.2020.00283

Negrao, S., Schmockel, S. M., and Tester, M. (2017). Evaluating physiological responses of plants to salinity stress. *Ann. Bot.* 119, 1–11. doi: 10.1093/aob/mcw191

Oxborough, K., and Baker, N. R. (1997). Resolving chlorophyll a fluorescence images of photosynthetic efficiency into photochemical and non-photochemical components – calculation of qP and Fv-/Fm-; without measuring Fo. *Photosynthesis Res.* 54, 135–142.

Pérez-López, U., Robredo, A., Lacuesta, M., Mena-Petite, A., and Muñoz-Rueda, A. (2012). Elevated CO2 reduces stomatal and metabolic limitations on photosynthesis caused by salinity in *Hordeum vulgare*. *Photosynthesis Res.* 111, 269–283. doi: 10.1007/s11120-012-9721-1

Qadir, M., Quillerou, E., Nangia, V., Murtaza, G., Singh, M., Thomas, R. J., et al. (2014). Economics of salt-induced land degradation and restoration. *Nat. Resour. Forum* 38, 282–295.

Schulte, M., Offer, C., and Hansen, U. (2003). Induction of CO2-gas exchange and electron transport: comparison of dynamic and steady-state responses in Fagus sylvatica leaves. *Trees Struct. Funct.* 17, 153–163.

Sharp, R. E., Hsiao, T. C., and Silk, W. K. (1990). Growth of the maize primary root at low water potentials II. Role of growth and deposition of hexose and potassium in osmotic adjustment. *Plant Physiol.* 93, 1337–1346. doi: 10.1104/pp.93.4.1337

Tezara, W., Mitchell, V. J., Driscoll, S. D., and Lawlor, D. W. (1999). Water stress inhibits plant photosynthesis by decreasing coupling factor and ATP. *Nature* 401, 914–917.

Timm, S., Giese, J., Engel, N., Wittmiß, M., Florian, A., Fernie, A. R., et al. (2018). T-protein is present in large excess over the other proteins of the glycine cleavage system in leaves of *Arabidopsis*. *Planta* 247, 41–51. doi: 10.1007/s00425-017-2767-8

Tomás, M., Flexas, J., Copolovici, L., Galmés, J., Hallik, L., Medrano, H., et al. (2013). Importance of leaf anatomy in determining mesophyll diffusion conductance to CO2 across species: quantitative limitations and scaling up by models. *J. Exp. Bot.* 64, 2269–2281. doi: 10.1093/jxb/ert086

Von Caemmerer, S. (2000). *Biochemical Models of Leaf Photosynthesis*. Clayton, VIC: CSIRO Publishing.

Wang, X., Wang, W., Huang, J., Peng, S., and Xiong, D. (2017). Diffusional conductance to CO2 is the key limitation to photosynthesis in salt-stressed leaves of rice (*Oryza sativa*). *Physiol. Plant.* 163, 45–58. doi: 10.1111/ppl.12653

Way, D. A., Katul, G. G., Vico, G., and Manzoni, S. (2014). Increasing water use efficiency along the C3 to C4 evolutionary pathway: a stomatal optimization perspective. *J. Exp. Bot.* 65, 3683–3693. doi: 10.1093/jxb/eru205

Zandalinas, S. I., Mittler, R., Balfagon, D., Arbona, V., and Gomezcadenas, A. (2018). Plant adaptations to the combination of drought and high temperatures. *Physiol. Plant.* 162, 2–12. doi: 10.1111/ppl.12540

Conflict of Interest: The authors declare that the research was conducted in the absence of any commercial or financial relationships that could be construed as a potential conflict of interest.

frontiers in Plant Science

REVIEW
published: 06 July 2020
doi: 10.3389/fpls.2020.00882

Photosynthesis in a Changing Global Climate: Scaling Up and Scaling Down in Crops

Marouane Baslam[1], Toshiaki Mitsui[1,2], Michael Hodges[3], Eckart Priesack[4], Matthew T. Herritt[5], Iker Aranjuelo[6]* and Álvaro Sanz-Sáez[7]**

[1] Laboratory of Biochemistry, Faculty of Agriculture, Niigata University, Niigata, Japan, [2] Graduate School of Science and Technology, Niigata University, Niigata, Japan, [3] Institute of Plant Sciences Paris-Saclay (IPS2), CNRS, INRAE, Université Paris-Saclay, Université Evry, Université Paris Diderot, Paris, France, [4] Institute of Biochemical Plant Pathology, Helmholtz Zentrum München, German Research Center for Environmental Health, Neuherberg, Germany, [5] USDA-ARS Plant Physiology and Genetics Research, US Arid-Land Agricultural Research Center, Maricopa, AZ, United States, [6] Agrobiotechnology Institute (IdAB-CSIC), Consejo Superior de Investigaciones Científicas-Gobierno de Navarra, Mutilva, Spain, [7] Department of Crop, Soil, and Environmental Sciences, Auburn University, Auburn, AL, United States

OPEN ACCESS

Edited by:
Sonia Negrao,
University College Dublin, Ireland

Reviewed by:
Alexander Gallé,
BASF (Belgium), Belgium
Keshav Dahal,
Fredericton Research and Development Centre, Agriculture and Agri-Food Canada, Canada
Yasutomo Hoshika,
Institute for Sustainable Plant Protection, Italian National Research Council, Italy

***Correspondence:**
Marouane Baslam
mbaslam@gs.niigata-u.ac.jp
Iker Aranjuelo
iker.aranjuelo@csic.es
Álvaro Sanz-Sáez
azs0223@auburn.edu

Specialty section:
This article was submitted to Plant Abiotic Stress, a section of the journal Frontiers in Plant Science

Received: 29 November 2019
Accepted: 29 May 2020
Published: 06 July 2020

Citation:
Baslam M, Mitsui T, Hodges M, Priesack E, Herritt MT, Aranjuelo I and Sanz-Sáez Á (2020) Photosynthesis in a Changing Global Climate: Scaling Up and Scaling Down in Crops. Front. Plant Sci. 11:882. doi: 10.3389/fpls.2020.00882

Photosynthesis is the major process leading to primary production in the Biosphere. There is a total of 7000bn tons of CO_2 in the atmosphere and photosynthesis fixes more than 100bn tons annually. The CO_2 assimilated by the photosynthetic apparatus is the basis of crop production and, therefore, of animal and human food. This has led to a renewed interest in photosynthesis as a target to increase plant production and there is now increasing evidence showing that the strategy of improving photosynthetic traits can increase plant yield. However, photosynthesis and the photosynthetic apparatus are both conditioned by environmental variables such as water availability, temperature, [CO_2], salinity, and ozone. The "omics" revolution has allowed a better understanding of the genetic mechanisms regulating stress responses including the identification of genes and proteins involved in the regulation, acclimation, and adaptation of processes that impact photosynthesis. The development of novel non-destructive high-throughput phenotyping techniques has been important to monitor crop photosynthetic responses to changing environmental conditions. This wealth of data is being incorporated into new modeling algorithms to predict plant growth and development under specific environmental constraints. This review gives a multi-perspective description of the impact of changing environmental conditions on photosynthetic performance and consequently plant growth by briefly highlighting how major technological advances including omics, high-throughput photosynthetic measurements, metabolic engineering, and whole plant photosynthetic modeling have helped to improve our understanding of how the photosynthetic machinery can be modified by different abiotic stresses and thus impact crop production.

Keywords: photosynthesis, climate change, crop improvement, -omics, phenotyping, modeling

INTRODUCTION

Owing to the expected increase in the world's population, yields of major crops must increase by over 70% in the next 30 years to sustain human requirements (FAO, 2009) and this should be attained without increasing the use of arable land and detrimental effects on nutritional quality while limiting the use of fertilizers and pesticides This means that breeders must increase crop yield at a rate of +2.4% per year, while the current rate is only +1.3% (FAO, 2009). In addition, abiotic stresses such as heat, drought, and flooding among others will tend to decrease yields up to 50% by 2050, if management techniques such as precision irrigation and breeding for abiotic stress tolerance are not implemented (Bierbaum et al., 2007).

Photosynthesis is a complex process that for simplification can be divided into light reactions driven by electrons passing through different protein complexes associated with chloroplast thylakoid membranes and the Calvin cycle reactions of photosynthetic CO_2 fixation taking place in the chloroplast stroma (Renger, 2007). In the light, the photosynthetic electron transfer chain consisting of photosystem II (PSII), the cytochrome b_6f complex (cytb_6f), photosystem I (PSI), and the free electron carriers plastoquinone (PQ) and plastocyanin, lead to the production of ATP and NADPH that fuel the Calvin-Benson cycle (CBC) and other assimilatory processes (Rochaix, 2011; Foyer et al., 2012). Three main stages operate during the CBC reactions namely carbon fixation, reduction, and regeneration. In all plants, CO_2 can be fixed by ribulose-1,5-bisphosphate carboxylase/oxygenase (RuBisCO), an enzyme catalyzing the carboxylation of ribulose-1,5-bisphosphate (RuBP) and leading to two molecules of 3-phosphoglycerate (3-PGA). Instead of CO_2, RuBisCO can also add O_2 to RuBP, resulting in one molecule each of 3-PGA and 2-phosphoglycolate (2-PG). Since 2-PG is toxic, it has to be removed in a metabolic pathway called photorespiration that is not only energy demanding, but also leads to a loss of carbon in the form of CO_2. Thus the efficiency of photosynthesis can be substantially decreased under environmental conditions favoring photorespiration (Ehleringer et al., 1991) and this would be associated with factors altering CO_2 entry and diffusion within the leaf such as stomatal density and aperture.

Furthermore, photosynthesis is highly sensitive to abiotic stresses such as drought, high temperatures, and ozone, since they inactivate photosynthetic electron transfer and photophosphorylation, adversely affect photosynthetic metabolic processes, and lead to damage of thylakoid membranes and organelle ultrastructure (Ainsworth et al., 2013; Lobell et al., 2014; Sieber et al., 2016). In fact, an increase in atmospheric temperature can reduce crop yields by between 6 to 25% depending on the region and the crop (Sieber et al., 2016; Zhao et al., 2017). However, drought is the major abiotic stress that impairs crop production (Mishra and Cherkauer, 2010; Lobell et al., 2014; Lesk et al., 2016; Zipper et al., 2016; Matiu et al., 2017) due to photosynthetic limitations imposed by stomatal and non-stomatal processes (Tissue et al., 2005; Kohzuma et al., 2009; Dahal et al., 2014). It has been estimated that drought has caused the loss of 1820 million tons of cereal production during the last 4 decades (Lesk et al., 2016). In the future, drought occurrence and severity are projected to rise, increasing the risk of yield loss by 24% in soybean, 21% in maize, 18% in rice, and 20% in wheat (Leng and Hall, 2019). On the other hand, the predicted increase in atmospheric CO_2 levels, as a substrate of photosynthesis, is expected to increase yields by up to 30% depending on plant species and other environmental conditions (Ainsworth and Long, 2005; Long et al., 2006; Sanz-Saez et al., 2017). It has been shown that elevated temperature and drought can negate the positive effects of elevated CO_2 on yield (Ruiz-Vera et al., 2013; Gray et al., 2016). While plant breeders and plant biologists have worked extensively over the years to increase yields and improve plant responses to abiotic stresses, photosynthesis was often overlooked (Long et al., 2015). Advances in genomics, genetics, and modeling tools have now paved the way for improving photosynthesis to increase yields within climate change scenarios (Zhu et al., 2010; Long et al., 2015; Ort et al., 2015).

The effects of abiotic stresses on photosynthesis have given rise to numerous review articles (Hikosaka et al., 2006; Pinheiro and Chaves, 2011; Ainsworth et al., 2013; Song et al., 2014; Dusenge et al., 2019); however, many of them only focused on specific aspects. In this review, the effects of abiotic stresses are considered from a holistic point of view. It covers the use of "omics" techniques (genomics, transcriptomics, proteomics, and hormonomics) (Section "-Omics" Analyses to Identify Novel Targets and Networks Underlying the Function of the Photosynthesis Machinery: Roads to Develop Engineered Environmental Stress-Tolerant Crops Through Photosynthesis") to identify potential target genes that could improve photosynthesis and crop yield. Whole plant physiological responses (Section "Physiological Traits Involved in the Maintenance of Photosynthesis as Tools for Crop Improvement in a Context of Climate Change") and the development of semi- and high-throughput phenotyping techniques (Section "Semi- and High-Throughput Phenotyping Techniques to Measure Photosynthetic Traits") are described that allow for a better understanding of major physiological traits associating the maintenance of photosynthesis with abiotic stress tolerance. To bring together the wealth of knowledge and to extrapolate the effects of the environment on photosynthetic capacity and plant development at the whole plant land canopy levels, Section "Modeling Photosynthesis in Crop Growth Models" reviews the application of photosynthetic models to calculate carbon gain for biomass production and to estimate possible future impacts of a changing climate on global crop production and grain yield. Finally, Section "Metabolic Engineering to Improve Photosynthesis and Elevated CO_2 Acclimation" gives an overview of the application of metabolic engineering and examples of what has been successfully achieved already to improve photosynthesis and how elevated CO_2 acclimation might limit yield improvement and quality of certain C3-plant species.

"-OMICS" ANALYSES TO IDENTIFY NOVEL TARGETS AND NETWORKS UNDERLYING THE FUNCTION OF THE PHOTOSYNTHESIS MACHINERY: ROADS TO DEVELOP ENGINEERED ENVIRONMENTAL STRESS-TOLERANT CROPS THROUGH PHOTOSYNTHESIS

The emergence of omics technologies, such as genomics, transcriptomics, proteomics, metabolomics, ionomics, and hormonomics have permitted to identify components associated with photosynthesis including molecular regulatory circuitries, photosynthetic machinery and functioning, and photoprotective mechanisms, thus underpinning factors paving the way to photosynthesis efficiency-boosting and the improved productivity and quality of modern crop varieties (**Figure 1**).

Genomics to Study the Natural Variation of Plant Photosynthetic Efficiency

This section does not intend to give a detailed account of genomics and the reader is directed to other publications to read about general genomic innovation for crop improvement (Bevan et al., 2017), development of new genomic technologies (Huang et al., 2010; Takagi et al., 2013; Schlotterer et al., 2014; Varshney et al., 2014; Pandey et al., 2016; Crossa et al., 2017; Rasheed et al., 2017; Scheben et al., 2017; Watson et al., 2018), and the use of genomics in crop breeding (Varshney et al., 2012, 2018).

Evolution has been continually shaping photosynthesis, so fine-tuning this rather inefficient metabolic process could help to boost crop yields under normal and adverse conditions. This could be achieved using new plant breeding technologies to target photosynthetic processes and thus to contribute substantially to improving global food security under climate change scenarios. Conventional quantitative trait locus (QTL) mapping using recombinant inbred lines (RIL) and near-isogenic lines (NIL) is an effective tool to identify quantitative traits associated with photosynthesis and the modulation of photosynthetic parameters in response to environmental cues (Adachi et al., 2011; Gehan et al., 2015; Yan et al., 2015; de Oliveira Silva et al., 2018; Oakley et al., 2018). Indeed, RIL and NIL populations have been used to discover genetic variation and genes associated with photosynthetic efficiency, while some specific photosynthesis-related traits were found to be influenced by functional genetic variation in a limited number of genes (Oakley et al., 2018). Indeed, putative QTLs have been detected for Single-Photon Avalanche Diode (SPAD) value, chlorophyll content, stomatal conductance, sink size, source strength, carbon isotope discrimination, and carbohydrate translocation (Ulloa et al., 2000; Teng et al., 2004; Takai et al., 2010, 2013). Potential QTLs have been revealed also for net CO_2 assimilation rate (A_n) in rice (Ishimaru et al., 2001; Price et al., 2002; Zhao et al., 2011; Hirotsu et al., 2017; Ye et al., 2017; Adachi et al., 2019), barley (Teulat et al., 2002; Cantalapiedra et al., 2015; Liu et al., 2017; Du et al., 2019), maize (Fracheboud et al., 2002), soybean (Jun et al., 2014; Lv et al., 2018; Liu D. et al., 2019), cucumber (Zhang et al., 2004), and legumes (Muchero et al., 2009; Kumar et al., 2014; Li F. et al., 2015). In the case of rice, several loci enhancing leaf A_n have been detected on chromosomes 3, 4, 5, 6, 8, 9, and 11 (Adachi et al., 2011; Gu et al., 2012). In addition, some backcross inbred lines (BILs) derived from an *indica* variety, Takanari, and an elite *japonica* cultivar have 20–50% higher values of leaf A_n than those of the parental cultivars (Adachi et al., 2013). By using BILs and chromosome segment substitution lines (CSSLs), Adachi et al. (2019) detected 10 "qHP" (high photosynthesis) QTLs linked to an increased A_n during at least 2 years in the field and named qHP1a, qHP1b, qHP2, qHP3a, qHP3b, qHP4, qHP5, qHP7a, qHP7b, and qHP10. Takai et al. (2013) identified qHP4 in a chromosomal region containing the *GPS* (GREEN FOR PHOTOSYNTHESIS) gene by using the above-mentioned BIL mapping population. Similarly, a previous fine-mapping study revealed Carbon Assimilation Rate 8 (CAR8) as an A_n-enhancing QTL (Adachi et al., 2017). Whole-genome sequencing (WGS) is another genetic tool that can be used to identify genes susceptible to make photosynthesis more efficient. This requires the development of high-resolution mapping populations in the form of genotypically detailed diversity panels suitable for genome-wide association studies (GWAS). Together, natural variation associated with different traits can be determined, thereby providing breeders with marker-trait associations that can be directly exploited for crop design (Huang and Han, 2014; Ogura and Busch, 2015; Barabaschi et al., 2016). The use of natural variation to understand the genetic basis of photosynthetic efficiency represents a powerful tool. Indeed, this approach has been widely used to reveal the genetic basis of photosynthesis-related traits under changing environmental conditions in several crops (Panthee et al., 2006; Wang et al., 2016; Lv et al., 2018). Tsai et al. (2019) investigated photosynthetic efficiency under salinity stress and identified several chromosomal regions associated with chlorophyll fluorescence parameter variations, and identified some significant SNPs linked to genes involved in salt tolerance. It has been shown also that plants exhibit genetic variation for photosynthetic response to changing irradiance levels (van Rooijen et al., 2015). Additionally, the application of GWAS as a powerful tool to identify candidate genes for the improvement of crop productivity has been validated by its role in the discovery of many genome regions and genes associated to A_n and chlorophyll fluorescence under different stresses (Strigens et al., 2013; Fiedler et al., 2016; Ortiz et al., 2017; Su et al., 2019). Recently, a multi-parent advanced generation intercross (MAGIC) strategy was proposed to promote genome intercrossing and shuffling (Cavanagh et al., 2008). MAGIC populations have been developed for several plant species[1] and used to create ideotypes under climate change (Bandillo et al., 2013; Lucas et al., 2013; Muchero et al., 2013; Huynh et al., 2018).

The functional dissection of photosynthesis can be undertaken also by forward genetic screens. Strategies, identification, insights and mutant effects have been reviewed previously (Somerville, 1986; Parinov and Sundaresan, 2000; Page and Grossniklaus,

[1]https://sites.google.com/site/ijmackay/work/magic

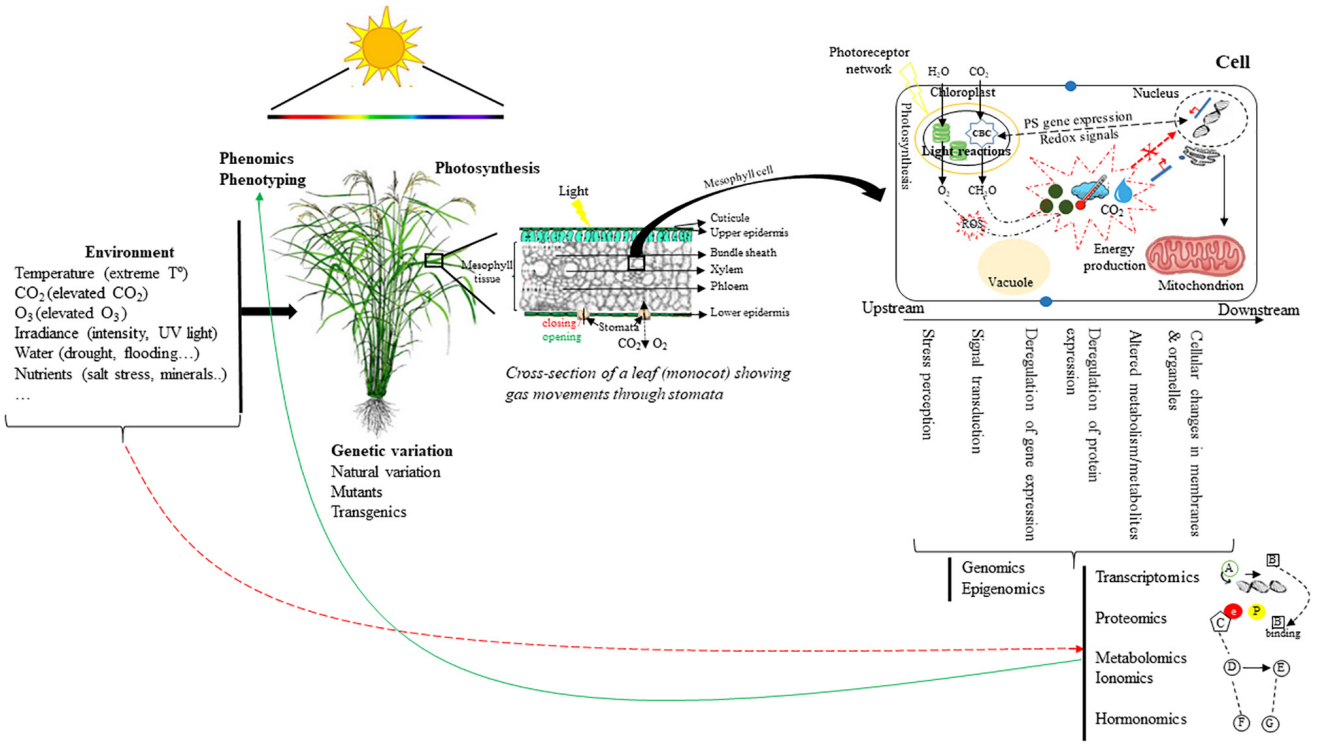

FIGURE 1 | Overview of the multi-scale level concept including molecular (genetic variation, gene expression networks, proteins, metabolites, hormones, etc.), cellular, plant (organ development), and ecosystem (canopy) levels. Systems biology methods can be used to analyze and model cellular networks to obtain a simplified description of cellular functioning (scaling down). The integration of these different scales can help improve photosynthesis. In the example, rice (monocot) plants are used as a higher-scale model. Phenomics technologies allow the physiological and/or temporal phenotypic dissection of quantitative traits (i.e., carbon assimilation) controlled by a subset of target genes, proteins, metabolites and/or pathways. ● represents external and internal factors (i.e., hormones, ROS, sugars, CO_2, T°) influencing the control of photosynthesis in plants. Red arrows show repression/activation of proteins/transcripts coordinating the expression of nuclear/plastid-encoded genes. Here, the upstream and downstream changes governing the above factors are summarized, on the one hand, by stress perception, signal transduction, and on the other hand, by genes, proteins, metabolites alterations, and reactions occurring in membranes and organelles.

2002; Luo et al., 2018; Döring et al., 2019). Knowledge obtained from mutant screenings can reveal new chloroplast functions, including those necessary for high photosynthetic performance, and accelerate the molecular characterization required for deciphering the genetic basis of plant photosynthesis for future improvements. For instance, Döring et al. (2019) identified genomic segments that contained mutated candidate genes to create a more C4–like bundle sheath by using a mapping-by-sequencing approach. However, a successful forward genetic screen needs an easily identifiable trait followed by a validation of the identified mutated genes by state-of-the-art technologies such as T-DNA knock-out lines, RNAi lines, or by gene-editing tools (Hahn et al., 2017). Indeed, genome editing approaches, such as transcription activator-like effector nucleases (TALENs) (Bedell et al., 2012; Li et al., 2012) and the CRISPR (clustered regularly interspaced short palindromic repeats)/Cas9 RNA-guided system (Cong et al., 2013; Feng et al., 2014), will enable precise genome engineering that could be useful to improve photosynthesis by generating targeted variations for precision breeding (Scheben and Edwards, 2017; Scheben et al., 2017). Crop breeding programs will benefit from the integration of modern genomics approaches, and the use of high-throughput genotyping/phenotyping platforms (see section "Semi- and High-Throughput Phenotyping Techniques to Measure Photosynthetic Traits"). Indeed, within the context of modern plant breeding, several molecular breeding approaches have been applied to introgress genomic regions into elite lines (Varshney et al., 2012). Marker-assisted selection (MAS), marker-assisted backcrossing (MABC), and gene pyramiding programs have been widely used in crop improvement to create desirable characters including high photosynthetic efficiency under (a) biotic stress conditions (Singh and Singh, 2015; Varshney, 2016; Cobb et al., 2018). While transgenic approaches have been successful in improving plant yield through improved photosynthesis (as highlighted in section "Modeling Photosynthesis in Crop Growth Models"), the genetic mapping of desired photosynthesis-related traits will require an efficient implementation of high-throughput, non-destructive phenotyping (see section "Semi- and High-Throughput Phenotyping Techniques to Measure Photosynthetic Traits" for more details) to assess them between plant genotypes (van Bezouw et al., 2018). The gap between genomes and phenotypes will be bridged by "omics" approaches, including transcriptomics, proteomics, hormononics, and metabolomics.

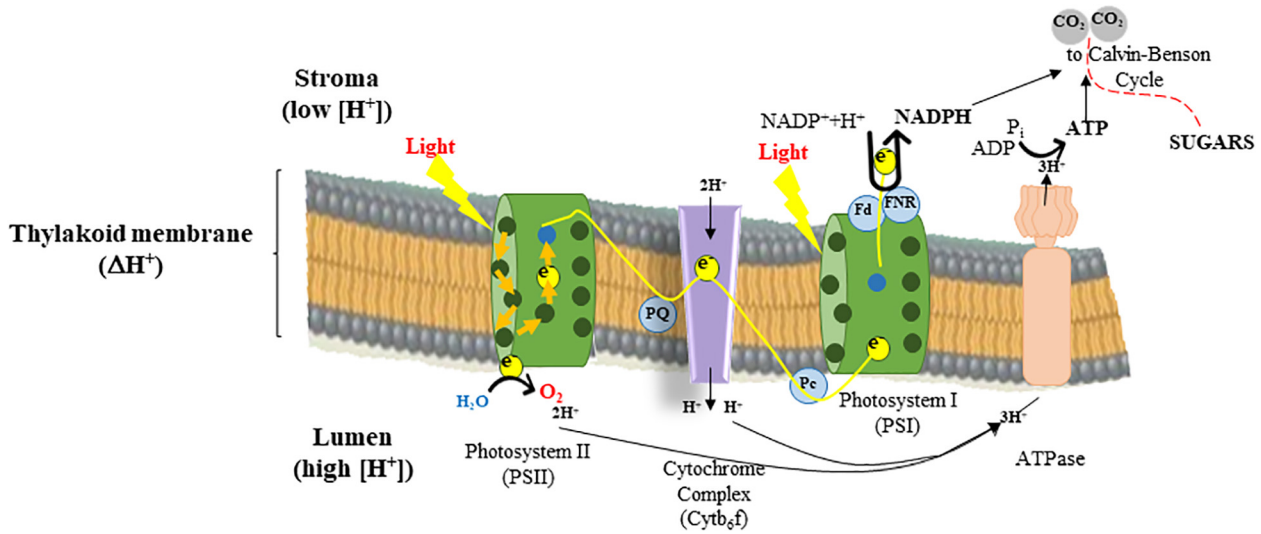

FIGURE 2 | Light energy drives mainstream electron flow used by photosystem II (PSII) to reduce plastoquinone (PQ) to plastoquinol. The reducing equivalents on plastoquinol move through the electron transfer chain (ETC) to the cytochrome b_6f complex and plastocyanin (Pc), releasing protons (H^+) into the thylakoid lumen, while the electrons are used by photosystem I (PSI) to reduce ferredoxin (Fd), again driven by light-supported ETC through PSI. Reduced Fd is coupled to Fd:NADP(H) oxidoreductase (FNR) that catalyzes the reduction of $NADP^+$ to NADPH. The oxidation of water by PSII and the oxidation of plastoquinol by the cytochrome b_6f complex allows the generation of a ΔpH between the thylakoid lumen and the stroma, essential for generating ATP via the ATPase and balancing the proportion of ATP:NADPH produced by electron transfer that is required to function the Calvin cycle that assimilates CO_2 and leads to sugar production, and plant growth.

Photosynthesis and Transcriptional Regulation

About 3000 genes are required for a plant to carry out photosynthesis and high-throughput sequencing to quantify transcripts will help determine when and where a gene is turned on/off. The analysis of deregulated gene expression patterns controlling photosynthesis-related processes across a wide array of cellular responses, phenotypes, and conditions would help to engineer multiple aspects of photosynthesis in the future. This could be achieved by the manipulation of gene regulatory networks. For instance, genes encoding the four major multi-component complexes of the thylakoid membrane [PSII-LHC (light harvesting complex) II, cytb$_6$f, PSI-LHCI, and ATP synthase] (*cf.* **Figure 2**) that work together to carry out light-dependent energy-production must be co-regulated to be efficient.

Photoreceptors regulate the expression of many genes important for plant performance including the initiation of chloroplast biogenesis, chloroplast gene transcription, chlorophyll biosynthesis and photosynthetic-associated processes like chloroplast movements and stomatal opening (Lepistö and Rintamäki, 2012; Legris et al., 2019), therefore engineering these genes could be of great interest to improve photosynthetic traits. The modulation of certain phytochrome gene families, especially PHYA and PHYB, in several crops of interest plays an important role in determining the enhancement of quality and yield as well as the development of agronomically important traits including abiotic stress tolerance (Franklin and Whitelam, 2007; Abdurakhmonov et al., 2014; Gupta et al., 2014; Gururani et al., 2015; Martín et al., 2016; Shin et al., 2016).

At least 41 transcription factors (TFs) have been described in Arabidopsis to act downstream of photoreceptor genes, the most characterized being PHYTOCHROME INTERACTING FACTOR (PIF) and PIFLIKE (PIL) families of basic helix-loop-helix (bHLH) proteins. Most plastid-encoded genes appear to be regulated by several sigma factors with overlapping functions. Stress-responsive TFs such as MYC (myelocytomatosis oncogene)/MYB (myeloblastosis oncogene), bZIP, NAC (NAM, ATAF, and CUC) and ZF-HD (zinc-finger homeodomain), CBF/DREB, and AREB/ABF (ABA-responsive element-binding protein/ABA-binding factor) are known to regulate the expression of photosynthetic genes in response to abiotic stresses. Homeobox homeodomain leucine-zipper (HD-Zip) TFs have diverse functions during plant development and stress adaptation, and some members of this family are under the control of the phytochrome system such as ARABIDOPSIS THALIANA HOMEOBOX 2 (ATHB2) (Kunihiro et al., 2011). *ATHB17*-overexpressing plants enhance abiotic stress tolerance by coordinating both photosynthesis-associated nuclear genes (PhANGs) involved in the light reactions and an essential nucleus-encoded Arabidopsis σ-Like Factor (*AtSig5*) (Zhao et al., 2017). The functional analysis of transgenic wheat overexpressing Nuclear Factor Y (*TaNF-YB3*) provided evidence for the positive involvement of the TF gene *TaNF-YB3* in the regulation of photosynthesis genes leading to an increase in leaf chlorophyll content and photosynthetic rate (Stephenson et al., 2011). Rice plants over-expressing *HARDY (HRD)*, an AP2-EREF-like TF, showed drought tolerance, thicker leaves, more chloroplast-bearing mesophyll cells, and improved water use efficiency by enhancing photosynthetic assimilation

and reducing transpiration thus contributing to increased biomass in a water-limiting environment (Karaba et al., 2007). Genetically engineering stress-responsive TFs regulating photosynthesis-related genes to modulate stress tolerance may hold promising beneficial traits of agronomic interest including improved productivity.

Further targets for improving photosynthetic traits could be to modulate TFs known to directly control the photosynthetic machinery. GOLDEN TWO-LIKE (GLK) TFs, key mediators of developmental control, have been implicated in positively regulating both chloroplast formation and coordinating the expression of photosynthetic apparatus genes, such as *LIGHT HARVESTING COMPLEX PROTEIN* genes and tetrapyrrole synthesis genes *HEMA1*, *GUN4*, *GUN5*/*CHLH*, and *CHLOROPHYLL A*/*B OXIDASE* (*CAO*) (Waters et al., 2009; Powell et al., 2012; Nguyen et al., 2014). Furthermore, the nuclear GATA NITRATE-INDUCIBLE CARBON-METABOLISM-INVOLVED (GNC) TF is involved in the control of both chloroplast development from the proplastid and control of chloroplast growth and division (Bastakis et al., 2018).

Since the ectopic overexpression of some genes might result in the overexpression of other genes (since many genes are coordinately regulated, for instance by photoreceptors) and increase the levels of associated proteins with undesired phenotypic modifications that could increase trade-offs within the agronomic characteristics and worsen productivity, even when photosynthetic performance has been improved. Therefore, it might be required to modulate only photosynthesis-related genes to accomplish the desired boosting of crops under adverse environmental conditions.

The physiological and biochemical changes in plants under specific stress conditions are related to altered gene expression, with a common set of about 750 nuclear-regulated genes responsive to changes in photosynthetic redox state (Jung et al., 2013). Genes showing redox-regulated expression characteristics are either directly involved in or connected to photosynthesis (Pfannschmidt, 2003). Adverse environmental conditions often lead to chloroplast damage including photoinhibition but this can be limited by acclimation mechanisms, many of which are based on ROS generation and/or the triggering of regulatory redox-reactive molecules (e.g., thioredoxins, and reduced glutathione). These redox-molecules can regulate transcription by interacting with TFs and other signaling molecules and thus deregulate the expression of photosynthetic component genes at multiple levels of signal transduction cascades and signaling pathways. Targeting such acclimation mechanisms, at the gene level, could help improve photosynthesis and plant adaptability under abiotic stresses. To achieve this, a better understanding of how triggered regulatory redox-reactive molecules deregulate the expression of photosynthetic component genes is required. Furthermore, the identification of redox signal targets and/or stress-responsive TFs could help identify unknown photosynthesis-related genes.

Although redox-associated changes in nuclear gene expression have been described, only a limited number of TFs that mediate transduction of redox signals controlling chloroplast signaling have been identified (Pesaresi et al., 2009; Petrillo et al., 2014). The over-expression of the zinc finger transcription factor, ZAT10, altered photosynthetic rates and resulted in enhanced tolerance to light and exogenous H_2O_2 photoinhibition, and increased expression of ROS detoxification genes whose products were targeted to multiple subcellular compartments (Rossel et al., 2007). Also, three A-type heat-shock transcription factors (HSFs) -HSFA1D, HSFA2, and HSFA3- were found to be key factors regulating the gene encoding ASCORBATE PEROXIDASE 2 (APX2) in response to a redox-generated plastid stress signal (Jung et al., 2013). Furthermore, *RADICAL INDUCED CELL DEATH PROTEIN 1 (RCD1)* stabilized the TF Rap2.4-dependent redox-regulation of genes encoding chloroplast antioxidant enzymes, although it was also found to be essential for protecting cells from photooxidative stress, in a widely redox-independent manner (Hiltscher et al., 2014). Recent promising approaches targeting chloroplast energy balance via AOX, a mitochondrial terminal alternative oxidase (Vanlerberghe, 2013; Vanlerberghe et al., 2016; Dahal and Vanlerberghe, 2017, 2018) and the overexpression of CBF (C-repeat binding factor) transcription factors (Dahal et al., 2012; Kurepin et al., 2013; Hüner et al., 2014) have been reported to enhance plant photosynthetic performance under stress conditions.

It can be seen that the manipulation of TF to modulate gene networks and gene expression is an avenue that could be exploited to engineer crops for enhanced photosynthesis and productivity under adverse environmental conditions. To achieve such aims, efforts are required to identify the appropriate TFs. Also, deep learning techniques that exploit large scale data set analyses (chromatin accessibility assays, microarray, RNA-seq expression, ChIP-seq data, gene expression profiles, DNA affinity purification sequencing, ampDAP-seq) to help resolve complex biological problems in transcriptomics need to be developed further.

Proteomics

Photosynthesis is mediated by the coordinated action of ca. 3000 nuclear-encoded preproteins synthesized in the cytosol and imported into organelles through special machineries (Nakai, 2015; Baslam et al., 2016) in envelope membranes. About 2400 of these proteins are found in the chloroplast (Friso et al., 2004), while only ca. 100 proteins are encoded by the chloroplast genome. Many environmental changes lead to an imbalance in photosynthetic electron transfer due to a modification of the redox potential of ETC components as well as functionally coupled pools of redox-active compounds (e.g., thioredoxins and glutathiones) thus affecting photosynthetic efficiency (Roach and Krieger-Liszkay, 2014; Larosa et al., 2018; Jimbo et al., 2019; Takagi et al., 2019). This imbalance can be redressed by the photosynthetic control of LHC, PS, and cytb_6f stoichiometry.

In order to prevent ROS generation, PSI must be induced to accept electrons when PSII is strongly active in the daytime by shorter-wavelength light. The mechanism of induction of PSI occurs through the de-phosphorylation of sigma factors by redox signals monitoring PQ status (Shimizu et al., 2010). Redox proteomics has been developed to monitor the redox dynamics of cellular proteins under environmental stimuli (Ansong et al., 2014; Sadler et al., 2014; Ameztoy et al., 2019).

Application of this technology to plants and chloroplasts has identified novel protein targets undergoing thiol modifications [e.g., NADPH-dependent thioredoxin reductase C (NTRC), chloroplastic fructose 1,6-bisphosphatase (FBPase)] and plastid redox signaling networks to maintain a high photosynthesis efficiency which is important for the global adjustment of plant metabolism (Lindahl and Kieselbach, 2009; Hall et al., 2010; Dietz and Pfannschmidt, 2011; Ameztoy et al., 2019). Quantitative phosphoproteomic profiling using isobaric tags for relative and absolute quantitation (iTRAQ) showed that ROS generated by an oxidative burst under drought stress could trigger NO synthesis to protect the photosynthetic apparatus by modulating the phosphorylation of diverse proteins such as LHC, thylakoid-bound Ser/Thr kinase STN7, and chloroplast post-illumination chlorophyll-fluorescence-increase protein (PIFI). ROS produced under drought conditions provoked an increase of the cellular concentration of Fe^{2+} ions, resulting in an increased electron transfer to oxygen *via* the Fenton reaction (de Carvalho, 2008). Similar effects are observed under nutrient starvation, including Mg^{2+} and Fe^{2+}, which are essential co-factors for several redox-active proteins in the photosynthetic ETC. More recently, Inomata et al. (2018) reported the chloroplast phosphoproteome profile of a rice *nucleotide pyrophosphatase/phosphodiesterase 1 (NPP1)* mutant. This study highlighted that the loss-of-function of NPP1 in rice leaves increased stomatal conductance, photosynthesis, starch, and sucrose storage while also impacting proteins involved in carbohydrate metabolism and protein synthesis system under high temperature and CO_2 conditions. Their data indicated that NPP1 plays a crucial role in carbon flux by transporting carbon taken up from starch and from cell wall polysaccharide biosynthesis to other metabolic pathways in response to the physiological needs of the cell.

Using proteomics, five new photosynthetic activity responsive transcriptional regulators were classed as redox-active in response to nutrient limitation in the photosynthetic cyanobacteria *Synechococcus* sp. PCC 7002. These were RbcR regulating the rbc LXS operon, Fur and Zur regulating iron and zinc homeostasis, respectively, cyAbrB regulating N and C metabolisms, and a TetR family regulator (Sadler et al., 2014). Furthermore, proteomics has led to the identification of proteins that mediate redox control during RNA maturation and transcription. These RNA plastid-encoded polymerase (PEP)-associated proteins are plastid transcription kinases (PTKs) (such as STN, CSK, and cpCK2), which respond to changes in thiol/disulfide redox state mediated by glutathione (Baginsky et al., 1999), and can phosphorylate the sigma-like TF, *SIG6*, involved in the regulation of chloroplast gene transcription. Similarly, these PTKs are under the control of the chloroplast GSH (glutathione) pool, suggesting a GSH-mediating redox control of their activities (Baena-González et al., 2002). Proteomics has identified also several heat-responsive TFs and proteins, such as MYB, WRKY, DnaJ protein (LeCDJ1), heat shock proteins (HSPs), filamentous temperature-sensitive H (ftsH11), sedoheptulose-1,7-bisphosphatase (SBPase), and constitutive or stress-inducible key enzymes (Chen et al., 2006; Rushton et al., 2012; Yang et al., 2012; Grover et al., 2013; Kong et al., 2014). (Phospho)-proteomic analyses suggested that heat-responsive phosphorylation levels of some important proteins [e.g., protochlorophyllide reductase (POR), oxygen-evolving complex (OEC), RuBisCO, and phosphoenolpyruvate carboxykinase (PEPCK)] were modulated, thus indicating that post-translational modifications (PTMs) were critical processes for plant heat tolerance (Hu et al., 2015; Walker et al., 2016). A proteomic approach has shown the role of PSII protein phosphorylation [e.g., the minor antenna polypeptide Lhcb4 (CP29)] in PSII protection and in the photoinhibition-repair cycle (reviewed in Aro et al., 2004).

In order to optimize leaf gas exchange under stressful environmental conditions, proteins related to stomatal development have been identified. Indeed, plants can modulate stomatal aperture, density, and placement through signaling pathways involving peptide ligands, transmembrane receptors, and mitogen-activated protein kinase (MAPK) modules. The TFs bHLH [including both MUTE and FAMA, inducer of CBF expression 1 (ICE1/SCRMI), HIGH CARBON DIOXIDE (HIC) protein, PHYTOCROME INTERACTING FACTOR (PIF), mitogen-activated protein kinases (MPKs), and their upstream MKK, YODA, SPCH, C2/H2-type zinc-finger proteins (SZT and AZF2)] have been described to regulate stomatal response to environmental perturbations and improve stress tolerance (Gray et al., 2000; Chinnusamy et al., 2003; Sakamoto et al., 2004; MacAlister et al., 2007; Wang et al., 2007; Kanaoka et al., 2008; Casson et al., 2009; Pillitteri and Dong, 2013). EPIDERMAL PATTERNING FACTOR 1 and 2, and STOMAGEN are secreted peptides that regulate the function and development of stomata (Hara et al., 2007; Hunt and Gray, 2009; Sugano et al., 2010). Furthermore, the α-subunit of the heterodimeric G protein (GPA1) and ERECTA protein are known to regulate plant transpiration efficiency by regulating stomatal density (Masle et al., 2005).

Interestingly, chloroplast proteome turnover is crucial to cell homeostasis and adaptation to changing conditions. In their review, Izumi and Nakamura analyzed the influence of extra-plastidial processes on the turnover of chloroplast proteins (Izumi and Nakamura, 2018). Fine-tuning protein turnover, and/or increasing the efficiency of respiratory ATP production can help "maintenance respiration" -the energy required to maintain mature tissue biomass when growth rate is zero (Thornley, 2011; O'Leary et al., 2017; Machacova et al., 2019)-, and hence reduce carbon loss. This process can be a primordial factor in determining growth rate and it may also impact biomass formation. Indeed, growth rate is negatively correlated with protein turnover among Arabidopsis accessions (Ishihara et al., 2017). For instance, eliminating THI4 (a suicide enzyme in thiamin biosynthesis) protein turnover, increased crop biomass accumulation by 4% by essentially reducing the high energy costs and loss of photosynthetically fixed carbon to produce thiamin (Hanson et al., 2018).

As thousands of different proteins make up the machinery of plant cells, proteomics and its derivatives (phosphoproteomics, redox proteomics, and peptidomics) are important tools to better understand processes that regulate protein synthesis and degradation in plants such as protein turnover, abundance, location, compartment-specific proteases/peptidases, protein

interactors, and PTMs (e.g., phosphorylation, ubiquitination, nitrosylation, and carbonylation) in steady and non-steady state scenarios. Establishing an integrated understanding of the processes that underpin changes in protein expression under several physiological and developmental scenarios could define new targets to rationally engineer photosynthesis for agronomic gain.

Hormonomics

Chloroplasts synthesize hormones that are known to play a critical role in photosynthesis gene expression and to participate as signaling molecules in stress signal transduction. Phytohormones including brassinosteroids (BRs), abscisic acid (ABA), cytokinins (CKs), salicylic acid (SA), ethylene, jasmonate, and auxins have been implicated in the control of stomatal development and function in response to environmental stresses, which ultimately impact photosynthesis. The importance of ABA as a central regulator and integrator of long-term changes in stomatal behavior was revealed by Dittrich et al. (2019). Under stress environments, such as drought, ABA induces stomatal closure through calcium-sensing receptor signaling driven by NO accumulation via H_2O_2 production in guard cell chloroplasts leading to membrane depolarization and loss of guard cell volume and turgor (Wang et al., 2012). ABA-dependent guard cell closure has been shown also to be regulated by the guard cell anion channel SLAC1, together with the protein kinase OST1 (Hedrich and Geiger, 2017). Using genetic approaches, Chater et al. (2015) showed that either guard cell ABA or ABA receptors, PYR/PYL/RCAR, were sufficient to mediate a [CO_2]-induced stomatal density response. However, recently a model for the convergence of CO_2 and ABA signal transduction downstream of OST1 protein kinase activation has been reported (Hsu et al., 2018). Transgenic rice and Arabidopsis plants overexpressing the pyrabactin resistance 1-like (*PYL*) family of ABA receptors promoted resistance to extreme drought stress by reducing transpiration rate and stomatal conductance thus enhancing the photosynthetic rate and water use efficiency (Zhao et al., 2016). Efforts have been made to improve photosynthetic efficiency by engineering the photosynthesis-related transcription factor, ABA-responsive 17 (*ABR17*) (Grover et al., 2013). Constitutive expression of ABA-responsive element-binding protein (*ABP9*) increased photosynthetic capacity, carbon use efficiency and tolerance to high temperature and water stress (Zhang et al., 2008). Xiong and Zhu (2003) suggested that genotypes with putative constitutive high ABA concentrations could be more tolerant to environmental stresses. ABA can also protect the photosynthetic apparatus against photoinhibition by modulating the xanthophyll cycle and by increasing the recovery rate of photo-inactivated PSII complexes (Saradhi et al., 2000). Therefore, altering stomatal sensitivity to ABA could allow plant acclimation to changing environments by optimizing gas exchange for photosynthesis.

A water deficit stimulates not only ABA synthesis but inhibits the production of CKs resulting in an imbalance between the two hormones in leaf tissues and this can control physiological responses (e.g., stomatal closure) that lead to whole plant higher adaptive fitness (Pospisilova et al., 2005; Tanaka et al., 2006). The action of CKs is mediated mainly by AHK3 receptors and several TFs (i.e., *ARR1*, *ARR10*, and *ARR12*) that regulate nuclear gene expression encoding plastid proteins (e.g., LHC, RuBisCO), plastid-related protein abundance [e.g., gamma-subunit of ATP synthase, glyceraldehyde-3-phosphate dehydrogenase (GAPDH), ClpP, ribosomal protein L21], and downstream TFs (i.e., *CGA1*, *GNC*, *HY5*, *GLK2*, *CRF2*). In this way, CKs modulate chloroplast development, division, and function (Chiang et al., 2012; Cortleven and Schmülling, 2015; Okazaki et al., 2015). Transcriptomic responses to CKs include over 100 different photosynthesis genes (Brenner et al., 2012) while a (phospho)-proteomic study identified about 50% of CK-regulated proteins to be localized in the chloroplast (Černý et al., 2011). Under high light stress, CKs show a protective function by decreasing photoinhibition, mediated by AHK2 and AHK3 receptors and the TFs ARR1 and ARR12 (Cortleven et al., 2014).

Genetic and pharmacological studies have implicated BRs in stomatal development and patterning. Kim et al. (2012) reported that the BR-insensitive mutants *bri1-116* and *bsu-q* (*amiRNA-BSL2,3 bsu1 bsl1* quadruple mutant) contained only paired guard cells, and lacked other epidermal cells. Genetic analyses indicated that receptor kinase-mediated BR signaling inhibited stomatal development through glycogen synthase kinase 3 (GSK3)-like kinase BIN2, which acts upstream of the MAPKKK YODA, and mediates signaling by ERECTA family receptor kinases. Previous studies had also demonstrated key functions of BRs in inhibiting photosynthetic gene expression, and promoting cell elongation, chloroplast senescence, and floral induction (Li et al., 1996). Furthermore, it was found in leaves and cotyledons that BR-promoted stomatal formation was via a cross-communication of the YDA-MKK4/5-MPK3/6 cascade and the basic helix-loop-helix transcription factor SPEECHLESS (SPCH), a regulator of the entry, amplifying and spacing divisions that occur during stomatal lineage development (Gudesblat et al., 2012).

As photosynthetic gas exchange and transpiration balance are impacted by altered stomatal patterning under changing environmental conditions, auxin control of stem cell compartment size, as well as auxin depletion as the switch from unequal to equal divisions, play key roles during stomatal development. High auxin activity has been observed during unequal cell divisions in stomatal patterning, whereas a decrease in auxin activity promoted guard mother cell (GMC) fate and its subsequent equal division into two guard cells. Similarly, an auxin-resistant mutant where AUX/IAA proteins failed to interact with the auxin receptor, leading to auxin insensitivity, was defective in the suppression of stomatal development in dark-grown seedlings (Balcerowicz et al., 2014). Zhang et al. (2014) reported that auxin negatively regulated stomatal development through MONOPTEROS (MP) repression of mobile peptide STOMAGEN gene expression in mesophyll cells where photosynthesis mainly takes place (Zhang et al., 2014). The regulation of stomatal and vascular developments by MP indicated that MP should play a role in photosynthesis and the transpiration system for optimizing plant growth and development. Loss-of-function quadruple mutants, *pin2, 3, 4, 7* and *pin1, 3, 4, 7* of the PIN gene family, controlling PIN protein-mediated auxin transport, showed stomatal defects

(Le et al., 2014). Moreover, Ogura et al. (2019) identified a new gene, *EXOCYST70A3* that directly regulated root system architecture by affecting the distribution of PIN4 and hence controlling the auxin pathway without disrupting other pathways. This study suggested that EXO70A3-dependent variation in the control of root system architecture could result in improved photosynthesis and help plants fight climate change. Taken together, such studies showed the important roles of stomata in photosynthesis and global carbon and water circulation and suggest that coordinating stomatal development with photosynthesis could be achieved by manipulating auxin signaling specifically in the mesophyll cells without disturbing whole plant development.

Salicylic acid (SA) acts as an important signaling molecule and influences various physiological and biochemical functions in plants, playing an important role in plant responses to biotic and abiotic stresses. Under chilling stress conditions, inhibition of SA biosynthesis by L-α-aminooxy-β-phenyl propionic acid (AOPP) increased PSII photooxidation, leading to the generation of ROS and impairment of photosynthesis and growth, whereas applying SA at moderate concentrations induced a stress tolerance by restoring the photosynthetic machinery (Cheng et al., 2016). Other studies have shown that SA treatment alleviated carbon assimilation and several components of PSII electron transfer under heat stress by increasing proline production through the increase in γ-glutamyl kinase (GK) and a decrease in proline oxidase (PROX) activity, resulting in the promotion of both osmotic and water potentials necessary for maintaining photosynthetic activity (Wang et al., 2010; Nazar et al., 2011). Under salt stress, it was revealed that SA could modulate photosynthetic capacity due to its interaction with metabolic signaling by ROS (including H_2O_2), and glutathione (Arfan et al., 2007; Nazar et al., 2011; Sewelam et al., 2016). Indeed, Miura et al. (2013) reported that SA accumulation in *siz1* [small ubiquitin-like modifier (SUMO) E3 ligase] mutant plants enhanced stomatal closure and drought tolerance by controlling guard cell ROS accumulation, while the introduction of salicylate hydroxylase (*NAHG*) into *siz1*, which reduced SA accumulation, restored stomatal opening (Miura et al., 2013). Furthermore, other SA-accumulating mutants, *cpr5* and *acd6*, exhibited stomatal closure thus reducing the entry of sufficient CO_2 for optimal photosynthesis while hindering the movement of water vapor and hence leading to drought tolerance (Miura et al., 2013).

In addition to the SA pathway, jasmonic acid (JA)-signaling (co)-regulates a wide-range of plant developmental processes and responses to biotic and abiotic stresses that probably involve the photosynthesis machinery. Indeed, the examination of high-throughput gene expression data for heat stress and methyl jasmonate (MeJA) responsive genes using GENEVESTIGATOR (Zimmermann et al., 2004), an online tool for large-scale expression data analysis, revealed a preponderance of genes associated with protein translation and photosynthetic electron transport, which could represent features associated with cellular recovery following heat stress (Clarke et al., 2009).

Ethylene receptor mutants show altered photosynthetic properties and they are sensitive to abiotic stresses. Indeed, Arabidopsis *etr1* mutants have demonstrated the role of ethylene receptor ETR1 in guard cell H_2O_2 signaling (Desikan et al., 2005). Other studies showed that ethylene-insensitive mutants, *etr1-1* and *ein2*, had smaller stomata, possessed lower chlorophyll and CAB (chlorophyll a/b binding complex) contents, RuBisCO activities, and had a lower whole-plant and leaf photosynthetic capacity, suggesting the role of basal ethylene perception in controlling stomatal conductance and photosynthetic capacity (Grbic and Bleecker, 1995; Tholen et al., 2007). Other seminal works suggested that ethylene-responsiveness was required for the fine regulation of PSII photochemical efficiency (Kim et al., 2017) and carbon fixation by achieving maximal RuBisCO activities through ethylene-responsive factors (ERFs) (Bracher et al., 2017; Xie et al., 2017). The control of photosynthesis by ethylene also affected plant biomass production by influencing final plant size (Ceusters and Van de Poel, 2018). Ethylene was found to directly control photosynthesis in juvenile non-senescing leaves and acted indirectly in mature leaves by promoting senescence.

In conclusion, it can be seen that hormonal networks influence plant photosynthesis and therefore they could assist us to develop new strategies to improve plant productivity and to help plants tolerate severe environmental conditions.

PHYSIOLOGICAL TRAITS INVOLVED IN THE MAINTENANCE OF PHOTOSYNTHESIS AS TOOLS FOR CROP IMPROVEMENT IN A CONTEXT OF CLIMATE CHANGE

Crop growth is linked to the assimilation of ambient CO_2 through photosynthesis, in which green plants convert sunlight, water, and CO_2 into O_2 and carbohydrates. During the last decade, different studies have highlighted that the improvement of plant photosynthetic rates can be a strategic tool to increase crop yields (Reynolds et al., 2011). Several studies analyzing the impact of overexpression of proteins linked with CO_2 assimilation have shown an increase in photosynthesis and plant growth (Driever et al., 2017; Kubis and Bar-Even, 2019; Ermakova et al., 2019; see section "Metabolic Engineering to Improve Photosynthesis and Elevated CO_2 Acclimation" for details). Further, as described by Parry et al. (2011), increases in wheat yield potential during the last decades have been associated with increased photosynthesis while Flood et al. (2011) have shown that variations in either the efficiency or capacity of photosynthesis can lead to variations in growth rate and productivity. Within this context, the adaptive potential of photosynthesis to changing environments depends on the degree of genetic variation for photosynthesis that is present within a population (Flood et al., 2011). Indeed, different studies (Peng et al., 2001; Hubbart et al., 2007) show that since 1980, increases in rice yield, rather than harvest index, correlate better with increases in biomass. Furthermore, the fact that varieties released after the 1980's show higher saturating photosynthetic rates when compared to older varieties suggest that varieties with higher biomass values would be the

ones with improved photosynthesis. This suggests that breeding programs aiming to improve crop biomass production will also have an effect on photosynthetic physiology (Flood et al., 2011). Supporting this observation, the increase in crop yields detected in plants grown under elevated [CO_2] (Ainsworth and Long, 2005; Long et al., 2006; Sanz-Saez et al., 2017; Torralbo et al., 2019) are also associated with higher photosynthetic rates measured under such conditions.

Yield depends on many factors such as the efficiency of light interception (LI), the radiation use efficiency of light energy conversion to biomass (RUE) and the fraction of biomass that is contained in harvested organs. Leaf morphological and physiological characteristics are two target factors conditioning variation in photosynthetic properties of individual leaves that are influenced by environment and genetics (Flood et al., 2011). Furthermore, genetically based differences in leaf morphology are commonly encountered at the interspecific level, and often correlate with growth (Hikosaka, 2010). During the last decade, the enhancement of plant light capturing surface and conversion of light energy has been a major target of crop breeders (Murchie et al., 2009). Within this context, a clear example of this strategy has been the increase in the development of erect leaves with a higher leaf area per unit ground area that enables more efficient radiation capture (Murchie et al., 2009). Despite this, it should be noted that the major step that is not yet near to the maximum is light conversion efficiency to biomass which is only at 50% of its theoretical level (see Zhu et al., 2008; Long et al., 2015; Slattery and Ort, 2015). However, despite its potential, selection based on improving photosynthesis was not properly considered during the last decades.

The assimilation of CO_2 is a complex process that involves multiple genes, regulatory mechanisms, and different metabolic pathways and plant structures working together. The overall photosynthetic process is determined by CO_2 diffusion to the chloroplast (conditioned by stomatal opening and mesophyll conductance), the capture and conversion of light energy to make ATP and NADPH (the light reactions) required for the assimilation of CO_2 to produce sugar-phosphates used to regenerate RuBP, the molecule used to fix CO_2 by RuBisCO, and to produce complex sugars like starch and sucrose. However, as mentioned in the introduction, O_2 competes with CO_2 at the RuBisCO active site thus reducing photosynthetic CO_2 assimilation capacity and producing toxic 2-PG (Flugel et al., 2017) that is removed by the photorespiratory cycle. Photorespiration has a high energetic cost and it leads to the potential loss of carbon and nitrogen in the form of CO_2 and ammonium. It has been calculated that photorespiration can reduce photosynthetic energy conversion to yield of certain important C3 grain plants by 20−50% (see South et al., 2019), including soybean and wheat (Walker et al., 2016). Therefore, photorespiration became a target for crop improvement (see section "Metabolic Engineering to Improve Photosynthesis and Elevated CO_2 Acclimation"). However recent studies (Betti et al., 2016; Eisenhut et al., 2017) suggest that reducing photorespiration may not always have beneficial effects since a higher photorespiratory capacity would contribute to: (1) maintaining Calvin cycle activity; (2) decreasing excess reducing power (a target under stressful growth conditions such as exposure to drought, salinity, cold, etc.); (3) improving nitrate assimilation under elevated CO_2 conditions. Similarly, it was found that under low CO_2 availability conditions, unrestricted photorespiratory metabolism favored plant performance (Eisenhut et al., 2017). Therefore, modulating photorespiration would probably be important to maintain or improve crop yield under certain environmental conditions that alter the chloroplast CO_2/O_2 ratio in favor of O_2.

SEMI- AND HIGH-THROUGHPUT PHENOTYPING TECHNIQUES TO MEASURE PHOTOSYNTHETIC TRAITS

Within the context of climate change, it is crucial to identify the crops that will perform better under the current and near-future conditions in the field. However, current breeding programs are constrained by the limitations of field phenotyping methods (Araus et al., 2018). During the last decade, different phenotyping platforms have emerged as a strategic tool to characterize crop performance. The light reactions can be studied by measuring chlorophyll fluorescence, whereas photosynthesis and respiration are studied by measuring CO_2 exchange between the plant and the atmosphere using infrared gas analyzers (IRGA). Depending on the type of parameter, measurements can take a few minutes, such as leaf chlorophyll fluorescence or respiration measurements, to 30−90 min, as is the case of photosynthetic parameters such as maximum rate of RuBisCO carboxylation (V_{cmax}) and maximal rate of electron transport (J_{max}) that are calculated using photosynthesis to CO_2 curves, named A-Ci curves (Farquhar et al., 1980; Bernacchi et al., 2003).

These parameters can be used to distinguish differences of photosynthetic efficiency under different environments allowing researchers to identify better-adapted cultivars (Aranjuelo et al., 2009, 2013; Sanz-Saez et al., 2017); or be used as input parameters for earth systems models that predict ecosystem responses to environmental changes (Rogers, 2014). However, a lack of information about V_{cmax} and J_{max} in some species in several ecosystems is the major source of error using earth systems models (Rogers, 2014). Another parameter that can be useful for the selection of abiotic stress-tolerant cultivars is dark respiration (R_d) (Vanlerberghe and McIntosh, 1997; Millar et al., 2011). Recently, high-throughput methodologies based on O_2 consumption have been developed (O'Leary et al., 2017; Scafaro et al., 2017), and they can rapidly (in 1−2 min) measure precise respiration rates. However, this requires the leaf to be removed from the plant and introduced into a measuring chamber, therefore it is destructive and thus not the best option. The latest technology used to estimate this parameter is a non-destructive technique that uses leaf reflectance spectroscopy, and it will be described below.

With the rise of the genomic era, screening of entire populations for traits of interest has become paramount to associate specific genomic regions with a given plant trait (see Section "Genomics to Study the Natural Variation of Plant Photosynthetic Efficiency"). Genomic approaches need

the implementation of technologies that allow the rapid measurement of photosynthetic and fluorescence traits to screen hundreds of cultivars in the shortest amount of time. Here, we will summarize semi- and high-throughput phenotyping methods to estimate parameters related to: (1) gas exchange such as V_{cmax}, J_{max}, and R_d using the latest LI-COR 6400 and LI-COR 6800 methodologies as well as hyperspectral reflectance; and (2) chlorophyll fluorescence such as solar-induced fluorescence (SIF) and stimulated fluorescence by a known source of light.

Semi- and High-Throughput Phenotyping Methods Related to Gas Exchange Parameters

In this subsection, the most recent literature focusing on two aspects of high-throughput phenotyping (HTP) of photosynthetic parameters are summarized and discussed: (1) New semi-HTP methodologies to estimate V_{cmax} and J_{max} using the Rapid A-Ci Response (RACiR) method for LICOR IRGA equipment and the use of the leaf excision method to estimate V_{cmax}, J_{max}, and light-saturated photosynthesis. (2) The use of hyperspectral reflectance technology to estimate gas exchange parameters such as V_{cmax}, J_{max}, and R_d.

Semi High Throughput Phenotyping Methods to Measure Gas Exchange Parameters

In order to estimate V_{cmax} and J_{max}, A-Ci curves need to be performed using an IRGA system. In regular A-Ci curves, the leaf receives different CO_2 concentrations ($[CO_2]$) in the IRGA chamber containing the leaf, usually from 50 μmol CO_2 mol^{-1} up to 2000 μmol CO_2 mol^{-1} (Long and Bernacchi, 2003). During this measurement, each time that $[CO_2]$ is increased, leaf photosynthesis and stomatal conductance are measured after reaching a steady-state equilibrium (Long and Bernacchi, 2003), which may take between 3 and 6 min per step. In this way, 30 to 90 min are needed per one A-Ci curve, which makes this method a Low Throughput Phenotyping technique.

Due to modifications in the way that the reference and sample IRGAs are placed in the new LI6800, Stinziano et al. (2017) were able to develop a Rapid A-Ci response curve protocol with a duration of approximately 12 min. The new design can minimize lags between the reference and the sample IRGAs thus generating a constant ramp rate for CO_2 control. In this method, the leaf is first stabilized at a $[CO_2]$ of 500 μmol mol^{-1} before being reduced to 0 μmol mol^{-1} at a rate of 100 μmol mol^{-1} min^{-1}. Data is recorded at a rate of 0.5 Hz, which is equivalent to a measurement every 2 s, therefore assuring that changes in photosynthetic response can be recorded. In order not to miss data near the inflection point of the A-Ci response curve, Stinziano et al. (2017) added another set of measurements from 300 μmol mol^{-1} to 800 μmol mol^{-1} to complete the curve (**Figure 3**). Plotting together these 2 curves, the authors were able to fit the data to the Farquhar-von Caemmerer-Berry (FvCB) model, thus obtaining V_{cmax} and J_{max} estimates that were very close to those calculated from a standard A-Ci curve. However, this method has some limitations; for example, although the physical separation between the reference and the sample chamber has been reduced, it still produces a lag between the two signals that is increased when the volume of the sample chamber has to be mixed. This lag creates a differential in CO_2 concentration that if not corrected can cause very significant variations in the measurements. To correct this lag, an empty chamber rapid A-Ci curve is run for each CO_2 ramp (Stinziano et al., 2017). In addition, Stinziano et al. (2019) produced a best practices guide in which they indicated under which conditions an empty chamber A-Ci curve was needed. Taylor and Long (2019) found significant offsets in R_d (95% variation) and CO_2 compensation point (Γ, 11% variation). According to their published data, RACiR curves can be a good tool to perform semi-HTP measurements in plant populations, being able to perform up to 60−80 A-Ci curves per day (8-h day) and per machine. However, when starting any experiment, a set of standard A-Ci curves should be performed to test that the method is working for each species and/or environmental

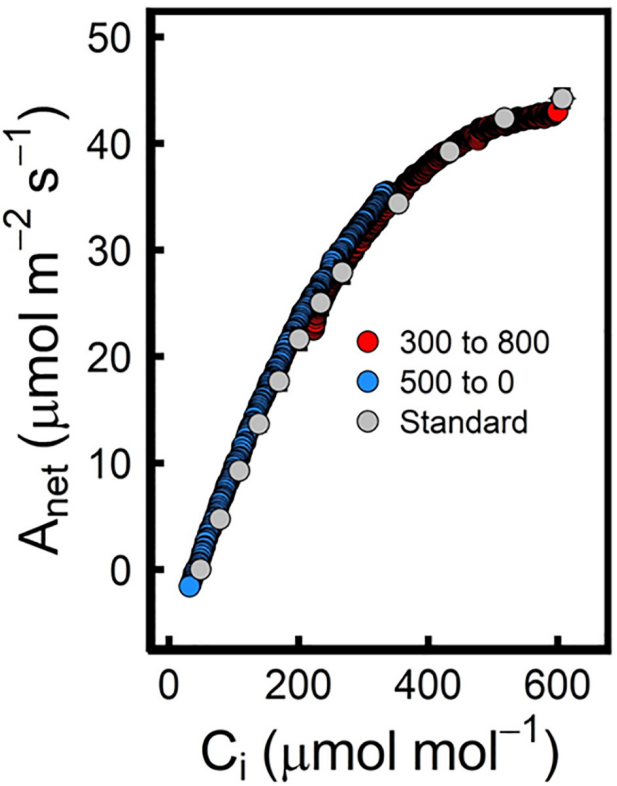

FIGURE 3 | The Rapid A-Ci curve method generates a wealth of data that when corrected to reduce the lags of the empty chamber, etc., overlay well onto the "standard" A-Ci curve. In this case, a modification of an A-Ci curve from Populus deltoides is shown. The graph has been adapted from **Figure 2** (Stinziano et al., 2017) by the author of the manuscript. Data for the "standard" A–Ci curve are presented as the mean of the mean (s.e.m.) for three measured responses on the same leaf of a single seedling (gray dots), while RACiRs were replicated once per CO_2 range per seedling on the same leaf at the same location as the "standard" A–Ci curve. The best RACiRs were produced by ramping $[CO_2]$ from 500 to 0 (blue) and from 300 to 800 (red). For statistical information about the curve fits and the calculated parameters, please check Stinziano et al. (2017).

condition. Therefore, this RACiR methodology only appears to be worth the effort when analyzing hundreds of samples at the same environmental condition as is often the case for GWAS and/or QTL experiments (Dhanapal et al., 2015; Herritt et al., 2018; Luo et al., 2018). For small experiments where only a few cultivars/species are to be analyzed, it is more reasonable to do standard A-Ci curve measurements even if it is more time consuming, as they can be used to obtain other important information such as C_c, g_m (Harley et al., 1992), R_d and Γ that can give further valuable information about the physiological state of the plant.

Other problems occurring when measuring A-Ci curves or mid-day photosynthesis under field conditions on hundreds of samples include a transient decrease in water potential, a decrease in chloroplast inorganic phosphate concentration, and a decrease in maximum PSII efficiency. These can all occur after a few hours of light exposure making it difficult to compare measurements at the beginning with those taken at the end of the day (Ainsworth et al., 2004). When measurements are performed in the field, changing environmental conditions can alter the photosynthetic response of the plants thus making it difficult to determine treatment effects. With this in mind, Ainsworth et al. (2004) developed the "leave scission method" where soybean leaves were cut pre-dawn under water, stored in the dark, and stimulated at saturating light, at least 30 min before measurements were recorded. Using this method, all samples were measured under the same temperature, light intensity, and biochemical state. A-Ci curves have been performed in this way for the last 15 years with successful results with soybean (Ainsworth et al., 2004; Bernacchi et al., 2005; Sanz-Saez et al., 2015, 2017) and corn (Leakey et al., 2006; Yendrek et al., 2017). Additionally, Choquette et al. (2019) used this methodology to phenotype light-saturated photosynthesis response to elevated ozone in a panel of 48 corn lines, measuring more than 200 plots per day. Although this technique cannot be considered high-throughput, we believe that it could be used to screen photosynthetic parameters in diversity panel populations of about 200 lines for several days to cover the different replications. The fact that all measurements are taken under the same conditions reduces the variability associated with weather changes that happen during sampling and allows differentiating between treatments and cultivars (Choquette et al., 2019).

Use of Hyperspectral Reflectance Technology to Estimate Gas Exchange Parameters

Hyperspectral sensors capture electromagnetic radiation reflected from vegetation in the visible (VIS, 400–700 nm), near-infrared (NIR, 700–1300 nm), and short-wavelength infrared regions (SWIR, 1400–3000 nm), which contain information about leaf physiological status, including pigments, structural constituents of biomass, and water content (Curran, 1989; Penuelas and Filella, 1998). Variation of foliar reflectance at different wavelengths is specific to variations in the chemical and structural characteristics of the leaf (Serbin et al., 2012). With the improvement of computational methods, predictive models using partial-least square regression (PLSR) have been used to create equations that predict other physiological parameters such as leaf isotopic ratio (Richardson and Reeves, 2005), specific leaf area (Asner and Martin, 2008; Asner et al., 2011), leaf carbohydrate content (Dreccer et al., 2014; Asner and Martin, 2015), and leaf mineral content (Mahajan et al., 2014). The use of hyperspectral reflectance spectroscopy as a HTP tool has been recognized as promising in agricultural research (Weber et al., 2012; Araus and Cairns, 2014), however, until recently its utility to differentiate between a big set of cultivars had not been tested. We will focus now on the methodologies used to produce models capable of predicting photosynthetic parameters such as V_{cmax} and J_{max} and R_d.

As measuring A-Ci curves is a tedious technique to calculate V_{cmax} and J_{max}, Serbin et al. (2012) tested the possibility to predict these parameters using hyperspectral reflectance and PLSR models in aspen and cottonwood seedlings grown at different atmospheric temperatures. Because of large phenotypic variations in V_{cmax} and J_{max} due to the temperature treatments and the inclusion of two different species, the correlation between the predicted data using hyperspectral reflectance measurements and the standard A-Ci curves was very high (R^2 of 0.89 and 0.93, respectively). This breakthrough publication demonstrated that it was possible to use hyperspectral reflectance data to estimate photosynthetic parameters. Following this discovery, Ainsworth et al. (2014) carried out a similar experiment with soybean grown at ambient and elevated ozone (O_3) in which standard A-Ci curves were combined with hyperspectral reflectance measurements using the Field Spec Hi-Res 4 (ASD technologies). Although the number of samples was not very high (59), the phenotypic variation due to the O_3 treatment resulted in a good correlation between the predicted and the standard A-Ci curve (R^2 of 0.88). More recently, similar correlations between standard and predicted V_{cmax} estimations have been found for corn (Yendrek et al., 2017; R^2 of 0.6) and wheat (Silva-Perez et al., 2018; R^2 of 0.62).

These results are very promising for applications using very big sample sets however, to date, nobody has applied this technique to estimate V_{cmax} without testing its accuracy with standard A-Ci curve measurements. Although it seems risky, this is the avenue to take if we want to increase the speed of analysis and contribute to future breeding. To break this barrier, Choquette et al. (2019) tested 45 F_1 corn hybrids with a differential response to elevated O_3 under field atmospheric conditions. The effect of elevated O_3 was studied by performing photosynthesis measurements under light-saturating conditions using a LI6400, and estimations of V_{cmax} using hyperspectral reflectance data and equations developed by Yendrek et al. (2017). In this way, Choquette et al. (2019) showed that they could detect both genotypic and O_3 effects on predicted V_{cmax} using hyperspectral data. They found good correlations between V_{cmax} and other variables estimated using the spectra such as chlorophyll content, a parameter that had a very strong correlation between predicted and measured values, and thus confirmed the quality of the general predictions.

R_d measurements using an O_2 electrode can be quick, around 2 min, allowing semi-HTP screening (O'Leary et al., 2017; Scafaro et al., 2017). However, the equipment is expensive and the technique requires destructive sampling of leaf material. To solve

these problems, Coast et al. (2019) adapted a piecewise linear regression splines (PLRS) model based on equations developed by Serbin et al. (2012) to estimate R_d from large and diverse sets of wheat cultivars. In their experiment, several wheat cultivars were tested under controlled and field conditions thus analyzing a total of 1,318 leaf samples using a standard R_d measurement and hyperspectral reflectance measurements (Coast et al., 2019). These authors found an overall R^2 between the measured and the predicted parameters of 0.50−0.63, which was higher than previous parameters used to estimate respiration such as leaf mass area (Wright et al., 2006) and leaf N content (Reich et al., 2008). As for V_{cmax} and J_{max}, it was theorized that some of the low predictability of the models could be due to low phenotypic differences for R_d. Indeed, low phenotypic variation has been identified as one of the problems when producing prediction models with NIRS technology as seen for the case of isotopic ratios (Cabrera-Bosquet et al., 2011). This limitation can be solved only by performing experiments with a diverse genetic background under different environmental conditions, or even better with stresses such as drought, elevated O_3, increasing temperatures, etc. that will increase the variability of the measured phenotype. Furthermore, a collaborative database sharing phenotypes and spectroscopy data could advance this technology much quicker, as suggested by Coast et al. (2019).

Although further validation is needed using other species and under other environmental conditions such as drought and high temperature, this could be the beginning of an era where researchers can estimate gas exchange related parameters using hyperspectral reflectance spectroscopy data that only takes 1−2 min to collect. Until then, if a researcher is thinking of performing large cultivar screenings using values estimated from hyperspectral reflectance data, it is still recommended to have a reduced set of samples that serve to undertake gold standard measurements (A-Ci curves, or R_d measurements) just to test whether predictions are coherent. For example, a solution would be to measure and compare hyperspectral data with standard measurements using cultivars identified as extremes with hyperspectral data just to test that standard measurements identify them as extremes.

High-Throughput Phenotyping Methods to Estimate Chlorophyll Fluorescence Parameters

Chlorophyll fluorescence measurements are based on capturing and measuring the light re-emitted by chlorophylls during a return from an excited to a non-excited state. Researchers measure chlorophyll fluorescence using different approaches: (1) After the leaf has been stimulated by solar radiation, and called "Solar Induced Fluorescence" (SIF). (2) After stimulation of the leaf with a light beam of known intensity and wavelength, and measurement at specific wavelengths, here referred to as "chlorophyll fluorescence."

Solar Induced Fluorescence

As previously mentioned, reflected light from vegetation can provide information about various plant traits. Light reflected from plants contains light remitted by chlorophyll that contributes to the reflectance signature. Chlorophyll remits absorbed light (fluorescence) at peak wavelengths of 690 and 740 nm associated with PSII and PSI, respectively (Krause and Weis, 1984). The reflectance signature of leaves is an outcome of various parameters that influence how incoming radiation is reflected. The deconvolution of reflectance and fluorescence can be observed in absorption bands of oxygen (centered at 687 and 760.4 nm) and hydrogen (centered at 656.4 nm) where solar radiation is absorbed by the atmosphere (Meroni et al., 2009). Reflectance recorded near these wavebands is from chlorophyll fluorescence and thus, it is possible to passively measure the amount of fluorescence being emitted from plant tissues while solar radiation is reaching the plants.

Multispectral measuring methods of SIF require the incident solar irradiance to be obtained along with the vegetative reflectance after which SIF is calculated by comparing the relative increase between a wavelength in and out of the absorption band (Carter et al., 1990). SIF can be also calculated using hyperspectral reflectance spectroscopy as it contains more information in the multitude of wavelengths (Alonso et al., 2008). However, the fluorescence measured under these conditions is a complex outcome of physiological processes. Previous studies have shown how SIF can be used to obtain information about photosynthesis (Rosema et al., 1998; Flexas et al., 2002; Evain et al., 2004). SIF can be measured remotely by satellites and at nearer to ground levels using multispectral and hyperspectral platforms. These multispectral and hyperspectral methods are especially amenable to high-throughput analyses and can be incorporated into different HTP platforms such as aerial drones (Sankaran et al., 2015; Kanning et al., 2018), tractors (Scotford and Miller, 2004; Andrade-Sanchez et al., 2014), and carts (Thompson et al., 2018). Previously, SIF had been shown to be correlated with canopy photosynthesis (Yang et al., 2015) and used to estimate gross primary productivity (Bacour et al., 2019). Passive measurements of photosynthetic traits like SIF can be carried out extremely rapidly and at multiple times during the growing season.

Chlorophyll Fluorescence

Chlorophyll fluorescence is an important tool used to investigate the light-dependent reactions of photosynthesis. This is achieved by removing or drastically decreasing one of the three routes of absorbed light energy. Without the addition of herbicides that inhibit PSII, this is achieved by applying a short saturating flash to the photosynthetic sample. With a short enough flash, no changes to non-photochemical quenching or photosynthetic efficiency occur and this allows the fluorescence maximum to be reached that can, with other fluorescence measurements, provide information about PSII efficiency (Maxwell and Johnson, 2000).

The commercial availability of handheld fluorometers has allowed researchers to use chlorophyll fluorescence measurements to study the effects of various stresses on the light-dependent reactions including nitrogen availability (Huang et al., 2004), salinity (Belkhodja et al., 1994), heat (Pastenes and Horton, 1996), cold (Fracheboud et al., 1999), and drought (Meyer and Genty, 1999; Sánchez-Rodríguez et al., 1999). While the use of such fluorometers in the field has yielded valuable

information, throughput is limited by the time required to walk from one plant to another and to initiate a new measurement. Additionally, the time frame in which photosynthetic traits are somewhat stable limits when measurements can be collected depending on the aim of the experiment. Because chlorophyll fluorescence is changing in response to irradiance, large data collections that span several hours can be influenced by when measurements were obtained (Huang et al., 2006). To avoid incorporating a large source of error, timing the measurements around solar noon, when chlorophyll fluorescence is relatively stable, produces better quality data. That said, several chlorophyll fluorescence studies involving large populations of genotypes have provided genetic information that could be used to improve photosynthesis and crop production (Guo et al., 2008; Kiani et al., 2008; Azam et al., 2015; Herritt et al., 2018).

Imaging-based methods for measuring chlorophyll fluorescence allow spatial details of leaf and plant canopy fluorescence that handheld devices cannot provide. This approach requires that the whole imaging area is provided with a rapid, homogenous, and saturating light flash. Thus, the field of view for the imaging system will dictate the number of light sources required to saturate the leaf area being imaged. Several studies have shown the sensitivity of fluorescence imaging concerning pathogen interactions (Meyer et al., 2001; Chaerle et al., 2004, 2007). More recently, several companies have offered systems that can obtain chlorophyll fluorescence images. However, the deployment of these and other custom-built systems in field experiments is often difficult. To achieve a high-throughput capacity with fluorescence imaging, automated systems that move the imaging system to the plants or move the plants to the imaging system are required (Fahlgren et al., 2015; Virlet et al., 2017). With the incorporation of such automated systems, chlorophyll fluorescence imaging can provide spatial information about the efficiency of the light-dependent reactions within large plant populations.

One emerging improvement in chlorophyll fluorometry is the use of light-emitting diodes (LEDs) to provide fast and repetitive flashes of sub-saturating light to obtain information about the primary electron acceptor of PSII as well as the reduction of the PQ pool. Previous fluorescence measurement methods relied on saturating light pulses to measure the relative changes in fluorescence required to describe biophysical and physiological aspects of photosynthesis (Avenson and Saathoff, 2018). The use of LEDs has allowed the development of multiphase flash techniques that use short sub-saturating light flashes to achieve a complete reduction of PSII primary quinone acceptors and PSII acceptor pools (Loriaux et al., 2013). Multiphase flash chlorophyll fluorescence allows for a more accurate measurement of light-adapted maximum fluorescence (F_m'). Despite these improvements, the multiphase flash technique has not been incorporated into HTP. The potential for high-throughput measurements has been realized with the fast repetition rate (FRR) protocol thus allowing for extremely rapid measurements of fluorescence (<0.2 s) (Kolber et al., 1998). The combination of LED systems with FRR capability into laser or light-induced fluorescence transient (LIFT) instruments can provide high-throughput fluorescence data. Thus, LIFT systems have been incorporated into HTP systems and used in the field and controlled environments to collect plant fluorescence data (Keller et al., 2018).

MODELING PHOTOSYNTHESIS IN CROP GROWTH MODELS

Over the last five decades, many crop growth models have been developed and applied to simulate agricultural production systems and to forecast crop yields (Priesack and Gayler, 2009). In particular, during the last years, a selection of these models have been tested and compared to characterize their ability to simulate crop production at different sites across the globe situated in different continents and representing different climatic conditions for major crops such as wheat (Asseng et al., 2013), maize (Bassu et al., 2014), rice (Li T. et al., 2015), and potato (Fleisher et al., 2017). The aim was also to apply the models to estimate possible future impacts of a changing climate on global crop production and grain yields (Asseng et al., 2019; Liu Y. et al., 2019).

Almost all crop growth models aim to estimate the carbon gain for biomass production at the field level based on models of photosynthesis and radiation absorbed by the canopy. Many models assume a linear relationship between net primary biomass production (NPP) and the photoactive radiation absorbed by the crop canopy (R_{PAR}). Models such as APSIM, CERES, EPIC, SALUS, LINTUL, Sirius, and STICS (Asseng et al., 2013 supplement, Bassu et al., 2014 supplement) follow the so-called "big-leaf" approach, where the whole canopy is treated as if it was one big leaf and photosynthetic carbon gain is described by the light-use-efficiency model. It is defined by the following direct proportionality with the parameterε_{LUE}, the light-use-efficiency, representing all photosynthetic and respiratory processes (Medlyn, 1998):

$$NPP = \varepsilon_{LUE}\, R_{PAR} \quad (1)$$

where NPP denotes net primary production [g m^{-2} d^{-1}], R_{PAR} is absorbed photoactive radiation [MJ m^{-2} d^{-1}] and ε_{LUE} is light-use-efficiency [g MJ^{-1}].

Other models such as Ecosys, ExpertN-SPASS, GECROS, HERMES, IXIM, LPJml, MCWLA, MONICA, SUCROS, WOFOST (Asseng et al., 2013 supplement, Bassu et al., 2014 supplement) simulate the photosynthesis rate of the canopy based on single leaf photosynthesis rates. This is achieved in three major steps by calculating (i) single leaf photosynthesis per leaf area of each leaf, (ii) the instantaneous photosynthesis rate of the whole canopy at given light conditions by integration over the canopy depth and plant leaf areas at each depth, (iii) the daily canopy photosynthesis by integration over the day. In these models, a distinction is made between shaded and sunlit leaves (Spitters, 1986; Goudriaan and van Laar, 1994; Wang and Leuning, 1998) and leaf photosynthesis is calculated for each leaf type separately. This modeling approach is known as the "two-leaf" model.

A further type of canopy photosynthesis model distinguishes different leaf classes depending on their height in the canopy

above the soil surface and it is called the "multi-layer" model (Leuning et al., 1995).

Besides the availability of light and CO_2, the impact of air temperature and the supply of water and nitrogen on leaf photosynthesis have to be modeled depending on the modeling approach at either canopy or both at the leaf and canopy-scales.

Leaf Photosynthesis Rate Models

In the case of the "big-leaf" approach, as with the LINTUL model, the daily net gain of carbon for biomass growth is described by:

$$\mu_B = \varepsilon_{LUE} \cdot \left\{R_{PAR}\left[1 - \exp(-\alpha_{ext} \cdot f_{LAI})\right]\right\} \cdot f_{CO_2} \cdot f_S \cdot f_T \cdot f_\vartheta \cdot f_N \quad (2)$$

where μ_B is the daily net carbon gain of the canopy biomass [g m^{-2} d^{-1}], ε_{LUE} the light-use-efficiency [g MJ^{-1}], R_{PAR} the absorbed photoactive radiation [MJ m^{-2} d^{-1}], α_{ext} the light extinction coefficient, f_{LAI} the leaf area index, f_{CO_2} the impact factor of atmospheric CO_2 concentration, f_S the impact factor of senescence, f_T the impact factor of daily average air temperature, f_ϑ the impact factor of available soil water content, and f_N the impact factor of available soil nitrogen. In a similar way this approach is used in the CERES model, where only the term representing the absorbed global radiation takes an empirically derived exponential form, i.e:

$$\mu_B = \varepsilon_{LUE} \cdot \left\{R_{PAR}\left[1 - \exp(-\alpha_{ext} \cdot f_{LAI})\right]\right\}^{0.6} \cdot f_{CO_2} \cdot f_S \cdot f_T \cdot f_\vartheta \cdot f_N \quad (3)$$

In cases of the "two-leaf" or the "multi-layer" approach, the description of leaf photosynthesis rates again follows the general scheme given by a maximal rate of carbon gain and additional reduction factors representing environmental conditions which are not often in an optimal state to allow maximal photosynthesis:

$$P_{gm} = P_{g\,max} \cdot f_{CO_2} \cdot f_S \cdot f_T \cdot f_\vartheta \cdot f_N \quad (4)$$

where P_{gm} denotes the gross leaf photosynthesis rate at light saturation [kg CO_2 m^{-2} d^{-1}] and $P_{g\,max}$the maximal gross leaf photosynthesis rate [kg CO_2 m^{-2} d^{-1}] with impact factors of CO_2, senescence S, temperature T, soil water ϑ and soil nitrogen availability *N*.

This scheme is similar to the mechanistic description of growth rates, which change by the impact of environmental factors, formulated in analogy to mechanics, i.e., to the description of the velocity change of a moving particle due to forces acting on the particle (Priesack et al., 2012).

The gross leaf photosynthesis rate P_{gl}[kg CO_2 m^{-2} d^{-1}] is then given by accounting for the absorbed photoactive radiation R_{PAR} [MJ m^{-2} d^{-1}] and by applying the light-use-efficiency parameter ε_{PAR}[kg CO_2 MJ^{-1}] of photosynthesis and the gross photosynthesis rate at light saturation P_{gm}[kg CO_2 m^{-2} d^{-1}]:

$$P_{gl} = P_{gm}\left\{1 - \exp\left(-\varepsilon_{PAR} \cdot R_{PAR} P_{gm}^{-1}\right)\right\} \quad (5)$$

Whole Canopy Photosynthesis Rate Models

The up-scaling calculation from leaf photosynthesis rate to whole canopy photosynthesis rate for a given time during the day often follows the method of Spitters et al. (1989). It is assumed that light-use-efficiency of photosynthesis ε_{PAR} and gross photosynthesis at light saturation P_{gm} are constant within the canopy. In a first step, photosynthesis rates of shaded and sunlit leaves at each depth of the canopy are calculated separately. In the case of sunlit leaves, an additional integration over the leaf angle distribution is performed to include an averaged value of the adsorbed direct radiation for the estimation of sunlit leaf photosynthesis rates at different canopy depths. Finally, the integration over the canopy depth of the photosynthesis rates of both sunlit plus shaded leaves gives gross canopy photosynthesis at any given time during the day.

$P_{g,l,z}$ [g CO_2 m^{-2} d^{-1}] denotes the total photosynthesis at depth z of the canopy given by the fraction of sunlit leaves $f_{slt,z}$ at depth z and the gross photosynthesis of sunlit *Pg*, *slt*, *z* or shaded leaves $P_{g,shd,z}$:

$$P_{g,l,z} = f_{slt,z} P_{g,slt,z} + \left(1 - f_{slt,z}\right) P_{g,shd,z} \quad (6)$$

Since the integration over the cumulative leaf area index $f_{LAI,z}$ at canopy depth z from zero at the soil surface to the total leaf area index f_{LAI} of the canopy corresponds to the integration over the canopy height, the total gross photosynthesis of the canopy P_g can be calculated using:

$$P_g = \int_0^{f_{LAI}} P_{g,l,z}\, df_{LAI,z} \quad (7)$$

The daily gross photosynthesis and hence the daily amount of assimilated carbon by the canopy is then estimated by integration over the day length (Spitters et al., 1989) from the time of sunrise t_0 to the time of sunset t_1:

$$P_g^{day} = \int_{t_0}^{t_1} P_g\, dt \quad (8)$$

Gaussian integration is usually applied as a fast and accurate method to calculate both instantaneous and daily canopy photosynthesis (Goudriaan, 1986; Spitters, 1986).

In the case of the GECROS model, upscaling from the leaf transpiration as determined by leaf stomatal conductance from either sunlit or shaded leaves to the whole canopy transpiration is achieved by the same integration procedures (Yin and van Laar, 2005).

Impact Factors of Temperature, Atmospheric CO_2 Concentration, Soil Water, and Soil Nitrogen Availability

Besides the differences between "big-leaf," "two-leaf," and "multi-layer" approaches, crop growth models mainly differ in their choice of impact functions.

The impact functions of air temperature are well documented in the supplementary information of Wang et al. (2017) an will not be mentioned further here.

To simulate the impact of atmospheric CO_2 concentration on photosynthesis, strongly different approaches have been incorporated into crop growth models especially if CO_2 enrichment experiments are considered. In the case of the "big-leaf" approach, the CO_2 impact factor is either a linear or a curvilinear multiplier leading to an increase of light-use-efficiency (Tubiello and Ewert, 2002), as in several models including CERES, Cropsyst, EPIC, Sirius and STICS (Vanuytrecht and Thorburn, 2017). In the case of leaf scale photosynthesis models, common and often documented approaches are the biochemical model of leaf photosynthesis of Farquhar et al. (1980) for C_3 plants and an equivalent version by Yin and Struik (2009) for C_4 plants. Both models are based on the calculation of intercellular CO_2 concentration and require the incorporation of a stomatal conductance model. However, for both photosynthesis models, several parameters have to be determined and the application of the model can be difficult. A simpler approach for leaf-level photosynthesis is the empirically determined increase of light-saturated photosynthetic rate prescribed by the impact factor f_{CO_2} in eq. (4). Additionally, photosynthetic light-use-efficiency ε_{PAR} can be modeled as influenced by atmospheric CO_2 concentrations (Nendel et al., 2009) and it is increased if higher CO_2 concentrations occur (Vanuytrecht and Thorburn, 2017). In contrast, the more complex structure of the GECROS model can simulate the acclimation of photosynthesis to higher CO_2 levels, which has been observed in FACE experiments. This good model performance is based on a better consideration of plant internal C−N interactions (Thornley, 1998, 2004) within the GECROS model (Biernath et al., 2013; Yin, 2013).

In several models, the impact factor of water availability on photosynthesis is set equal to the ratio of actual to potential evapotranspiration, which then reduces canopy light-use-efficiency or the maximal leaf photosynthesis rate if the actual transpiration, i.e., the root water uptake, is less than the potential demand. It is assumed that stomatal closure is controlled by the balance between available soil water and water demand caused by atmospheric conditions (Tubiello and Ewert, 2002). Less simple approaches calculate leaf stomatal conductance, which decreases under water stress, and thus limits photosynthetic rates by reducing CO_2 entry into leaves or fluxes within the canopy. This has to be based on simulations of energy balance either at the leaf or canopy level to adequately represent the impact of atmospheric conditions that determine transpiration demand.

Similar to the very simple approach to account for water availability, the impact factor of nitrogen availability can be defined as the ratio of actual nitrogen demand versus optimal nitrogen supply. This is often calculated as the ratio of the difference between actual and minimal nitrogen content about the difference between optimal and minimal nitrogen content of either the leaf in the case of leaf photosynthesis or of the aboveground canopy biomass in the case of canopy photosynthesis. It is assumed that nitrogen contents are not optimal if the mineral nitrogen uptake from the soil cannot fulfill plant nitrogen demand given as the sum of the differences between actual and optimal concentrations in the plant organs (Priesack and Gayler, 2009). More complex nitrogen uptake models can also simulate the observed increase in photosynthetic nitrogen-use-efficiency and decreased tissue N concentrations at elevated [CO_2] (Biernath et al., 2013; Vanuytrecht and Thorburn, 2017). This is achieved for example by incorporating a functional balance between root N acquisition and shoot C gain in GECROS (Yin and van Laar, 2005; Priesack and Gayler, 2009), or by including an adaptation of photosynthetic N demand to atmospheric [CO_2] as in the growth model AgPasture of APSIM (Cullen et al., 2009).

Most of the considered crop models are source driven assuming growth limitation by the supply of assimilates. Therefore, approaches to model either positive or negative environmental impacts on yields by factors increasing or reducing maximal leaf photosynthesis rate or crop light-use-efficiency strongly determine the simulation of crop growth. Determination of these factors needs numerous field experiments and extensive testing to provide a sound basis for adequate simulations of impacts on crop growth. By this rather simple and parsimonious approach, crop growth is conceived as carbon-source driven and described by balancing gains from assimilation and losses through respiration and plant tissue abscission.

METABOLIC ENGINEERING TO IMPROVE PHOTOSYNTHESIS AND ELEVATED CO_2 ACCLIMATION

As already stated in this review, improving photosynthesis has become a major aim for increasing plant yield (example: the RIPE project[2]) (Long et al., 2015; Ort et al., 2015; Simkin et al., 2019; Weber and Bar-Even, 2019). To date, targets to achieve this include: RuBisCO properties and activation, RuBP regeneration, photorespiration, CO_2 availability by improving mesophyll conductance and by introducing CO_2 concentrating mechanisms based on cyanobacterial, algal and C4-plant systems, photoprotection by modifying the relaxation of energy quenching processes, and by optimizing crop canopies to improve light capture (see Ort et al., 2015). Already, several studies have provided support by demonstrating that modifying photosynthetic processes through genetic engineering can improve photosynthetic CO_2 assimilation rates and yield potential (see reviews by Simkin et al., 2019; Weber and Bar-Even, 2019). Several major examples are highlighted below and include improving RuBP regeneration by overexpressing selected Calvin cycle enzymes and modifying photorespiration by creating artificial glycolate-metabolizing bypass pathways in the chloroplast (see **Figure 4**). These processes were found to be amongst the best targets to improve photosynthesis CO_2

[2]http://ripe.illinois.edu/

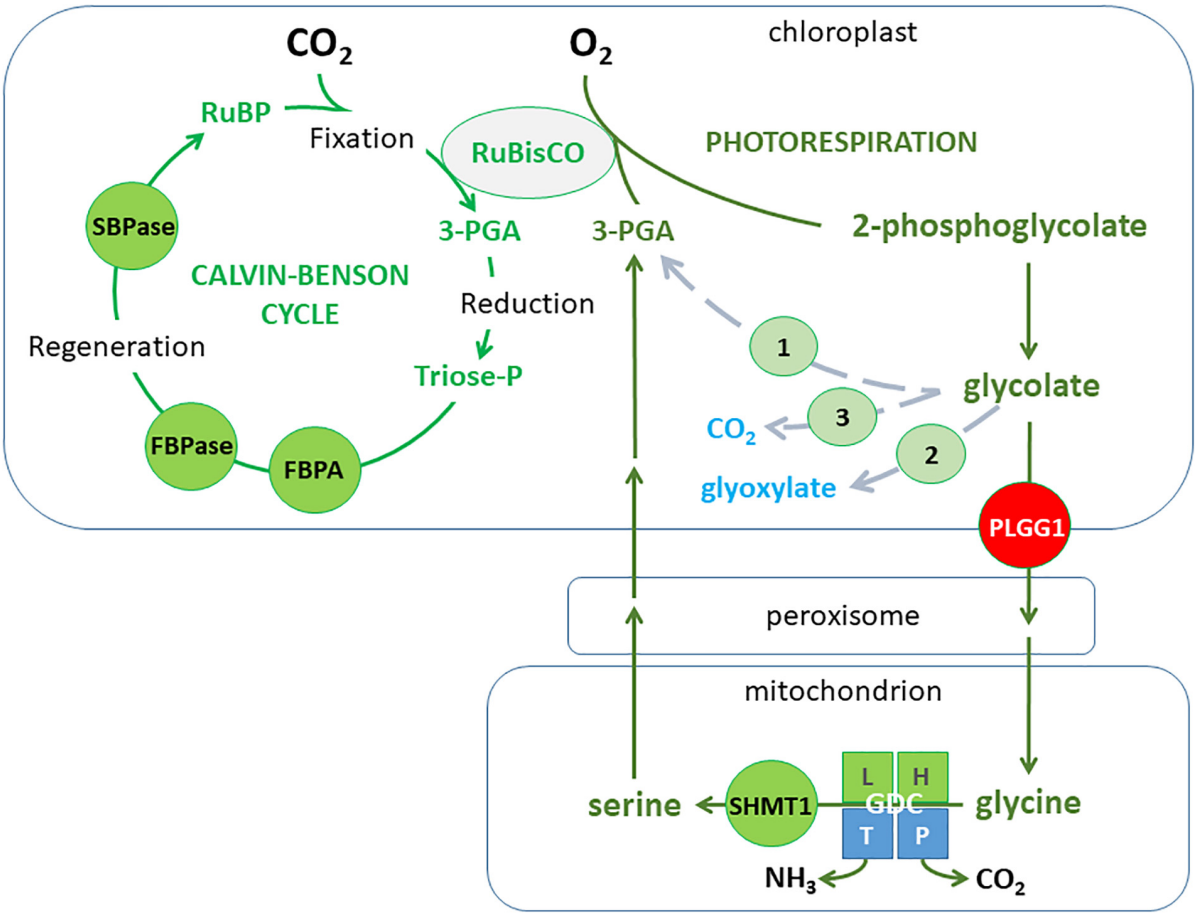

FIGURE 4 | A simplified scheme highlighting tested ways to increase photosynthesis and crop yield by overexpressing selected Calvin cycle enzymes and by creating synthetic chloroplastic photorespiratory bypasses. The enzymes in green circles/squares have been overexpressing either individually or together. Details of the different photorespiratory pathways can be found in the main text: 1 is based on the bacterial glycerate pathway leading to 3-PGA from glycolate (Kebeish et al., 2007; Dalal et al., 2015), 2 is an incomplete glycerate pathway leading to glyoxylate from glycolate (Nölke et al., 2014), 3 are pathways leading to the production of CO_2 from glycolate (Maier et al., 2012; Shen et al., 2019; South et al., 2019). The transporter in the red circle was repressed to improve photorespiratory bypasses (see South et al., 2019). Abbreviations can be found in the main text.

assimilation efficiency after *in silico* modeling studies pinpointed SBPase, fructose bisphosphate aldolase (FBPA), and photorespiration as potential limiting reactions (Zhu et al., 2007).

Plants over-expressing the redox-regulated Calvin cycle enzyme SBPase show improved photosynthetic activities and increased biomass. This has been seen to occur in *Arabidopsis thaliana* (Simkin et al., 2017a), tobacco (Lefebvre et al., 2005; Rosenthal et al., 2011; Simkin et al., 2015), tomato (Ding et al., 2016), and wheat (Driever et al., 2017). However, beneficial effects were found to be dependent on both developmental stage and growth conditions. An increase in photosynthesis was only observed in young expanding tobacco leaves but not in fully expanded ones and no effect on photosynthesis was seen when plants were grown under short days and low light (Lefebvre et al., 2005). When tobacco over-expressing Arabidopsis SBPase was grown outside under elevated CO_2 (585 ppm) an increase in photosynthesis and biomass was observed when compared to wild-type plants (Rosenthal et al., 2011). However, the increase in biomass was only 50% of the theoretical value due to C3-plant acclimation to elevated CO_2 (see below). Furthermore, higher CO_2 assimilation rates were variable over the growing season with no significant increase observed in August compared to July. Cyanobacterial and green algal Calvin cycle enzymes have also been used to improve plant productivity. The overexpression of either Chlamydomonas SBPase or cyanobacterial FBPase led to increases in both photosynthesis and biomass (Tamoi et al., 2006). A cyanobacterial bifunctional SBPase/FBPase enzyme has been overexpressed also in tobacco (Miyagawa et al., 2001), lettuce (Ichikawa et al., 2010), and soybean (Köhler et al., 2017) with increases in photosynthetic CO_2 fixation and biomass. In the work of Köhler et al. (2017), soybean overexpressing cyanobacterial SBPase/FBPase was grown in the field during three seasons under elevated CO_2 (600 ppm) and elevated temperature (+3°C) and compared to normal ambient conditions. Across the different treatments, the over-expressing lines exhibited higher carbon assimilation rates. Under ambient CO_2, elevated

temperature led to seed yield reductions in both control and transgenic genotypes. However, under elevated CO_2 and high temperature, the SBPase/FBPase plants maintained higher seed yield levels, while WT plants had reduced seed yields, compared with plants grown under only high CO_2. Therefore, perhaps Calvin cycle manipulation can offset the detrimental effects of future climate change conditions. Improved biomass has been observed also when overexpressing FBPA in tobacco (Uematsu et al., 2012) and the positive effect on photosynthesis and biomass was more pronounced when plants were grown at elevated CO_2 (700 ppm). When Arabidopsis FBPA was overexpressed in the photosynthetic tissues of Arabidopsis using a RuBisCO small subunit 2A promoter, similar increases in photosynthesis, dry weight, and seed yield occurred (Simkin et al., 2017a). However, when overexpression of SBPase and FBPA were stacked in Arabidopsis, no significant additional increases in maximal efficiency of CO_2 assimilation rate (A_{max}), dry weight and seed yield were observed when compared to individual transgene overexpressing lines (Simkin et al., 2017a).

Another major strategy for improving photosynthesis has been a synthetic biology approach to express within the chloroplast an alternative pathway to efficiently metabolize photorespiratory glycolate and thus alleviate the potential inhibitory action of 2-PG on photosynthesis, while preventing ammonium release and limiting CO_2 release to the chloroplast where RuBisCO is located (**Figure 4**). Since the first report (Kebeish et al., 2007), several photorespiratory bypass strategies have been used to improve photosynthetic CO_2 assimilation and biomass. The initial bypass tested was based on the bacterial glycerate pathway where glyoxylate was converted to glycerate by two enzymes; glyoxylate carboligase and tartronate semialdehyde reductase (**Figure 4**, pathway 1). The conversion of glycolate to glyoxylate in the chloroplast was achieved by expressing a bacterial glycolate dehydrogenase (GlycDH). When expressed in Arabidopsis chloroplasts, transgenic lines produced bigger rosettes and more biomass while increasing A_{max} (Kebeish et al., 2007). A similar strategy was used to increase biomass and seed yield in *Camelina sativa* (Dalal et al., 2015). Bacterial GlycDH alone was introduced into *Solanum tuberosum* using a single construct to produce a polyprotein to circumvent instability problems (Nölke et al., 2014). These potato lines exhibited an enhanced A_{max} at 400 ppm CO_2 (but not when measured at 2000 ppm CO_2) and an increase in tuber yield even though the complete glycerate pathway had not been introduced (**Figure 4**, pathway 2). This was observed also for GlycDH-expressing Arabidopsis (Kebeish et al., 2007) and *Camelina sativa* (Dalal et al., 2015). Another successful photorespiratory bypass was achieved by expressing glycolate oxidase, catalase and malate synthase in chloroplasts (Maier et al., 2012). Such a bypass has the potential to completely oxidize glycolate to CO_2 and it led to increases in leaf dry weight and net CO_2 fixation rates (**Figure 4** pathway 3). More recently, another chloroplastic photorespiratory bypass (named the GOC bypass) was expressed in rice to increase photosynthetic efficiency (Shen et al., 2019). It consisted of three rice enzymes; glycolate oxidase, oxalate oxidase, and catalase expressed in chloroplasts and designed to lead to the complete oxidation of glycolate to CO_2 (**Figure 4** pathway 3). Improved photosynthetic efficiency, biomass, and yield were found in both greenhouse and field experiments although there were differences according to seeding season and it was more advantageous under high light. To improve flux through chloroplastic photorespiratory bypasses, glycolate export out of the chloroplast was manipulated by down-regulating PLGG1 (a plastidial glycolate/glycerate transporter, Pick et al., 2013; South et al., 2019). The best results were obtained with a variant of the glycolate oxidation pathway where glycolate oxidase was replaced by *Chlamydomonas reinhardtii* GlycDH (**Figure 4**, pathway 3). Field-grown tobacco expressing this version of an alternative photorespiratory pathway exhibited a >25% increase in total vegetative biomass (without PLGG1 inhibition) and a 40% increase (with inhibited PLGG1) although the impact on net CO_2 assimilation was quite low (5−8%) and no significant increase in seed yield was observed (South et al., 2019).

The over-expression of specific photorespiratory enzymes has also led to increased biomass, A_{max}, and grain yield. This was observed when mitochondrial serine hydroxymethyltransferase (SHMT1) was overexpressed in rice (Wu et al., 2015) and when individual glycine decarboxylase (GDC) subunits were overexpressed in Arabidopsis either the H-protein (Timm et al., 2012) or the L-protein (Timm et al., 2015; **Figure 4**). When the H-protein was overexpressed in tobacco, improved biomass was only observed when under the control of a leaf-specific promoter and this only became significant at high light intensities while constitutively overexpressed H-protein led to a detrimental growth effect (López-Calcagno et al., 2019). In gene stacking experiments, the additional overexpression of the H-protein in Arabidopsis lines overexpressing SBPase and FBPA led to further improvements in seed weight per plant (under high light growth conditions) and leaf area with no further increase in A_{max} compared to SBPase-FBPA lines alone (Simkin et al., 2017a).

Improved photosynthesis has also been found in plants where the light-side of photosynthesis has been manipulated. In Arabidopsis, the overexpression of the Rieske-FeS protein of the cytb_6f complex led to plants exhibiting increased A_{max}, dry weight, leaf area and seed yield (Simkin et al., 2017b). Photosynthesis was improved also under fluctuating light conditions by overexpressing violaxanthin de-epoxidase, zeaxanthin epoxidase and *PsbS*, all components of a photoprotection mechanism involving light energy dissipation as heat (Kromdijk et al., 2016). Field-grown tobacco plants overexpressing these three proteins showed increases in dry weight, leaf area and plant height (Kromdijk et al., 2016).

As mentioned above, certain strategies to improve photosynthesis and yield have already been tested under one or more climate change condition(s) such as elevated temperature and CO_2 levels. In general, increased temperatures of only several °C have been shown to cancel the beneficial effects of elevated CO_2 (see Köhler et al., 2017). Multiple FACE experiments (carried out at around 600 ppm CO_2) have consistently shown that the increase in C3-crop yield in response to long-term elevated CO_2 conditions is 50% lower than predicted due to photosynthetic acclimation (see Ainsworth and Long, 2005; Kant et al., 2012). Many C3-plant species only exhibit

a small 15% increase in yield compared to a hypothetical 40% increase under predicted climate change CO_2 levels. This yield response to elevated CO_2 has been observed in both controlled growth conditions and FACE experiments (see Leakey et al., 2009 and references therein) where a significant reduction in N-content was also reported (Ainsworth and Long, 2005; Vicente et al., 2015). This underachievement of certain C3 model plants like *Arabidopsis thaliana* and major C3-cereal plants including wheat and rice to elevated CO_2 is due to modifications in plant metabolism, physiology, and development where acclimation is associated with a negative impact on leaf photosynthesis (Ainsworth and Rogers, 2007), root nitrate uptake and leaf nitrate assimilation (Rachmilevitch et al., 2004; Bloom et al., 2010), thus reducing the expected benefits of elevated CO_2. It includes a reduction in RuBisCO protein content, a reduction in stomatal conductance, and decreases in both photosynthetic and N-assimilation gene expression (e.g., Vicente et al., 2015) that brings about a reduction in leaf and seed N-content. In the literature, photosynthetic acclimation to elevated CO_2 has been explained by the inhibition of photosynthetic gene expression due to the accumulation of excess non-structural carbohydrates in source leaves (Moore et al., 1999; Ruiz-Vera et al., 2017). However, it is possible that this acclimation is also driven by N-limitations when N-assimilation cannot keep up with the increased C-assimilation rates. It has also been suggested that at elevated CO_2, a decrease in photorespiration impacts negatively both nitrate uptake and assimilation (Bloom, 2015). Several factors have been proposed to influence acclimation to elevated CO_2, such as sink strength, sugar signaling, and N-regime (see Long et al., 2004 and references therein). Several papers have suggested a link between improved sink strength and a reduction of this acclimation in tobacco (Ruiz-Vera et al., 2017), rice (Zhu et al., 2014), barley (Torralbo et al., 2019), and *Larrea tridentata* (Aranjuelo et al., 2011). Although a number of actors in sugar signaling and sensing are known (see Pego et al., 2000), a lack of information on how they are affected by elevated CO_2, especially in roots, has been stated (Thompson et al., 2017). This is similar to nitrate-signaling where actors of perception, signal transduction and even root to shoot communication have been discovered (see Wang et al., 2018) but little is known about how elevated CO_2 and other climate change factors affect such processes. Indeed, to date, there is no global understanding of the regulatory networks involved in the acclimation processes occurring to balance plant C and N metabolism under elevated CO_2. That said, a recent work using correlation network analyses confirmed the tight coordination between C and N metabolisms while carbohydrate levels were linked to the down-regulation of both photosynthetic and N metabolism genes (Vicente et al., 2018).

When light is saturating, photosynthesis can be limited by several factors including V_{cmax} (amount and maximal carboxylase activity of RuBisCO), RuBP regeneration, triose-phosphate utilization/carbohydrate export (source-sink properties) and, of course, photorespiration. Under future climate conditions of elevated CO_2 and temperature, major limitations will probably shift to RuBP regeneration and source-sink properties. Under elevated CO_2, plants reduce RuBisCO amounts since it is no longer a limiting factor but they need to improve their photosynthetic electron transport properties to produce enough NADPH and ATP to regenerate RuBP via the Calvin cycle. Less RuBisCO is a common feature of elevated CO_2 acclimation in C3-cereals while N reallocations to improve the light reactions are not adequate and there is an overall reduction in plant N-content.

Predicted climate change conditions of elevated CO_2 and temperature have been shown to affect the benefits of improved photosynthesis by current genetic manipulations, as mentioned above (Rosenthal et al., 2011; Köhler et al., 2017). That said, strategies used to improve RuBP regeneration have often given rise to the best increases in photosynthesis and yields under either elevated CO_2 or high light or both (see above). However, strategies to reduce the negative impact of photorespiratory carbon recycling might be expected to have a lesser impact under conditions that lower photorespiration like elevated CO_2 although benefits may still occur under elevated temperatures and high light in association with CO_2. It is probable that C3-plant acclimation to future atmospheric CO_2 and temperature levels could hamper strategies to improve photosynthesis and yield of actual plant genotypes. Therefore, perhaps additional strategies to reduce C3-plant acclimation by deregulating plant functions associated with known acclimation processes might be required. This would require extensive omics analyses to identify the regulating gene networks and proteins involved in photosynthetic acclimation to climate change conditions, this could be helped by photosynthetic performance measurements in the field using non-destructive HTP techniques and platforms while the data sets could be used to improve plant growth models to predict the benefits. In this way, the best gene targets will be identified and tested to create new crops for the future.

AUTHOR CONTRIBUTIONS

MB and ÁS-S integrated the contributions. All authors read and approved the final version of the manuscript.

FUNDING

This work was supported by IRUEC project funded by EIG CONCERT-Japan 3rd Joint Call on "Food Crops and Biomass Production Technologies" under the Strategic International Research Cooperative Program of the Japan Science and Technology Agency (JST) and the Spanish Innovation and Universities Ministry (Acciones de programación conjunta Internacional, PCIN-2017-007), and by the ANR-14-CE19-0015 grant REGUL3P. A Grant for Promotion of KAAB Projects (Niigata University) from the Ministry of Education, Culture, Sports, Science, and Technology-Japan is also acknowledged.

ACKNOWLEDGMENTS

We apologize to all colleagues whose work was not referenced due to space constraints.

REFERENCES

Abdurakhmonov, I. Y., Buriev, Z. T., Saha, S., Jenkins, J. N., Abdukarimov, A., and Pepper, A. E. (2014). Phytochrome RNAi enhances major fibre quality and agronomic traits of the cotton *Gossypium hirsutum* L. *Nat. Commun.* 5:3062. doi: 10.1038/ncomms4062

Adachi, S., Nakae, T., Uchida, M., Soda, K., Takai, T., Oi, T., et al. (2013). The mesophyll anatomy enhancing CO2 diffusion is a key trait for improving rice photosynthesis. *J. Exp. Bot.* 64, 1061–1072. doi: 10.1093/jxb/ers382

Adachi, S., Tsuru, Y., Nito, N., Murata, K., Yamamoto, T., Ebitani, T., et al. (2011). Identification and characterization of genomic regions on chromosomes 4 and 8 that control the rate of photosynthesis in rice leaves. *J. Exp. Bot.* 62, 1927–1938. doi: 10.1093/jxb/erq387

Adachi, S., Yamamoto, T., Nakae, T., Yamashita, M., Uchida, M., Karimata, R., et al. (2019). Genetic architecture of leaf photosynthesis in rice revealed by different types of reciprocal mapping populations. *J. Exp. Bot.* 70, 5131–5144. doi: 10.1093/jxb/erz303

Adachi, S., Yoshikawa, K., Yamanouchi, U., Tanabata, T., Sun, J., Ookawa, T., et al. (2017). Fine mapping of Carbon Assimilation Rate 8, a quantitative trait locus for flag leaf nitrogen content, stomatal conductance and photosynthesis in rice. *Front. Plant Sci.* 8:60. doi: 10.3389/fpls.2017.00060

Ainsworth, E. A., and Long, S. P. (2005). What have we learned from 15 years of free-air CO2 enrichment (FACE)? A meta-analytic review of the responses of photosynthesis, canopy properties and plant production to rising CO2. *New Phytol.* 165, 351–372. doi: 10.1111/j.1469-8137.2004.01224.x

Ainsworth, E. A., and Rogers, A. (2007). The response of photosynthesis and stomatal conductance to rising [CO2]: mechanisms and environmental interactions. *Plant Cell Environ.* 30, 258–270. doi: 10.1111/j.1365-3040.2007.01641.x

Ainsworth, E. A., Rogers, A., Nelson, R., and Long, S. P. (2004). Testing the "source–sink" hypothesis of down-regulation of photosynthesis in elevated [CO2] in the field with single gene substitutions in *Glycine max*. *Agric. Forest Meteor.* 122, 85–94. doi: 10.1016/j.agrformet.2003.09.002

Ainsworth, E. A., Serbin, S. P., Skoneczka, J. A., and Townsend, P. A. (2014). Using leaf optical properties to detect ozone effects on foliar biochemistry. *Photosynth. Res.* 119, 65–76. doi: 10.1007/s11120-013-9837-y

Ainsworth, E. A., Yendrek, C. R., Sitch, S., Collins, W. J., and Emberson, L. D. (2013). The effects of tropospheric ozone on net primary productivity and implications for climate change. *Annu. Rev. Plant Biol.* 63, 637–661. doi: 10.1146/annurev-arplant-042110-103829

Alonso, L., Gomez-Chova, L., Vila-Frances, J., Amoros-Lopez, J., Guanter, L., Calpe, J., et al. (2008). Improved fraunhofer line discrimination method for vegetation fluorescence quantification. *IEEE Geosci. Remote Sens. Lett.* 5, 620–624. doi: 10.1109/lgrs.2008.2001180

Ameztoy, K., Baslam, M., Sánchez-López, ÁM., Muñoz, F. J., Bahaji, A., Almagro, G., et al. (2019). Plant responses to fungal volatiles involve global posttranslational thiol redox proteome changes that affect photosynthesis. *Plant. Cell Environ.* 42:13601. doi: 10.1111/pce.13601

Andrade-Sanchez, P., Gore, M. A., Heun, J. T., Thorp, K. R., Carmo-Silva, A. E., French, A. N., et al. (2014). Development and evaluation of a field-based high-throughput phenotyping platform. *Funct. Plant Biol.* 41, 68–79.

Ansong, C., Sadler, N. C., Hill, E. A., Lewis, M. P., Zink, E. M., Smith, R. D., et al. (2014). Characterization of protein redox dynamics induced during light-to-dark transitions and nutrient limitation in cyanobacteria. *Front. Microbiol.* 5:325. doi: 10.3389/fmicb.2014.00325

Aranjuelo, I., Ebbets, A. L., Evans, R. D., Tissue, D. T., Nogués, S., van Gestel, N., et al. (2011). Maintenance of C sinks sustains enhanced C assimilation during long-term exposure to elevated [CO2] in Mojave Desert shrubs. *Oecologia* 167, 339–354. doi: 10.1007/s00442-011-1996-y

Aranjuelo, I., Pardo, A., Biel, C., Savé, R., Azcón-Bieto, J., and Nogués, S. (2009). Leaf carbon management in slow-growing plants exposed to elevated CO2. *Glob. Change Biol.* 15, 97–109. doi: 10.1111/j.1365-2486.2008.01829.x

Aranjuelo, I., Sanz-Saez, A., Jauregui, I., Irigoyen, J. J., Araus, J. L., Sanchez- Diaz, M., et al. (2013). Harvest index, a parameter conditioning responsiveness of wheat plants to elevated CO2. *J. Exp. Bot.* 64, 1879–1892. doi: 10.1093/jxb/ert081

Araus, J. L., and Cairns, J. E. (2014). Field high-throughput phenotyping: the new crop breeding frontier. *Trends Plant Sci.* 19, 52–61. doi: 10.1016/j.tplants.2013.09.008

Araus, J. L., Kefauver, S. C., Zaman-Allah, M., Olsen, M. S., and Cairns, J. E. (2018). Translating high-throughput phenotyping into genetic gain. *Trends Plant Sci.* 23, 451–466. doi: 10.1016/j.tplants.2018.02.001

Arfan, M., Athar, H. R., and Ashraf, M. (2007). Does exogenous application of salicylic acid through the rooting medium modulate growth and photosynthetic capacity in two differently adapted spring wheat cultivars under salt stress? *J. Plant Physiol.* 164, 685–694. doi: 10.1016/J.JPLPH.2006.05.010

Aro, E.-M., Suorsa, M., Rokka, A., Allahverdiyeva, Y., Paakkarinen, V., Saleem, A., et al. (2004). Dynamics of photosystem II: a proteomic approach to thylakoid protein complexes. *J. Exp. Bot.* 56, 347–356. doi: 10.1093/jxb/eri041

Asner, G. P., and Martin, R. E. (2008). Spectral and chemical analysis of tropical forests: Scaling from leaf to canopy levels. *Remote Sens. Environ.* 112, 3958–3970. doi: 10.1016/j.rse.2008.07.003

Asner, G. P., and Martin, R. E. (2015). Spectroscopic remote sensing of nonstructural carbohydrates in forest canopies. *Remote Sens.* 7, 3526–3547. doi: 10.3390/rs70403526

Asner, G. P., Martin, R. E., Knapp, D. E., Tupayachi, R., Anderson, C., Carranza, L., et al. (2011). Spectroscopy of canopy chemicals in humid tropical forests. *Remote Sens. Environ.* 115, 3587–3598. doi: 10.1016/j.rse.2011.08.020

Asseng, S., Ewert, F., Rosenzweig, C., Jones, J. W., Hatfield, J. L., Ruane, A., et al. (2013). Uncertainty in simulating wheat yields under climate change. *Nat. Climate Change* 3, 827–832.

Asseng, S., Martre, P., Maiorano, A., Rötter, R. P., O'Leary, G. J., Fitzgerald, G. J., et al. (2019). Climate change impact and adaptation for wheat protein. *Glob. Chang Biol.* 25, 155–173. doi: 10.1111/gcb.14481

Avenson, T. J., and Saathoff, A. J. (2018). *Sub-Saturating Multiphase Flash Irradiances to Estimate Maximum Fluorescence Yield Photosynthesis*. Cham: Springer, 105–120.

Azam, F., Chang, X., and Jing, R. (2015). Mapping QTL for chlorophyll fluorescence kinetics parameters at seedling stage as indicators of heat tolerance in wheat. *Euphytica* 202, 245–258. doi: 10.1007/s10681-014-1283-1

Bacour, C., Maignan, F., MacBean, N., Porcar-Castell, A., Flexas, J., Frankenberg, C., et al. (2019). Improving estimates of gross primary productivity by assimilating solar-induced fluorescence satellite retrievals in a terrestrial biosphere model using a process-based SIF model. *J. Geophys. Res. Biogeosci.* 124, 3281–3306. doi: 10.1029/2019jg005040

Baena-González, E., Baginsky, S., Mulo, P., Summer, H., Aro, E. M., and Link, G. (2002). Chloroplast transcription at different light intensities. Glutathione-mediated phosphorylation at the major RNA polymerase involved in redox-regulated organellar gene expression. *Plant Physiol.* 127, 1044–1052. doi: 10.1104/pp.010168

Baginsky, S., Tiller, K., Pfannschmidt, T., and Link, G. (1999). PTK, the chloroplast RNA polymerase-associated protein kinase from mustard (*Sinapis alba*), mediates redox control of plastid in vitro transcription. *Plant Mol. Biol.* 39, 1013–1023. doi: 10.1023/a:1006177807844

Balcerowicz, M., Ranjan, A., Rupprecht, L., Fiene, G., and Hoecker, U. (2014). Auxin represses stomatal development in dark-grown seedlings via Aux/IAA proteins. *Development* 141, 3165–3176. doi: 10.1242/dev.109181

Bandillo, N., Raghavan, C., Muyco, P. A., Sevilla, M. A. L., Lobina, I. T., Dilla-Ermita, C. J., et al. (2013). Multi-parent advanced generation inter-cross (MAGIC) populations in rice: progress and potential for genetics research and breeding. *Rice* 6:11. doi: 10.1186/1939-8433-6-11

Barabaschi, D., Tondelli, A., Desiderio, F., Volante, A., Vaccino, P., Valè, G., et al. (2016). Next generation breeding. *Plant Sci.* 242, 3–13. doi: 10.1016/J.PLANTSCI.2015.07.010

Baslam, M., Oikawa, K., Kitajima-Koga, A., Kaneko, K., and Mitsui, T. (2016). Golgi-to-plastid trafficking of proteins through secretory pathway: insights into vesicle-mediated import toward the plastids. *Plant Signal. Behav.* 11:e1221558. doi: 10.1080/15592324.2016.1221558

Bassu, S., Brisson, N., Durand, J.-L., Boote, K., Lizaso, J., Jones, J. W., et al. (2014). How do various maize crop models vary in their responses to climate change factors? *Glob. Change Biol.* 20, 2301–2320. doi: 10.1111/gcb.12520

Bastakis, E., Hedtke, B., Klermund, C., Grimm, B., and Schwechheimer, C. (2018). LLM-domain B-GATA transcription factors play multifaceted roles in

controlling greening in *Arabidopsis*. *Plant Cell* 30, 582–599. doi: 10.1105/tpc.17.00947

Bedell, V. M., Wang, Y., Campbell, J. M., Poshusta, T. L., Starker, C. G., Krug, R. G., et al. (2012). In vivo genome editing using a high-efficiency TALEN system. *Nature* 491, 114–118. doi: 10.1038/nature11537

Belkhodja, R., Morales, F., Abadia, A., Gomez-Aparisi, J., and Abadia, J. (1994). Chlorophyll fluorescence as a possible tool for salinity tolerance screening in barley (*Hordeum-vulgare* L). *Plant Physiol.* 104, 667–673. doi: 10.1104/pp.104.2.667

Bernacchi, C. J., Morgan, P. B., Ort, D. R., and Long, S. P. (2005). The growth of soybean under free air [CO2] enrichment (FACE) stimulates photosynthesis while decreasing in vivo RuBisCO capacity. *Planta* 220, 434–446. doi: 10.1007/s00425-004-1320-8

Bernacchi, C. J., Pimentel, C., and Long, S. P. (2003). In vivo temperature response functions of parameters required to model RuBP-limited photosynthesis. *Plant Cell Environ.* 26, 1419–1430. doi: 10.1046/j.0016-8025.2003.01050.x

Betti, M., Bauwe, H., Busch, F. A., Fernie, A. R., Keech, O., Levey, M., et al. (2016). Manipulating photorespiration to increase plant productivity: recent advances and perspectives for crop improvement. *J. Exp. Bot.* 67, 2977–2988. doi: 10.1093/jxb/erw076pmid:26951371

Bevan, M. W., Uauy, C., Wulff, B. B. H., Zhou, J., Krasileva, K., and Clark, M. D. (2017). Genomic innovation for crop improvement. *Nature* 543, 346–354.

Bierbaum, R. M., Holdren, J. P., MacCracken, M. C., Moss, R. H., and Raven, P. H. (2007). *Confronting Climate Change: Avoiding the Unmanageable and Managing the Unavoidable*. Washington, DC: The United Nations Foundation.

Biernath, C., Bittner, S., Klein, C., Gayler, S., Hentschel, R., Hoffmann, P., et al. (2013). Modeling acclimation of leaf photosynthesis to atmospheric CO2 enrichment. *Eur. J. Agron.* 48, 74–87. doi: 10.1016/j.eja.2013.02.008

Bloom, A. J. (2015). Photorespiration and nitrate assimilation: a major intersection between plant carbon and nitrogen. *Photosynth. Res.* 123, 117–128. doi: 10.1007/s11120-014-0056-y

Bloom, A. J., Burger, M., Rubio Asensio, J. S., and Cousins, A. B. (2010). Carbon dioxide enrichment inhibits nitrate assimilation in wheat and *Arabidopsis*. *Science* 328, 899–903. doi: 10.1126/science.1186440

Bracher, A., Whitney, S. M., Hartl, F. U., and Hayer-Hartl, M. (2017). Biogenesis and metabolic maintenance of RuBisCO. *Annu. Rev. Plant Biol.* 68, 29–60. doi: 10.1146/annurev-arplant-043015-111633

Brenner, W. G., Ramireddy, E., Heyl, A., and Schmülling, T. (2012). Gene regulation by cytokinin in *Arabidopsis*. *Front. Plant Sci.* 3:8. doi: 10.3389/fpls.2012.00008

Cabrera-Bosquet, L., Sanchez, C., Rosales, A., Palacios-Rojas, N., and Araus, J. L. (2011). Near-infrared reflectance spectroscopy (NIRS) assessment of δ18O and nitrogen and ash contents for improved yield potential and drought adaptation in maize. *J. Agric. Food Chem.* 59, 467–474. doi: 10.1021/jf103395z

Cantalapiedra, C. P., Boudiar, R., Casas, A. M., Igartua, E., and Contreras-Moreira, B. (2015). BARLEY MAP: physical and genetic mapping of nucleotide sequences and annotation of surrounding loci in barley. *Mol. Breed.* 35:253.

Carter, G., Theisen, A., and Mitchell, R. (1990). Chlorophyll fluorescence measured using the Fraunhofer line-depth principle and relationship to photosynthetic rate in the field. *Plant Cell Environ.* 13, 79–83. doi: 10.1111/j.1365-3040.1990.tb01302.x

Casson, S. A., Franklin, K. A., Gray, J. E., Grierson, C. S., Whitelam, G. C., and Hetherington, A. M. (2009). phytochrome B and PIF4 regulate stomatal development in response to light quantity. *Curr. Biol.* 19, 229–234. doi: 10.1016/J.CUB.2008.12.046

Cavanagh, C., Morell, M., Mackay, I., and Powell, W. (2008). From mutations to MAGIC: resources for gene discovery, validation and delivery in crop plants. *Curr. Opin. Plant Biol.* 11, 215–221. doi: 10.1016/j.pbi.2008.01.002

Černý, M., Dyčka, F., Bobáľová, J., and Brzobohatý, B. (2011). Early cytokinin response proteins and phosphoproteins of *Arabidopsis thaliana* identified by proteome and phosphoproteome profiling. *J. Exp. Bot.* 62, 921–937. doi: 10.1093/jxb/erq322

Ceusters, J., and Van de Poel, B. (2018). Ethylene exerts species-specific and age-dependent control of photosynthesis. *Plant Physiol.* 176, 2601–2612. doi: 10.1104/pp.17.01706

Chaerle, L., Hagenbeek, D., De Bruyne, E., Valcke, R., and Van Der Straeten, D. (2004). Thermal and chlorophyll-fluorescence imaging distinguish plant-pathogen interactions at an early stage. *Plant Cell Physiol.* 45, 887–896. doi: 10.1093/pcp/pch097

Chaerle, L., Hagenbeek, D., De Bruyne, E., and Van Der Straeten, D. (2007). Chlorophyll fluorescence imaging for disease-resistance screening of sugar beet. *Plant Cell Tissue Organ Cult.* 91, 97–106. doi: 10.1007/s11240-007-9282-9288

Chater, C., Peng, K., Movahedi, M., Dunn, J. A., Walker, H. J., Liang, Y.-K., et al. (2015). Elevated CO2-induced responses in stomata require ABA and ABA signaling. *Curr. Biol.* 25, 2709–2716. doi: 10.1016/J.CUB.2015.09.013

Chen, J., Burke, J. J., Velten, J., and Xin, Z. (2006). FtsH11 protease plays a critical role in *Arabidopsis* thermotolerance. *Plant J.* 48, 73–84. doi: 10.1111/j.1365-313X.2006.02855.x

Cheng, F., Lu, J., Gao, M., Shi, K., Kong, Q., Huang, Y., et al. (2016). Redox signaling and CBF-responsive pathway are involved in salicylic acid-improved photosynthesis and growth under chilling stress in watermelon. *Front. Plant Sci.* 7:1519. doi: 10.3389/fpls.2016.01519

Chiang, Y.-H., Zubo, Y. O., Tapken, W., Kim, H. J., Lavanway, A. M., Howard, L., et al. (2012). Functional characterization of the GATA transcription factors GNC and CGA1 reveals their key role in chloroplast development, growth, and division in *Arabidopsis*. *Plant Physiol.* 160, 332–348. doi: 10.1104/pp.112.198705

Chinnusamy, V., Ohta, M., Kanrar, S., Lee, B.-H., Hong, X., Agarwal, M., et al. (2003). ICE1: a regulator of cold-induced transcriptome and freezing tolerance in *Arabidopsis*. *Genes Dev.* 17, 1043–1054. doi: 10.1101/gad.1077503

Choquette, N. E., Ogut, F., Wertin, T. M., Montes, C. M., Sorgini, C. A., Morse, A. M., et al. (2019). Uncovering hidden genetic variation in photosynthesis of field-grown maize under ozone pollution. *Glob. Change Biol.* 25, 4327–4338. doi: 10.1111/gcb.14794

Clarke, S. M., Cristescu, S. M., Miersch, O., Harren, F. J. M., Wasternack, C., and Mur, L. A. J. (2009). Jasmonates act with salicylic acid to confer basal thermotolerance in *Arabidopsis thaliana*. *New Phytol.* 182, 175–187. doi: 10.1111/j.1469-8137.2008.02735.x

Coast, A., Shah, S., Ivakov, A., Gaju, O., Wilson, P. B., Posch, B. C., et al. (2019). Predicting dark respiration rates of wheat leaves from hyperspectral reflectance. *Plant Cell Environ.* 42, 2133–2150. doi: 10.1111/pce.13544

Cobb, J. N., Biswas, P. S., and Platten, J. D. (2018). Back to the future: revisiting MAS as a tool for modern plant breeding. *Theor. Appl. Genet.* 132, 647–667. doi: 10.1007/s00122-018-3266-4

Cong, L., Ran, F. A., Cox, D., Lin, S., Barretto, R., Habib, N., et al. (2013). Multiplex genome engineering using CRISPR/Cas systems. *Science* 15, 819–823.

Cortleven, A., Nitschke, S., Klaumuenzer, M., AbdElgawad, H., Asard, H., Grimm, B., et al. (2014). A novel protective function for cytokinin in the light stress response is mediated by the *Arabidopsis* histidine kinase2 and *Arabidopsis* histidine kinase3 receptors. *Plant Physiol.* 164, 1470–1483. doi: 10.1104/pp.113.224667

Cortleven, A., and Schmülling, T. (2015). Regulation of chloroplast development and function by cytokinin. *J. Exp. Bot.* 66, 4999–5013. doi: 10.1093/jxb/erv132

Crossa, J., Pérez-Rodríguez, P., Cuevas, J., Montesinos-López, O., Jarquín, D., de Los Campos, G., et al. (2017). Genomic selection in plant breeding: methods, models, and perspectives. *Trends Plant Sci.* 22, 961–975.

Cullen, B. R., Johnson, I. R., Eckard, R. J., Lodge, G. M., Walker, R. G., Rawnsley, R. P., et al. (2009). Climate change effects on pasture systems in south-eastern Australia. *Crop Pasture Sci.* 60, 933–942.

Curran, P. J. (1989). Remote sensing of foliar chemistry. *Remote Sens. Environ.* 30, 271–278. doi: 10.1016/0034-4257(89)90069-2

Dahal, K., Gadapati, W., Savitch, L. V., Singh, J., and Hüner, N. P. (2012). Cold acclimation and BnCBF17-over-expression enhance photosynthetic performance and energy conversion efficiency during long-term growth of *Brassica napus* under elevated CO2 conditions. *Planta* 236, 1639–1652. doi: 10.1007/s00425-012-1710-2

Dahal, K., and Vanlerberghe, G. C. (2017). Alternative oxidase respiration maintains both mitochondrial and chloroplast function during drought. *New Phytol.* 213, 560–571. doi: 10.1111/nph.14169

Dahal, K., and Vanlerberghe, G. C. (2018). Growth at elevated CO2 requires acclimation of the respiratory chain to support photosynthesis. *Plant Physiol.* 178, 82–100. doi: 10.1104/pp.18.00712

Dahal, K., Wang, J., Martyn, G. D., Rahimy, F., and Vanlerberghe, G. C. (2014). Mitochondrial alternative oxidase maintains respiration and preserves photosynthetic capacity during moderate drought in *Nicotiana tabacum*. *Plant Physiol.* 166, 1560–1574. doi: 10.1104/pp.114.247866

Dalal, J., Lopez, H., Vasani, N. B., Hu, Z., Swift, J. E., Yalamanchili, R., et al. (2015). A photorespiratory bypass increases plant growth and seed yield in biofuel crop *Camelina sativa*. *Biotechnol. Biofuels* 8:175. doi: 10.1186/s13068-015-0357-351

de Carvalho, M. H. C. (2008). Drought stress and reactive oxygen species. *Plant Signal. Behav.* 3, 156–165. doi: 10.4161/psb.3.3.5536

de Oliveira Silva, F. M., Lichtenstein, G., Alseekh, S., Rosado-Souza, L., Conte, M., Suguiyama, V. F., et al. (2018). The genetic architecture of photosynthesis and plant growth-related traits in tomato. *Plant. Cell Environ.* 41, 327–341. doi: 10.1111/pce.13084

Desikan, R., Hancock, J. T., Bright, J., Harrison, J., Weir, I., Hooley, R., et al. (2005). A role for ETR1 in hydrogen peroxide signaling in stomatal guard cells. *Plant Physiol.* 137, 831–834. doi: 10.1104/pp.104.056994

Dhanapal, A. P., Ray, J. D., Singh, S. K., Hoyos-Villegas, V., Smith, J. R., Purcell, L. C., et al. (2015). Genome-wide association analysis of diverse soybean genotypes reveals novel markers for Nitrogen derived from atmosphere (Ndfa), nitrogen concentration ([N]) and C/N ratio. *Plant Genome.* 8, 1–5.

Dietz, K. J., and Pfannschmidt, T. (2011). Novel regulators in photosynthetic redox control of plant metabolism and gene expression. *Plant Physiol.* 155, 1477–1485. doi: 10.1104/pp.110.170043

Ding, F., Wang, M., Zhang, S., and Ai, X. (2016). Changes in SBPase activity influence photosynthetic capacity, growth, and tolerance to chilling stress in transgenic tomato plants. *Sci. Rep.* 6, 1–14. doi: 10.1038/srep32741

Dittrich, M., Mueller, H. M., Bauer, H., Peirats-Llobet, M., Rodriguez, P. L., Geilfus, C.-M., et al. (2019). The role of *Arabidopsis* ABA receptors from the PYR/PYL/RCAR family in stomatal acclimation and closure signal integration. *Nat. Plants* 5, 1002–1011. doi: 10.1038/s41477-019-0490-490

Döring, F., Billakurthi, K., Gowik, U., Sultmanis, S., Khoshravesh, R., Das Gupta, S., et al. (2019). Reporter-based forward genetic screen to identify bundle sheath anatomy mutants in *A. thaliana*. *Plant J.* 97, 984–995. doi: 10.1111/tpj.14165

Dreccer, M. F., Barnesa, L. R., and Meder, R. (2014). carbohydrates in wheat can be monitored in the field using hyperspectral reflectance. *Field Crops Res.* 159, 70–80. doi: 10.1016/j.fcr.2014.01.001

Driever, S. M., Simkin, A. J., Alotaibi, S., Fisk, S. J., Madgwick, P. J., Sparks, C. A., et al. (2017). Increased sbpase activity improves photosynthesis and grain yield in wheat grown in greenhouse conditions. *Philos. Trans. R. Soc. B Biol. Sci.* 372:20160384. doi: 10.1098/rstb.2016.0384

Du, B., Liu, L., Wang, Q., Sun, G., Ren, X., Li, C., et al. (2019). Identification of QTL underlying the leaf length and area of different leaves in barley. *Sci. Rep.* 9:4431. doi: 10.1038/s41598-019-40703-40706

Dusenge, M. E., Duarte, A. G., and Way, D. A. (2019). Plant carbon metabolism and climate change: elevated CO2 and temperature impacts on photosynthesis, photorespiration and respiration. *New Phytol.* 221, 32–49. doi: 10.1111/nph.15283

Ehleringer, J. R., Sage, R. F., Flanagan, L. B., and Pearcy, R. W. (1991). Climate change and the evolution of C4 photosynthesis. *Trends Ecol. Evol.* 6, 95–99. doi: 10.1016/0169-5347(91)90183-x

Eisenhut, M., Bräutigam, A., Timm, S., Florian, A., Tohge, T., Fernie, A. R., et al. (2017). Photorespiration is crucial for dynamic response of photosynthetic metabolism and stomatal movement to altered CO2 availability. *Mol. Plant.* 10, 47–61. doi: 10.1016/j.molp.2016.09.011

Ermakova, M., Lopez-Calgagno, P. E., Raines, C. A., Furbank, R. T., and von Caemmerer, S. (2019). Overexpression of the Rieske FeS protein of the Cytochrome b6f complex increases C4 photosynthesis in *Setaria viridis*. *Commun. Biol.* 2:314.doi: 10.1038/s42003-019-0561-569

Evain, S., Flexas, J., and Moya, I. (2004). A new instrument for passive remote sensing: 2. Measurement of leaf and canopy reflectance changes at 531 nm and their relationship with photosynthesis and chlorophyll fluorescence. *Remote Sens. Environ.* 91, 175–185. doi: 10.1016/j.rse.2004.03.012

Fahlgren, N., Feldman, M., Gehan, M. A., Wilson, M. S., Shyu, C., Bryant, D. W., et al. (2015). A versatile phenotyping system and analytics platform reveals diverse temporal responses to water availability in Setaria. *Mol. Plant* 8, 1520–1535. doi: 10.1016/j.molp.2015.06.005

FAO (2009). *Feeding the World in 2050. World Agricultural Summit on Food Security*. Rome: FAO.

Farquhar, G. D., von Caemmerer, S., and Berry, J. A. (1980). A biochemical model of photosynthetic CO2 assimilation in leaves of C3 species. *Planta* 149, 78–90. doi: 10.1007/bf00386231

Feng, Z., Mao, Y., Xu, N., Zhang, B., Wei, P., Yang, D. L., et al. (2014). Multi-generation analysis reveals the inheritance, specificity, and patterns of CRISPR/Cas-induced gene modifications in *Arabidopsis*. *Proc. Natl. Acad. Sci. U.S.A.* 111, 4632–4637. doi: 10.1073/pnas.1400822111

Fiedler, K., Bekele, W. A., Matschegewski, C., Snowdon, R., Wieckhorst, S., Zacharias, A., et al. (2016). Cold tolerance during juvenile development in sorghum: a comparative analysis by genome-wide association and linkage mapping. *Plant Breed.* 135, 598–606. doi: 10.1111/pbr.12394

Fleisher, D. H., Condori, B., Quiroz, R., Alva, A., Asseng, S., Barreda, C., et al. (2017). A potato model inter-comparison across varying climates and productivity levels. *Glob. Change Biol.* 23, 1258–1281. doi: 10.1111/gcb.13411

Flexas, J., Escalona, J. M., Evain, S., Gulías, J., Moya, I., Osmond, C. B., et al. (2002). Steady-state chlorophyll fluorescence (Fs) measurements as a tool to follow variations of net CO2 assimilation and stomatal conductance during water-stress in C3 plants. *Physiol. Plant.* 114, 231–240. doi: 10.1034/j.1399-3054.2002.1140209.x

Flood, P. J., Harbinson, J., and Aarts, M. G. M. (2011). Natural genetic variation in plant photosynthesis. *Trends Plant Sci.* 16, 327–335. doi: 10.1016/j.tplants.2011.02.005

Flugel, F., Timm, S., Arrivault, S., Florian, A., Stitt, M., Fernie, A. R., et al. (2017). The photorespiratory metabolite 2-phosphoglycolate regulates photosynthesis and starch accumulation in *Arabidopsis*. *Plant Cell* 29, 2537–2551. doi: 10.1105/tpc.17.00256

Foyer, C. H., Neukermans, J., Queval, G., Noctor, G., and Harbinson, J. (2012). Photosynthetic control of electron transport and the regulation of gene expression. *J. Exp. Bot.* 63, 1637–1661. doi: 10.1093/jxb/ers013

Fracheboud, Y., Haldimann, P., Leipner, J., and Stamp, P. (1999). Chlorophyll fluorescence as a selection tool for cold tolerance of photosynthesis in maize (*Zea mays* L.). *J. Exp. Bot.* 50, 1533–1540. doi: 10.1093/jexbot/50.338.1533

Fracheboud, Y., Ribaut, J. M., Vargas, M., Messmer, R., and Stamp, P. (2002). Identification of quantitative trait loci for cold-tolerance of photosynthesis in maize (*Zea mays* L.). *J. Exp. Bot.* 53, 1967–1977. doi: 10.1093/jxb/erf040

Franklin, K. A., and Whitelam, G. C. (2007). Light-quality regulation of freezing tolerance in *Arabidopsis thaliana*. *Nat. Genet.* 39, 1410–1413. doi: 10.1038/ng.2007.3

Friso, G., Giacomelli, L., Ytterberg, A. J., Peltier, J.-B., Rudella, A., Sun, Q., et al. (2004). In-depth analysis of the thylakoid membrane proteome of *Arabidopsis thaliana* chloroplasts: new proteins, new functions, and a plastid proteome database. *Plant Cell* 16, 478–499. doi: 10.1105/tpc.017814

Gehan, M. A., Park, S., Gilmour, S. J., An, C., Lee, C.-M., and Thomashow, M. F. (2015). Natural variation in the C-repeat binding factor cold response pathway correlates with local adaptation of *Arabidopsis* ecotypes. *Plant J.* 84, 682–693. doi: 10.1111/tpj.13027

Goudriaan, J. (1986). A simple and fast numerical method for the computation of daily totals of crop photosynthesis. *Agric. For. Meteorol.* 38, 249–254. doi: 10.1016/0168-1923(86)90063-8

Goudriaan, J., and van Laar, H. H. (1994). *Modelling Potential Crop Growth Processes - Textbook with Exercises. Current Issues in Production Ecology 2*. Dordrecht: Kluwer Academic Publishers.

Gray, J. E., Holroyd, G. H., van der Lee, F. M., Bahrami, A. R., Sijmons, P. C., Woodward, F. I., et al. (2000). The HIC signalling pathway links CO2 perception to stomatal development. *Nature* 408, 713–716. doi: 10.1038/35047071

Gray, S. B., Dermody, O., Klein, S. P., Locke, A. M., McGrath, J. M., Paul, R. E., et al. (2016). Intensifying drought eliminates the expected benefits of elevated carbon dioxide for soybean. *Nat. Plants* 2:16132. doi: 10.1038/nplants.2016.132

Grbic, V., and Bleecker, A. B. (1995). Ethylene regulates the timing of leaf senescence in *Arabidopsis*. *Plant J.* 8, 595–602. doi: 10.1046/j.1365-313X.1995.8040595.x

Grover, A., Mittal, D., Negi, M., and Lavania, D. (2013). Generating high temperature tolerant transgenic plants: achievements and challenges. *Plant Sci.* 205–206, 38–47. doi: 10.1016/J.PLANTSCI.2013.01.005

Gu, J., Yin, X., Struik, P. C., Stomph, T. J., and Wang, H. (2012). Using chromosome introgression lines to map quantitative trait loci for photosynthesis parameters

in rice (*Oryza sativa* L.) leaves under drought and well-watered field conditions. *J. Exp. Bot.* 63, 455–469. doi: 10.1093/jxb/err292

Gudesblat, G. E., Schneider-Pizoń, J., Betti, C., Mayerhofer, J., Vanhoutte, I., van Dongen, W., et al. (2012). SPEECHLESS integrates brassinosteroid and stomata signalling pathways. *Nat. Cell Biol.* 14, 548–554. doi: 10.1038/ncb2471

Guo, P., Baum, M., Varshney, R. K., Graner, A., Grando, S., and Ceccarelli, S. (2008). QTLs for chlorophyll and chlorophyll fluorescence parameters in barley under post-flowering drought. *Euphytica* 163, 203–214. doi: 10.1007/s10681-007-9629-6

Gupta, S. K., Sharma, S., Santisree, P., Kilambi, H. V., Appenroth, K., Sreelakshmi, Y., et al. (2014). Complex and shifting interactions of phytochromes regulate fruit development in tomato. *Plant. Cell Environ.* 37, 1688–1702. doi: 10.1111/pce.12279

Gururani, M. A., Ganesan, M., and Song, P.-S. (2015). Photo-biotechnology as a tool to improve agronomic traits in crops. *Biotechnol. Adv.* 33, 53–63. doi: 10.1016/J.BIOTECHADV.2014.12.005

Hahn, F., Mantegazza, O., Greiner, A., Hegemann, P., Eisenhut, M., and Weber, A. P. M. (2017). An efficient visual screen for CRISPR/Cas9 activity in *Arabidopsis thaliana*. *Front. Plant Sci.* 08:39. doi: 10.3389/fpls.2017.00039

Hall, M., Mata-Cabana, A., Åkerlund, H.-E., Florencio, F. J., Schröder, W., Lindahl, M., et al. (2010). Thioredoxin targets of the plant chloroplast lumen and their implications for plastid function. *Proteomics* 10, 987–1001. doi: 10.1002/pmic.200900654

Hanson, A. D., Amthor, J. S., Sun, J., Niehaus, T. D., Gregory, J. F., Bruner, S. D., et al. (2018). Redesigning thiamin synthesis: prospects and potential payoffs. *Plant Sci.* 273, 92–99. doi: 10.1016/J.PLANTSCI.2018.01.019

Hara, K., Kajita, R., Torii, K. U., Bergmann, D. C., and Kakimoto, T. (2007). The secretory peptide gene EPF1 enforces the stomatal one-cell-spacing rule. *Genes Dev.* 21, 1720–1725. doi: 10.1101/gad.1550707

Harley, P. C., Loreto, F., Di Marco, G., and Sharkey, T. D. (1992). Theoretical considerations when estimating the mesophyll conductance to CO2 flux by analysis of the response of photosynthesis to CO2. *Plant Phys.* 98, 1429–1436. doi: 10.1104/pp.98.4.1429

Hedrich, R., and Geiger, D. (2017). Biology of SLAC1-type anion channels - from nutrient uptake to stomatal closure. *New Phytol.* 216, 46–61. doi: 10.1111/nph.14685

Herritt, M., Dhanapal, A. P., Purcell, L. C., and Fritschi, F. B. (2018). Identification of genomic loci associated with 21chlorophyll fluorescence phenotypes by genome-wide association analysis in soybean. *BMC Plant Biol.* 18:312. doi: 10.1186/s12870-018-1517-1519

Hikosaka, K. (2010). Mechanisms underlying interspecific variation in photosynthetic capacityacross wild plant species. *Plant Biotech.* 27, 223–229. doi: 10.5511/plantbiotechnology.27.223

Hikosaka, K., Ishikawa, K., Borjigidai, A., Muller, O., and Onoda, Y. (2006). Temperature acclimation of photosynthesis: mechanisms involved in the changes in temperature dependence of photosynthetic rate. *J. Exp. Bot.* 57, 291–302. doi: 10.1093/jxb/erj049

Hiltscher, H., Rudnik, R., Shaikhali, J., Heiber, I., Mellenthin, M., Meirelles Duarte, I., et al. (2014). The radical induced cell death protein 1 (RCD1) supports transcriptional activation of genes for chloroplast antioxidant enzymes. *Front. Plant Sci.* 5:475. doi: 10.3389/fpls.2014.00475

Hirotsu, N., Ujiie, K., Perera, I., Iri, A., Kashiwagi, T., and Ishimaru, K. (2017). Partial loss-of-function of NAL1 alters canopy photosynthesis by changing the contribution of upper, and lower canopy leaves in rice. *Sci. Rep.* 7:15958. doi: 10.1038/s41598-017-15886-15885

Hsu, P. K., Takahashi, Y., Munemasa, S., Merilo, E., Laanemets, K., Waadt, R., et al. (2018). Abscisic acid-independent stomatal CO2 signal transduction pathway and convergence of CO2 and ABA signaling downstream of OST1 kinas. *Proc. Natl. Acad. Sci. U.S.A.* 115, E9971–E9980. doi: 10.1073/pnas.1809204115

Hu, X., Wu, L., Zhao, F., Zhang, D., Li, N., Zhu, G., et al. (2015). Phosphoproteomic analysis of the response of maize leaves to drought, heat and their combination stress. *Front. Plant Sci.* 6:298. doi: 10.3389/fpls.2015.00298

Huang, J., Taylor, J. P., Chen, J. G., Uhrig, J. F., Schnell, D. J., Nakagawa, T., et al. (2006). The plastid protein THYLAKOID FORMATION1 and the plasma membrane G-protein GPA1 interact in a novel sugar-signaling mechanism in *Arabidopsis*. *Plant Cell* 18, 1226–1238. doi: 10.1105/tpc.105.037259

Huang, X., and Han, B. (2014). Natural variations and genome-wide association studies in crop plants. *Annu. Rev. Plant Biol.* 65, 531–551. doi: 10.1146/annurev-arplant-050213-35715

Huang, X., Wei, X., Sang, T., Zhao, Q., Feng, Q., Zhao, Y., et al. (2010). Genome-wide association studies of 14 agronomic traits in rice landraces. *Nat. Genet.* 42, 961–967.

Huang, Z. A., Jiang, D. A., Yang, Y., Sun, J. W., and Jin, S. H. (2004). Effects of nitrogen deficiency on gas exchange, chlorophyll fluorescence, and antioxidant enzymes in leaves of rice plants. *Photosynthetica* 42, 357–364. doi: 10.1023/B:PHOT.0000046153.08935.4c

Hubbart, S., Peng, S., Horton, P., Chen, Y., and Murchie, E. H. (2007). Trends in leaf photosynthesis in historical rice varieties developed in the Philippines since 1966. *J. Exp. Bot.* 58, 3429–3438. doi: 10.1093/jxb/erm192

Hüner, N. P., Dahal, K., Kurepin, L. V., Savitch, L., Singh, J., Ivanov, A. G., et al. (2014). Potential for increased photosynthetic performance and crop productivity in response to climate change: role of CBFs and gibberellic acid. *Front. Chem.* 2:18. doi: 10.3389/fchem.2014.00018

Hunt, L., and Gray, J. E. (2009). The signaling peptide EPF2 controls asymmetric cell divisions during stomatal development. *Curr. Biol.* 19, 864–869. doi: 10.1016/J.CUB.2009.03.069

Huynh, L., Ehlers, J. D., Huang, B. E., Munoz-Amatriain, M., Lonardi, S., Santos, J. R. P., et al. (2018). A multi-parent advanced generation inter-cross (MAGIC) population for genetic analysis and improvement of cowpea (*Vigna unguiculata* L. Walp.). *Plant J.* 93, 1129–1142. doi: 10.1111/tpj.13827

Ichikawa, Y., Tamoi, M., Sakuyama, H., Maruta, T., Ashida, H., Yokota, A., et al. (2010). Generation of transplastomic lettuce with enhanced growth and high yield. *GM Crops* 1, 322–326. doi: 10.4161/gmcr.1.5.14706

Inomata, T., Baslam, M., Masui, T., Koshu, T., Takamatsu, T., Kaneko, K., et al. (2018). Proteomics analysis reveals non-controlled activation of photosynthesis and protein synthesis in a rice npp1 mutant under high temperature and elevated CO2 conditions. *Int. J. Mol. Sci.* 19:2655. doi: 10.3390/ijms19092655

Ishihara, H., Moraes, T. A., Pyl, E.-T., Schulze, W. X., Obata, T., Scheffel, A., et al. (2017). Growth rate correlates negatively with protein turnover in *Arabidopsis* accessions. *Plant J.* 91, 416–429. doi: 10.1111/tpj.13576

Ishimaru, K., Yano, M., Aoki, N., Ono, K., Hirose, T., Lin, S. Y., et al. (2001). Toward the mapping of physiological and agronomic characters on a rice function map: QTL analysis and comparison between QTLs and expressed sequence tags. *Theor. Appl. Genet.* 102, 793–800. doi: 10.1007/s001220000467

Izumi, M., and Nakamura, S. (2018). Chloroplast protein turnover: the influence of extraplastidic processes, including autophagy. *Int. J. Mol. Sci.* 19:828. doi: 10.3390/ijms19030828

Jimbo, H., Izuhara, T., Hihara, Y., Hisabori, T., and Nishiyama, Y. (2019). Light-inducible expression of translation factor EF-Tu during acclimation to strong light enhances the repair of photosystem II. *Proc. Natl. Acad. Sci. U.S.A.* 116, 21268–21273. doi: 10.1073/pnas.1909520116

Jun, T., Freewalt, K., Michel, A. P., Mian, R., and Singh, R. (2014). Identification of novel QTL for leaf traits in soybean. *Plant Breed.* 133, 61–66. doi: 10.1111/pbr.12107

Jung, H.-S., Crisp, P. A., Estavillo, G. M., Cole, B., Hong, F., Mockler, T. C., et al. (2013). Subset of heat-shock transcription factors required for the early response of *Arabidopsis* to excess light. *Proc. Natl. Acad. Sci. U.S.A.* 110, 14474–14479. doi: 10.1073/pnas.1311632110

Kanaoka, M. M., Pillitteri, L. J., Fujii, H., Yoshida, Y., Bogenschutz, N. L., Takabayashi, J., et al. (2008). SCREAM/ICE1 and SCREAM2 specify three cell-state transitional steps leading to *Arabidopsis* stomatal differentiation. *Plant Cell* 20:1775. doi: 10.1105/TPC.108.060848

Kanning, M., Kuhling, I., Trautz, D., and Jarmer, T. (2018). High-Resolution UAV-based hyperspectral imagery for LAI and chlorophyll estimations from wheat for yield prediction. *Remote Sens.* 10:2000. doi: 10.3390/rs10122000

Kant, S., Seneweera, S., Rodin, J., Materne, M., Burch, D., Rothstein, S. J., et al. (2012). Improving yield potential in crops under elevated CO2: integrating the photosynthetic and nitrogen utilization efficiencies. *Front. Plant Sci.* 3:162. doi: 10.3389/fpls.2012.00162

Karaba, A., Dixit, S., Greco, R., Aharoni, A., Trijatmiko, K. R., Marsch-Martinez, N., et al. (2007). Improvement of water use efficiency in rice by expression of HARDY, an *Arabidopsis* drought and salt tolerance gene. *Proc. Natl. Acad. Sci. U.S.A.* 104, 15270–15275. doi: 10.1073/pnas.0707294104

Kebeish, R., Niessen, M., Thiruveedhi, K., Bari, R., Hirsch, H. J., Rosenkranz, R., et al. (2007). Chloroplastic photorespiratory bypass increases photosynthesis and biomass production in *Arabidopsis thaliana*. *Nat. Biotechnol.* 25, 593–599. doi: 10.1038/nbt1299

Keller, B., Vass, I., Matsubara, S., Paul, K., Jedmowski, C., Pieruschka, R., et al. (2018). Maximum fluorescence and electron transport kinetics determined by light-induced fluorescence transients (LIFT) for photosynthesis phenotyping. *Photosynth. Res.* 140, 221–233. doi: 10.1007/s11120-018-0594-599

Kiani, S. P., Maury, P., Sarrafi, A., and Grieu, P. (2008). QTL analysis of chlorophyll fluorescence parameters in sunflower (*Helianthus annuus* L.) under well-watered and water-stressed conditions. *Plant Sci.* 175, 565–573. doi: 10.1016/j.plantsci.2008.06.002

Kim, G.-D., Cho, Y.-H., and Yoo, S.-D. (2017). Phytohormone ethylene-responsive *Arabidopsis* organ growth under light is in the fine regulation of Photosystem II deficiency-inducible AKIN10 expression. *Sci. Rep.* 7:2767. doi: 10.1038/s41598-017-02897-2895

Kim, T.-W., Michniewicz, M., Bergmann, D. C., and Wang, Z.-Y. (2012). Brassinosteroid regulates stomatal development by GSK3-mediated inhibition of a MAPK pathway. *Nature* 482, 419–422. doi: 10.1038/nature10794

Köhler, I. H., Ruiz-Vera, U. M., VanLoocke, A., Thomey, M. L., Clemente, T., Long, S. P., et al. (2017). Expression of cyanobacterial FBP/SBPase in soybean prevents yield depression under future climate conditions. *J. Exp. Bot.* 68, 715–726. doi: 10.1093/jxb/erw435

Kohzuma, K., Cruz, J. A., Akashi, K., Hoshiyasu, S., Munekage, Y. N., Yokota, A., et al. (2009). The long-term responses of the photosynthetic proton circuit to drought. *Plant Cell Environ.* 32, 209–219. doi: 10.1111/j.1365-3040.2008.01912.x

Kolber, Z. S., Prasil, O., and Falkowski, P. G. (1998). Measurements of variable chlorophyll fluorescence using fast repetition rate techniques: defining methodology and experimental protocols. *Biochim. Biophys. Acta Bioenerget.* 1367, 88–106. doi: 10.1016/S0005-2728(98)00135-132

Kong, F., Deng, Y., Wang, G., Wang, J., Liang, X., and Meng, Q. (2014). LeCDJ1, a chloroplast DnaJ protein, facilitates heat tolerance in transgenic tomatoes. *J. Integr. Plant Biol.* 56, 63–74. doi: 10.1111/jipb.12119

Krause, G. H., and Weis, E. (1984). Chlorophyll fluorescence as a tool in plant physiology. II. Interpretation of fluorescence signals. *Photosynth. Res.* 5, 139–157. doi: 10.1007/Bf00028527

Kromdijk, J., Głowacka, K., Leonelli, L., Gabilly, S. T., Iwai, M., Niyogi, K. K., et al. (2016). Improving photosynthesis and crop productivity by accelerating recovery from photoprotection. *Science* 354, 857–861. doi: 10.1126/science.aai8878

Kubis, A., and Bar-Even, A. (2019). Synthetic biology approaches for improving photosynthesis. *J. Exp. Bot.* 70, 1425–1433. doi: 10.1093/jxb/erz029

Kumar, B., Talukdar, A., Bala, I., Verma, K., Kumar-Lal, S., Sapra, R., et al. (2014). Population structure and association mapping studies for important agronomic traits in soybean. *J. Genet.* 93, 775—-784.

Kunihiro, A., Yamashino, T., Nakamichi, N., Niwa, Y., Nakanishi, H., and Mizuno, T. (2011). Phytochrome-interacting factor 4 and 5 (PIF4 and PIF5) activate the homeobox ATHB2 and auxin-inducible IAA29 genes in the coincidence mechanism underlying photoperiodic control of plant growth of *Arabidopsis thaliana*. *Plant Cell Physiol.* 52, 1315–1329. doi: 10.1093/pcp/pcr076

Kurepin, L. V., Dahal, K. P., Savitch, L. V., Singh, J., Bode, R., Ivanov, A. G., et al. (2013). Role of CBFs as integrators of chloroplast redox, phytochrome and plant hormone signaling during cold acclimation. *Int. J. Mol. Sci.* 14, 12729–12763. doi: 10.3390/ijms140612729

Larosa, V., Meneghesso, A., La Rocca, N., Steinbeck, J., Hippler, M., Szabò, I., et al. (2018). Mitochondria affect photosynthetic electron transport and photosensitivity in a green alga. *Plant Physiol.* 176, 2305–2314. doi: 10.1104/pp.17.01249

Le, J., Liu, X.-G., Yang, K.-Z., Chen, X.-L., Zou, J.-J., Wang, H.-Z., et al. (2014). Auxin transport and activity regulate stomatal patterning and development. *Nat. Commun.* 5:3090. doi: 10.1038/ncomms4090

Leakey, A. D. B., Ainsworth, E. A., Bernacchi, C. J., Rogers, A., Long, S. P., and Ort, D. R. (2009). Elevated CO2 effects on plant carbon, nitrogen, and water relations; six important lessons from FACE. *J. Exp. Bot.* 60, 2859–2876. doi: 10.1093/jxb/erp096

Leakey, A. D. B., Uribelarrea, M., Ainsworth, E. A., Naidu, S. L., Rogers, A., Ort, D. R., et al. (2006). Photosynthesis, productivity, and yield of maize are not affected by open-air elevation of CO2 concentration in the absence of drought. *Plant Physiol.* 140, 779–790. doi: 10.1104/pp.105.073957

Lefebvre, S., Lawson, T., Zakhleniuk, O. V., Lloyd, J. C., Raines, C. A., and Fryer, M. (2005). Increased sedoheptulose-1,7-bisphosphatase activity in transgenic tobacco plants stimulates photosynthesis and growth from an early stage in development. *Plant Physiol.* 138, 451–460. doi: 10.1104/pp.104.055046

Legris, M., Ince, Y. Ç, and Fankhauser, C. (2019). Molecular mechanisms underlying phytochrome-controlled morphogenesis in plants. *Nat. Commun.* 10:5219. doi: 10.1038/s41467-019-13045-0

Leng, G., and Hall, J. (2019). Crop yield sensitivity of global major agricultural countries to droughts and the projected changes in the future. *Sci. Total Environ.* 654, 811–821. doi: 10.1016/j.scitotenv.2018.10.434

Lepistö, A., and Rintamäki, E. (2012). Coordination of plastid and light signaling pathways upon development of *Arabidopsis* leaves under various photoperiods. *Mol. Plant.* 5, 799–816. doi: 10.1093/mp/ssr106

Lesk, C., Rowhani, P., and Ramankutty, N. (2016). Influence of extreme weather disasters on global crop production. *Nature* 529, 84–87. doi: 10.1038/nature16467

Leuning, R., Kelliher, F. M., De Pury, D. G. G., and Schultze, E.-D. (1995). Leaf nitrogen, photosynthesis, conductance and transpiration: scaling from leaves to canopies. *Plant Cell Environ.* 18, 1183–1200. doi: 10.1111/j.1365-3040.1995.tb00628.x

Li, F., Chen, B., Xu, K., Gao, G., Yan, G., Qiao, J., et al. (2015). A genome-wide association study of plant height and primary branch number in rapeseed (*Brassica napus*). *Plant Sci.* 242, 169–177. doi: 10.1016/j.plantsci.2015.05.012

Li, J., Nagpal, P., Vitart, V., McMorris, T. C., and Chory, J. (1996). A role for brassinosteroids in light-dependent development of *Arabidopsis*. *Science* 272, 398–401. doi: 10.1126/science.272.5260.398

Li, T., Hasegawa, T., Yin, X., Zhu, Y., Boote, K., Adam, M., et al. (2015). Uncertainties in predicting rice yield by current crop models under a wide range of climatic conditions. *Glob. Change Biol.* 21, 1328–1341. doi: 10.1111/gcb.12758

Li, T., Liu, B., Spalding, M. H., Weeks, D. P., and Yang, B. (2012). High-efficiency TALEN-based gene editing produces disease-resistant rice. *Nat. Biotechnol.* 30, 390–392. doi: 10.1038/nbt.2199

Lindahl, M., and Kieselbach, T. (2009). Disulphide proteomes and interactions with thioredoxin on the track towards understanding redox regulation in chloroplasts and cyanobacteria. *J. Proteomics* 72, 416–438. doi: 10.1016/J.JPROT.2009.01.003

Liu, D., Chen, S., Liu, X., Yang, F., Liu, W. G., She, Y. H., et al. (2019). Genetic map construction and QTL analysis of leaf-related traits in soybean under monoculture and relay intercropping. *Sci. Rep.* 9;2716. doi: 10.1038/s41598-019-39110-8

Liu, X., Fan, Y., Mak, M., Babla, M., Holford, P., Wang, F., et al. (2017). QTLs for stomatal and photosynthetic traits related to salinity tolerance in barley. *BMC Genomics* 18:9. doi: 10.1186/s12864-016-3380-0

Liu, Y., Wei, H., Ma, M., Li, Q., Kong, D., Sun, J., et al. (2019). *Arabidopsis* FHY3 and FAR1 proteins regulate the balance between growth and defense responses under shade conditions. *Plant Cell* 31, 2089–2106. doi: 10.1105/tpc.18.00991

Lobell, D. B., Roberts, M. J., Schlenker, W., Braun, N., Little, B. B., Rejesus, R. M., et al. (2014). Greater sensitivity to drought accompanies maize yield increase in the U.S. Midwest. *Science* 344, 516–519. doi: 10.1126/science.1251423

Long, S. P., Ainsworth, E. A., Rogers, A., and Ort, D. R. (2004). Rising atmospheric carbon dioxide: plants FACE the future. *Annu. Rev. Plant Biol.* 55, 591–628. doi: 10.1146/annurev.arplant.55.031903.141610

Long, S. P., and Bernacchi, C. J. (2003). Gas exchange measurements, what can they tell us about the underlying limitations to photosynthesis? Procedures and sources of error. *J. Exp Bot.* 54, 2393–2401. doi: 10.1093/jxb/erg262

Long, S. P., Marshall-Colon, A., and Zhu, X.-G. (2015). Meeting the global food demand of the future by engineering crop photosynthesis and yield potential. *Cell* 161, 56–66. doi: 10.1016/J.CELL.2015.03.019

Long, S. P., Zhu, X. G., Naidu, S. L., and Ort, D. R. (2006). Can improvement in photosynthesis increase crop yields? *Plant Cell Environ.* 29, 315–330. doi: 10.1111/j.1365-3040.2005.01493.x

López-Calcagno, P. E., Fisk, S., Brown, K. L., Bull, S. E., South, P. F., and Raines, C. A. (2019). Overexpressing the H-protein of the glycine cleavage system increases biomass yield in glasshouse and field-grown transgenic tobacco plants. *Plant Biotechnol. J.* 17, 141–151. doi: 10.1111/pbi.12953

Loriaux, S., Avenson, T., Welles, J., McDermitt, D., Eckles, R., Riensche, B., et al. (2013). Closing in on maximum yield of chlorophyll fluorescence using a single multiphase flash of sub-saturating intensity. *Plant Cell Environ.* 36, 1755–1770. doi: 10.1111/pce.12115

Lucas, M. R., Ehlers, J. D., Huynh, B., Diop, N. N., Roberts, P. A., and Close, T. J. (2013). Markers for breeding heat-tolerant cowpea. *Mol. Breed.* 31, 529–536. doi: 10.1007/s11032-012-9810-z

Luo, M., Zhang, S., Tang, C., Jia, G., Tang, S., Zhi, H., et al. (2018). Screening of mutants related to the C4 photosynthetic kranz structure in foxtail millet. *Front. Plant Sci.* 14:1650. doi: 10.3389/fpls.2018.01650

Lv, H., Yang, Y., Li, H., Liu, Q., Zhang, J., Yin, J., et al. (2018). Genome-wide association studies of photosynthetic traits related to phosphorus efficiency in soybean. *Front. Plant Sci.* 9:1226. doi: 10.3389/fpls.2018.01226

MacAlister, C. A., Ohashi-Ito, K., and Bergmann, D. C. (2007). Transcription factor control of asymmetric cell divisions that establish the stomatal lineage. *Nature* 445, 537–540. doi: 10.1038/nature05491

Machacova, K., Vainio, E., Urban, O., and Pihlatie, M. (2019). Seasonal dynamics of stem N2O exchange follow the physiological activity of boreal trees. *Nat. Commun.* 10:4989. doi: 10.1038/s41467-019-12976-y

Mahajan, G. R., Sahoo, R. N., Pandey, R. N., Gupta, V. K., and Kumar, D. (2014). Using hyperspectral remote sensing techniques to monitor nitrogen, phosphorus, sulphur and potassium in wheat (*Triticum aestivum* L.). *Precision Agric.* 15, 227–240.

Maier, A., Fahnenstich, H., von Caemmerer, S., Engqvist, M. K. M., Weber, A. P. M., Flügge, U.-I., et al. (2012). Transgenic introduction of a glycolate oxidative cycle into *A. thaliana* chloroplasts leads to growth improvement. *Front. Plant Sci.* 3:38. doi: 10.3389/fpls.2012.00038

Martín, G., Leivar, P., Ludevid, D., Tepperman, J. M., Quail, P. H., and Monte, E. (2016). Phytochrome and retrograde signalling pathways converge to antagonistically regulate a light-induced transcriptional network. *Nat. Commun.* 7:11431. doi: 10.1038/ncomms11431

Masle, J., Gilmore, S. R., and Farquhar, G. D. (2005). The ERECTA gene regulates plant transpiration efficiency in *Arabidopsis*. *Nature* 436, 866–870. doi: 10.1038/nature03835

Matiu, M., Ankerst, D. P., and Menzel, A. (2017). Interactions between temperature and drought in global and regional crop yield variability during 1961-2014. *PLoS One* 12:e0178339. doi: 10.1371/journal.pone.0178339

Maxwell, K., and Johnson, G. N. (2000). Chlorophyll fluorescence-a practical guide. *J. Exp. Bot.* 51, 659–668. doi: 10.1093/jexbot/51.345.659

Medlyn, B. E. (1998). Physiological basis of the light use efficiency model. *Tree Physiol.* 18, 167–176. doi: 10.1093/treephys/18.3.167

Meroni, M., Rossini, M., Guanter, L., Alonso, L., Rascher, U., Colombo, R., et al. (2009). Remote sensing of solar-induced chlorophyll fluorescence: review of methods and applications. *Remote Sens. Environ.* 113, 2037–2051. doi: 10.1016/j.rse.2009.05.003

Meyer, S., and Genty, B. (1999). Heterogeneous inhibition of photosynthesis over the leaf surface of *Rosa rubiginosa* L. during water stress and abscisic acid treatment: induction of a metabolic component by limitation of CO2 diffusion. *Planta* 210, 126–131. doi: 10.1007/s004250050661

Meyer, S., Saccardy-Adji, K., Rizza, F., and Genty, B. (2001). Inhibition of photosynthesis by Colletotrichum lindemuthianum in bean leaves determined by chlorophyll fluorescence imaging. *Plant Cell Environ.* 24, 947–955. doi: 10.1046/j.0016-8025.2001.00737.x

Millar, A. H., Whelan, J., Soole, K. L., and Day, D. A. (2011). Organization and regulation of mitochondrial respiration in plants. *Annu. Rev. Plant Biol.* 62, 79–104. doi: 10.1146/annurev-arplant-042110-103857

Mishra, V., and Cherkauer, K. A. (2010). Retrospective droughts in the crop growing season: implications to corn and soybean yield in the Midwestern United States. *Agric. For. Meteorol.* 150, 1030–1045. doi: 10.1016/j.agrformet.2010.04.002

Miura, K., Okamoto, H., Okuma, E., Shiba, H., Kamada, H., Hasegawa, P. M., et al. (2013). SIZ1 deficiency causes reduced stomatal aperture and enhanced drought tolerance via controlling salicylic acid-induced accumulation of reactive oxygen species in *Arabidopsis*. *Plant J.* 73, 91–104. doi: 10.1111/tpj.12014

Miyagawa, Y., Tamoi, M., and Shigeoka, S. (2001). Overexpression of a cyanobacterial. *Nat. Biotechnol.* 19, 965–969. doi: 10.1038/nbt1001-965

Moore, B. D., Cheng, S. H., Sims, D., and Seemann, J. R. (1999). The biochemical and molecular basis for photosynthetic acclimation to elevated atmospheric CO2. *Plant Cell Environ.* 22, 567–582. doi: 10.1046/j.1365-3040.1999.00432.x

Muchero, W., Ehlers, J. D., Close, T. J., and Roberts, P. A. (2009). Mapping QTL for drought stress-induced premature senescence and maturity in cowpea [*Vigna unguiculata* (L.) Walp.]. *Theor. Appl. Genet.* 118, 849–863. doi: 10.1007/s00122-008-0944-947

Muchero, W., Roberts, P. A., Diop, N. N., Drabo, I., Cisse, N., Close, T. J., et al. (2013). Genetic architecture of delayed senescence, biomass, and grain yield under drought stress in cowpea. *PLoS One* 8:e70041. doi: 10.1371/journal.pone.0070041

Murchie, E. H., Pinto, M., and Horton, P. (2009). Agriculture and the new challenges for photosynthesis research. *New Phytol.* 181, 532–552. doi: 10.1111/j.1469-8137.2008.02705.x

Nakai, M. (2015). The TIC complex uncovered: the alternative view on the molecular mechanism of protein translocation across the inner envelope membrane of chloroplasts. *Biochim. Biophys. Acta Bioenerg.* 1847, 957–967. doi: 10.1016/J.BBABIO.2015.02.011

Nazar, R., Iqbal, N., Syeed, S., and Khan, N. A. (2011). Salicylic acid alleviates decreases in photosynthesis under salt stress by enhancing nitrogen and sulfur assimilation and antioxidant metabolism differentially in two mungbean cultivars. *J. Plant Physiol.* 168, 807–815. doi: 10.1016/J.JPLPH.2010.11.001

Nendel, C., Kersebaum, K. C., Mirschel, W., Manderscheid, R., Weigel, H.-J., and Wenkel, K.-O. (2009). Testing different CO2 response algorithms against a FACE crop rotation experiment. *NJAS Wageningen J. Life Sci.* 57, 17–25. doi: 10.1016/j.njas.2009.07.005

Nguyen, C. V., Vrebalov, J. T., Gapper, N. E., Zheng, Y., Zhong, S., Fei, Z., et al. (2014). Tomato GOLDEN2-LIKE transcription factors reveal molecular gradients that function during fruit development and ripening. *Plant Cell* 26, 585–601. doi: 10.1105/tpc.113.118794

Nölke, G., Houdelet, M., Kreuzaler, F., Peterhänsel, C., and Schillberg, S. (2014). The expression of a recombinant glycolate dehydrogenase polyprotein in potato (*Solanum tuberosum*) plastids strongly enhances photosynthesis and tuber yield. *Plant Biotechnol. J.* 12, 734–742. doi: 10.1111/pbi.12178

Oakley, C. G., Savage, L., Lotz, S., Larson, G. R., Thomashow, M. F., Kramer, D. M., et al. (2018). Genetic basis of photosynthetic responses to cold in two locally adapted populations of *Arabidopsis thaliana*. *J. Exp. Bot.* 69, 699–709. doi: 10.1093/jxb/erx437

Ogura, T., and Busch, W. (2015). From phenotypes to causal sequences: using genome wide association studies to dissect the sequence basis for variation of plant development. *Curr. Opin. Plant Biol.* 23, 98–108. doi: 10.1016/J.PBI.2014.11.008

Ogura, T., Goeschl, C., Filiault, D., Mirea, M., Slovak, R., Wolhrab, B., et al. (2019). Root system depth in *Arabidopsis* is shaped by EXOCYST70A3 via the dynamic modulation of auxin transport. *Cell* 178, 400.e16–412.e16. doi: 10.1016/j.cell.2019.06.021

Okazaki, K., Kabeya, Y., Suzuki, K., Mori, T., Ichikawa, T., Matsui, M., et al. (2015). The PLASTID DIVISION1 and 2 components of the chloroplast division machinery determine the rate of chloroplast division in land plant cell differentiation. *Plant Cell* 21, 1769–1780. doi: 10.1105/tpc.109.067785

O'Leary, B. M., Lee, C. P., Atkin, O. K., Cheng, R., Brown, T. B., and Millar, A. H. (2017). Variation in leaf respiration rates at night correlates with carbohydrate and amino acid supply. *Plant Physiol.* 174, 2261–2273. doi: 10.1104/pp.17.00610

Ort, D. R., Merchant, S. S., Alric, J., Barkan, A., Blankenship, R. E., Bock, R., et al. (2015). Redesigning photosynthesis to sustainably meet global food and bioenergy demand. *Proc. Natl. Acad. Sci. U.S.A.* 112, 8529–8536. doi: 10.1073/pnas.1424031112

Ortiz, D., Hu, J., and Salas-Fernandez, M. G. (2017). Genetic architecture of photosynthesis in Sorghum bicolor under non-stress and cold stress conditions. *J. Exp. Bot.* 68, 4545–4557. doi: 10.1093/jxb/erx276

Page, D. R., and Grossniklaus, U. (2002). The art and design of genetic screens: *Arabidopsis thaliana*. *Nat. Rev. Genet.* 3, 124–136. doi: 10.1038/nrg730

Pandey, M. K., Roorkiwal, M., Singh, V. K., Ramalingam, A., Kudapa, H., Thudi, M., et al. (2016). Emerging genomic tools for legume breeding: current status and future prospects. *Front. Plant Sci.* 7:455. doi: 10.3389/fpls.2016.00455

Panthee, D. R., Pantalone, V. R., Saxton, A. M., West, D. R., and Sams, C. (2006). Genomic regions associated with amino acid composition in soybean. *Mol. Breed.* 17, 79–89. doi: 10.1007/s11032-005-2519-5

Parinov, S., and Sundaresan, V. (2000). Functional genomics in *Arabidopsis*: large-scale insertional mutagenesis complements the genome sequencing project. *Curr. Opin. Biotechnol.* 11, 157–161. doi: 10.1016/s0958-1669(00)00075-6

Parry, M. A. J., Reynolds, M., Salvucci, M. E., Raines, C., Andralojc, P. J., Zhu, X. G., et al. (2011). Raising yield potential of wheat. II. Increasing photosynthetic capacity and efficiency. *J. Exp. Bot.* 62, 453–467. doi: 10.1093/jxb/erq304

Pastenes, C., and Horton, P. (1996). Effect of high temperature on photosynthesis in beans (I. Oxygen evolution and chlorophyll fluorescence). *Plant Physiol.* 112, 1245–1251. doi: 10.1104/pp.112.3.1245

Pego, J. V., Kortstee, A. J., Huijser, C., and Smeekens, S. C. (2000). Photosynthesis, sugars and the regulation of gene expression. *J. Exp. Bot.* 51, 407–416. doi: 10.1093/jexbot/51.suppl_1.407

Peng, S., Laza, R. C., Visperas, R. M., Sanico, A. L., and Cassman, K. G. K. G. (2001). Grain yield of rice cultivars and lines developed in the Philippines since 1966. *Crop Sci.* 40, 307–314. doi: 10.2135/cropsci2000.402307x

Penuelas, J., and Filella, I. (1998). Visible and near-infrared reflectance techniques for diagnosing plant physiological status. *Trends Plant Sci.* 3, 151–156. doi: 10.1016/s1360-1385(98)01213-8

Pesaresi, P., Hertle, A., Pribil, M., Kleine, T., Wagner, R., Strissel, H., et al. (2009). *Arabidopsis* STN7 kinase provides a link between short- and long-term photosynthetic acclimation. *Plant Cell* 21, 2402–2423. doi: 10.1105/tpc.108.064964

Petrillo, E., Godoy Herz, M. A., Fuchs, A., Reifer, D., Fuller, J., Yanovsky, M. J., et al. (2014). A chloroplast retrograde signal regulates nuclear alternative splicing. *Science* 344, 427–430. doi: 10.1126/science.1250322

Pfannschmidt, T. (2003). Chloroplast redox signals: how photosynthesis controls its own genes. *Trends Plant Sci.* 8, 33–41. doi: 10.1016/S1360-1385(02)00005-5

Pick, T. R., Brautigam, A., Schulz, M. A., Obata, T., Fernie, A. R., and Weber, A. P. M. (2013). PLGG1, a plastidic glycolate glycerate transporter, is required for photorespiration and defines a unique class of metabolite transporters. *Proc. Natl. Acad. Sci. U.S.A.* 110, 3185–3190. doi: 10.1073/pnas.1215142110

Pillitteri, L. J., and Dong, J. (2013). Stomatal development in *Arabidopsis*. *Arab. B.* 11:e0162. doi: 10.1199/tab.0162

Pinheiro, C., and Chaves, M. M. (2011). Photosynthesis and drought: can we make metabolic connections from available data? *J. Exp. Bot.* 62, 869–882. doi: 10.1093/jxb/erq340

Pospisilova, J., Vagner, M., Malbeck, J., Travnickova, A., and Batkova, P. (2005). Interactions between abscisic acid and cytokinins during water stress and subsequent rehydration. *Biol. Plant.* 49, 533–540. doi: 10.1007/s10535-005-0047-0

Powell, A. L. T., Nguyen, C. V., Hill, T., Cheng, K. L., Figueroa-Balderas, R., Aktas, H., et al. (2012). Uniform ripening encodes a Golden 2-like transcription factor regulating tomato fruit chloroplast development. *Science* 336, 1711–1715. doi: 10.1126/science.1222218

Price, A. H., Cairns, J. E., Horton, P., Jones, H. G., and Griffiths, H. (2002). Linking drought-resistance mechanisms to drought avoidance in upland rice using a QTL approach: progress and new opportunities to integrate stomatal and mesophyll responses. *J. Exp. Bot.* 53, 989–1004. doi: 10.1093/jexbot/53.371.989

Priesack, E., and Gayler, S. (2009). "Agricultural crop models: Concepts of resource acquisition and assimilate partitioning," in *Progress in Botany 70*, eds U. E. Lüttge, W. Beyschlag, and J. Murata (Berlin: Springer-Verlag), 195–222. doi: 10.1007/978-3-540-68421-3_9

Priesack, E., Gayler, S., Rötzer, T., Seifert, T., and Pretzsch, H. (2012). "Mechanistic modelling of soil–plant–atmosphere systems," in *Growth and Defence in Plants, Ecological Studies 220*, eds R. Matyssek, H. Schnyder, W. Oßwald, D. Ernst, J. C. Munch, and H. Pretzsch (Berlin: Springer-Verlag), 335–353. doi: 10.1007/978-3-642-30645-7_15

Rachmilevitch, S., Cousins, B., and Bloom, J. (2004). Nitrate assimilation in plant shoots depends on photorespiration. *Proc. Natl. Acad. Sci. U.S.A.* 101, 11506–11510. doi: 10.1073/pnas.0404388101

Rasheed, A., Hao, Y., Xia, X., Khan, A., Xu, Y., Varshney, R. K., et al. (2017). Crop breeding chips and genotyping platforms: progress, challenges, and perspectives. *Mol. Plant.* 10, 1047–1064. doi: 10.1016/j.molp.2017.06.008

Reich, P. B., Tjoelker, M. G., Pregitzer, K. S., Wright, I. J., Oleksyn, J., and Machado, J. L. (2008). Scaling of respiration to nitrogen in leaves, stems and roots of higher land plants. *Ecol. Lett.* 11, 793–801. doi: 10.1111/j.1461-0248.2008.01185.x

Renger, G. (2007). *Primary Processes of Photosynthesis: Principles and Apparatus, 2 Parts*. Cambridge: Royal Society of Chemistry Publishers.

Reynolds, M., Bonnett, D., Chapman, S. C., Furbank, R. T., Manès, Y., Mather, D. E., et al. (2011). Raising yield potential of wheat. I. Overview of a consortium approach and breeding strategies. *J. Exp. Bot.* 62, 439–452. doi: 10.1093/jxb/erq311

Richardson, A. D., and Reeves, J. B. (2005). Quantitative reflectance spectroscopy as an alternative to traditional wet lab analysis of foliar chemistry: near-infrared and mid-infrared calibrations compared. *Can. J. Res.* 35, 1122–1130. doi: 10.1139/x05-037

Roach, T., and Krieger-Liszkay, A. K. (2014). Regulation of photosynthetic electron transport and photoinhibition. *Curr. Protein Pept. Sci.* 15, 351–362. doi: 10.2174/1389203715666140327105143

Rochaix, J. D. (2011). Reprint of: regulation of photosynthetic electron transport. *Biochim. Biophys. Acta* 1807, 878–886. doi: 10.1016/j.bbabio.2011.05.009

Rogers, A. (2014). The use and misuse of V_{cmax} in earth system models. *Photosynth. Res.* 119, 15–29. doi: 10.1007/s11120-013-9818-1

Rosema, A., Snel, J. F. H., Zahn, H., Buurmeijer, W. F., and Van Hove, L. W. A. (1998). The relation between laser-induced chlorophyll fluorescence and photosynthesis. *Remote Sens. Environ.* 65, 143–154. doi: 10.1016/s0034-4257(98)00020-0

Rosenthal, D. M., Locke, A. M., Khozaei, M., Raines, C. A., Long, S. P., and Ort, D. R. (2011). Over-expressing the C3photosynthesis cycle enzyme Sedoheptulose-1-7 Bisphosphatase improves photosynthetic carbon gain and yield under fully open air CO2 fumigation (FACE). *BMC Plant Biol.* 11:123. doi: 10.1186/1471-2229-11-123

Rossel, J. B., Wilson, P. B., Hussain, D., Woo, N. S., Gordon, M. J., Mewett, O. P., et al. (2007). Systemic and intracellular responses to photooxidative stress in *Arabidopsis*. *Plant Cell* 19, 4091–4110. doi: 10.1105/tpc.106.045898

Ruiz-Vera, U. M., De Souza, A. P., Long, S. P., and Ort, D. R. (2017). The role of sink strength and nitrogen availability in the down-regulation of photosynthetic capacity in field-grown *Nicotiana tabacum* L. at elevated CO2 concentration. *Front. Plant Sci.* 8:998. doi: 10.3389/fpls.2017.00998

Ruiz-Vera, U. M., Siebers, M., Gray, S. B., Drag, D. W., Rosenthal, D. M., Kimball, B. A., et al. (2013). Global warming can negate the expected CO2 stimulation in photosynthesis and productivity for soybean grown in the Midwestern United States. *Plant Physiol.* 162, 410–423. doi: 10.1104/pp.112.211938

Rushton, D. L., Tripathi, P., Rabara, R. C., Lin, J., Ringler, P., Boken, A. K., et al. (2012). WRKY transcription factors: key components in abscisic acid signalling. *Plant Biotechnol. J.* 10, 2–11. doi: 10.1111/j.1467-7652.2011.00634.x

Sadler, N. C., Melnicki, M. R., Serres, M. H., Merkley, E. D., and Chrisler, W. B. (2014). Live cell chemical profiling of temporal redox dynamics in a photoautotrophic cyanobacterium. *ACS Chem. Biol.* 9, 291–300. doi: 10.1021/cb400769v

Sakamoto, H., Maruyama, K., Sakuma, Y., Meshi, T., Iwabuchi, M., Shinozaki, K., et al. (2004). *Arabidopsis* Cys2/His2-type zinc-finger proteins function as transcription repressors under drought, cold, and high-salinity stress conditions. *Plant Physiol.* 136, 2734–2746. doi: 10.1104/pp.104.046599

Sánchez-Rodríguez, J., Pérez, P., and Martínez-Carrasco, R. (1999). Photosynthesis, carbohydrate levels and chlorophyll fluorescence-estimated intercellular CO2 in water-stressed *Casuarina equisetifolia* Forst. & Forst. *Plant Cell Environ.* 22, 867–873. doi: 10.1046/j.1365-3040.1999.00447.x

Sankaran, S., Khot, L. R., and Carter, A. H. (2015). Field-based crop phenotyping: multispectral aerial imaging for evaluation of winter wheat emergence and spring stand. *Comput. Electron. Agric.* 118, 372–379. doi: 10.1016/j.compag.2015.09.001

Sanz-Saez, A., Heath, K. D., Burke, P. V., and Ainsworth, E. A. (2015). Inoculation with an enhanced N2-fixing *Bradyrhizobium japonicum* strain (USDA110) does not alter soybean (Glycine max Merr.) response to elevated [CO2]. *Plant Cell Environ.* 38, 2589–2602. doi: 10.1111/pce.12577

Sanz-Saez, A., Koester, R. P., Rosenthal, D. M., Montes, C. M., Ort, D. R., and Ainsworth, E. A. (2017). Leaf and canopy scale drivers of genotypic variation in soybean response to elevated carbon dioxide concentration. *Glob. Change Biol.* 23, 3908–3920. doi: 10.1111/gcb.13678

Saradhi, P. P., Suzuki, I., Katoh, A., Sakamoto, A., Sharmila, P., Shi, D.-J., et al. (2000). Protection against the photo-induced inactivation of the photosystem II complex by abscisic acid. *Plant Cell Environ.* 23, 711–718. doi: 10.1046/j.1365-3040.2000.00579.x

Scafaro, A. P., Negrini, A. C. A., O'Leary, B., Rashid, F. A. A., Hayes, L., Fan, Y., et al. (2017). The combination of gas-phase fluorophore technology and automation to enable high-throughput analysis of plant respiration. *Plant Methods* 13:16. doi: 10.1186/s13007-017-0169-163

Scheben, A., and Edwards, D. (2017). Genome editors take on crops. *Science* 355, 1122–1123. doi: 10.1126/science.aal4680

Scheben, A., Wolter, F., Batley, J., Puchta, H., and Edwards, D. (2017). Towards CRISPR/Cas crops-bringing together genomics and genome editing. *New Phytol.* 216, 682–698. doi: 10.1111/nph.14702

Schlotterer, C., Tobler, R., Kofler, R., and Nolte, V. (2014). Sequencing pools of individuals - mining genome-wide polymorphism data without big funding. *Nat. Rev. Genet.* 15, 749–763. doi: 10.1038/nrg3803

Scotford, I. M., and Miller, P. C. H. (2004). Estimating tiller density and leaf area index of winter wheat using spectral reflectance and ultrasonic sensing techniques. *Biosyst. Eng.* 89, 395–408. doi: 10.1016/j.biosystemseng.2004.08.019

Serbin, S. P., Dillaway, D. N., Kruger, E. L., and Townsend, P. A. (2012). Leaf optical properties reflect variation in photosynthetic metabolism and its sensitivity to temperature. *J. Exp. Bot.* 63, 489–502. doi: 10.1093/jxb/err294

Sewelam, N., Kazan, K., and Schenk, P. M. (2016). Global plant stress signaling: reactive oxygen species at the cross-road. *Front. Plant Sci.* 7:187. doi: 10.3389/fpls.2016.00187

Shen, B.-R., Wang, L.-M., Lin, X.-L., Yao, Z., Xu, H.-W., Zhu, C.-H., et al. (2019). Engineering a new chloroplastic photorespiratory bypass to increase photosynthetic efficiency and productivity in rice. *Mol. Plant* 12, 199–214. doi: 10.1016/J.MOLP.2018.11.013

Shimizu, M., Kato, H., Ogawa, T., Kurachi, A., Nakagawa, Y., and Kobayashi, H. (2010). Sigma factor phosphorylation in the photosynthetic control of photosystem stoichiometry. *Proc. Natl. Acad. Sci. U.S.A.* 107, 10760–10764. doi: 10.1073/pnas.0911692107

Shin, A.-Y., Han, Y.-J., Baek, A., Ahn, T., Kim, S. Y., Nguyen, T. S., et al. (2016). Evidence that phytochrome functions as a protein kinase in plant light signalling. *Nat. Commun.* 7:11545. doi: 10.1038/ncomms11545

Sieber, M. H., Thomsen, M. B., and Spradling, A. C. (2016). Electron transport chain remodeling by GSK3 during oogenesis connects nutrient state to reproduction. *Cell* 164, 420–432. doi: 10.1016/j.cell.2015.12.020

Silva-Perez, V., Molero, G., Serbin, S. P., Condon, A. G., Reynolds, M. P., Furbank, R. T., et al. (2018). Hyperspectral reflectance as a tool to measure biochemical and physiological traits in wheat. *J. Exp. Bot.* 69, 483–496. doi: 10.1093/jxb/erx421

Simkin, A. J., Lopez-Calcagno, P. E., Davey, P. A., Headland, L. R., Lawson, T., Timm, S., et al. (2017a). Simultaneous stimulation of sedoheptulose 1,7-bisphosphatase, fructose 1,6-bisphophate aldolase and the photorespiratory glycine decarboxylase-H protein increases CO2 assimilation, vegetative biomass and seed yield in *Arabidopsis*. *Plant Biotechnol. J.* 15, 805–816. doi: 10.1111/pbi.12676

Simkin, A. J., López-Calcagno, P. E., and Raines, C. A. (2019). Feeding the world: improving photosynthetic efficiency for sustainable crop production. *J. Exp. Bot.* 70, 1119–1140. doi: 10.1093/jxb/ery445

Simkin, A. J., McAusland, L., Headland, L. R., Lawson, T., and Raines, C. A. (2015). Multigene manipulation of photosynthetic carbon assimilation increases CO2 fixation and biomass yield in tobacco. *J. Exp. Bot.* 66, 4075–4090. doi: 10.1093/jxb/erv204

Simkin, A. J., McAusland, L., Lawson, T., and Raines, C. A. (2017b). Overexpression of the RieskeFeS protein increases electron transport rates and biomass yield. *Plant Physiol.* 175, 134–145. doi: 10.1104/pp.17.00622

Singh, B. D., and Singh, A. K. (2015). *Marker-Assisted Plant Breeding: Principles and Practices*. Cham: Springer.

Slattery, R. A., and Ort, D. R. (2015). Photosynthetic energy conversion efficiency: setting a baseline for gauging future improvements in important food and biofuel crops. *Plant Physiol.* 168, 383–392. doi: 10.1104/pp.15.00066

Somerville, C. R. (1986). Analysis of photosynthesis with mutants of higher plants and algae. *Annu. Rev. Plant. Physiol.* 37, 467–507.

Song, Y., Chen, Q., Ci, D., Shao, X., and Zhan, D. (2014). Effects of high temperature on photosynthesis and related gene expression in poplar. *BMC Plant Biol.* 14:111. doi: 10.1186/1471-2229-14-111

South, P. F., Cavanagh, A. P., Liu, H. W., and Ort, D. R. (2019). Synthetic glycolate metabolism pathways stimulate crop growth and productivity in the field. *Science* 363:eaat9077. doi: 10.1126/science.aat9077

Spitters, C. J. T. (1986). Separating the diffuse and direct component of global radiation and its implications for modeling canopy photosynthesis Part II. Calculation of canopy photosynthesis. *Agric. For. Meteorol.* 38, 231–242. doi: 10.1016/0168-1923(86)90060-90062

Spitters, C. J. T., van Keulen, H., and van Kraalingen, D. W. G. (1989). "A simple and universal crop growth simulator: SUCROS87," in *Simulation and Systems Management in Crop Production*, eds R. Rabbinge, S. A. Ward, and H. H. van Laar (Wageningen: Backhuys Publishers), 147–181.

Stephenson, T. J., McIntyre, C. L., Collet, C., and Xue, G. P. (2011). TaNF-YB3 is involved in the regulation of photosynthesis genes in *Triticum aestivum*. *Funct. Integr. Genom.* 11, 327–340. doi: 10.1007/s10142-011-0212-9

Stinziano, J. R., McDermitt, D. K., Lynch, D. J., Saathoff, A. J., Morgan, P. B., and Hanson, D. T. (2019). The rapid A/Ci response: a guide to best practices. *New Phytol.* 221, 625–627. doi: 10.1111/nph.15383

Stinziano, J. R., Morgan, P. B., Lynch, D. J., Saathoff, A. J., McDermitt, D. K., and Hanson, D. T. (2017). The rapid A-Ci response: photosynthesis in the phenomic era. *Plant Cell Environ.* 40, 1256–1262. doi: 10.1111/pce.12911

Strigens, A., Freitag, N. M., Gilbert, X., Grieder, C., Riedelsheimer, C., Schrag, T. A., et al. (2013). Association mapping for chilling tolerance in elite flint and dent maize inbred lines evaluated in growth chamber and field experiments. *Plant Cell Environ.* 36, 1871–1887. doi: 10.1111/pce.12096

Su, J., Zhang, F., Chong, X., Song, A., Guan, Z., Fang, W., et al. (2019). Genome-wide association study identifies favorable SNP alleles and candidate genes for waterlogging tolerance in chrysanthemums. *Hortic. Res.* 6:21. doi: 10.1038/s41438-018-0101-107

Sugano, S. S., Shimada, T., Imai, Y., Okawa, K., Tamai, A., Mori, M., et al. (2010). Stomagen positively regulates stomatal density in *Arabidopsis*. *Nature* 463, 241–244. doi: 10.1038/nature08682

Takagi, D. H., Ihara, S., and Takumi, C. (2019). Miyake growth light environment changes the sensitivity of photosystem I photoinhibition depending on common wheat cultivars. *Front. Plant. Sci.* 10:686. doi: 10.3389/fpls.2019.00686

Takagi, H., Abe, A., Yoshida, K., Kosugi, S., Natsume, S., Mitsuoka, C., et al. (2013). QTL-seq: rapid mapping of quantitative trait loci in rice by whole genome resequencing of DNA from two bulked populations. *Plant J.* 74, 174–183. doi: 10.1111/tpj.12105

Takai, T., Adachi, S., Taguchi-Shiobara, F., Sanoh-Arai, Y., Iwasawa, N., Yoshinaga, S., et al. (2013). A natural variant of NAL1, selected in high-yield rice breeding programs, pleiotropically increases photosynthesis rate. *Sci. Rep.* 3:2149. doi: 10.1038/srep02149

Takai, T., Kondo, M., Yano, M., and Yamamoto, T. (2010). A quantitative trait locus for chlorophyll content and its association with leaf photosynthesis in rice. *Rice* 3, 172–180. doi: 10.1007/s12284-010-9047-6

Tamoi, M., Nagaoka, M., Miyagawa, Y., and Shigeoka, S. (2006). Contribution of fructose-1,6-bisphosphatase and sedoheptulose-1,7- bisphosphatase to the photosynthetic rate and carbon flow in the Calvin cycle in transgenic plants. *Plant Cell Physiol.* 47, 380–390. doi: 10.1093/pcp/pcj004

Tanaka, Y., Sano, T., Tamaoki, M., Nakajima, N., Kondo, N., and Hasezawa, S. (2006). Cytokinin and auxin inhibit abscisic acid-induced stomatal closure by enhancing ethylene production in *Arabidopsis*. *J. Exp. Bot.* 57, 2259–2266. doi: 10.1093/jxb/erj193

Taylor, S. H., and Long, S. P. (2019). Phenotyping photosynthesis on the limit – a critical examination of RACiR. *New Phytol.* 221, 621–624. doi: 10.1111/nph.15382

Teng, S., Qian, Q., Zeng, D. L., Kunihiro, Y., Fujimoto, K., Huang, D. N., et al. (2004). QTL analysis of leaf photosynthetic rate and related physiological traits in rice (*Oryza sativa* L.). *Euphytica* 135, 1–7. doi: 10.1023/b:euph.0000009487.89270.e9

Teulat, B., Merah, O., Sirault, X., Borries, C., Waugh, R., and This, D. (2002). QTLs for grain carbon isotope discrimination in field-grown barley. *Theor. Appl. Genet.* 106, 118–126. doi: 10.1007/s00122-002-1028-8

Tholen, D., Pons, T. L., Voesenek, L. A. C. J., and Poorter, H. (2007). Ethylene insensitivity results in down-regulation of RuBisCO expression and

photosynthetic capacity in tobacco. *Plant Physiol.* 144, 1305–1315. doi: 10.1104/pp.107.099762

Thompson, A. L., Thorp, K. R., Conley, M., Andrade-Sanchez, P., Heun, J. T., Dyer, J. M., et al. (2018). Deploying a proximal sensing cart to identify drought-adaptive traits in upland cotton for high-throughput phenotyping. *Front. Plant Sci.* 9:507. doi: 10.3389/fpls.2018.00507

Thompson, M., Gamage, D., Hirotsu, N., Martin, A., and Seneweera, S. (2017). Effects of elevated carbon dioxide on photosynthesis and carbon partitioning: a Perspective on root sugar sensing and hormonal crosstalk. *Front. Physiol.* 8:578. doi: 10.3389/fphys.2017.00578

Thornley, J. H. M. (1998). Dynamic model of leaf photosynthesis with acclimation to light and nitrogen. *Ann. Bot.* 81, 421–430. doi: 10.1006/anbo.1997.0575

Thornley, J. H. M. (2004). Acclimation of photosynthesis to light and canopy nitrogen distribution: an interpretation. *Ann. Bot.* 93, 473–475. doi: 10.1093/aob/mch051

Thornley, J. H. M. (2011). Plant growth and respiration re-visited: maintenance respiration defined – it is an emergent property of, not a separate process within, the system-and why the respiration : photosynthesis ratio is conservative. *Ann. Bot.* 108, 1365–1380. doi: 10.1093/aob/mcr238

Timm, S., Florian, A., Arrivault, S., Stitt, M., Fernie, A. R., and Bauwe, H. (2012). Glycine decarboxylase controls photosynthesis and plant growth. *FEBS Lett.* 586, 3692–3697. doi: 10.1016/j.febslet.2012.08.027

Timm, S., Wittmiß, M., Gamlien, S., Ewald, R., Florian, A., Frank, M., et al. (2015). Mitochondrial dihydrolipoyl dehydrogenase activity shapes photosynthesis and photorespiration of *Arabidopsis thaliana*. *Plant Cell* 27, 1968–1984. doi: 10.1105/tpc.15.00105

Tissue, D. T., Griffin, K. L., Turnbull, M. H., and Whitehead, D. (2005). Stomatal and nonL. Griffinlimitations to photosynthesis in four tree species in a temperate rainforest dominated by *Dacrydium cupressinum* in New Zealand. *Tree Physiol.* 25, 447–456. doi: 10.1093/treephys/25.4.447

Torralbo, F., Vicente, R., Morcuende, R., González-Murua, C., and Aranjuelo, I. (2019). C and N metabolism in barley leaves and peduncles modulates responsiveness to changing CO2. *J. Exp. Bot.* 70, 599–611. doi: 10.1093/jxb/ery380

Tsai, Y., Chen, K., Cheng, T., Lee, C., Lin, S. H., and Tung, C. W. (2019). Chlorophyll fluorescence analysis in diverse rice varieties reveals the positive correlation between the seedlings salt tolerance and photosynthetic efficiency. *BMC Plant Biol.* 19:403. doi: 10.1186/s12870-019-1983-8

Tubiello, F., and Ewert, F. (2002). Simulating the effects of elevated CO2 on crops: approaches and applications for climate change. *Eur. J. Agron.* 18, 57–74. doi: 10.1016/S1161-0301(02)00097-97

Uematsu, K., Suzuki, N., Iwamae, T., Inui, M., and Yukawa, H. (2012). Increased fructose 1,6-bisphosphate aldolase in plastids enhances growth and photosynthesis of tobacco plants. *J. Exp. Bot.* 63, 3001–3009. doi: 10.1093/jxb/ers004

Ulloa, M. R., Cantrell, G. R., Percy, G., Zeiger, E., and Lu, Z. M. (2000). QTL analysis of stomatal conductance and relationship to lint yield in an interspecific cotton. *J. Cotton Sci.* 4, 10–18.

van Bezouw, R. F. H. M., Keurentjes, J. J. B., Harbinson, J., and Aarts, M. G. M. (2018). Converging phenomics and genomics to study natural variation in plant photosynthesis efficiency. *Plant J.* 97, 112–133. doi: 10.1111/tpj.14190

van Rooijen, R., Aarts, M. G., and Harbinson, J. (2015). Natural genetic variation for acclimation of photosynthetic light use efficiency to growth irradiance in *Arabidopsis*. *Plant Physiol.* 167, 1412–1429. doi: 10.1104/pp.114.252239

Vanlerberghe, G. C. (2013). Alternative oxidase: a mitochondrial respiratory pathway to maintain metabolic and signaling homeostasis during abiotic and biotic stress in plants. *Int. J. Mol. Sci.* 2013, 6805–6847. doi: 10.3390/ijms14046805

Vanlerberghe, G. C., Martyn, G. D., and Dahal, K. (2016). Alternative oxidase: a respiratory electron transport chain pathway essential for maintaining photosynthetic performance during drought stress. *Physiol. Plant.* 157, 322–337. doi: 10.1111/ppl.12451

Vanlerberghe, G. C., and McIntosh, L. (1997). Alternative oxidase: from gene to function. *Annu. Rev. Plant Biol.* 48, 703–734. doi: 10.1146/annurev.arplant.48.1.703

Vanuytrecht, E., and Thorburn, P. J. (2017). Responses to atmospheric CO2 concentrations in crop simulation models: a review of current simple and semi-complex representations and options for model development. *Glob. Change Biol.* 23, 1806–1820. doi: 10.1111/gcb.13600

Varshney, R. K. (2016). Exciting journey of 10 years from genomes to fields and markets: some success stories of genomics-assisted breeding in chickpea, pigeonpea and groundnut. *Plant Sci.* 242, 98–107. doi: 10.1016/j.plantsci.2015.09.009

Varshney, R. K., Ribaut, J. M., Buckler, E. S., Tuberosa, R., and Rafalski, J. A. (2012). Langridge P. Can genomics boost productivity of orphan crops? *Nat. Biotechnol.* 30, 1172–1176. doi: 10.1038/nbt.2440

Varshney, R. K., Singh, V. K., Kumar, A., Powell, W., and Sorrells, M. E. (2018). Can genomics deliver climate-change ready crops? *Curr. Opin. Plant Biol.* 45, 205–211. doi: 10.1016/j.pbi.2018.03.007

Varshney, R. K., Terauchi, R., and McCouch, S. R. (2014). Harvesting the promising fruits of genomics: applying genome sequencing technologies to crop breeding. *PLoS Biol.* 12:e1001883. doi: 10.1371/journal.pbio.1001883

Vicente, R., Martínez-Carrasco, R., Pérez, P., and Morcuende, R. (2018). New insights into the impacts of elevated CO2, nitrogen, and temperature levels on the regulation of C and N metabolism in durum wheat using network analysis. *Nat. Biotechnol.* 40, 192–199. doi: 10.1016/j.nbt.2017.08.003

Vicente, R., Pérez, P., Martínez-Carrasco, R., Usadel, B., Kostadinova, S., and Morcuende, R. (2015). Quantitative RT-PCR platform to measure transcript levels of C and N metabolism-related genes in durum wheat: transcript profiles in elevated CO2 and high temperature at different levels of N supply. *Plant Cell Physiol.* 56, 1556–1573. doi: 10.1093/pcp/pcv079

Virlet, N., Sabermanesh, K., Sadeghi-Tehran, P., and Hawkesford, M. J. (2017). Field scanalyzer: an automated robotic field phenotyping platform for detailed crop monitoring. *Funct. Plant Biol.* 44, 143–153. doi: 10.1071/Fp16163

Walker, R. P., Paoletti, A., Leegood, R. C., and Famiani, F. (2016). Phosphorylation of phosphoenolpyruvate carboxykinase (PEPCK) and phosphoenolpyruvate carboxylase (PEPC) in the flesh of fruits. *Plant Physiol. Biochem.* 108, 323–327. doi: 10.1016/J.PLAPHY.2016.07.021

Wang, E., Martre, P., Asseng, S., Ewert, F., Zhao, Z., Maiorano, A., et al. (2017). Improved temperature response functions reduce uncertainty in wheat yield projections. *Nat. Plants* 3:17102. doi: 10.1038/nplants.2017.102

Wang, H., Ngwenyama, N., Liu, Y., Walker, J. C., and Zhang, S. (2007). Stomatal development and patterning are regulated by environmentally responsive mitogen-activated protein kinases in *Arabidopsis*. *Plant Cell* 19, 63–73. doi: 10.1105/tpc.106.048298

Wang, J., Chu, S., Zhang, H., Zhu, Y., Cheng, H., and Yu, D. (2016). Development and application of a novel genome-wide SNP array reveals domestication history in soybean. *Sci. Rep.* 9:20728.

Wang, L., Fan, L., Loescher, W., Duan, W., Liu, G., Cheng, J., et al. (2010). Salicylic acid alleviates decreases in photosynthesis under heat stress and accelerates recovery in grapevine leaves. *BMC Plant Biol.* 10:34. doi: 10.1186/1471-2229-10-34

Wang, W.-H., Yi, X.-Q., Han, A.-D., Liu, T.-W., Chen, J., Wu, F.-H., et al. (2012). Calcium-sensing receptor regulates stomatal closure through hydrogen peroxide and nitric oxide in response to extracellular calcium in *Arabidopsis*. *J. Exp. Bot.* 63, 177–190. doi: 10.1093/jxb/err259

Wang, Y.-P., and Leuning, R. (1998). A two-leaf model for canopy conductance, photosynthesis and partitioning of available energy I: model description and comparison with a multi-layered model. *Agric. For. Meteorol.* 91, 89–111. doi: 10.1016/S0168-1923(98)00061-6

Wang, Y. Y., Cheng, Y. H., Chen, K. E., and Tsay, Y.-F. (2018). Nitrate transport, signaling, and use efficiency. *Annu. Rev. Plant Biol.* 69, 85–122. doi: 10.1146/annurev-arplant-042817-40056

Waters, M. T., Wang, P., Korkaric, M., Capper, R. G., Saunders, N. J., and Langdale, J. A. (2009). GLK transcription factors coordinate expression of the photosynthetic apparatus in *Arabidopsis*. *Plant Cell* 21, 1109–1128. doi: 10.1105/tpc.108.065250

Watson, A., Ghosh, M. J., Williams, W. S., Cuddy, J., Simmonds, M. D., Rey, M. A., et al. (2018). Speed breeding is a powerful tool to accelerate crop research and breeding. *Nat. Plants* 4, 23–29.

Weber, A. P. M., and Bar-Even, A. (2019). Update: improving the efficiency of photosynthetic carbon reactions. *Plant Physiol.* 179, 803–812. doi: 10.1104/pp.18.01521

Weber, V. S., Araus, J. L., Cairns, J. E., Sanchez, C., Melchinger, A. E., and Orsini, E. (2012). Prediction of grain yield using reflectance spectra of canopy and

leaves in maize plants grown under different water regimes. *Field Crops Res.* 128, 82–90. doi: 10.1016/j.fcr.2011.12.016

Wright, I. J., Reich, P. B., Atkin, O. K., Lusk, C. H., Tjoelker, M. G., and Westoby, M. (2006). Irradiance, temperature and rainfall influence leaf dark respiration in woody plants: evidence from comparisons across 20 sites. *New Phytol.* 169, 309–319. doi: 10.1111/j.1469-8137.2005.01590.x

Wu, J., Zhang, Z., Zhang, Q., Han, X., Gu, X., and Lu, T. (2015). The molecular cloning and clarification of a photorespiratory mutant, oscdm1, using enhancer trapping. *Front. Genet.* 6:226. doi: 10.3389/fgene.2015.00226

Xie, X., Xia, X., Kuang, S., Zhang, X., Yin, X., Yu, J., et al. (2017). A novel ethylene responsive factor CitERF13 plays a role in photosynthesis regulation. *Plant Sci.* 256, 112–119. doi: 10.1016/J.PLANTSCI.2016.11.001

Xiong, L., and Zhu, J. K. (2003). Regulation of abscisic acid biosynthesis. *Plant Physiol.* 133, 29–36. doi: 10.1104/pp.103.025395

Yan, X., Qu, C., Li, J., Chen, L., and Liu, L. (2015). QTL analysis of leaf photosynthesis rate and related physiological traits in *Brassica napus*. *J. Integr. Agric.* 14, 1261–1268. doi: 10.1016/s2095-3119(14)60958-8

Yang, X., Tang, J., Mustard, J. F., Lee, J. E., Rossini, M., Joiner, J., et al. (2015). Solar-induced chlorophyll fluorescence that correlates with canopy photosynthesis on diurnal and seasonal scales in a temperate deciduous forest. *Geophys. Res. Lett.* 42, 2977–2987. doi: 10.1002/2015gl063201

Yang, Y., Chen, J., Liu, Q., Ben, C., Todd, C. D., Shi, J., et al. (2012). Comparative proteomic analysis of the thermotolerant plant *Portulaca oleracea* acclimation to combined high temperature and humidity stress. *J. Proteome Res.* 11, 3605–3623. doi: 10.1021/pr300027a

Ye, W., Hu, S., Wu, L., Ge, C., Cui, Y., Chen, P., et al. (2017). Fine mapping a major QTL qFCC7 L for chlorophyll content in rice (*Oryza sativa* L.) cv. PA64s. *Plant Growth Regul.* 81, 81–90. doi: 10.1007/s10725-016-0188-185

Yendrek, C. R., Tomaz, T., Montes, C. M., Cao, Y., Morse, A. M., Brown, P. J., et al. (2017). High-throughput phenotyping of maize leaf physiological and biochemical traits using hyperspectral reflectance. *Plant Physiol.* 173, 614–626. doi: 10.1104/pp.16.01447

Yin, X. (2013). Improving ecophysiological simulation models to predict the impact of elevated atmospheric CO2 concentration on crop productivity. *Ann. Bot.* 112, 465–475. doi: 10.1093/aob/mct016

Yin, X., and Struik, P. C. (2009). C3 and C4 photosynthesis models: an overview from the perspective of crop modelling. *NJAS Wageningen J. Life Sci.* 57, 27–38. doi: 10.1016/j.njas.2009.07.001

Yin, X., and van Laar, H. H. (2005). *Crop Systems Dynamics – An Ecophysiological Simulation Model for Genotype-by-Environment Interactions*. Wageningen: Wageningen Academic Publishers.

Zhang, H. Y., Chen, Q. J., Wang, Y. J., Xu, Y., and Zhang, F. (2004). Identification of QTLs for cucumber poor light tolerance. *Mol. Plant Breed.* 2, 795–799.

Zhang, J.-Y., He, S.-B., Li, L., and Yang, H.-Q. (2014). Auxin inhibits stomatal development through MONOPTEROS repression of a mobile peptide gene STOMAGEN in mesophyll. *Proc. Natl. Acad. Sci. U.S.A.* 111, E3015–E3023. doi: 10.1073/pnas.1400542111

Zhang, X., Wollenweber, B., Jiang, D., Liu, F., and Zhao, J. (2008). Water deficits and heat shock effects on photosynthesis of a transgenic *Arabidopsis thaliana* constitutively expressing ABP9, a bZIP transcription factor. *J. Exp. Bot.* 59, 839–848. doi: 10.1093/jxb/erm364

Zhao, K., Tung, C.-W., Eizenga, G. C., Wright, M. H., Ali, M. L., Price, A. H., et al. (2011). Genome-wide association mapping reveals a rich genetic architecture of complex traits in *Oryza sativa*. *Nat. Commun.* 2:467. doi: 10.1038/ncomms1467

Zhao, P., Cui, R., Xu, P., Wu, J., Mao, J. L., Chen, Y., et al. (2017). ATHB17 enhances stress tolerance by coordinating photosynthesis associated nuclear gene and ATSIG5 expression in response to abiotic stress. *Sci. Rep.* 7:45492. doi: 10.1038/srep45492

Zhao, Y., Chan, Z., Gao, J., Xing, L., Cao, M., Yu, C., et al. (2016). ABA receptor PYL9 promotes drought resistance and leaf senescence. *Proc. Natl. Acad. Sci. U.S.A.* 113, 1949–1954. doi: 10.1073/pnas.1522840113

Zhu, C., Zhu, J., Cao, J., Jiang, Q., Liu, G., and Ziska, L. H. (2014). Biochemical and molecular characteristics of leaf photosynthesis and relative seed yield of two contrasting rice cultivars in response to elevated [CO2]. *J. Exp. Bot.* 65, 6049–6056. doi: 10.1093/jxb/eru344

Zhu, X. G., de Sturler, E., and Long, S. P. (2007). Optimizing the distribution of resources between enzymes of carbon metabolism can dramatically increase photosynthetic rate: a numerical simulation using an evolutionary algorithm. *Plant Physiol.* 145, 513–526. doi: 10.1104/pp.107.103713

Zhu, X. G., Long, S. P., and Ort, D. R. (2008). What is the maximum efficiency with which photosynthesis can convert solar energy into biomass? *Curr. Opin. Biotechnol.* 19, 153–159. doi: 10.1016/j.copbio.2008.02.004

Zhu, X. G., Long, S. P., and Ort, D. R. (2010). Improving photosynthetic efficiency for greater yield. *Annu. Rev. Plant Biol.* 61, 235–261. doi: 10.1146/annurev-arplant-042809-112206

Zimmermann, P., Hirsch-Hoffmann, M., and Hennig, L. G. W. (2004). GENEVESTIGATOR. *Arabidopsis* microarray database and analysis toolbox. *Plant Physiol.* 136, 2621–2632. doi: 10.1104/pp.104.046367

Zipper, S. C., Qiu, J., and Kucharik, C. J. (2016). Drought effects on US maize and soybean production: spatiotemporal patterns and historical changes. *Enviro. Res. Lett.* 11:094021. doi: 10.1088/1748-9326/11/9/094021

Conflict of Interest: The authors declare that the research was conducted in the absence of any commercial or financial relationships that could be construed as a potential conflict of interest.

frontiers in Plant Science

ORIGINAL RESEARCH
published: 23 October 2020
doi: 10.3389/fpls.2020.516818

Biofertilizers as Strategies to Improve Photosynthetic Apparatus, Growth, and Drought Stress Tolerance in the Date Palm

Mohamed Anli[1,2], Marouane Baslam[3], Abdelilah Tahiri[1,2], Anas Raklami[1,2], Sarah Symanczik[4], Abderrahim Boutasknit[1], Mohamed Ait-El-Mokhtar[1], Raja Ben-Laouane[1], Salma Toubali[1], Youssef Ait Rahou[1], Mustapha Ait Chitt[5], Khalid Oufdou[2], Toshiaki Mitsui[3], Mohamed Hafidi[2,6] and Abdelilah Meddich[1]**

[1] Laboratory of Agro-Food, Biotechnologies and Valorization of Plant Bioresources (AGROBIOVAL), Department of Biology, Faculty of Science Semlalia, Cadi Ayyad University (UCA), Marrakesh, Morocco, [2] Laboratory of Microbial Biotechnologies, Agrosciences, and Environment (BioMAgE), Faculty of Science Semlalia, Cadi Ayyad University (UCA), Marrakesh, Morocco, [3] Laboratory of Biochemistry, Faculty of Agriculture, Niigata University, Niigata, Japan, [4] Department of Soil Sciences, Research Institute of Organic Agriculture Frick (FiBL), Frick, Switzerland, [5] Domaines Agricoles, Laboratoire El Bassatine, Domaine El Bassatine, Meknès, Morocco, [6] Mohammed VI Polytechnic University (UM6P), Agrobiosciences program (AgBs), Benguerir, Morocco

OPEN ACCESS

Edited by:
Thomas Roitsch,
University of Copenhagen, Denmark

Reviewed by:
Arafat Abdel Hamed Abdel Latef,
South Valley University, Egypt
Nieves Goicoechea,
University of Navarra, Spain

***Correspondence:**
Marouane Baslam
mbaslam@gs.niigata-u.ac.jp
Abdelilah Meddich
a.meddich@uca.ma

Specialty section:
This article was submitted to Plant Abiotic Stress, a section of the journal Frontiers in Plant Science

Received: 02 December 2019
Accepted: 22 September 2020
Published: 23 October 2020

Citation:
Anli M, Baslam M, Tahiri A, Raklami A, Symanczik S, Boutasknit A, Ait-El-Mokhtar M, Ben-Laouane R, Toubali S, Ait Rahou Y, Ait Chitt M, Oufdou K, Mitsui T, Hafidi M and Meddich A (2020) Biofertilizers as Strategies to Improve Photosynthetic Apparatus, Growth, and Drought Stress Tolerance in the Date Palm. Front. Plant Sci. 11:516818. doi: 10.3389/fpls.2020.516818

Rainfall regimes are expected to shift on a regional scale as the water cycle intensifies in a warmer climate, resulting in greater extremes in dry versus wet conditions. Such changes are having a strong impact on the agro-physiological functioning of plants that scale up to influence interactions between plants and microorganisms and hence ecosystems. In (semi)-arid ecosystems, the date palm (*Phoenix dactylifera* L.) -an irreplaceable tree- plays important socio-economic roles. In the current study, we implemeted an adapted management program to improve date palm development and its tolerance to water deficit by using single or multiple combinations of exotic and native arbuscular mycorrhizal fungi (AMF1 and AMF2 respectively), and/or selected consortia of plant growth-promoting rhizobacteria (PGPR: B1 and B2), and/or composts from grasses and green waste (C1 and C2, respectively). We analyzed the potential for physiological functioning (photosynthesis, water status, osmolytes, mineral nutrition) to evolve in response to drought since this will be a key indicator of plant resilience in future environments. As result, under water deficit, the selected biofertilizers enhanced plant growth, leaf water potential, and electrical conductivity parameters. Further, the dual-inoculation of AMF/PGPR amended with composts alone or in combination boosted the biomass under water deficit conditions to a greater extent than in non-inoculated and/or non-amended plants. Both single and dual biofertilizers improved physiological parameters by elevating stomatal conductance, photosynthetic pigments (chlorophyll and carotenoids content), and photosynthetic efficiency. The dual inoculation and compost significantly enhanced, especially under drought stress, the concentrations of sugar and protein content, and antioxidant enzymes (polyphenoloxidase and peroxidase) activities as a defense strategy as compared with controls. Under water stress, we demonstrated that phosphorus was improved in the inoculated and

amended plants alone or in combination in leaves (AMF2: 807%, AMF1+B2: 657%, AMF2+C1+B2: 500%, AMF2+C2: 478%, AMF1: 423%) and soil (AMF2: 397%, AMF1+B2: 322%, AMF2+C1+B2: 303%, AMF1: 190%, C1: 188%) in comparison with controls under severe water stress conditions. We summarize the extent to which the dual and multiple combinations of microorganisms can overcome challenges related to drought by enhancing plant physiological responses.

Keywords: arbuscular mycorrhizal fungi, climate change, compost, PGPR, plant fitness, photosynthesis, agro-physiological responses, water deficit

INTRODUCTION

Owing to rapid climate change, drought is becoming one of the most important environmental stresses that is outside of plants' physiological limits and is causing a substantial decline in crop productivity (Shaw and Etterson, 2012; Sarwat and Tuteja, 2017). Drought influences transport and availability of soil nutrients (Vurukonda et al., 2016), and it affects morphological, physiological, and nutritional traits of plants especially water content, leaf water potential, photosynthetic pigment, stomatal conductance and phosphorus (P) and nitrogen (N) absorption (Jaleel et al., 2009; Augé et al., 2014; Baslam et al., 2014; Meddich et al., 2015a, 2018; Symanczik et al., 2018). Drought also affects antioxidant defense leading to oxidative stress owing to the accumulation of reactive oxygen species (ROS) such as hydrogen peroxide (Maheshwari et al., 2012; Vurukonda et al., 2016; Abdel Latef et al., 2019a,b). On a higher scale, when plants are exposed to drought that alters their photosynthesis machinery, this can shift source/sink relationships of photosynthate, symbiotic interactions, plant growth, and fitness (Becklin et al., 2016; Sever et al., 2018). The inhibition and degradation of chlorophyll synthesis through ROS over-accumulation leads to a decrease of photosynthetic activity (Abd El-Mageed et al., 2018; Duo et al., 2018).

The date palm (*Phoenix dactylifera* L.) is a dioecious evergreen tree with major ecological and socio-economic roles in many countries, mainly arid zones (Chao and Krueger, 2007). Indeed, the economic importance of the palm family of plants (Arecaceae) ranks second only to the grass family (Poaceae) among monocotyledons and the third in the world (after the Gramineae and Leguminosae families) (FAO[1]). The economic utility of these palms is based on their fruits and derived beverages as a staple food, their wood, as palms are used in building and the artisanal sector, where they are used for ornamental purposes (Arias et al., 2016). In addition, in oasis ecosystems, date palms create a microclimate that is essential for the cultivation of underlying crops such as fruit trees, vegetables and forage species (Meddich et al., 2019). However, date palm groves are subjected to biotic (primary *fusarium* wilt) and abiotic (mainly drought and salinity) constraints as well as low soil fertility and management that have decimated this crop thus deteriorating oasis ecosystems, hindering agricultural production under this environmental instability, and driving higher levels of migration (Oihabi, 1991; Meddich et al., 2015a, 2018; Arias et al., 2016; Meddich and Boumezzough, 2017; FAO, 2018; Whitman, 2019). Factors such as drought, exacerbated by climate change, will affect plant physiology by altering plant-organism interactions since plant species evolve in complex environments with networks of interacting species. Although studies have examined various ways of handling stress inducers to increase plant survival and performance, little has been done on the integrative aspect of this improvement approach to protecting and empowering plants to resist and grow better under drought conditions. In this regard, management practices and strategies that allow plants to resist abiotic and biotic stresses are urgently required and should be exploited to improve agricultural production (Meddich et al., 2018, 2019), reduce the use of pesticides and chemical fertilizers, and protect crops and soil quality (Shen et al., 2013). It should be noted that the plant nursery industry – being trees and fruit plants the most important nursery crops- constitutes a large and growing sector of agriculture. The regular practice of cultivating vitro plants by farmers under nursery conditions prior to field transplantation involves growing the plants only in sandy soil without any amendments. At the time of planting is especially apparent when outplants face stresses and/or strong competition from other vegetation. At this stage, the growth potential of planting stock plays a primordial role for the transplanting success. The application of biofertilizers such as organic fertilizers and beneficial soil microorganisms has emerged as a potential solution to promote plant fitness, boost yield, and tolerance to environmental constraints (Abdel Latef and Chaoxing, 2011; Meddich et al., 2015b; Abdel Latef et al., 2016; Padilla et al., 2017; Júnior et al., 2018; Symanczik et al., 2018; Ait-El-Mokhtar et al., 2019; Ben-Laouane et al., 2019; Raklami et al., 2019). The appropriate management of plant nutrition, growth, and tolerance to drastic constraints such as drought, salinity and soil poverty is becoming a key component in increasing crop yield under changing environmental conditions (Zou and Wu, 2011; Baslam and Goicoechea, 2012; Maheshwari et al., 2012; Hidri et al., 2016; De Pascale et al., 2017; Meddich et al., 2018). In addition to regulating nutrient acquisition, inoculation with Arbuscular Mycorrhizal Fungi (AMF) and Plant Growth Promoting Rhizobacteria (PGPR) are successfully being seen to be an effective substitute to ensure stable, safe and sustainable agricultural and biomass production (Wu and Zou, 2017; Zhang et al., 2018; Kumar et al., 2019; Kumari et al., 2019; Abdel Latef et al., 2020). Indeed, the beneficial effects of the inoculation by the rhizosphere microbial communities are linked with nutrient recycling,

[1]http://www.fao.org

mineral nutrition. solubilisation of nutrients such as P, potassium (K) and iron (Fe), biodegradation of soil organic matter, phytohormone and antibiotics productions, improvements in soil structure and aggregation, and enhancement of plant resistance to pests and diseases (Al-Karaki, 2000, 2006; Al-Karaki et al., 2004; Nadeem et al., 2014; Rillig et al., 2014; Grobelak et al., 2015; Kumar et al., 2015; Meddich et al., 2018, 2019; Symanczik et al., 2018; Raklami et al., 2019; Wu et al., 2019). The (co)-inoculants of PGPR and/or AMF can advance the nutrient use efficiency of fertilizers (Adesemoye et al., 2009). Moreover, AMF and/or PGPR inoculation could mitigate the detrimental effect of stresses through the enhancement of photosynthetic efficiency, overproduction of antioxidant enzymes and/or non-enzymatic antioxidants, and/or activation of the mycorrhizal induced resistance (MIR) mechanism by bypassing plant defense (Pozo and Azcón-Aguilar, 2007; Bompadre et al., 2014; Nadeem et al., 2014; Pieterse et al., 2014; Gusain et al., 2015; Lenoir et al., 2016; Duo et al., 2018; Javan Gholiloo et al., 2019). Although PGPR and AMF are commonly applied as beneficial microorganisms in agriculture and several studies have been devoted to studying the influence of this symbiosis on the plant response to abiotic stress, the mechanisms responsible for increased plant tolerance to stress have yet to be fully elucidated. Also, little is known about the agro-physiological changes occurring in the plants when these microorganisms are applied together. It has been suggested that the combined application of both microorganisms has positive effects on the nutritional composition of several plant species (Nadeem et al., 2014; Ben-Laouane et al., 2019).

Furthermore, the exogenous introduction of beneficial organic substances such as compost has been evaluated previously (Nikitas et al., 2008) as a soil conditioner in agriculture or a substitute to chemical fertilizers to improve resilience, yield, and tolerance of plants to the toxicity of these stress-imposed conditions. The use of local composts represents an eco-friendly alternative for plant growth, mineral nutrition, soil organic matter content, and soil properties such as water retention capacity and soil suppressiveness (Shen et al., 2013; Luciens et al., 2014; Mehta et al., 2014; Kwey et al., 2015; Ning et al., 2017). Previous studies have suggested that compost application in soil increased the supply of organic carbon and N for microbial communities and improved soil health and plant yield (Shen et al., 2013; Liu et al., 2018). Further, compost application triggers plant resistance to different environmental stresses (Tartoura et al., 2014; Ortuño et al., 2018) by increasing the photosynthetic activity (Abd El-Mageed et al., 2019; Khosravi Shakib et al., 2019). In the current research, we explored the agro-physiological and biochemical responses involved in drought adaptation in date palms, and the functionality of the single and dual-use of selected strains of PGPR and native and exotic AMF with or without the addition of two composts. The objective of this study was to evaluate the morpho-physiological basis of drought responses in date palms under implementation of eco-friendly cultivation practices. The results obtained here will provide a deeper understanding of the mechanisms of date palm tolerance to long-term drought stress as well as paving the way for identification of the best factors that led to successful outcomes in the biofertilization experiments for other crops.

MATERIALS AND METHODS

Biofertilizer Materials

Two types of AMF inoculants were used in our experiment: (i) an exogenous AMF strain (*Rhizoglomus irregulare*, DAOM 197198) provided by the Plant Biotechnology Institute of Montreal (Canada) and (ii) an indigenous consortium of AMF isolated from the Tafilalet palm grove located 500 km southeast of Marrakesh and containing a mixture of native species: (i) *Glomus* sp. (15 spores/g of substrate), (ii) *Sclerocystis* sp. (9 spores/g substrate), and (iii) *Acaulospora* sp. (1 spore/g of substrate) (Meddich et al., 2015a). The inoculum was enriched in propagules by co-cultivation with *Zea mays* L. as the host plant under controlled greenhouse conditions. Corn roots containing hyphae, vesicles, and spores were harvested, cut into small pieces and used as the inoculum. Inoculation of date palm was performed by adding 40 g of the inoculum (roots and substrate containing spores) to the date palm root system. Non-mycorrhizal (NM) treatments received an equal quantity of both non-inoculated (and non-mycorrhizal) *Z. mays* roots to match 'organic matter' in the pots and filtered inoculum in an attempt to restore other soil free-living microorganisms accompanying the AMF. The filtrate for each pot was obtained by passing the mycorrhizal inoculum in 20 mL of distilled water through a layer of 15- to 20-μm filter papers (Whatman, GE Healthcare, Buckinghamshire, United Kingdom).

The bacterial inocula used in our study consisted of four PGPR isolates (Z1, Z2, Z4, and ER21 strains) isolated from the date palm groves rhizosphere (Tafilalet, Morocco). The inocula were prepared by growing the strains in Tryptic Soy Broth (TSB) liquid culture at 28°C to an optical density of 1 at 600 nm (about 10^9 CFU/mL). The plant inoculations were carried out by adding 4 mL of the bacterial suspension formed from the four abovementioned strains into equal volumes closer to the roots. After 15 days, a second inoculation (booster) was carried out by placing another 4 mL of the bacterial suspension next to the plant roots to increase the bacterial rate in the soil and ensure the infection of the newly formed roots.

The quantification *in vitro* of plant growth-promoting traits of the strains used was examined by standard protocols: phosphate solubilization was performed by the production of halo on agar medium as described by Alikhani et al. (2006) and the tolerance to water deficiency was tested by the resistance to polyethylene glycol. A confrontation assay was carried out to confirm the absence of inhibition between the four strains. The PGPR characteristics of the four strains are listed in **Table 1**.

The composts used were prepared from grass (C1) and a mixture of green (C2) waste as described by Meddich et al. (2016). The composts (5% *W*/*W* with respect to culture soil) were added

TABLE 1 | Phosphate solubilization and resistance to polyethylene glycol (tolerance to water deficiency) of the four tested PGPR strains (Z1, Z2, Z4, and ER21).

Activity	Z1	Z2	Z4	ER21
Phosphate solubilization	+	+	+	+
Resistance to polyethylene glycol 6000	+	+	−	−

to the corresponding pots at date palm vitroplants transplanting (Anli et al., 2020). The physicochemical and microbiological properties of the two composts are presented in **Table 2**.

Experimental Design

Date palm vitroplants (*Phoenix dactylifera* L.) of variety Boufgouss -an elite variety with high commercial importance- were transplanted at the two leaf stage into 2.4 L plastic buckets filled (4/5) with sterilized soil (at 180°C for 3 h on 3 consecutive days) alone or mixed with compost at 5%. The soil used (bulk density: 1.32 ± 0.01 g cm^{-3}) had the following characteristics: sand, 51%; clay, 19%; loam, 30%, available phosphorus, 11 ppm; organic matter, 1%; total organic carbon, 0.58%; nitrogen, 0.84 mg/g; EC 0.19 mS/cm; and pH, 8.6. The soil bulk density did not vary in every treatment. The finely textured soil to successfully grow date palm, instead of sand, has been used to achieve fast equilibrium rates during drying. The plants were watered and maintained at 75% field capacity (FC). During the pre-sowing period, irrigation was applied to FC to ensure full stand establishment in all treatments. Soil moisture was measured randomly in untreated and treated pots in each treatment using a TDR meter (Delta UK Ltd., Clacton-on-Sea, United Kingdom) in the morning and evening of each day. According to the measured soil water content, soil bulk density, soil moisture maximum field capacity and soil weight, the amount of needed water under different water conditions was calculated. Plants were grown in the greenhouse at 25.5°C (16/8 h light/dark) with fluorescent lighting (500 μmol m^{-2} s^{-1}) and average relative humidity of 68.5%.

The experiment was carried out in a fully randomized design with 10 biological replicates for each treatment (in total 54 treatments) and all plants were placed randomly in the greenhouse (**Table 3**).

Three months after experiment start, two water regimes were imposed 75 and 25% FC (Baslam et al., 2014; Meddich et al., 2015a, 2018).

Chlorophyll Fluorescence and Stomatal Conductance Determinations

Chlorophyll fluorescence was measured by a fluorometer (OPTI-SCIENCE, OS30p). Dark adaptation was made on the upper side of the second fully developed leaf from the apex by obscuring for 20 min. This parameter was measured by transmission at 650 nm on a leaf area of 12.5 mm^2. The fluorescence signal was recorded for a second at an acquisition speed of 10 μs (Strasser and Strasser, 1995). Stomatal conductance (g_s) was determined as described by Harley et al. (1992).

Photosynthetic Pigments Quantification

The concentration of chlorophyll *a*, *b*, total chlorophyll, and carotenoids was determined according to the method described by Arnon (1949). Photosynthetic pigments were extracted from the frozen leaf powder subsample using cold acetone 80%. Following centrifugation at 10,000 × *g* for 10 min, supernatant absorbance was read at 480, 645, and 663 nm using a UV–visible spectrophotometer (UV-3100PC spectrophotometer, VWR).

Leaf Water Potential

Leaf water potential (Ψ_w) was measured using a pressure chamber (Model 600-EXP Super Pressure Chamber, PMS instrument, Albany, OR, United States) at predawn (06:00–08:00 h). The measurements were taken on mature fully expanded leaves from the upper part of the stem. Cutting leaves water potential were measured over the same days and immediately after gas exchange measurements.

Growth Assessment and Mineral Analysis

The growth performance of date palm plants was assessed by measuring the number of leaves, shoot height, root length, leaf area, and total dry matters (DM; obtained after drying samples at 80°C until the weight remained constant). The first fully expanded leaf of date palms in each treatments was harvested at the end of the light period, snap-frozen, ground to a fine powder in liquid N using a pestle and mortar, and kept at −80°C for the subsequent biochemical analyses.

For mineral analyses, the dried shoots were grounded using a coffee mill. Shoot N concentration was measured according to the method described by Rodier (1984). Shoot P concentration was estimated using the Olsen method (Olsen and Sommers, 1982) by incinerating the shoot powder (500 mg) in a muffle furnace before acid extraction.

Mycorrhization Assessment

Root samples were washed with distilled water and cleaned with 10% of KOH at 90°C for 30 min. Then, they were washed again and acidified with 2% HCl for 10 min and stained with Trypan blue at 90°C for 20 min according to Phillips and Hayman (1970). The microscopic assessment of mycorrhizal root colonization rates was performed according to the method of Trouvelot et al. (1986).

Total Soluble Sugars Quantification

Total soluble sugars (TSS) were determined in 0.1 g of the frozen leaf powder in 80% (v/v) ethanol. The quantity of TSS was determined according to Dubois et al. (1956) in

TABLE 2 | Physico-chemical and microbiological properties of the composts used in this study.

Composts	pH	EC (mS/cm)	COT (%)	NTK (%)	C/N	P (mg/g)	Bacterial population (CFU/g)	Fungal population (CFU/g)
Compost (C1)	7.86	7.10	30.65	2.19	14.00	0.270	1.65×10^8	4.30×10^5
Compost (C2)	7.80	8.50	27.24	1.32	20.64	0.266	2.12×10^5	9.75×10^4

EC, electrical conductivity; TOC, total organic carbon; TKN, total Kjeldahl-nitrogen; C/N, carbon-to-nitrogen ratio; P, phosphorous; CFU, colony-forming unit.

TABLE 3 | Different treatments (and their nomenclature) applied in this study.

Treatments	Water regime	
Control	75% FC	Plants non-amended with compost and no-inoculated with AMF/PGPR
B1	25% FC	Plants non-amended with compost, no-inoculated with AMF, and inoculated with PGPR consortia B1 (Z1+Z2)
B2		Plants non-amended with compost, no-inoculated with AMF, and inoculated with PGPR consortia B2 (Z1+Z2+Z4+ER21)
C1		Plants amended with compost C1 (grass waste), no-inoculated with AMF/PGPR
C1 + B1		Plants amended with compost C1, no-inoculated with AMF, and inoculated with PGPR consortia B1
C1 + B2		Plants amended with compost C1. no-inoculated with AMF, and inoculated with PGPR consortia B2
C2		Plants amended with compost C2 (mixture of green waste) and no-inoculated with AMF/PGPR
C2 + B1		Plants amended with compost C2, no-inoculated with AMF, and inoculated with PGPR consortia B1
C2 + B2		Plants amended with compost C2. no-inoculated with AMF and inoculated with PGPR consortia B2
AMF1		Plants inoculated with AMF1 (exogenous *R. irregulare*), non-amended with compost, and no-inoculated with PGPR
AMF1 + B1		Plants inoculated with AMF1, inoculated with PGPR consortia B1, and non-amended with compost
AMF1 + B2		Plants inoculated with AMF1, inoculated with PGPR consortia B2, and non-amended with compost
AMF1 + C1		Plants inoculated with AMF1, amended with C1, and no-inoculated with PGPR
AMF1 + C1 + B1		Plants inoculated with AMF1, inoculated with PGPR consortia B1, and amended with C1
AMF1 + C1 + B2		Plants inoculated with AMF1, inoculated with PGPR consortia B2, and amended with C1
AMF1 + C2		Plants inoculated with AMF1, amended with C2, and no-inoculated with PGPR
AMF1 + C2 + B1		Plants inoculated with AMF1, inoculated with PGPR consortia B1, and amended with C2
AMF1 + C2 + B2		Plants inoculated with AMF1, inoculated with PGPR consortia B2, and amended with C2
AMF2		Plants inoculated with AMF2 (indigenous consortium of AMF), non-amended with compost, and no-inoculated with PGPR
AMF2 + B1		Plants inoculated with AMF2, inoculated with PGPR consortia B1, and non-amended with compost
AMF2 + B2		Plants inoculated with AMF2, inoculated with PGPR consortia B2, and non-amended with compost
AMF2 + C1		Plants inoculated with AMF2, amended with C1, and no-inoculated with PGPR
AMF2 + C1 + B1		Plants inoculated with AMF2, inoculated with PGPR consortia B1, and amended with C1
AMF2 + C1 + B2		Plants inoculated with AMF2, inoculated with PGPR consortia B2, and amended with C1
AMF2 + C2		Plants inoculated with AMF2, amended with C2, and no-inoculated with PGPR
AMF2 + C2 + B1		Plants inoculated with AMF2, inoculated with PGPR consortia B1, and amended with C2
AMF2 + C2 + B2		Plants inoculated with AMF2, inoculated with PGPR consortia B2, and amended with C2

0.2 mL of the supernatant mixed with 0.2 mL of phenol and 1 mL of concentrated sulfuric acid. After 15 min, TSS content was determined by measuring the absorbance at 485 nm and calculated using the standard glucose curve.

Total Soluble Proteins and Antioxidant Enzymes

Frozen leaf powder subsamples (0.1 g) were homogenized in a cold mortar with 4 mL of 1 M phosphate buffer (pH 7) containing 5% polyvinylpolypyrrolidone (PVPP). The homogenate was centrifuged at 18,000 × *g* for 15 min at 4°C and the supernatant was used to measure antioxidant enzyme activities (Tejera García et al., 2004). Total soluble proteins were determined according to the technique described by Bradford (1976). Peroxidase (POX) activity was measured as described previously (Hori et al., 1997). The reaction mixture (3 mL) contained 1 M phosphate buffer (pH 7.0), 20 mM guaiacol, 40 mM H_2O_2, and 0.1 mL of the enzymatic extract which was added to start the reaction. POX activity was determined at 470 nm by its ability to convert guaiacol to tetraguaiacol ($\varepsilon = 26.6\ mM^{-1} \cdot cm^{-1}$) One unit of POX activity was defined as an absorbance change of 0.01 unit min^{-1}. Polyphenol oxidase (PPO) was estimated by the method of Hori et al. (1997). The assay solution contained 20 mM catechol in 0.1 M phosphate buffer (pH 7). The reaction was started by addition of 100 μL of the enzymatic extract. PPO activity was expressed in enzyme unit mg^{-1} protein. One unit of PPO activity was defined as the amount of enzyme causing an increase in the absorbance of 0.001/min at 420 nm.

Malondialdehyde and Hydrogen Peroxide Content

Malondialdehyde (MDA) content in leaves was estimated by homogenizing the frozen leaf powder subamples (0.25 g) in 10 mL of 0.1% (w/v) trichloroacetic acid (TCA) and centrifuging at 18,000 *g* for 10 min as described by Madhava Rao and Sresty (2000). Two milliliters of supernatant were mixed with 2 mL of 20% TCA containing 0.5% Thiobarbituric acid (TBA). The mixture was then heated in a water bath at 100°C for 30 min and immediately cooled in an ice bath. The absorbance was read at 532 nm. The nonspecific turbidity was corrected by subtracting A600 from A532, and the MDA content was calculated as follows: $[MDA] = 6.45\ (A_{532} - A_{600}) - 0.56A_{450}$.

Hydrogen peroxide (H_2O_2) concentration in leaves was determined by the method described by Velikova et al. (2000). Briefly, 0.25 g of the frozen leaf powder were homogenized with 5 mL 10% (w/v) TCA and then centrifuged at 15,000 *x g* for 15 min at 4°C. The supernatant (0.5 mL) was recovered to determine the content of H_2O_2 and 0.5 mL of potassium phosphate buffer (10 mM, pH 7) and 1 mL of iodic potassium (1 M) was added. After 1 h of incubation, the absorbance at 390 nm

was recorded and plotted against a standard H_2O_2 curve. The blank was made by replacing the sample extract by 10% TCA.

Soil Analyses

At plant harvest, soil physicochemical properties were analyzed on samples taken near the roots. The pH and electrical conductivity (EC) were measured in a diluted soil suspension 1/5 (v/v) using a pH meter HI 9025 and a conductivity meter HI-9033 (Hanna Instruments, Padua, Italy), respectively. Total organic carbon (TOC) and organic matter (OM) were measured according to the method described by Aubert (1978), which consists of the oxidation of organic matter by potassium dichromate in the presence of sulfuric acid. Available P was determined according to Olsen and Sommers method (1982). The amount mineral N available in soil was measured according to the method described by Rodier (1984).

Statistical Analysis

Data are presented as mean ± SE (standard error) of six independent biological replicates. Data were analyzed by employing one-way analysis of variance (ANOVA) followed by Tukey's honest significant difference test using a significance level of 5% ($p \leq 0.05$). Normality of residuals was tested using the Shapiro-Wilk test. Mycorrhizal root colonization rates were arcsin-square root transformed to fit the assumption of normal distribution. Multivariate analysis of variance (MANOVA) was performed using SPSS 10.0 software to determine the interaction among the tested factors (AMF × Bacteria × Compost × Drought). Different lower cases indicate significant differences among treatments at $p \leq 0.05$. In order to integrate all the data, a complete dataset comprising all growth, physiological, and biochemical data was subjected to Principal Components Analysis (PCA). The PCA was performed using XLSTAT v. 2014.

RESULTS

Mycorrhization Parameters

Our results showed that no mycorrhizal structure was observed in the roots of non-treatment controls. The frequency and intensity of AMF in date palm roots was significantly decreased by drought stress (**Supplementary Table 1**). The plants inoculated with AMF, especially for AMF1, without compost and PGPR showed the higher root colonization intensity compared to plants treated with compost and PGPR (**Figures 1A,B**). AMF infection frequency and intensity showed no significant difference between date palm inoculated with AMF alone or combined with PGPR and/or composts (bi- and tripartite combinations) under drought stress conditions (**Figures 1A,B**). The interactions between AMF and drought were significant for these two parameters (**Supplementary Tables 1A** and **B**).

Growth Assessment and Mineral Nutrition

Drought caused a significant decrease ($P < 0.001$) (**Supplementary Table 1**) in all the growth parameters such as leaf number, plant height, root length, leaf area (**Table 4**), and total dry weight (**Figure 2**). Our results showed that the un-inoculated and un-amended control performed very weak response in all these parameters compared to the treated plants under both well-watered and drought stress conditions (**Figure 2**, **Table 4**, and **Supplementary Figure 1**). Under drought stress, however, the application of bi- and tripartite combinations of biofertilizers (AMF1+C1, AMF1+C1+B1, AMF2+C2+B1, and AMF2+C1+B2) showed positive effects by promoting date palm shoot height and root length to a greater extent than in non-inoculated and non-amended plants. Moreover, the compost alone, bi and tripartite combinations (AMF1+C2+B1, AMF2+C2, C2) increased the number of leaves as compared to non-inoculated and non-amended date palm plants under well-watered and water deficit conditions. The plants treated with AMF1+C1, AMF2+B2, and AMF2+C2 improved the leaf area compared to non-inoculated and non-amended vitroplants under water deficit. A positive effect on the total dry weight of vitroplants subjected to water stress was recorded after application of biofertilizers (**Figure 2**). Indeed, the AMF and compost alone, bi and tripartite combinations (5 g in AMF2+C2 and C2, 4.8 g in AMF1+C1, and 4.6 g in AMF2, AMF1+B1, and AMF2+C1+B1) showed the highest values of this parameter under water deficit in comparison with non-inoculated and non-amended vitroplants (ca. 2.4 g).

We assayed the P and N content in shoots of date palm plants under drought and different biofertilizers, since the degree of stress and growth depend on their uptake and translocation. Under the control condition (75% FC), shoot P was significantly increased in plants treated with AMF (**Figure 3A**) as compared to non-amended and non-inoculated control plants, whereas under drought stress, it was decreased. Under water deficit, shoot P content was significantly increased by C1+B1, AMF1, AMF1+B2, AMF1+C1+B1, AMF2, AMF1+B1+C1AMF2+C1+B2, and AMF2+C2 in comparison with non-treated plants (**Figure 3A**). Under 75% FC, N levels in leaves of all treated plants remained significantly higher than in control conditions. Drought stress decreased N content in all treatments, and all the biofertilizer treatments were able to maintain higher content than non-amended and non-inoculated control plants (**Figure 3B**). The interaction between drought × C1 × B1 (**Supplementary Table 1A**), drought × B2, and drought × C1 × B2 (**Supplementary Table 1B**) had a significant effect ($P < 0.01$) on P, while N showed a significant effect between drought × AMF2 (**Supplementary Table 1B**).

Physiological Traits

All physiological parameters were significantly decreased by drought ($P < 0.001$) (**Supplementary Table 1**). Under water scarcity, the leaf water potential values were decreased in non-inoculated and non-amended control plants. Plant inoculation with AMF and/or PGPR amended or not with the compost yielded an improvement in leaf water potential under water deficit, especially AMF1 (−1 MPa), AMF1+C1+B1 (−1.15 MPa), and AMF2+C2+B2 (−1.20 MPa) versus non-inoculated and no-amended plants (−2.18 MPa) (**Figure 4A**).

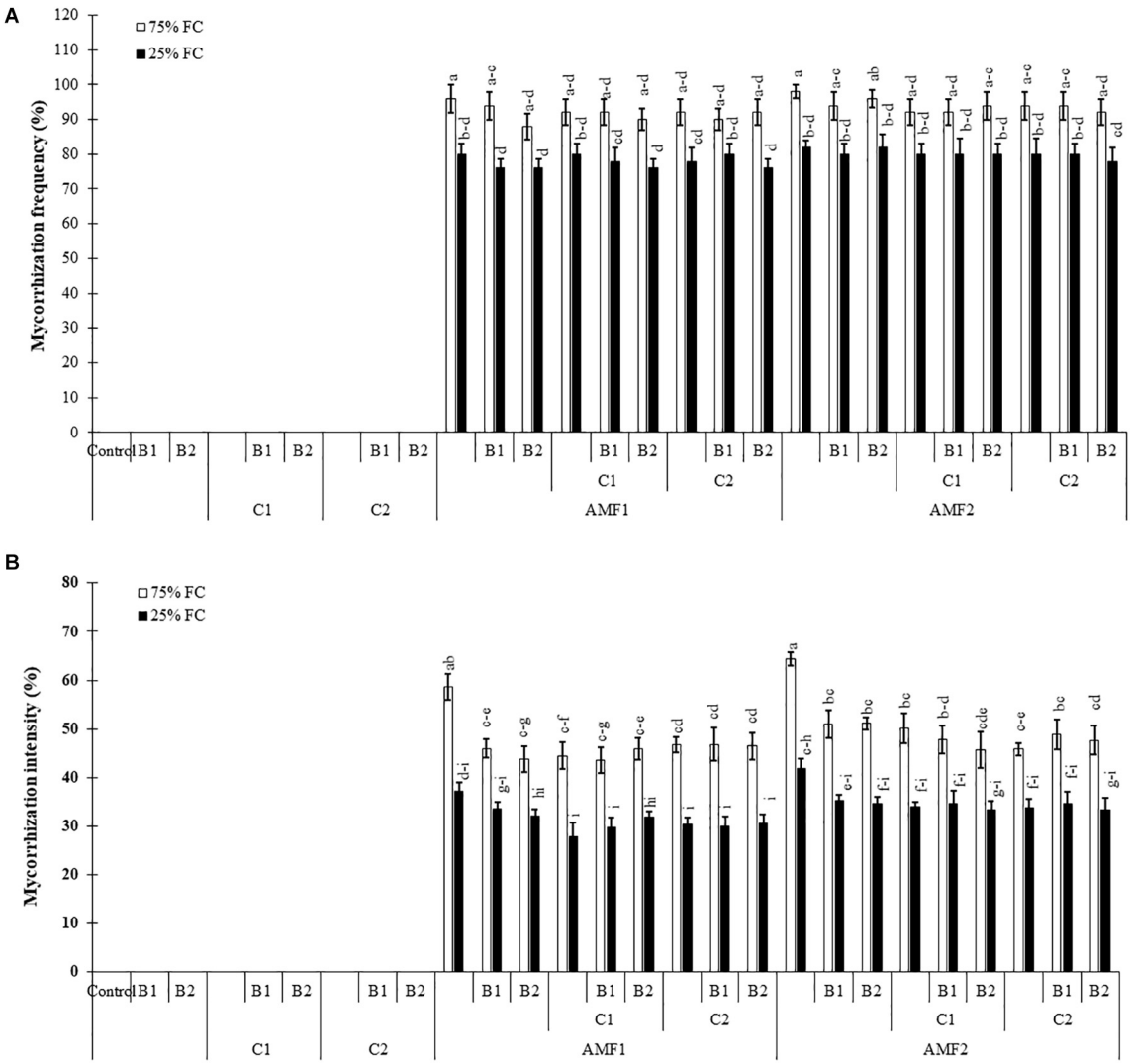

FIGURE 1 | Influence of different water regimes [75% field capacity (FC); open bars and 25% FC; filled bars] on **(A)** mycorrhization frequency and **(B)** intensity in control plants (non-amended, non-inoculated), and plants amended with composts (C1 or C2) and/or inoculated with arbuscular mycorrhizal fungi (AMF, exogenous AMF1 or native AMF2) or plant growth promoting rhizobacteria (PGPR) strains (B1 or B2). Data are mean ± SE of six biological replicates. Means followed by the same letters are not significantly different at $P < 0.05$ (Tukey's HSD).

Under water control condition, there was obvious stomatal conductance differences between non-amended/non-inoculated and treated plants with AMF and/or PGPR. Under water stress, stomatal conductance values decreased in date palm plants. However, the application of biofertilizers increased stomatal conductance, with AMF1 alone, the bi- (C2+B1, AMF1+B1, AMF1+B2, AMF1+C2, and AMF2+B1) and tripartite (AMF1+C2+B1, AMF1+C2+B2, AMF2+C1+B2, and AMF2+C2+B2) combinations being the most effective in improving this parameter compared to control plants (**Figure 4B**).

As shown in **Figure 4C**, the chlorophyll fluorescence (F_v/F_m) was only slightly affected by drought stress. Biofertilizer application improved F_v/F_m in date palm plants under water shortage. The single (AMF1, PGPR B2 and compost C1), bi- (AMF1+C2), and tripartite (AMF2+C1+B2) combinations presented the most effective treatments to increase chlorophyll fluorescence under water deficit conditions compared to non-inoculated and non-amended plants.

In response to drought stress and inoculation with AMF, PGPR and compost application, chlorophyll *a*, *b*, total chlorophyll, and carotenoid content are shown in **Figure 5**. Under water deficit, the photosynthetic pigment content was reduced. However, the application of AMF, compost, and PGPR especially the combination C2+B1, AMF2+C1+B2, AMF2+C2+B1, AMF1, and AMF2+C2+B2 increased pigments contents compared to control plants, under water stress conditions. As for carotenoid content, this was positively affected by biofertilizers applied alone (B1, B2, C2, C1, AMF2, and AMF1) or in combination (AMF2+C1, AMF2+C1+B1, AMF1+B2,

TABLE 4 | Influence of different water regimes on growth parameters of non-amended and non-inoculated plants (control), and plants amended and inoculated date palm plants with composts (C1 or C2) and/or arbuscular mycorrhizal fungi (AMF, exogenous AMF1 and native AMF2), and/or plant growth promoting rhizobacteria (PGPR) (B1 or B2).

Treatments	Leaf number		Shoot height (cm)		Root length (cm)		Leaf area (cm^2)	
	75% FC	25% FC	75% FC	25% FC	75% FC	25% FC	75% FC	25% FC
Control	4.6 ± 0.2 fg	3.8 ± 0.2 g	23.6 ± 0.8 lm	21.1 ± 0.6 m	21.9 ± 0.6 n–p	18.5 ± 0.9 p	29.8 ± 1.4 g–j	21.7 ± 0.9 j
B1	5.2 ± 0.2 c–f	4.6 ± 0.2 fg	25.7 ± 0.5 c–m	23.4 ± 0.7 lm	25.2 ± 0.7 d–n	23.2 ± 1.6 i–o	35.0 ± 1.8 c–h	22.7 ± 1.4 ij
B2	6.4 ± 0.2 a–c	5.4 ± 0.2 b–f	27.2 ± 0.4 b–l	23.0 ± 0.7 lm	26.3 ± 1.1 a–m	22.4 ± 1.4 m–p	34.0 ± 1.8 d–h	26.3 ± 1.6 h–j
C1	6.4 ± 0.2 a–c	5.4 ± 0.2 b–f	28.8 ± 1.2 a–j	24.1 ± 0.6 j–m	26.1 ± 0.8 a–m	22.5 ± 1.0 l–p	39.8 ± 1.9 a–f	28.3 ± 1.0 g–j
C1+B1	6.2 ± 0.2 a–d	4.6 ± 0.2 fg	27.5 ± 0.9 b–l	25.0 ± 0.8 f–m	26.7 ± 1.1 a–k	21.9 ± 0.9 n–p	42.5 ± 0.9 a–d	32.7 ± 0.9 f–h
C1+B2	6.0 ± 0.3 a–e	5.0 ± 0.3 d–g	29.8 ± 0.8 a–f	26.6 ± 1.0 b–l	26.6 ± 0.5 a–l	23.4 ± 1.3 i–o	43.3 ± 2.1 a–c	29.3 ± 1.3 g–j
C2	6.8 ± 0.2 a	5.6 ± 0.2 a–f	30.1 ± 0.6 a–d	25.7 ± 0.5 c–m	27.1 ± 0.5 a–j	22.8 ± 0.8 k–o	45.3 ± 1.5 a	34.5 ± 0.8 c–h
C2+B1	6.2 ± 0.2 a–d	5.4 ± 0.2 b–f	27.6 ± 0.9 a–l	25.1 ± 0.9 e–m	24.5 ± 0.2 g–o	21.0 ± 0.4 op	42.0 ± 1.2 a–e	32.0 ± 0.7 f–h
C2+B2	5.8 ± 0.2 a–f	5.4 ± 0.2 b–f	31.0 ± 1.1 ab	26.7 ± 0.9 b–l	28.7 ± 0.9 a–f	23.4 ± 0.5 i–o	48.5 ± 1.7 a	33.0 ± 1.6 f–h
AMF1	6.4 ± 0.2 a–c	5.4 ± 0.2 b–f	30.0 ± 1.3 a–d	27.2 ± 0.5 b–l	27.9 ± 1.3 a–h	23.1 ± 0.4 j–o	43.3 ± 1.7 a–c	31.5 ± 0.7 f–i
AMF1+B1	6.2 ± 0.3 a–d	5.2 ± 0.2 c–f	30.2 ± 0.7 a–c	25.6 ± 0.9 c–m	29.3 ± 0.8 a–d	25.3 ± 0.5 d–n	44.0 ± 1.6 ab	33.0 ± 1.3 f–h
AMF1+B2	6.6 ± 0.2 ab	5.4 ± 0.2 b–f	29.6 ± 0.9 a–g	26.4 ± 0.6 b–l	29.2 ± 1.3 a–d	24.4 ± 0.5 g–o	43.0 ± 1.1 a–c	34.0 ± 1.1 d–h
AMF1+C1	5.6 ± 0.2 a–f	4.8 ± 0.2 e–g	29.9 ± 1.0 a–e	27.6 ± 0.7 a–l	30.0 ± 1.1 a	25.0 ± 0.5 e–o	46.0 ± 1.9 a	34.7 ± 1.5 c–h
AMF1+C1+B1	6.8 ± 0.2 a	5.2 ± 0.2 c–f	30.4 ± 1.3 a–c	27.5 ± 1.1 a–l	29.5 ± 0.5 a–c	27.1 ± 0.5 a–j	45.0 ± 2.2 a	31.3 ± 0.9 f–i
AMF1+C1+B2	5.8 ± 0.2 a–f	5.2 ± 0.2 c–f	29.5 ± 0.5 a–h	26.8 ± 0.9 b–l	30.0 ± 0.8 a	24.9 ± 0.6 e–o	42.0 ± 2.0 a–e	33.0 ± 1.3 f–h
AMF1+C2	6.4 ± 0.2 a–c	5.4 ± 0.2 b–f	28.6 ± 1.2 a–j	24.7 ± 0.7 h–m	28.2 ± 1.2 a–g	26.2 ± 0.6 a–m	45.3 ± 1.7 a	31.7 ± 1.1 f–h
AMF1+C2+B1	5.8 ± 0.2 a–f	5.8 ± 0.2 a–f	27.2 ± 0.8 b–l	24.4 ± 0.7 j–m	27.3 ± 0.4 a–i	24.7 ± 0.5 f–o	44.3 ± 1.9 ab	31.7 ± 1.6 f–h
AMF1+C2+B2	6.2 ± 0.2 a–d	5.0 ± 0.3 d–g	30.2 ± 0.6 a–c	24.8 ± 0.7 g–m	29.0 ± 0.7 a–e	25.6 ± 0.7 b–n	47.8 ± 1.7 a	32.6 ± 1.5 f–h
AMF2	6.2 ± 0.2 a–d	5.4 ± 0.2 b–f	28.9 ± 0.7 a–j	24.8 ± 0.6 g–m	28.8 ± 0.9 a–f	24.4 ± 0.5 g–o	47.8 ± 2.4 a	32.3 ± 1.1 f–h
AMF2+B1	6.0 ± 0.3 a–e	5.2 ± 0.2 c–f	29.5 ± 1.2 a–h	25.9 ± 0.6 c–m	27.9 ± 0.6 a–h	25.2 ± 0.3 d–n	46.3 ± 1.4 a	33.7 ± 1.7 d–h
AMF2+B2	6.2 ± 0.2 a–d	5.4 ± 0.2 b–f	28.5 ± 0.7 a–k	24.6 ± 0.6 i–m	28.8 ± 0.9 a–f	25.4 ± 0.5 c–n	47.5 ± 1.5 a	35.0 ± 0.9 c–h
AMF2+C1	5.8 ± 0.2 a–f	5.0 ± 0.0 d–g	32.3 ± 1.2 a	27.0 ± 0.7 b–l	26.0 ± 0.4 a–n	22.6 ± 0.7 k–p	43.3 ± 1.2 a–c	32.8 ± 1.1 f–h
AMF2+C1+B1	6.2 ± 0.2 a–d	5.4 ± 0.2 b–f	29.4 ± 0.9 a–i	23.8 ± 0.7 k–m	26.1 ± 0.5 a–m	24.0 ± 0.7 h–o	44.5 ± 2.0 ab	34.0 ± 1.4 d–h
AMF2+C1+B2	5.8 ± 0.2 a–f	5.2 ± 0.2 c–f	31.0 ± 0.6 ab	28.4 ± 0.8 a–k	29.6 ± 1.2 ab	27.1 ± 0.7 a–j	45.3 ± 2.2 a	33.5 ± 1.6 e–h
AMF2+C2	6.2 ± 0.2 a–d	5.6 ± 0.2 a–f	29.9 ± 1.3 a–e	26.8 ± 0.4 b–l	26.2 ± 0.8 a–m	23.5 ± 0.5 i–o	46.0 ± 2.1 a	36.0 ± 1.1 b–g
AMF2+C2+B1	6.0 ± 0.3 a–e	4.8 ± 0.2 e–g	32.3 ± 1.1 a	27.3 ± 0.9 b–l	28.5 ± 0.4 a–g	24.8 ± 0.6 f–o	45.0 ± 1.9 a	32.3 ± 1.4 f–h
AMF2+C2+B2	6.0 ± 0.0 a–e	4.8 ± 0.0 e–g	29.9 ± 0.6 a–d	25.3 ± 0.5 d–m	26.5 ± 0.6 a–m	22.7 ± 0.7 k–o	44.5 ± 0.8 ab	33.8 ± 1.6 d–h

Means followed by the same letters are not significantly different $P < 0.05$ (Tukey's HSD).

AMF2+C2+B2, AMF2+C1+B2, and AMF2+C2+B1) as compared with non-inoculated with AMF/PGPR and non-amended with composts, under water deficit.

Biochemical Traits

Treatment effects on biochemical traits were significantly decreased by drought ($P < 0.001$) (**Supplementary Table 1**). Results related to the effect of drought stress and biofertilizer applications on sugar and protein content and POX and PPO activities in date palm plants are presented in **Figure 6**. Under normal water conditions, both compost and AMF increased sugar and protein content. Exposure to water deficit caused a significant decrease in sugar and protein content (**Figures 6A,B**). The addition of biofertilizers yielded a significant increase in sugar and protein compared to stressed control plants. Under 75% FC conditions, POX and PPO did not differ significantly among the biofertilizers treatments (**Figures 6C,D**) Exposure to drought stress led to a considerable increase in the POX and PPO specific activities as compared to non-treated control plants.

To characterize damage caused by drought stress, we carried out MDA and H_2O_2 analyses (**Figure 7**). The exposure of date palm plants to severe water deficit resulted in an increase in MDA and H_2O_2 content. Under water stress, in contrast, the application of single or combined biofertilizers showed reduced MDA and H_2O_2 content compared to non-inoculated and non-amended controls. The interactions AMF1 × C2 × Drought, and AMF1 × B1 × Drought (**Supplementary Table 1A**), AMF2 × C2 × Drought, B1 × Drought, and B1 × Drought (**Supplementary Table 1B**) had a significant effect on H_2O_2 content.

Soil Analysis

We assayed the pH, electrical conductivity, total organic carbon, total organic matter, N, and P content in the soil just after harvesting the plants, since the degree of soil quality depends on their values after the culture (**Table 5**). Under control conditions, the addition of composts increased the soil quality more than controls. Under drought stress, soil analyses at harvest time showed that biofertilizers application - mainly composts - improved soil quality as compared to the controls (**Table 5**). As a result, relative to control plants, the soil pH was decreased following the application of biofertilizers

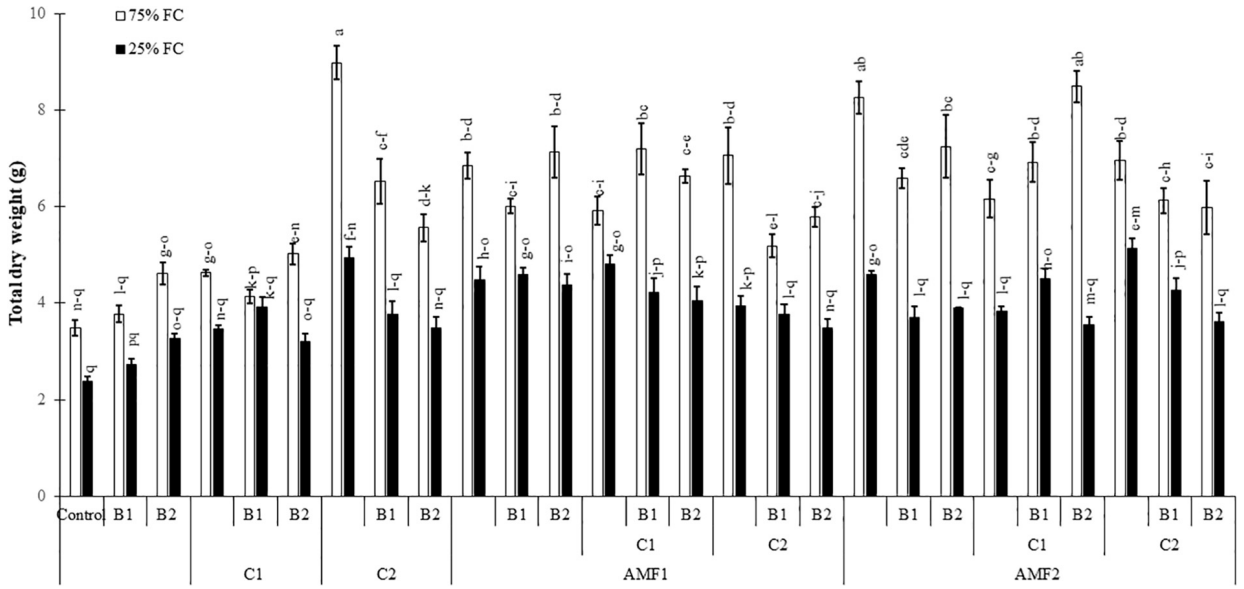

FIGURE 2 | Influence of different water regimes (75% field capacity (FC); open bars and 25% FC; filled bars) on date palm total dry matter in control (non-amended, non-inoculated), and plants amended with composts (C1 or C2) and/or inoculated with arbuscular mycorrhizal fungi (AMF, exogenous AMF1 or native AMF2) or plant growth promoting rhizobacteria (PGPR) strains (B1 or B2) date palms. Data are mean ± SE of six biological replicates. Means followed by the same letters are not significantly different at $P < 0.05$ (Tukey's HSD).

after prolonged drought. Under these conditions, EC, TOC, and OM were improved by biofertilizers. Moreover, under drought stress, both total N and P content in the soil were improved when biofertilizers were applied, especially in the treatments AMF1+B2, AMF1+C2+B1, AMF2, AMF2+B2, AMF2+C1+B2, and AMF2+C2.

Principal Component Analysis (PCA)

The PCA showed that AMF alone or combined with compost and/or PGPR were the most effective treatments to improve growth, nutrition, osmolytes and antioxidant traits (shown in the right panel of **Figure 8A**) under drought stress (**Figure 8A**). PC1 explained 40.8% and PC2 explained 11.9% of the total variance. **Figure 8B** showed that all biofertilizer treatments, single or combined (right panel of **Figure 8B**), were separate from the control. In **Figure 8A**, we observed in the right lower panel of the PC1 component, that the traits PPO, F_v/F_m, OM, TOC, Total Chlorophyll, chlorophyll *a* and *b*, shoot height, carotenoid, and leaf water potential were closely related to soil P and N concentration, shoot P and N content, sugar, root length, leaf area, leaf number, POX, protein, mycorrhizal frequency and intensity, and EC. In contrast, relative to biofertilizer treatments, the non-treatment control separated in the left of the PC1 component (**Figure 8B**) and was related to H_2O_2, MDA and pH traits (**Figure 8A**).

DISCUSSION

In the present study, the application of composts together with inoculation of the exotic and native AMF and PGPR strains inoculations either as single or combined treatments were very effective in helping date palm plants to attenuate the detrimental effects of drought stress on growth, photosynthetic apparatus, nutrient uptake, physiological traits, and oxidative stress. The treated biofertilizers assayed showed a high level of osmotic stress tolerance under water deficit. Our results show that no mycorrhizal structure was observed in the roots of non-treatment controls, but the plants inoculated with AMF were successfully infected by the native or exogenous mycorrhizal consortium under both well-watered and drought conditions. In the presence of water stress, mycorrhization intensity decreased in the AMF treatments alone or in combination with compost and/or PGPR. Our results are in line with several studies showing that mycorrhizal infection decreased when the host plants were exposed to drought stress (Baslam and Goicoechea, 2012; Meddich et al., 2015a; Paymaneh et al., 2019). Under drought stress, however, our findings show an increase of the mycorrhization intensity in date palms treated by compost and PGPR alone or in combination. Cavagnaro (2014) and Kohler et al. (2015) reported that the application of compost at a low dose (2 and 12.5%) increased AMF infection in the root system. Other studies have shown a positive effect of PGPR on enhancing root infection by AMF (Ben-Laouane et al., 2019; Raklami et al., 2019). On the other hand, Sghir et al. (2014) noted that mycorrhizal frequencies and arbuscular content decreased significantly in palm trees inoculated with the combination AMF-PGPR *Trichoderma harzianum* as compared to plants inoculated only with AMF because it colonizes the same space as AMF. However, dual-inoculation AMF-Trichoderma led to the best date palm growth (Sghir et al., 2014). The application of different biofertilizers (alone or in combination) benefited plant growth

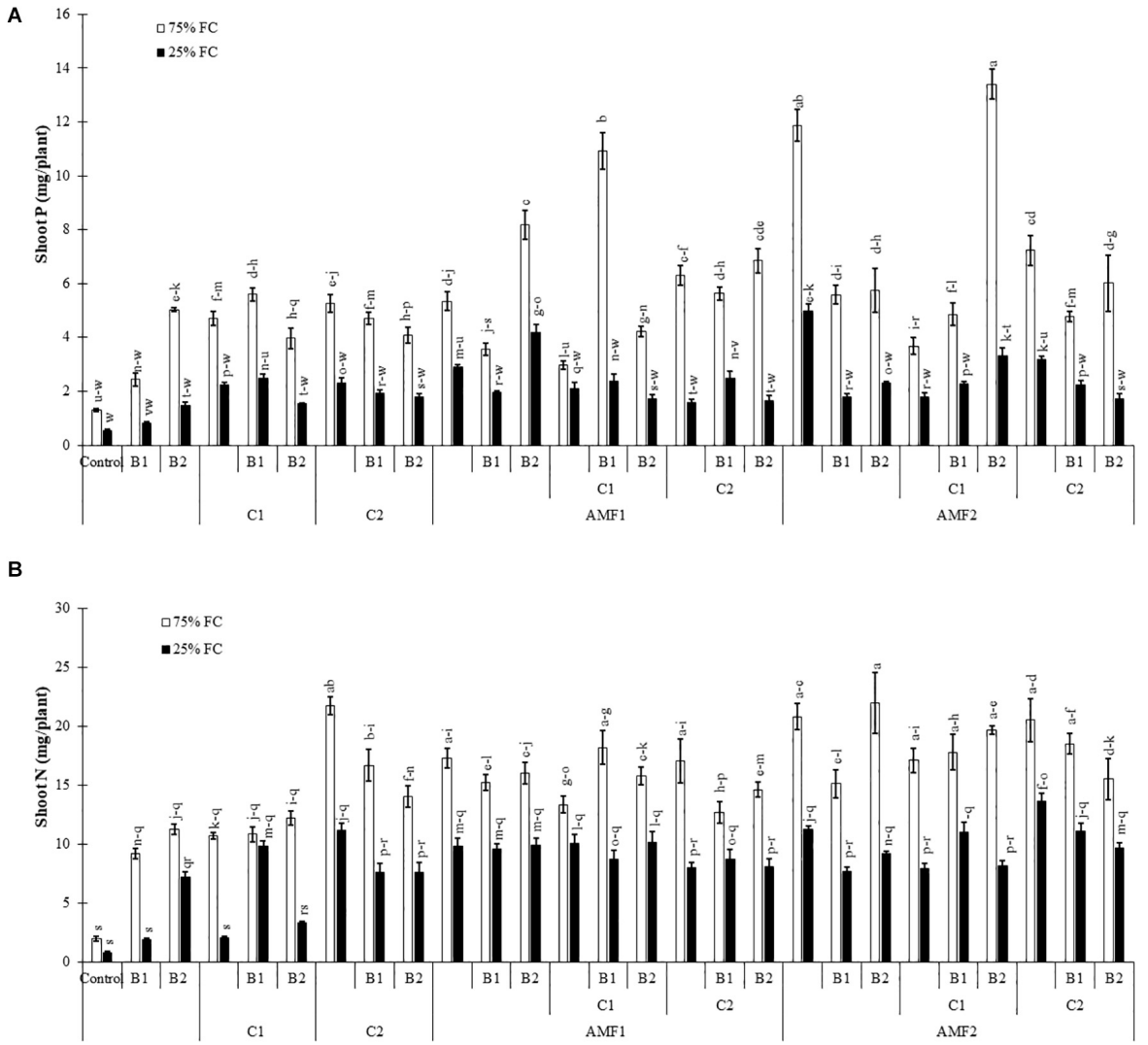

FIGURE 3 | (A) Phosphorous (P) and **(B)** nitrogen (N) content in date palm shoots under two water regimes [75% field capacity (FC); open bars and 25% FC; filled bars] of the tested control (non-amended and non-inoculated) and biofertilizers treatments [composts C1 or C2, arbuscular mycorrhizal fungi (AMF, exogenous AMF1 and native AMF2), and/or plant growth promoting rhizobacteria (PGPR) (B1 or B2)]. Data are mean ± SE of six biological replicates. Means followed by the same letters are not significantly different at $P < 0.05$ (Tukey's HSD).

(mainly leaf number, shoot height, root length, leaf area, and total dry biomass production). The beneficial effect of mycorrhizal and PGPR associations and compost amendment on growth of date palms, under water deficit, could be explained by the greater uptake of nutrients with low mobility such as P and N contained in the substrate. Previous studies demonstrated that date palm and other plants inoculated with AMF accumulated more N and P in leaves than non-mycorrhizal plants when subjected to drought stress (Meddich et al., 2015c; Hao et al., 2019). Javan Gholiloo et al. (2019) showed that the application of biofertilizers (AMF and PGPR) improve the P and N nutrition and consequently enhances date palm plant growth under deficit conditions. Nadeem and colleagues (2014) showed that AMF and PGPR can regulate mineral nutrition by solubilizing nutrients in the soil and producing plant growth regulators (i.e., hormones). Several studies have indicated that compost, AMF and PGPR improve plant growth through the assimilation of immobile soil nutrients such as N and P (Yadav et al., 2013; Baslam et al., 2014; Al-Karaki, 2016; Barje et al., 2016; Frosi et al., 2016; Yang et al., 2018; Raklami et al., 2019; Yu et al., 2019). Here we showed that inoculated and amended date palm plants had considerably higher mineral nutrient content (P and N) as compared to controls under water deficit conditions allowing higher plant performance. This resulted from the better absorption of the surface area provided by extensive fungal hyphae (Wu and Zou, 2017; Zhang et al., 2018) and/or a direct uptake from compost to plant root (Kohler et al., 2015) and/or the mobilization and absorption of various nutrients from soil to plants by PGPR (Grobelak et al., 2015). AMF-colonization results in the establishment of extensive hyphal networks and glomalin

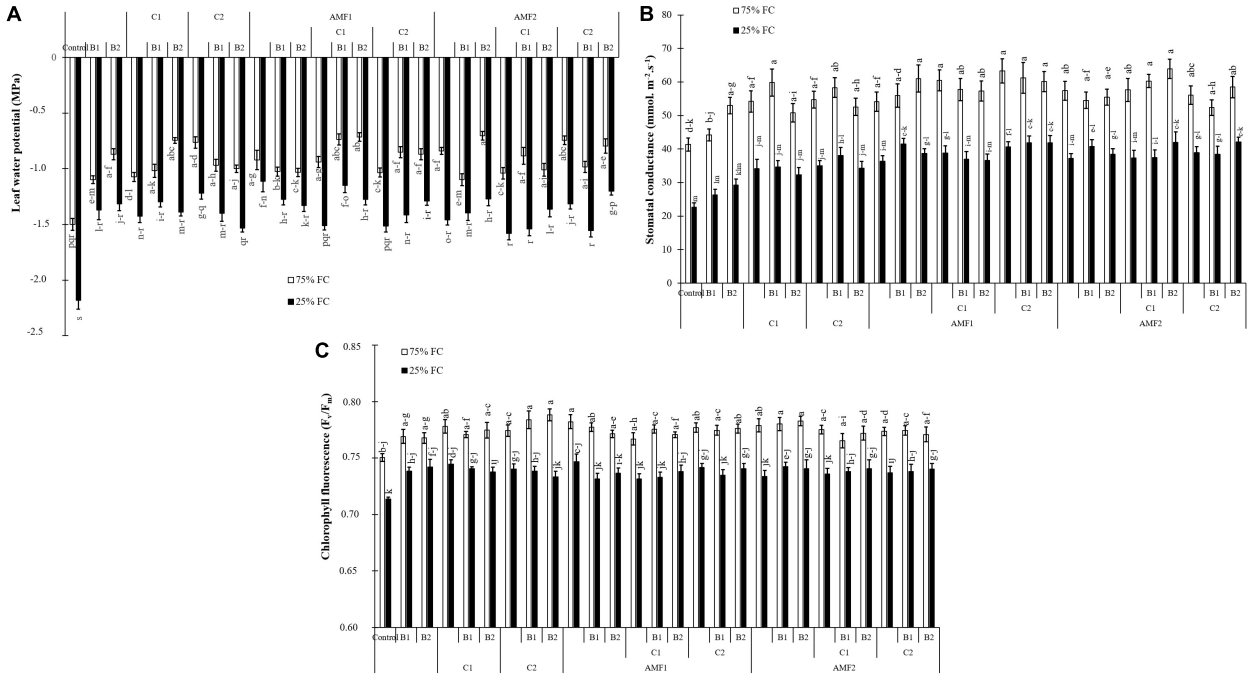

FIGURE 4 | (A) Leaf water potential, **(B)** stomatal conductance, and **(C)** chlorophyll fluorescence of date palm plants under two water regimes [75% field capacity (FC); open bars and 25% FC; filled bars] and grown under control (non-amended and non-inoculated) or biofertilizer applications [composts C1 or C2, arbuscular mycorrhizal fungi (exogenous AMF1 and native AMF2), and/or plant growth promoting rhizobacteria (PGPR) (B1 or B2)]. Data are mean ± SD of six biological replicates. Means followed by the same letters are not significantly different at $P < 0.05$ (Tukey's HSD).

secretion, fueling plants with water and nutrient, and thereby, enhancing soil structure (Pagano, 2014). Recently, Volpe et al. (2016) reported the role of PT family genes as components of the Pi-sensing machinery in root tips, which is up-regulated in AMF colonized plants. In addition to P and N, evidence of the role of AMF and PGPR symbiosis in the "transportome" of several mineral nutrients has been obtained in studies on several plant species (Hogekamp et al., 2011; Casieri et al., 2013).

Physiological traits constitute an important tool to study the effect of drought stress on many plants. Our results showed an increase in leaf water potential, stomatal conductance, F_v/F_m, and chlorophyll pigment synthesis in plants inoculated with AMF and PGPR and/or amended by composts. This improvement of physiological traits can lead to an increase in CO_2 assimilation for photosynthesis. Similarly, several studies have demonstrated the capacity of AMF inoculation to reduce the negative effect of drought stress on date palm growth by improving photosynthesis, water status, and antioxidant activity (Baslam et al., 2014; Meddich et al., 2015a). In our research under drought stress, treated plants reduced the degradation of total chlorophyll *a* and *b* and carotenoid. A higher photosynthetic pigment under drought stress conditions suggests a better performance of the photosynthetic apparatus. Our data show that biofertilizers not only increase water and nutrient uptake to mitigate the negative effect of drought but also improve stomatal conductance. Several studies have reported the existence of a positive correlation between photosynthetic efficiency maintenance and tolerance to drought stress in plants amended with compost and/or inoculated with AMF/PGPR (Wu et al., 2006; Sandhya et al., 2010; Tartoura, 2010; Abd El-Mageed et al., 2018, 2019; Duo et al., 2018; Khosravi Shakib et al., 2019). In response to drought stress, plants treated with biofertilizers showed lower levels of potentials and higher water content, allowing the inoculated and amended plants to sustain high organ hydration and turgor level which maintain overall physiological activities of the cells, especially those linked to the photosynthetic apparatus. Another study showed that the positive effect of compost on soil was related to the improvement of water retention (Tartoura, 2010). The association with AMF amends the plants' water regulation by triggering hormonal signaling such as ABA-mediating stomatal conductance or by stimulating osmolytes. Other studies showed, under drought stress, the development of microorganisms-mediated mechanisms including modifications in the content of plant hormones (e.g., strigolactones, jasmonic acid, and abscisic acid) and improvement in plant water status by increasing hydraulic conductivity (Chaumont and Tyerman, 2014; Fernández-Lizarazo and Moreno-Fonseca, 2016). The increase in root hydraulic conductivity can be related to an enhanced expression in fungal or plant AQPs (Sánchez-Romera et al., 2016). Chitarra et al. (2016) showed an enhancement in the water transport capacity of treated roots, which correlated with overexpression of the NIP AQP-encoding gene (LeNIP3;1). Recently, Xie et al. (2018) found up-regulation of the root AQP gene PIP expression under moderate water deficit in AMF roots.

Soil organic matter and total organic carbon were improved by the biofertilizers used. This improvement could be explained

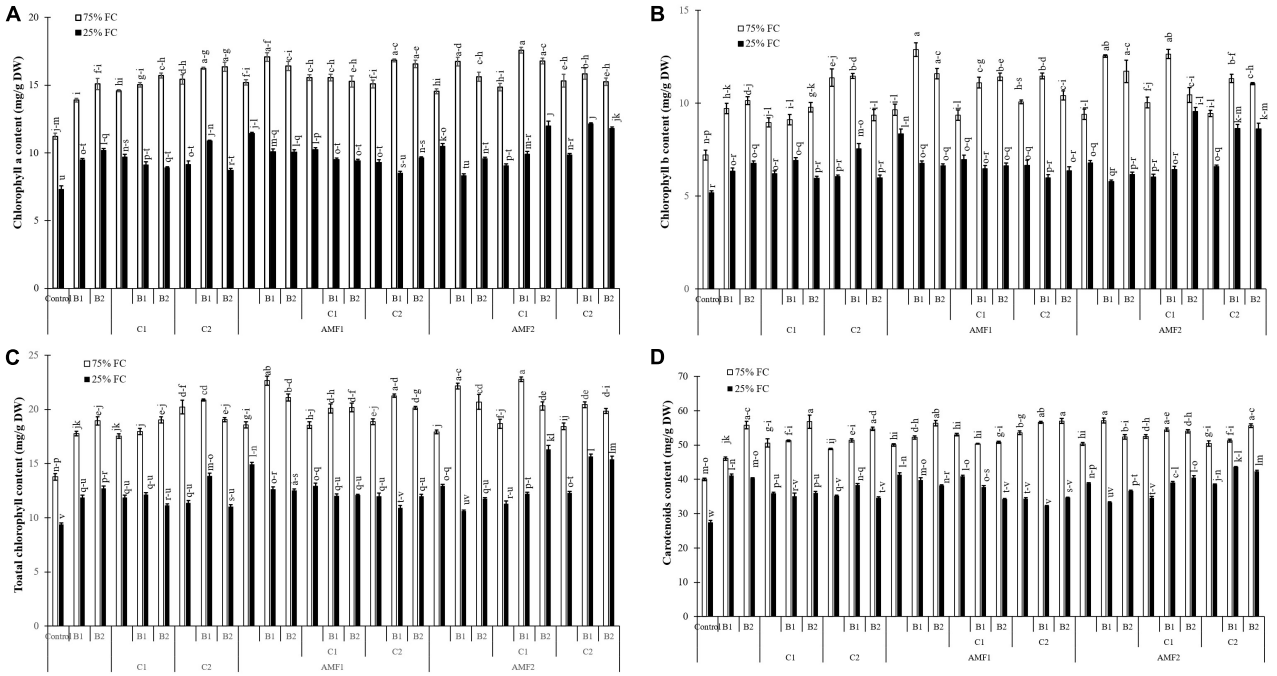

FIGURE 5 | (A) Chlorophyll *a*, **(B)** chlorophyll *b*, **(C)** total chlorophyll, and **(D)** carotenoid content in leaves of date palm plants under two water regimes [75% field capacity (FC); open bars and 25% FC; filled bars] and further grown without (control; non-amended and non-inoculated) or with biofertilizers [composts C1 or C2, arbuscular mycorrhizal fungi (AMF, exogenous AMF1 and native AMF2), and/or PGPR (B1 or B2)]. Data are mean ± SE of six independent biological replicates. Means followed by the same letters are not significantly different at $P < 0.05$ (Tukey's HSD).

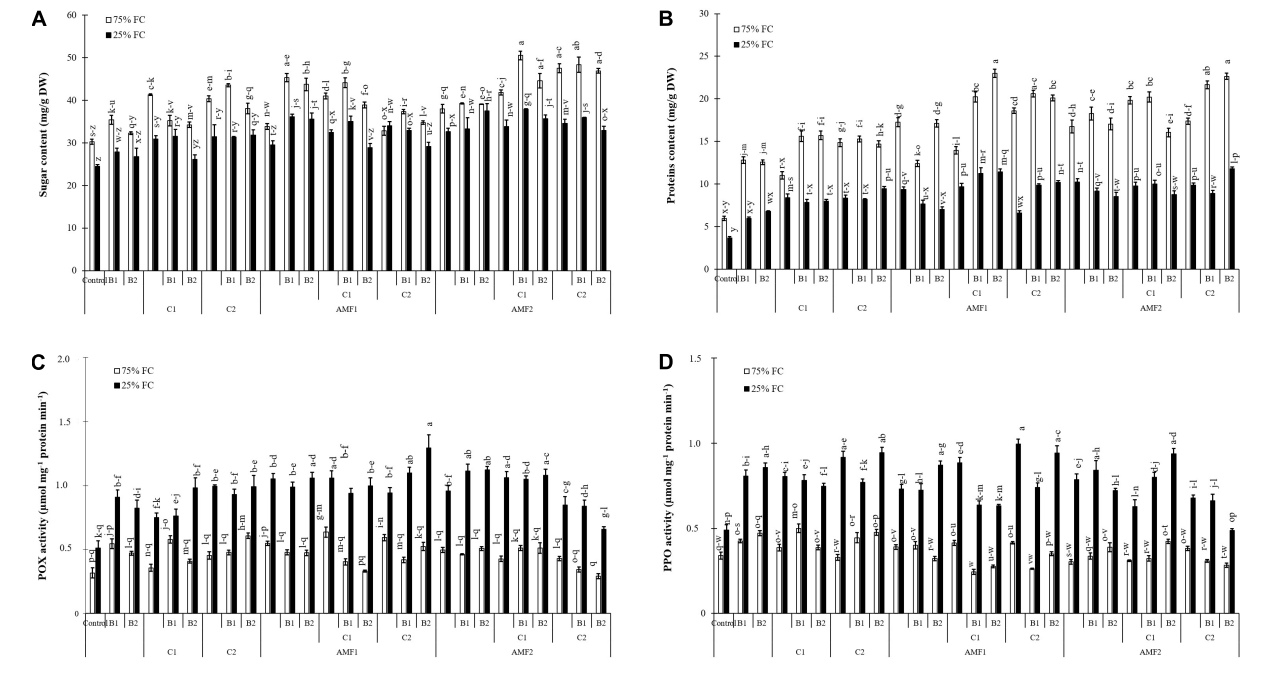

FIGURE 6 | (A) Total soluble sugar content, **(B)** protein content, **(C)** peroxidase (POX) activity, and **(D)** polyphenol oxidase (PPO) activity in date palm shoots under two water regimes [75% field capacity (FC); open bars and 25% FC; filled bars] of the tested control treatments (non-amended and non-inoculated) and biofertilizers treatments [composts C1 or C2, arbuscular mycorrhizal fungi (exogenous AMF1 and native AMF2), and/or plant growth promoting rhizobacteria (PGPR) (B1 or B2)]. Data are mean ± SE of six biological replicates. Means followed by the same letters are not significantly different at $P < 0.05$ (Tukey's HSD).

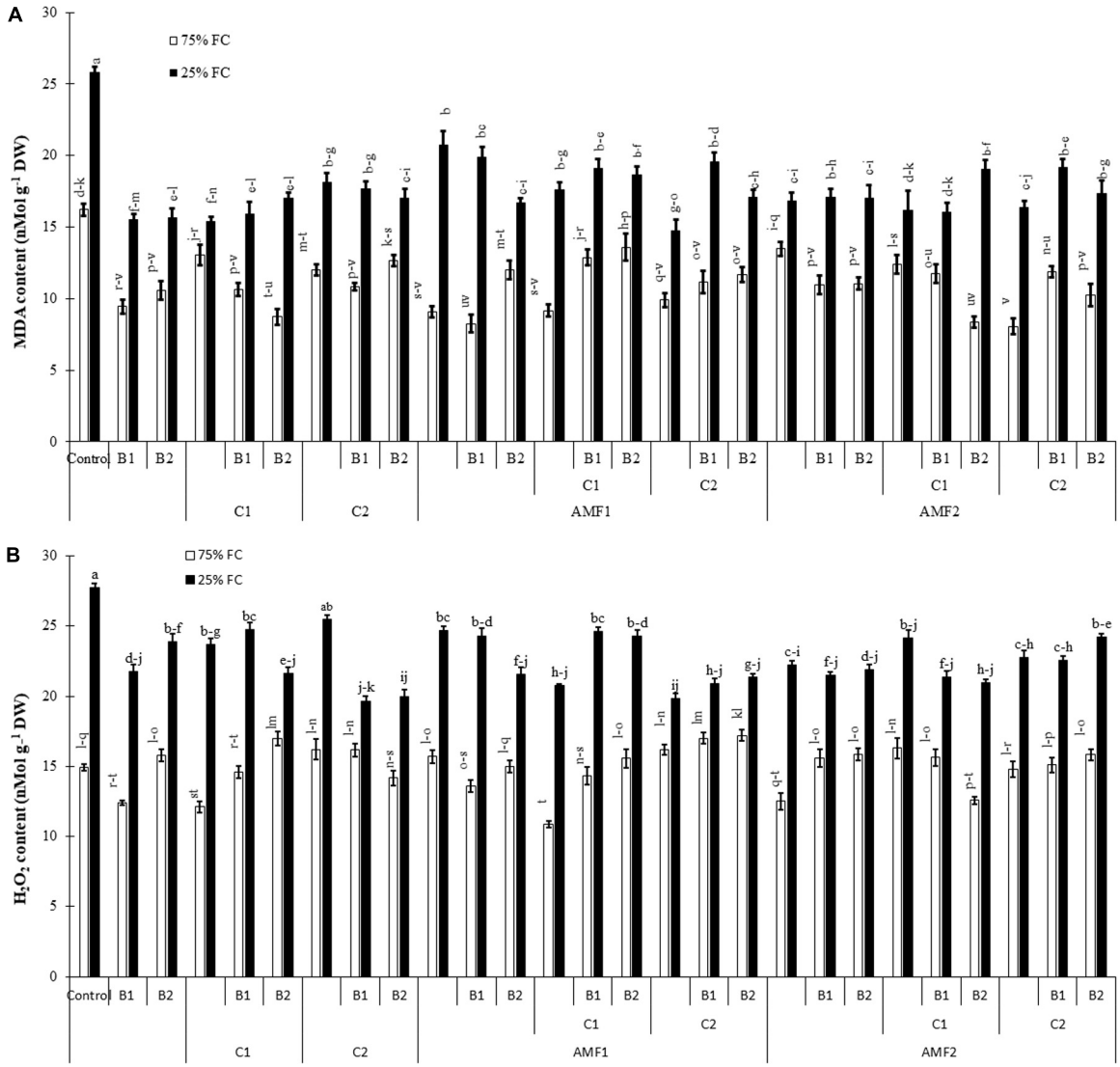

FIGURE 7 | (A) Malondialdehyde (MDA) and **(B)** hydrogen peroxide (H_2O_2) content in date palm shoots under two water regimes (75% field capacity (FC); open bars and 25% FC; filled bars) of the tested control treatments (non-amended and non-inoculated) and biofertilizers treatments [composts C1 or C2, arbuscular mycorrhizal fungi (AMF, exogenous AMF1 and native AMF2), and/or plant growth promoting rhizobacteria (PGPR) (B1 or B2)]. Data are mean ± SE of six independent biological replicates. Means followed by the same letters are not significantly different at $P < 0.05$ (Tukey's HSD).

by a direct contribution from compost or by the ability of AMF and PGPR to metabolize different compounds produced by plant roots mainly carbohydrates and organic acids. Shen et al. (2013) and Ning et al. (2017) showed that inoculation with microorganisms and compost application to plants was very effective in improving soil quality especially in organic matter, water retention, and mineral nutrition. The results obtained showed that biological treatments had an important effect on N and P in soil. However, a high amount of N and P in the rhizosphere soil of plants amended with compost and inoculated with AMF and PGPR could be due to a direct absorption via compost or by the fact that AMF and PGPR efficiently and directly take up from the soil to the plant nutrients such as N and P (Grobelak et al., 2015; Liu et al., 2018). In order to tolerate drought stress, plant adaptation is associated with high concentration of solutes such as soluble sugars and protein to regulate the osmotic potential of cells which, in turn, induce an improvement in water absorption under unfavorable condition (Zhang et al., 2010; Liao et al., 2019). Our data indicated that the concentrations of soluble sugars and protein in leaves increased during drought stress in treated plants as compared to microbes-free controls. These results are in agreement with previous reports using AMF or PGPR (Abbaspour et al., 2012; Vurukonda et al., 2016; Javan Gholiloo et al., 2019). In fact, PGPR were shown to secrete osmolytes to mitigate drought stress, which act synergistically with plants internal osmolytes boosting plant growth (Paul et al., 2008). Bano et al. (2013) and Sandhya et al. (2010) reported that plants inoculated with PGPR and

TABLE 5 | Soil physic-chemical analysis at harvest time of date palm grown under two water regimes (75 and 25% Field Capacity (FC)) of the tested control (non-amended and no-inoculated) and biofertilizers (composts C1 or C2, arbuscular mycorrhizal fungi (AMF, exogenous AMF1 and native AMF2), and/or plant growth promoting rhizobacteria (PGPR) (B1 or B2). Data are mean ± SE of six biological replicates.

Treatments	pH		EC (mS/cm)		TOC (%)		OM (%)		N (mg/g of soil)		P (ppm)	
	75% FC	25% FC	75% FC	25% FC	75% FC	25% FC	75% FC	25% FC	75% FC	25% FC	75% FC	25% FC
Control	7.96 ± 0.05 a	7.88 ± 0.06 ab	0.28 ± 0.01 v–x	0.20 ± 0.01 A	0.40 ± 0.02 v	0.52 ± 0.01 u	0.70 ± 0.03 v	0.89 ± 0.02 u	0.16 ± 0.02 lm	0.06 ± 0.02 m	51.97 ± 1.47 u–w	30.05 ± 1.44 w
B1	7.50 ± 0.07 c–e	7.46 ± 0.02 c–e	0.23 ± 0.00 y–A	0.21 ± 0.01 zA	0.75 ± 0.01 n–s	0.71 ± 0.01 p–t	1.29 ± 0.02 n–s	1.22 ± 0.02 p–t	0.30 ± 0.03 e–k	0.22 ± 0.02 j–l	86.53 ± 5.37 m–t	41.34 ± 1.64 vw
B2	7.38 ± 0.04 c	7.42 ± 0.02 de	0.25 ± 0.01 x–z	0.21 ± 0.01 zA	0.68 ± 0.06 st	0.74 ± 0.02 o–s	1.16 ± 0.10 st	1.28 ± 0.04 o–s	0.30 ± 0.03 e–k	0.22 ± 0.02 j–l	151.48 ± 7.02 c–e	57.97 ± 3.46 s–w
C1	7.46 ± 0.05 c–e	7.56 ± 0.02 c–e	0.30 ± 0.01 s–w	0.31 ± 0.01 r–v	0.87 ± 0.03 e–l	0.83 ± 0.01 h–o	1.51 ± 0.05 e–l	1.43 ± 0.03 h–o	0.24 ± 0.02 j–l	0.34 ± 0.04 b–k	140.04 ± 11.28 c–g	86.59 ± 3.88 m–s
C1+B1	7.44 ± 0.05 c–e	7.54 ± 0.02 c–e	0.39 ± 0.01 h–n	0.39 ± 0.01 h–n	0.94 ± 0.02 b–g	0.90 ± 0.00 e–k	1.62 ± 0.03 b–g	1.55 ± 0.01 e–k	0.34 ± 0.04 b–k	0.22 ± 0.02 j–l	190.18 ± 9.77 b	80.89 ± 1.68 n–u
C1+B2	7.52 ± 0.04 c–e	7.48 ± 0.04 c–e	0.38 ± 0.01 i–o	0.21 ± 0.01 zA	0.92 ± 0.01 d–i	0.84 ± 0.01 g–n	1.58 ± 0.03 d–i	1.46 ± 0.02 g–n	0.32 ± 0.02 c–k	0.25 ± 0.01 j–l	105.63 ± 8.57 h–n	64.06 ± 1.36 q–v
C2	7.42 ± 0.04 de	7.48 ± 0.04 c–e	0.38 ± 0.01 h–o	0.37 ± 0.01 j–p	0.94 ± 0.02 b–g	0.87 ± 0.02 e–l	1.62 ± 0.03 b–g	1.50 ± 0.03 e–l	0.47 ± 0.02 ab	0.28 ± 0.02 g–l	79.43 ± 3.91 n–u	61.90 ± 2.57 r–v
C2+B1	7.52 ± 0.05 c–e	7.58 ± 0.02 c–e	0.32 ± 0.00 q–v	0.31 ± 0.00 r–v	0.95 ± 0.02 b–f	0.84 ± 0.02 g–o	1.64 ± 0.03 b–f	1.44 ± 0.03 g–o	0.35 ± 0.02 a–k	0.21 ± 0.02 kl	96.76 ± 3.17 k–p	71.07 ± 3.07 o–u
C2+B2	7.50 ± 0.04 c–e	7.58 ± 0.04 c–e	0.35 ± 0.01 n–r	0.33 ± 0.01 p–u	0.91 ± 0.02 e–j	0.68 ± 0.01 r–t	1.57 ± 0.03 e–j	1.16 ± 0.03 r–t	0.32 ± 0.02 c–k	0.26 ± 0.02 i–l	100.34 ± 2.42 j–o	69.50 ± 4.30 p–v
AMF1	7.56 ± 0.02 c–e	7.52 ± 0.04 c–e	0.25 ± 0.01 x–z	0.23 ± 0.00 y–A	0.75 ± 0.01 n–s	0.68 ± 0.01 r–t	1.29 ± 0.02 n–s	1.17 ± 0.03 r–t	0.29 ± 0.02 f–l	0.32 ± 0.02 c–k	114.85 ± 5.74 g–m	87.29 ± 4.24 m–s
AMF1+B1	7.64 ± 0.02 b–d	7.56 ± 0.02 c–e	0.25 ± 0.01 x–z	0.27 ± 0.01 w–y	0.70 ± 0.03 p–t	0.78 ± 0.00 l–q	1.21 ± 0.05 p–t	1.35 ± 0.01 l–q	0.39 ± 0.03 a–i	0.34 ± 0.02 b–k	80.54 ± 2.33 n–u	57.87 ± 2.25 s–w
AMF1+B2	7.68 ± 0.04 bc	7.56 ± 0.02 c–e	0.30 ± 0.01 t–w	0.29 ± 0.01 u–x	0.70 ± 0.01 q–t	0.64 ± 0.02 t	1.20 ± 0.01 q–t	1.10 ± 0.04 t	0.32 ± 0.02 c–k	0.28 ± 0.02 g–l	156.47 ± 8.83 cd	126.84 ± 1.00 e–j
AMF1+C1	7.48 ± 0.04 c–e	7.54 ± 0.02 c–e	0.39 ± 0.01 h–o	0.31 ± 0.01 r–w	0.90 ± 0.00 e–j	0.80 ± 0.01 k–p	1.56 ± 0.00 e–j	1.38 ± 0.02 k–p	0.41 ± 0.03 a–g	0.31 ± 0.01 d–k	68.55 ± 1.05 p–v	58.47 ± 3.04 r–w
AMF1+C1+B1	7.50 ± 0.09 c–e	7.48 ± 0.04 c–e	0.45 ± 0.01 d–g	0.34 ± 0.01 o–t	0.97 ± 0.01 a–e	0.77 ± 0.02 m–r	1.67 ± 0.01 a–e	1.32 ± 0.03 m–r	0.31 ± 0.03 d–k	0.25 ± 0.01 j–l	207.15 ± 3.30 ab	74.39 ± 3.45 o–u
AMF1+C1+B2	7.64 ± 0.02 b–d	7.68 ± 0.04 bc	0.41 ± 0.01 g–k	0.32 ± 0.01 q–v	1.07 ± 0.00 a	0.89 ± 0.02 e–k	1.85 ± 0.00 a	1.54 ± 0.04 e–k	0.36 ± 0.03 a–j	0.31 ± 0.01 d–k	86.99 ± 1.47 m–s	57.06 ± 2.51 t–w
AMF1+C2	7.65 ± 0.05 c–e	7.68 ± 0.04 bc	0.49 ± 0.01 cd	0.41 ± 0.01 f–j	0.90 ± 0.01 e–k	1.03 ± 0.01 a–c	1.55 ± 0.02 e–k	1.78 ± 0.01 a–c	0.44 ± 0.02 a–e	0.31 ± 0.02 d–k	127.90 ± 12.23 d–j	58.22 ± 3.26 s–w
AMF1+C2+B1	7.66 ± 0.06 b–d	7.68 ± 0.04 bc	0.55 ± 0.01 b	0.42 ± 0.01 e–i	1.05 ± 0.02 ab	0.93 ± 0.00 c–h	1.80 ± 0.03 ab	1.60 ± 0.01 c–h	0.32 ± 0.02 c–k	0.29 ± 0.02 f–l	149.41 ± 8.46 c–f	87.94 ± 3.18 m–r
AMF1+C2+B2	7.48 ± 0.07 c–e	7.68 ± 0.04 bc	0.45 ± 0.00 d–f	0.40 ± 0.01 h–m	1.02 ± 0.01 a–d	0.82 ± 0.01 i–o	1.77 ± 0.02 a–d	1.41 ± 0.02 i–o	0.31 ± 0.02 a–d	0.29 ± 0.02 f–l	157.48 ± 7.11 c	66.08 ± 3.09 q–v
AMF2	7.60 ± 0.03 c–e	7.66 ± 0.04 b–d	0.35 ± 0.01 m–r	0.32 ± 0.01 q–v	0.53 ± 0.00 u	0.64 ± 0.01 t	0.91 ± 0.00 u	1.10 ± 0.02 t	0.35 ± 0.03 a–k	0.34 ± 0.03 b–k	198.64 ± 8.48 ab	149.41 ± 8.35 c–f

(Continued)

TABLE 6 | Continued

Treatments	pH		EC (mS/cm)		TOC (%)		OM (%)		N (mg/g of soil)		P (ppm)	
	75% FC	25% FC	75% FC	25% FC	75% FC	25% FC	75% FC	25% FC	75% FC	25% FC	75% FC	25% FC
AMF2+B1	7.56 ± 0.05 c–e	7.68 ± 0.04 bc	0.33 ± 0.01 p–u	0.28 ± 0.01 v–x	0.66 ± 0.01 st	0.78 ± 0.01 l–q	1.14 ± 0.02 st	1.35 ± 0.01 l–q	0.45 ± 0.03 a–d	0.31 ± 0 01 d–k	121.65 ± 2.58 f–k	65.12 ± 2.55 q–v
AMF2+B2	7.66 ± 0.04 b–d	7.60 ± 0.03 c–e	0.37 ± 0.01 k–p	0.36 ± 0.01 l–q	0.85 ± 0.02 f–m	0.84 ± 0.01 g–o	1.47 ± 0.04 f–m	1.44 ± 0.03 g–o	0.35 ± 0.03 a–k	0.36 ± 0.03 a–j	108.20 ± 5.69 h–n	83.21 ± 0.96 n–t
AMF2+C1	7.58 ± 0.04 c–e	7.64 ± 0.02 b–d	0.43 ± 0.01 e–h	0.38 ± 0.01 i–o	1.05 ± 0.01 ab	0.75 ± 0.01 n–s	1.80 ± 0.02 ab	1.30 ± 0.02 n–s	0.45 ± 0.02 a–d	0.29 ± 0.02 f–l	82.05 ± 1.52 n–t	62.10 ± 3.00 r–v
AMF2+C1+B1	7.64 ± 0.05 b–d	7.56 ± 0.04 c–e	0.42 ± 0.01 e–i	0.34 ± 0.01 n–s	0.92 ± 0.02 d–i	0.69 ± 0.01 q–t	1.59 ± 0.03 d–i	1.19 ± 0.01 q–t	0.40 ± 0.03 a–h	0.32 ± 0.02 c–k	92.03 ± 2.27 l–q	64.32 ± 1.73 q–v
AMF2+C1+B2	7.66 ± 0.04 b–d	7.52 ± 0.04 c–e	0.48 ± 0.01 cd	0.40 ± 0.01 h–l	0.81 ± 0.01 i–o	0.92 ± 0.02 d–i	1.40 ± 0.01 i–o	1.58 ± 0.04 d–i	0.48 ± 0.02 a	0.32 ± 0.02 c–k	223.33 ± 3.07 a	121.35 ± 6.35 f–l
AMF2+C2	7.54 ± 0.04 c–e	7.58 ± 0.05 c–e	0.65 ± 0.01 a	0.51 ± 0.01 bc	0.85 ± 0.02 f–m	0.90 ± 0.01 e–j	1.47 ± 0.03 f–m	1.55 ± 0.02 e–j	0.43 ± 0.03 a–f	0.32 ± 0.04 c–k	134.55 ± 6.93 c–h	81.90 ± 3.92 n–t
AMF2+C2+B1	7.64 ± 0.02 b–d	7.52 ± 0.04 c–e	0.51 ± 0.01 bc	0.42 ± 0.01 e–i	0.83 ± 0.01 h–o	0.84 ± 0.01 g–n	1.42 ± 0.02 h–o	1.45 ± 0.03 g–n	0.46 ± 0.02 a–c	0.27 ± 0.02 h–l	104.17 ± 3.09 i–n	70.97 ± 4.55 o–u
AMF2+C2+B2	7.68 ± 0.06 bc	7.54 ± 0.04 c–e	0.62 ± 0.01 a	0.46 ± 0.01 de	1.07 ± 0.00 a	0.90 ± 0.02 e–k	1.84 ± 0.01 a	1.55 ± 0.03 e–k	0.36 ± 0.03 a–j	0.26 ± 0.01 i–l	132.43 ± 9.97 c–i	61.90 ± 2.82 r–v

Means followed by the same letters are not significantly different at $P < 0.05$ (Tukey's HSD). EC, electrical conductivity; TOC, total organic carbon; OM, organic matter, N, nitrogen concentration; P, phosphorous concentration.

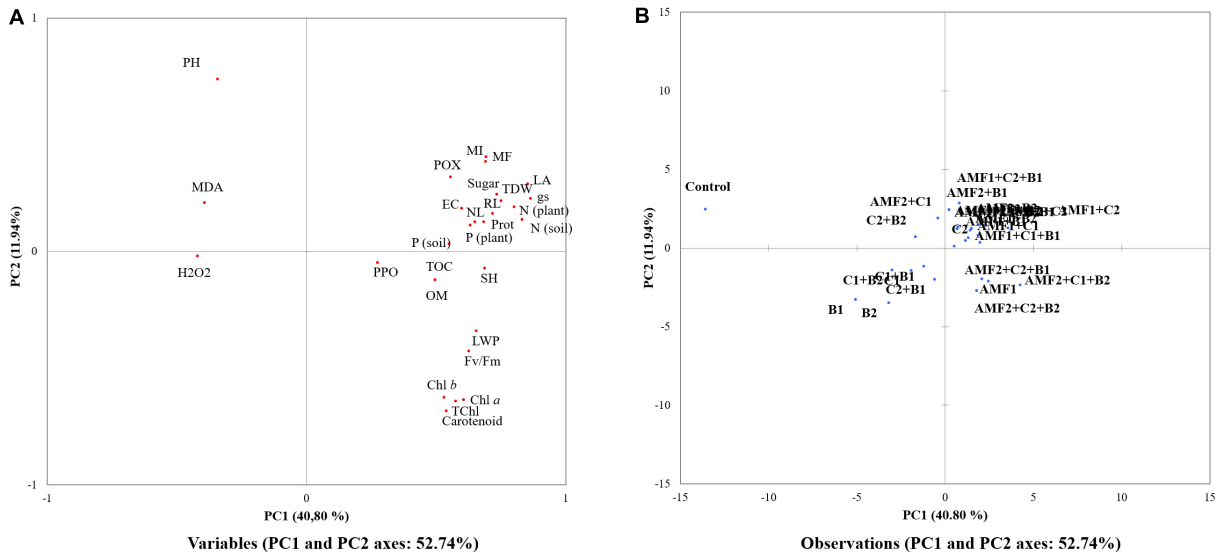

FIGURE 8 | Principal component analysis (PCA) of the different studied **(A)** traits and **(B)** treatments under drought stress conditions (25% FC). Chl a, chlorophyll *a*; Chl b, chlorophyll *b*; EC, electrical conductivity; Fv/Fm, chlorophyll fluorescence; g_s, stomatal conductance; H_2O_2, hydrogen peroxide; LA, leaf area; LWP, leaf water potential; MDA, malondialdehyde; MI, mycorrhizal intensity; MF, mycorrhizal frequency; N (soil), nitrogen content in soil; N (plant); nitrogen content in plant; NL, leaf numbers; OM, organic matter; P (soil), Phosphorous content in soil; P (plant), Phosphorous content in plant shoot; POX, peroxidase; PPO, polyphenol oxidase; RL, root length; SH, shoot height; TOC, total organic carbon; T Chl, total chlorophylls.

grown under drought stress improved their growth by soluble sugars and protein accumulations compared to non-treated plants. However, our results suggest that the application of compost and inoculation with AMF and PGPR were propitious to carbohydrate accumulation, mainly soluble sugars, in drastic conditions resulting in reduced osmotic potentials in host cells. Indeed, the osmotic stress induced by drought is tolerated by the host plant by altering biochemical responses via the enhancement of metabolite biosynthesis (e.g., sugars and proline) that function as osmolytes, and thereby maintaining the water potential, hydration and turgor level which maintain overall physiological activities under harsh environments. Previous studies showed that sugar metabolism-related genes tend to be enriched in plants treated with beneficial microbes under drought stress (Ahanger et al., 2014; Bárzana et al., 2015). Our results demonstrated that levels of MDA and H_2O_2 in leaves were lower under drought stress in treated plants compared to beneficial microbe-free control plants. To explain the low lipid peroxidation damage in AMF-treated plants, two possibilities were suggested by Abbaspour et al. (2012): (1) either inoculated plants with AMF suffered less drought stress owing to a primary drought avoidance effect by symbiosis (e.g., direct water uptake by fungal hyphae from the soil to the host plant) or (2) AMF colonization improved the activities of antioxidant enzymes as a defense to eliminate the ROS. Our results suggest that the application of compost and inoculation with AMF and PGPR could improve the defense against drought stress by reducing and eliminating ROS diffusion and production. Plants treated with AMF/PGPR counteract water deficit-induced oxidative stress by upregulating ROS-scavenging antioxidant compounds and antioxidant enzymatic activities. It is well known that plants protect against the damage caused by this oxidative stress by mechanisms that detoxify ROS which can be enzymatic (superoxide dismutase, catalase, ascorbate peroxidase, glutathione reductase, and monodehydroascorbate reductase) and non-enzymatic (flavanones, anthocyanins, carotenoids, and ascorbic acid). Our results showed a significant increase in POX and PPO in plants subjected to water deficit and inoculated with beneficial microbes and/or amended with compost than controls. Duo et al. (2018) revealed that nano-compost alone or combined with bacterial strains minimized the effects of drought stress by increasing antioxidant enzymes and decreasing MDA. Other studies suggested that drought tolerance is acquired by bacteria through the improvement of plant cell membrane stability and elasticity by activating the antioxidant defense system (Dimkpa et al., 2009; Gusain et al., 2015).

The results highlight a physiological and biochemical switching mechanism in microbe association and provide additional confirmation of the hypothesis that, as illustrated in **Figure 9**, microbial association and compost operate at multiple (including photosynthesis machinery, antioxidant system, osmolytes biosynthesis, gene regulation) levels. Our study showed an improvement in the parameters studied in date palms growing in soil treated by the autochthonous biofertilizers mainly the consortium AMF2 alone and its combination with compost (C2) and/ or PGPR (B2) under drought stress, especially AMF2+C2 and AMF2+C2+B2 treatments. This improvement in growth, mineral uptake, and physio-biochemical traits together with the decrease in MDA and H_2O_2 could be due to the synergy between AMF, compost, and PGPR: (1) the compost (C2) with low dose 5% allows good mycorrhizal infectivity, the presence of essential mineral elements such as N, P, and K for plant growth, and improves the soil quality by

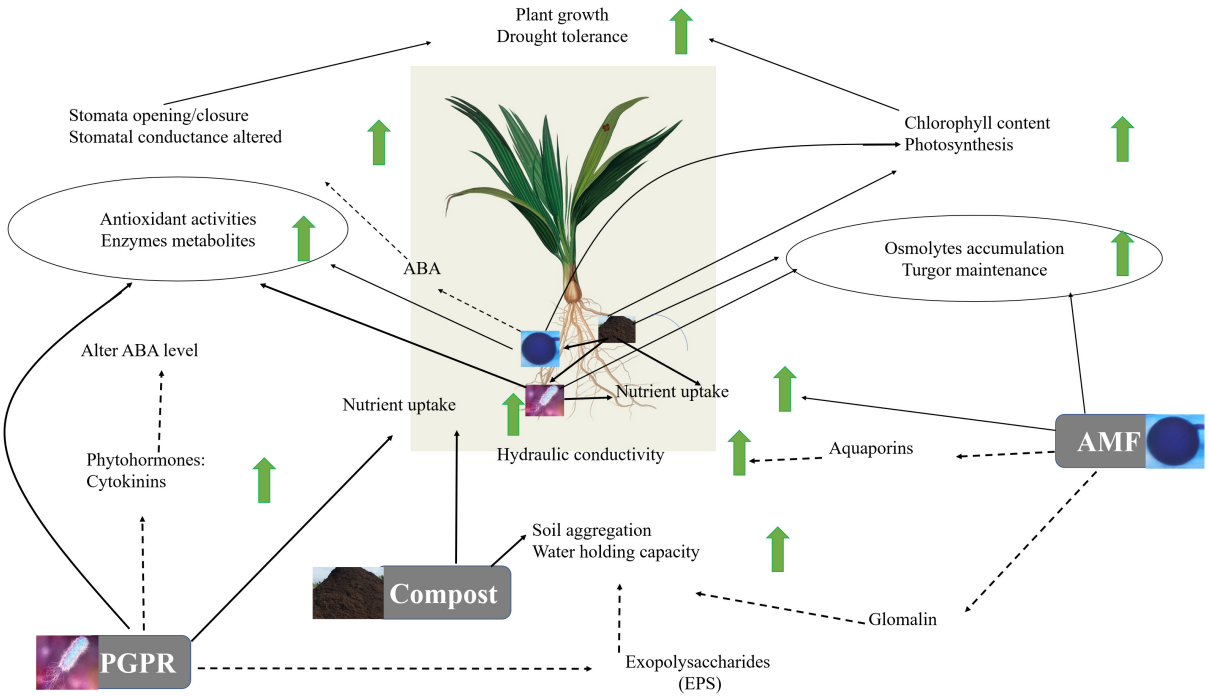

FIGURE 9 | Suggested model for the regulatory network involved in date palm growth and tolerance to drought in response to compost, arbuscular mycorrhizal fungi (AMF) and plant growth promoting rhizobacteria (PGPR). According to this model, AMF colonization of a plant root permits the extension of hyphae extending into the surrounding soil, providing availability and storage of nutrients such as phosphorus and nitrogen for the plant. Also, AMF help to promote the synthesis of aquaporins which by changing the root hydraulic conductivity can enhance water uptake and water homeostasis maintenance under drought conditions. PGPR function as plant enhancer and facilitate the drought-exposed plants by improving nutrient uptake (N), water balance and osmoregulation through hormones (CKs and ABA)-mediating stomatal pores and regulating plant biochemical mechanisms (reducing the degradation of chlorophyll content and lipid peroxidation, increasing production of protein that reduces the damaging effect of ROS and can help maintain photosystem functionality under drought stress). Further, PGPR affect the EPS, allowing the increase of the water holding capacity. The compost functions as a soil conditioner in the process of decomposition and nutrient cycling (capture and delivery), which are driven by the activity of soil microorganisms affecting the soil microorganism activity (e.g., AMF and PGPR). The resulting changes in soil characteristics permit soil aggregation and enhance water holding capacity. Additionally, the plant–AMF/PGPR-compost associations act on physiological (increases in the photosynthetic pigments, and ABA-mediating higher stomatal conductance, permitting the increase of internal CO_2 and photosynthetic capacity) and biochemical (accumulation of osmolytes and activation of antioxidant metabolites/activities allowing leaf osmotic adjustment, ROS scavenging, and alleviation of oxidative stresses) parameters. Solid lines represent the analyses carried out in this study. Dashed lines indicate mechanisms found in the literature.

enhancing carbon, organic matter, and available P and N, (2) the native AMF hyphal structure might allow the uptake of water and nutrients needed by the plants and/or the changes in the level of phytohormones that participate in symbiosis. Furthermore, the stimulation of AMF symbiosis by root exudates could constitute an important source of organic carbon in the rhizosphere and a route of chemical communication between root plants and the fungi and (3) the PGPR (B2) could enhance phosphate solubilization resulting in increased phosphate available in the soil absorbed by plants through the production of organic acids and phosphatase. Furthermore, PGPR could modulate the tolerance of date palms via other mechanisms, yet to be elucidated, such as phytohormones (auxin, cytokinins), siderophores, and exopolysaccharide production.

Altogether, the general pattern that can be observed in the dataset is that an amendment of the soil reflects in better growth, in better soil properties and this also mirrors in stress related properties of photosynthesis; gas exchange or compound accumulation. It is worthy of note that the use of autochthonous biofertilizers (i.e., AMF2, C2, and B2) could constitute an original approach to improving the boost in growth and tolerance and may be a suitable combination for date palms in arid climates.

CONCLUSION

Global agriculture will not only have to face the task of improving stress resistance and yields for food and biomass production but also that of reducing the dependence of producers on agrochemicals for a sustainable food system and environmental health. Therefore, the need to implement or revitalize eco-friendly technologies, such as compost and beneficial microbe-based biofertilization is of great importance for agriculture and the environment. Despite its enormous potential, the application of AMF, as yet, has not been fully adopted by farmers and the underlying mechanisms have not been sufficiently examined over recent decades. Moreover, since native AMF have demonstrated a great potential versus commercial isolates, in this work, it has been pointed out that native AMF, PGPR inoculation and compost overall produces positive outcomes on plant production,

mainly owing to the several nutrition-related benefits that this class of soil beneficial microbes, symbionts and compost are able to provide to their host-plants. Furthermore, our data suggest that biofertilizers develop drought-adaptive strategies through the influence of plant mechanisms, such as photosynthetic machinery, better efficiency of PSII, root hydraulic conductivity, osmolyte accumulation, antioxidant enzyme production, higher membrane stability, and lower lipid peroxidation. Our findings are a first step toward encouraging farmers to autonomously produce their AMF inocula, starting from native soils. Further, this work makes biofertilization technology more likely to be affordable for farmers in harsh areas, and also those in developing countries for a sustainable crop growing system. For these reasons, the next significant step (an on-going study) toward the stable use of biofertilizers in agriculture and to better understand the potential effects of indigenous biofertilizers is carrying out field trials.

DATA AVAILABILITY STATEMENT

The datasets generated for this study are available on request to the corresponding author.

AUTHOR CONTRIBUTIONS

MA and MB designed and supervised the research. AM performed the experiments and carried out the analysis. AT, AR, AB, MA-E-M, RB-L, ST, and YA contributed analytic tools. MA, MB, and AM interpreted the data. MA, KO, MH, SS, and TM contributed to the conception and design of the work. AM and MB wrote the manuscript. AM, MB, and AM revised and finalized the manuscript. All authors read and approved the final version of the manuscript.

FUNDING

This work was supported by "Application of organic bio-fertilizer technology to improve the sustainability of date palm production and cultivation" project (IZ07Z0_160904) funded by the r4d program, the Swiss Program for Research on Global Issues for Development, a partnership of the Agency for Development and Cooperation, and the Swiss National Science Foundation. The Grant-in-Aid for Young Scientists to MB (JST, Japan), KAKENHI Grants-in-Aid for Scientific Research (A) (15H02486) from the Japan Society for the Promotion of Sciences, Strategic International Collaborative Research Program by the Japan Science and Technology Agency (JPMJSC16C5), and Grant for Promotion of KAAB Projects (Niigata University) from the Ministry of Education, Culture, Sports, Science, and Technology, Japan are also acknowledged. The funders had no role in the data collection, decision to publish, or preparation of the manuscript.

SUPPLEMENTARY MATERIAL

The Supplementary Material for this article can be found online at: https://www.frontiersin.org/articles/10.3389/fpls.2020.516818/full#supplementary-material

Supplementary Figure 1 | Phenotypic comparison in control date palm plants (non-amended, non-inoculated), and plants amended with composts (C1 or C2) and/or inoculated with arbuscular mycorrhizal fungi (AMF; exogenous AMF1 or native AMF2) or plant growth-promoting rhizobacteria (PGPR) strains (B1 or B2) under two water regimes [75 and 25% field capacity (FC)].

Supplementary Table 1A | Result of multivariate analysis of variance MANOVA test for independent variables including Drought treatment, Composts (C1 and C2) amendment and exotic AMF (AMF1) and Bacteria (B1 and B2) inoculation and interaction among them.

Supplementary Table 1B | Result of multivariate analysis of variance MANOVA test for independent variables including Drought treatment, Composts (C1 and C2) amendment and autochthonous AMF (AMF2) and Bacteria (B1 and B2) inoculation and interaction among them.

REFERENCES

Abbaspour, H., Saeidi-Sar, S., Afshari, H., and Abdel-Wahhab, M. A. (2012). Tolerance of Mycorrhiza infected Pistachio (*Pistacia vera* L.) seedling to drought stress under glasshouse conditions. *J. Plant Physiol.* 169, 704–709. doi: 10.1016/j.jplph.2012.01.014

Abd El-Mageed, T. A., El-Samnoudi, I. M., Ibrahim, A. E. A. M., and Abd El Tawwab, A. R. (2018). Compost and mulching modulates morphological, physiological responses and water use efficiency in *Sorghum bicolor* L. (Moench) under low moisture regime. *Agric. Water Manag.* 208, 431–439. doi: 10.1016/j.agwat.2018.06.042

Abd El-Mageed, T. A., El-Sherif, A. M. A., Abd El-Mageed, S. A., and Abdou, N. M. (2019). A novel compost alleviate drought stress for sugar beet production grown in Cd-contaminated saline soil. *Agric. Water Manag.* 226:105831. doi: 10.1016/j.agwat.2019.105831

Abdel Latef, A. A. H., Abu Alhmad, M. F., Kordrostami, M., Abo–Baker, A. B. A. E., and Zakir, A. (2020). Inoculation with *Azospirillum lipoferum* or *Azotobacter chroococcum* reinforces maize growth by improving physiological activities under saline conditions. *J. Plant Growth Regul.* 39, 1293–1306. doi: 10.1007/s00344-020-10065-9

Abdel Latef, A. A. H., and Chaoxing, H. (2011). Effect of arbuscular mycorrhizal fungi on growth, mineral nutrition, antioxidant enzymes activity and fruit yield of tomato grown under salinity stress. *Sci. Hortic.* 127, 228–233. doi: 10.1016/j.scienta.2010.09.020

Abdel Latef, A. A. H., Hashem, A., Rasool, S., Abd_Allah, E. F., Alqarawi, A. A., Egamberdieva, D., et al. (2016). Arbuscular mycorrhizal symbiosis and abiotic stress in plants: a review. *J. Plant Biol.* 59, 407–426. doi: 10.1007/s12374-016-0237-7

Abdel Latef, A. A. H., Mostofa, M. G., Rahman, M. M., Abdel-Farid, I. B., and Tran, L.-S. P. (2019a). Extracts from yeast and carrot roots enhance maize performance under seawater-induced salt stress by altering physio-biochemical characteristics of stressed plants. *J. Plant Growth Regul.* 38, 966–979. doi: 10.1007/s00344-018-9906-8

Abdel Latef, A. A. H., Kordrostami, M., Zakir, A., Zaki, H., and Saleh, O. (2019b). Eustress with H_2O_2 facilitates plant growth by improving tolerance to salt stress in two wheat cultivars. *Plants* 8:303. doi: 10.3390/plants8090303

Adesemoye, A. O., Torbert, H. A., and Kloepper, J. W. (2009). Plant growth-promoting rhizobacteria allow reduced application rates of chemical fertilizers. *Micro Ecol.* 58, 921–929. doi: 10.1007/s00248-009-9531-y

Ahanger, M. A., Tyagi, S. R., Wani, M. R., and Ahmad, P. (2014). "Drought tolerance: role of organic osmolytes, growth regulators, and mineral nutrients," in *Physiological Mechanisms and Adaptation Strategies in Plants Under Changing Environment*, Vol. 1, eds P. Ahmad and M. R. Wani (New York, NY: Springer), 25–55. doi: 10.1007/978-1-4614-8591-9_2

Ait-El-Mokhtar, M., Ben-Laouane, R., Anli, M., Boutasknit, A., Wahbi, S., and Meddich, A. (2019). Use of mycorrhizal fungi in improving tolerance of the date palm (*Phoenix dactylifera* L.) seedlings to salt stress. *Sci. Hortic.* 253, 429–438. doi: 10.1016/j.scienta.2019.04.066

Alikhani, H. A., Saleh-Rastin, N., and Antoun, H. (2006). Phosphate solubilization activity of rhizobia native to Iranian soils. *Plant Soil* 287, 35–41. doi: 10.1007/s11104-006-9059-6

Al-Karaki, G., McMichael, B., and Zak, J. (2004). Field response of wheat to arbuscular mycorrhizal fungi and drought stress. *Mycorrhiza* 14, 263–269. doi: 10.1007/s00572-003-0265-2

Al-Karaki, G. N. (2000). Growth of mycorrhizal tomato and mineral acquisition under salt stress. *Mycorrhiza* 10, 51–54. doi: 10.1007/s005720000055

Al-Karaki, G. N. (2006). Nursery inoculation of tomato with arbuscular mycorrhizal fungi and subsequent performance under irrigation with saline water. *Sci. Hortic.* 109, 1–7. doi: 10.1016/j.scienta.2006.02.019

Al-Karaki, G. N. (2016). Application of mycorrhizal fungi in landscape turfgrass establishment under arid and semiarid environments. *AGROFOR* 1, 154–161. doi: 10.7251/agreng1602154a

Anli, M., Symanczik, S., El Abbassi, A., Ait-El-Mokhtar, M., Boutasknit, A., Ben-Laouane, R., et al. (2020). Use of arbuscular mycorrhizal fungus *Rhizoglomus irregulare* and compost to improve growth and physiological responses of *Phoenix dactylifera* "Boufgouss". *Plant Biosyst.* 1–14. doi: 10.1080/11263504.2020.1779848

Arias, E., Hodder, A. J., and Oihabi, A. (2016). FAO support to date palm development around the world: 70 years of activity. *Emirates J. Food Agric.* 28, 1–11. doi: 10.9755/ejfa.2015-10-840

Arnon, D. I. (1949). Copper enzymes in isolated chloroplasts. Polyphenoloxidase in *Beta vulgaris*. *Plant Physiol.* 24, 1–15. doi: 10.1104/pp.900074

Aubert, G. (1978). *Méthodes d'analyses des sols*, 2ème Edn. Marseille: Centre régional de Documentation Pédagogique, 191.

Augé, R. M., Toler, H. D., and Saxton, A. M. (2014). Arbuscular mycorrhizal symbiosis alters stomatal conductance of host plants more under drought than under amply watered conditions: a meta-analysis. *Mycorrhiza* 25, 13–24. doi: 10.1007/s00572-014-0585-4

Bano, Q., Ilyas, N., Bano, A., Zafar, N., Akram, A., and Hassan, F. (2013). Effect of *Azospirillum* inoculation on maize (*Zea mays* L.) under drought stress. *Pakistan J. Bot.* 45, 13–20.

Barje, F., Meddich, A., El Hajjouji, H., El Asli, A., Ait Baddi, G., El Faiz, A., et al. (2016). Growth of date palm (*Phoenix dactylifera* L.) in composts of olive oil mill waste with organic household refuse. *Compost Sci. Util.* 24, 273–280. doi: 10.1080/1065657X.2016.1171738

Bárzana, G., Aroca, R., and Ruiz-Lozano, J. M. (2015). Localized and nonlocalized effects of arbuscular mycorrhizal symbiosis on accumulation of osmolytes and aquaporins and on antioxidant systems in maize plants subjected to total or partial root drying. *Plant Cell Environ.* 38, 1613–1627. doi: 10.1111/pce.12507

Baslam, M., and Goicoechea, N. (2012). Water deficit improved the capacity of arbuscular mycorrhizal fungi (AMF) for inducing the accumulation of antioxidant compounds in lettuce leaves. *Mycorrhiza* 22, 347–359. doi: 10.1007/s00572-011-0408-9

Baslam, M., Qaddoury, A., and Goicoechea, N. (2014). Role of native and exotic mycorrhizal symbiosis to develop morphological, physiological and biochemical responses coping with water drought of date palm, *Phoenix dactylifera*. *Trees* 28, 161–172. doi: 10.1007/s00468-013-0939-0

Becklin, K. M., Mullinix, G. W. R., and Ward, J. K. (2016). Host plant physiology and mycorrhizal functionining shift across a glacial through future [CO_2] gradient. *Plant Physiol.* 172, 789–801. doi: 10.1104/pp.16.00837

Ben-Laouane, R., Meddich, A., Bechtaoui, N., Oufdou, K., and Wahbi, S. (2019). Effects of arbuscular mycorrhizal fungi and rhizobia symbiosis on the tolerance of *Medicago sativa* to salt stress. *Gesunde Pflanz.* 71, 135–146. doi: 10.1007/s10343-019-00461-x

Bompadre, M. J., Silvani, V. A., Bidondo, L. F., Rios de Molina, M. C., Colombo, R. P., and Pardo, A. G. (2014). Arbuscular mycorrhizal fungi alleviate oxidative stress in pomegranate plants growing under different irrigation conditions. *Botany* 92, 187–193. doi: 10.1139/cjb-2013-0169

Bradford, M. M. (1976). A rapid and sensitive method for the quantitation of microgram quantities of protein utilizing the principle of protein-dye binding. *Anal. Biochem.* 72, 248–254. doi: 10.1016/0003-2697(76)90527-3

Casieri, L., Ait Lahmidi, N., Doidy, J., Veneault-Fourrey, C., Migeon, A., Bonneau, L., et al. (2013). Biotrophic transportome in mutualistic plant-fungal interactions. *Mycorrhiza* 23, 597–625.

Cavagnaro, T. R. (2014). Impacts of compost application on the formation and functioning of arbuscular mycorrhizas. *Soil Biol. Biochem.* 78, 38–44. doi: 10.1016/j.soilbio.2014.07.007

Chao, C. T., and Krueger, R. R. (2007). The date palm (*Phoenix dactylifera* L.): Overview of biology, uses, and cultivation. *HortScience* 42, 1077–1082. doi: 10.21273/HORTSCI.42.5.1077

Chaumont, F., and Tyerman, S. D. (2014). Aquaporins: highly regulated channels controlling plant water relations. *Plant Physiol.* 164, 1600–1618. doi: 10.1104/pp.113.233791

Chitarra, W., Pagliarani, C., Maserti, B., Lumini, E., Siciliano, I., Cascone, P., et al. (2016). Insights on the impact of arbuscular mycorrhizal symbiosis on tomato tolerance to water stress. *Plant Physiol.* 171, 1009–1023. doi: 10.1104/pp.16.00307

De Pascale, S., Rouphael, Y., and Colla, G. (2017). Plant biostimulants: Innovative tool for enhancing plant nutrition in organic farming. *Eur. J. Hortic. Sci.* 82, 277–285. doi: 10.17660/eJHS.2017/82.6.2

Dimkpa, C., Weinand, T., and Asch, F. (2009). Plant-rhizobacteria interactions alleviate abiotic stress conditions. *Plant Cell Environ.* 32, 1682–1694. doi: 10.1111/j.1365-3040.2009.02028.x

Dubois, M., Gilles, K. A., Hamilton, J. K., Rebers, P. A., and Smith, F. (1956). Colorimetric method for determination of sugars and related substances. *Anal. Chem.* 28, 350–356. doi: 10.1021/ac60111a017

Duo, L. A., Liu, C. X., and Zhao, S. L. (2018). Alleviation of drought stress in turfgrass by the combined application of nano-compost and microbes from compost. *Russ. J. Plant Physiol.* 65, 419–426. doi: 10.1134/S102144371803010X

FAO (2018). *Drought characteristics and management in North Africa and the Near East*. Available online at: www.fao.org/3/CA0034EN/ca0034en.pdf

Fernández-Lizarazo, J. C., and Moreno-Fonseca, L. P. (2016). Mechanisms for tolerance to water-deficit stress in plants inoculated with arbuscular mycorrhizal fungi. A review. *Agron. Colomb.* 34, 179–189. doi: 10.15446/agron.colomb.v34n2.55569

Frosi, G., Barros, V. A., Oliveira, M. T., Santos, M., Ramos, D. G., Maia, L. C., et al. (2016). Symbiosis with AMF and leaf Pi supply increases water deficit tolerance of woody species from seasonal dry tropical forest. *J. Plant Physiol.* 207, 84–93. doi: 10.1016/j.jplph.2016.11.002

Grobelak, A., Napora, A., and Kacprzak, M. (2015). Using plant growth-promoting rhizobacteria (PGPR) to improve plant growth. *Ecol. Eng.* 84, 22–28. doi: 10.1016/j.ecoleng.2015.07.019

Gusain, Y. S., Singh, U. S., and Sharma, A. K. (2015). Bacterial mediated amelioration of drought stress in drought tolerant and susceptible cultivars of rice (*Oryza sativa* L.). *Afr. J. Biotechnol.* 14, 764–773. doi: 10.5897/AJB2015.14405

Hao, Z., Xie, W., Jiang, X., Wu, Z., Zhang, X., and Chen, B. (2019). Arbuscular mycorrhizal fungus improves Rhizobium–glycyrrhiza seedling symbiosis under drought stress. *Agronomy* 9, 1–12. doi: 10.3390/agronomy9100572

Harley, P. C., Loreto, F., Di Marco, G., and Sharkey, T. D. (1992). Theoretical considerations when estimating the mesophyll conductance to CO_2 flux by the analysis of the response of photosynthesis to CO_2. *Plant Physiol.* 98, 1429–1436. doi: 10.1104/pp.98.4.1429

Hidri, R., Barea, J. M., Mahmoud, O. M., Abdelly, C., and Azcón, R. (2016). Impact of microbial inoculation on biomass accumulation by *Sulla carnosa* provenances, and in regulating nutrition, physiological and antioxidant activities of this species under non-saline and saline conditions. *J. Plant Physiol.* 201, 28–41. doi: 10.1016/j.jplph.2016.06.013

Hogekamp, C., Arndt, D., Pereira, P. A., Becker, J. D., Hohnjec, N., and Küster, H. (2011). Laser microdissection unravels cell-type-specific transcription in arbuscular mycorrhizal roots, including CAAT-box transcription factor gene expression correlating with fungal contact and spread. *Plant Physiol.* 157, 2023–2043. doi: 10.1104/pp.111.186635

Hori, K., Wada, A., and Shibuta, T. (1997). Changes in phenoloxidase activities of the galls on leaves of *Ulmus davidiana* formed by *Tetraneura fusiformis* (Homoptera: Eriosomatidae). *Appl. Entomol. Zool.* 32, 365–371. doi: 10.1303/aez.32.365

Jaleel, C. A., Manivannan, P., Wahid, A., Farooq, M., Al-Juburi, H. J., Somasundaram, R., et al. (2009). Drought stress in plants: a review on morphological characteristics and pigments composition. *Int. J. Agric. Biol.* 11, 100–105.

Javan Gholiloo, M., Yarnia, M., Ghorttapeh, A. H., Farahvash, F., and Daneshian, A. M. (2019). Evaluating effects of drought stress and bio-fertilizer on quantitative and qualitative traits of valerian (*Valeriana officinalis* L.). *J. Plant Nutr.* 42, 1417–1429. doi: 10.1080/01904167.2019.1628972

Júnior, A. G. G., Pereira, R. A., Sodré, G. A., do Sacramneto, C. K., and Gross, E. (2018). Inoculation with arbuscular micorrizhal fungi and organic compost from cocoa shell positively influence the growth and mineral nutrition of soursop plants (*Annona muricata* L.). *Rev. Bras. Frutic.* 40, 1–11.

Khosravi Shakib, A., Rezaei Nejad, A., Khandan Mirkohi, A., and Kalate Jari, S. (2019). Vermicompost and manure compost reduce water-deficit stress in pot marigold (*Calendula officinalis* L. cv. Candyman Orange). *Compost Sci. Util.* 27, 61–68. doi: 10.1080/1065657X.2019.1602489

Kohler, J., Caravaca, F., Azcón, R., Díaz, G., and Roldán, A. (2015). The combination of compost addition and arbuscular mycorrhizal inoculation produced positive and synergistic effects on the phytomanagement of a semiarid mine tailing. *Sci. Total Environ.* 514, 42–48. doi: 10.1016/j.scitotenv.2015.01.085

Kumar, A., Patel, J. S., Meena, V. S., and Srivastava, R. (2019). Recent advances of PGPR based approaches for stress tolerance in plants for sustainable agriculture. *Biocatal. Agric. Biotechnol.* 20:101271. doi: 10.1016/j.bcab.2019.101271

Kumar, R. K., Singh, K. P., and Raju, D. V. S. (2015). Effect of different strains of arbuscular mycorrhizal fungi (AMF) on macro and micro nutrient uptake in micropropagated chrysanthemum plantlets. Vegetos-An Int. *J. Plant Res.* 28, 47–54. doi: 10.5958/2229-4473.2015.00036.1

Kumari, B., Mallick, M. A., Solanki, M. K., Solanki, A. C., Hora, A., and Guo, W. (2019). "Plant growth promoting rhizobacteria (PGPR): Modern prospects for sustainable agriculture," in *Plant Health Under Biotic Stress*, eds R. A. Ansari and I. Mahmood (Singapore: Springer Singapore), 109–127. doi: 10.1007/978-981-13-6040-4_6

Kwey, M. M., Banze, S. K., and Mukalay, J. B. (2015). Etude de cas sur l'impact des amendements organiques vis-à-vis de la salinité en culture de bananier. *Afrique Sci.* 11, 152–160.

Lenoir, I., Fontaine, J., and Lounès-Hadj Sahraoui, A. (2016). Arbuscular mycorrhizal fungal responses to abiotic stresses: a review. *Phytochemistry* 123, 4–15. doi: 10.1016/j.phytochem.2016.01.002

Liao, L., Dong, T., Qiu, X., Rong, Y., Wang, Z., and Zhu, J. (2019). Nitrogen nutrition is a key modulator of the sugar and organic acid content in citrus fruit. *PLoS One* 14:e0223356. doi: 10.1371/journal.pone.0223356

Liu, X., Rezaei Rashti, M., Dougall, A., Esfandbod, M., Van Zwieten, L., and Chen, C. (2018). Subsoil application of compost improved sugarcane yield through enhanced supply and cycling of soil labile organic carbon and nitrogen in an acidic soil at tropical Australia. *Soil Tillage Res.* 180, 73–81. doi: 10.1016/j.still.2018.02.013

Luciens, N. K., Yannick, U. S., Yambayamba, K., Michel, M. M., and Louis, B. L. (2014). Amélioration des propriétés physiques et chimiques du sol sous l'apport combiné des biodéchets et des engrais minéraux et influence sur le comportement du maïs (*Zea mays* L. variété Unilu). *J. Appl. Biosci.* 6130, 6121–6130.

Madhava Rao, K. V., and Sresty, T. V. S. (2000). Antioxidative parameters in the seedlings of pigeonpea (*Cajanus cajan* (L.) Millspaugh) in response to Zn and Ni stresses. *Plant Sci.* 157, 113–128. doi: 10.1016/S0168-9452(00)00273-9

Maheshwari, D. K., Kumar, S., Maheshwari, N. K., Patel, D., and Saraf, M. (2012). "Nutrient availability and management in the rhizosphere by microorganisms," in *Bacteria in Agrobiology: Stress Management*, ed. D. K. Maheshwari (Berlin: Springer), 301–326. doi: 10.1007/978-3-642-23465-1

Meddich, A., Ait El Mokhtar, M., Bourzik, W., Mitsui, T., Baslam, M., and Hafidi, M. (2018). "Optimizing growth and tolerance of date palm (*Phoenix dactylifera* L.) to drought, salinity, and vascular fusarium-induced wilt (*Fusarium oxysporum*) by application of arbuscular mycorrhizal fungi (AMF)," in *Root Biology*, eds B. Giri, R. Prasad, and A. Varma (Cham: Springer), 239–258. doi: 10.1007/978-3-319-75910-4

Meddich, A., and Boumezzough, A. (2017). First detection of *Potosia opaca* larva attacks on *Phoenix dactylifera* and *P. canariensis* in Morocco: focus on pests control strategies and soil quality of prospected palm groves. *J. Entomol. Zool. Stud.* 5, 984–991.

Meddich, A., Elouaqoudi, F., Khadra, A., and Bourzik, W. (2016). Valorization of green and industrial waste by composting process. *J. Rev. Compos. Adv. Mater.* 26, 451–469.

Meddich, A., Jaiti, F., Bourzik, W., El Asli, A., and Hafidi, M. (2015a). Use of mycorrhizal fungi as a strategy for improving the drought tolerance in date palm (*Phoenix dactylifera*). *Sci. Hortic.* 192, 468–474. doi: 10.1016/j.scienta.2015.06.024

Meddich, A., Mézy, M., Allain, E., and Toutain, G. (2015b). Optimisation de la croissance et du developpement du palmier dattier en pepiniere par l'utilisation d'amendements biologiques, organiques et chimiques. *Eur. Sci. J.* 11, 396–408.

Meddich, A., Oihabi, A., Jaiti, F., Bourzik, W., and Hafidi, M. (2015c). Rôle des champignons mycorhiziens arbusculaires dans la tolérance du palmier dattier (*Phoenix dactylifera*) à la fusariose vasculaire et au déficit hydrique. *Botany* 93, 1–9.

Meddich, A., Oufdou, K., Boutasknit, A., Raklami, A., Tahiri, A., Ben-Laouane, R., et al. (2019). "Use of organic and biological fertilizers as strategies to improve crop biomass, yields and physicochemical parameters of soil," in *Nutrient Dynamics for Sustainable Crop Production*, ed. R. S. Meena (Singapore: Springer Singapore), 247–288. doi: 10.1007/978-981-13-8660-2_9

Mehta, C. M., Palni, U., Franke-Whittle, I. H., and Sharma, A. K. (2014). Compost: Its role, mechanism and impact on reducing soil-borne plant diseases. *Waste Manag.* 34, 607–622. doi: 10.1016/j.wasman.2013.11.012

Nadeem, S. M., Ahmad, M., Zahir, Z. A., Javaid, A., and Ashraf, M. (2014). The role of mycorrhizae and plant growth promoting rhizobacteria (PGPR) in improving crop productivity under stressful environments. *Biotechnol. Adv.* 32, 429–448. doi: 10.1016/j.biotechadv.2013.12.005

Nikitas, C., Pocock, R., Toleman, I., and Gilbert, E. J. (2008). *The State of Composting and Biological Waste Treatment in the UK 2005/06*. Wellingborough: The composting Association.

Ning, C. C., Gao, P. D., Wang, B. Q., Lin, W. P., Jiang, N. H., and Cai, K. Z. (2017). Impacts of chemical fertilizer reduction and organic amendments supplementation on soil nutrient, enzyme activity and heavy metal content. *J. Integr. Agric.* 16, 1819–1831. doi: 10.1016/S2095-3119(16)61476-4

Oihabi, A. (1991). *Effet des endomycorhizes V.A sur la croissance et la nutrition minérale du palmier dattier*. Thèse de Doctorat d'Etat. Université Cadi Ayyad de Marrakech, Maroc/Univ. Bourgogne Dijon France, 117.

Olsen, S., and Sommers, L. (1982). Methods of soil analysis. Part 2. Chemical and microbiological properties of phosphorus. *ASA Monograp.* 9, 403–430.

Ortuño, M. F., Lorente, B., Hernández, J. A., and Sánchez-Blanco, M. J. (2018). Mycorrhizal inoculation on compost substrate affects nutritional balance, water uptake and photosynthetic efficiency in *Cistus albidus* plants submitted to water stress. *Rev. Bras. Bot.* 41, 299–310. doi: 10.1007/s40415-018-0457-9

Padilla, F. M., Peña-Fleitas, M. T., Fernández, M. D., Del Moral, F., Thompson, R. B., and Gallardo, M. (2017). Responses of soil properties, crop yield and root growth to improved irrigation and N fertilization, soil tillage and compost addition in a pepper crop. *Sci. Hortic.* 225, 422–430. doi: 10.1016/j.scienta.2017.07.035

Pagano, M. C. (2014). "Drought stress and mycorrhizal plants," in *Use of Microbes for the Alleviation of Soil Stress*, ed. M. Miransai (New York, NY: Springer), 97–110.

Paul, M. J., Primavesi, L. F., Jhurreea, D., and Zhang, Y. (2008). Trehalose metabolism and signaling. *Annu. Rev. Plant Biol.* 59, 417–441. doi: 10.1146/annurev.arplant.59.032607.092945

Paymaneh, Z., Sarcheshmehpour, M., Bukovská, P., and Jansa, J. (2019). Could indigenous arbuscular mycorrhizal communities be used to improve tolerance of pistachio to salinity and/or drought? *Symbiosis* 79, 269–283. doi: 10.1007/s13199-019-00645-z

Phillips, J. M., and Hayman, D. S. (1970). Improved procedures for clearing roots and staining parasitic and vesicular-arbuscular mycorrhizal fungi for rapid assessment of infection. *Trans. Br. Mycol. Soc.* 55, 158–161. doi: 10.1016/S0007-1536(70)80110-3

Pieterse, C. M., Zamioudis, C., Berendsen, R. L., Weller, D. M., Van Wees, S. C., and Bakker, P. A. (2014). Induced systemic resistance by beneficial microbes. *Annu. Rev. Phytopathol.* 52, 347–375. doi: 10.1146/annurev-phyto-082712-102340

Pozo, M. J., and Azcón-Aguilar, C. (2007). Unraveling mycorrhiza-induced resistance. *Curr. Opin. Plant Biol.* 10, 393–398. doi: 10.1016/j.pbi.2007.05.004

Raklami, A., Bechtaoui, N., Tahiri, A., Anli, M., Meddich, A., and Oufdou, K. (2019). Use of rhizobacteria and mycorrhizae consortium in the open field as a strategy for improving crop nutrition, productivity and soil fertility. *Front. Microbiol.* 10:1106. doi: 10.3389/fmicb.2019.01106

Rillig, M. C., Wendt, S., Antonovics, J., Hempel, S., Kohler, J., Wehner, J., et al. (2014). Interactive effects of root endophytes and arbuscular mycorrhizal fungi on an experimental plant community. *Oecologia* 174, 263–270. doi: 10.1007/s00442-013-2759-8

Rodier, J. (1984). *L'analyse de l'eau: eaux Naturelles, eaux résiduaires, eau de mer*, 7 ème Edn. Paris: Dunod, 1365.

Sánchez-Romera, B., Ruiz-Lozano, J. M., Zamarreño, ÁM., García-Mina, J. M., and Aroca, R. (2016). Arbuscular mycorrhizal symbiosis and methyl jasmonate avoid the inhibition of root hydraulic conductivity caused by drought. *Mycorrhiza* 26, 111–122. doi: 10.1007/s00572-015-0650-7

Sandhya, V., Ali, S. Z., Grover, M., Reddy, G., and Venkateswarlu, B. (2010). Effect of plant growth promoting *Pseudomonas* spp. on compatible solutes, antioxidant status and plant growth of maize under drought stress. *Plant Growth Regul.* 62, 21–30. doi: 10.1007/s10725-010-9479-4

Sarwat, M., and Tuteja, N. (2017). Hormonal signaling to control stomatal movement during drought stress. *Plant Gene* 11, 143–153. doi: 10.1016/j.plgene.2017.07.007

Sever, K., Bogdan, S., Franjiæ, J., and Škvorc, Ž (2018). Nondestructive estimation of photosynthetic pigment concentrations in pedunculate oak (*Quercus robur* L.) leaves. *Sumar. List* 142, 247–256.

Sghir, F., Chliyeh, M., Touati, J., Mouria, B., Touhami, O.-A., Filali-Maltouf, A., et al. (2014). Effect of a dual inoculation with endomycorrhizae and *Trichoderma harzianum* on the growth of date palm seedlings. *Int. J. Pure Appl. Biosci.* 2, 12–26.

Shaw, R. G., and Etterson, J. R. (2012). Rapid climate change and the rate of adaptation: insight from experimental quantitative genetics. *New Phytol.* 195, 752–765. doi: 10.1111/j.1469-8137.2012.04230.x

Shen, Z., Zhong, S., Wang, Y., Wang, B., Mei, X., Li, R., et al. (2013). Induced soil microbial suppression of banana fusarium wilt disease using compost and biofertilizers to improve yield and quality. *Eur. J. Soil Biol.* 57, 1–8. doi: 10.1016/j.ejsobi.2013.03.006

Strasser, B. J., and Strasser, R. J. (1995). "Measuring fast fluorescence transients to address environmental questions: the JIP-test," in *Photosynthesis: From Light to Biosphere*, ed. P. Mathis (Dordrecht: Springer Netherlands), 4869–4872. doi: 10.1007/978-94-009-0173-5_1142

Symanczik, S., Lehmann, M. F., Wiemken, A., Boller, T., and Courty, P.-E. (2018). Effects of two contrasted arbuscular mycorrhizal fungal isolates on nutrient uptake by Sorghum bicolor under drought. *Mycorrhiza* 28, 779–785. doi: 10.1007/s00572-018-0853-9

Tartoura, K. A. H. (2010). Alleviation of oxidative-stress induced by drought through application of compost in wheat (*Triticum aestivum* L.) plants. *Am. J. Agric. Environ. Sci.* 9, 208–216.

Tartoura, K. A. H., Youssef, S. A., and Tartoura, E.-S. A. A. (2014). Compost alleviates the negative effects of salinity via up- regulation of antioxidants in *Solanum lycopersicum* L. plants. *Plant Growth Regul.* 74, 299–310. doi: 10.1007/s10725-014-9923-y

Tejera García, N. A., Olivera, M., Iribarne, C., and Lluch, C. (2004). Partial purification and characterization of a non-specific acid phosphatase in leaves and root nodules of *Phaseolus vulgaris*. *Plant Physiol. Biochem.* 42, 585–591. doi: 10.1016/j.plaphy.2004.04.004

Trouvelot, A., Kough, J. L., and Gianinazzi-Pearson, V. (1986). Du taux de mycorhization VA d'un système radiculaire. Recherche de méthodes d'estimation ayant une signification fonctionnelle. *Mycorhizes Physiol. Génétique* 217–221. doi: 10.1177/004057368303900411

Velikova, V., Yordanov, I., and Edreva, A. (2000). Oxidative stress and some antioxidant systems in acid rain-treated bean plants. *Plant Sci.* 151, 59–66. doi: 10.1016/s0168-9452(99)00197-1

Volpe, V., Giovannetti, M., Sun, X. G., Fiorilli, V., and Bonfante, P. (2016). The phosphate transporters LjPT4 and MtPT4 mediate early root responses to phosphate status in non mycorrhizal roots. *Plant Cell Environ.* 39, 660–671. doi: 10.1111/pce.12659

Vurukonda, S. S. K. P., Vardharajula, S., Shrivastava, M., and SkZ, A. (2016). Enhancement of drought stress tolerance in crops by plant growth promoting rhizobacteria. *Microbiol. Res.* 184, 13–24. doi: 10.1016/j.micres.2015.12.003

Whitman, E. (2019). A land without water: the scramble to stop Jordan from running dry. *Nature* 573, 20–23. doi: 10.1038/d41586-019-02600-w

Wu, H., Xiang, W., Chen, L., Ouyang, S., Xiao, W., Li, S., et al. (2019). Soil phosphorus bioavailability and recycling increased with stand age in chinese fir plantations. *Ecosystems* 23, 973–988. doi: 10.1007/s10021-019-00450-1

Wu, Q., Xia, R., and Hu, Z. (2006). Effect of arbuscular mycorrhiza on the drought tolerance of *Poncirus trifoliata* seedlings. *Front. Forst. China* 1, 100–104. doi: 10.1007/s11461-005-0007-z

Wu, Q., and Zou, Y. (2017). "Arbuscular mycorrhizal fungi and tolerance of drought stress in plants," in *Arbuscular Mycorrhizas and Stress Tolerance of Plants*, ed. Q.-S. Wu (Singapore: Springer Singapore), 25–41. doi: 10.1007/978-981-10-4115-0

Xie, W., Hao, Z., Zhou, X., Jiang, X., Xu, L., Wu, S., et al. (2018). Arbuscular mycorrhiza facilitates the accumulation of glycyrrhizin and liquiritin in *Glycyrrhiza uralensis* under drought stress. *Mycorrhiza* 28, 285–300. doi: 10.1007/s00572-018-0827-y

Yadav, K., Aggarwal, A., and Singh, N. (2013). Arbuscular mycorrhizal fungi (AMF) induced acclimatization, growth enhancement and colchicine content of micropropagated *Gloriosa superba* L. plantlets. *Ind. Crops Prod.* 45, 88–93. doi: 10.1016/j.indcrop.2012.12.001

Yang, W., Gu, S., Xin, Y., Bello, A., Sun, W., and Xu, X. (2018). Compost addition enhanced hyphal growth and sporulation of arbuscular mycorrhizal fungi without affecting their community composition in the soil. *Front. Microbiol.* 9:169. doi: 10.3389/fmicb.2018.00169

Yu, Y. Y., Li, S. M., Qiu, J. P., Li, J. G., Luo, Y. M., and Guo, J. H. (2019). Combination of agricultural waste compost and biofertilizer improves yield and enhances the sustainability of a pepper field. *J. Plant Nutr. Soil Sci.* 182, 560–569. doi: 10.1002/jpln.201800223

Zhang, F., Zou, Y.-N., and Wu, Q.-S. (2018). Quantitative estimation of water uptake by mycorrhizal extraradical hyphae in citrus under drought stress. *Sci. Hortic.* 229, 132–136. doi: 10.1016/j.scienta.2017.10.038

Zhang, Y., Zhong, C. L., Chen, Y., Chen, Z., Jiang, Q. B., Wu, C., et al. (2010). Improving drought tolerance of *Casuarina equisetifolia* seedlings by arbuscular mycorrhizas under glasshouse conditions. *New For.* 40, 261–271. doi: 10.1007/s11056-010-9198-8

Zou, Y. N., and Wu, Q. S. (2011). Efficiencies of five arbuscular mycorrhizal fungi in alleviating salt stress of trifoliate orange. *Int. J. Agric. Biol.* 13, 991-995.

Conflict of Interest: The authors declare that the research was conducted in the absence of any commercial or financial relationships that could be construed as a potential conflict of interest.

Advantages of publishing in Frontiers

OPEN ACCESS
Articles are free to read for greatest visibility and readership

FAST PUBLICATION
Around 90 days from submission to decision

HIGH QUALITY PEER-REVIEW
Rigorous, collaborative, and constructive peer-review

TRANSPARENT PEER-REVIEW
Editors and reviewers acknowledged by name on published articles

Frontiers
Avenue du Tribunal-Fédéral 34
1005 Lausanne | Switzerland

Visit us: www.frontiersin.org
Contact us: frontiersin.org/about/contact

REPRODUCIBILITY OF RESEARCH
Support open data and methods to enhance research reproducibility

DIGITAL PUBLISHING
Articles designed for optimal readership across devices

FOLLOW US
@frontiersin

IMPACT METRICS
Advanced article metrics track visibility across digital media

EXTENSIVE PROMOTION
Marketing and promotion of impactful research

LOOP RESEARCH NETWORK
Our network increases your article's readership